C–H Activation by Ruthenium(II), Cobalt(III) and Manganese(I) Catalysis

Dissertation

for the award of the degree

"Doctor rerum naturalium"

of the Georg-August-Universität Göttingen

within the doctoral program of chemistry

of the Georg-August-University School of Science (GAUSS)

submitted by

Daniel Zell

from Bad Karlshafen

Göttingen, 2017

Thesis Committee

Prof. Dr. Lutz Ackermann, Institute of Organic and Biomolecular Chemistry

PD Dr. Alexander Breder, Institute of Organic and Biomolecular Chemistry

Members of the Examination Board

Reviewer: Prof. Dr. Lutz Ackermann, Institute of Organic and Biomolecular Chemistry

Second Reviewer: PD Dr. Alexander Breder, Institute of Organic and Biomolecular Chemistry

Further Members of the Examination Board

Prof. Dr. Konrad Koszinowski, Institute of Organic and Biomolecular Chemistry

Prof. Dr. Dietmar Stalke, Institute of Inorganic Chemistry

Dr. Shoubik Das, Institute of Organic and Biomolecular Chemistry

Dr. Franziska Thomas, Institute of Organic and Biomolecular Chemistry

Date of the Oral Examination: 04.07.2017

Contents

List of Abbreviations

Ac	acetyl
acac	acetyl acetonate
Ad	adamantyl
Alk	alkyl
AMLA	ambiphilic metal-ligand activation
aq.	aqueous
Ar	aryl
atm	atmospheric pressure
ATR	attenuated total reflectance
BHT	2,6-di-*tert*-butyl-4-methylphenol
BIES	base-assisted internal electrophilic substitution
BINAP	2,2'-bis(diphenylphosphino)-1,1'-binaphthyl
Bn	benzyl
Boc	*tert*-butyloxycarbonyl
Bu	butyl
Bz	benzoyl
calc.	calculated
cat.	catalytic
cf.	*confer*
CMD	concerted metalation deprotonation
cod	1,5-cyclooctadiene
conv.	conversion
Cp	cyclopentadienyl
Cp*	pentamethylcyclopentadienyl
Cy	cyclohexyl
δ	chemical shift
d	doublet
DCE	1,2-dichloroethane
DCM	dichloromethane
dd	doublet of doublet
DFT	density functional theory
DG	directing group
DMA	*N,N*-dimethylacetamide
DME	1,2-dimethoxyethane
DMF	*N,N*-dimethylformamide
DMSO	dimethyl sulfoxide
DMPU	1,3-dimethyl-3,4,5,6-tetrahydro-2(1*H*)-pyrimidinone
DPPH	2,2-diphenyl-1-picrylhydrazyl
dt	doublet of triplet
E	electron-withdrawing group
Ed.	edition

ee	enantiomeric excess
e.g.	*exempli gratia*
EI	electron ionization
equiv	equivalent
ESI	electronspray ionization
Et	ethyl
FG	functional group
g	gram
GC	gas chromatography
GPC	gel permeation chromatography
h	hour
Hal	halogen
Het	hetero(aryl)
Hept	heptyl
Hex	hexyl
HFIP	1,1,1,3,3,3-hexafluoro-2-propanol
HPLC	high performance liquid chromatography
HR-MS	high resolution mass spectrometry
Hz	Hertz
i	*iso*
IES	internal electrophilic substitution
IMes	1,3-bis(2,4,6-trimethylphenyl)imidazol-2-ylidene
IR	infrared spectroscopy
J	coupling constant
KIE	kinetic isotope effect
L	ligand
LDA	lithium diisopropylamide
LiHMDS	lithium bis(trimethylsilyl)amide
LLHT	ligand-to-ligand hydrogen transfer
m	*meta*
m	multiplet
M	molar
$[M]^+$	molecular ion peak
Me	methyl
Mes	mesityl
mg	milligram
MHz	megahertz
min	minute
mL	milliliter
mmol	millimol
M. p.	melting point
MS	mass spectrometry
MTBE	methyl *tert*-butyl ether
m/z	mass-to-charge ratio
NCFS	*N*-cyano-*N*-(4-fluorophenyl)-4-methylbenzenesulfonamide
NCTS	*N*-cyano-4-methyl-*N*-phenyl benzenesulfonamide
NHC	*N*-heterocyclic carbene
NMP	*N*-methylpyrrolidinone

NMR	nuclear magnetic resonance
o	*ortho*
OPV	oil pump vacuum
p	*para*
PA	phosphinous acid
pent	pentyl
Ph	phenyl
PMP	*para*-methoxyphenyl
Piv	pivaloyl
ppm	parts per million
Pr	propyl
Py	pyridyl
q	quartet
ref.	reference
r.r.	regioisomeric ratio
RT	room temperature
s	singlet and second
sat.	saturated
SET	single electron transfer
SPO	secondary phosphine oxide
SPS	solvent purification system
t	*tert*
t	triplet
T	temperature
TEMPO	2,2,6,6-tetramethylpiperidine-*N*-oxide
Tf	trifluoromethanesulfonyl
TFE	2,2,2-Trifluoroethanol
TFA	trifluoroacetic acid
THF	tetrahydrofuran
TLC	thin layer chromatography
TM	transition metal
TMP	3,4,5-trimethoxyphenyl
TMS	trimethylsilyl
Ts	*para*-toluenesulfonyl
TS	transition state
wt%	weight percent
X	(pseudo)halide

1   Introduction

1.1   Transition Metal-Catalyzed C–H Activation

The past five decades have witnessed prosperous advances in the development of highly efficient transition metal-catalyzed C–C/C–Het bond forming processes that tremendously expanded the toolbox of modern organic synthesis. Thus far, predominantly transition metal-catalyzed cross coupling reactions, such as *Hiyama-*,[1] *Kumada-Corriu-*,[2] *Mizoroki-Heck-*,[3] *Negishi-*,[4] *Sonogashira-*,[5] *Stille-*,[6] and *Suzuki-Miyaura*-couplings,[7] have found widespread applications in agrochemical and pharmaceutical industry and streamlined the total synthesis of complex natural products.[8] Consequently, these significant innovations culminated in the Nobel Prize for Chemistry in 2010 for *Heck*, *Negishi* and *Suzuki*.

Despite this enormous progress, cross-coupling reactions are associated with a series of drawbacks like prefunctionalization to often sensitive starting materials and the generation of toxic by-products (Figure 1).[9] However, climate change and severe environmental pollution due to chemicals have created a strong demand for atom-[10] and step-economical[11] processes, giving rise to the concept of green chemistry.[12]

In striking contrast, C–H bond functionalizations[13] have become an invaluable and powerful strategy to achieve synthetic versatility in excellent atom- and step-economies by obviating typical prefunctionalization steps and directly functionalizing C–H bonds.
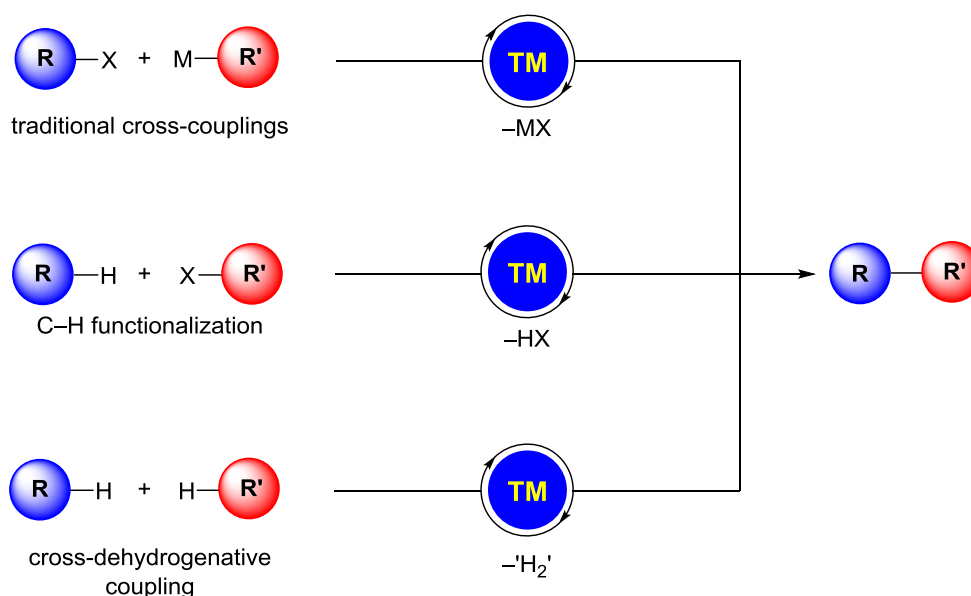
Figure 1. Comparison of general methods for C–C/C–Het bond formation.

Nonetheless, environmentally benign and sustainable transition metal-catalyzed transformations should not only match substrate availability: the use of earth-abundant 3d base and particularly cost-effective metals is also of prime importance. Thus, a boost in the development of *inter alia*

manganese-[14] and cobalt-catalyzed[15] C–H functionalizations has revolutionized sustainable organic synthesis.

The most important basis for the development of new efficient metal-catalyzed C–H functionalizations is a detailed mechanistic understanding. Consequently, considerable efforts have been made to elucidate several mechanistically distinct pathways for the crucial C–H activation step (Scheme 1).[16] In this respect, a) oxidative addition was observed for late metals in low oxidation states. Furthermore, for *e.g.* alkylidene-, amide-, imide-, or alkoxide complexes of early as well as late transition metals, b) 1,2 addition to the C–H bond is favored *via* formal $[2_\sigma + 2_\pi]$ reaction.[17] In addition, c) an electrophilic substitution mechanism was observed for *inter alia* Pd^{2+} and Pt^{2+} in polar media and involves the electrophilic attack of the metal to carbon.[18] For *inter alia* actinides, lanthanides, and early transition metals which are not prone to oxidations state changes d) σ-bond metathesis is a commonly proposed pathway.[16c] Closely related to σ-bond metathesis, *Periana*/*Goddard*[19] coined the term internal electrophilic substitution (IES) for mechanisms involving electrophilic attack of the metal and deprotonation by *e.g.* alkoxy-ligands *via* a four-membered transition state.
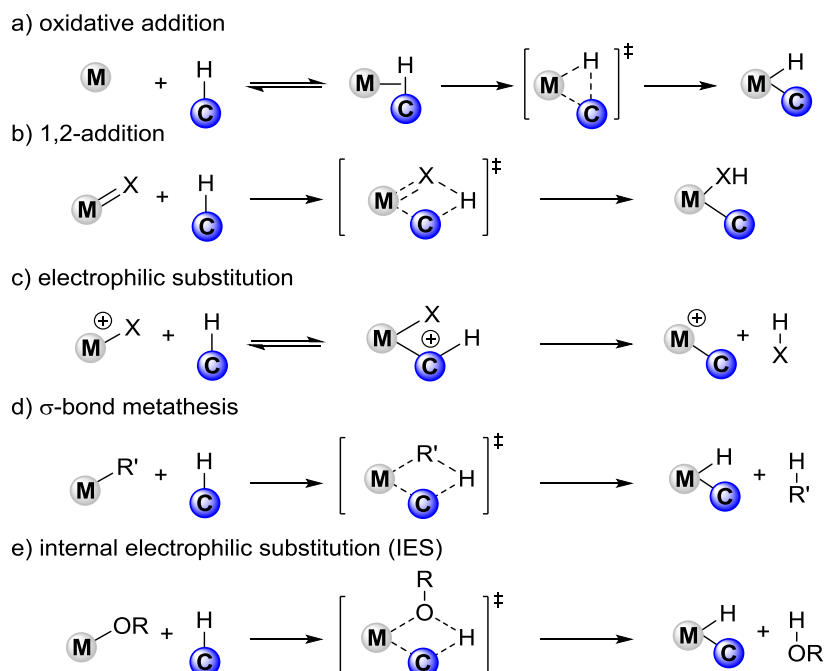
Scheme 1. Common mechanistic pathways for C–H activation.

In contrast to the above mentioned mechanistic scenarios, numerous reports have highlighted base-assisted C–H metalation events (Scheme 2).[20] While *Fagnou*/*Gorelsky*[20c] have coined the term CMD (concerted metalation deprotonation), computational studies by *MacGregor*/*Davies*[21] revealed an agostic metal-hydrogen interaction, being rationalized by the term ambiphilic metal-ligand activation (AMLA). In both mechanisms, the metalation and deprotonation steps proceed in a concerted fashion *via* a six-membered transition state (Scheme 2a). Additionally, typical experimental characteristics of

CMD-type C–H functionalizations are often high kinetic isotope effects (KIEs) and a clear preference for acidic C–H bonds.[22]

Nevertheless, in recent years several reports have emphasized a significant rate acceleration of electrophilic substitution type C–H activations by bifunctional acetate or carboxylate additives, which are suggested to proceed *via* a six-membered transition state. Based on detailed mechanistic studies, this manifold was termed base-assisted internal electrophilic substitution (BIES) (Scheme 2b). Thus, intermolecular competition experiments have revealed a preference for more electron-rich substrates and typically low KIEs have been observed which clearly underline the unique mechanism of this pathway. Hence, in contrast to CMD-type C–H activation, the site-selectivity of BIES-type C–H transformations was not governed by kinetic C–H acidity.[23]
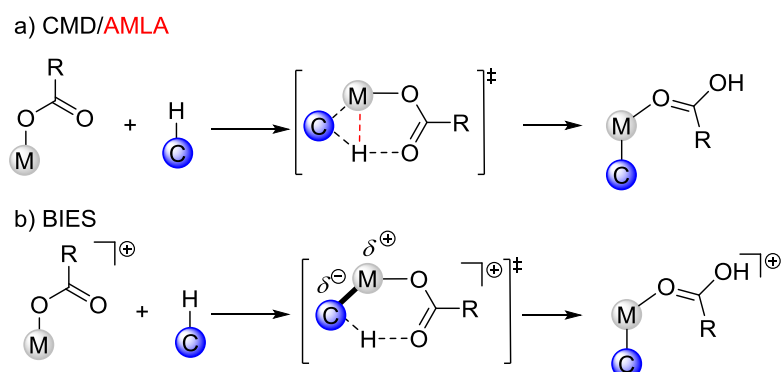
Scheme 2. Base-assisted C–H activation mechanisms.

Moreover, a major challenge in C–H functionalizations includes achieving regioselectivity in complex molecules which display C–H bonds with similar dissociation energies. Besides the preference for the activation of somewhat more acidic positions *e.g.* in azoles, a strategy involving *Lewis* basic functionalities, which direct the transition metal into close proximity, has been well established in the field of C–H activation (Scheme 3).
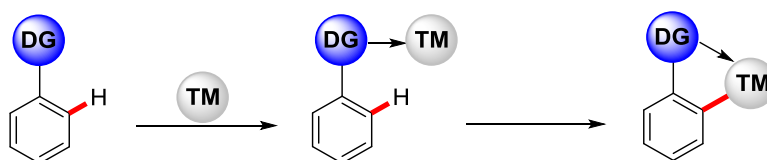
Scheme 3. Regioselective C–H activation by directing groups.

In recent years, numerous efforts have been made to explore weak,[24] modifiable or even removable directing groups (Figure 2),[25] which have overall strongly contributed to the versatility of C–H functionalizations and their impact on sustainable organic synthesis.
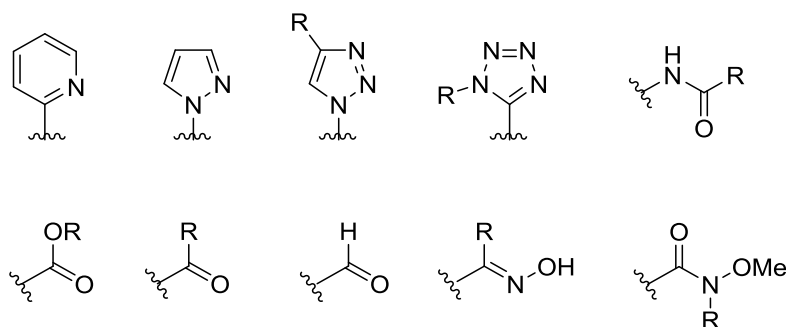
Figure 2. Selected examples of important directing groups in C–H activation catalysis.

1.2   Ruthenium-Catalyzed C–H Arylations

The development of cost-effective methods for the preparation of biaryls has gained tremendous interest in the past decades since biaryls are common structural motifs in *inter alia* agrochemically and pharmaceutically relevant molecules. In addition, there is a lack of generally applicable classical methods for their synthesis.[26]

Thus far, a number of synthetic methods have been developed for the synthesis of biaryls, with cross-coupling reactions being particularly powerful.[8] As mentioned above, a more sustainable strategy to accomplish C–C bond formations involves the direct C–H functionalization by cost-effective metals, such as ruthenium. Until now, ruthenium complexes have been employed for numerous C–H transformations, including C–C, but also a wealth of C–Het bond formations.[26b, 27]

As early as 2001, the first ruthenium-catalyzed C–H arylation was reported by *Oi/Inoue*, who used the dimeric [RuCl$_2$(benzene)]$_2$ complex and triphenylphosphine as the crucial additive for the *ortho-* selective C–H arylation of 2-phenylpyridine (**1a**) with aryl bromides **2** (Scheme 4). Remarkably, their studies already revealed that ruthenium(II) catalysts are able to undergo oxidative addition with challenging aryl chlorides **3** as well as aryl triflates **4**.[28] In this regard, the authors disclosed the following reactivity order for the mono-arylation of 2-phenylpyridine (**1a**): PhCl < PhOTf < PhI < PhBr.

Interestingly, a series of additives, including phosphines, phosphites, and bidendate diphosphines rendered phosphines as the optimal choice. It is noteworthy that the di-arylated product **5aa'** was obtained solely by drastically increasing the amount of the aryl bromide **2**.
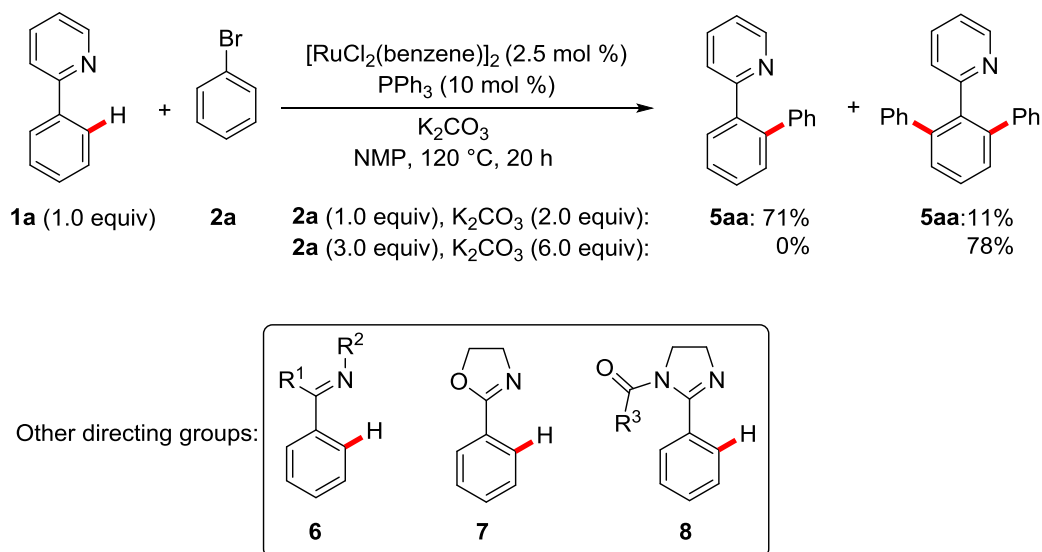
Scheme 4. Ruthenium(II)-catalyzed C–H arylation.

Further studies by *Oi/Inoue* and coworkers[29] have extended the applicability of these arylation methods to valuable directing groups, such as ketimines **6**,[30] oxazolines **7**, and imidazolines **8**.[31] Remarkably, the authors accomplished a highly *Z*-selective ruthenium(II)-catalyzed arylation of (*E*)-2-styrylpyridines **9**, which displayed a wide substrate scope of arylated (*E*)-2-styrylpyridines **10** (Scheme 5).[32] Nevertheless, the arylation of 2-vinylpyridines **11** was not achieved and there was no example for acyclic tetrasubstituted alkenes **11**. However, the reaction system of *Oi/Inoue* was later shown to be irreproducible due to impurities in the solvent NMP.[33]
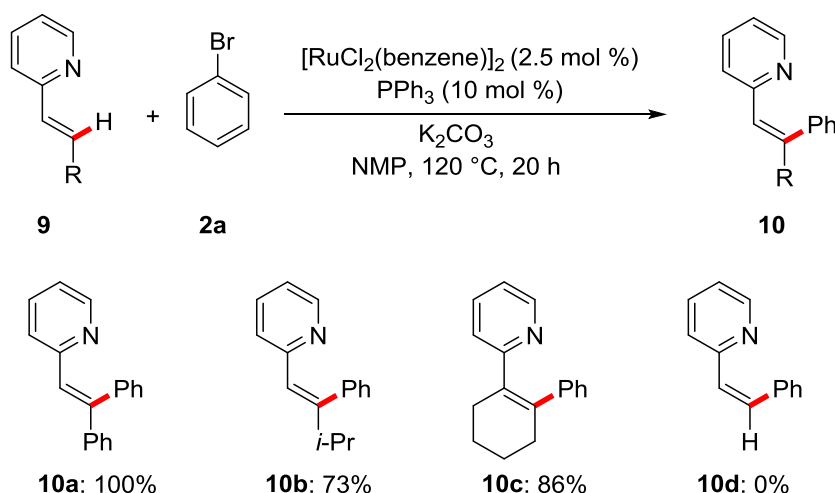
Scheme 5. Ruthenium(II)-catalyzed arylation of alkenes (*E*)-styrylpyridines **9**.

At around the same time, *Kakiuchi* and coworkers accomplished a ruthenium(0)-catalyzed C–H arylations with arylboronates **12** as the arylating reagents, utilizing valuable ketones **13** as the directing group (Scheme 6a).[34] The authors proposed that the ruthenium complex first undergoes oxidative addition with the C–H bond, then transmetalation, and finally reductive elimination occur. However, a major drawback of this reaction is the formation of one equivalent of the corresponding

benzylic alcohols by reduction of ketone **13**. Subsequently, the efficiency of this reaction has been improved by the addition of acetone or pinacolone, which suppressed the reduction and thus avoided excess amounts of the ketone **13a** (Scheme 6b).

a)

13a (2.0 equiv)   **12a** (1.0 equiv)   **14aa**: 80%

[RuH$_2$(CO)(PPh$_3$)$_3$] (2.0 mol %)
PhMe, reflux, 1 h

b)

13a (1.0 equiv)   **12a** (1.1 equiv)   **14aa**: 76%

[RuH$_2$(CO)(PPh$_3$)$_3$] (2.0 mol %)
pinacolone, reflux, 1 h
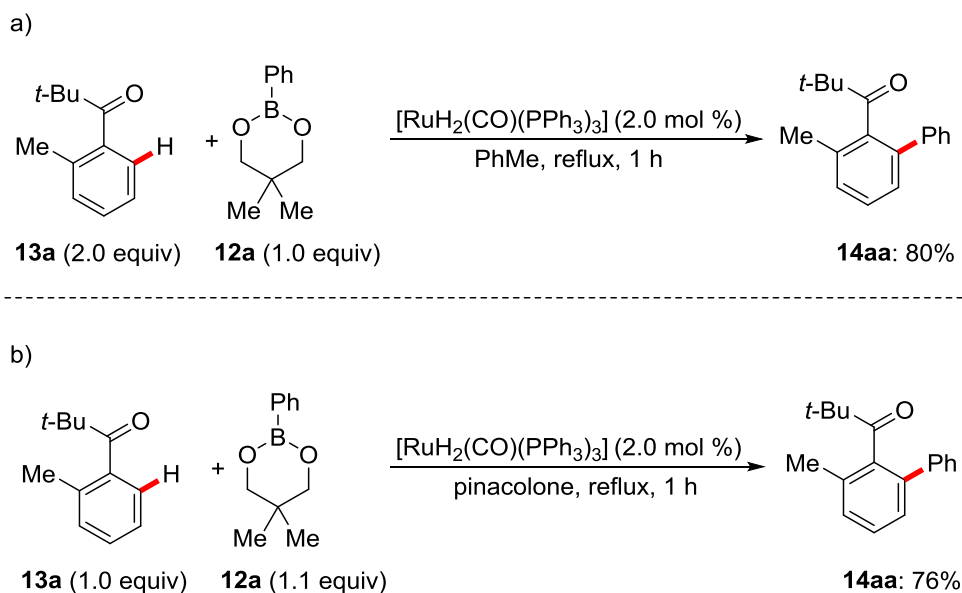
Scheme 6. Ruthenium(0)-catalyzed C–H arylation with arylboronate **12a**.

Interestingly, the authors presented compelling evidence for the coordination of the ketone **13** to the ruthenium-hydride complex, which they inferred from a difference between intra- and intermolecular kinetic isotope effects (KIEs). Under optimal reaction conditions, the authors showed a broad applicability towards electron-donating and electron-withdrawing substituents. Nonetheless, valuable functional groups such as esters, cyano-, chloro-, bromo-, and iodo-substituents not being within the reaction scope represented a major limitation.[35]

Despite these undisputed advances, a general and efficient ruthenium-catalyzed arylation using inexpensive aryl chlorides **3** had not yet been disclosed at that time, and all protocols were limited to phosphine ligands.

As early as 2005, *Ackermann* presented a significant breakthrough in ruthenium(II)-catalyzed arylations by employing structurally diverse (heteroatom-substituted) secondary phosphine oxides[36] ((HA)SPOs) as powerful preligands (Scheme 7).
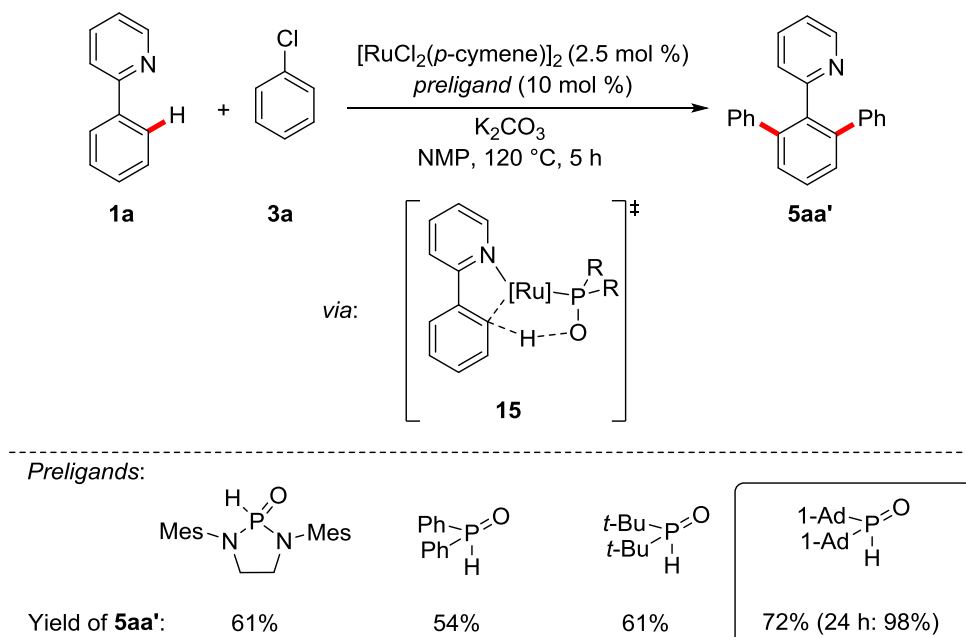
Scheme 7. Ruthenium(II)-catalyzed C–H arylations using SPOs as additives.

Hence, a large variety of different air-stable SPOs and HASPOs was tested, somewhat counterintuitively rendering the sterically most hindered di-adamantyl-substituted SPO as the optimal additive. Under the optimized reaction conditions a series of valuable functional groups, such as esters, ketones, and nitriles, was well tolerated and, moreover, it was demonstrated that modifiable ketimines **6** as the directing group delivered the corresponding mono-arylated products **5** in overall higher efficiency than *Oi/Inoue* had previously achieved by using phosphine additives (*vide supra*).[30] Thereafter, the mechanistic working mode of the SPO preligands was proposed to be a ruthenium(II)-phosphinous acid (PA) cooperative C–H activation *via* a five-membered transition state **15** (Scheme 7).[36a]

Subsequently, *Ackermann* and coworkers reported on a (HA)SPO-preligand enabled ruthenium-catalyzed C–H arylation with aryl tosylates, highlighting the catalytic system to enable oxidative addition through C–O[37] bond cleavage.[36b]

Inspired by the successful strategy of applying bifunctional ligands like SPOs, *Ackermann* and coworkers introduced –for the first time in ruthenium-catalyzed C–H functionalizations– carboxylates as additives (Scheme 8).[36a] The mechanistic pathway of the C–H activation by carboxylate-assistance was suggested to proceed *via* a six-membered CMD-type transition state **16** that had first been proposed by *Reutov* and coworkers[38] and was thereafter computationally studied by *Fagnou/Gorelsky* for the palladium-catalyzed C–H activation.[20c, 39]

Hence, a significant rate acceleration by carboxylates as compared to phosphines and phosphates was also observed for the ruthenium(II)-catalyzed C–H arylation of triazoles **17**. Notably, triazoles **17** are valuable directing groups due to their considerable impact on bioorganic chemistry and material sciences.[40] In contrast to previous reports, less polar toluene was successfully employed as the

solvent, since NMP is hygroscopic and often led to irreproducible results due to carboxylic acid impurities (*vide supra*).[26a, 33]
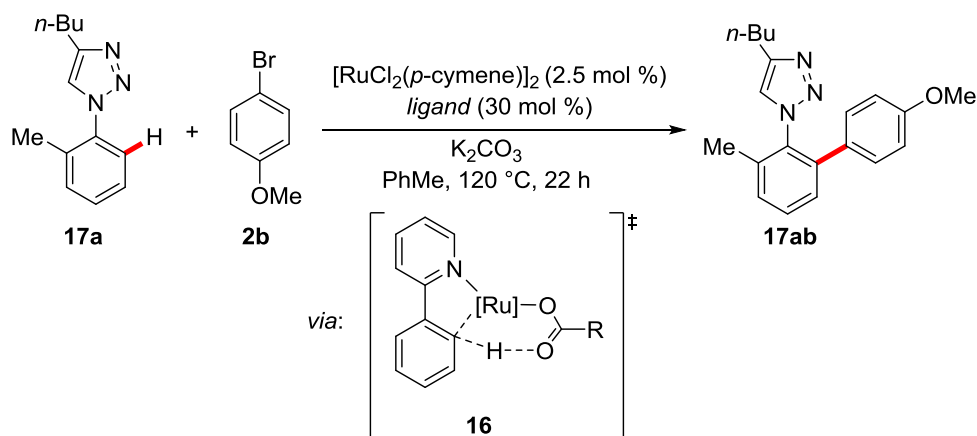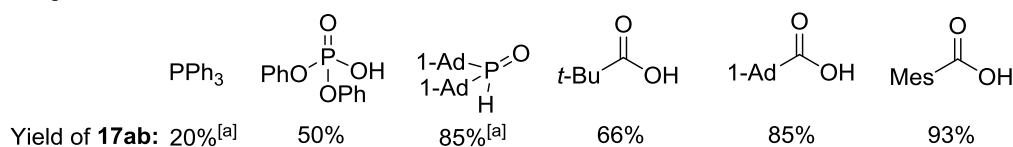
Scheme 8. Ruthenium(II)-catalyzed C–H arylation through carboxylate-assistance. [a] 10 mol %.

Thereafter, the idea of using carboxylate additives was picked up by *Dixneuf* and coworkers, as they utilized the well-defined ruthenium(II)-acetate complex [Ru(OAc)$_2$(*p*-cymene)] as a competent catalyst for the construction of poly-heterocyclic molecules by C–H arylation.[41]

The first detailed mechanistic insights for carboxylate-assisted ruthenium-catalyzed C–H activations were reported by *Ackermann* and coworkers in 2010.[42] The authors achieved the synthesis of a well-defined ruthenium(II)biscarboxylate complex [Ru(O$_2$CMes)$_2$(*p*-cymene)] (**20**), which displayed an excellent reactivity for the C–H arylation of *inter alia* pyrazoles **18**, triazoles **17**, oxazolines **7**, imidazoles **19**, as well as 2-styrylpyridines **9**.

Besides these synthetically useful contributions, a set of important mechanistic findings shed light on the reaction mechanism. First, H/D-exchange experiments indicated the C–H activation to be reversible (Scheme 9a). Second, the 2-phenylpyridine derivative **1b** was shown to form the ruthenium cyclometalated complex **21** through a stoichiometric reaction with [Ru(O$_2$CMes)$_2$(*p*-cymene)] (**20**). Third, the complex **21** was demonstrated to be catalytically active and thus delivered the arylated product **5bb** (Scheme 9b) in high yield. Finally, various intermolecular competition experiments revealed a clear preference for electron-deficient aryl bromides **2**, which suggested that the oxidative addition is the turnover-limiting elementary step in this transformation.[42]
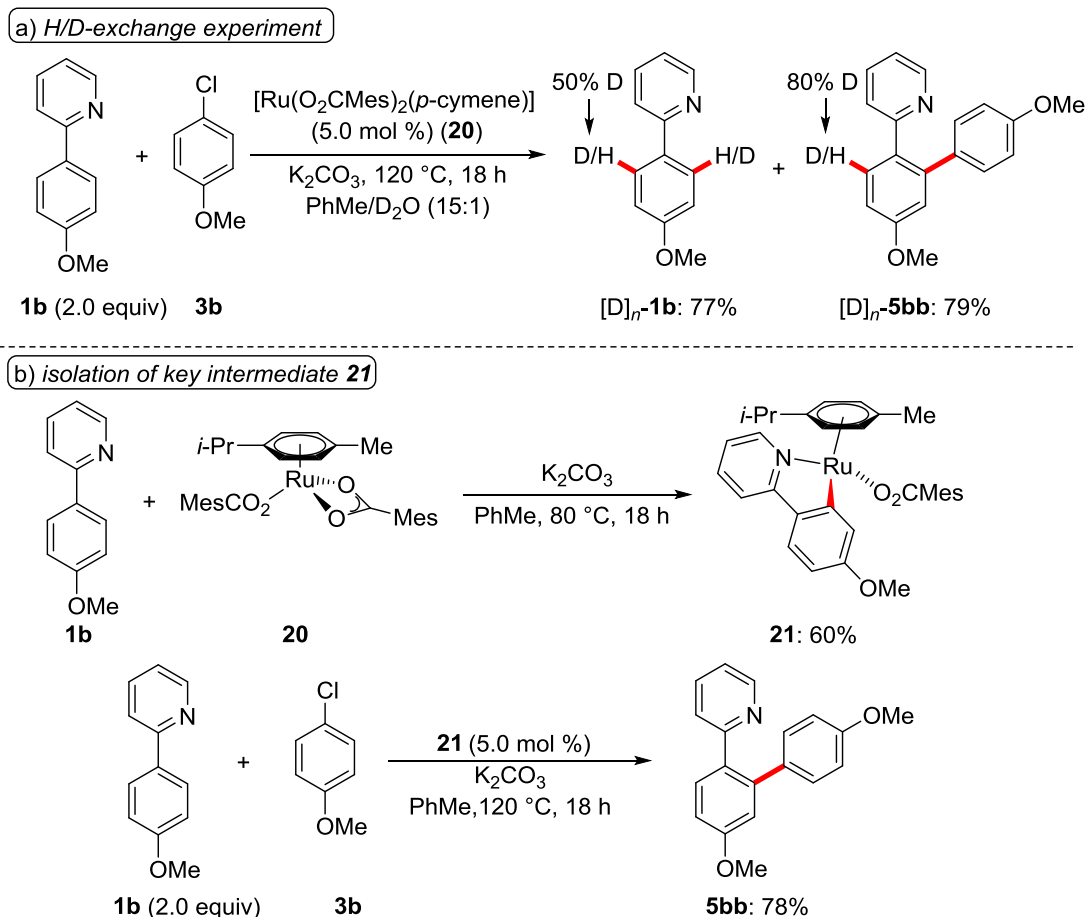
Scheme 9. Key mechanistic findings for the carboxylate-assisted C–H arylation.

To summarize all these mechanistic results, the authors proposed a general catalytic cycle (Scheme 10), which is initiated by a reversible carboxylate-assisted C–H ruthenation *via* a CMD-type six-membered transition state **16** to deliver ruthenacycle **23**. Subsequently, a turnover-limiting oxidative addition of the aryl halide **24** to the ruthenium(II) complex **23** occurs and generates a ruthenium(IV) intermediate **25**. Ultimately, a reductive elimination produces the desired arylated product **26** and regenerates the active ruthenium complex **27**.
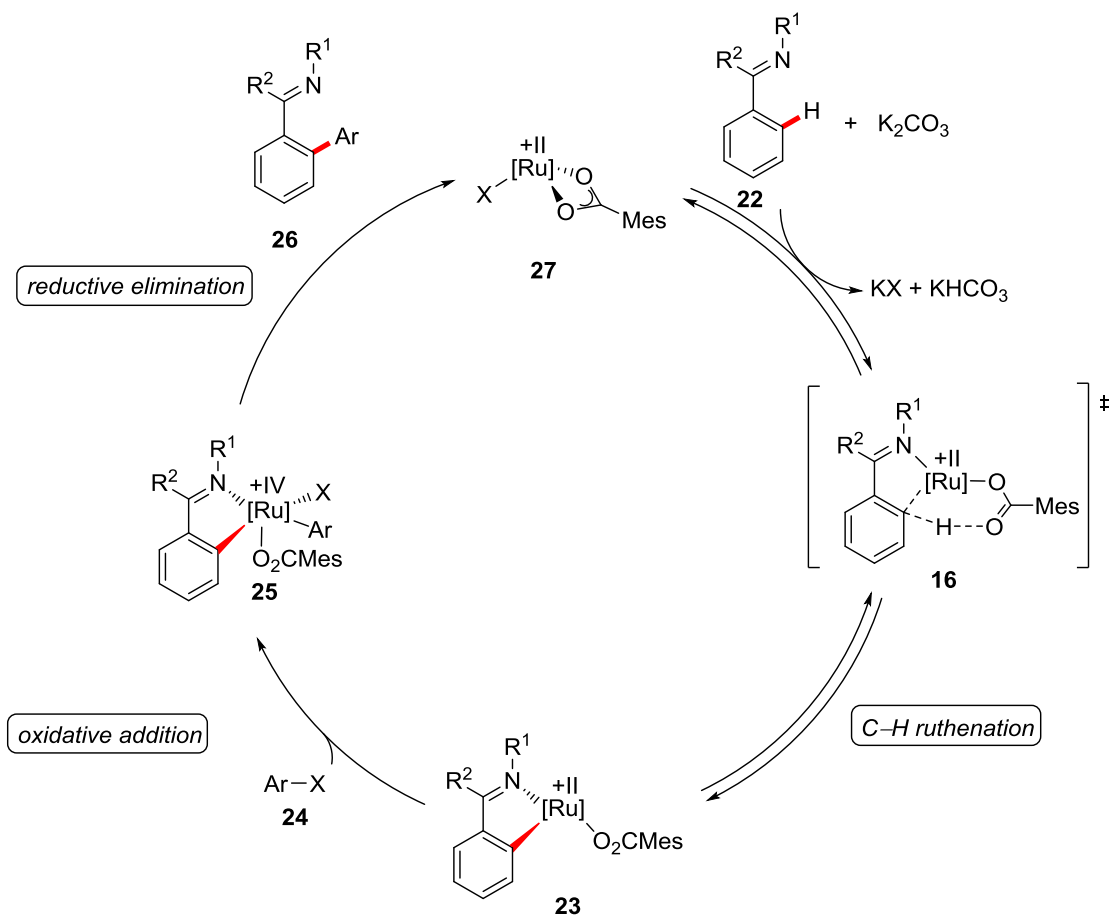
Scheme 10. Proposed catalytic cycle for the carboxylate-assisted ruthenium(II)-catalyzed C–H arylation. X = Br⁻, Cl⁻, MesCO₂⁻.

Furthermore, the excellent performance and broad applicability of ruthenium(II)-carboxylate complexes was highlighted by regioselective arylations of diversely substituted heterocycles, such as pyrroles **28,** thiophenes **29** and indoles **30**, which bear a removable pyrimidyl directing group.[43]

Based on seminal observations by *Ackermann* (*vide supra*) using water as additive in ruthenium-catalyzed C–H arylations,[36c] *Dixneuf* and coworkers demonstrated the robustness of ruthenium-catalyzed C–H arylations by establishing water as an economically attractive and environmentally benign reaction medium (Scheme 11).[44]
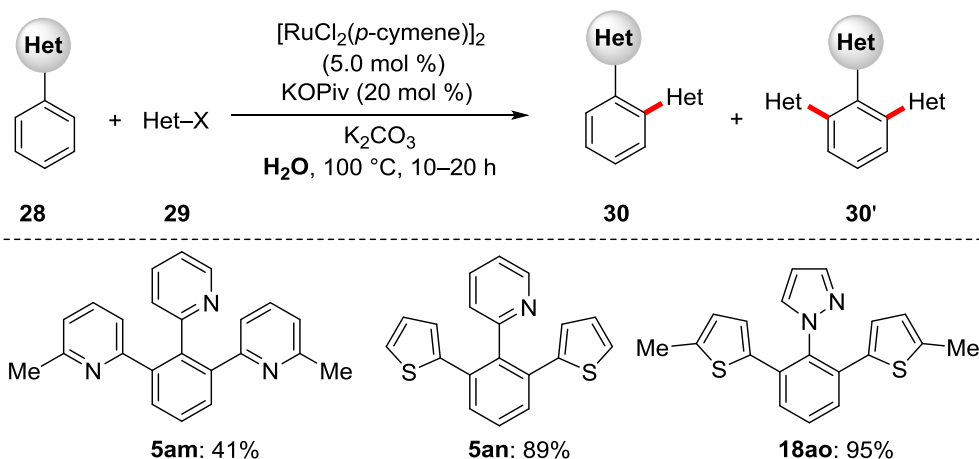
Scheme 11. Water-tolerant ruthenium(II)-catalyzed C–H arylation.

Notably, *Ackermann* and coworkers presented a ruthenium(II) biscarboxylate-catalyzed arylation in PhMe as the solvent and tetrazoles **31** as the directing group. Thereby, the authors highlighted a step-economical access to the angiotensin(II)-receptor blocker Valsartan (Scheme 12). *Seki* reported on a comparable method, but with the irreproducible triphenylphosphine and NMP system (*vide supra*).[45]
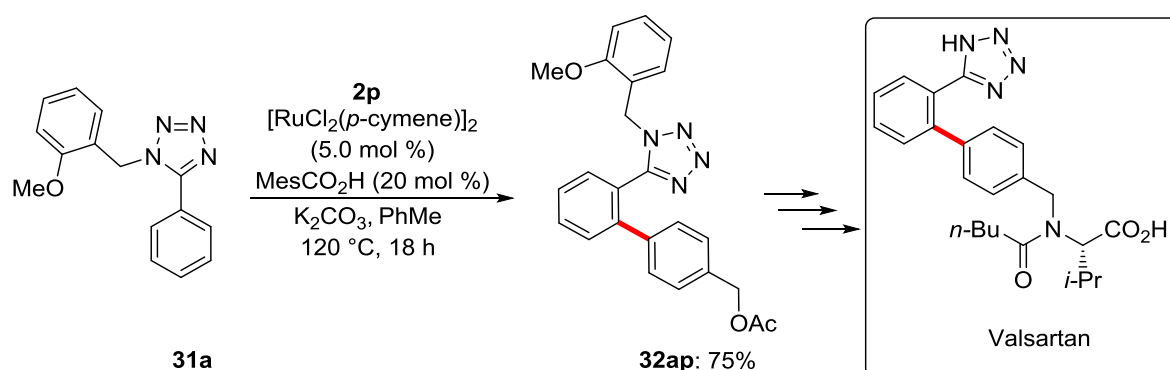
Scheme 12. Step-economical access to a Valsartan building block.

Furthermore, *Pratap* and coworkers disclosed a ruthenium(II)-catalyzed C–H arylation on a purine derivative by using triphenylphosphine as an additive and aryl iodides **3** as arylating reagent.[46]

In striking contrast, ruthenium-catalyzed C–H arylations were not only accomplished by the corresponding dimer $[RuCl_2(arene)]_2$/RCO_2H or well-defined ruthenium(II)biscarboxylate complexes, but also by the simple $[RuCl_3 \cdot xH_2O]$ salt (Scheme 13). In this regard, *Ackermann* and coworkers reported on a $[RuCl_3 \cdot xH_2O]$-catalyzed C–H arylation with aryl bromides **2** in NMP in the absence of additives.[47]

Moreover, *Yu* and coworkers presented a similar system comprising the same ruthenium-catalyst and NMP as the solvent to accomplish C–H arylations with aryl chlorides **3**. However, PPh_3 as the additive and Na_2CO_3 as the base were shown to be crucial for achieving high efficiencies.[48] However, in these systems the exact structure of the active catalyst has so far remained unknown. Preliminary studies

suggested the *in situ* reduction of the ruthenium(III)-precursor to the catalytically active ruthenium(II)-complex.[48]
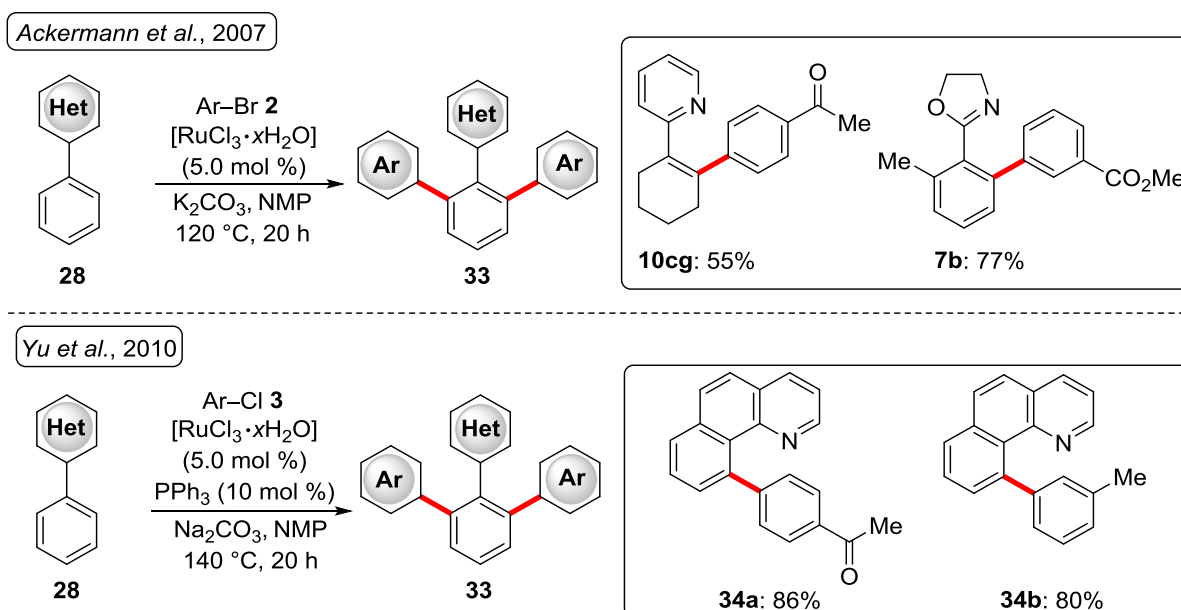
Scheme 13. [RuCl$_3$·xH$_2$O]-catalyzed C–H arylations.

1.3   Cobalt-Catalyzed C–H Activation

In 1938, *Otto Roelen* made a groundbreaking advance in homogenous catalysis by reporting on the first metal-catalyzed hydroformylation reaction.[49] Remarkably, after testing a variety of catalytic systems, he suggested that the simple and inexpensive cobalt complex [CoH(CO)$_4$] is the optimal catalyst.[50] After these pioneering studies, the following decades have witnessed enormous progress in cobalt catalysis, *e.g.* the development of the *Pauson-Khand*-reaction.[51] Nowadays, the great importance of cobalt catalysts is reflected by numerous industrial processes using economically attractive cobalt complexes, such as the *Fischer-Tropsch*-process[52] and the hydrodesulfurization of petroleum.[53]

Due to the earth abundance and thus inexpensiveness[54] of cobalt as well as the beneficial step- and atom-economical features of C–H activation catalysis, it appeared particularly attractive to investigate the performance of cobalt catalysts in C–H functionalizations. Thus, *Murahashi* and coworkers accomplished one of the first examples of C–H functionalizations in 1955, as they reported on a cobalt-catalyzed carbonylative cyclization of azobenzenes **35**. However, extremely harsh conditions were shown to be necessary for achieving overall moderate yields (Scheme 14).[55]
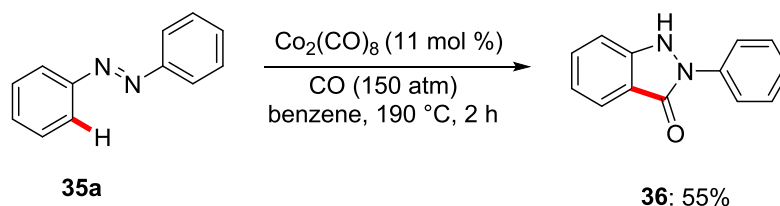
Scheme 14. Cobalt-catalyzed carbonylative cyclization.

Almost 40 years later, one of the first examples for a stoichiometric C–H activation by a cobalt complex was reported by *Klein* and coworkers in 1993 by again using azobenzene (**35a**) as the substrate and [CoMe(PMe$_3$)$_4$] as the cobalt source (Scheme 15).[56] The authors suggested that the reaction is initiated by a dissociation of one PMe$_3$ ligand. Subsequently, oxidative addition of the *ortho*-C–H bond to the cobalt complex occurs, and finally a reductive elimination of methane provides the cyclometalated species **37**.
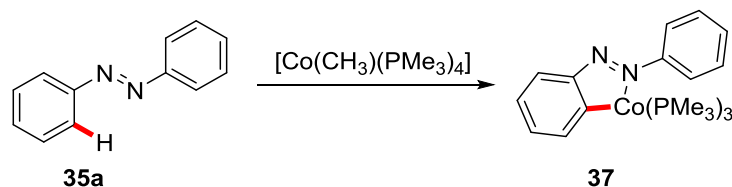
Scheme 15. Stoichiometric formation of a cobaltacycle through C–H activation.

Based on these findings, *Klein* and coworkers reported on the synthesis of several cobaltacycles by C−H activation, directed by *Lewis* basic directing groups with nitrogen-, phosphorous-, sulfur-, or oxygen-functionalities.[57]

These fundamental studies paved the way for a blossom of cobalt-catalyzed C–H functionalizations by initially low-valent cobalt catalytic systems, with numerous contributions by *inter alia Ackermann* and *Yoshikai*.[15] Despite the broad synthetic applicability of low-valent cobalt-catalyzed C–H functionalizations, one of the major drawbacks of some low-valent cobalt catalytic systems is often the need for stoichiometric amounts of *Grignard* reagents, which limit the overall atom-efficiency and the substrate scope with respect to base-labile functional groups.

1.3.1   Cobalt(III)-Catalyzed C–H Functionalization

Matsunaga/*Kanai* and coworkers devised an elegant strategy to implement [Co^{III}Cp*]-complexes,[58] which obviate the use of *Grignard* reagents and usually follow the reactivity features of the well-established rhodium(III) C–H activation catalysis.[13o, 59] As an early example in 2013, they investigated the catalytic performance of several cobalt complexes in addition reactions of 2-phenylpyridine (**1a**) to highly electrophilic sulfonylimines **38** as well as *α,β*-unsaturated ketones, esters and amides **39** (Scheme 16).[60] During their optimization studies, the authors emphasized that only

[Co^{III}Cp*]- complexes were powerful catalysts for these transformations, whereas CoCl$_2$ did not furnish the desired products.
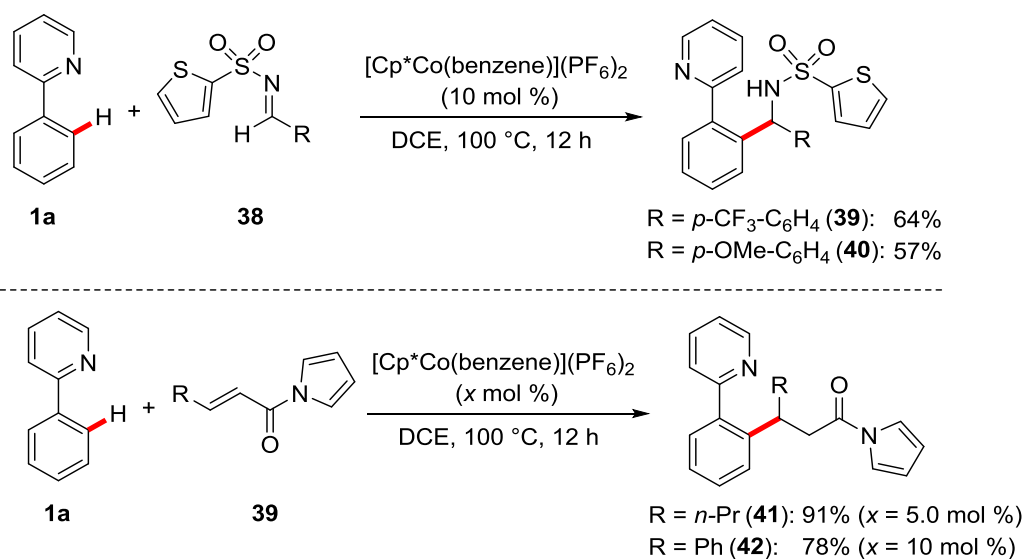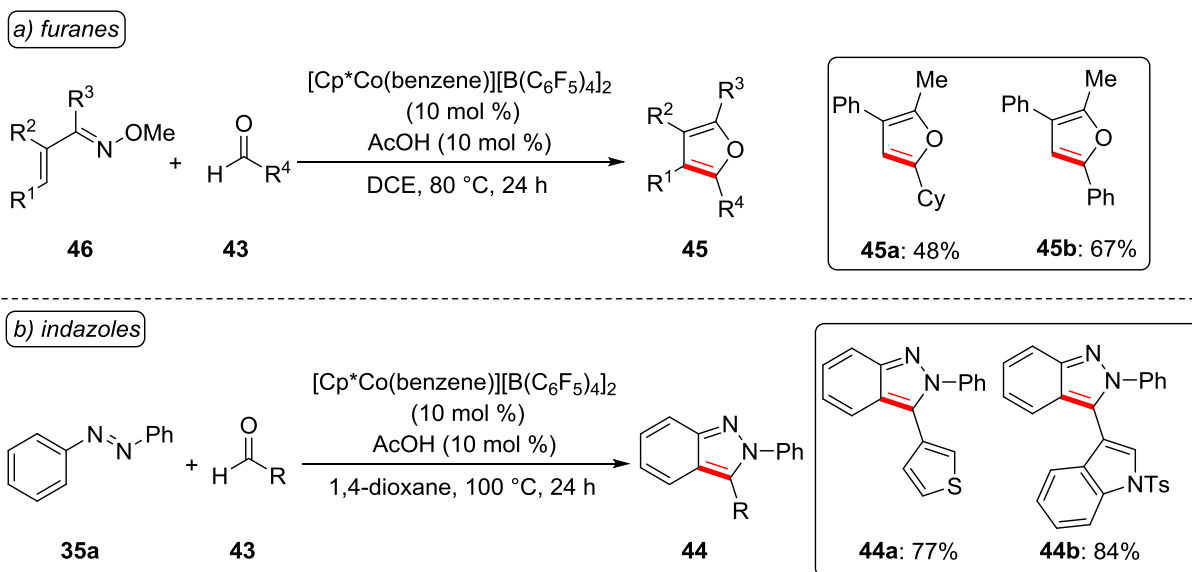

Scheme 16. Cobalt(III)-catalyzed C–H functionalization and addition to electrophiles.

Under comparably mild reaction conditions, various functional groups, such as enolizable ketones, hydroxyls as well as ester-groups, were tolerated, contrasting the often limited substrate scope of low-valent cobalt-catalyzed reactions.

Remarkably, a related [Rh^{III}Cp*]-catalyzed C–H functionalization[61] was shown to be inefficient in addition reactions to less electrophilic *α,β*-unsaturated esters and amides, indicating the unique reactivity profile of [Co^{III}Cp*]-catalysts. Presumably, the higher nucleophilicity of the cobalt-carbon bond enables the addition reaction to even less electrophilic functionalities. In this regard, the *Pauling* electronegativity of cobalt is $\chi_F \approx 1.9$ and of rhodium it is $\chi_F \approx 2.3$.[62]

Capitalizing on this distinct reactivity feature of [Co^{III}Cp*]-complexes, a plethora of new synthetic methods were developed, with partly new reactivities and selectivities as compared to the analogous [Rh^{III}Cp*]-catalysis. Shortly afterwards, the same group reported on a similar reaction with indoles **30**, but using KOAc as the crucial additive to accomplish a significant rate acceleration.[63] The authors proposed that the C–H activation elementary step proceeds either *via* an electrophilic or acetate-assisted CMD-type mechanism.

Encouraged by these seminal reports of *Matsunaga*/*Kanai*, *Ellman* and coworkers probed the reactivity of cobalt(III) complexes to aldehyde **43** functionalities in addition reactions.[64] The reported reaction comprised a sequence of an addition and successive cylization reaction to furnish indazoles **44** with azobenzenes **35** or furanes **45** employing *α,β*-unsaturated oximes **46** (Scheme 17).

Scheme 17. Cobalt(III)-catalyzed synthesis of a) furanes **45** and b) indazoles **44**.

In addition, the isohypsic synthesis of heterocycles, such as isoquinolines[65] **49** (Scheme 18a) and indoles **50** (Scheme 18b),[23c] by cobalt(III)-catalyzed C–H/N–O functionalizations was accomplished by *Ackermann* and coworkers, employing oximes **46** and nitrones **47** as the directing groups. These reactions exhibited a broad scope with respect to both substrates. Intriguingly, the overall high efficiency of cobalt(III) catalysis was highlighted by a reaction time of only 15 min (Scheme 18a). Further notable contributions to this reaction type by cobalt(III) catalysis were independently reported by *Chang*,[66] *Jiao*,[67] *Kanai/Matsunaga*[68] and *Sundaraju*.[69]
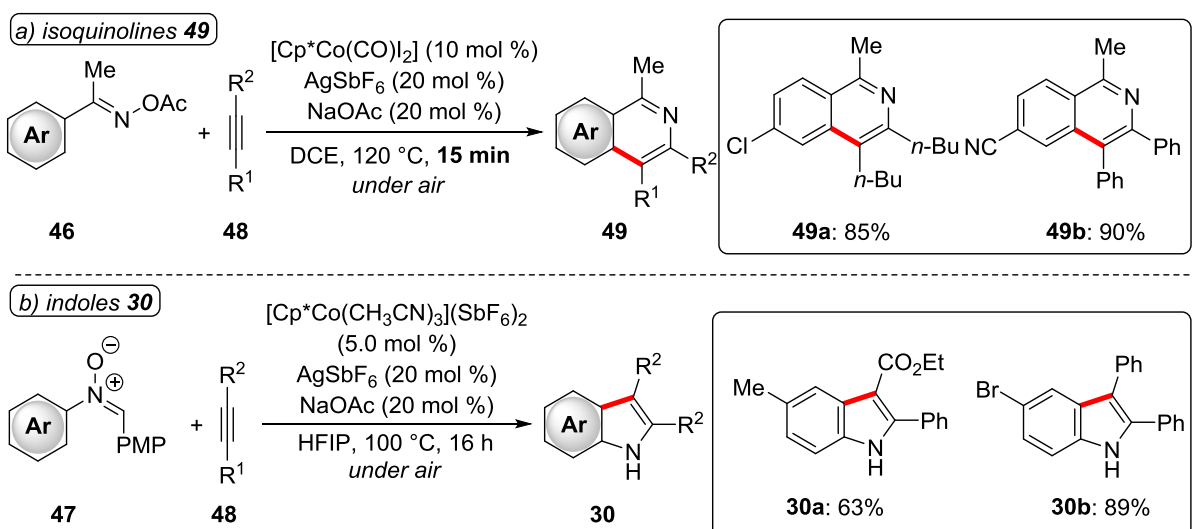
Scheme 18. Cobalt(III)-catalyzed C–H/N–O functionalizations for the synthesis of heterocycles.

The syntheses presented above already indicated the great importance of nitrogen-containing heterocycles.[70] Along this line, *Matsunaga/Kanai* published an amidation of 2-pyrimidylindoles **50** with sulfonyl azides **51**[71] (Scheme 19) with ample scope and excellent yields. Thereafter, the same

group extended the applicability of cobalt(III) catalysis to an analogous phosphoramidation[72] utilizing phosphorylazides **53**.
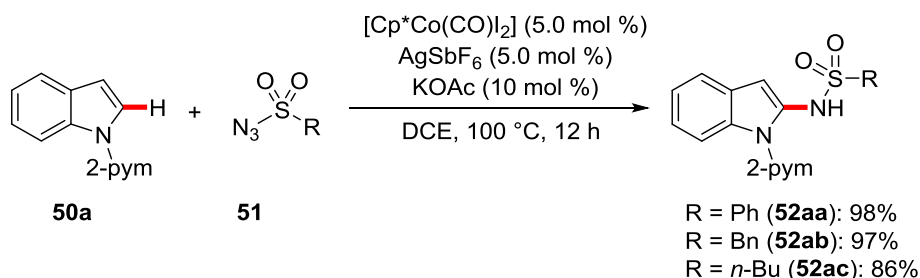
Scheme 19. Cobalt(III)-catalyzed amidation with sulfonyl azides **51**.

Another important and easily modifiable nitrogen-containing functional group is the cyano-group.[73] Accordingly, *Ackermann*[74] and *Glorius*[75] independently reported on cobalt(III)-catalyzed cyanations. The reaction system of *Ackermann* and coworkers is cha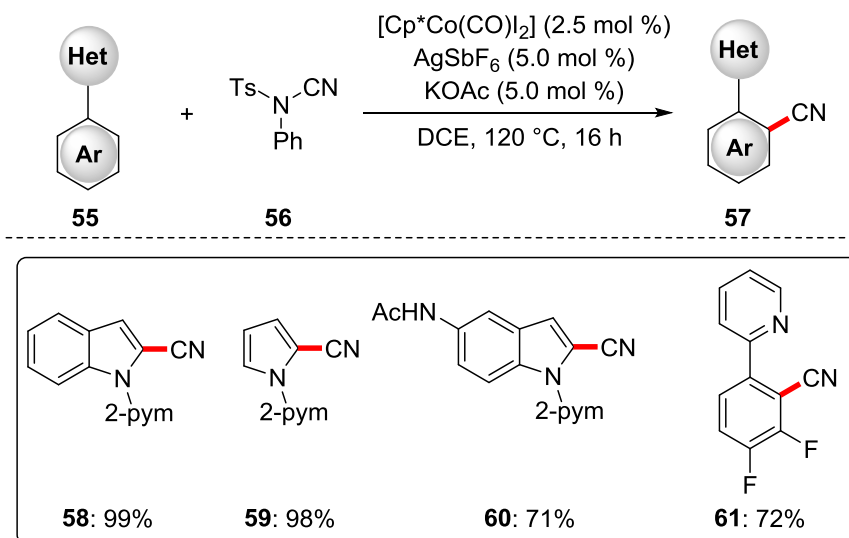racterized by a low catalyst loading of only 2.5 mol % and functionalizations of valuable heteroarenes to *inter alia* cyanated 2-pyrimidylindoles **58**/**60** and 2-pyrimidylpyrroles **59** (Scheme 20). The corresponding products were obtained in almost quantitative yield, good functional group tolerance, and very good mono/di-selectivities.

Scheme 20. Cobalt(III)-catalyzed C–H cyanation of heteroarenes.

Moreover, the authors proposed a catalytic cycle of the cobalt(III)-catalyzed C–H cyanation (Scheme 21), which is initiated by reversible C–H cobaltation involving an acetate-assisted deprotonation pathway to deliver cobaltacycle **62a**. After coordination of the cyanation reagent **56**, a *β*-nitrogen elimination takes place. Subsequently, proto-demetalation with the *in situ* generated acetic acid delivers the cyanated product **66** and regenerates the catalytically active cobalt(III)-acetate species **62a**.
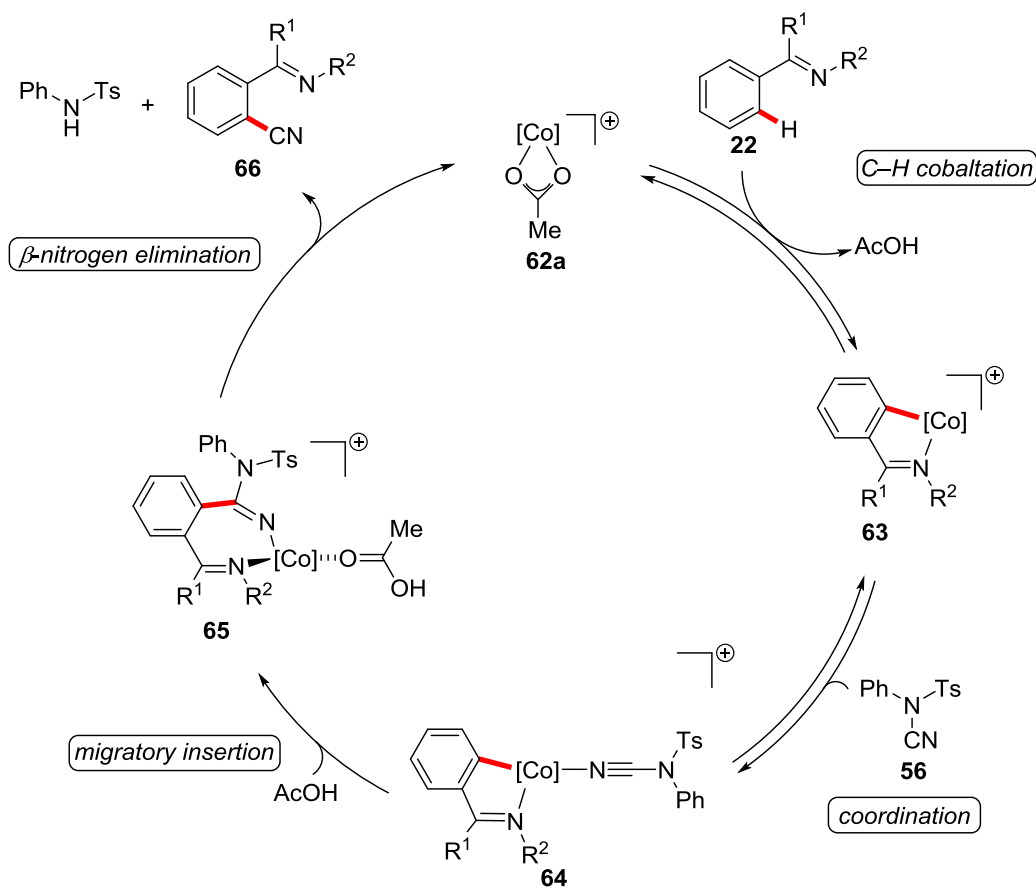
Scheme 21. Proposed catalytic cycle for the cobalt(III)-catalyzed cyanation. [Co] = Cp*Co^{III}.

Generally, the β-nitrogen elimination described above was found to be an energetically preferred step due to the formation of strong metal-nitrogen bonds. Likewise, the same pathway should be favored for oxygen, which is in β-position to a metal center. Consequently, a process involving C–H functionalization and subsequent β-oxygen elimination is a step-economical approach for installing functionalities, such as synthetically versatile allyl-groups, which have found widespread applications in organic synthesis.[76] In this context, *Ackermann*,[77] *Glorius*[75] and *Kanai/Matsunaga*[78] and coworkers have independently devised several methods merging cobalt(III)-catalyzed C–H activation with C–O bond cleavage by β-oxygen elimination to accomplish C–H allylations with a variety of directing groups and allylating reagents (Scheme 22). Accompanied by a report on cobalt(III)-catalyzed cyanations, brominations, and iodinations, *Glorius* and coworkers showed that allyl carbonates **67** are competent reagents for the allylation of 2-pyrimidylindoles **50**. In a follow-up work, the same group demonstrated that benzamides **68** (Scheme 22a) and acrylamides **69** could also be efficiently allylated.[79] The reaction system of *Ackermann* and coworkers highlighted the use of simple allyl acetates **71** to accomplish C−H allylations of *inter alia* 2-pyrimidylindoles **50** as well as less eletron-rich pyridyl- and pyrimidylarenes. Surprisingly, the crucial β-oxygen elimination step turned out to be such a strong driving force that even weak leaving groups like hydroxyls could be

eliminated by using allyl alcohols **74** directly, as *Kanai/Matsunaga* and coworkers demonstrated. In addition, the authors emphasized that the reactivity of the cobalt(III) complex was much higher as compared to the well-established complex [Cp*RhCl$_2$]$_2$ under otherwise unchanged reaction conditions.
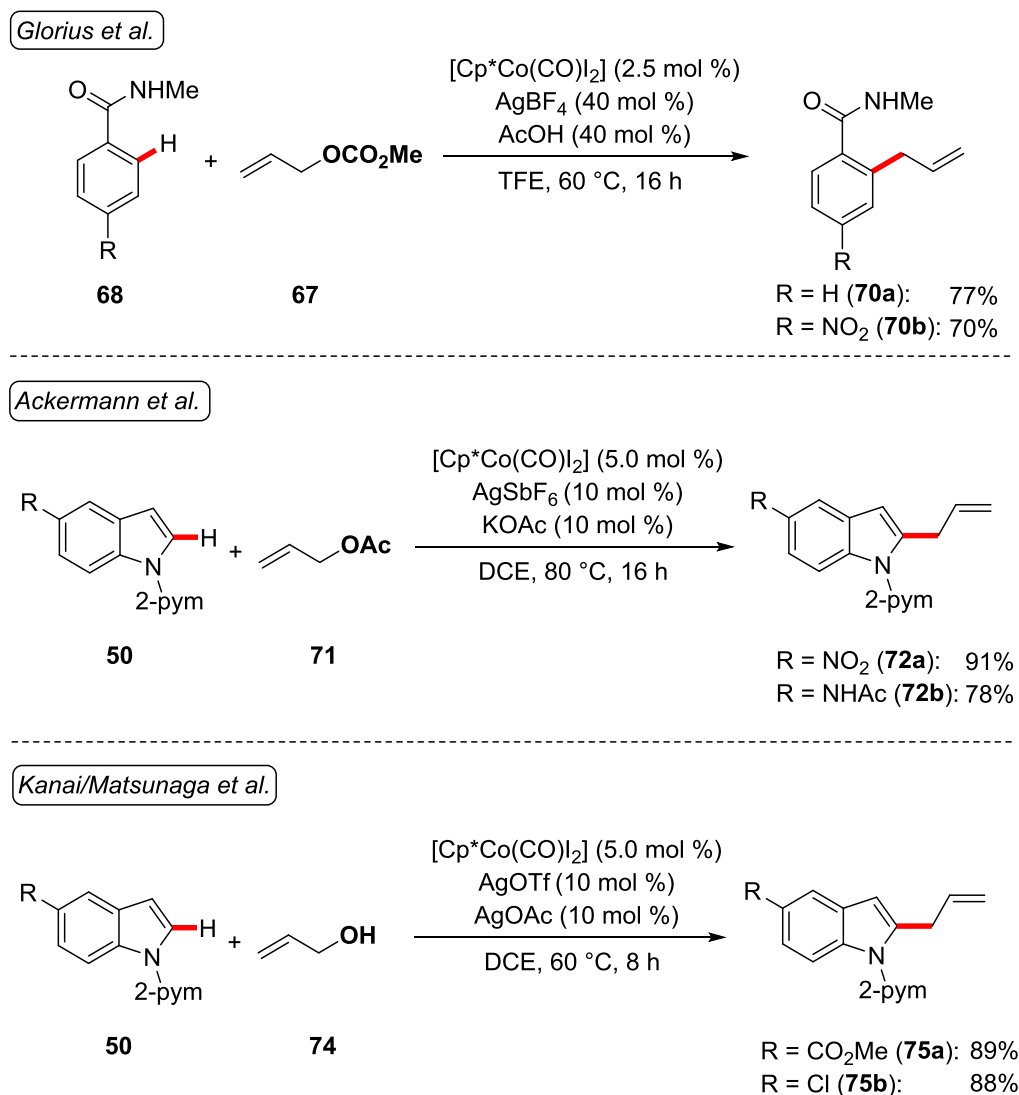
Scheme 22. Cobalt(III)-catalyzed C–H allylations.

Furthermore, a catalytic cycle for the general leaving group OR can be postulated (Scheme 23). Interestingly, all reported catalytic systems featured a significant rate acceleration by carboxylates or carboxylic acid additives, which leads to the assumption that the cationic cobalt-carboxylate **62** (*cf.* Scheme 21) might be catalytically active species.

Initially, a base-assisted C–H cobaltation takes place, which was shown to be reversible and not turnover-limiting, at least in the case of indole substrates.[77] After reversible coordination of the allyl substrate **76** to form complex **77**, a migratory insertion furnishes intermediate **78**, which undergoes a *β*-oxygen elimination step to release the allylated product **79** and a cobalt(III)-alkoxy species.

Additionally, *Kanai/Matsunaga* showed by DFT-studies that a competing S_N2' pathway is unfavorable.[78] Finally, a reaction of the cobalt(III)-alkoxy species with carboxylic acid regenerates the active cobalt(III)-carboxylate catalyst **62**.
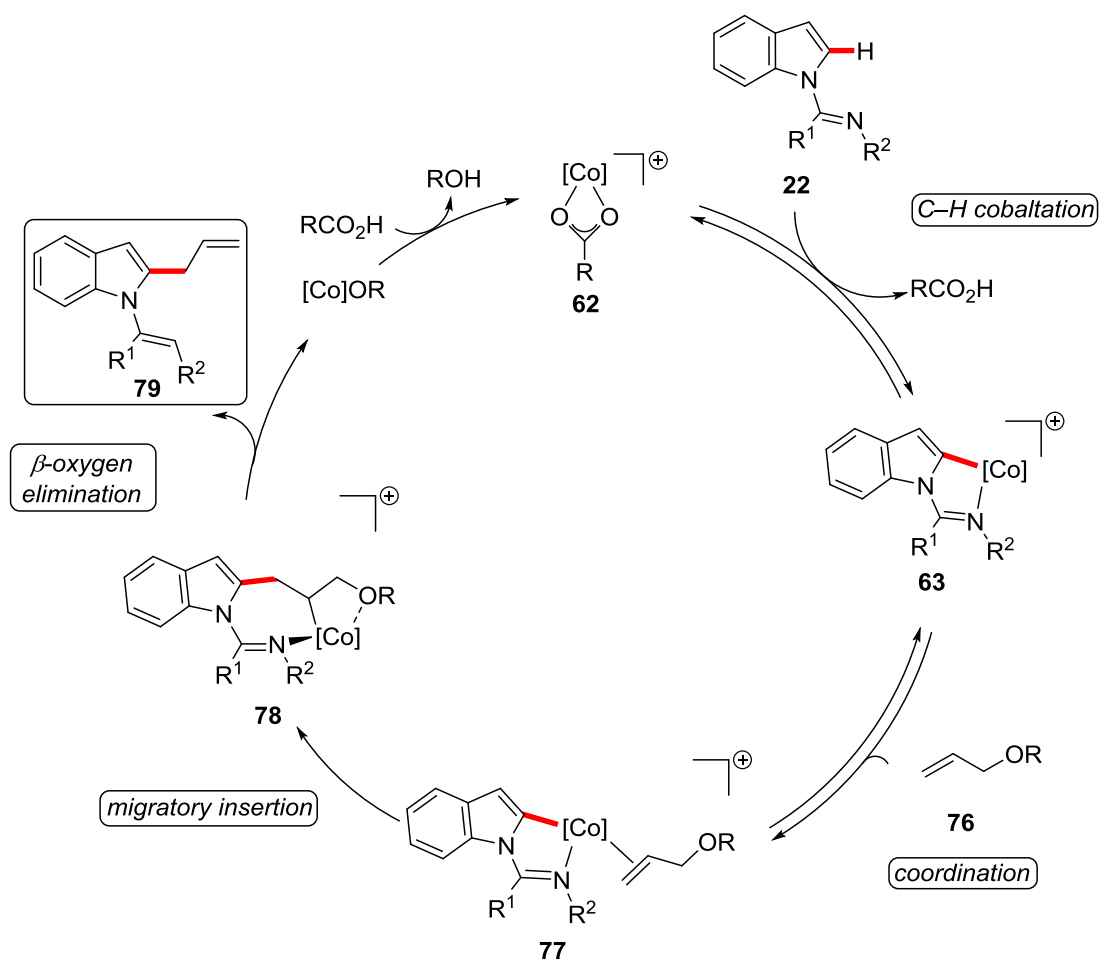
Scheme 23. Proposed catalytic cycle for the cobalt(III)-catalyzed allylation. [Co] = Cp*Co^{III}.

1.3.2   Cobalt-Catalyzed Hydroarylations

The first example of a cobalt-catalyzed C–H hydroarylation reaction was reported by *Kisch* and coworkers in 1994, using azobenzenes **35** and tolane **48a** as substrates.[80] The corresponding di-functionalized products **80** were obtained in good isolated yields of around 70–80% (Scheme 24).
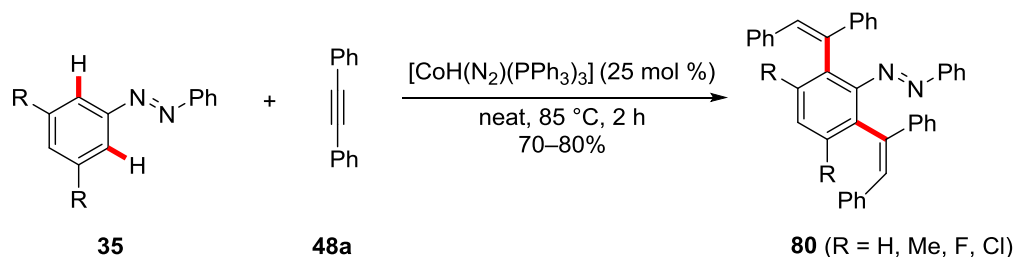
Scheme 24. Cobalt(I)-catalyzed C–H hydroarylation.

These fundamental findings inspired *Yoshikai* and coworkers to develop a cobalt-catalyzed C–H hydroarylation of internal alkynes **48** (Scheme 25). The catalytic system comprised comparably low amounts of a simple cobalt salt as the catalytic precursor, a phosphine ligand, and stoichiometric amounts of a *Grignard* reagent as the reductant. In this context, the authors first succeeded in functionalizing 2-phenylpyridines **1**.[81] Afterwards they extended the substrate scope to ketimines **6**[82] and indoles **30** as well.[83] Under the optimal reaction conditions, the desired alkenylated products **81** were delivered in very good yields and an excellent regiocontrol was achieved in the case of unsymmetrical alkynes **48**. Most of th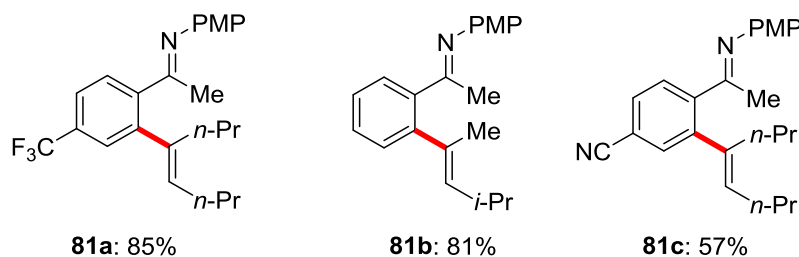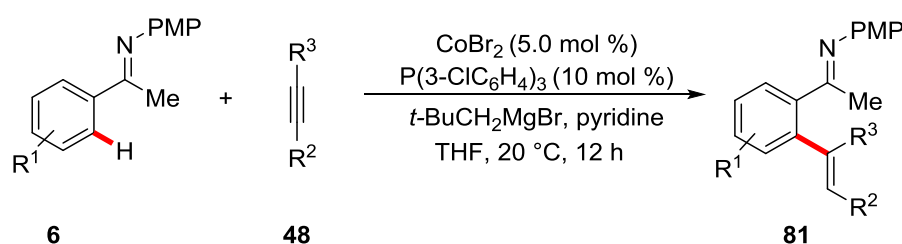e reactions proceeded at ambient temperature so that even sensitive functional groups such as nitriles were well tolerated.

Scheme 25. Low-valent cobalt-catalyzed C–H hydroarylation with ketimines **6**.

Thereafter, the excellent performance of low valent cobalt catalysis in hydroarylation reactions was successfully extended to more challenging alkenes by *Yoshikai*[84] and *Nakamura*.[85] *Yoshikai* and coworkers developed a cobalt-catalyzed C–H hydroarylation with styrenes **82** and 2-phenylpyridines **1** (Scheme 26). Remarkably, the authors accomplished a complete switch in *Markovnikov/anti-Markovnikov* selectivity by the judicious choice of the ligand. While bulky NHC ligands afforded linear products **83**, phosphine ligands completely reversed the selectivity and delivered the branched products **84** in overall good to excellent regioselectivities.
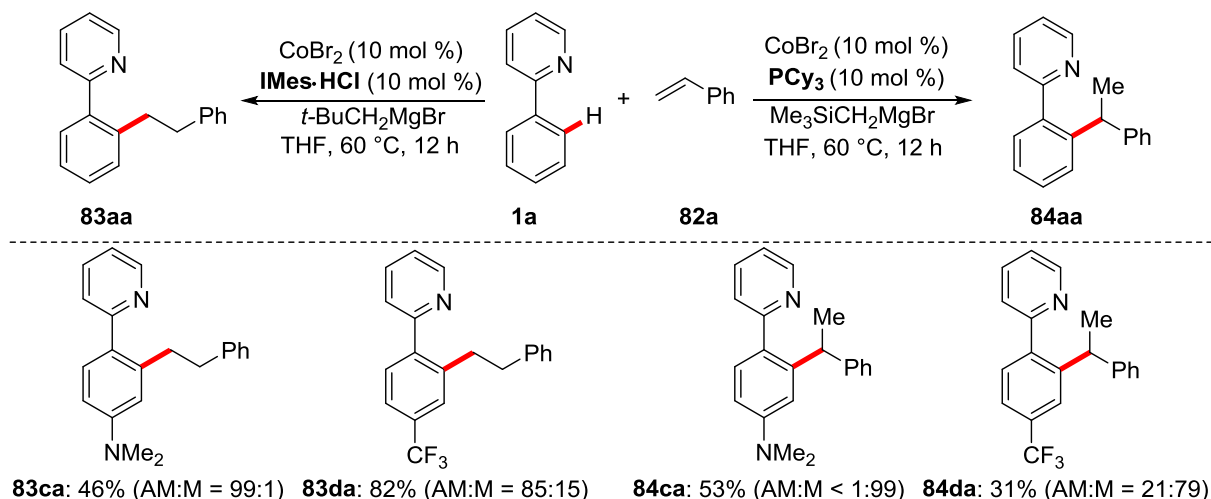
Scheme 26. Low-valent cobalt-catalyzed regioselective C–H hydroarylations.

Moreover, the authors conducted deuterium labeling experiments with deuterated 2-phenylpyridine-d_5 ([D]$_5$-**1a**). In the case of the branched product **84aa** a higher content of deuterium was observed in the α-position of the styrene moiety. In contrast, for the linear product **83aa** a larger deuterium incorporation could be detected in β-position.[84] These findings led to the mechanistic hypothesis that the C–H activation *via* oxidative addition as well as the migratory insertion steps are reversible for both reactions, while the reductive elimination is turnover-limiting as well as regioselectivity-determining (Scheme 27). The bulky NHC ligand forces the styrene **82** to insert linearly into the carbon-cobalt bond to avoid steric interactions, whereas the linear-selective reaction is controlled by the electronically favored formation of a benzylic cobalt species,[86] as the authors claimed.[84]
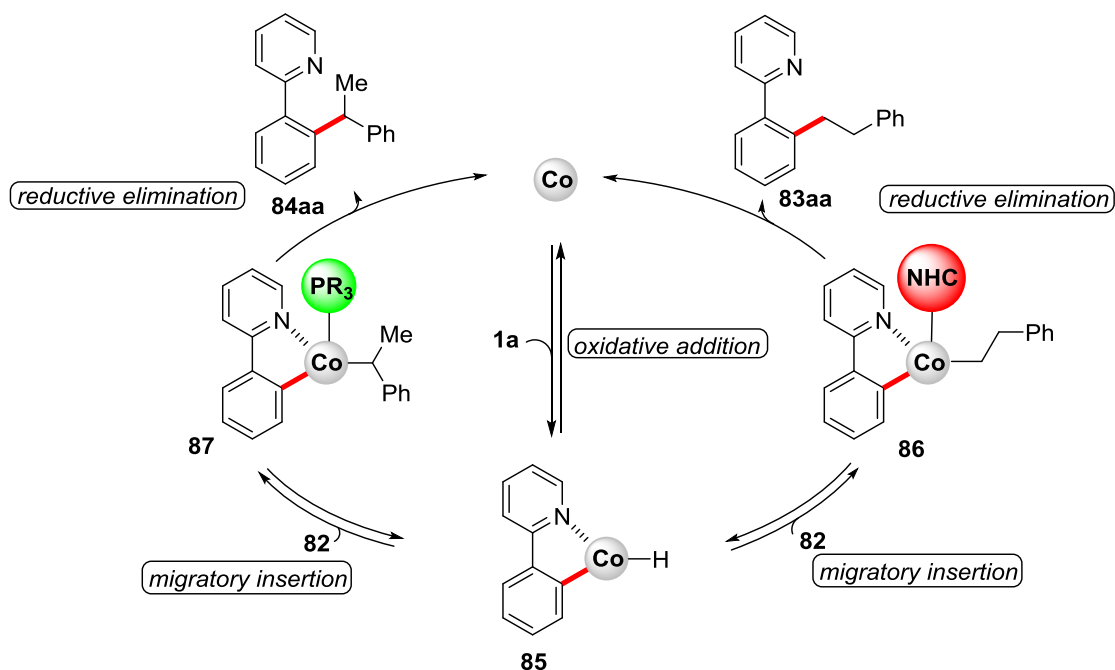
Scheme 27. Proposed mechanism for the regioselective cobalt-catalyzed C–H hydroarylation.

Thereafter, *Nakamura* and coworkers disclosed a low-valent cobalt-catalyzed C–H hydroarylation of benzamides **68** with mostly electronically unactivated alkenes **88**. However, the authors also presented a few examples comprising styrenes **82** (Scheme 28).[85] The catalytic system was characterized by an inexpensive Co(acac)₃ catalyst, stoichiometric amounts of a *Grignard* reagent, and a reaction temperature as low as 25 °C. The authors proposed DMPU to be an essential ligand, which they had previously shown for a related reaction.[87] Importantly, under very mild reaction conditions, even base-labile functional groups like esters were well tolerated. Interestingly, electronically unactivated alkenes **88** delivered solely the linear-selective product **89** in excellent yields and regioselectivities. In contrast, the use of styrene (**82a**) afforded the linear product **89ca** in only moderate regioselectivity. Nevertheless, the authors did not propose a mechanistic reason for this interesting change in selectivity, which is obviously related to *Yoshikai's* observation (*vide supra*).
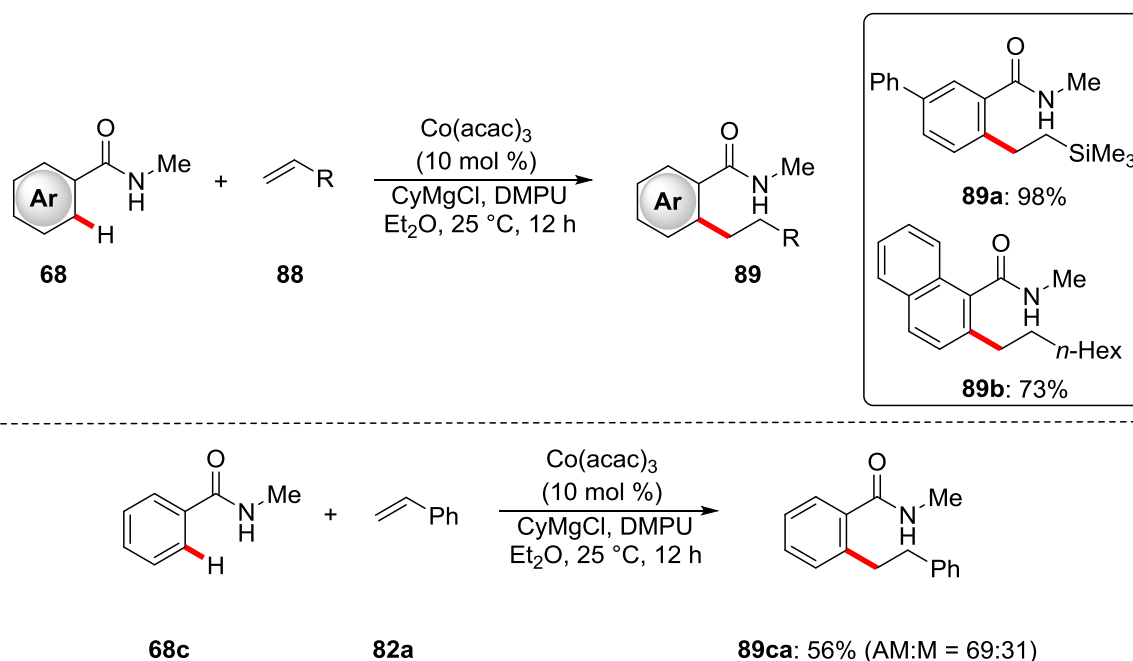
Scheme 28. Low-valent cobalt-catalyzed C–H hydroarylation of benzamides **68** with alkenes **88**.

Intriguingly, *Yoshikai* and coworkers accomplished an enantioselective low-valent cobalt-catalyzed hydroarylation with styrenes **82** in the C2-position of indole **90**, which bear a ketimine directing group in C3-position (Scheme 29).[88] The key to success in achieving moderate to good enantioselectivity was the use of phosphoramidite ligands,[89] featuring a BINOL-derived backbone.[88] Overall, good yields and enantioselectivities were obtained, albeit sterically demanding indoles **90** led to a clear decrease in yield and enantioselectivity, as it was demonstrated for the 7-ethyl substituted indole **90b**.
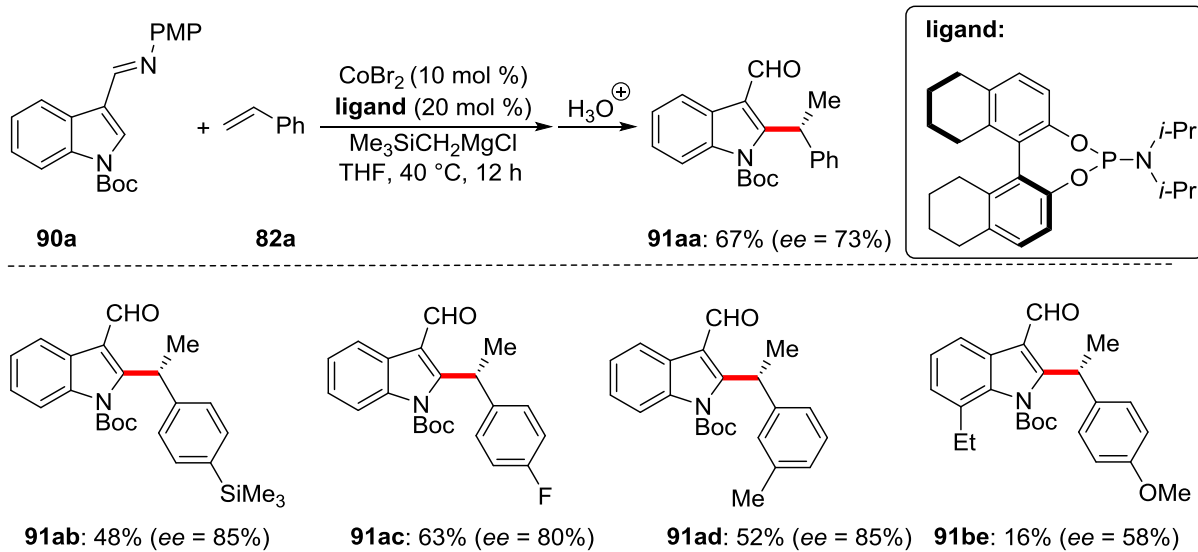
Scheme 29. Low-valent cobalt catalyzed enantioselective C–H hydroarylation.

Based on a previous report by *Fagnou* and coworkers on a rhodium(III)-catalyzed C–H hydroarylation[90] with alkynes **48** and low-valent cobalt-catalyzed reaction of *Yoshikai*,[83] *Kanai*/*Matsunaga* and coworkers presented a cobalt(III)-catalyzed hydroarylation of 2-carbamoylindoles **92**.[91]

Remarkably, the authors achieved a full control of chemoselectivity depending on the directing group (Scheme 30). While carbamoyl-substituted indoles **92** furnished the expected hydroarylation products **93** with excellent regioisomeric ratios and a broad scope (Scheme 30a), a morpholine unit on the carbamoyl residue in substrate **94** almost exclusively afforded the corresponding pyrroloindolones **95** (Scheme 30b) *via* a hydroarylation/annulation sequence.

The authors emphasized the unique selectivity features of cobalt(III) catalysis by comparison with the chemoselectivity of the corresponding rhodium(III)-catalyzed hydroarylation. Notably, rhodium(III) catalysis exclusively yielded the hydroarylated product **93**, regardless of the carbamoyl-moiety.

a) hydroarylation

92a   **48**

R^1 =Me, R^2 = Ph (**93a**): 90% (r.r. = 17:1)
R^1 =Me, R^2 = 4-CO$_2$Et-C$_6$H$_4$ (**93b**): 88% (r.r. = 17:1)

b) hydroarylation/annulation

94a   **48**

R^1 =Me, R^2 = Ph (**95a**): 78%
R^1 =Me, R^2 = 4-CO$_2$Et-C$_6$H$_4$ (**95b**): 63%
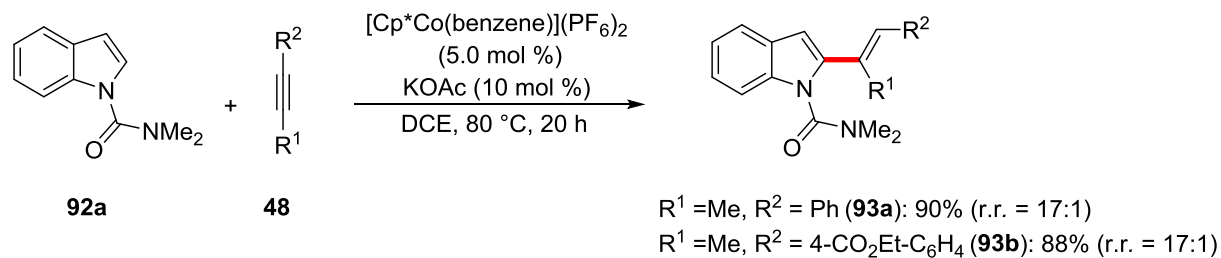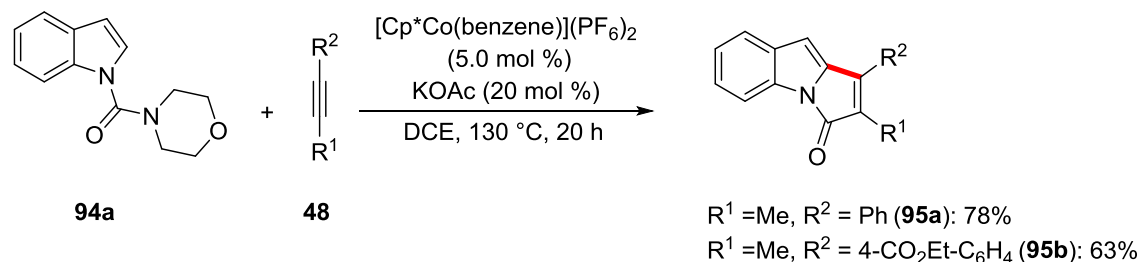
Scheme 30. Cobalt(III)-catalyzed chemoselective C–H hydroarylations with alkynes **48**.

Finally, the authors proposed a catalytic cycle (Scheme 31), which is initiated by the formation of the catalytically active cobalt(III)-monoacetate species **62a**. Subsequently, a reversible cobaltation delivers the cobaltacycle **96** *via* an acetate-assisted C–H activation mechanism. The exact pathway of this C–H activation step is presumably not fully concerted, as it was shown by DFT calculations. Rather, a stepwise mechanism was proposed, which is initiated by a weak interaction between cobalt and the C2-position of indole, followed by deprotonation through acetate-assistance.[20] After reversible coordination of the alkyne **48** and migratory insertion, the crucial cobalt-alkenyl-intermediate **98** is produced. Depending on the leaving group ability of the dialkylamine unit, either a proto-demetalation follows, delivering the product **93**, or an annulation reaction by nucleophilic attack of the cobalt-carbon bond with following *β*-nitrogen elimination affords the pyrroloindolone **95**. In addition, DFT calculations and charge estimation by a natural population analysis led to the assumption that a crucial cobalt(III)-alkenyl intermediate **98** is more nucleophilic than the analogous rhodium(III)-intermediate due the diminished electrophilicity of cobalt (*vide supra*). In this respect, a simple change to a better leaving group, such as the morpholino-unit, energetically favoured the successive annulation reaction.
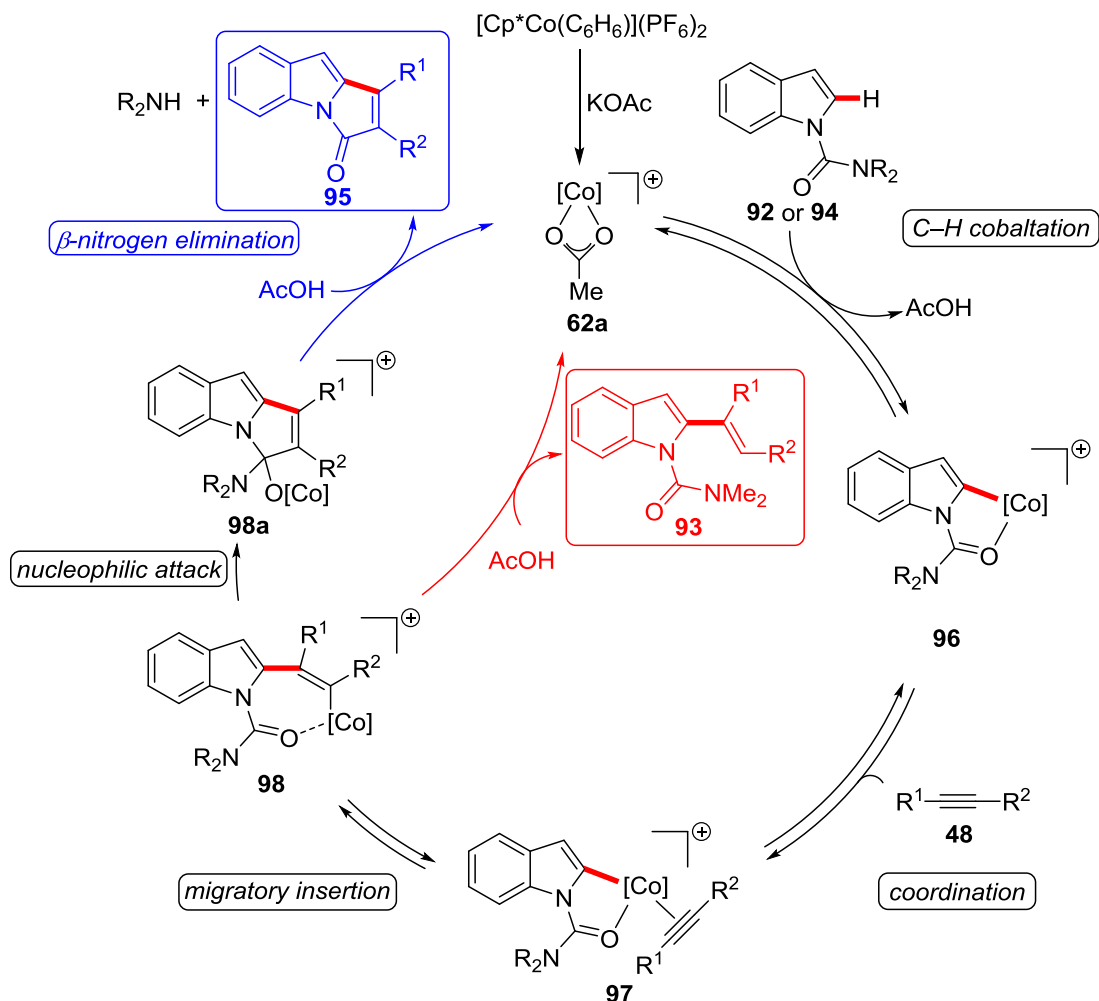
Scheme 31. Postulated catalytic cycle of the cobalt(III)-catalyzed hydroarylation of alkynes. $[Co] = Cp^*Co^{III}$.

1.4   Manganese-Catalyzed C–H Activation

The achievement of sustainable chemical processes ideally involves the use of earth-abundant reagents and catalysts. In this regard, manganese represents an ideal candidate for C–H activation catalysis, since it is the twelfth most abundant element in the earth crust, and the third most abundant transition metal after iron and titanium.[54] However, manganese could be an appealing metal for new catalysts not only from an economical viewpoint, but also due to its usually low toxicity,[54, 92] which matches the principles of green chemistry.[12] In addition, there are several manganese co-factors in enzymes that are involved in the human metabolism of *inter alia* carbohydrates and amino acids, rendering manganese essential for human life.[93]

Thus, by strong analogy with the stoichiometric cobalt-mediated C–H activation by *Klein* and coworkers (*cf.* chapter 1.3), *Stone/Bruce* and coworkers presented a manganese-mediated C(sp^2)–H activation of azobenzene (**35a**) to deliver the manganacycle **99** (Scheme 32).[94]
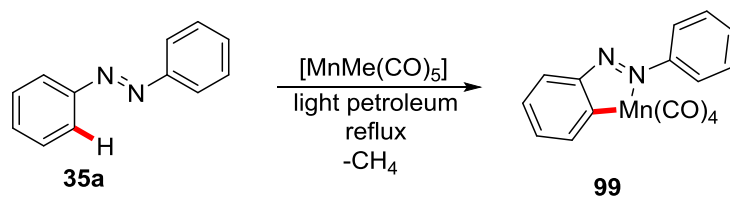
Scheme 32. Stoichiometric manganese(I)-mediated C(sp^2)–H activation.

Thereafter, a number of reactivities with these well-defined manganacycles were disclosed by *inter alia Liebeskind* for the synthesis of indenoles,[95] and by *Nicholson*[96] and *Woodgate*.[97] These accomplishments have already predicted the great potential of manganese in C–H activation catalysis. However, almost 40 years had passed since the report of *Stone/Bruce* until the first example of manganese-catalyzed C–H activation was reported by *Kuninobu/Takai* in 2007 (Scheme 33).[98] Here, the authors presented a manganese(I)-catalyzed C–H activation of imidazoles **19** and a subsequent addition reaction of the manganacycle to electrophilic aldehydes **43**. Notably, triethylsilane turned out to be a crucial reagent for catalytic turnover, delivering the silyl-protected benzylic alcohols **100** in overall moderate to good yields. The authors emphasized that only a manganese-catalyst was efficient, whereas other representative metal-catalysts based on *inter alia* rhenium, ruthenium, and iridium-complexes were not active. Within a comprehensive scope it was demonstrated that even sterically demanding substrates like *ortho*-substituted phenyl-groups led to only a slight decrease in yield.

R = 4-CF$_3$C$_6$H$_4$ (**100aa**): 87%
R = 2-OMeC$_6$H$_4$ (**100ab**): 59%
R = *n*-C$_8$H$_{17}$ (**100ac**):   75%

Scheme 33. Manganese(I)-catalyzed C–H addition to aldehydes **43**.

Moreover, a plausible mechanistic scenario was proposed (Scheme 34). The yet undefined structure of the catalytically active manganese(I) species **101** undergoes C–H activation by oxidative addition, furnishing the manganese(III)-hydride species **102**. Afterwards, migratory insertion of the polar carbonyl bond into the nucleophilic carbon-manganese bond takes place. Finally, triethylsilane promotes a reductive elimination to release the silyl-protected product **100**, the active catalyst, and molecular hydrogen.
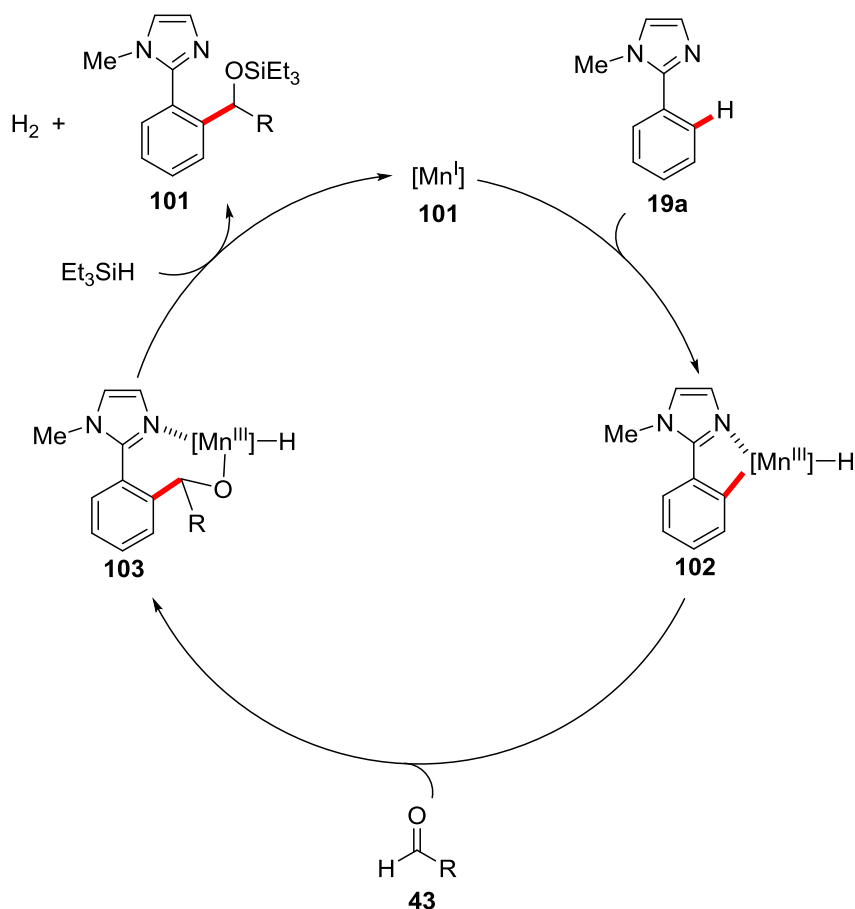
Scheme 34. Proposed catalytic cycle for the manganese(I)-catalyzed C–H addition to aldehydes **43**.

Even though this reaction represented a significant breakthrough in manganese C–H activation catalysis, a serious limitation was represented by the need for triethylsilane to achieve catalytic turnover. In contrast, *Wang* and coworkers succeeded in the development of a more general manganese(I)-catalyzed C–H addition to aldehydes **43** by using $ZnBr_2$ and Me_2Zn (Scheme 35).[99] The optimal reaction conditions allowed for aromatic as well as olefinic C–H activation and various functional groups like halogens, ester-, and methoxy- groups were tolerated. Likewise, detailed mechanistic studies led to the hypothesis that Me_2Zn was crucial for the *in situ* formation of the active catalytic species $[MnMe(CO)_5]$, which facilitates the C–H cyclomanganation step *via* oxidative addition.
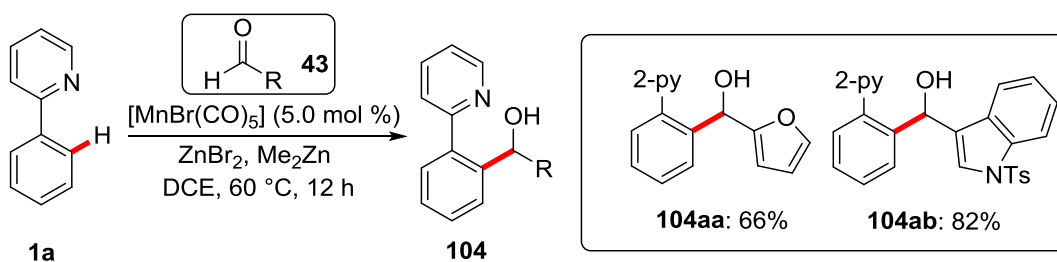
Scheme 35. Manganese(I)-catalyzed C–H addition to aldehydes **43**.

Additionally, *Ackermann* and coworkers reported on a manganese(I)-catalyzed aminocarbonylation of heteroarenes through C–H addition to furnish isocyanates.[100] The authors presented an ample scope of differently substituted 2-pyridylindoles **105** and a large variety of isocyanates **106** to afford the corresponding aminocarbonylated products **107** in very good yields. Notably, sensitive functional groups, such as ketones and esters, were well tolerated under the optimal reaction conditions.

105   **106**   **107**

107a: 81%   **107b**: 82%   **107c**: 62%
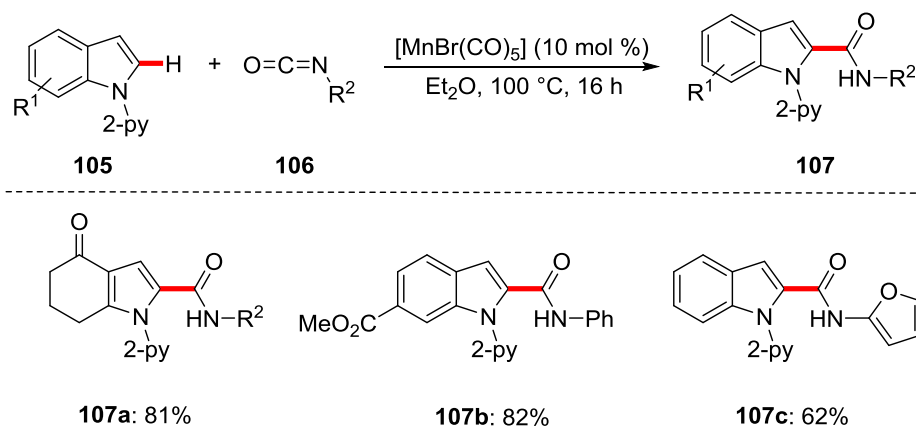
Scheme 36. Manganese(I)-catalyzed aminocarbonylation.

Recently, *Ackermann* and coworkers disclosed a manganese(I)-catalyzed cyanation reaction on several heterocycles (Scheme 37).[101] Overall, a variety of functional groups was tolerated, including esters, ketones, and tryptophans. The authors introduced the new and more electrophilic cyanation reagent *N*-cyano-*N*-(4-fluorophenyl)-4-methylbenzenesulfonamide (NCFS) (**108**) and compared its reactivity with *Beller's* well-established *N*-cyano-*N*-phenyl-*p*-toluenesulfonamide (NCTS) (**56**).[102] Thus, with respect to the cyanation of very challenging tryptophan **110**, NCFS was shown to be a more powerful cyanation reagent than NCTS.[101]

55   **56**   **57**

58: 70%   **59**: 86%   **109**: 83%   **110**: 58% (NCTS)
   **110**: 68% (NCFS)
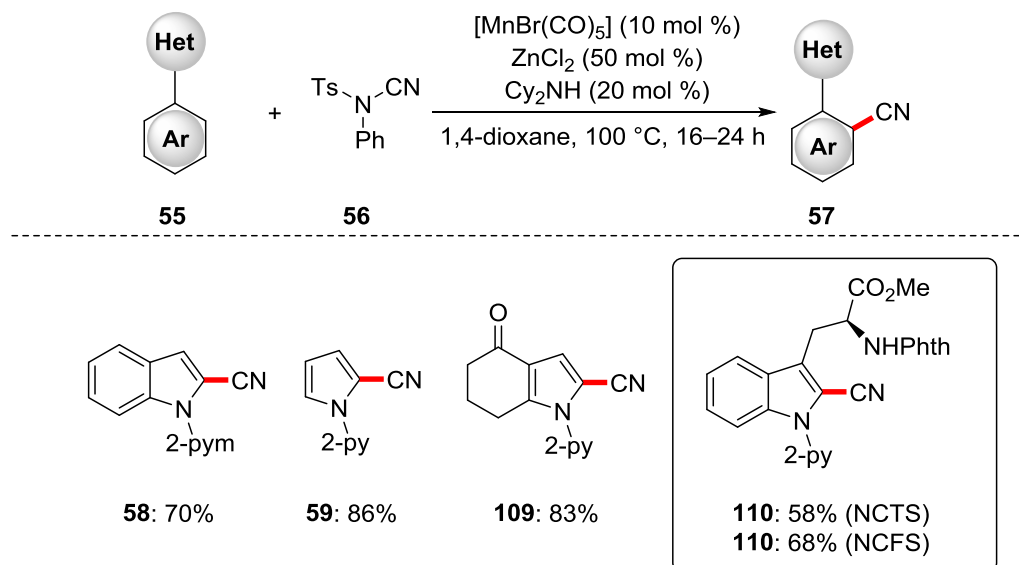
Scheme 37. Manganese(I)-catalyzed C–H cyanation.

Intermolecular competition experiments with electron-donating and electron-withdrawing substituents indicated a clear preference for electron-rich substrates. Moreover, H/D-exchange experiments and a KIE study revealed a fully reversible C–H activation step to be at work. In addition, detailed DFT studies were supportive of $ZnCl_2$ to act as a *Lewis* acid and to facilitate the turnover-limiting migratory insertion step in a hetero-bimetallic fashion.

However, the reactivity of manganacycles was not only limited to addition reactions with strong electrophiles. Indeed, the insertion of inherently less polar carbon-carbon multiple bonds proved to be viable as well. Thus, *Wang* and coworkers accomplished the first manganese(I)-catalyzed alkenylation reaction with terminal alkynes **111** using [MnBr(CO)$_5$] as the catalyst and Cy$_2$NH as the crucial base additive.[103]
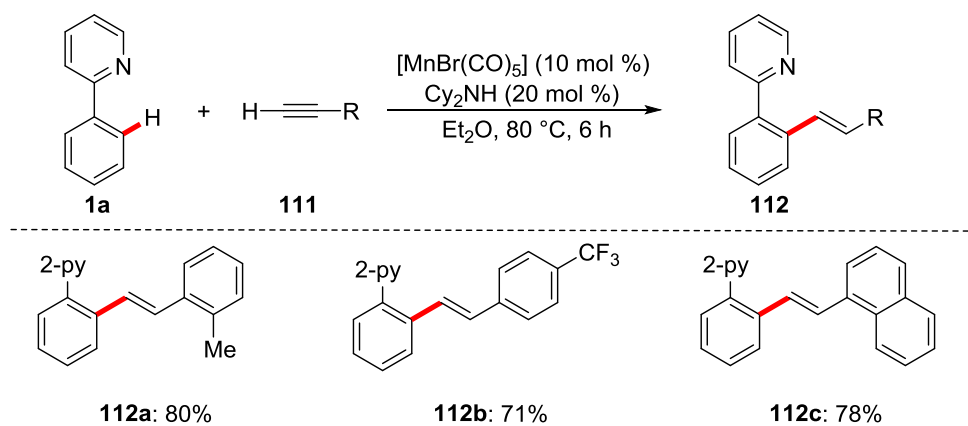
Scheme 38. Manganese(I)-catalyzed C–H alkenylation.

In this reaction, a variety of aryl- as well as alkyl-substituted terminal alkynes **111** reacted smoothly to provide the (*E*)-configured alkenes **112** with perfect *anti-Markovnikov* selectivity. Finally, the authors performed DFT calculations to shed light on the reaction mechanism. Based on these studies, it was proposed that Cy$_2$NH facilitates the C–H activation step *via* a base-assisted deprotonative pathway.

Thereafter, the same group extended the manganese(I)-catalyzed hydroarylation protocol to electronically activated *α,β*-unsaturated carbonyls **113** (Scheme 39).[104] The reaction proceeded with excellent mono-selectivities, delivering the corresponding products **114** in satisfactory yields.
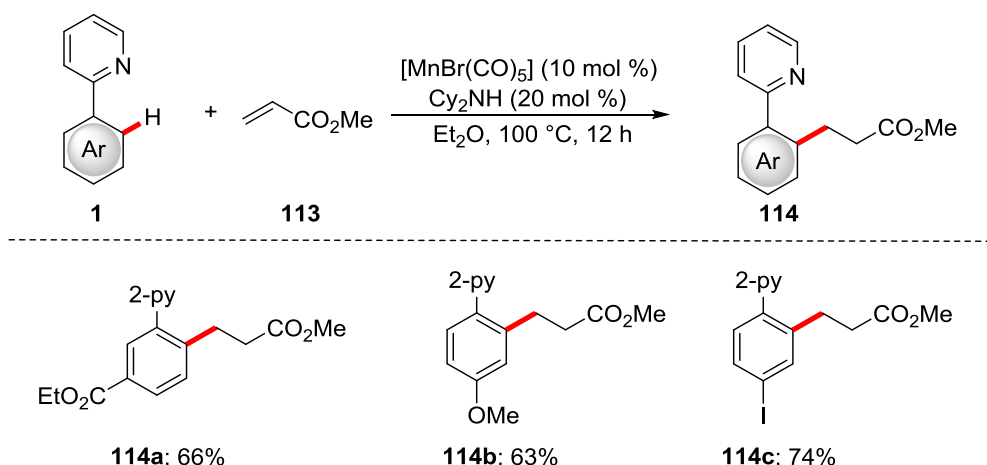
Scheme 39. Manganese(I)-catalyzed hydroarylation of α,β-unsaturated carbonyls **113**.

Furthermore, *Wang* and coworkers demonstrated that the C–H hydroarylation strategy turned out to be applicable in C–H/N–H annulation reactions with imines **115** and terminal **111** as well as internal alkynes **48** to deliver isoquinolines **116** (Scheme 40).[105] In addition to a broad substrate scope with good yields and regioselectivities, the authors unraveled large parts of the reaction mechanism.
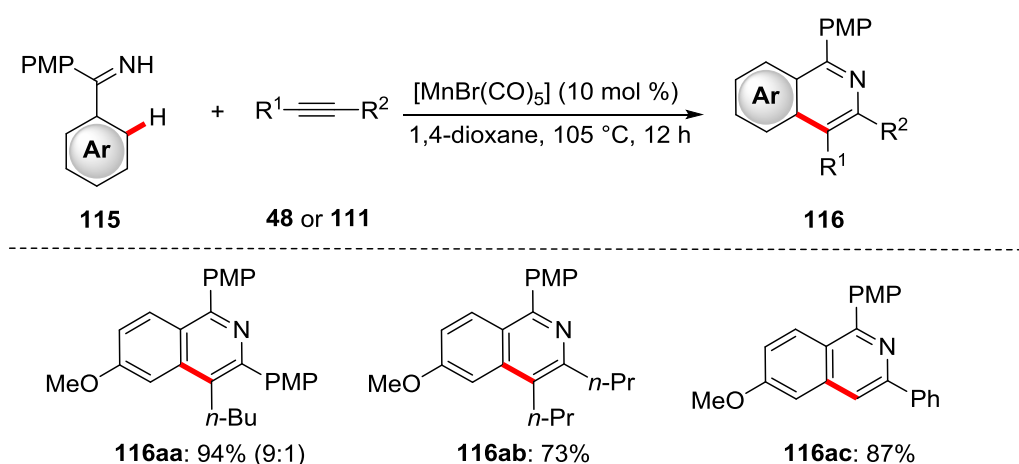
Scheme 40. Manganese(I)-catalyzed C–H/N–H annulation.

Thus, the authors proposed a catalytic cycle (Scheme 41), which is commenced by a presumably turnover-limiting C–H activation step to form manganacycle **117**. After ligand exchange of CO by alkyne-coordination, a migratory insertion leads to intermediate **119**, which is prone to undergo reductive elimination to release the desired product **116** and generates a manganese-hydride species **120**. The latter reacts with a new imine **115** to again deliver manganacycle **117** through C–H manganation under evolution of hydrogen.

Scheme 41. Postulated catalytic cycle for the manganese(I)-catalyzed C–H/N–H annulation.
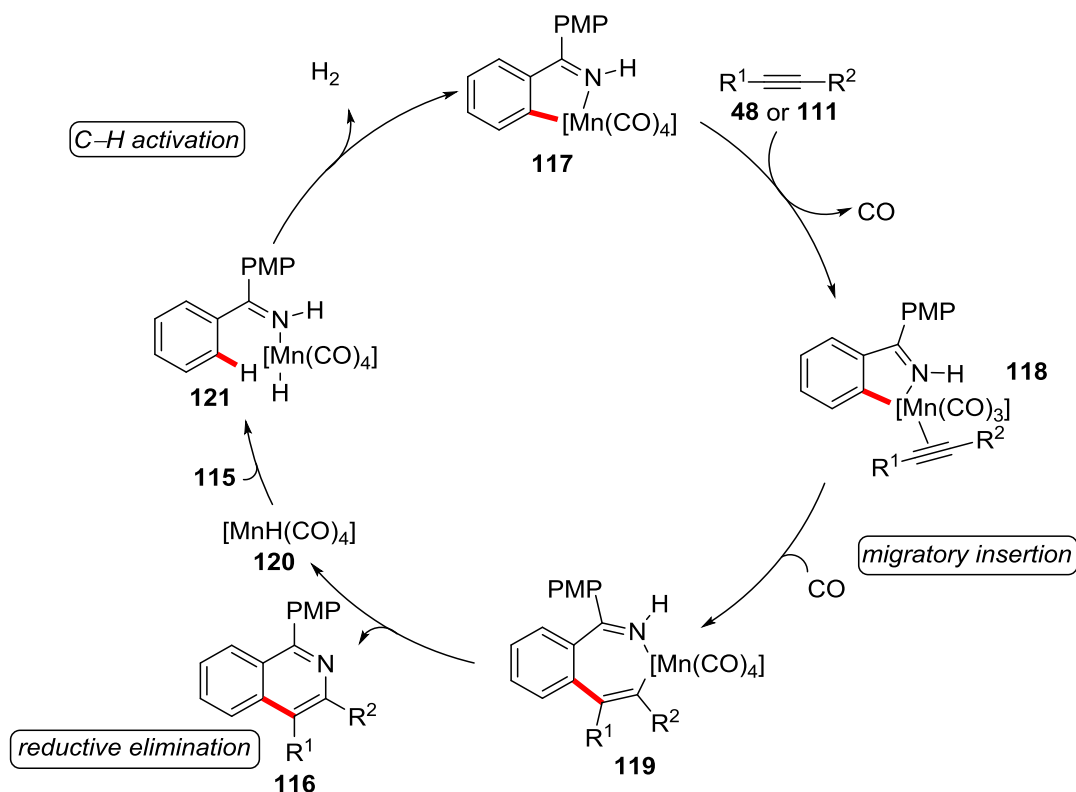
Ackermann and coworkers reported on an manganese-catalyzed C–H annulation with acrylates[106] to afford highly valuable *β*-amino esters[107] **122** (Scheme 42) in good yields and overall intriguing levels of diastereoselectivities.
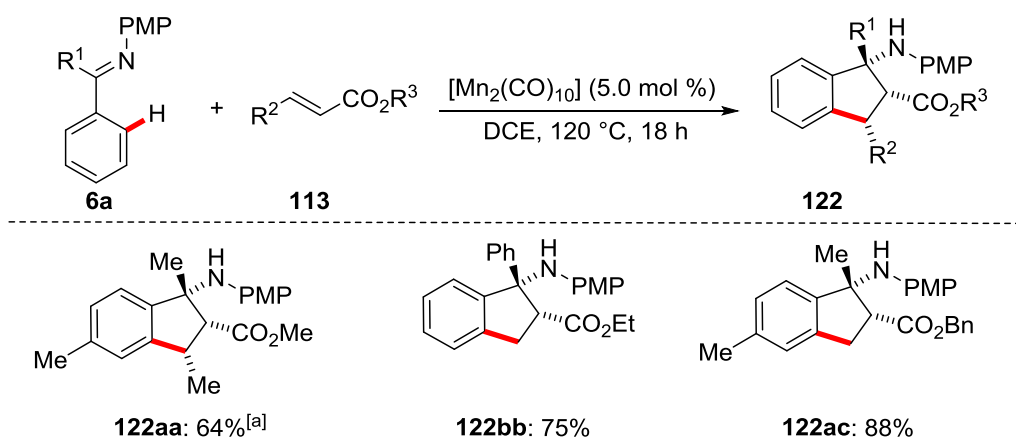
Scheme 42. Manganese-catalyzed synthesis of *β*-amino esters *via* a C–H annulation process. [a] [Mn$_2$(CO)$_{10}$] (10 mol %) in PhMe.

In addition to the previously described substitutive cobalt(III)-catalyzed C–H allylation with allyl carbonates **67** (*cf.* Scheme 22), manganese catalysis was shown to be a competent alternative to enable C–H allylations.

In this regard, the *Ackermann* group reported on a C–H allylation of ketimines **6** with allyl carbonates **67**, delivering the corresponding allylated ketones **123** in excellent yields and good diastereoselectivities upon acidic workup (Scheme 43).[108]
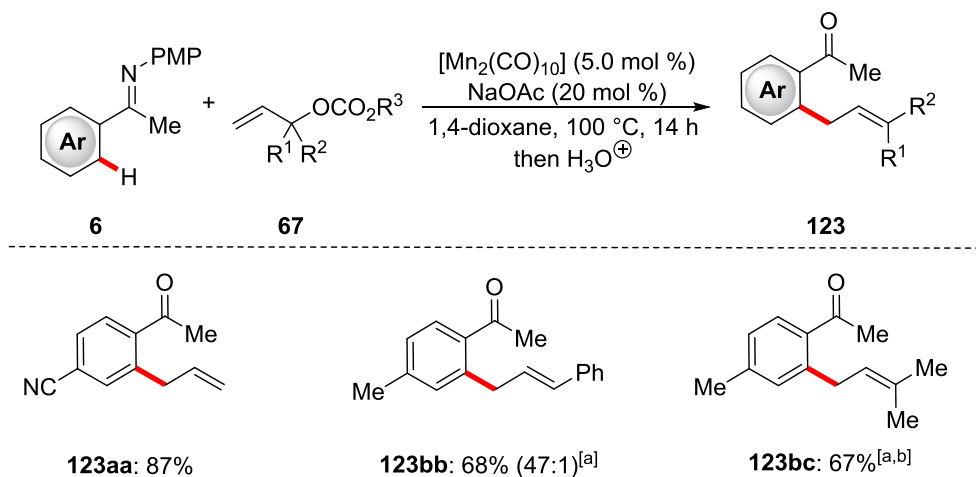
Scheme 43. Manganese-catalyzed C–H allylation with allyl carbonates **67**. [a] At 120 °C. [b] [Mn$_2$(CO)$_{10}$] (10 mol %).

2   Objectives

The development of novel strategies for highly stereoselective transition metal-catalyzed C–C bond forming processes is of prime importance for expanding the toolbox of modern organic synthesis. In recent years, C–H bond functionalizations[13] have emerged as a powerful reaction class due to their synthetic versatility and excellent atom-[10] and step-economy.[11] Thus, the focus of this thesis is directed towards exploring novel cost-effective and environmentally benign C–H functionalizations.[12b] In this context, particularly the efficiency of catalysts should be studied that are based on rather inexpensive ruthenium as well as earth-abundant base metals such as cobalt and manganese.[54]

In the past decade, invaluable advances in ruthenium-catalyzed C–H arylations were *inter alia* achieved by *Ackermann* and coworkers, highlighting powerful carboxylates as the additives of choice.[20a, 109] Nevertheless, also the use of secondary phosphine oxides (SPOs) as preligands has been revealed to be highly beneficial.[36] Within this thesis, the performance of well-defined and easily modifiable ruthenium(II)-phosphinous acid (PA) complexes **124** in the C–H arylation of (*E*)-styrylpyridines **9** as challenging acyclic alkene substrates should be explored (Scheme 44). Moreover, detailed mechanistic studies should elucidate the pathways of the C–H and the C–X bond activation steps.
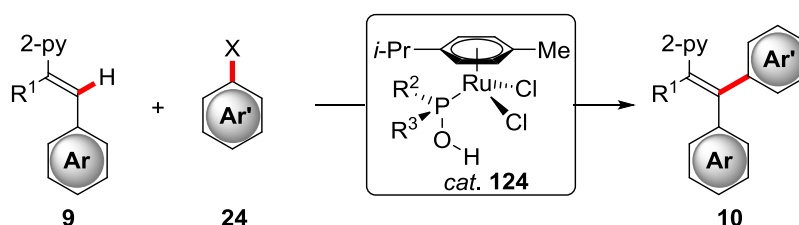
Scheme 44. Ruthenium(II)-PA-catalyzed C−H arylation.

Despite of undisputed progress in the field of cobalt(III)-catalyzed C–H bond activations,[15] there is still a lack of methods that merge C–H with C–C[110] functionalizations in a tandem process. In this regard, vinylcyclopropanes **125**[111] are due to their ring strain ideal synthons for achieving the first cobalt-catalyzed C–H/C–C functionalization, along with detailed mechanistic studies (Scheme 45).
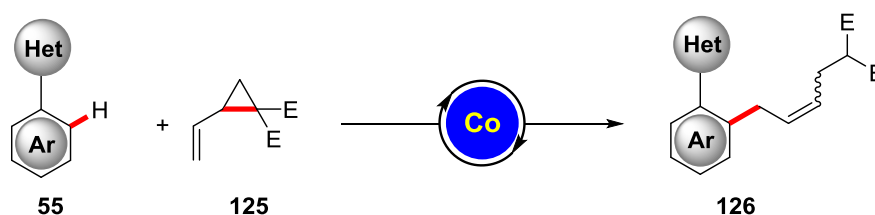
Scheme 45. Cobalt(III)-catalyzed C–H/C–C functionalization.

So far, there have been numerous reports on transition metal-catalyzed C–H hydroarylations,[112] with a plethora of metals and broad synthetic applicability. Thus far, the control of *Markovnikov*/*anti-*

Markovnikov regioselectivity has relied on the use of expensive ligands[113] and was mostly restricted to electronically activated styrenes **82**.[114] Within this thesis, a new concept for regiocontrol in C–H hydroarylations of unactivated alkenes should be developed (Scheme 46). This approach should encompass the design of reaction conditions to easily switch between branched and linear selectivity.
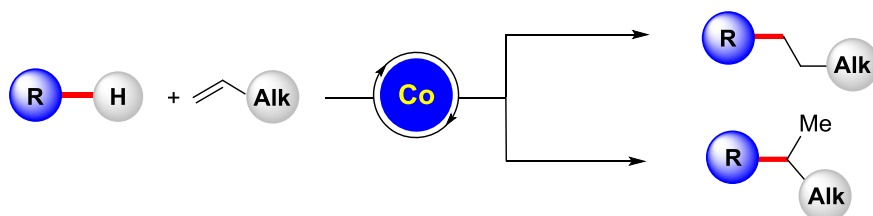
Scheme 46. Control of branched/linear selectivity in cobalt(III)-catalyzed C–H hydroarylations.

There is a strong demand for novel synthetic methods to install fluorine in organic molecules,[115] because fluorine is known to improve several physicochemical properties of *e.g.* pharmaceuticals, such as metabolic stability, lipophilicity and membrane permeability.[116] So far, several methods for C–H/C–X functionalizations are known that are based on feasible *β*-carbon,[117] -oxygen,[75, 77-78] or -nitrogen[74, 91, 117a] eliminations. Thus, a cobalt(III)-catalyzed C–H activation was intended to be combined with C–F functionalizations[118] through *β*-fluoride elimination[119] using perfluoroalkylalkenes **127** and 1,1-difluoroalkenes **128** (Scheme 47).
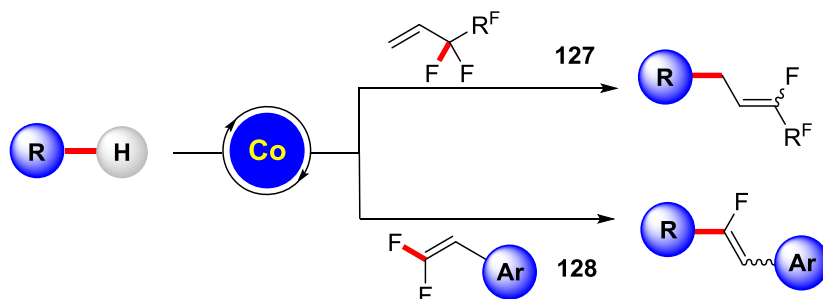
Scheme 47. Cobalt(III)-catalyzed allylative and alkenylative C–H/C–F functionalization.

In recent years, a tremendous progress has been achieved in utilizing manganese(I) catalysts for C–H functionalizations[14] with partly unique levels of selectivity control.[117d, 120] Thus, the development of a novel manganese(I)-catalyzed C–H/C–F functionalization was intended (Scheme 48). Particularly, a comparison with the analogous cobalt(III)-catalyzed reaction in terms of reactivities and selectivities should be of prime importance for revealing unique features of metals in C–H activation catalysis.
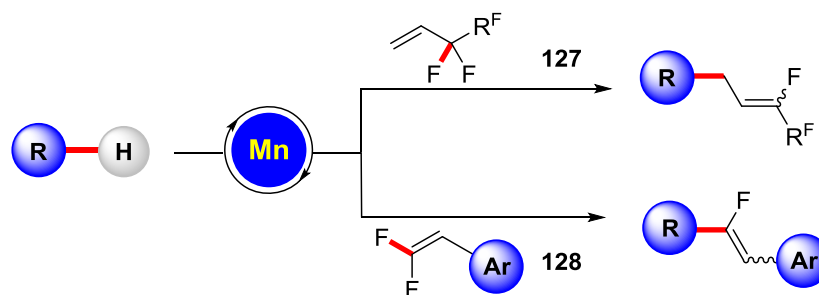
Scheme 48. Manganese(I)-catalyzed allylative and alkenylative C–H/C–F functionalization.

3   Results and Discussion

3.1   C−H Arylations by Ruthenium(II)-Phosphinous Acid Catalysts

The last years have witnessed significant progress in the development of ruthenium catalyzed C–H arylations. In this context, especially well-defined ruthenium(II)-carboxylate catalysts have proven to be powerful catalysts with a broad applicability and excellent functional group tolerance.[20a, 109a]

However, there is still a strong demand for the synthesis of novel and efficient ruthenium catalysts, which could be used for applications in *inter alia* polymer chemistry and material sciences.[121]

For this purpose, highly reactive and bench-stable catalysts are needed which bear an easily modifiable ligand such as phosphinous acid. Thus, the exploration of versatile single-component ruthenium(II)-PA complexes **124**, their use in C–H arylations, and new mechanistic insights represent a great opportunity to raise the potential of ruthenium-catalyzed C–H arylation methods.

3.1.1   Optimization Studies

We initiated our optimization studies by probing the effect of different ruthenium(II) catalysts on the desired C−H arylation of (*E*)-2-styrylpyridine (**9a**) (Table 1). In this context, conventionally used catalytic precursors like [RuCl$_3$·xH$_2$O][47-48] and [RuCl$_2$(*p*-cymene)]$_2$ (entries 1 and 2) were clearly outcompeted by well-defined single component phosphinous acid (PA) ruthenium(II) catalysts **124**,[122] that have been synthesized following an optimized protocol by *S. Warratz*.[123] It is noteworthy that in the absence of any ruthenium precursor the desired product **10ab** was not formed (entry 3). To elucidate the role of the substitution pattern on the phosphorous atom of the phosphinous acid ligand, the reactivity of different ruthenium(II)-PA complexes **124** with aliphatic as well as aromatic substituents has been studied (entries 4–10). Aromatic substituents only led to moderate yields, with a decrease in reactivity for electron-poor substituents (entry 5). In contrast, a clearly higher reactivity was achieved by employing alkyl-substituted PA-ligands (entries 7 and 8). However, a sterically more congested substitution pattern led to only unsatisfactory results (entries 9 and 10), which reveals that a balanced situation between the repulsive steric interactions and electronic parameters of the PA-ligand is necessary for an efficient transformation.

Generally, it can be speculated that electron-donating substituents on the phosphorous atom increase the basicity of the deprotonated phosphinous acid ligand, which acts as internal base during the metal-ligand cooperated C–H activation.[36a, 123] Consequently, a faster C–H activation elementary step would occur. In addition, the contribution of attractive *London* dispersion interactions[124] to the stabilization of the C–H activation transition state should be considered as well, since a significant rate acceleration by using diadamantyl-phosphine oxides as preligands has been observed for previously reported ruthenium(II)-catalyzed C–H arylations.[36]

Table 1. Optimization for the C–H arylation of (*E*)-2-styrylpyridine (**9a**) with aryl bromides **2**.
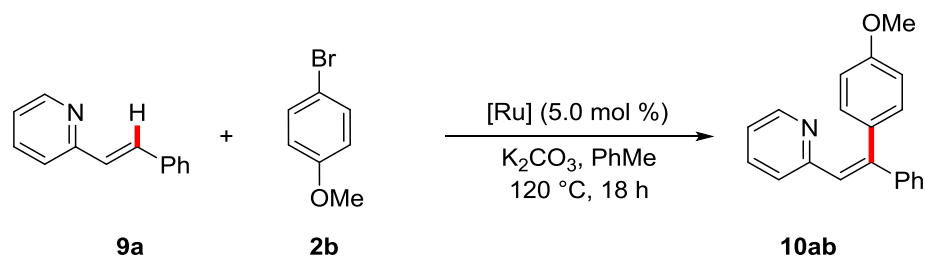
Entry	[Ru]	yield / %[a]
1	[RuCl$_3$·*x*H$_2$O]	<5[b]
2	[RuCl$_2$(*p*-cymene)]$_2$	9
3	---	---[b,c]
4	[RuCl$_2$(*p*-cymene)(Ph$_2$POH)] (**124a**)	77
5	[RuCl$_2$(*p*-cymene){(*p*-FC$_6$H$_4$)$_2$POH}] (**124b**)	60
6	[RuCl$_2$(*p*-cymene)(*t*-BuPhPOH)] (**124c**)	51
7	[RuCl$_2$(*p*-cymene)(*i*-Pr$_2$POH)] (**124d**)	92
8	**[RuCl$_2$(*p*-cymene)(*n*-Bu$_2$POH)] (124e)**	**96**
9	[RuCl$_2$(*p*-cymene)(Cy$_2$POH)] (**124f**)	53
10	[RuCl$_2$(*p*-cymene)(*o*-Tol$_2$POH)] (**124g**)	71

[a] Reaction conditions: **9a** (0.50 mmol), **2b** (0.75 mmol), [Ru] (5.0 mol %), K$_2$CO$_3$ (1.00 mmol), PhMe (0.25 M), 120 °C, 18 h, isolated yield. [b] Determined by GC with *n*-dodecane as the internal standard. [c] *n*-Bu$_2$P(O)H (20 mol %) as additive.

Encouraged by these preliminary optimization results, the catalytic performance of the optimal ruthenium(II)-PA complex **124e** was furthermore tested by reducing the catalyst loading (Table 2), employing slightly higher concentrations and reaction temperatures. Surprisingly, catalyst loadings as low as 0.90 mol % still provided an excellent conversion to the desired product **10ab** (entry 4), while even lower catalyst loadings led to a slightly decreased reactivity (entry 5).

Table 2. Reduction of the catalyst loading.
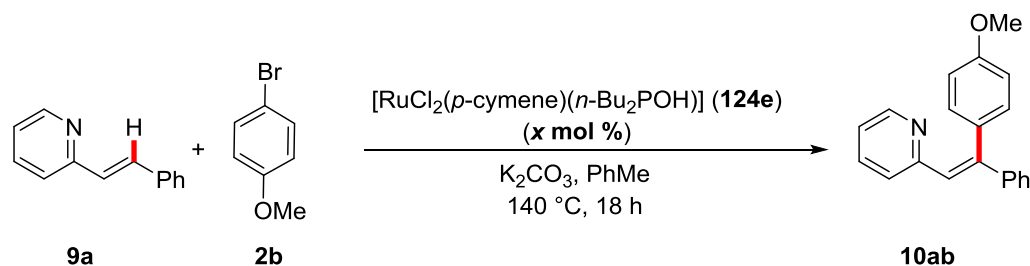
Entry	x / mol %	yield / % [a]
1	5.00	99
2	2.50	99
3	1.00	98
4	0.90	98
5	0.75	82
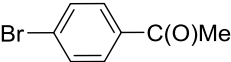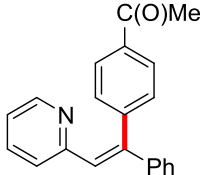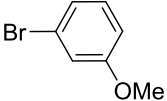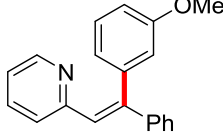
[a] Reaction conditions: **9a** (0.50 mmol), **2b** (0.75 mmol), [Ru] (5.0 mol %), K_2CO_3 (1.00 mmol), PhMe (1.00 M), 140 °C, 18 h. Conversions determined by means of GC with *n*-dodecane as the internal standard.

3.1.2   Scope of the C–H Arylation with Aryl Bromides

With the optimized catalytic system in hand, the substrate scope for the C–H arylation of (*E*)-2-styrylpyridine (**9a**) with aryl bromides **2** was explored. To start with, different substitution patterns as well as valuable functional groups on the aryl bromide **2** were extensively tested (Table 3). Furthermore, a variation of substituents in *para*-position of the aryl bromide **2** led to overall good to excellent yields. However, no clear reactivity trend with respect to the electronic nature of the aryl bromide **2** (entries 1–8) could be disclosed. Notably, even challenging functional groups, such as esters, amines, as well as enolizable ketones, were well tolerated under the optimal reaction conditions. Furthermore, substituents in *meta-* and *ortho*-positions (entries 9 and 10) were well accepted and afforded the desired arylated products **10** in good yields under slightly altered reaction conditions for the *ortho*-substituted aryl bromide **2j**. Nevertheless, a significant limitation was observed by using the sterically very congested aryl bromide **2k** (entry 11).[125] The electron-rich heteroarene 3-bromothiophene (**2l**) afforded the corresponding product **10l** in very good yield (entry 12), together with detectable amounts of the diastereomer (*Z/E* = 96:4), which might be rationalized in terms of a thermal isomerization.

Table 3. Scope of the ruthenium(II)-PA-catalyzed C–H arylation with aryl bromides **2**.

Entry	aryl bromide	2	product	10a	yield / %[a]
1	Br—⟨⟩—NMe₂	2c		10ac	94
2	Br—⟨⟩—OMe	2b		10ab	96
3	Br—⟨⟩—Me	2d		10ad	93
4	Br—⟨⟩	2a		10aa	80
5	Br—⟨⟩—F	2e		10ae	92
6	Br—⟨⟩—CF₃	2f		10af	71
7	Br—⟨⟩—CO₂Et	2g		10ag	87

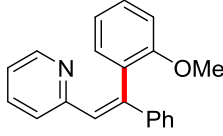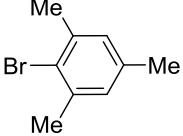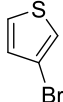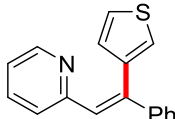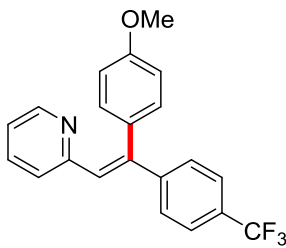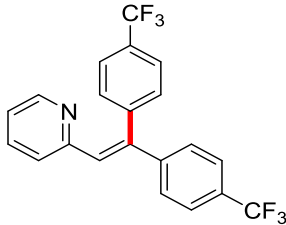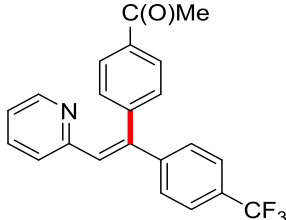| 8 | Br—⟨ ⟩—C(O)Me | **2h** | | **10ah** | 87 |
9	Br-aryl-OMe	**2i**		**10ai**	80
10	Br-aryl-MeO	**2j**		**10aj**	81[b]
11	Me-Br-aryl-Me-Me	**2k**	---	**10ak**	---[b]
12	thiophene-Br	**2l**		**10al**	87[c]

[a] Reaction conditions: **9a** (0.50 mmol), **2** (0.75 mmol), [Ru] (5.0 mol %), K_2CO_3 (1.00 mmol), PhMe (2.0 mL, 0.25 M), 120 °C, 18 h, isolated yields. [b] At 140 °C, PhMe (1.00 M). [c] Z/E = 96:4, determined by means of ^{1}H-NMR spectroscopy.

Having revealed the broad applicability of the reaction with respect to electronic and steric parameters of the aryl bromide **2**, the substitution pattern of (*E*)-2-styrylpyridine (**9a**) was tested next (Table 4). Herein, a slight preference for electron-rich substrates with methyl- (**9b**) and methoxy-substituents (**9c**) (entries 1–5) as compared to the electron-poor trifluoromethyl-substituted (*E*)-2-styrylpyridine (**9d**) (entries 6–8) was observed, albeit the overall high reactivity of the catalytic system might have levelled this effect.

Table 4. Scope of (*E*)-2-styrylpyridines **9**.
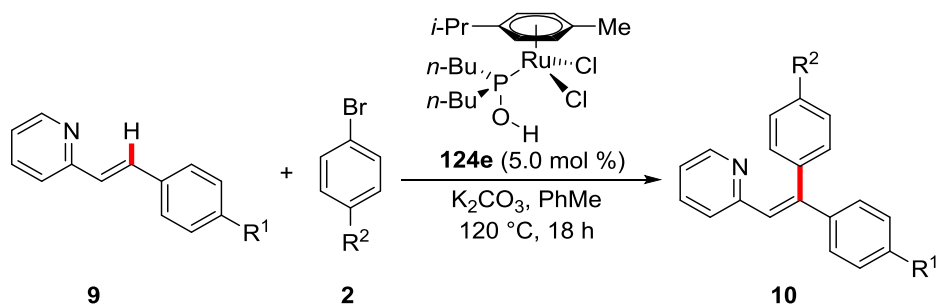
Entry	R^1	R^2	product	**10**	yield / %[a]
1	Me	OMe		**10bb**	90
2	Me	CF_3		**10bf**	85
3	Me	CO_2Et		**10bg**	87
4	OMe	OMe		**10cb**	93
5	OMe	CF_3		**10cf**	84

6	CF$_3$	OMe		**10db**	90
7	CF$_3$	CF$_3$		**10df**	77
8	CF$_3$	C(O)Me		**10dh**	78

[a] Reaction conditions: **9** (0.50 mmol), **2** (0.75 mmol), [Ru] (5.0 mol %), K$_2$CO$_3$ (1.00 mmol), PhMe (0.25 M), 120 °C, 18 h, isolated yield.

It is noteworthy that the sterically encumbered trisubstituted alkene **9e** was successfully converted to the fully substituted acyclic alkene **10eb**, displaying the first synthesis of tetrasubstituted acyclic alkenes by ruthenium-catalyzed C–H arylation (Scheme 49). Tetrasubstituted alkenes are important key motifs in *inter alia* pharmaceuticals and thus far considerable efforts have been made to devise highly stereoselective methods for their synthesis.[126]
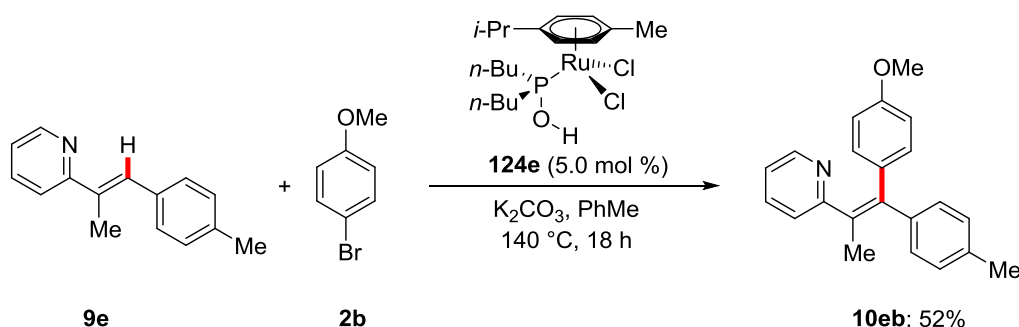
Scheme 49. Ruthenium(II)-PA-catalyzed synthesis of the tetrasubstitued acyclic alkene **10eb**.

Given the overall excellent performance of the catalytic system, more challenging aryl chlorides **3** with an inherently higher C–Cl dissociation energy[37b] were probed as arylating reagents under otherwise identical reaction conditions (Table 5). In summary, all the tested aryl chlorides **3** were efficiently converted into the desired products **10** in good to excellent yields, demonstrating that ruthenium(II)-PA complexes are very competent arylating catalysts, disregarding the C–X bond

strength. In this context, it should be emphasized that *S. Warratz* succeeded in using aryl tosylates as arylating reagents by employing a ruthenium(II)-PA complex.[123, 127]

Table 5. Scope of the ruthenium(II)-PA-catalyzed C–H arylation with aryl chlorides **3**.

Entry	aryl chloride	3	product	10a	yield / %[a]
1	Cl—⬡—OMe	3b		10ab	96
2	Cl—⬡—F	3e		10ae	92
3	Cl—⬡—CF₃	3f		10af	84
4	Cl—⬡—C(O)Me	3h		10ah	77

[a] Reaction conditions: **9a** (0.50 mmol), **3** (0.75 mmol), [Ru] (5.0 mol %), K₂CO₃ (1.00 mmol), PhMe (0.25 M), 120 °C, 18 h, isolated yield.

The overall reactivity of the optimized catalytic system seemed to be only moderately affected by the electronic nature of both reagents. In summary, the substitution pattern of the (*E*)-2-styrylpyridines **9** had a slight impact on the reactivity, whereas the electronics of the organic electrophile exerted only a minor influence. Only the steric effects of the aryl bromide **2** had a major influence on the reactivity, with a significant drop in reactivity for di-*ortho*-substituted aryl bromides **2** (*cf.* Table 3, entry 11).

3.1.3 Mechanistic Studies

3.1.3.1 Experiments with Radical Scavengers

A key step in the mechanism of C–H arylation reactions involves the activation and cleavage of C–Hal bonds. So far, the mechanism of this process has remained elusive and underexplored, as it has been unclear whether a single electron transfer (SET)-type process is operative. In this context, there are a few reports on oxidative additions of aryl halides to metals, such as nickel,[128] palladium[129] and platinum,[130] proceeding *via* SET-type activation of the C–Hal bond.

To delineate the C–Hal bond activation pathway, a set of well-established radical scavengers in stoichiometric amounts was added to the catalytic system (Table 6). In all cases, the catalytic reaction was significantly inhibited, which might suggest that a SET-type C–Br cleavage process occurred. Interestingly, a similar observation for ruthenium(II)-catalyzed C–H arylations was recently reported by *Ackermann* and coworkers[131] Nevertheless, no radical adduct of the scavenger and any reaction intermediate could be detected by means of GC- and ^{1}H-NMR- analysis. To shed light on this interesting mechanistic pathway, further studies should include for instance spin trapping experiments, since some radical scavengers like TEMPO possibly not only inhibit by radical, but also oxidative processes.[132]

Table 6. Experiments with radical scavengers.
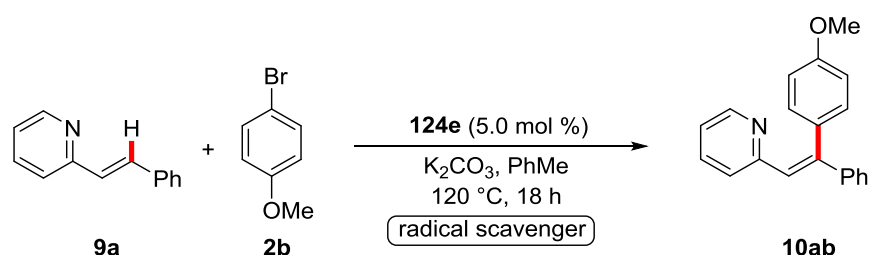
Entry	radical scavenger	conversion
1	TEMPO	2 %
2	$Ph_2C=CH_2$	---
3	BHT	---
4	Galvinoxyl	---
5	DPPH	---

[a] Reaction conditions: **9a** (0.50 mmol), **2b** (0.75 mmol), [Ru] (5.0 mol %), K_2CO_3 (1.00 mmol), scavenger (0.50 mmol), PhMe (2.0 mL, 0.25 M), 120 °C, 18 h. Conversions were determined by GC with *n*-dodecane as the internal standard.

3.1.3.2 *Hammett* Plot Analysis

Besides the exact working mode of the C–Hal bond activation, a particularly interesting question in ruthenium(II)-catalyzed C–H arylations encompasses the nature of the turnover-limiting step in the catalytic cycle. So far, there has been limited evidence for the oxidative addition to be turnover-limiting, albeit detailed kinetic studies have not been presented.[42] In this regard, a *Hammett* plot analysis[133] is a suitable analysis tool, which relies on a logarithmic relationship between the reaction rate k and a specific substitution parameter σ of the reacting substrate as well as a reaction parameter ρ (Equation 1).

$$\log k = \sigma \times \rho \qquad \text{(Equation 1)}$$

Notably, a *Hammett* plot analysis is particularly interesting for C–H arylations with *para*-substituents on aryl halides because of the overall minor steric effects and the availability of known values for commonly used arylating substrates.[134] Based on the initial reaction rates k_X, employing differently *para*-substituted aryl bromides **2** and the known σ_p-values, the resulting *Hammett* plots could indicate whether electronic effects of the aryl halide have a considerable impact on the overall reaction rate. Depending on the sign of the slope, it can furthermore elucidate whether oxidative addition or reductive elimination are turnover-limiting.[135]

Thus, a *Hammett* plot analysis of the C–H arylation on (*E*)-2-styrylpyridines **9** with differently *para*-substituted aryl bromides **2** was performed by comparing initial rates and correlating them with literature known σ_p-values (Scheme 50, Figure 3 and Figure 4).
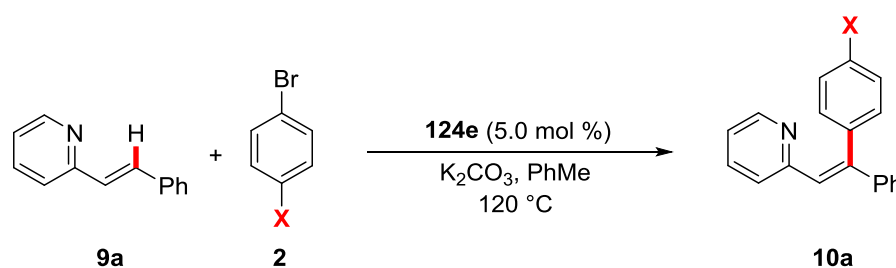
Scheme 50. *Hammett* plot analysis of differently *para*-substituted aryl bromides **2**.
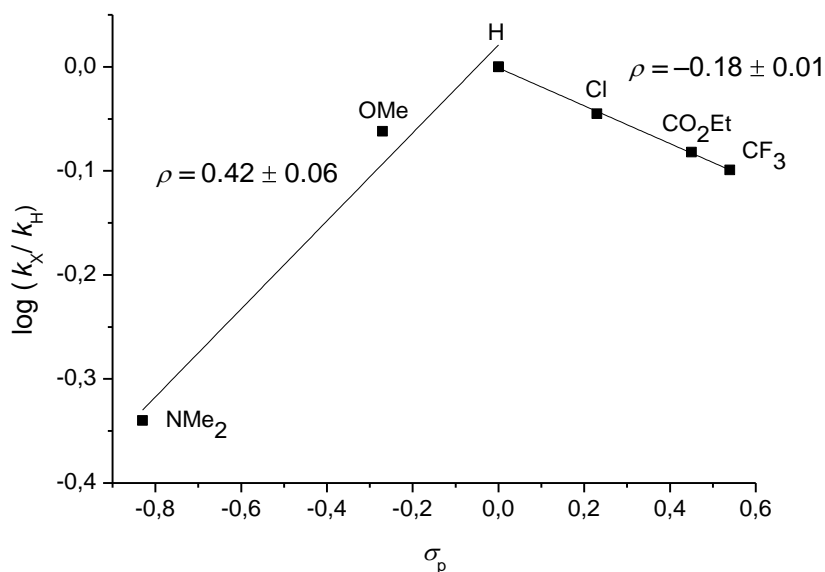
Figure 3. Hammett plot of the ruthenium(II)-PA-catalyzed arylation of (*E*)-2-styrylpyridine (**9a**).
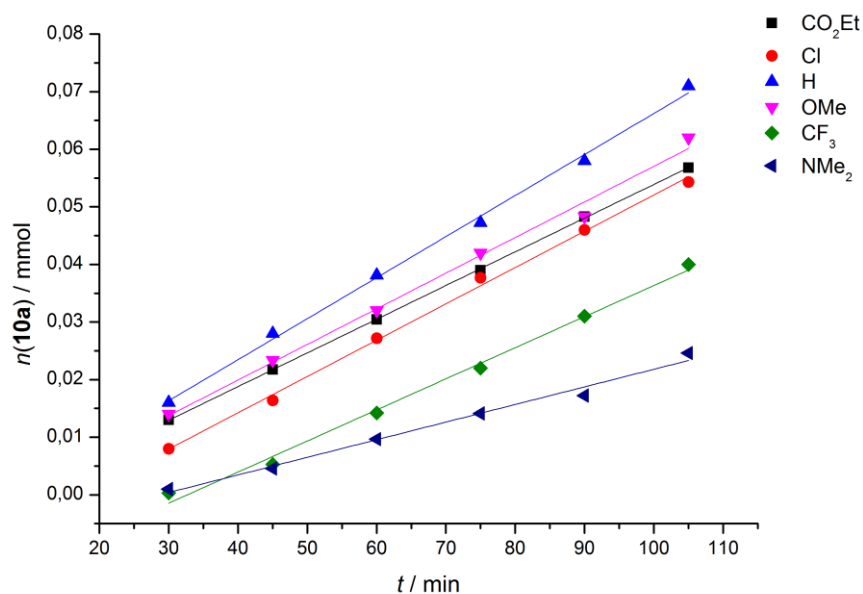
Figure 4. Initial rates using different aryl bromides **2**.

Remarkably, the obtained *Hammett* plot exhibited an unusual V-shape with slopes of $\rho = 0.42 \pm 0.06$ and $\rho = -0.18 \pm 0.01$. Likewise, a similar behaviour has been disclosed by *Chatani* and coworkers for a ruthenium(II)-catalyzed arylation with a bidentate directing group.[135b]

This unusual finding can be interpreted by a change in the turnover-limiting step from oxidative addition in the regime of electron-donating substituents to reductive elimination with electron-deficient aryl bromides **2**. Nevertheless, the observed ρ-value within the electron-deficient substitution

regime is not significantly high enough for drawing a reliable conclusion and the absolute reaction rates for electron-deficient aryl bromides **2** were still found to be comparably high. Overall, it can be concluded that rather oxidative addition is the turnover-limiting step, while for highly electron-deficient aryl bromides **2** the reductive elimination becomes energetically less feasible.

3.1.3.3   KIE Studies

Based on the results of the *Hammett* plot analysis, further mechanistic evidence for a turnover-limiting oxidative addition were indeed necessary. For this purpose, a study of the kinetic isotope effect (KIE) could elucidate the impact of the C–H activation elementary step on the overall reaction rate.
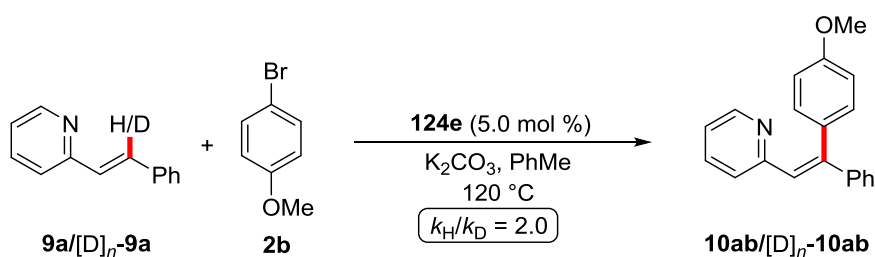
Scheme 51. KIE of the ruthenium(II)-PA-catalyzed arylation.

In this regard, a comparison of the independent reaction rates[136] with **9a** and the isotopically labeled [D]$_1$-**9a** was conducted by an *in situ* ReactIR analysis (Scheme 51, Figure 5 and Figure 6). For this purpose, the initial rates were followed by integration of a characteristic IR-band of the products **10ab** and [D]$_n$-**10ab** at 1520 cm^{-1} during the reaction progress (*vide infra*). In this way, a KIE of $k_H/k_D \approx 2.0$ was measured.
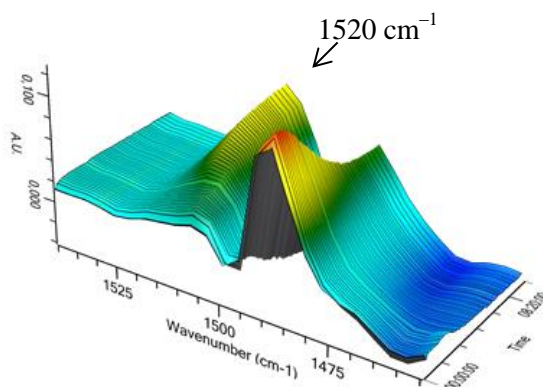
Figure 5. Kinetic profile of the C–H arylation followed by *in situ*-IR analysis.

This observation reveals that the C–H cleavage is a kinetically relevant elementary step, either being the turnover-limiting step itself or happening before turnover-limiting step as an equilibrium reaction. The latter assumption is in agreement with studies of *S. Warratz* who detected a significant H/D-exchange in the *ortho*-positions of 2-phenyloxazoline **7a** in a ruthenium(II)-PA catalyzed C–H arylation, which indicates a reversible C–H activation to be operative.[123] Therefore, the observed KIE

value can be interpreted in terms of a reversible, but kinetically relevant C–H activation before the turnover-limiting formal oxidative addition.
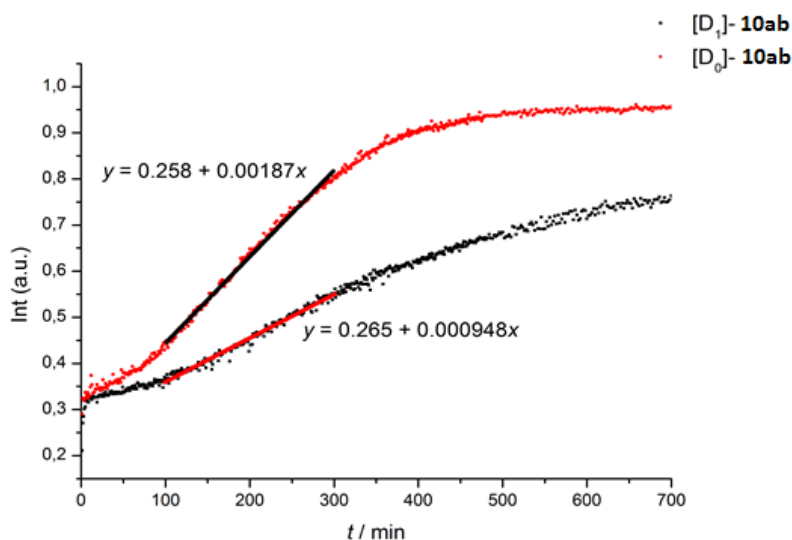
Figure 6. KIE of the ruthenium(II)-PA-catalyzed C–H arylation of **9a** by ReactIR analysis.

3.1.3.4   Kinetic Reaction Order

3.1.3.4.1   Reaction Order with respect to the concentration of (*E*)-2-styrylpyridine (9a)

Generally, an analysis of the kinetic reaction order in dependence on the concentration of each reactant as well as the catalyst represents a powerful mechanistic tool to elucidate the nature of the turnover-limiting step.[137]

Thus, the overall reaction rate showed a first order dependence ($n = 0.87 \pm 0.02$) on the concentration of (*E*)-2-styrylpyridine (**9a**), which is a hint for the C–H activation elementary step to be kinetically relevant (Figure 7).
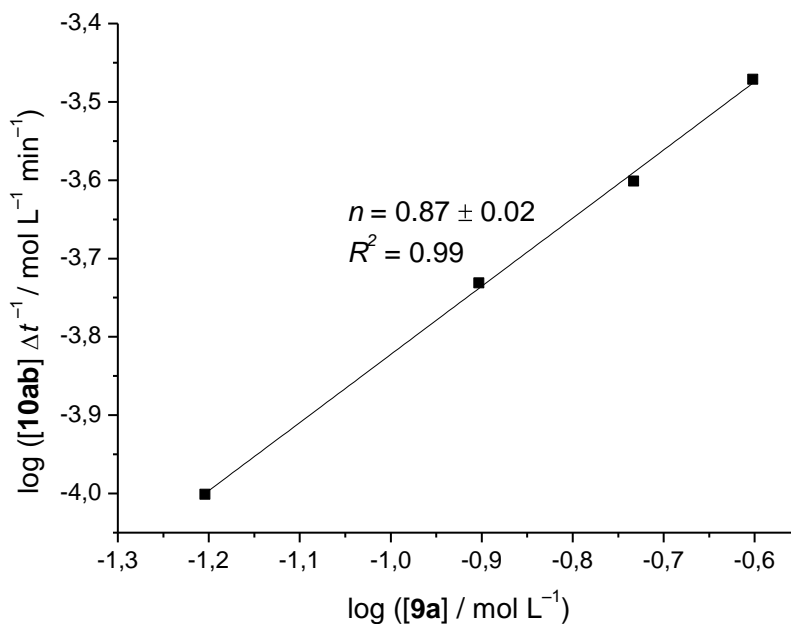
Figure 7. Reaction order *n* in [(*E*)-2-styrylpyridine] (**9a**).

3.1.3.4.2 Reaction Order with respect to the concentration of 4-bromoanisole (2b)

The kinetic order with respect to the concentration of the arylating reagent 4-bromoanisole (**2b**) exhibited saturation kinetics (Figure 8).
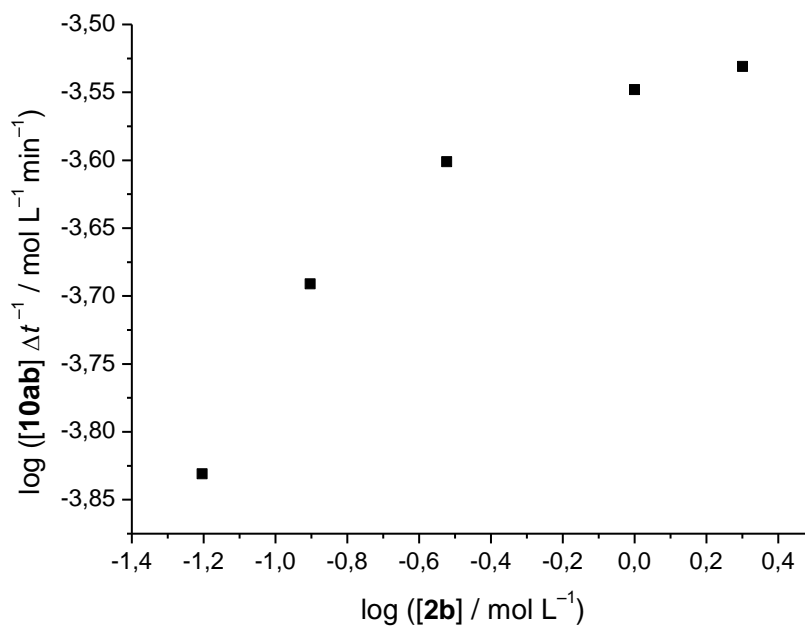
Figure 8. Reaction order *n* in [4-bromoanisole] (**2b**).

This observation is indicative of the oxidative addition to be the turnover-limiting step of the catalytic cycle. For the studied reaction, a simplified reaction is depicted in Scheme 52. Assuming that the

concentration of ruthenacycle **127** follows steady-state kinetics (Equation 2) and the subsequent steps after oxidative addition are fast and neglectable for the reaction rate, the overall rate law for the formation of the product **10ab** (Equation 3) simplifies to Equation 4.[137c]

$$\frac{d[\mathbf{127}]}{dt} = k_1[\mathbf{9a}][\mathbf{126}] - k_{-1}[\mathbf{127}] - k_2[\mathbf{127}][\mathbf{2b}] = 0 \qquad \text{(Equation 2)}$$

$$\frac{d[\mathbf{10ab}]}{dt} = k_1[\mathbf{2b}][\mathbf{127}] \qquad \text{(Equation 3)}$$

$$\frac{d[\mathbf{10ab}]}{dt} = \frac{k_1 k_2[\mathbf{9a}][\mathbf{126}][\mathbf{2b}]}{k_{-1} + k_2[\mathbf{2b}]} \qquad \text{(Equation 4)}$$

If there is a very high concentration of 4-bromoanisole (**2b**), the term $k_2[\mathbf{2b}]$ could become larger than k_{-1} and consequently the overall reaction rate becomes independent on the concentration of the 4-bromoanisole (**2b**). That could be reasonable explanation for the observed saturation kinetics.
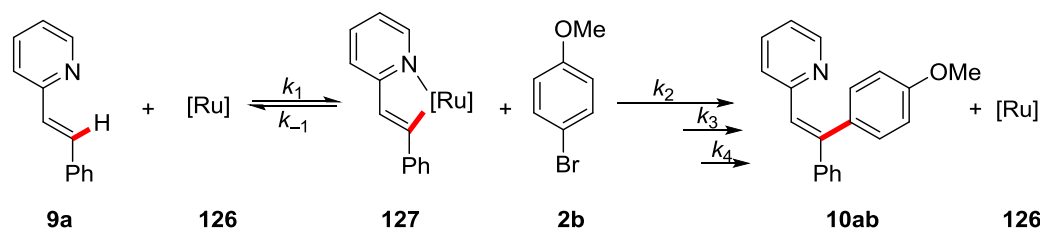
Scheme 52. Simplified kinetic scheme of the ruthenium(II)-PA-catalyzed C–H arylation.

3.1.3.4.3   Reaction Order with respect to the concentration of complex 124e

Further kinetic investigations established a first order dependence on the concentration of the single-component ruthenium(II)-PA complex **124e** (Figure 9), which reveals the presence of a mononuclear ruthenium-complex within the turnover-limiting step of the catalytic cycle.
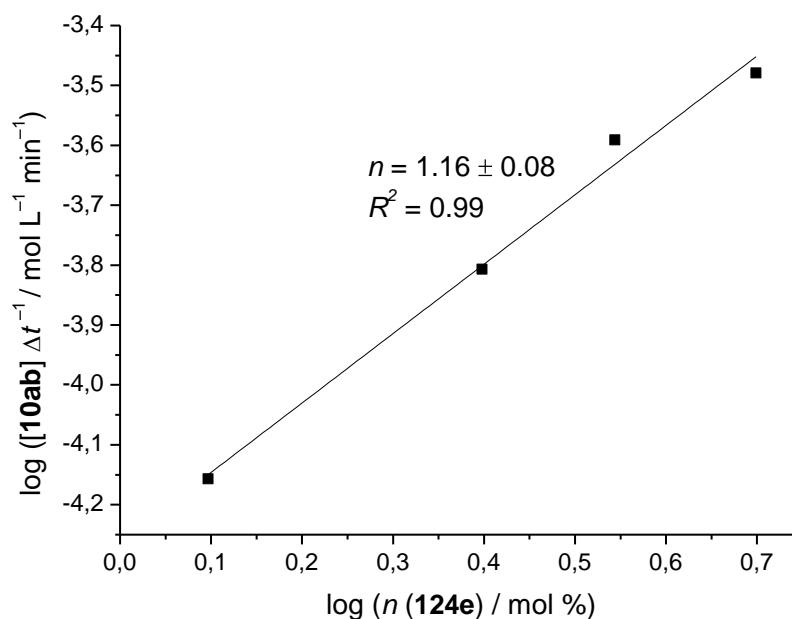
Figure 9. Reaction order in [**124e**].

3.1.4   Proposed Catalytic Cycle

In summary, it can be concluded that the C–H activation is a reversible, but kinetically relevant elementary step (Scheme 53). Presumably, the C–H activation proceeds by metal-ligand-cooperation, in which the *in situ* formed phosphinite acts as an internal base for the deprotonation step. Likewise, a *Hammett* plot analysis, KIE studies as well as kinetic order experiments supported the oxidative addition to be the turnover-limiting step. However, for electron-deficient aryl bromides **2** a slight trend to a slower reductive elimination step was observed. Additionally, computational studies involving DFT-calculations, performed by *S. J. Garden*, confirmed that the PA-ligand assisted the deprotonation during a metal-ligand-cooperative C–H activation step (transition state **127**).[123]

Thereafter, a SET-type oxidative addition of the aryl bromide **2** to the cyclometalated complex **128** occurs and furnishes the ruthenium(IV) complex **129**. After reductive elimination, the product **10a** is released and the active ruthenium(II)-PA catalyst **126** is regenerated.

However, the exact structures of some assumed intermediates have thus far remained unclear and some efforts should be made to investigate possible hapticity changes or even a decoordination of the *p*-cymene ligand in the course of the reaction. In this regard, a possible dissociation of the *p*-cymene ligand has already been proposed in related reactions.[138] Additionally, *Ackermann* and coworkers reported on C–H arylation catalysis which is enabled by a powerful and *p*-cymene-free [RuCl$_3$·xH$_2$O]-precursor.[47-48]
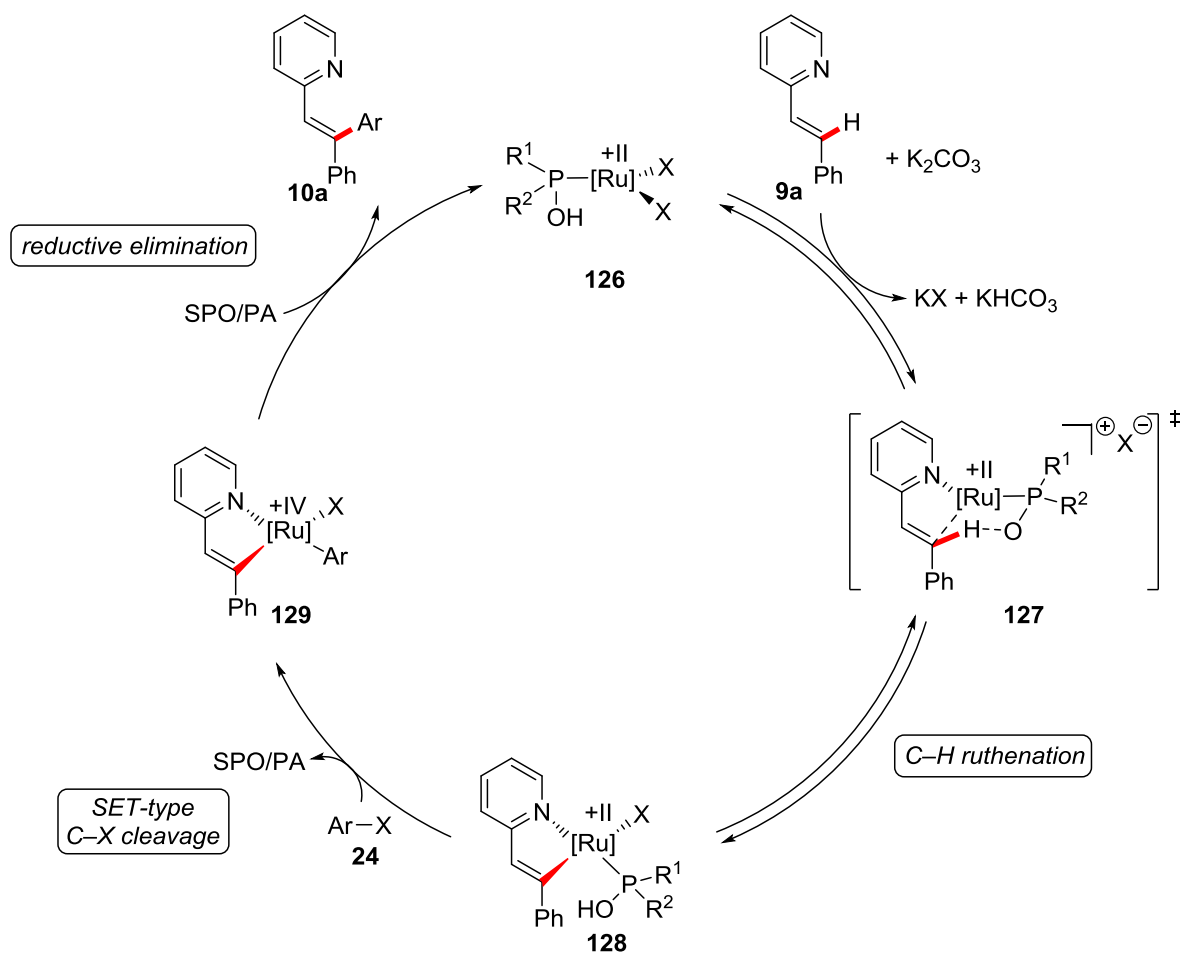
Scheme 53. Proposed catalytic cycle of the ruthenium(II)-PA-catalyzed C–H arylation. [Ru] = Ru(II)(*p*-cymene). X = Cl or Br.

3.2 Cobalt(III)-Catalyzed C−H/C−C Functionalization

The use of inexpensive 3d base metals, such as *inter alia* manganese[14a, 139] and cobalt,[15] for C–H functionalization reaction has been intensively studied in the last few years. In this regard, not only the cost-efficiency of these metals is of prime importance, but also a systematic study of their unique reactivity profile is essential for making considerable advances in transition metal-catalysis.

There are indeed aspects in C–H functionalizations like reactivity and stereoselectivity that can be controlled not only by the judicious choice of ligands, but also by the distinctive features of any metal. In this regard, there are several reports of *inter alia Ackermann*,[23c] *Glorius*,[140] *Kanai/Matsunaga*,[91] and *Wang*[141] on higher reactivities and distinct chemoselectivities for cobalt(III) complexes as compared to the corresponding rhodium(III) C–H activation catalysis.

Despite these intriguing advances, there is still demand for the exploration of distinct selectivity features in cobalt(III) catalysis. Therefore, the control of diastereoselectivity in C–H/C–C activations[117a, 117c, 117d] with vinylcyclopropanes **125** represents a promising objective.
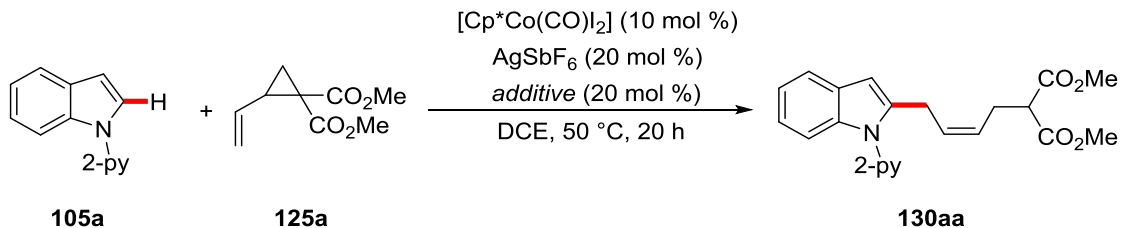
3.2.1 Optimization Studies

The optimization studies were commenced by probing the effect of various acetate- and pivalate bases with different alkali metal counter cations (Table 7). Lithium, sodium and potassium acetate as additives delivered the desired product **130aa** in satisfactory yields, whereas cesium acetate was by far the least effective additive (entries 1–4). The same trend was observed for pivalate bases, with sodium pivalate being the optimal base for this transformation (entry 6). In contrast, potassium- and cesium pivalate led to a significant drop in reactivity (entries 7 and 8).

Furthermore, no reaction was observed by omitting the cobalt(III) catalyst, which is a clear hint for cobalt catalysis to be operative in this reaction (entry 9). In addition, the silver additive $AgSbF_6$ was found to be essential for catalytic activity (entry 10). Based on previous results in C–H activation by cobalt(III) catalysis, no further optimization of the silver additive was performed.[15a] A reaction without base additive led to only moderate yield and 10% of a double bond regioisomer was detected, in which the double bond was shifted into conjugation with the indole nucleus (entry 11). In contrast, efficient conversion can only be accomplished in the presence of a base additive, which is a hint for a BIES-type C–H activation pathway.

Notably, all tested reaction conditions exclusively furnished the thermodynamically less favored *Z*-diastereomer in very good selectivities, which is in contrast to *E*-selective manganese(I)[117a, 117d] and rhodium(III) catalysis.[117c] Furthermore, *Q. Bu* tested different cobalt(III) sources, indicating that silver is not necessary for the reaction (entry 15) and other ligands are inferior to the electron-rich Cp* (entries 16 and 17). In this context, she detected a slight decrease in *E*/*Z*-ratio to 8:1, which could be interesting for future developments of ligand-controlled diastereoselective C–H/C–C functionalizations.

Remarkably, the catalytic performance was only moderately affected by decreasing the reaction temperature to 25 °C (entry 18).

Table 7. Optimization for the cobalt(III)-catalyzed C–H/C–C functionalization.

Entry	additive	yield / %[a]
1	LiOAc	74
2	NaOAc	88
3	KOAc	76
4	CsOAc	11
5	LiOPiv	61
6	**NaOPiv**	**93**
7	KOPiv	51
8	CsOPiv	39
9	NaOPiv	---[c]
10	---	---[d]
11	---	68[e]
12	$NaO_2C(3\text{-}CF_3)C_6H_4$	68
13	KO_2CMes	27
14	Na(O-Piv-Val)	84
15	NaOPiv	91[f]
16	NaOPiv	18[g]
17	NaOPiv	10[h]
18	NaOPiv	64[i]

[a] Reaction conditions: **105a** (0.50 mmol), **125a** (0.60 mmol), [Cp*Co(CO)I$_2$] (10 mol %), AgSbF$_6$ (20 mol %), additive (20 mol %), DCE (1.0 mL), 20 h, isolated yield. py = pyridyl, E = CO$_2$Me; all E/Z = 1:11. [b] Additive (10 mol %). [c] Without [Co]. [d] Without AgSbF$_6$. [e] Double bond regioisomer (10%) observed. [f] [Cp*Co(CH$_3$CN)$_3$](SbF$_6$)$_2$ (10 mol %). [g] [1,3-(t-Bu)$_2$C$_5$H$_3$Co(CO)I$_2$] (10 mol %), E/Z = 1:8. [h] [CpCo(CO)I$_2$] (10 mol %), E/Z = 1:8. [i] At 25 °C.

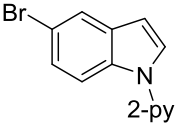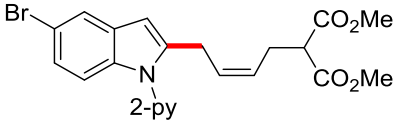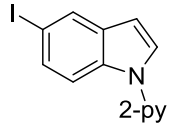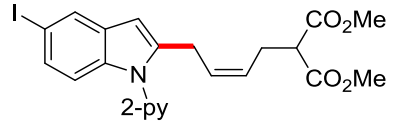### 3.2.2 Scope of the Cobalt(III)-Catalyzed C–H/C–C Functionalization
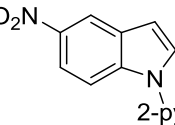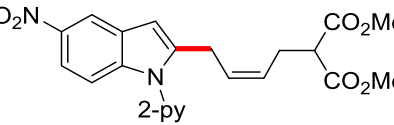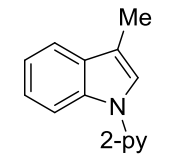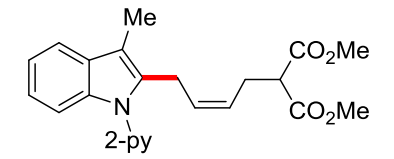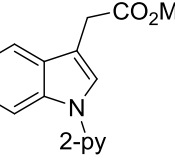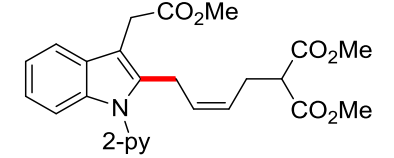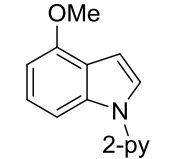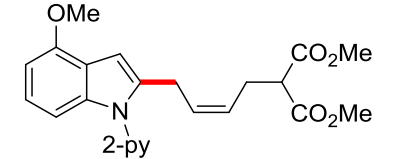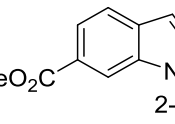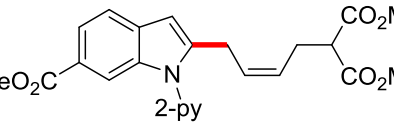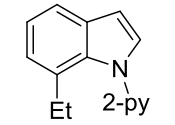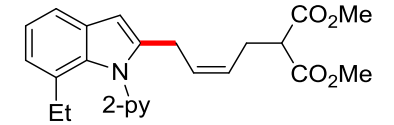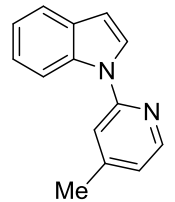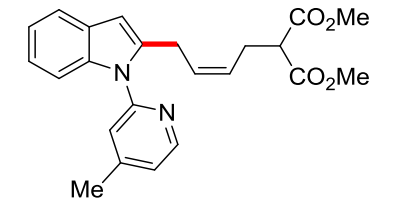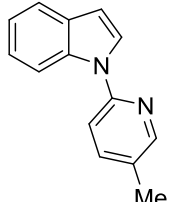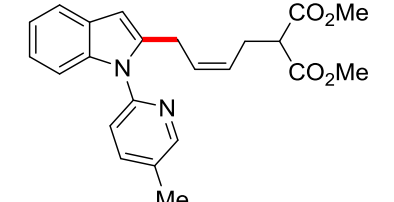
Under the optimized reaction conditions for the cobalt(III)-catalyzed C–H/C–C functionalization, an extensive substrate scope was probed (Table 8). At first, various substituents in C5-position of the indole were tested, such as methoxy, bromo, iodo, and nitro groups (entries 2–5). Notably, all functional groups were fully tolerated, delivering the desired *Z*-configured product in very good yields ranging from 88% to 92% and good diastereoselectivities.

Furthermore, sterically demanding substituents in C3-position were employed, furnishing the desired products **100fa** and **100ga** still in good to excellent yield (entries 6 and 7), with a minor drop in diastereoselectivity for product **100fa**, probably due to steric effects. The substituent in C3-position of **105g** can flexibly rotate and is sterically less demanding than the methyl-substituted analogue. Substituents in C4- and C6-position (entries 8 and 9) were well tolerated, affording the corresponding products **105ha** and **105ia** in excellent yields. For the C7-substituted product **105ja** (entry 10) the diastereoselectivities were somewhat reduced, presumably due to steric interactions, which is in good agreement with the observation for the C3-methyl-substituted product **130fa** (entry 6). The pyridyl-directing group of the products **130** was shown to be removable (*cf.* chapter 5.3.2). However, a chemoselective method, that tolerated the alkene functionality, has not been disclosed so far.

Finally, a sterically more congested substitution pattern on the pyridyl-directing group did not influence the reactivity, with overall very good yields of **130ka** and **130la** (entries 11 and 12). Only the diastereoselectivity profited somewhat from the changed substitution on the pyridyl-ring, affording the product in excellent selectivities of *Z/E* = 14:1. A reasonable explanation for this unexpected finding could be the involvement of stabilizing *London* dispersion interactions,[124, 142] partly exhibited by the pyridyl-ring, which was highlighted by DFT-calculations of *M. Feldt*.[143]

Table 8. Scope of the cobalt(III)-catalyzed C–H/C–C functionalization of indoles **105**.

Entry	2-pyridylindole	105	product	130	Z/E	yield/ %[a]
1		**105a**		**130aa**	11:1	93
2	MeO	**105b**	MeO	**130ba**	13:1	92

Entry	Substrate 105		Product 130		Z:E	Yield
3	5-Br indole, 2-py (**105c**)		**130ca**		9:1	89
4	5-I indole, 2-py (**105d**)		**130da**		14:1	89
5	5-O₂N indole, 2-py (**105e**)		**130ea**		17:1	88
6	3-Me indole, 2-py (**105f**)		**130fa**		5:1	93
7	3-CH₂CO₂Me indole, 2-py (**105g**)		**130ga**		11:1	74
8	4-OMe indole, 2-py (**105h**)		**130ha**		13:1	77
9	6-MeO₂C indole, 2-py (**105i**)		**130ia**		8:1	84
10	7-Et indole, 2-py (**105j**)		**130ja**		8:1	68
11	indole, 4-Me-2-py (**105k**)		**130ka**		14:1	81
12	indole, 5-Me-2-py (**105l**)		**130la**		14:1	92

[a] Reaction conditions: **105** (0.50 mmol), **125a** (0.60 mmol), [Cp*Co(CO)I₂] (10 mol %), AgSbF₆ (20 mol %), NaOPiv (20 mol %), DCE (1.0 mL), 50 °C, 20 h, isolated yield.

Furthermore, the scope was extended to vinylcyclopropane **125b** derived from meldrums acid[144] (Table 9). Herein, a remarkable switch in diastereoselectivity to the *E*-configured products was found. In all cases, the main isomer was the *E*-configured product, but the selectivities were overall poor. By comparison with the analogous rhodium(III)-catalyzed reaction, the same reactivity and similar selectivity were obtained, with an even higher *E*/*Z*-ratio (entry 1).

The reason for this unexpected switch in diastereocontrol is not yet fully elucidated and there is need for detailed computational studies dealing with this kind of substrate-controlled stereoselectivity. In this respect, a detailed understanding of this observation would possibly give rise to the development of a switchable control in diastereoselectivity of C–H/C–C bond activations by the substitution pattern on the vinylcyclopropane **125**.

Table 9. Scope of the cobalt(III)-catalyzed C–H/C–C functionalization with meldrums acid-derived vinylcyclopropane **125b**.

Entry	2-pyridylindole **105**		product	**130b**	*E*/*Z*	yield / % [a]
1		**105a**		**130ab**	3.7:1	83[b]
2		**105m**		**130mb**	2.6:1	81
3		**105n**		**130nb**	2.4:1	75

[a] Reaction conditions: **105** (0.50 mmol), **125b** (0.60 mmol), [Cp*Co(CO)I$_2$] (10 mol %), AgSbF$_6$ (20 mol %), NaOPiv (20 mol %), DCE (1.0 mL), 50 °C, 20 h, isolated yield. [b] With [Cp*Rh(CH$_3$CN)$_3$](SbF$_6$)$_2$ (10 mol %) product **130ab** (83%, *Z*/*E* = 1:5.9) was obtained.

Besides the applicability of this reaction to the functionalization of 2-pyridylindoles **105**, also the inherently less electron-rich heterocycles were tested (Table 10). Thus, also 2-phenylpyridines **1** were

successfully converted with comparable efficiency, but somewhat decreased diastereoselectivities (entries 1 and 2). In contrast, rhodium(III) catalysis furnished the *E*-configured product **132ba'** in lower yield, poor selectivity of *E/Z* = 2:1 and a significant amount of the di-functionalized product **132ba''** was observed (entry 3). These findings emphasize the unique diastereo- and site-selectivities of the cobalt(III)-catalyzed C–H/C–C activation.

In this respect, a reasonable explanation for the mono-selectivity could be the overall shorter cobalt-carbon bond lengths,[117b] which presumably increase steric interactions in catalytic intermediates towards the mono-functionalized product **132ba**. Furthermore, 1-(thiophen-2-yl)-1*H*-pyrazole (**131**) reacted with moderate yield, but excellent diastereoselectivity (entry 4). In this regard, *Q. Bu* could extend the heteroarene-scope to valuable examples of functionalized phenylpyrazoles **18** with excellent levels of site- and diastereoselectivity.[117b]

Table 10. Scope of the cobalt(III)-catalyzed C–H/C–C functionalization with 2-phenylpyridines **1**.

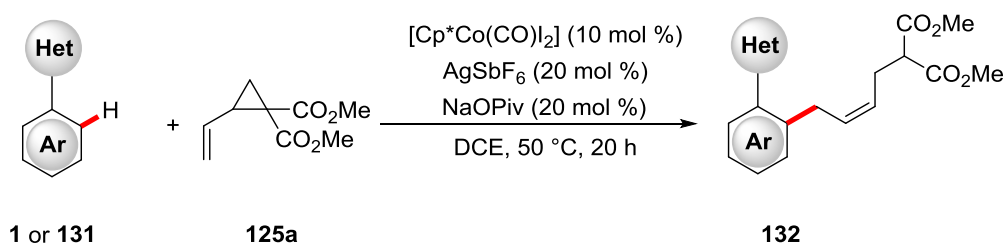| Entry	heteroarene **1**		product **132**		*Z/E*	yield / %[a]
1	**1a**		**132aa**		9:1	86
2	**1b**		**132ba**		4:1	75
3	**1b**		**132ba'**		1:2	45[b]

| 4 | | **131** | | **133** | 12:1 | 40 |
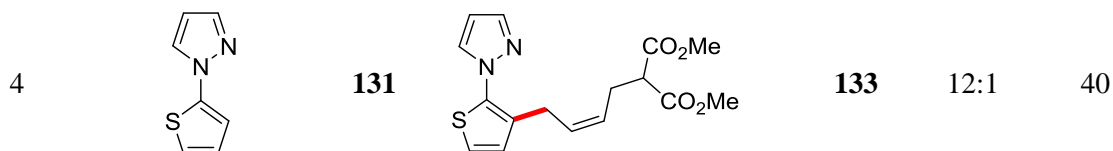
[a] Reaction conditions: **1** or **131** (0.50 mmol), **125a** (0.60 mmol), [Cp*Co(CO)I$_2$] (10 mol %), AgSbF$_6$ (20 mol %), NaOPiv (20 mol %), DCE (1.0 mL), 20 h, isolated yields. [b] With [Cp*Rh(CH$_3$CN)$_3$](SbF$_6$)$_2$ (10 mol %) di-substituted **132ba''** (12%, Z/E = 1:3) was obtained.

Additionally, some limititations in the scope were disclosed (Scheme 54). Benzamides **68**, oximes **48** as well as oxazolines **7** unfortunately delivered no or only traces of the desired products under otherwise identical reaction condition. Moreover, the use of weaker directing groups like tetrazoles **31** and the functionalization *via* a six-membered cobaltacycle with substrate **136a** turned out to be unfavorable. However, it cannot be excluded that extensive optimization studies on a certain substrate might lead to the desired transformation.
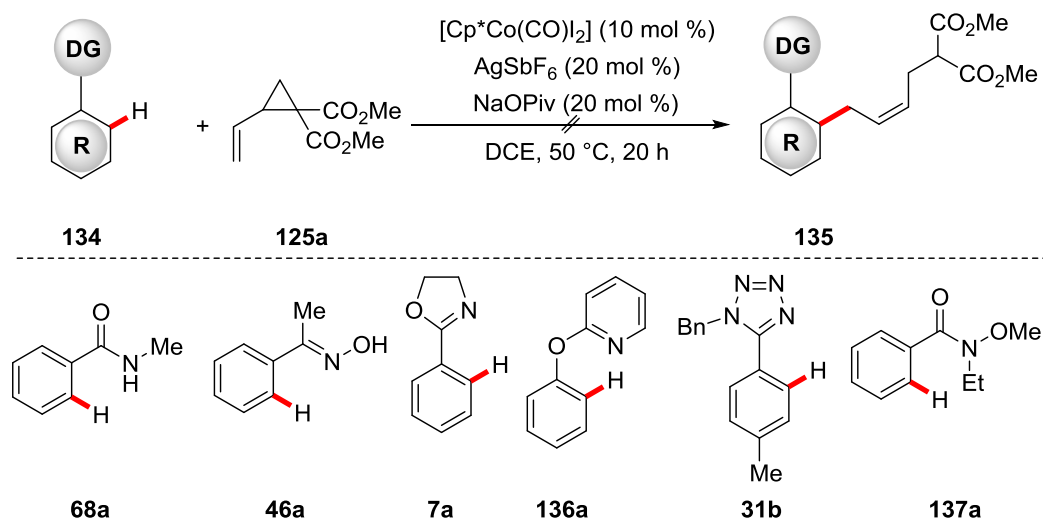
Scheme 54. Limitations of the cobalt(III)-catalyzed C–H/C–C functionalization.

Subsequently, it was explored whether the developed catalytic reaction could proceed under even milder conditions, at an ambient temperature of 25 °C (Table 11). In this manner, a minor decrease in reactivity was observed, with yields being around 10% less than under the optimized reaction conditions, except for the unsubstituted substrate **105a** (entry 1). Overall, the observed diastereoselectivities are comparable with those at 50 °C (*cf.* Table 8).

Table 11. Scope of the cobalt(III)-catalyzed C–H/C–C functionalization at 25 °C.
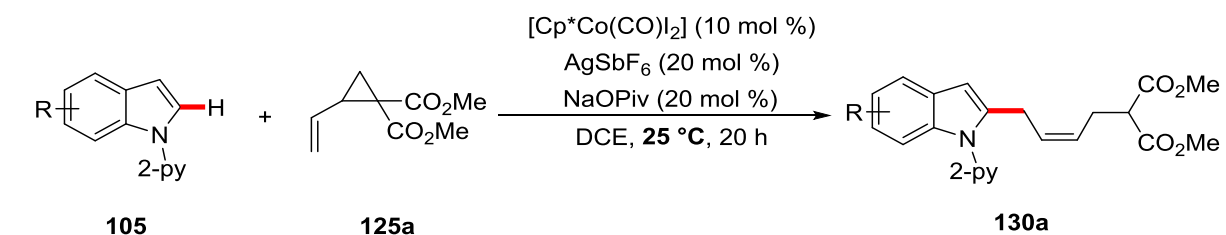
Entry	2-pyridylindole	**105**	product	**130**	*Z/E*	yield / %[a]
1		**105a**		**130aa**	11:1	64
2		**105b**		**103ba**	11:1	82
3		**105d**		**130da**	14:1	78
4		**105f**		**130fa**	9:1	87
5		**105h**		**130ha**	10:1	75

[a] Reaction conditions: **105** (0.50 mmol), **125a** (0.60 mmol), [Cp*Co(CO)I$_2$] (10 mol %), AgSbF$_6$ (20 mol %), NaOPiv (20 mol %), DCE (1.0 mL), 25 °C, 20 h, isolated yield.

3.2.3   Mechanistic Studies

3.2.3.1   H/D-Exchange Experiment

To rationalize the C–H activation mechanism, a catalytic reaction in the presence of deuterated co-solvent CD$_3$OD was carried out under otherwise unchanged reaction conditions. In the reisolated starting material **105a** as well as in the product **130aa** a significant H/D-scrambling was observed (Scheme 55). In the case of the reisolated starting material **105a**, a deuterium incorporation of 41% in C2-position is indicative of a reversible C–H activation step.

Furthermore, in the starting material **105a** and the product **130aa** significant amounts of H/D-exchange in C7- as well as in C3-position of the indole were detected. Deuterium incorporation in C7-position can be explained by the formation of a six-membered cobaltacycle, which has been reported

for indoles and indolines in *inter alia* copper-,[145] rhodium-[146] and iridium-catalyzed[147] C–H functionalizations. Nevertheless, the corresponding C7-substituted product could not be detected, which might be due to the unfavored formation of an expected eight-membered intermediate after migratory insertion of the alkene. The H/D-scrambling in C3-position can be explained by a reversible electrophilic activation and following deutero-demetalation.
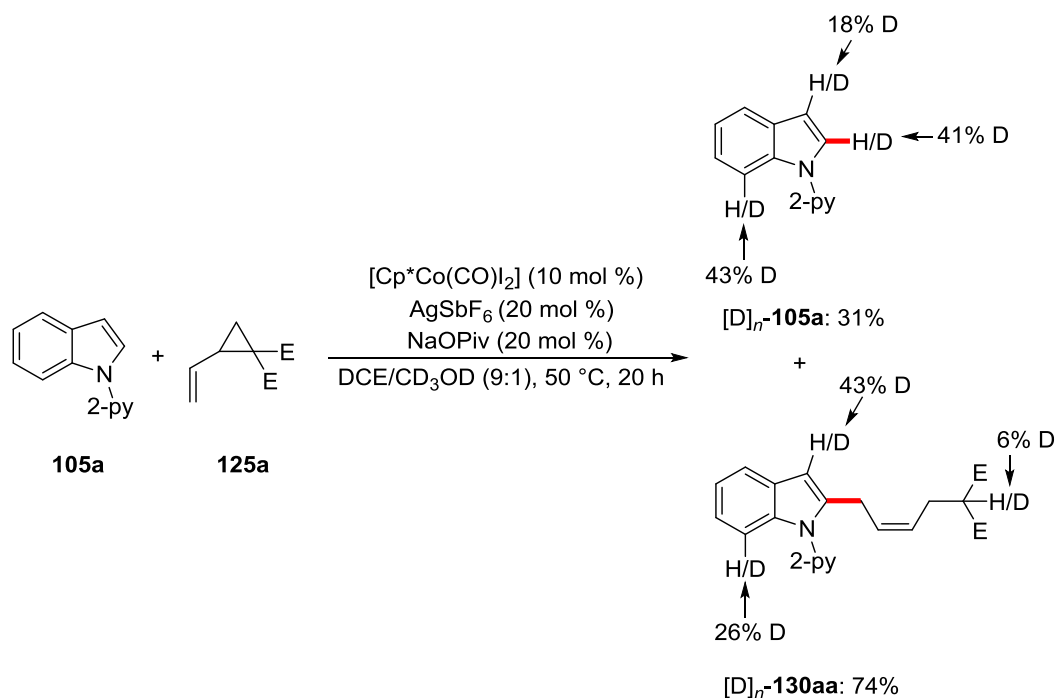
Scheme 55. H/D-exchange study of the cobalt(III)-catalyzed C–H/C–C functionalization. E = CO$_2$Me.

3.2.3.1.1   H/D-exchange in the Absence of Cobalt(III) Catalyst

Based on the observed deuterium incorporation in C3-position of the indole nucleus, a reaction in the presence of deuterated co-solvent CD$_3$OD without the cobalt(III) catalyst and vinylcyclopropane **125a** was performed. Herein, no detectable H/D-scrambling in any position of the recovered indole **105a** (Scheme 56) was observed. These findings emphasize that the C–H activation occurs solely *via* an organometallic cobalt(III) catalysis, and the previously described H/D-scrambling C7-position (*vide supra*) is a result of cobalt(III)-catalyzed C–H activation *via* a six-membered cobaltacycle.
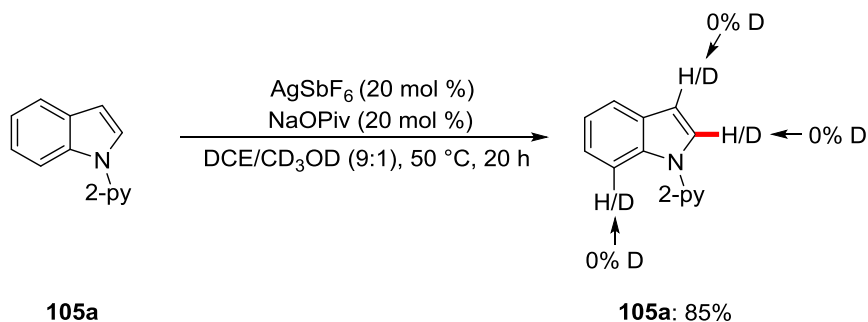
Scheme 56. H/D-exchange study in the absence of the cobalt(III) catalyst.

3.2.3.2   Kinetic Isotope Effect

To gain a deeper mechanistic understanding of the C–H activation elementary step, a KIE-experiment by comparison of independent reaction rates of 2-pyridylindole (**105a**) and [D]$_1$-**105a** was performed (Scheme 57). In this reaction, a KIE of $k_H/k_D = 1.3$ was obtained, which suggests a facile and not turnover-limiting C−H activation to be operative.
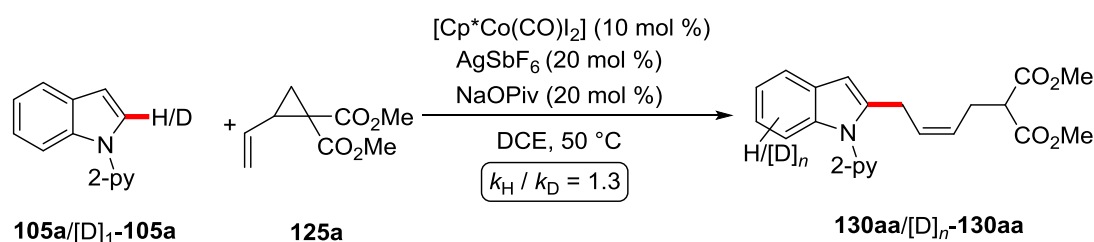
Scheme 57. KIE experiment for the cobalt(III)-catalyzed C–H/C–C functionalization.
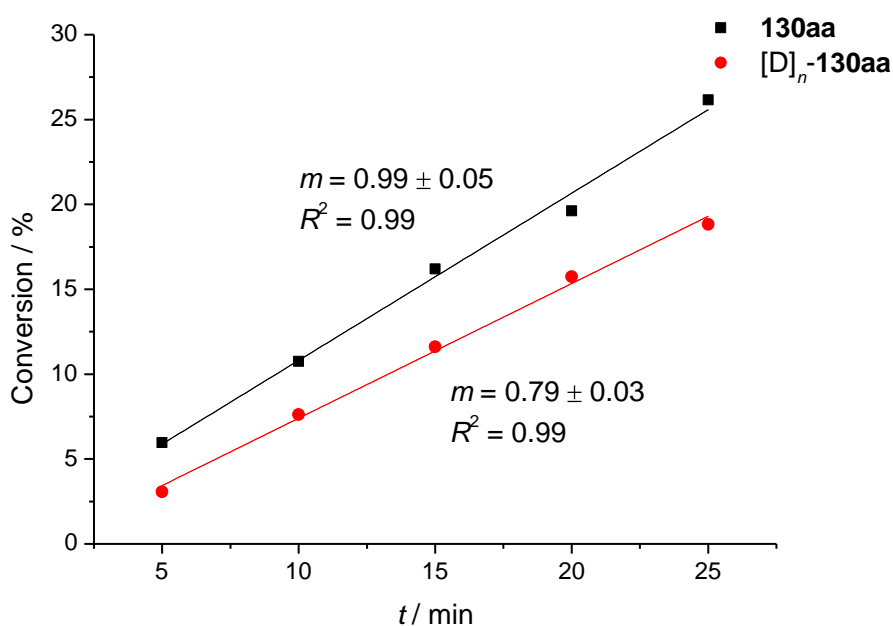
Figure 10. KIE-experiment for the cobalt(III)-catalyzed C–H/C–C functionalization.

3.2.4   Proposed Catalytic Cycle

Based on these mechanistic findings, a catalytic cycle was proposed (Scheme 58). The active catalytic species **138** might be a cationic cobalt(III)-pivalate complex formed by reaction between the cobalt(III) precursor and silver hexafluoroantimonate.[91] In this respect, hexafluoroantimonate is a non-nucleophilic and weakly-coordinating anion[148] and it is proposed to energetically stabilize the catalytically active species as well as the following cationic reaction intermediates. The first step comprises a facile and reversible C–H cobaltation that is assisted by the pivalate additive and presumably proceeds *via* a BIES-type mechanistic pathway to furnish the cobaltacycle **139** (*cf.* Table

7). For the following steps, extensive computational studies by DFT calculations were performed by *M. Feldt*.[117b] Accordingly, a coordination of the vinylcyclopropane **125a** leads to intermediate **140**, in which a migratory insertion of the coordinated vinylcyclopropane **125a** into the carbon-cobalt bond occurs. An oxygen-coordination of the ester group to the cobalt center is suggested to energetically stabilize the following intermediate **141**. Thereafter, a diastereoselectivity-determining C–C cleavage process leads to the favored *Z*-configurated intermediate **142**.

By applying the energetic span model[149] to the energetic profile, the activation barrier difference for this selectivity-determining C–C cleavage process amounts to 6.5 kcal/mol in favor of the *Z*-configurated transition state. The origin of this diastereocontrol presumably lies in attractive *London* dispersion interactions that are more pronounced for the compact *Z*-configurated transition state.[143] Along the same line, the diastereodivergence between cobalt(III) and rhodium(III) catalysis is proposed to be an effect of dispersion interactions due to the smaller carbon-cobalt bonds. The reduced bond lengths in cobalt(III) intermediates of this reaction lead to larger dispersion contributions, which are strongly dependent on the interaction distance r by proportionality to r^{-6}. Finally, a proto-demetalation step by the *in situ* formed pivalic acid regenerates the active catalyst and releases the product **130aa**. Notably, *Q. Bu* did not observe any post catalytic-isomerization of the double bond, when the *E*-configurated product was subjected to the optimal reaction conditions.[117b]
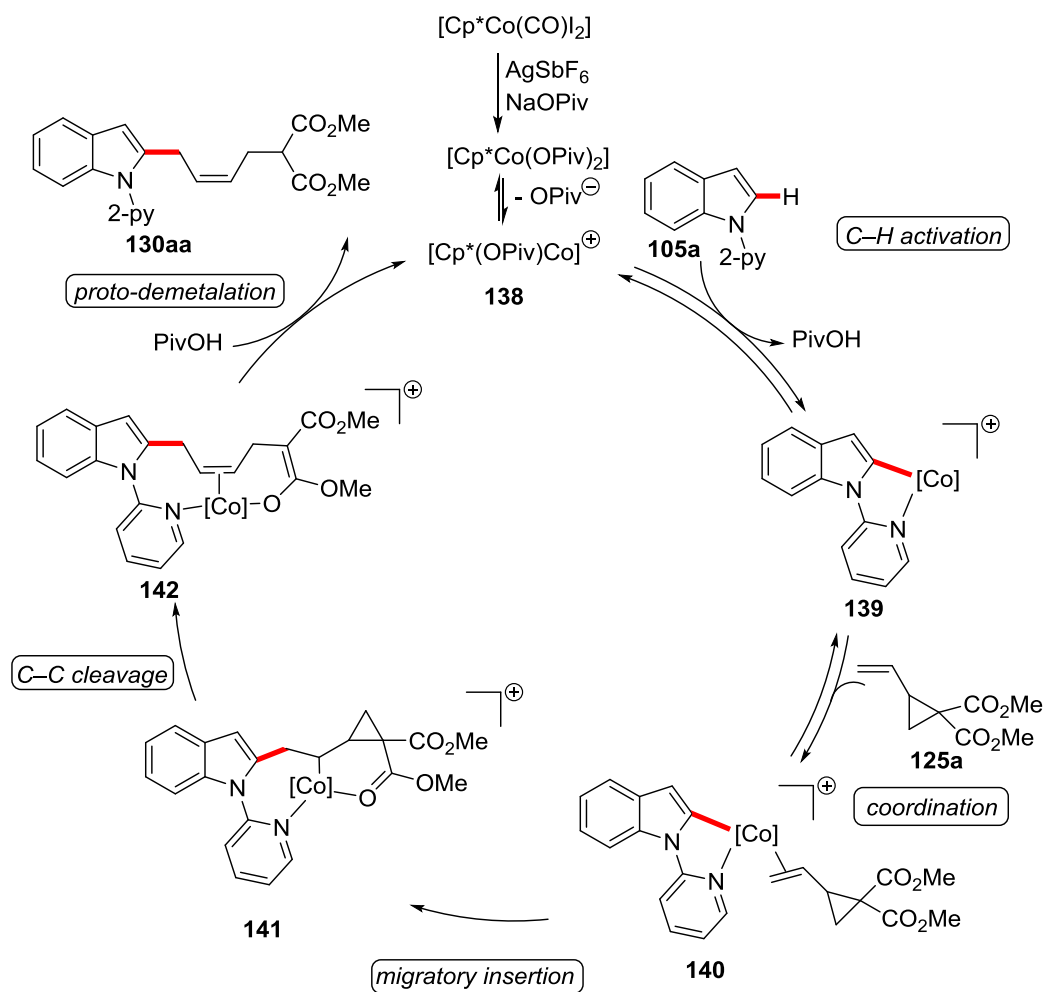
Scheme 58. Proposed catalytic cycle for the cobalt(III)-catalyzed C–H/C–C activation. [Co] = Cp*Co^{III}.

3.3   Regioselective Cobalt(III)-Catalyzed C−H Alkylations

Transition metal-catalyzed C–H alkylations by alkene hydroarylation reactions represent a versatile and powerful strategy to achieve highly atom-economical alkylations.[110c, 150] However, in these reactions there is an inherent requirement for *Markovnikov/anti-Markovnikov* selectivity control, which has so far been mainly restricted to electronically activated alkenes and the use of complex ligands.[113-114, 151] *Yoshikai* and coworkers have indeed demonstrated a switchable regiocontrol in low valent cobalt-catalyzed C–H hydroarylations, but stoichiometric amounts of *Grignard* reagents were required, which translated into a considerable limitation regarding the substrate scope.[114]

Consequently, a new and sustainable concept to achieve regiocontrol in cobalt(III) catalysis is indispensable. The new catalytic system must obviate the use of *Grignard* reagents, laborious ligand design and should ideally be applicable to hydroarylations with unactivated alkenes. In this regard, a full control of linear/branched selectivity is of prime importance.

3.3.1   Optimization Studies for the Linear-Selective C–H Alkylation

The optimization studies for the cobalt(III)-catalyzed *anti-Markovnikov*-selective C–H alkylation were commenced by testing the effect of a few selected acetate and pivalate additives (Table 12, entries 1−5). Among a series of alkali metal cations, especially lithium and sodium performed well, while the cesium analogue delivered the desired linear product **144aa** in only unsatisfactory yield or trace amount (entries 3 and 5). Remarkably, acetate bases displayed a slightly higher selectivity up to an excellent ratio of AM:M = 99:1. Thereafter, the effect of different reaction temperatures on the regioselectivity was studied by using pivalic acid as the additive. Interestingly, the selectivity dropped with decreasing temperature in favor of the *Markovnikov*-product **145aa** (entries 6–8). Moreover, the use of sterically much more congested 1-adamantanecarboxylic acid as additive (entries 9–11) led to a further drop in linear selectivity. Notably, by increasing the acid loading up to one equivalent, an intriguing inversion of selectivity (entry 11) towards the branched product **145aa** was observed.

In summary, lower temperatures and carboxylic acids as additives tend to favor the formation of the branched product, although the temperature-dependence is much less pronounced.

To achieve an excellent linear selectivity of AM:M > 99:1, the temperature was kept at 120 °C and no additive was utilized (entry 14). Noteworthily, no reactivity was observed by omitting the essential AgSbF$_6$ or the catalyst (entries 12 and 13). Silver was found to play no role in the catalytic reaction, because silver-free conditions with [Cp*Co(CH$_3$CN)$_3$](SbF$_6$)$_2$ as the catalyst still furnished the desired product **144aa** in satisfactory yield (entry 15). Additionally, cobalt(III) complexes with differently substituted Cp-ligands performed overall poorly as catalysts (entries 17 and 18).

Table 12. Optimization studies for the *anti-Markovnikov*-selective C–H alkylation.
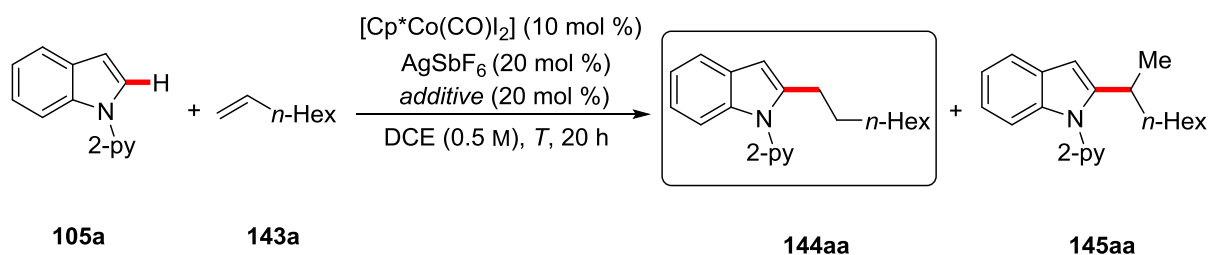
Entry	additive	T / °C	**144aa**:**145aa**[a]	yield / %[a]
1	LiOAc	120	99:1	82
2	NaOAc	120	98:2	77
3	CsOAc	120	98:2	15
4	NaOPiv	120	88:12	46
5	CsOPiv	120	---	traces
6	PivOH	120	93:7	80
7	PivOH	100	85:15	67
8	PivOH	60	52:48	56
9	1-AdCO$_2$H	120	88:12	82
10	1-AdCO$_2$H (40 mol %)	120	46:54	74
11	1-AdCO$_2$H (100 mol %)	120	37:63	81
12	---	120	---	---[b]
13	---	120	---	---[c]
14	---	**120**	**>99:1**	**82**
15	---	100	>99:1	75
16	---	120	>99:1	76[d]
17	---	120	95:5	7[e]
18	---	120	>99:1	traces[f]

[a] Reaction conditions: **105a** (0.50 mmol), **143a** (1.50 mmol), [Cp*Co(CO)I$_2$] (10 mol %), AgSbF$_6$ (20 mol %), additive (20 mol %), DCE (1.0 mL), 120 °C, 20 h, isolated yield; selectivities determined by means of ^{1}H-NMR spectroscopy. [b] No AgSbF$_6$. [c] No [Cp*Co(CO)I$_2$]. [d] [Cp*Co(CH$_3$CN)$_3$](SbF$_6$)$_2$. [e] [1,3-(t-Bu)$_2$C$_5$H$_3$Co(CO)I$_2$]. [f] [CpCo(CO)I$_2$].

3.3.2 Optimization Studies for the Branched-Selective C–H Alkylation

With the results from the previous optimization study in hand (*vide supra*), it was initially tested whether the formation of the *Markovnikov*-selective product **145aa** is mainly controlled by reaction temperature. However, still the linear product **144aa** (Table 13, entry 1) was formed in the absence of additives although the reaction temperature was decreased to as low as 50 °C. Furthermore, the steric effect of the additives was investigated by comparing a set of carboxylates (entries 2–6). Therein, it could be pointed out that the sterically encumbered 1-adamantylcarboxylate delivered the branched product **145aa** in moderate yield, but very good regioselectivity (entries 3 and 6). Moreover, a series

of carboxylic acids (entries 7–12) was studied, similarly leading to very good selectivities and moderate yields. The use of bulky pivalic and 1-adamantanecarboxylic acid (entries 8 and 12) furnished the *Markovnikov*-selective product **145aa** in good yields. Notably, an increase of the 1-adamantanecarboxylic acids concentration furthermore improved the selectivity up to an excellent ratio of M:AM = 95:5 (entries 14–16). Interestingly, carboxylic acids delivered the branched product **145aa** with comparable selectivities, whereas a clear trend in steric effects along a series of carboxylates was observed (*vide supra*). These observations might indicate that the branched-selective mechanistic pathway is generally preferred by using acid additives. As it had previously been observed (*vide supra*), no product was formed in the absence of AgSbF$_6$ or the catalyst (entries 17 and 18). Noteworthily, under silver-free conditions and [Cp*Co(CH$_3$CN)$_3$](SbF$_6$)$_2$ as the catalyst (entry 19), the product **145aa** was still afforded in good yields, but the selectivity decreased slightly to M:AM = 75:25. In this regard, it can be assumed that the acetonitrile ligands of [Cp*Co(CH$_3$CN)$_3$](SbF$_6$)$_2$ reduce the selectivity by hampering the reaction between the catalyst or a catalytic intermediate and the acid additive. As observed before (Table 12), cobalt(III) complexes with differently substituted Cp-ligands performed poorly (entries 20 and 21).

Table 13. Optimization studies for the *Markovnikov*-selective C–H alkylation.
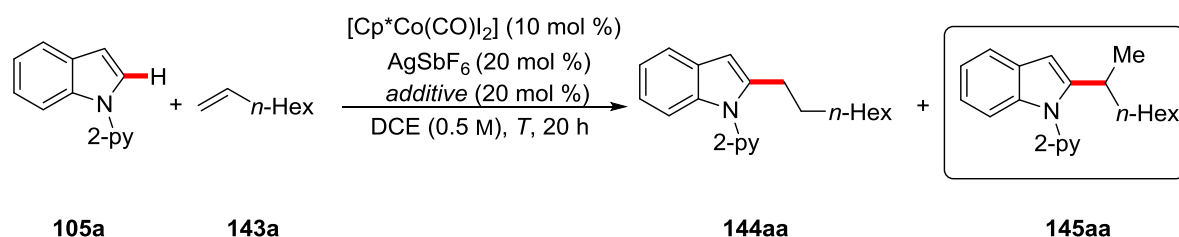
Entry	additive	T / °C	**144aa**:**145aa**[a]	yield / %[a]
1	---	50	>99:1	9
2	LiOAc	50	27:73	6
3	LiO$_2$C-(1-Ad)	50	8:92	48
4	NaOAc	50	35:65	11
5	NaOPiv	50	22:78	44
6	NaO$_2$C-(1-Ad)	50	12:88	50
7	AcOH	50	14:86	43
8	PivOH	50	17:83	68
9	CyCO$_2$H	50	14:86	58
10	C$_6$H$_5$CO$_2$H	50	14:86	57
11	CF$_3$CO$_2$H	50	---	---
12	1-AdCO$_2$H	50	13:87	68
13	1-AdCO$_2$H	60	20:80	71
14	1-AdCO$_2$H (40 mol %)	50	10:90	79

15	**1-AdCO$_2$H (100 mol %)**	**50**	**5:95**	**80**
16	1-AdCO$_2$H (100 mol %)	40	>1:99	48
17[b]	---	50	---	---
18[c]	1-AdCO$_2$H	50	---	---
19[d]	1-AdCO$_2$H	50	25:75	65
20[e]	1-AdCO$_2$H	50	---	traces
21[f]	1-AdCO$_2$H	50	---	traces

[a] Reaction conditions: **105a** (0.50 mmol), **143a** (1.50 mmol), [Cp*Co(CO)I$_2$] (10 mol %), AgSbF$_6$ (20 mol %), additive (20 mol %), DCE (0.5 mL, 1.0 M), 50 °C, 20 h, isolated yield; selectivities determined by ^{1}H-NMR spectroscopy. [b] No AgSbF$_6$. [c] No [Cp*Co(CO)I$_2$]. [d] [Cp*Co(CH$_3$CN)$_3$](SbF$_6$)$_2$. [e] [1,3-(t-Bu)$_2$C$_5$H$_3$Co(CO)I$_2$]. [f] [CpCo(CO)I$_2$].

3.3.3 Scope of the Linear-Selective C–H Alkylation

Under the optimized conditions for the linear-selective C–H alkylation, the effect of various 2-pyridylindoles **105** was probed (Table 14). Among a series of substituents in C5-position of the indole nucleus, halogens were well tolerated and delivered the corresponding products in good yields (entries 3–5). Even in the presence of a very challenging and redox-active nitro-substituent, a moderate yield of **144ea** was achieved (entry 6), although substrate **105e** displayed a low solubility in DCE. It is noteworthy that methyl- and ester-substituents in C3-position performed with similar reactivities (entries 7 and 8). Substitution in the C4-position (entries 9 and 10) furnished the desired products **144ha** and **144oa** in good yields. Nonetheless, a slight drop in yield was observed for indole **105j** bearing an ethyl-substituent in the C7-position, which is possibly due to steric effects (entry 11). Remarkably, the pyridyl-directing group was shown to be removable and the corresponding free indoles were obtained in excellent yields (*cf.* chapter 5.4.2).

With respect to limitations of the substrate scope, 1-(thiophen-2-yl)-1*H*-pyrazole (**131**) was not converted under otherwise unchanged reaction conditions (entry 12). In this regard, *V. Müller* showed that substrate **131** only reacted by addition of pivalic acid at 140 °C, delivering the corresponding product in good yield and selectivity of AM:M = 55:45.[152]

In addition, 2-pyridyl-1*H*-pyrrole (**146**) delivered the desired product **147** with an excellent selectivity of AM:M > 99:1, but only unsatisfactory yields were obtained and significant amounts of di-functionalized product **147'** were formed (entry 13). In summary, all products were afforded with an excellent linear selectivity of AM:M > 99:1.

Table 14. Scope of different 2-pyridylindoles **105** under linear-selective reaction conditions.
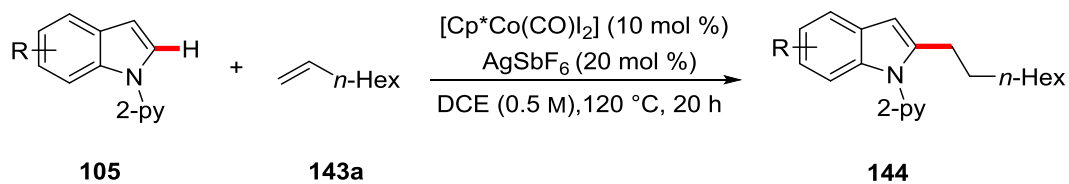
Entry	2-pyridylindole	105	product	144	yield / %[a]
1		**105a**		**144aa**	82
2		**105b**		**144ba**	74
3		**105m**		**144ma**	76
4		**105c**		**144ca**	79
5		**105d**		**144da**	77
6		**105e**		**144ea**	42
7		**105f**		**144fa**	65
8		**105n**		**144na**	77
9		**105h**		**144ha**	79

Entry	alkene	143	product	144	yield / %[a]
10	[CO₂Me indole, 2-py]	**105o**	[CO₂Me indole, 2-py, n-Hex]	**144oa**	83
11	[Et indole, 2-py]	**105j**	[Et indole, 2-py, n-Hex]	**144ja**	61
12	[thiophene-pyrazole]	**131**	---		---
13	[pyrrole, 2-py]	**146**	[pyrrole, 2-py, n-Hex]	**147**	31[b]

[a] Reaction conditions: **105** (0.50 mmol), **143a** (1.50 mmol), [Cp*Co(CO)I₂] (10 mol %), AgSbF₆ (20 mol %), DCE (1.0 mL, 0.5 M), 120 °C, 20 h, isolated yield; all AM:M > 99:1, determined by ¹H-NMR spectroscopy. [b] 45% of di-substituted product **147'** (AM:M > 99:1) was isolated.

Furthermore, alkenes **143** with selected functional groups were examined under the linear-selective reaction regime (Table 15). Initially, allyl benzene (**143b**) reacted with excellent regioselectivities and no by-products from isomerization of the double bond were observed. Likewise, alkenes with different chain lengths performed well (entries 2–4), with somewhat higher yields for longer alkyl chains, which might be attributed to lower boiling points. The boiling point of 1-hexene (**143e**) at ambient pressure is 63 °C,[153] presumably leading to evaporation under elevated reaction temperatures. Notably, ester- (**143f**) and challenging hydroxyl-groups (**143g**) on the alkene were well tolerated (entries 5 and 6). The good performance of 1,7-octadiene (**143h**) demonstrated that double bonds did not isomerize during the reaction. In addition, only selective monofunctionalization occurred (entry 7), albeit the overall yield was somewhat diminished. In this regard, the polymerization of 1,7-octadiene (**143h**) as a potential side reaction should be considered. Furthermore, internal alkenes, such as cis/trans-2-octene (**143i**), did not react under otherwise unchanged reaction conditions (entry 8).

Table 15. Scope of different alkenes **143** under the linear-selective reaction regime.

Entry	alkene	143	product	144	yield / %[a]
1	[allyl-Ph]	**143b**	[indole, 2-py, Ph]	**144ab**	85

2	⌇⌇n-C$_{13}$H$_{27}$	**143c**	(indol-2-yl with 2-py, CH$_2$CH$_2$-n-C$_{13}$H$_{27}$)	**144ac**	79
3	⌇⌇n-Oct	**143d**	(indol-2-yl with 2-py, CH$_2$CH$_2$-n-Oct)	**144ad**	75
4	⌇⌇n-Bu	**143e**	(indol-2-yl with 2-py, CH$_2$CH$_2$-n-Bu)	**144ae**	65
5	(allyl)$_4$-O-C(O)-Me	**143f**	(indol-2-yl with 2-py, (CH$_2$)$_5$-O-C(O)Me)	**144af**	76
6	(allyl)$_8$-OH	**143g**	(indol-2-yl with 2-py, (CH$_2$)$_9$-OH)	**144ag**	67
7	(diene)$_4$	**143h**	(indol-2-yl with 2-py, (CH$_2$)$_5$-allyl)	**144ah**	66
8	Me⌇⌇n-Pent	**143i**	---		---

[a] Reaction conditions: **105a** (0.50 mmol), **143** (1.50 mmol), [Cp*Co(CO)I$_2$] (10 mol %), AgSbF$_6$ (20 mol %), DCE (1.0 mL, 0.5 M), 120 °C, 20 h, isolated yield; all AM:M > 99:1, determined by ^{1}H-NMR spectroscopy.

3.3.4 Scope of the Branched-Selective C–H Alkylation

The substrate scope under the *Markovnikov*-selective reaction regime was initially explored by probing various substituents in C5-position, such as methoxy and halogens (Table 16, entries 2–5). Fortunately, all reactions performed with good yields and selectivities in the range of M:AM = 95:5.

However, a methyl-substituent in C3-position of the indole nucleus obviously disfavored the formation of the branched product **145fa** likely due to repulsive steric effects. Thus, the undesired *anti-Markovnikov* product **144fa** was afforded (entry 7). In contrast, substituents in C4- or C7-position again resulted in overall satisfactory yields and very good selectivities (entries 8 and 9). Remarkably, 1-(thiophen-2-yl)-1*H*-pyrazole (**131**) was successfully C–H alkylated in acceptable selectivity and very good yield at 80 °C (entry 10). Unfortunately, 2-pyridyl-1*H*-pyrrole (**146**) delivered mainly the linear-selective product **149** in lower yield (entry 11).

In summary, only substitution in C3-position affected the branched/linear-selectivity, while different functional groups had no observable impact on the selectivity. The overall reactivity was obviously not controlled by electronic parameters of the indole substrate. Interestingly, the pyridyl-directing group was shown to be removable in an excellent yield (*cf.* chapter 5.4.2).

Table 16. Scope of different 2-pyridylindoles **105** and heteroarenes **145** for the branched-selective regime.

entry	2-pyridylindole	105	product	145	M:AM[a]	yield / %[a]
1		105a		145aa	95:5	80
2		105b		145ba	94:6	69
3		105m		145ma	96:4	85
4		105c		145ca	95:5	80
5		105d		145da	94:6	82
7		105f		144fa	21:79	61
8		105h		145ha	95:5	76
9		105j		145ja	96:4	71
10		131		148	81:19	83[b]

| 11 | (pyrrole, 2-py) | **146** | (product, 2-py, n-Hex) | **149** | 40:60 | 16 |
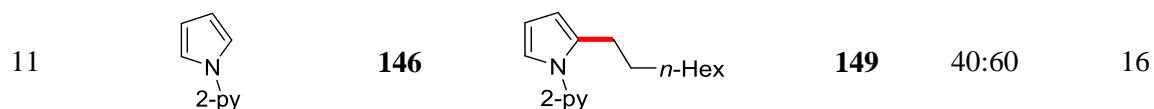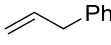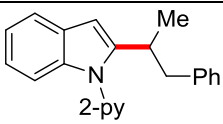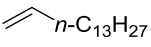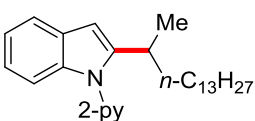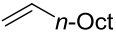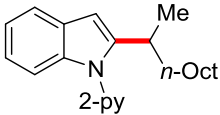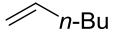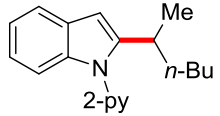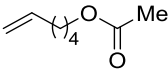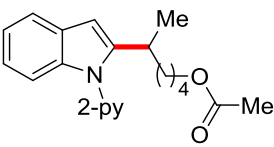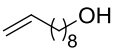
[a] Reaction conditions: **105** (0.50 mmol), **143a** (1.50 mmol), [Cp*Co(CO)I$_2$] (10 mol %), AgSbF$_6$ (20 mol %) and 1-AdCO$_2$H (0.50 mmol), DCE (0.5 mL, 1.0 M), 50 °C, 20 h, isolated yield; all AM:M ratios determined by ^{1}H-NMR spectroscopy. [b] At 80 °C.

Subsequently, a comprehensive study as to the scope of the alkene **143** was analogously performed under the branched-selective reaction conditions (Table 17). Herein, allylbenzene (**143b**) delivered the corresponding product **145ab** with an outstanding selectivity of M:AM = 99:1 and a good yield of 82% (entry 1). Thereafter, a variation of the alkyl chain showed no effect on the selectivity, and only a moderate decrease in yield with shorter chain lenght was found (entries 2–4). Remarkably, an ester-group on the alkene **143f** was well tolerated and the corresponding product **143af** was afforded with an excellent selectivity of M:AM = 99:1 (entry 5). A challenging hydroxyl-group performed moderately (entry 6) with slightly lower yield of the corresponding product **145ag**. As observed before, a selective mono-functionalization of 1,7-octadiene **143h** was observed with a higher yield of 78% of the corresponding branched product **145ah** than under linear-selective conditions (*cf.* Table 15, entry 7). This finding could be either explained by a reduced evaporation of 1,7-octadiene (**143h**) or the diminished polymerization tendency at the lower reaction temperatures. Furthermore, it was shown that internal alkenes, such as *cis/trans*-2-octene **143i**, were not converted under otherwise unchanged reaction conditions (entry 8).

Table 17. Scope of different alkenes **143** for the branched-selective regime.
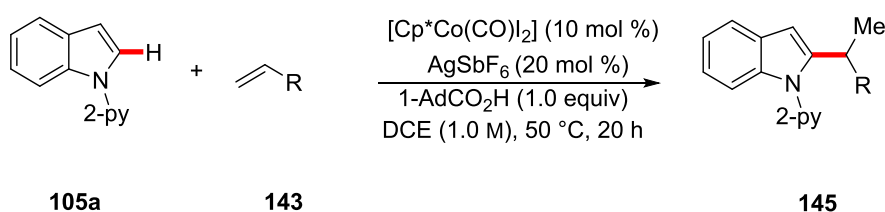
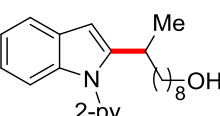| entry	alkene	**143**	product	**145**	M:AM	yield / %[a]
1	⤳Ph	**143b**	(indole, 2-py, Me, Ph)	**145ab**	99:1	82
2	⤳n-C$_{13}$H$_{27}$	**143c**	(indole, 2-py, Me, n-C$_{13}$H$_{27}$)	**145ac**	95:5	76

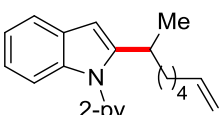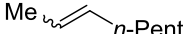| #	Alkene		Product		AM:M	Yield
3	n-Oct	**143d**	2-py, Me, n-Oct indolyl product	**145ad**	94:6	71
4	n-Bu	**143e**	2-py, Me, n-Bu indolyl product	**145ae**	96:4	68
5	($\cdot$)$_4$ O Me O	**143f**	2-py, Me, ($\cdot$)$_4$O–Me O indolyl product	**145af**	99:1	73
6	($\cdot$)$_8$ OH	**143g**	2-py, Me, ($\cdot$)$_8$OH indolyl product	**145ag**	92:8	62
7	($\cdot$)$_4$	**143h**	2-py, Me, ($\cdot$)$_4$ indolyl product	**145ah**	94:6	78
8	Me n-Pent	**143i**	---		---	---

[a] Reaction conditions: **105a** (0.50 mmol), **143** (1.50 mmol), [Cp*Co(CO)I$_2$] (10 mol %), AgSbF$_6$ (20 mol %), 1-AdCO$_2$H (0.50 mmol), DCE (0.5 mL, 1.0 M), 50 °C, 20 h, isolated yield; all AM:M ratios determined by means of ^{1}H-NMR spectroscopy.

3.3.5   Enantioselective Cobalt(III)-Catalyzed C–H Hydroarylations

Given the inherent possibility to induce enantioselectivity within the presented branched-selective cobalt(III)-catalyzed C–H hydroarylation, extensive optimization studies were performed by employing chiral carboxylic acids (Table 18). In this respect, the use of natural amino acids as chiral additives is particularly attractive because of their synthetic versatility[154] and natural availability. Thus far, a considerable number of C–H functionalizations involving metals like *inter alia* ruthenium[131, 155] and palladium[156] have been reported, in which mono-protected amino acids have been utilized as beneficial additives. However, their role in these transformations has been mainly limited to the *in situ* formation of the corresponding bases for a CMD-type C–H activation pathway.

In stark contrast, the utilization of their chirality to enable asymmetric C–H functionalizations is restricted to only a few examples.[157] So far, considerable efforts have been made by *inter alia* Cramer,[158] You[159] and Lam[160] to synthesize costly, but efficient chiral Cp-ligands for asymmetric C–H functionalizations.

In the herein described branched-selective C–H hydroarylation reaction, the acid additive is presumably not only involved in the BIES-type C–H activation, but also serves as a proton source for the product releasing proto-demetalation (*vide infra*: Scheme 70). If the step before the turnover-limiting proto-demetalation, namely the migratory insertion of the alkene **143**, is a reversible step, then potentially enantioselectivity might be induced by the amino acid (*cf.* Scheme 70).

To start with, the *N*-pthalimide protected L-isoleucine was tested (Table 18) at different concentrations and reaction temperatures, and indeed an intriguing *ee* of 23% (entries 1–3) was observed in product **145aa**. Subsequently, different *N*-pthalimide-protected amino acids were probed, with an optimal *ee* of 25% for mono-protected L-leucine (entries 4–7).[161] In summary, no clear trend in steric effects of the amino acid backbone was observed. It is noteworthy that different *N*-pivaloyl and -1-adamantoyl protected amino acids delivered the product as racemic mixture (entries 8–11). Additionally, *N*-acetyl, -ester and -*t*-butyloxycarbonyl (Boc) protecting groups furnished the products in only unsatisfactory enantioselectivities and partly very low branched/linear selectivities (entries 12–16). Moreover, two selected dipeptides were tested, with overall low enantioselectivities and conversions (entries 17 and 18). Interestingly, the stronger Brønsted acid (*R*)-BINOL-phosphoric acid failed to provide the desired product.

In summary, phthalimide was found to be the optimal protecting group. However, the exact reason for that observation has remained unclear. Notably, extensive optimization studies by *V. Müller* and *F. Pesciaioli* concerning different protecting groups, including a structural diversification of the phthalimide-protecting group as well as different amino acids, led thus far to a slight increase in enantioselectivity of up to 36% *ee*.[162]

Table 18. Optimization studies for the enantioselective cobalt(III)-catalyzed C–H alkylation.

Entry	additive	**145aa:144aa**	yield / %[a] (GC-conversion)	*ee* / %[a]
1	Phth-Ile-OH	92:8	33 (67)	23
2	Phth-Ile-OH	93:7	37 (69)[b]	23
3	Phth-Ile-OH	98:2	(45)[c]	23
4	**Phth-Leu-OH**	**90:10**	**25 (41)**	**25**
5	Phth-Ala-OH	89:11	18 (35)	19
6	Phth-Trp-OH	93:7	27 (48)	21
7	Phth-Phe-OH	93:7	(67)	21
8	1-Ad-Val-OH	---	(5)	---
9	1-Ad-*t*-Leu-OH	85:15	25[b]	1
10	Piv-Ile-OH	80:20	(37)	---
11	Piv-Asp-OH	45:55	18[b]	---
12	Ac-Ile-OH	80:20	(33)[b]	18

13	CO$_2$Me-Ile-OH	96:4	(81)	7
14	Boc-Ile-OH	95:5	(35)	10
15	Boc-Tyr-OH	---	---[b]	---
16	Boc$_2$-Val-OH	90:10	31[b]	12
17	Boc-Val-Gly-OH	80:20	(25)[b]	3
18	Boc-Trp-Gly-OH	99:1	(4)[b]	2
19	(R)-BINOL-phosphoric acid	---	---	---

[a] Reaction conditions: **105a** (0.50 mmol), **143a** (1.50 mmol), [Cp*Co(CO)I$_2$] (10 mol %), AgSbF$_6$ (20 mol %), additive (20 mol %), DCE (0.5 mL, 1.0 M), 50 °C, 20 h, isolated yield. For all entries, L-amino acids were used. Branched/linear selectivities and conversions were determined by GC-analysis with *n*-dodecane as the internal standard. Enantioselectivities were determined by means of analytical HPLC. [b] Additive (1.00 equiv), DCE (1.0 M). [c] At 40 °C.

3.3.6   Mechanistic Studies

3.3.6.1   H/D-Exchange Experiments

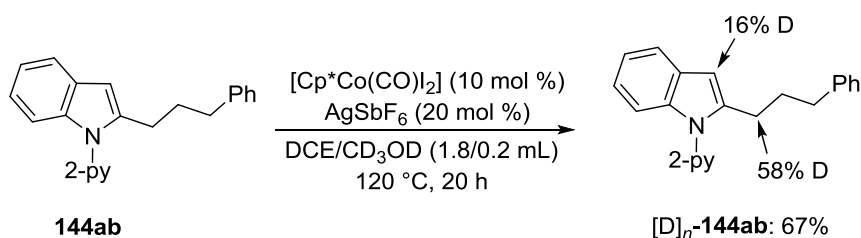##### 3.3.6.1.1   H/D-Exchange for the linear-selective reaction
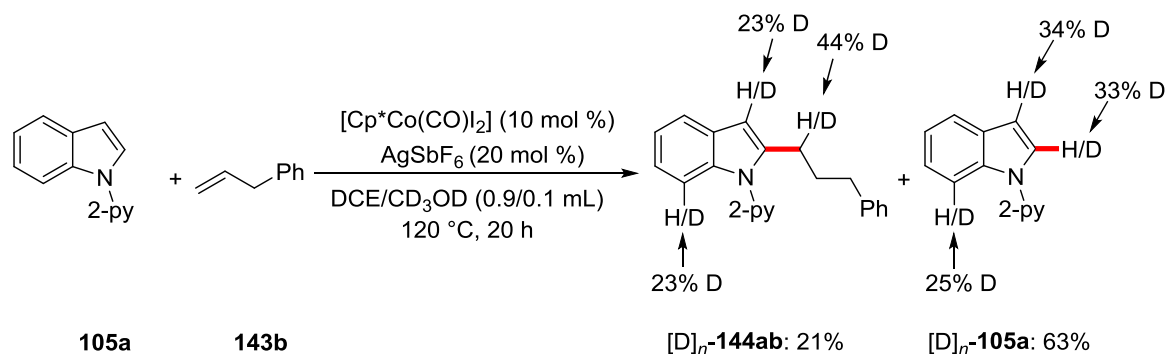
Scheme 59. H/D-exchange under the linear-selective reaction conditions.

To study the mechanism of the C–H activation elementary step, an H/D-exchange experiment under the linear-selective reaction regime with CD$_3$OD as the co-solvent was conducted. As a result, a significant deuterium incorporation was observed in C3- and C7-positions of the product **144ab** and the starting material **105a** (Scheme 59), as it had previously been shown for the cobalt(III)-catalyzed C–H/C–C activation (*cf.* chapter 3.2.3.1). Importantly, a significant H/D-exchange in C2-position of the reisolated starting material **105a** suggested a facile and reversible cobalt(III)-catalyzed C–H activation event to be operative.

Notably, a considerable amount of deuterium incorporation could be exclusively detected in α-position of the alkyl chain in product **144ab**. Based on this result, a H/D-exchange reaction with product **144ab** under otherwise unchanged reaction conditions resulted again in a significant H/D-scrambling in α-

position of the alkyl chain (Scheme 60), rendering a post-catalytic H/D-exchange likely. A reasonable mechanistic pathway for this H/D-exchange could be a cobalt(III)-catalyzed C(sp^3)–H activation.[163]

Scheme 60. H/D-exchange with product **144ab** under the linear-selective reaction conditions.

3.3.6.1.2   H/D-Exchange for the branched-selective reaction

Under the *Markovnikov*-selective reaction conditions a significant H/D scrambling was detected in C3- as well in C7-position (Scheme 61). Additionally, the reisolated starting material **105a** displayed a moderate H/D-exchange in C2-position, however, in slightly less amount than under the linear-selective conditions (*cf.* Scheme 59). Overall, the C–H activation under the branched-selective reaction regime seems to be reversible, but proceeds less readily than under linear-selective conditions. Furthermore, a minor deuterium incorporation in the methyl group of the alkyl chain was observed, which might be in agreement with the proposed mechanism to involve a proto-demetalation step (*vide infra*).
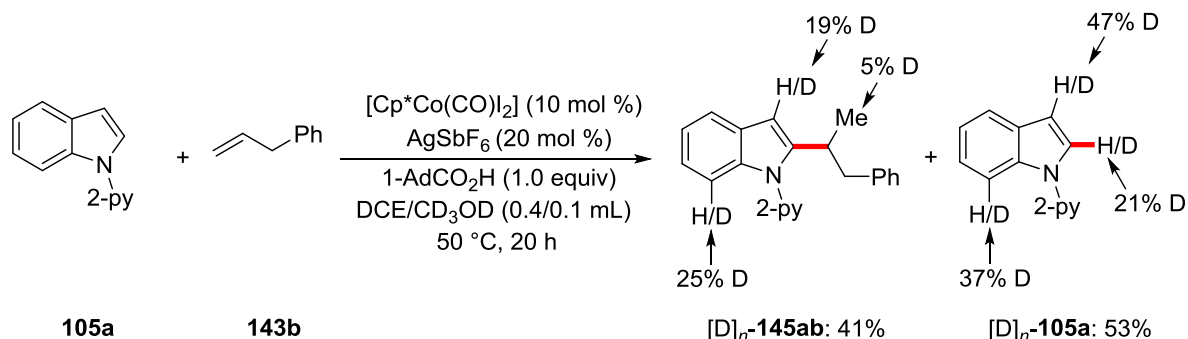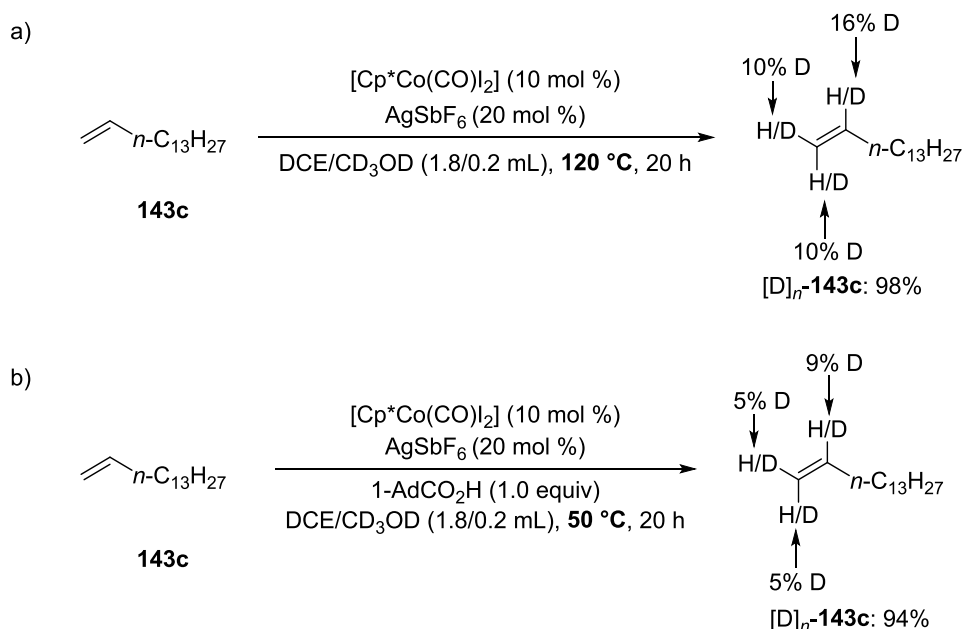

Scheme 61. H/D-exchange under the branched-selective reaction conditions.

3.3.6.1.3   H/D-exchange with alkenes 143

The previously shown experiments revealed that H/D-exchange can occur after the catalytic reaction (*cf.* Scheme 60) in product **144ab**. In addition to this observation, also H/D-exchange with solely the alkene **143c** was studied under the otherwise unchanged reaction conditions.

First, 1-pentadecene (**143c**) could be reisolated in almost quantitative yield under linear-selective conditions, which showed that no detectable side reactions like dimerization or isomerization of the double bond occurred (Scheme 62a). However, significant H/D-scramblings in both alkene positions were detected. Even under the milder branched-selective reaction conditions, H/D-scrambling was observed (Scheme 62b). Based on these observations, H/D-exchange studies of the cobalt(III)-

catalyzed C–H alkylation should be cautiously interpreted with respect to the prediction of possible mechanistic pathways. However, these preliminary results bear potential for the development of isomerization-free and mild isotope labeling reactions with terminal alkenes.[164]

a)

b)

Scheme 62. H/D-exchange with alkene **143c** under a) linear- and b) branched-selective conditions.

3.3.6.1.4   H/D-exchange with [D]₁-105a during the reaction progress

Under otherwise unchanged linear-selective reaction conditions, but in the absence of any external deuterium-/proton-source, a H/D-exchange experiment was performed with isotopically labeled [D]₁-**105a** (Scheme 63). Besides the previously observed H/D-scrambling in C2, C3- and C7-positions of the reisolated starting material **105a** as well as the product **144aa** (*cf.* Scheme 59) a significant deuteration in α-position of the alkyl sidechain was detected.
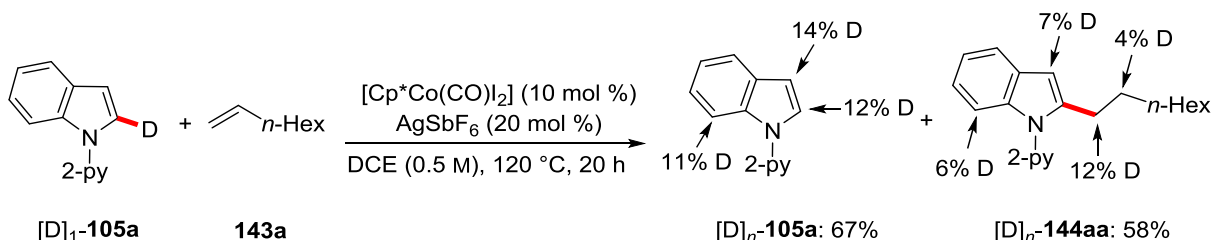
Scheme 63. H/D-exchange with [D]₁-**105a** under linear-selective reaction conditions.

With respect to the previously observed H/D-exchange study of the product **144ab** (*cf.* Scheme 60), this finding can be most likely explained by post-catalytic deuterium exchange with product **144aa**. Remarkably, minor deuteration was detected in β-position, which might proceed by deutero-demetalation of a catalytically relevant intermediate (*vide infra* Scheme 69).

3.3.6.1.5 H/D-exchange with [D]₁-105a

Moreover, a H/D-exchange reaction with substrate [D]$_1$-**105a** was conducted under linear-selective reaction conditions, but in the absence of any alkene (Scheme 64). The substrate [D]$_1$-**105a** could be almost quantitatively reisolated in 93%, with significant H/D-scramblings in C2-, C3- and C7-position. A reasonable explanation for this observation is a reversible C–H activation in C2-position and proto-demetalation, likely by traces of water in the solvent DCE.
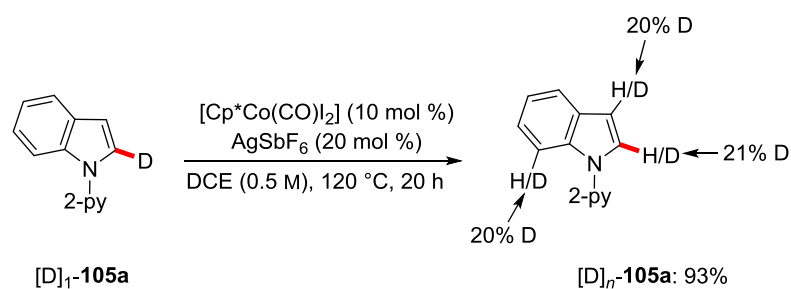
Scheme 64. H/D-exchange experiment with deuterated substrate [D]$_1$-**105a**.

3.3.6.1.6 Intermolecular competition experiment

In addition, an intermolecular competition experiment under the branched-selective reaction conditions was carried out by comparing the reaction rates of the electronically distinct 2-pyridylindoles **105b** and **105m** (Scheme 65). As a result, the electron-rich 5-methoxypyridylindole (**105b**) reacted preferentially, which possibly supports a BIES-type C–H activation.
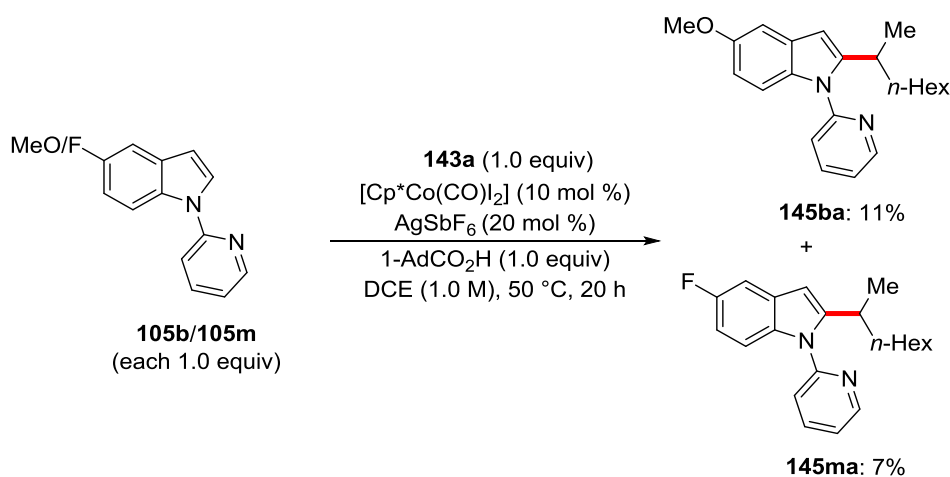
***Scheme 65.*** Intermolecular competition experiment for the branched-selective C–H alkylation.

Notably, *V. Müller* showed a significant preference for the electron-rich 1-(*p*-tolyl)-1*H*-pyrazole (**18a**) as compared to [1-(4-(trifluoromethyl)phenyl]-1*H*-pyrazole (**18b**), which is in agreement with the above mentioned findings. Here, the electron-rich pyrazole **18a** reacted almost nine times faster than substrate **18b**.

3.3.6.2   KIE Studies

3.3.6.2.1   KIE of the linear-selective reaction
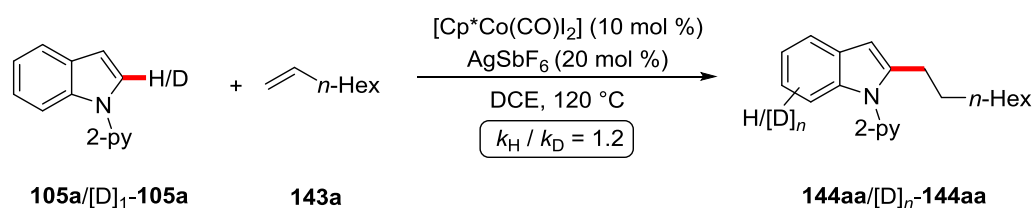
Scheme 66. KIE of the linear-selective reaction.

The kinetic isotope effect (KIE) of the *anti-Markovnikov*-selective reaction was measured by comparison of independent reaction rates for substrate **105a** and its isotopically labeled analogue [D]$_1$-**105a**, resulting in a minor value of $k_H/k_D \approx 1.2$ (Scheme 66). The observed KIE is in good agreement with the results obtained from the H/D-exchange experiments, suggesting the reversible C–H activation not to be the turnover-limiting step of the catalytic cycle.
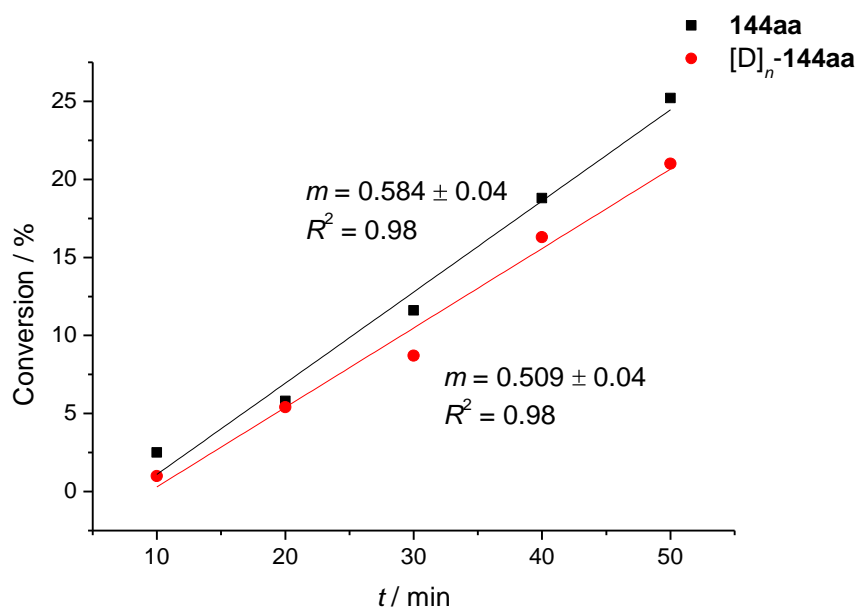
Figure 11. KIE under the linear-selective reaction conditions.

3.3.6.2.2 KIE of the branched-selective reaction
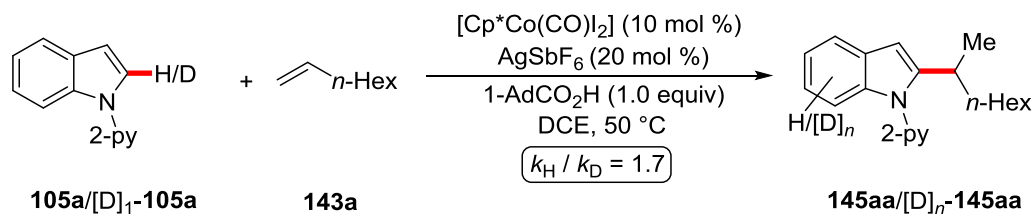

Scheme 67. KIE of the branched-selective reaction.

The kinetic isotope effect (KIE) of the *Markovnikov*-selective reaction was analogously determined to be $k_H/k_D \approx 1.7$ (Scheme 67 and Figure 12). The comparatively lower H/D-exchange in C2-position of the starting material **105a** for the branched-selective reaction (*vide supra*) and the higher KIE value show that the C–H activation step under the *Markovnikov*-selective reaction regime presumably does not follow an electrophilic activation pathway. Along this line, a rate acceleration by acids as well as carboxylate additives has been observed (*cf.* Table 13). Overall, these findings might support a BIES-type C–H activation mechanism by assistance of the *in situ* formed 1-adamantylcarboxylate to be operative for the branched-selective reaction regime.
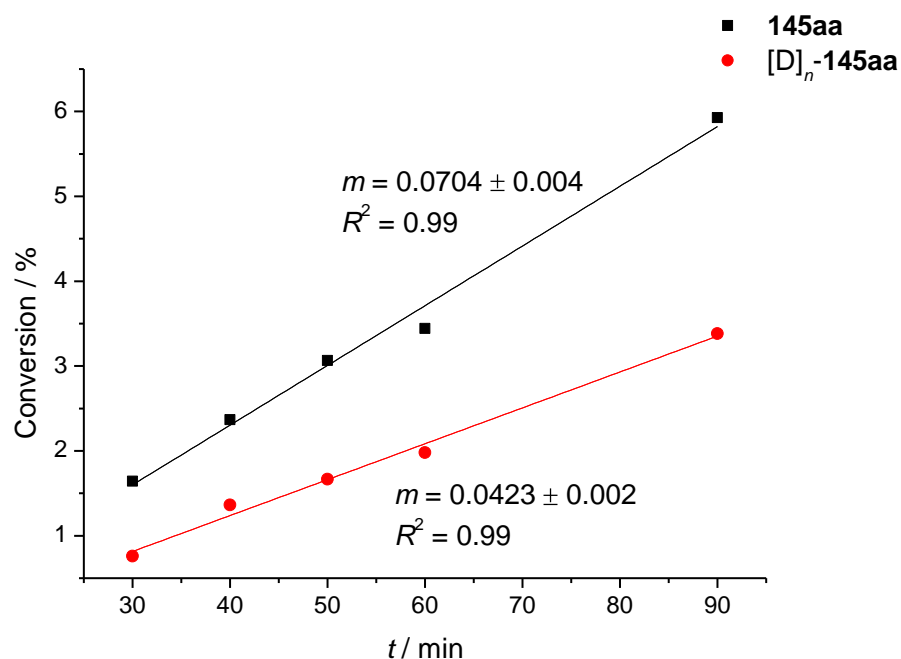

Figure 12. KIE under the branched-selective reaction conditions.

3.3.6.3   Kinetic reaction orders

3.3.6.3.1   Kinetic reaction order for the linear-selective reaction

3.3.6.3.1.1   Reaction order with respect to the concentration of 2-pyridylindole (105a)

The kinetic order of the reaction with respect to the concentration of 2-pyridylindole (**105a**) equals $n = 1.24 \pm 0.11$, which might correspond to a reaction order of one (Figure 13). This result can be interpreted as a clear hint for the participation of 2-pyridylindole (**105a**) in the turnover-limiting step of the reaction.
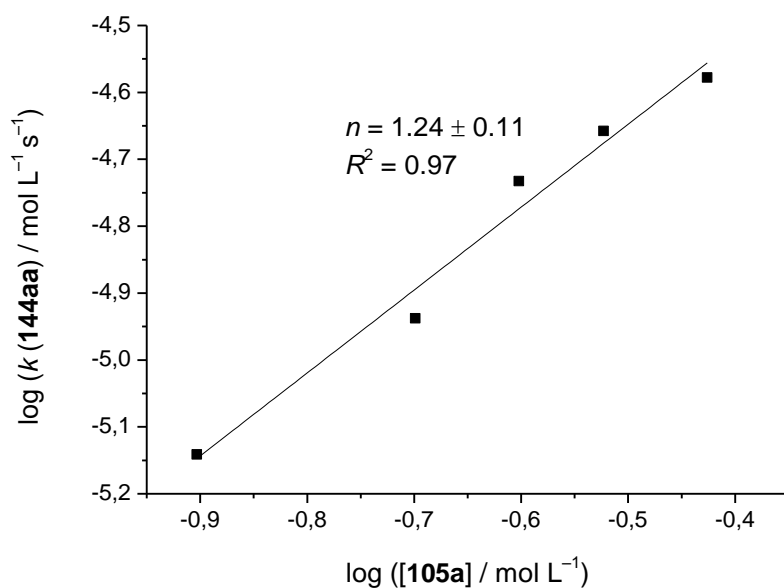
Figure 13. Kinetic order in [2-pyridylindole] (**105a**) under linear-selective conditions.

3.3.6.3.1.2   Reaction order with respect to the concentration of 1-octene (143a)

Interestingly, a non-integer reaction order[165] of $n = 0.30 \pm 0.02$ with respect to the alkene-concentration **143a** was observed (Figure 14), suggesting a complex rate law for this reaction. One possible explanation could be that the step after alkene-insertion is turnover-limiting and both the coordination and the following migratory insertion of the alkene **143a** are two interdepending equilibrium reactions, which are kinetically relevant for the following turnover-limiting step.

Figure 14. Kinetic order in [1-octene] (**143a**) under linear-selective conditions.

3.3.6.3.1.3   Reaction order with respect to the concentration of [Cp*Co(CO)I₂]

The reaction order with respect to the catalyst concentration is roughly one, with $n = 1.08 \pm 0.12$ (Figure 15), showing that the catalyst is part of the turnover-limiting step of the catalytic cycle.

Figure 15. Kinetic order in [[Cp*Co(CO)I₂]] under the linear-selective reaction regime.

3.3.6.3.2   Kinetic reaction order for the branched-selective reaction

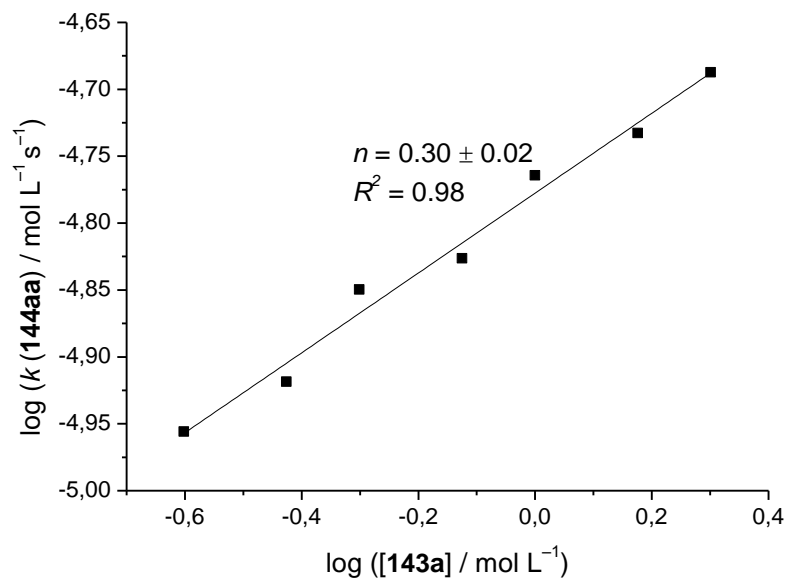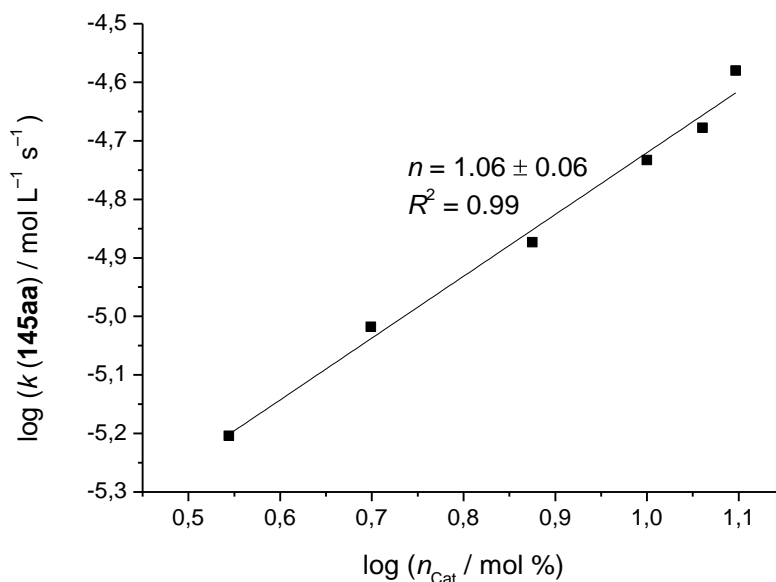### 3.3.6.3.2.1   Reaction order with respect to the concentration of 2-pyridylindole (105a)

In stark contrast to the observed first-order-dependence for the linear-selective reaction regime, a zero-order-dependence with respect to the concentration of 2-pyridylindole (**105a**) with $n = 0.00 \pm 0.09$ was

observed (Figure 16). Notably, a similar result was obtained by *V. Müller*, who performed ^{19}F-NMR studies of the same reaction system utilizing 5-fluoro-1-(pyridin-2-yl)-1*H*-indole (**105m**).[162b] Based on these results, it can be proposed that the concentration of 2-pyridylindole (**105a**) is not kinetically relevant and it is neither part of an equilibrium reaction before nor of the turnover-limiting step itself.
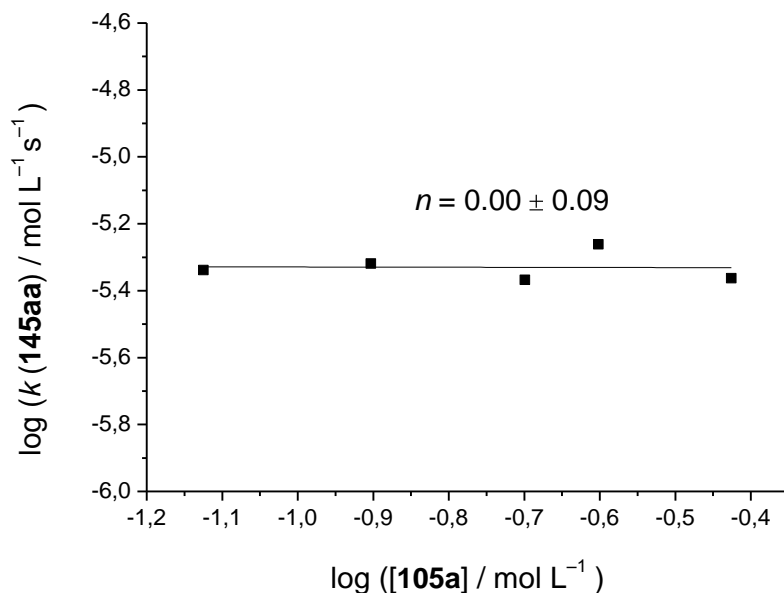
Figure 16. Kinetic order in [2-pyridylindole] (**105a**) under branched-selective conditions.

3.3.6.3.2.2   Reaction order with respect to the concentration of 1-octene (143a)

In contrast to the non-integer reaction order for the linear-selective regime (*cf.* Figure 14), the *Markovnikov*-selective reaction displayed a first order dependence with respect to [1-octene] (**143a**), which reveals the participation of 1-octene (**143a**) within or before the turnover-limiting step (Figure 17).
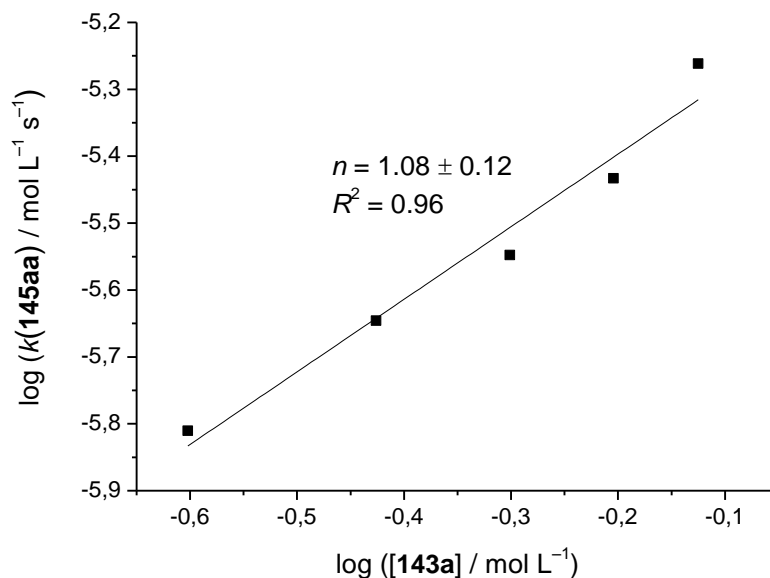
Figure 17. Kinetic order in [1-octene] (**143a**) under branched-selective conditions.

3.3.6.3.2.3   Reaction order with respect to the concentration of [Cp*Co(CO)I$_2$]

As for the linear-selective reaction (*cf.* Figure 15), a first-order dependence was observed with respect to the concentration of the cobalt(III) catalyst (Figure 18).
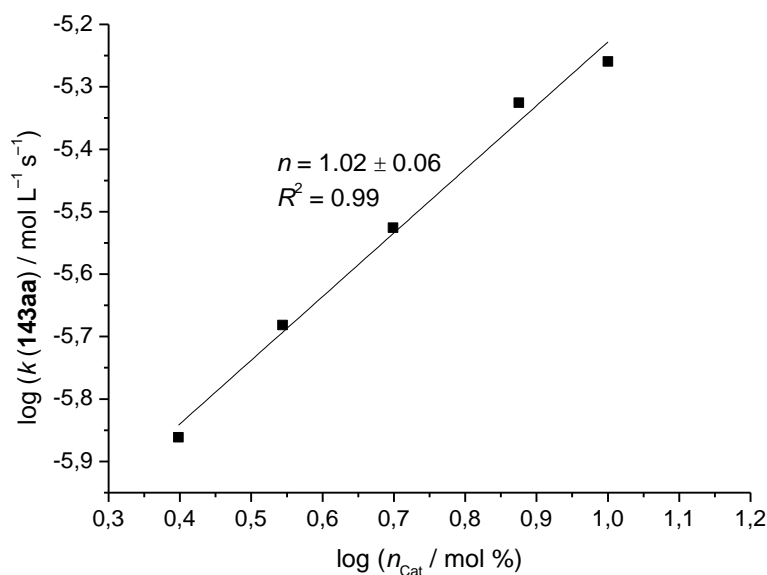
Figure 18. Kinetic order in [[Cp*Co(CO)I$_2$]] under branched-selective conditions.

3.3.6.4   *Arrhenius* Activation Energies

A common approximation for the measurement of activation barriers E_A of *inter alia* catalytic reactions is the *Arrhenius* plot, in which the natural logarithm of the reaction rate k is plotted against

the inverse reaction temperature T (Equation 5).[166] The slope of the thus obtained graph corresponds to the activation energy E_A divided by the ideal gas constant R and the y-axis intercept represents the natural logarithm of the preexponential factor A.

$$\ln k = \ln(A) - \frac{E_A}{R} \times \frac{1}{T} \qquad \text{(Equation 5)}$$

Thus, the activation energy of the linear-selective reaction was determined to be $E_A = 22.3 \pm 1.7$ kcal/mol (Figure 20) and the branched-selective reaction displayed a barrier of $E_A = 14.4 \pm 1.6$ kcal/mol (Figure 22), which were obtained by comparison of the initial rates at different reaction temperatures for both reactions (Figure 19 and Figure 21). The difference in activation energy for both reactions amounts to roughly 8.0 kcal/mol, which is in good agreement with the difference in each optimized reaction temperature of 120 °C and 50 °C, respectively.
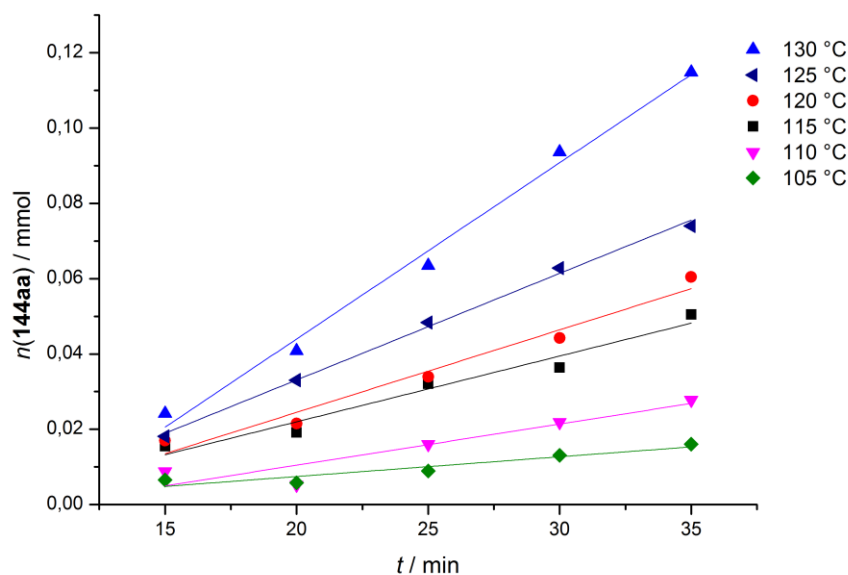
Figure 19. Initial rates at different reaction temperatures for the linear-selective reaction.
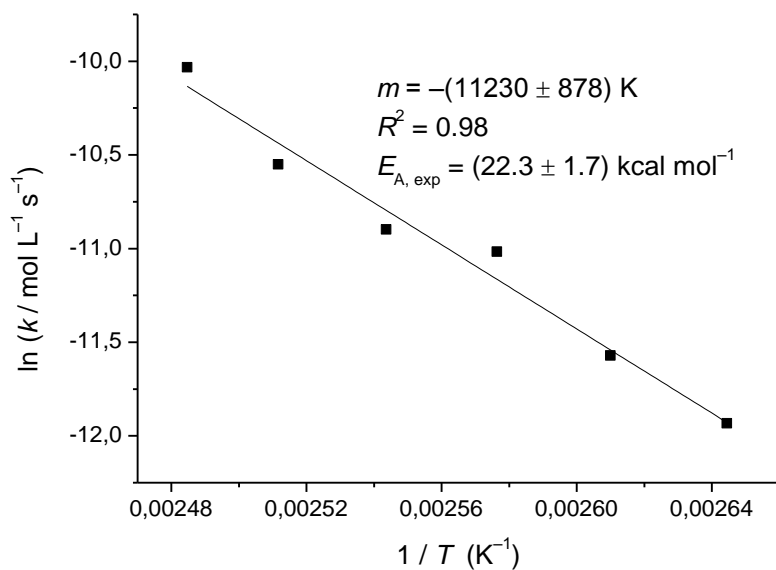
Figure 20. Arrhenius plot for the linear-selective reaction regime.
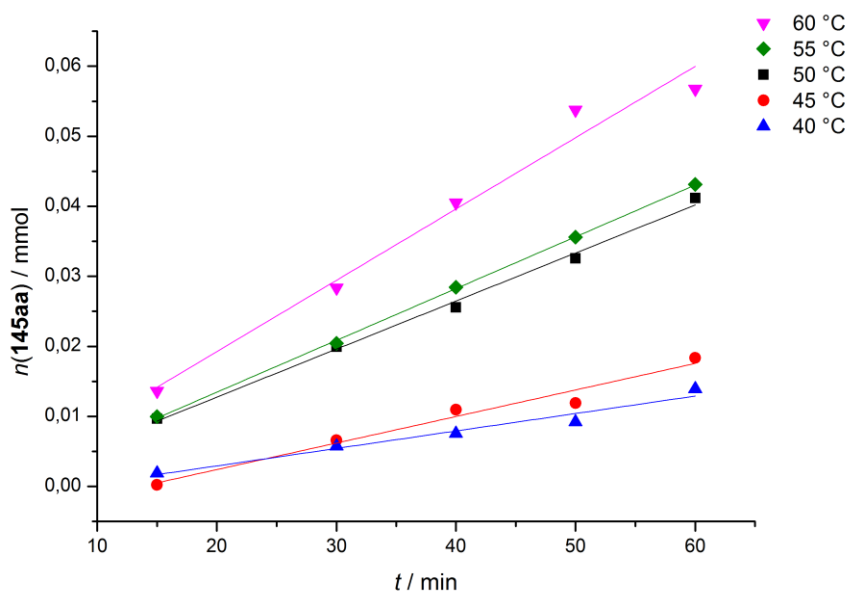
Figure 21. Initial rates at different temperatures for the branched-selective reaction.
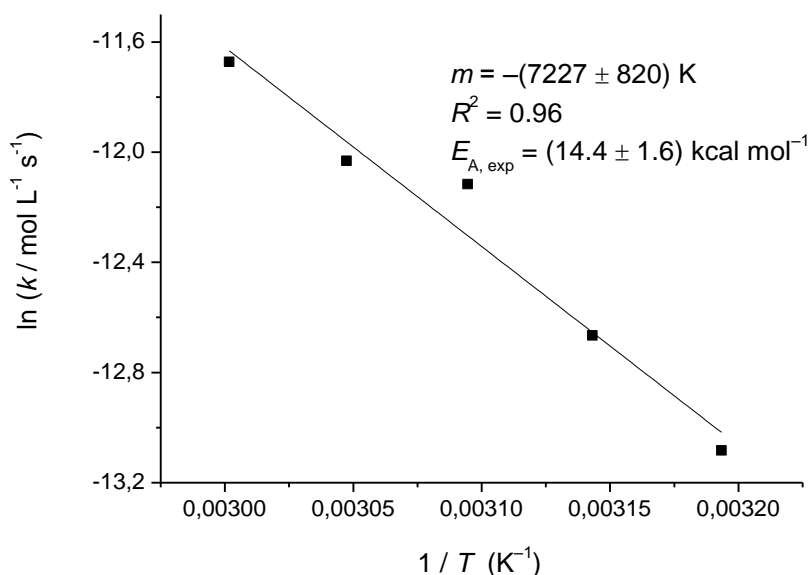
Figure 22. Arrhenius plot for the branched-selective reaction regime.

3.3.6.5   Attempted Post-Synthetic Isomerization Studies

Furthermore, it was studied whether a post-catalytic isomerization through cobalt(III)-catalyzed C–C bond cleavage could occur for the linear product **144aa** under branched-selective conditions (Scheme 68a) and *vice versa* (Scheme 68b). Overall, there was no change in connectivity, which indicates that both products are thermodynamically stable under the catalytic reaction conditions.
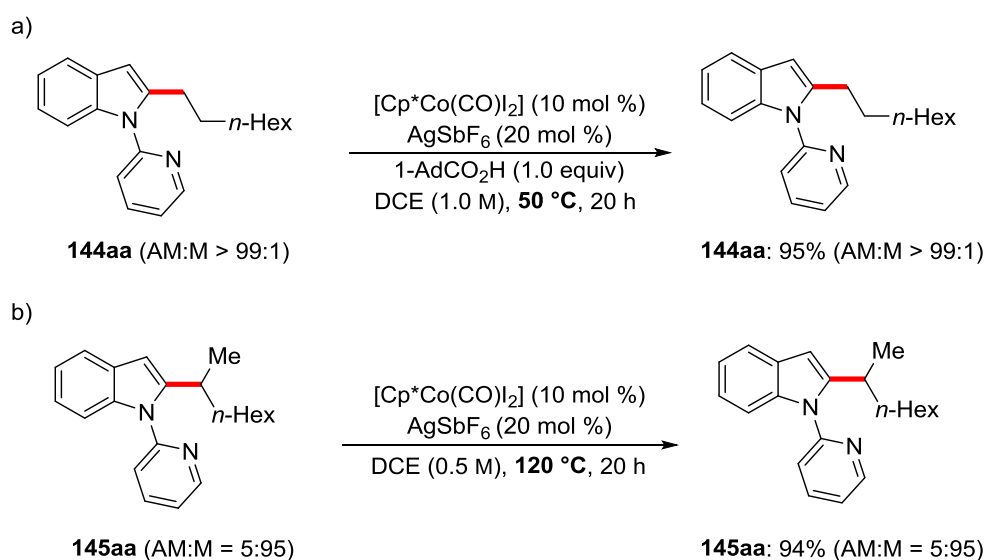
Scheme 68. Attempted isomerization of a) the linear **144aa** and b) the branched product **145aa**.

3.3.7   Proposed Catalytic Cycles

In summary, there are several mechanistically distinct characteristics of the presented regiodivergent catalytic reactions. The linear-selective reaction seems to involve a feasible C–H activation step which

is indicated by the significant H/D-scrambling in C2-position and the minor KIE of 1.2, overall rendering the C–H activation to be facile and reversible. For the branched-selective reaction (*i*) a clear rate acceleration was accomplished using carboxylic acids (*cf.* Table 13), (*ii*) a reversible H/D-exchange was detected, (*iii*) a higher KIE of 1.7 was measured and (*iv*) a clear preference for electron-rich substrates was observed. Altogether, these results indicate that the C–H activation for the *Markovnikov*-selective reaction follows a BIES-type mechanistic pathway, which is clearly different from the linear-selective reaction.

The kinetic order studies reveal a first-order-dependence on [2-pyridylindole] (**105a**) for the linear-selective regime, whereas a zero-order-dependence was found for the branched one. With respect to [1-octene] (**143a**), a non-integer order of roughly 0.3 was observed in the case of the linear-selective reaction, and a first-order-dependence could be shown for the branched-selective one. The kinetic order of the reaction with respect to the catalysts concentration equaled one for both reactions. In summary, these differences clearly reveal that the regiodivergence of the studied reactions is possibly rooted in two mechanisms with distinct rate-determining steps.

To gain a deeper mechanistic insight, DFT-studies were performed in collaboration with *S. Grimme* and *M. Bursch*.[161] The computational results showed the selectivity control to be a consequence of two mechanistically different pathways for the proto-demetalation elementary step.

On the one hand, linear selectivity is clearly preferred by a ligand-to-ligand hydrogen transfer (LLHT), which enabled the proto-demetalation by delivering the proton from a second substrate **105a** to intermediate **153** (Scheme 69, **TS1**). The energetic difference of both regioisomers amounts to 7.9 kcal/mol. These theoretical results match the experimentally observed regioselectivities as well as the first-order-dependence on substrate **105a** because the recoordination with the second 2-pyridylindole (**105a**) seems to be the overall highest calculated activation barrier.
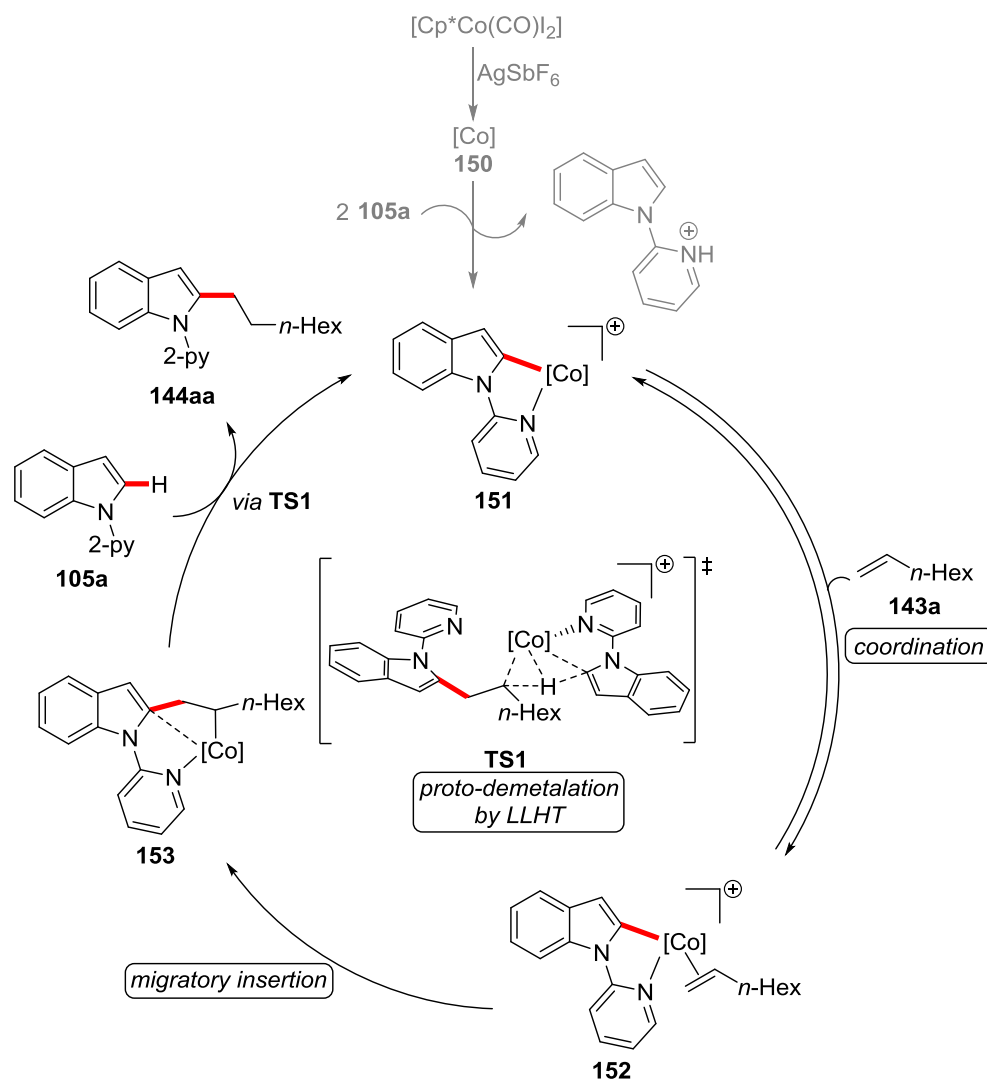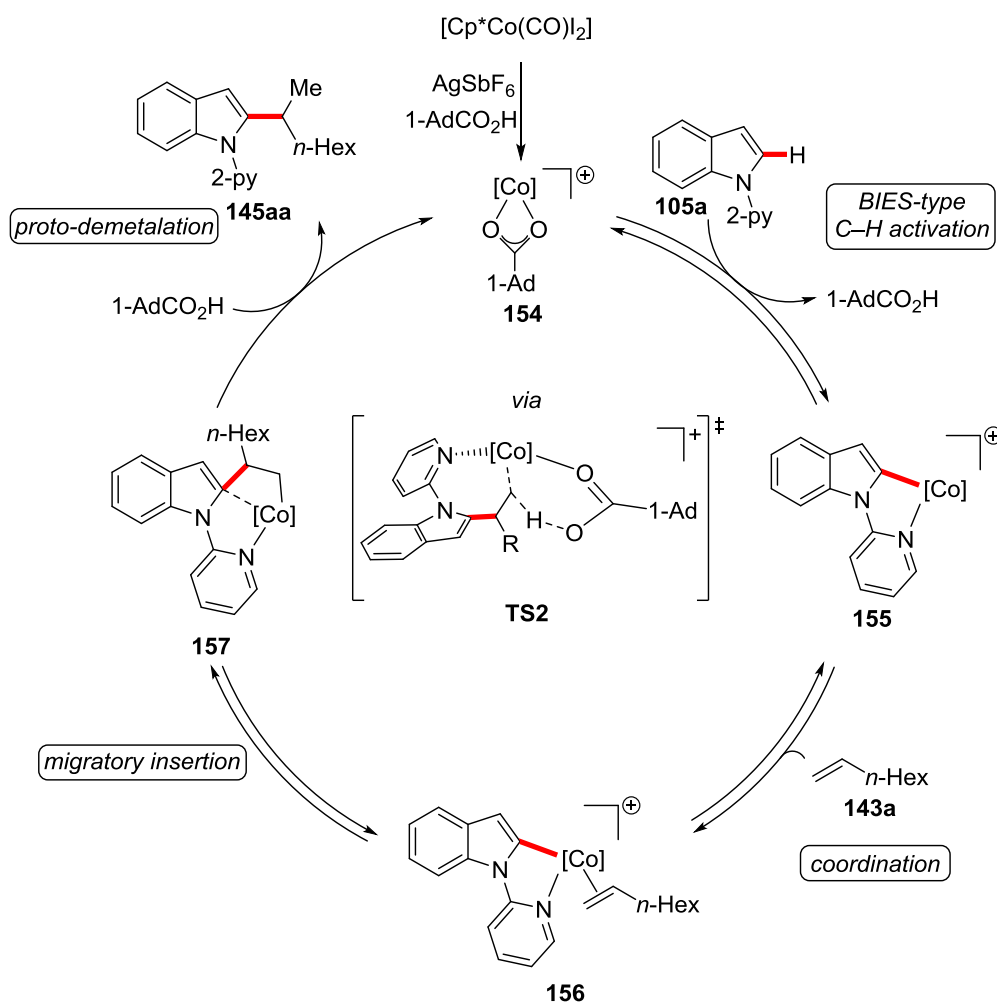
Scheme 69. Proposed catalytic cycle for the linear-selective reaction with only the preferred linear intermediates depicted. [Co] = Cp*Co^{III}.

In the case of the branched-selective reaction, the turnover-limiting proto-demetalation step proceeds *via* **TS2** (Scheme 70) with 1-adamanantanecarboxylic acid as the proton source and results in the formation of the favored branched product **145aa**. The energy difference of the overall activation barriers equals 6.5 kcal/mol, which reflects the excellent experimental regioselectivities. A minor amount of linear product **144aa** under the branched-selective reaction conditions might possibly be caused by the *anti-Markovnikov*-selective LLHT mechanism being in parallel operative, but it is clearly the less favored mechanistic pathway under these conditions (*cf.* Table 13, entry 1).

The regiocontrol in the *Markovnikov*-selective reaction is presumably caused by steric interactions in the unfavored linear transition state **TS2$_l$** (Figure 23), which was disclosed by DFT-calculations of *M. Bursch*. The linear product formation is considerably less favored because the alkyl-chain R = *n*-Hex hinders the approach of the sterically congested 1-adamantanecarboxylic acid, which is needed as proton source for the proto-demetalation step. In this context, it could be shown that attractive *London* dispersion interactions[124, 142] significantly contribute to a stabilization of all catalytically relevant

intermediates as well as transition states, but they do not compensate for the energetic destabilization by steric interactions and overall do not influence *Markovnikov/anti-Markovnikov* selectivity.[161]

Generally, the proto-demetalation step is kinetically favored by the presence of carboxylic acids as compared to their carboxylate analogues, which can only form the corresponding acid *in situ* during the BIES-type C–H activation. This hypothesis is in good agreement with the previously described observation that acids, even in high concentrations and regardless of their steric demand, favor the branched product formation, whereas only sterically demanding carboxylates lead to comparably good selectivities (*cf*. Table 13, entries 2–12).

Scheme 70. Proposed catalytic cycle for the branched-selective reaction with only the preferred branched intermediates depicted. [Co] = Cp*Co^{III}.
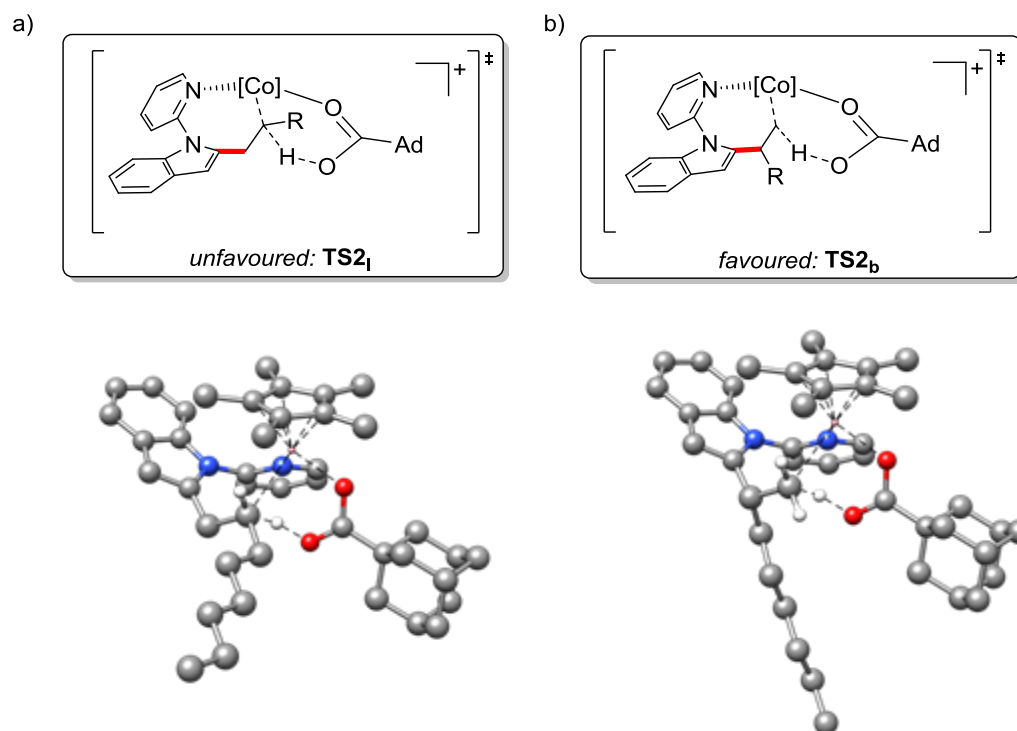
Figure 23. Calculated transition states of the proto-demetalation for the branched-selective reaction with a) the unfavored linear arrangement and b) the energetically favored branched transition state shown; R = *n*-Hex.[161]

3.4 Cobalt(III)-Catalyzed Allylative and Alkenylative C–H/C–F Functionalizations

The selective synthetis of fluorinated molecules is a major challenge in organic synthesis, since about 20–30% of all agrochemicals and pharmaceuticals contain fluorine for the improvement of *inter alia* their metabolic stability and lipophilicity (Figure 24).[118h, 118k, 167] Consequently, there is a continued demand for selective and mild conditions to install fluorinated motifs in late-stage modifications of complex molecules.[13k, 118] A particularly sustainable and step-economical access to highly functionalized fluorine-containing molecules can be achieved by merging C–H with C–F functionalization in a tandem process.[168]
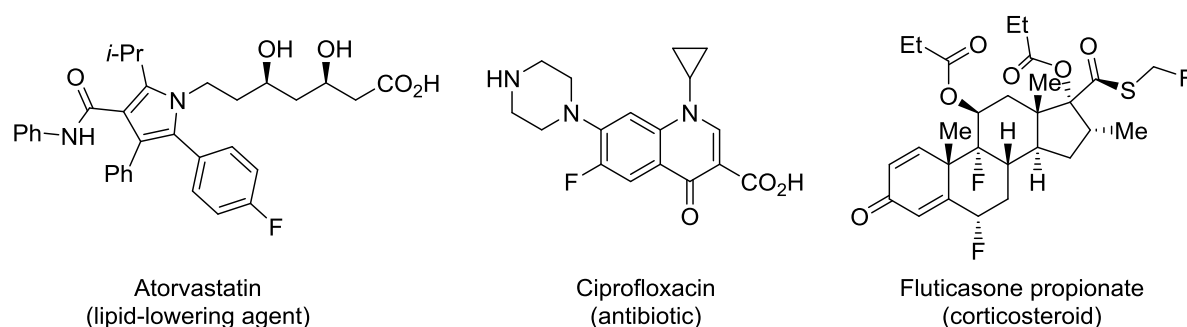
Figure 24. Selected examples of fluorine-containing pharmaceuticals.

### 3.4.1 Optimization Studies for the Allylative C–H/C–F Functionalizations

The optimization studies for the cobalt(III)-catalyzed C–H/C–F functionalization were started by probing the effect of representative solvents for cobalt(III)-catalyzed C–H activation (Table 19). Interestingly, fluorinated solvents[169] such as HFIP and TFE by far outcompeted DCE and MeOH (entries 1–4), with TFE delivering the desired product **158aa** in an almost quantitative yield of 97% with a good diastereoselectivity of Z/E = 86:14. According to a report of *Berkessel* and coworkers on the beneficial effects of fluorinated solvents,[170] it can be assumed that TFE and HFIP form higher order solvent aggregates that significantly stabilize cationic intermediates in catalysis by enhanced H-bond donor abilities. In the absence of any cobalt(III) catalyst, no reactivity was observed (entry 5). Furthermore, a catalyst loading of 0.25 mol % still provided the product **158aa** in excellent yield, albeit reduced catalyst loadings as low as 0.10 mol % seemed to be less efficient (entries 6 and 7). Notably, the reaction still proceeded at 0 °C and furnished the product in overall moderate yield, but with an improved diastereoselectivity of Z/E = 93:7 (entry 8).

Thereafter, various bases were tested, especially mild bases like carbonates. Within a series of alkali metal carbonates, an increased reactivity from lithium to potassium carbonate was found, but with cesium carbonate a significant drop in yield to only 8% was noticed (entries 4 and 9–12). The preference for potassium as countercation in this reaction was furthermore revealed by obtaining excellent yields with potassium hydrogen carbonate and potassium acetate as the bases (entries 13

and 14). Among significantly more basic hydroxides, potassium hydroxide was found to be the most efficient base (entries 15 and 16). Based on these findings, it can be assumed that potassium-containing bases are generally favored regardless of their pK_B-values.

Importantly, qualitative solubility experiments in TFE as solvent showed an increasing solubility in a row from lithium to cesium fluoride, which is agreement with quantitative experiments of *Wynn* and coworkers.[171] Thus, by only taking the solubility of fluorides into account, lithium carbonate as base would create the strongest driving force for the reaction. However, the solubility of the corresponding carbonate bases should be considered as well. In this regard, qualitative solubility experiments indicated an increasing solubility from lithium to cesium carbonate, which would lead to the highest reactivity for cesium carbonate. Based on these results, only well-balanced solubilities of the carbonate bases as well as the precipitating alkali metal fluorides can account for this reactivity trend, resulting in the overall highest efficiency for potassium carbonate.

Table 19. Optimization study for the cobalt(III)-catalyzed C–H/C–F functionalization.
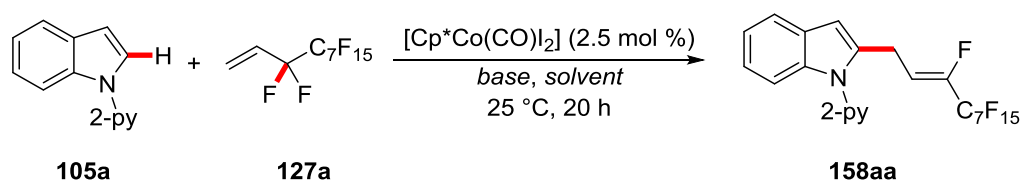
Entry	base	solvent	yield / %[a]
1	K_2CO_3	DCE	3
2	K_2CO_3	MeOH	12
3	K_2CO_3	HFIP	91
4	**K_2CO_3**	**TFE**	**97**
5	K_2CO_3	TFE	---[b]
6	K_2CO_3	TFE	95[c]
7	K_2CO_3	TFE	44[d]
8	K_2CO_3	TFE	46[e]
9	Li_2CO_3	TFE	18
10	Na_2CO_3	TFE	81
11	Rb_2CO_3	TFE	49
12	Cs_2CO_3	TFE	8
13	$KHCO_3$	TFE	94
14	KOAc	TFE	87
15	KOH	TFE	93

| 16 | Ca(OH)$_2$ | TFE | 45 |

[a] Reaction conditions: **105a** (0.50 mmol), **127a** (0.60 mmol), [Co] (2.5 mol %), base (1.00 equiv), solvent (0.5 mL, 1.0 M), 25 °C, 20 h, isolated yield; all Z/E = 86:14. [b] Without [Co]. [c] 0.25 mol % [Co]. [d] 0.10 mol % [Co]. [e] At 0 °C, Z/E = 93:7.

To explore this reaction with respect to even more cost-efficient cobalt sources, a comprehensive screening of some well-established cobalt-complexes[15a] was performed (Table 20). Catalysts with Cp or substituted (t-Bu)$_2$-Cp-ligands delivered only traces of the desired product **158aa** (entries 2 and 3). In striking contrast, the beneficial influence on stereoselectivities by substituents on the Cp-ligand had previously been disclosed by *Rovis* and coworkers in rhodium(III)-catalyzed C–H activation catalysis.[172] Unfortunately, also simple cobalt salts, such as cobalt(III) fluoride (entry 4) and cobalt(II) bromide (entry 8), failed to furnish any desired product as well as other salts, such as cobalt acetylacetonate and cobalt acetate (entries 5–7). In summary, these findings show the great importance of the Cp*-ligand for efficient catalysis, probably due to its very good donor abilities and rigid structure.

Table 20. Screening of different cobalt sources as catalysts.
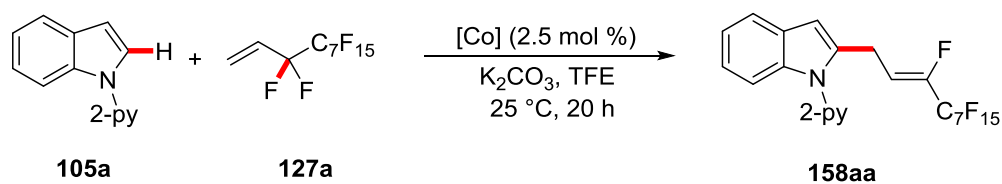
| Entry	[Co]	yield / %[a]
1	[Cp*Co(CO)I$_2$]	97
2	[CpCo(CO)I$_2$]	traces
3	[1,3-(t-Bu)$_2$C$_5$H$_3$Co(CO)I$_2$]	traces
4	CoF$_3$	---
5	Co(acac)$_3$	---
6	Co(acac)$_2$	---
7	Co(ac)$_2$	---
8	CoBr$_2$	---

[a] Reaction conditions: **105a** (0.50 mmol), **127a** (0.60 mmol), [Co] (2.5 mol %), K$_2$CO$_3$ (1.00 equiv), solvent (0.5 mL, 1.0 M), 25 °C, 20 h. Conversions were determined by GC with n-dodecane as the internal standard.

3.4.2 Optimization Studies for the Alkenylative C–H/C–F Functionalization

Based on the optimization studies for the allylative C–H/C–F functionalization, it was studied whether 1,1-difluorostyrenes **128** can be efficiently converted by cobalt(III) catalysis (Table 21). 1,1-difluorostyrenes **128** are synthetically easily accessible and biologically relevant substrates.[173] For this purpose, it was initially observed that the reaction performed poorly in the absence of base (entry 1), whereas AgSbF$_6$ had a beneficial influence on the reactivity (entry 2). Thereafter, a significant increase in product yield was achieved by utilizing potassium carbonate as the base (entry 3), while no improvement by additional AgSbF$_6$ (entry 4) was observed. Moreover, the optimal base loading was found to be 1.50 equivalents (entries 5–7). Noteworthily, after screening different metal carbonates the corresponding potassium salt turned out to be optimal (entries 5–11), showing same reactivity trend as it was previously observed for the C–H/C–F allylative functionalization (*cf.* Table 19, entries 8–12).

Importantly, a slight increase of the 1,1-difluorostyrenes (**128a**) concentration furnished the desired alkenylated product **159aa** in almost quantitative yield and excellent *Z*-diastereoselectivity (entry 12). Moreover, a control reaction revealed that this reaction is indeed cobalt(III)-catalyzed (entry 13). Subsequently, selected solvents were tested, with an unsatisfactory result for the more expensive perfluorinated HFIP (entry 14). Unfortunately, more economic solvents, such as MeOH and H$_2$O, showed no reactivity (entries 16 and 17). It is noteworthy that in all cases excellent diastereoselectivities of *Z/E* > 99:1 were achieved.

Table 21. Optimization of cobalt(III)-catalyzed alkenylative C–H/C–F functionalizations.
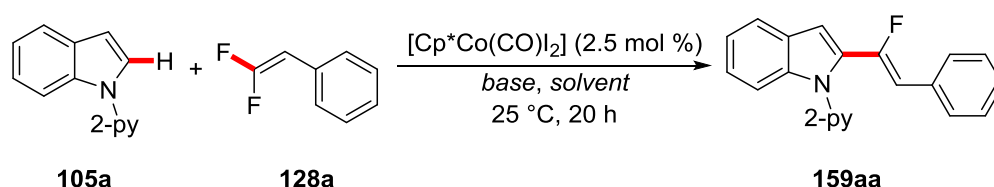
Entry	base	solvent	yield / %[a]
1	---	TFE	---
2	---	TFE	37[b]
3	K$_2$CO$_3$	TFE	77
4	K$_2$CO$_3$	TFE	73[b]
5	K$_2$CO$_3$ (0.50 equiv)	TFE	33
6	K$_2$CO$_3$ (1.50 equiv)	TFE	86
7	K$_2$CO$_3$ (2.00 equiv)	TFE	67
8	Li$_2$CO$_3$	TFE	---

9	Na$_2$CO$_3$	TFE	18
10	Rb$_2$CO$_3$	TFE	60
11	Cs$_2$CO$_3$	TFE	30
12	**K$_2$CO$_3$**	**TFE**	**98[c]**
13	K$_2$CO$_3$	TFE	---[d]
14	K$_2$CO$_3$	HFIP	46
15	K$_2$CO$_3$	DCE	---
16	K$_2$CO$_3$	MeOH	---
17	K$_2$CO$_3$	H$_2$O	---

[a] Reaction conditions: **105a** (0.50 mmol), **128a** (0.60 mmol), [Co] (2.5 mol %), base (1.00 equiv), solvent (0.5 mL, 1.0 M), 25 °C, 20 h, isolated yield; all *Z/E*-ratios > 99:1, determined by ^{1}H-NMR spectroscopy. [b] With AgSbF$_6$ (5.0 mol %). [c] **128a** (1.50 equiv). [d] Without [Co].

### 3.4.3   Scope of the Allylative Cobalt(III)-Catalyzed C–H/C–F Functionalization

Under the optimized reaction conditions several heterocycles, including indoles **105**, pyrroles **146** and phenylpyrazoles **18** were probed (Table 22). Initially, 1*H*,1*H*,2*H*-perfluorohexene (**127b**) furnished the corresponding product **158ab** in excellent yield and good *Z/E*-ratio (entry 2), displaying a considerable variability with respect to the perfluoroalkyl chain length. Subsequently, various substituents in the C5-position of 2-pyridylindole (**105a**) were tested, with overall very good yields and good diastereoselectivities (entries 3–7). It is noteworthy that even sterically demanding substrates like **105p** were successfully converted although an elevated reaction temperature and higher catalyst loading were necessary (entry 8). Notably, due to the higher reaction temperature the diastereoselectivity dropped to moderate *Z/E* = 80:20. Moreover, it was demonstrated that also 1-(pyridin-2-yl)-1*H*-pyrrole (**146**) and phenylpyrazoles **18** could deliver the desired products (entries 9−11). In the latter case, an optimal reactivity was achieved by using AgSbF$_6$ (20 mol %) as the additive, which is presumably due to an unfavored BIES-type C–H activation step, as the arene is less electron-rich than indoles and pyrroles.

Table 22. Scope of the cobalt(III)-catalyzed allylative C–H/C–F funtionalization with different heterocycles.

Entry	substrate	105	product	158	Z/E	yield / %[a]
1		105a		158aa	86:14	97
2		105a		158ab	86:14	94[b]
3		105b		158ba	86:14	90
4		105f		158fa	86:14	77
5		105m		158ma	86:14	85
6		105c		158ca	84:16	93
7		105d		158da	82:18	93
8		105p		158pa	80:20	67[c]
9		146		160	84:16	61[d]
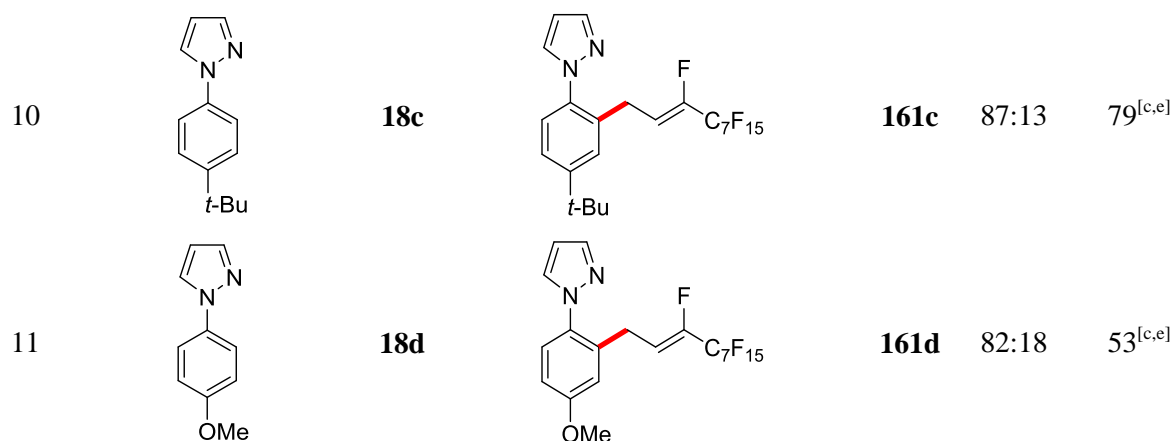
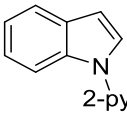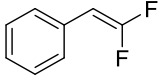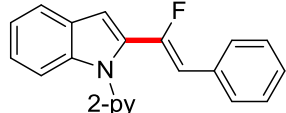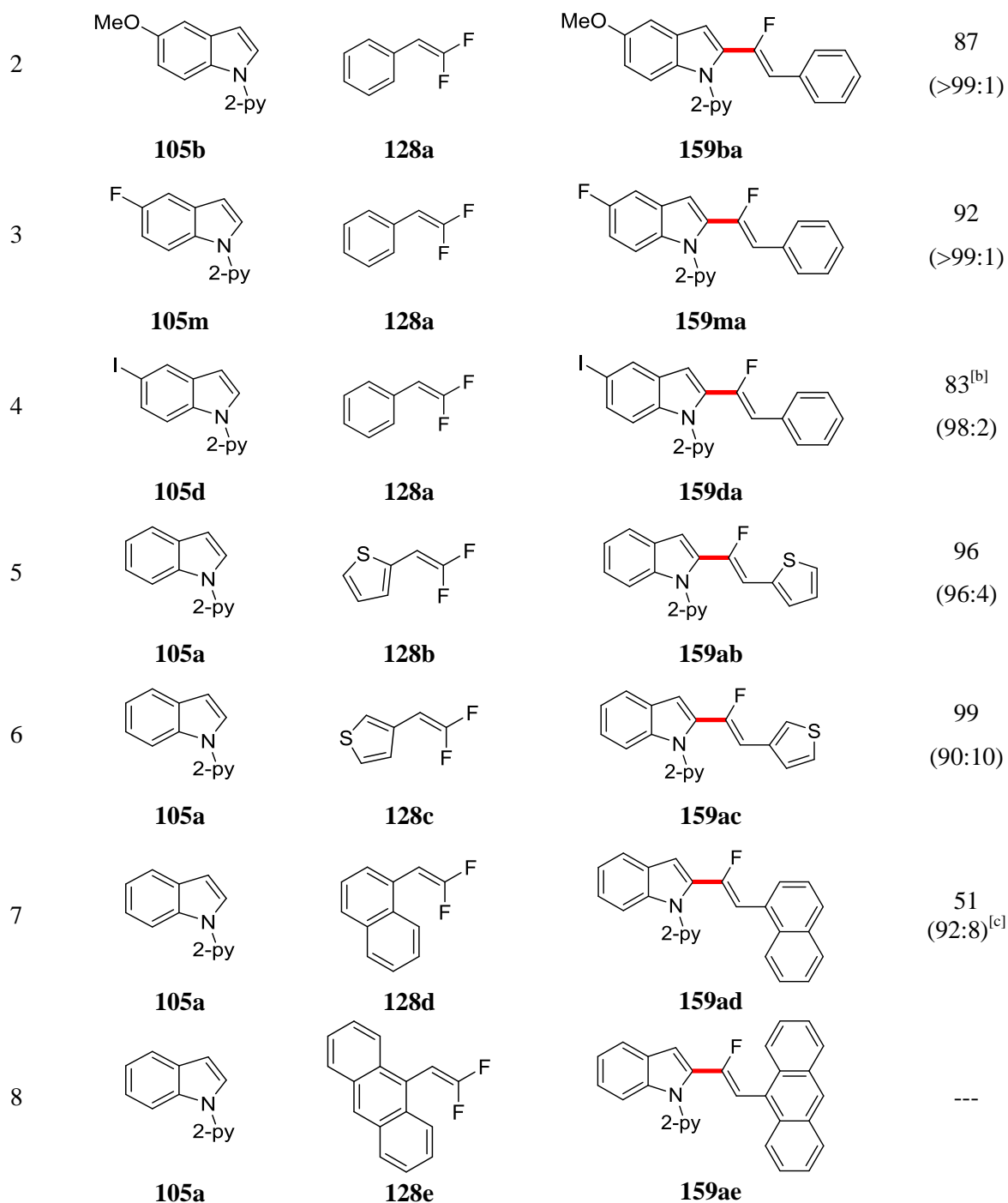|					
10	**18c**		**161c**	87:13	79[c,e]
11	**18d**		**161d**	82:18	53[c,e]

[a] Reaction conditions: **105a** (0.50 mmol), **127a** (0.60 mmol), [Co] (2.5 mol %), K_2CO_3 (1.00 equiv), TFE (0.5 mL, 1.0 M), 25 °C, 20 h, isolated yield; Z/E-ratio determined by ^{1}H-NMR spectroscopy. [b] 1*H*,1*H*,2*H*-perfluorohex-1-ene (**127b**) (0.60 mmol) was used. [c] At 70 °C and [Co] (10 mol %). [d] 8% of di-substituted **160'** (Z/E = 84:16) was detected. [e] With $AgSbF_6$ (20 mol %).

3.4.4 Scope of the Alkenylative Cobalt(III)-Catalyzed C–H/C–F Functionalization

With the optimized catalytic reaction conditions in hand, the substrate scope with respect to various indoles **105** and 1,1-difluorostyrenes **128** was performed (Table 23). Electron-rich as well as electron-poor indoles reacted in very good yields and excellent diastereoselectivities (entries 1–4). Notably, *V. Müller* and *R. R. Presa* extended the scope to more examples of *ortho-* and *meta*-substituted 1,1-difluorostyrenes **128**. [174] Furthermore, it was demonstrated that the thiophene-derived substrates (entries 5 and 6) performed well, delivering the desired products **159ab** and **159ac** in almost quantitative yield. However, a slightly decreased diastereoselectivity for the 3-substituted thiophene **128c** was observed. Elevated temperatures were necessary to convert the naphthalene-derived substrate **128d** (entry 7). In this manner, the sterically even more biased fluorescent anthracene-derivative **128e** failed to yield the corresponding product, revealing a limitation for this reaction with respect to bulky 1,1-difluoroalkenes **128**.

Table 23. Scope of the alkenylative cobalt(III)-catalyzed C–H/C–F functionalization.

Entry	indole **105**	alkene **128**	product **159**	yield / % (Z/E)[a]
1	**105a**	**128a**	**159aa**	97 (>99:1)

|	105	128	159	Yield (Z/E)
2	MeO-indole, 2-py **105b**	Ph-CF=CF₂ **128a**	MeO-indole-2-py product **159ba**	87 (>99:1)
3	F-indole, 2-py **105m**	Ph-CF=CF₂ **128a**	F-indole-2-py product **159ma**	92 (>99:1)
4	I-indole, 2-py **105d**	Ph-CF=CF₂ **128a**	I-indole-2-py product **159da**	83[b] (98:2)
5	indole, 2-py **105a**	thienyl-CF=CF₂ **128b**	indole-2-py thiophene product **159ab**	96 (96:4)
6	indole, 2-py **105a**	thienyl-CF=CF₂ **128c**	indole-2-py thiophene product **159ac**	99 (90:10)
7	indole, 2-py **105a**	naphthyl-CF=CF₂ **128d**	indole-2-py naphthyl product **159ad**	51 (92:8)[c]
8	indole, 2-py **105a**	anthracenyl-CF=CF₂ **128e**	indole-2-py anthracenyl product **159ae**	---

[a] Reaction conditions: **105a** (0.50 mmol), **128a** (0.75 mmol), [Co] (2.5 mol %), K_2CO_3 (1.00 equiv), TFE (0.5 mL, 1.0 M), 25 °C, 20 h, isolated yield; *Z/E*-ratios in parentheses, determined by ¹H-NMR spetroscopy. [b] At 50 °C. [c] At 70 °C.

Remarkably, under the same reaction conditions as well as the reported one by *Loh* and coworkers,[168d] rhodium(III) catalysis was clearly shown to be less efficient. Indeed, the desired product **159aa** was delivered with the same excellent diastereoselectivity of *Z/E* > 99:1, but with a considerably reduced efficacy (Scheme 71). The exact reason for this significant difference has yet not been fully elucidated. It can be speculated that the increased nucleophilicity of the cobalt-carbon bond (*Pauling*-electronegativity of cobalt is $\chi_F \approx 1.9$ and for rhodium it is $\chi_F \approx 2.3$)[62] presumably enables an

accelerated migratory insertion of the very polarized 1,1-difluorostyrene **128a** into the carbon-cobalt bond.[115]
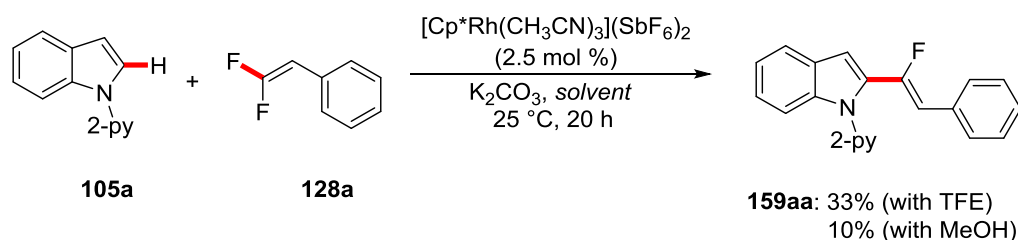

Scheme 71. Performance of a rhodium(III) catalyst in C–H/C–F functionalizations at 25 °C.

3.4.5   Mechanistic Studies

3.4.5.1   H/D-Exchange Experiments

Initially, a H/D-exchange study was conducted with deuterated 2-pyridylindole [D]$_1$-**105a** in the presence of TFE as solvent and proton source (Scheme 72). In the reisolated starting material **105a** and the product **158aa** minor amounts of deuterium incorporation in C3-positions were detected, which was previously observed for the cobalt(III)-catalyzed C–H/C–C functionalization as well (*cf.* Scheme 55). This finding might be explained by an electrophilic activation at the C3-position with cobalt(III) and subsequent deutero-demetalation. In contrast to previous observations, no deuteration was detected in the C7-position, which is possibly due to the kinetically unfavored formation of a six-membered cobaltacycle at the lower reaction temperature. It is noteworthy that almost full protonation in C2-position of the reisolated starting material was observed, which indicated that the C–H activation step is fully reversible and not turnover-limiting. Furthermore, it should be mentioned that no H/D-scrambling in any position of the perfluoroalkyl chain could be detected. These results might suggest that the migratory insertion is irreversible.
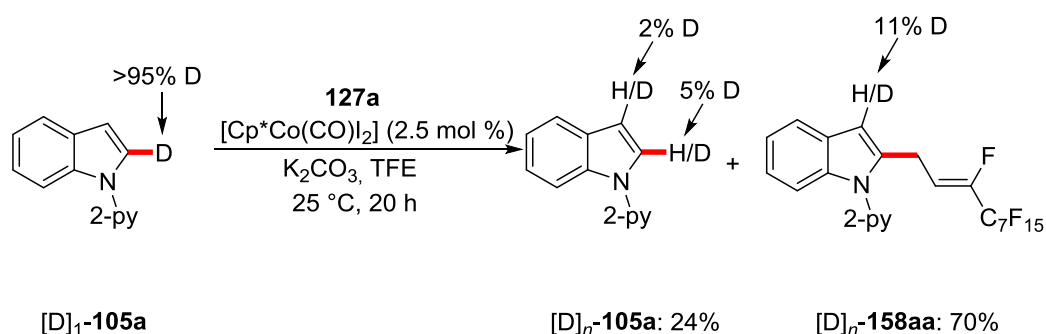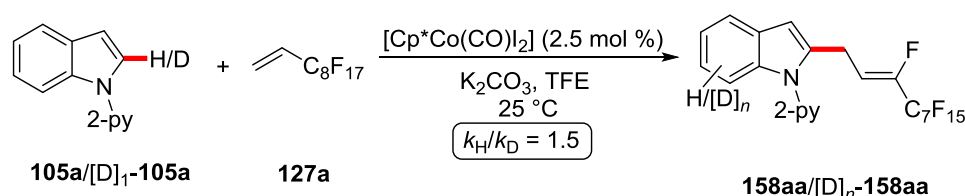

Scheme 72. H/D-exchange study for the cobalt(III)-catalyzed allylative C–H/C–F functionalization.

3.4.5.2   KIE Studies

The KIE of the allylative cobalt(III)-catalyzed C–H/C–F functionalization was determined by comparison of independent reaction rates for substrate **105a** and its isotopically labeled analogue [D]$_1$-**105a**, resulting in a value of $k_H/k_D \approx 1.5$ (Scheme 73 and Figure 25). The KIE value is in good agreement with the H/D-exchange experiment, which altogether indicate that the C–H activation is

facile and reversible. Nevertheless, the slightly larger KIE as compared to previously studied reactions (*cf.* Figure 11) leads to the mechanistic hypothesis that the C–H activation could be a kinetically relevant equilibrium step before the turnover-limiting migratory insertion.

Scheme 73. KIE study of the allylative cobalt(III)-catalyzed C–H/C–F functionalization.
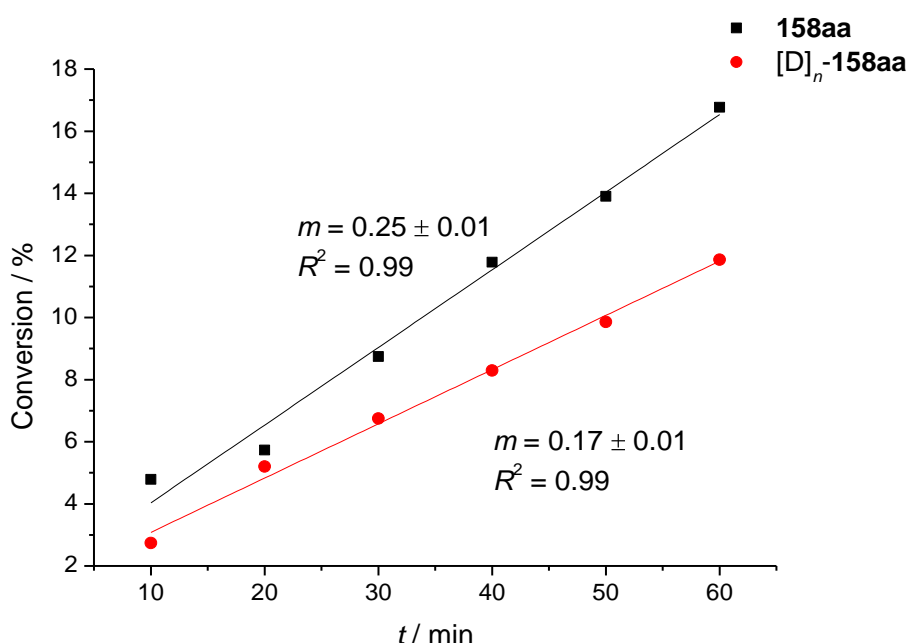

Figure 25. KIE study of the allylative cobalt(III)-catalyzed C–H/C–F functionalization.

3.4.5.3   Intermolecular Competition Experiments

To gain further insight regarding the C–H activation mechanism, an intermolecular competition experiment between the electron-rich substrate **18a** and electron-poor trifluoromethyl-substituted **18b** was conducted (Scheme 74).

Importantly, a strong preference for the electron-rich substrate **18a** was found which reacted almost four times faster than the corresponding electron-poor substrate **18b**. Along with the slightly higher KIE of 1.5, this finding reveals that the C–H activation possibly follows a BIES-type pathway, which is clearly favored for electron-rich substrates. Furthermore, a kinetically relevant migratory insertion, which benefits from a more nucleophilic carbon-cobalt bond in electron-rich substrates, could be a reasonable explanation for this reactivity trend.
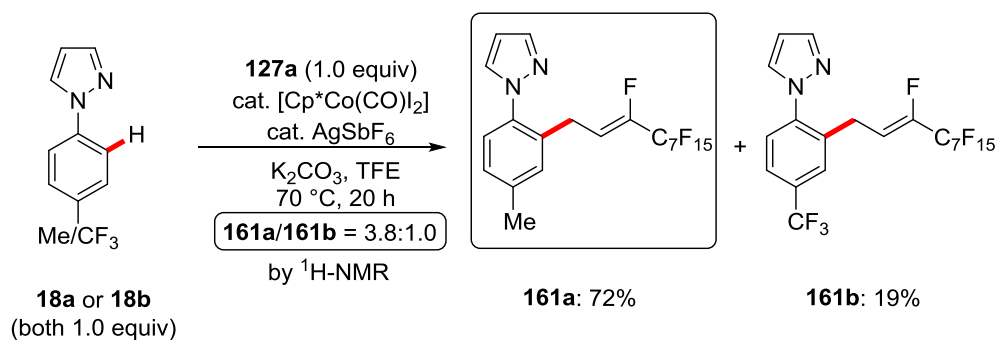
Scheme 74. Intermolecular competition experiment.

3.4.6   Proposed Catalytic Cycle

In summary, the C–H activation presumably occurs *via* a reversible and facile BIES-type pathway, in which the C–H cleavage likely is assisted by the carbonate, which *in situ* forms the active cobalt(III)carbonate catalyst **162**. Afterwards, the generated cobaltacycle **163** first undergoes a reversible coordination of the perfluoroalkylalkene **127a** to furnish intermediate **164**. Thereafter, a migratory insertion into the cobalt-carbon bond proceeds to form intermediate **165**. The migratory insertion step is proposed to be irreversible because the H/D-exchange study revealed no H/D-scrambling in the perfluoroalkylalkene side-chain (Scheme 72). Afterwards, a process involving the *β*-fluoride elimination[119f] and reaction with the initially formed bicarbonate regenerates the active catalytic species **162** and releases the product **158aa**. In principle, the same sequence of elementary steps can be proposed for the alkenylative C–H/C–F functionalization.
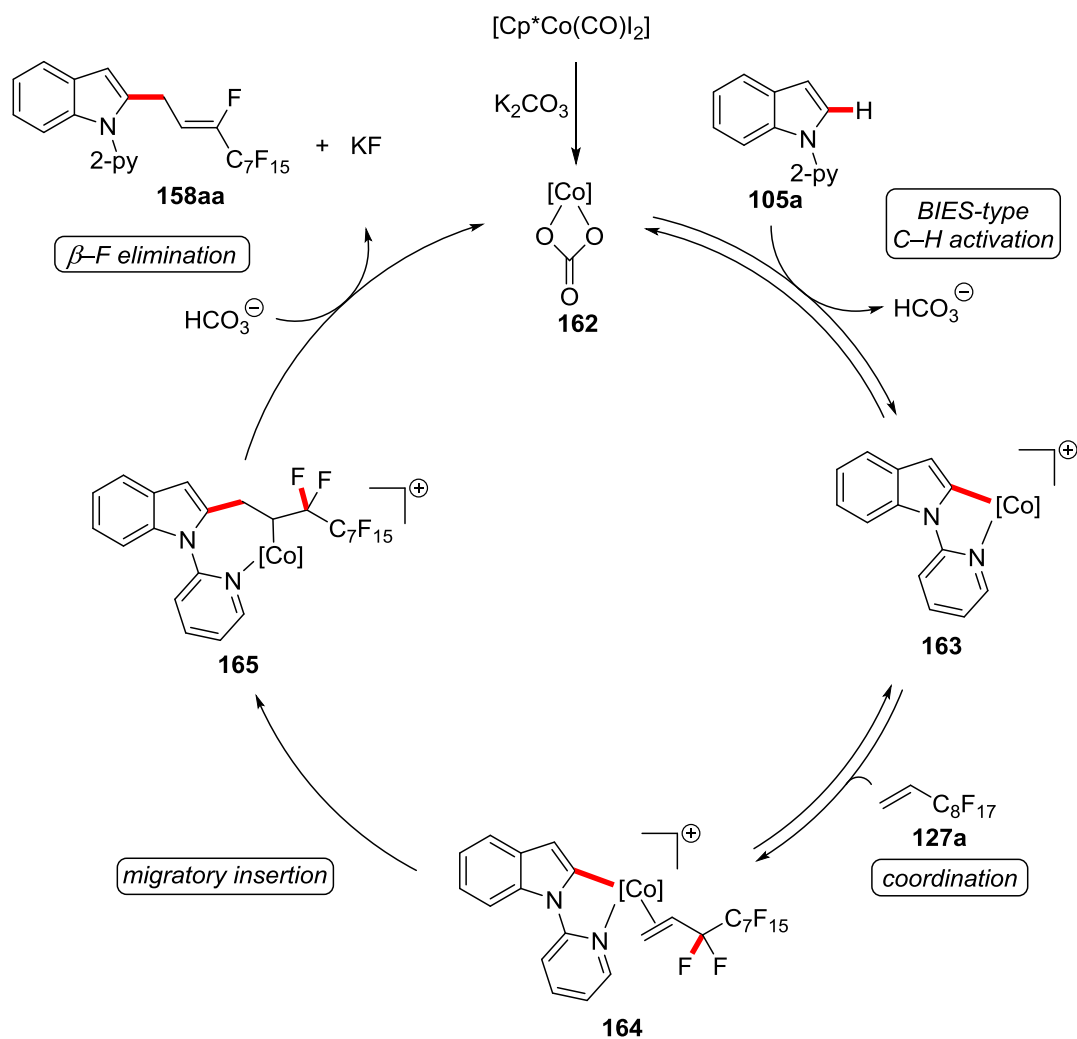
Figure 26. Proposed catalytic cycle for the cobalt(III)-catalyzed allylative C–H/C–F functionalization. [Co] = Cp*Co^{III}.

3.5 Manganese(I)-Catalyzed Allylative C–H/C–F Funtionalizations

The use of very inexpensive and less toxic[54, 92] manganese complexes in catalysis has been intensively studied in recent years.[14] In this regard, it has been reported that manganese catalysts allowed for C–H/C–Het functionalizations by β-oxygen, -nitrogen or -carbon elimination.[108, 117a, 117d] As it was previously reported, β-fluoride elimination is a feasible process[119] that allows for the metal-catalyzed installation of fluorine into organic molecules. Thus, it appears to be very attractive to explore the efficiency of manganese catalysts for allylative and alkenylative C–H/C–F functionalizations[168] on a variety of valuable substrates. Additionally, detailed mechanistic studies should eventually lead to the development of related C–H/C–Het transformations.

3.5.1 Optimization Studies for Indoles as Substrates

The optimization study for the desired transformation was commenced by screening various solvents, initially with unsatisfactory yields of the desired product **158aa** (Table 24, entries 1–6). In stark contrast, 1,4-dioxane turned out to be the optimal solvent for this reaction (entry 7) and by far outcompeted other prevalent solvents for manganese(I)-catalyzed C–H activations, such as DCE and n-Bu$_2$O. Subsequently, the effect of bases was probed which were shown to be essential for an efficient conversion (entry 8). Stronger bases like calcium and potassium hydroxide only performed poorly to moderately, with the same observation for potassium phosphate (entries 9–11). These findings are comparable with a related cobalt(III)-catalyzed reaction (*cf*. chapter 3.4.1) and clearly demonstrate that no direct correlation between reactivity and base strength was observed for this transformation. In this manner, also considerably weaker bases like potassium hydrogen carbonate and sodium acetate, which is a common base in manganese(I)-catalyzed C–H activation catalysis,[14] displayed a moderate to good reactivity (entries 12 and 13). As it has been previously observed (*cf*. Table 7 and Table 24), a comparison between several alkali metal carbonates showed that the reactivity increased from lithium to potassium carbonate, but significantly dropped, when heavier analogues like rubidium and cesium carbonate were employed (entries 15–18). Notably, qualitative solubility experiments in 1,4-dioxane revealed an increasing solubility of alkali metal fluorides as well as carbonates from lithium to cesium salts. This observation is in good agreement with the previously observed trend for the cobalt(III)-catalyzed C–H/C–F functionalization in TFE (*cf*. chapter 3.4.1). Finally, a reaction in the absence of the manganese(I) catalyst afforded no detectable amounts of the desired product **158aa** (entry 19). It is noteworthy that the diastereoselectivity of $Z/E = 90{:}10$ was found unaltered by the probed reaction conditions.

Table 24. Optimization for the manganese(I)-catalyzed allylative C–H/C–F functionalization.
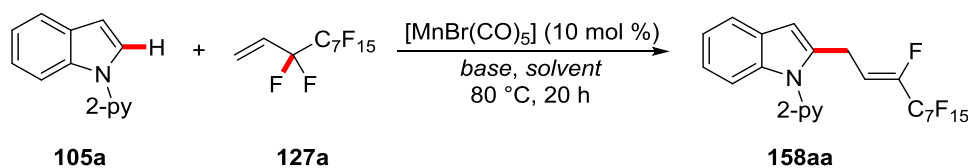
| Entry	base	solvent	yield / %[a]
1	K_2CO_3	DCE	23
2	K_2CO_3	TFE	8
3	K_2CO_3	PhMe	6
4	K_2CO_3	acetone	23
5	K_2CO_3	H_2O	14
6	K_2CO_3	*n*-Bu$_2$O	14
7	K_2CO_3	1,4-dioxane	97
8	---	1,4-dioxane	7
9	$Ca(OH)_2$	1,4-dioxane	37
10	KOH	1,4-dioxane	78
11	K_3PO_4	1,4-dioxane	19
12	$KHCO_3$	1,4-dioxane	70
13	NaOAc	1,4-dioxane	52
14	K_2CO_3	1,4-dioxane	45[b]
15	Li_2CO_3	1,4-dioxane	8
16	Na_2CO_3	1,4-dioxane	92
17	Rb_2CO_3	1,4-dioxane	25
18	Cs_2CO_3	1,4-dioxane	5
19	K_2CO_3	1,4-dioxane	---[c]

[a] Reaction conditions: **105a** (0.50 mmol), **127a** (0.60 mmol), [MnBr(CO)$_5$] (10 mol %), base (0.50 mmol), solvent (0.5 mL, 1.0 M), 20 h, isolated yield; all *Z/E* = 90:10, determined by ¹H-NMR spectroscopy. [b] At 50 °C. [c] Without [Mn].

3.5.2   Optimization Studies for Ketimines as Substrates

Ketimines **6** are a powerful and transformable class of directing groups[14a, 175] which could give access to the corresponding ketones **166** after hydrolysis. Thus, a comprehensive optimization study with

mainly *para*-methoxyphenyl- (PMP)-substituted ketimines **6** was attempted (Table 25). Indeed, the desired ketone **166aa** was furnished even in the absence of any base additive (entry 1). To increase the reactivity, acetate bases were utilized (entries 2 and 3), revealing the sodium salt to be optimal, as it was reported before for manganese-catalyzed C–H activations.[14] Furthermore, the influence of the reaction temperature was probed, giving optimal yields at 105 °C (entry 5). In contrast, higher reaction temperatures, such as 120 °C, led to a slight decrease in yield. However, the observed reactivity difference was overall less pronounced. Interestingly, an increase of the perfluoroalkylalkene **127a** concentration turned out to be the optimal condition (entry 8). Importantly, in the absence of manganese(I) catalysis no reactivity was observed (entry 9). A variation of the protecting group to more electron-rich TMP (3,4,5-trimethoxyphenyl) provided the corresponding product **166aa** with a slight decrease in yield (entry 10). The dimeric manganese precursor [$Mn_2(CO)_{10}$] showed some catalytic activity, albeit the product **166aa** was delivered in only unsatisfactory yield (entry 11).

Table 25. Optimization for the allylative C–H/C–F functionalization of ketimines **6**.
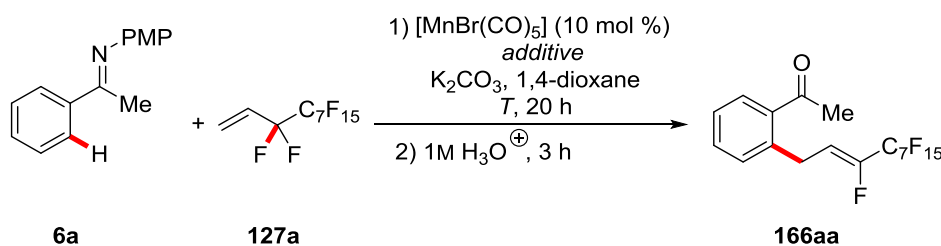
Entry	additive	T / °C	yield / %[a]
1	---	120	8[b]
2	NaOAc	120	44
3	KOAc	120	15
4	NaOAc	110	50
5	NaOAc	105	53
6	NaOAc	90	38
7	NaOAc	105	54[c]
8	NaOAc	105	72[d]
9	NaOAc	105	---[e]
10	NaOAc	105	61[d,f]
11	NaOAc	105	32[g]

[a] Reaction conditions: **6a** (0.50 mmol), **127a** (0.75 mmol), [MnBr(CO)$_5$] (10 mol %), additive (40 mol %), base (0.50 mmol), solvent (0.50 mL, 1.00 M), 20 h, isolated yield; all *Z/E* = 97:3, determined by ^{1}H-NMR

spectroscopy. [b] Without K_2CO_3. [c] 2.00 equiv of **127a**. [d] 3.00 equiv of **127a**. [e] Without [Mn]. [f] With TMP-substituted ketimine. [g] $[Mn_2(CO)_{10}]$ (5.0 mol %) as catalyst.

### 3.5.3   Scope of the Allylative C–H/C–F Functionalizations

Subsequently, an extensive study on the scope for the allylative and alkenylative manganese(I)-catalyzed C–H/C–F functionalization on 2-pyridylindoles **105** was carried out by *U. Dhawa* and *V. Müller*, including various heterocycles like pyrroles, pyrazoles, tryptophan-derivatives, and dipeptides.[176] These results highlighted the broad applicability and excellent functional group tolerance of the optimized catalytic system.

Besides these significant advances, a strong focus has been directed at the generality of the catalytic reaction with respect to valuable ketimines **6** (Table 26). Initially, the change of methyl- to ethyl-substituted ketimine **6b** altered the yield of the desired product **166b** only marginally (entries 1 and 2). Subsequently, different substituents in *para*-position to the directing group were tested (**6c–h**, entries 3–8), revealing no clear trend concerning the electronic properties of the functionalized ketimine **6**, with overall moderate to good yields. Interestingly, the sterically congested naphthalene-derived ketimine **6i** afforded the corresponding product **166i** with moderate yield, but an excellent diastereoselectivity (entry 9). Notably, the *meta*-fluorine substituted ketimine **6j** delivered the corresponding product *via* C–H activation at the more acidic *ortho*-position next to fluorine, indicating a CMD-type C–H activation pathway to be likely (entry 10). This assumption is in agreement with the finding that there is no clear preference for electron-rich substrates (*vide supra*) as it would be indicative for a BIES-type C−H activation. In contrast, a BIES-type pathway has been previously shown as a potential C–H activation mechanism in manganese-catalyzed C–H functionalizations.[14a, 117d] Thereafter, a methylene-dioxy substituent of the ketimine **6k** presumably acted as a secondary directing group to direct the manganese(I) catalyst by the *Lewis* basic oxygen to the sterically more congested position (entry 11). This site-selectivity is well-established for *inter alia* manganese catalysis.[106, 108] In summary, all ketimines **6** reacted with excellent diastereoselectivities and moderate to good yields.

Table 26. Scope of the manganese(I)-catalyzed allylative C–H/C–F functionalization of ketimines **6**.

entry	ketimine	**6**	product	**166**	*Z/E*	yield[a] [%]
1		**6a**		**166a**	97:3	72
2		**6b**		**166b**	97:3	65
3		**6c**		**166c**	97:3	63
4		**6d**		**166d**	97:3	51
5		**6e**		**166e**	97:3	47
6		**6f**		**166f**	97:3	69
7		**6g**		**166g**	97:3	71
8		**6h**		**166h**	97:3	74

9		**6i**		**166i**	98:2	60
10		**6j**		**166j**	97:3	53
11		**6k**		**166k**	98:2	65
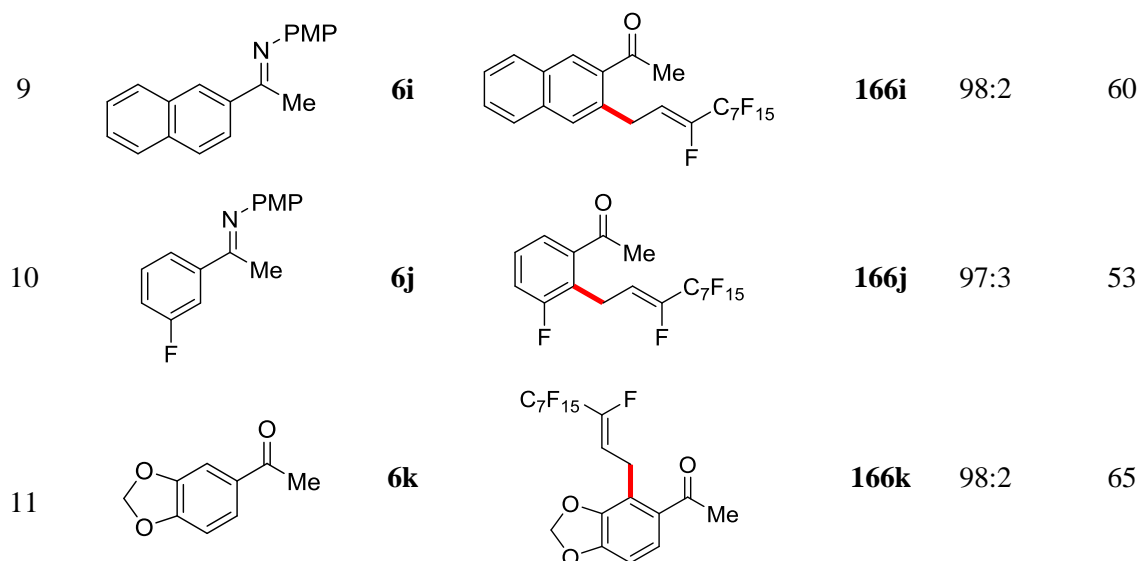
[a] Reaction conditions: **6** (0.50 mmol), **127a** (1.50 mmol), [MnBr(CO)$_5$] (10 mol %), NaOAc (40 mol %), K$_2$CO$_3$ (0.75 mmol), 1,4-dioxane (0.5 mL, 1.0 M), 105 °C, 20 h, isolated yield; *Z/E* ratios determined by ^{1}H-NMR spectroscopy.

Moreover, under the optimized reaction conditions, a removable[177] phenylpyrazole **18** was successfully converted with high yield and good diastereoselectivity (Scheme 75).
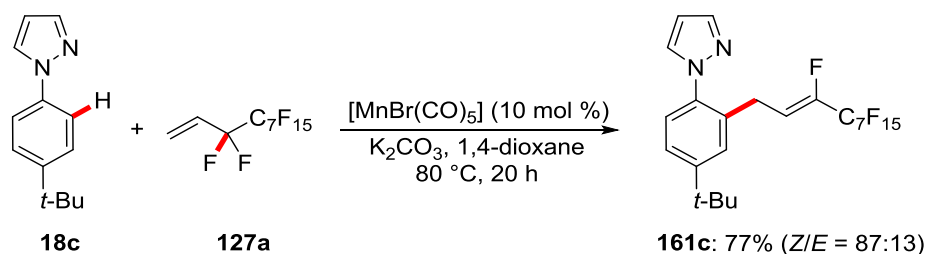
Scheme 75. Manganese(I)-catalyzed C–H/C–F functionalization of phenylpyrazoles **18**.

3.5.4 Mechanistic Studies

3.5.4.1 H/D-Exchange Experiments

To delineate the manganese(I) catalysts mode of action, H/D-exchange experiments in either the presence of fully isotopically labeled CD$_3$OD (Scheme 76a) or partly deuterated CD$_3$OH (Scheme 76b) were conducted. By using CD$_3$OD, a minor deuteration in both C3-positions of the reisolated starting material **105a** and the product **158aa** was detected. This H/D-exchange presumably proceeded through an electrophilic activation pathway, which is less pronounced for manganese(I) catalysis than in the case of the more electrophilic cobalt(III) catalyst (*cf.* Scheme 59). Considerably stronger H/D exchange was observed in C2-position of the reisolated starting material **105a**, indicating a reversible C–H bond activation step to be operative. In presence of the partly deuterated CD$_3$OH (Scheme 76b), no deuterium incorporation in any position was found by means of ^{1}H-NMR spectroscopy. This

finding supports that the H/D-exchange by using CD$_3$OD cannot originate from a radical mechanism, but rather from an organometallic C–H activation by manganese catalysis.
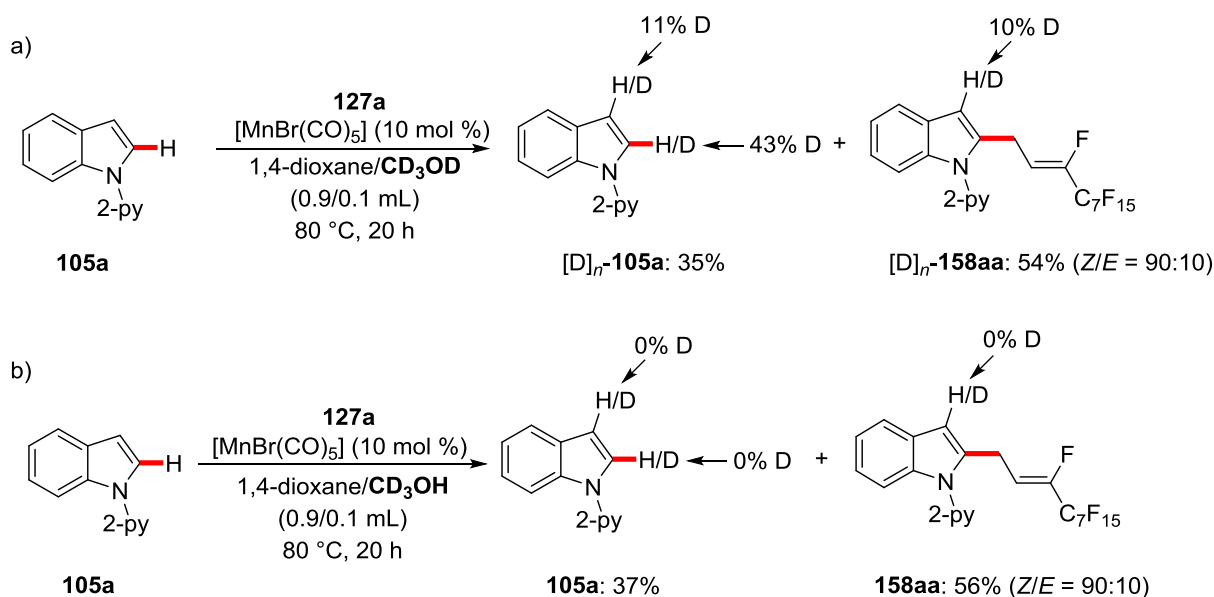
Scheme 76. H/D-exchange experiments with a) CD$_3$OD and b) CD$_3$OH.

3.5.4.2 KIE Studies

Subsequently, a KIE experiment by comparison of the initial rates of independent reactions with substrate **105a** and its deuterated analogue [D]$_1$-**105a** was conducted (Scheme 77 and Figure 27). The experiments revealed a KIE of $k_H/k_D = 1.1$, showing that the C–H activation event is facile and not turnover-limiting.
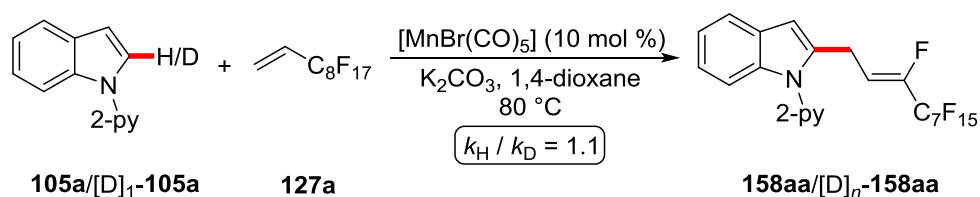
Scheme 77. KIE-experiment for the manganese(I)-catalyzed C–H/C–F functionalization.
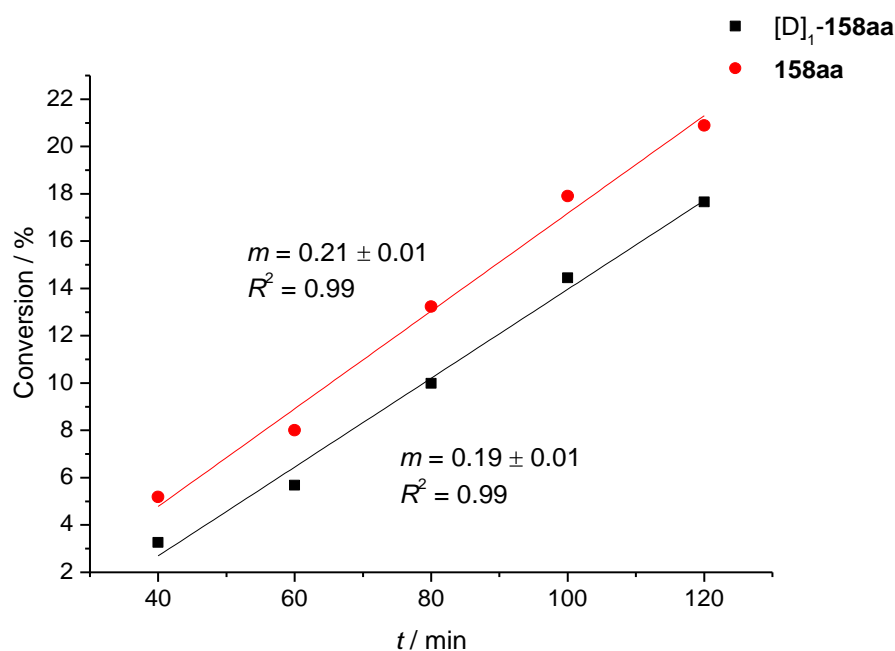
Figure 27. Conversion-time curves for the KIE-experiment.

3.5.4.3   Experiments with Cyclometalated Complexes

Furthermore, it was studied whether the desired product **158aa** can be provided by reaction of the perfluoroalkylalkene **127a** with the well-defined manganacycle **167** (Scheme 78). The reaction proved viable in an almost quantitative fashion with the same diastereoselectivity as for the catalytic transformation. Based on this result, a manganese(I)-catalyzed C–H activation pathway *via* the formation of manganacycle **167** can be assumed.

Moreover, the importance of the carbonate-base for subsequent elementary steps after the C–H activation was studied by performing the same reaction in the absence of base. The corresponding reaction displayed a slight decrease in yield, but the same diastereoselectivity was observed. This observation possibly indicates that the C–H activation step is assisted by the carbonate base, which is in full agreement with the poor reactivity of the catalytic reaction by omitting the base (*cf.* Table 24 entry 8). However, these findings cannot exclude a dual role of the carbonate base: On the one hand it could facilitate the C–H activation step, while on the other hand it could participate in a reaction to regenerate the active catalytic species and stabilize the fluoride anion by precipitation of potassium fluoride.

a)

b)
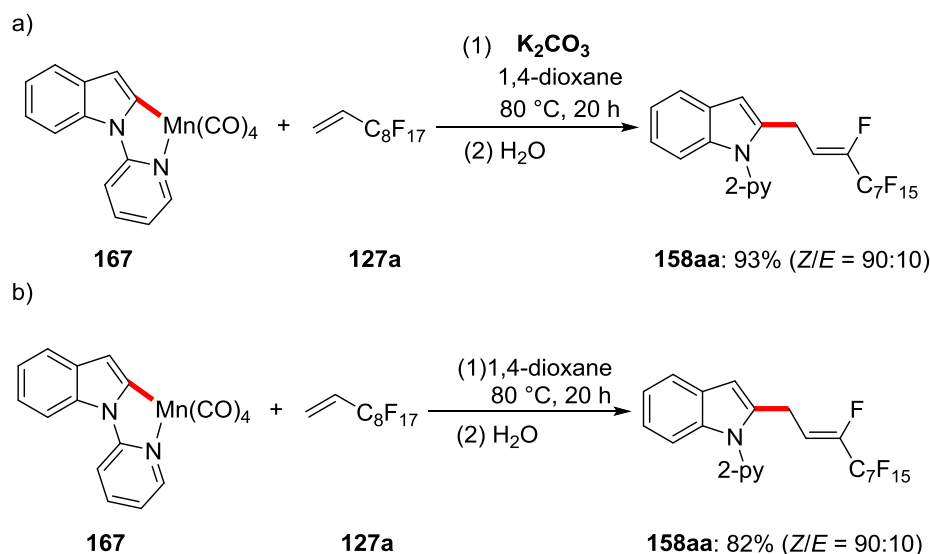
Scheme 78. Stoichiometric reaction of manganacycle **167** in a) the presence and b) absence of potassium carbonate.

In addition, a catalytic reaction with manganacycle **167** as the catalyst afforded the desired product **158aa** in good yield, which indicates that the manganese(I) complex **167** is possibly an intermediate in the catalytic cycle (Scheme 79).
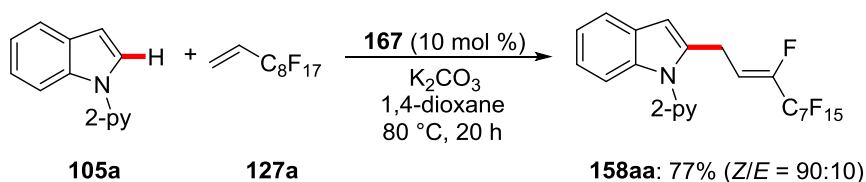

Scheme 79. Catalytic reaction with manganacycle **167** as catalyst.

3.5.5   Proposed Catalytic Cycle

In conclusion, the allylative manganese(I)-catalyzed C–H/C–F functionalization of indoles **105** most likely proceeds *via* a reversible and facile BIES-type mechanistic pathway, which is supported by the results obtained from the H/D-exchange experiments (Scheme 76) and the KIE study (Scheme 77). The active catalyst **168** is proposed to be a manganese(I) carbonate complex, in which the carbonate assists the deprotonation step in an intramolecular manner (Scheme 80). Likewise, DFT studies by *M. Bursch* and *S. Grimme* support a BIES-type C–H activation mechanism to proceed and notably to be favored in an intramolecular fashion by carbonate as internal base.[176] These studies contrast previous theoretical results by *Maseras* and *Echavarran*, who pointed out that the carbonate-assisted palladium-catalyzed C–H activation proceeds favorably *via* an intermolecular deprotonation.[178]

Thereafter, the manganacycle **169** is coordinated by the perfluoroalkylalkene **127a** in a rapid and reversible process. Subsequently, a migratory insertion into the manganese-carbon bond forms intermediate **171**. According to the H/D-exchange study, which disclosed no deuterium incorporation

in any position of the perfluoroalkylalkene side-chain, the migratory insertion is presumably an irreversible step (Scheme 76). Additionally, DFT-calculations by *M. Bursch* showed that the subsequent *β*-fluoride elimination step forms the preferred *Z*-configured product **158aa** and regenerate the active catalyst by the initially formed bicarbonate.[176] Future mechanistic investigations, including competition experiments, should reveal the C–H activation mechanism in the case of *e.g.* less electron-rich substrates like ketimines **6**. Interestingly, during the scope of ketimines **6** a preference for particularly acidic C–H bonds was found (Table 26, entry 10). These findings indicate that there might be rather a CMD- instead of BIES-type C–H activation operative for ketimines **6**.
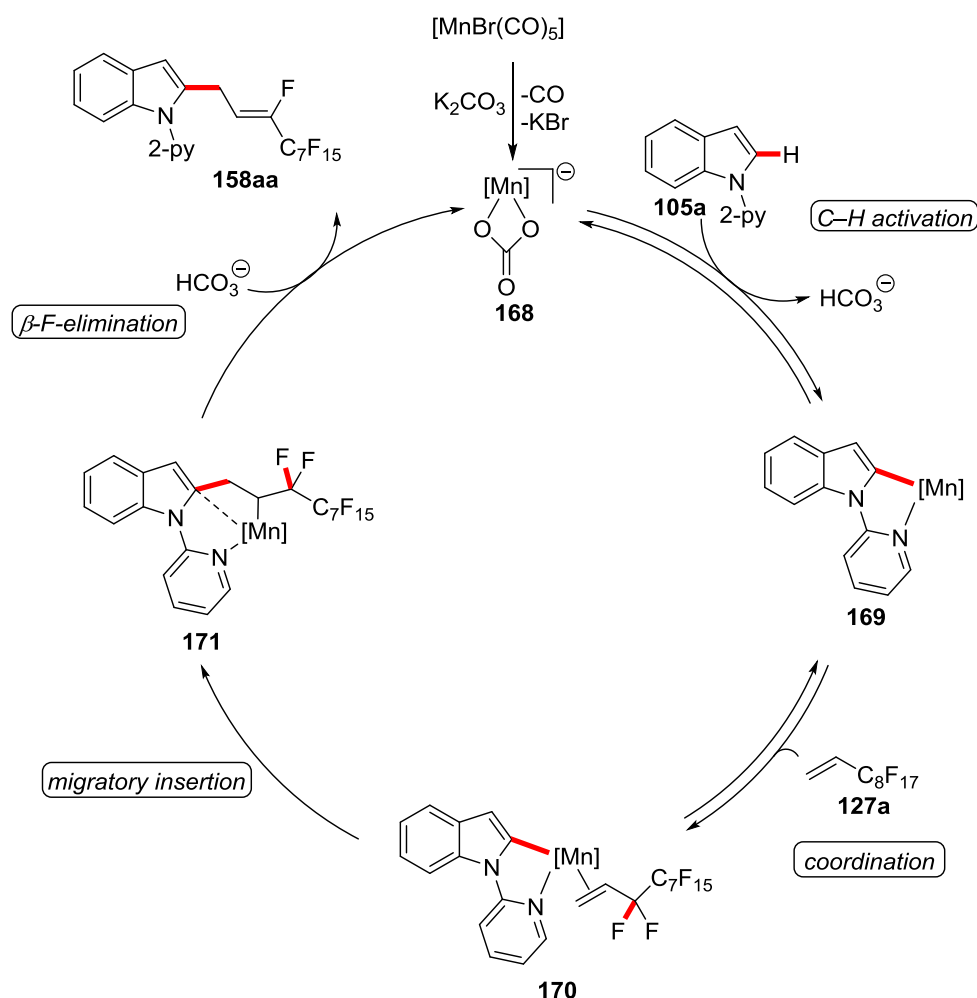
Scheme 80. Proposed catalytic cycle of the allylative manganese(I)-catalyzed C–H/C–F functionalization. [Mn] = Mn^I(CO)$_3$.

4   Summary and Outlook

The development of highly step- and atom-economical C–H functionalizations by inexpensive and earth-abundant metals streamlines organic synthesis and offers new tools for *inter alia* pharmaceutical, agrochemical chemistry, and material sciences. In this thesis, several new synthetic methods have been devised that reveal the remarkable efficiency and synthetic diversity of ruthenium(II), cobalt(III), and manganese(I) complexes in C−H activation catalysis.

In the first project, well-defined single component phosphinous acid (PA) complexes of ruthenium(II) have been employed as powerful catalyst for the C–H arylation of valuable and omnipresent alkene motifs, including challenging aryl chlorides **3** as arylating reagents (Scheme 81). For the first time, detailed kinetic studies, such as kinetic orders and *Hammett* plot analyses, revealed the mechanistic nature of the turnover-limiting step and gave hints on a SET-type C–X bond activation process.[123]
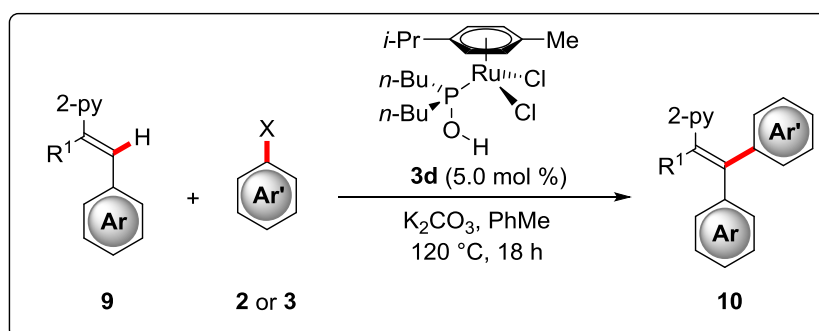
Scheme 81. Ruthenium(II)-PA-catalyzed C–H arylation of alkenes **9**.

These findings might give rise to the design of new tailor-made catalysts with enhanced efficiencies by adjusting the electronic features or attractive *London* dispersion and repulsive steric interactions on the easily modifiable phosphinous acid ligand. In this context, insightful studies concerning steric effects on the reactivity might be conducted, *e.g.* by comparing the buried volume of several PA ligands, which is a concept that has been developed for *inter alia* NHC and phosphine ligands by *Cavallo*.[179]

In the next project, a cobalt(III)-catalyzed C–H/C–C functionalization of valuable heteroarenes and arenes by using vinylcyclopropanes **125** was achieved (Scheme 82).[117b] Under very mild reaction conditions, the thermodynamically less stable *Z*-configured diastereomer was obtained in excellent yields as well as very good positional- and diastereoselectivities. In striking contrast to the analogous *E*-selective rhodium[117c] and manganese[117d] catalyses, this reaction appeared to be stereo-complementary, which bears great potential for new uniquely selective synthetic methods based on cobalt(III) catalysis.
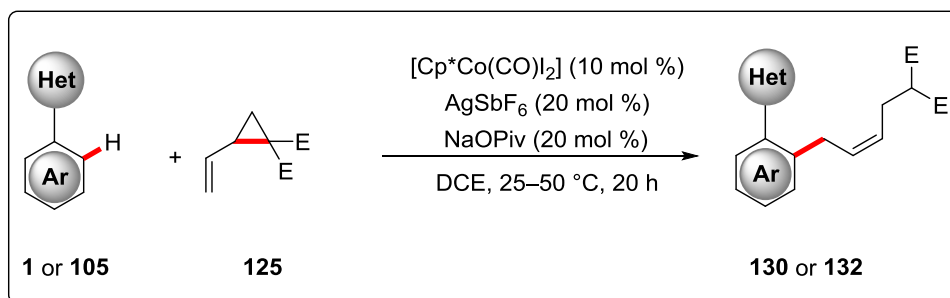
Scheme 82. Cobalt(III)-catalyzed C–H/C–C functionalization.

In the third project, a new concept for *Markovnikov/anti-Markovnikov* regiocontrol in C–H hydroarylations was devised (Scheme 83).[161] Here, the control of regioselectivity was accomplished by a tunable switch of the regiodetermining proto-demetalation step. Within this reaction, an expedient substrate scope was highlighted with excellent and fully complementary branched/linear selectivities, notably using unactivated alkenes. Likewise, extensive mechanistic studies, including detailed kinetic experiments, revealed a switch in the C–H activation manifold from a linear-selective LLHT to a branched-selective BIES-type pathway to be stereodiscriminating. Herein, *inter alia* a change from zeroth-order dependence on the concentration of indoles **105** for the branched- to a first order-dependence for the linear-selective regime supported the mechanistic hypothesis.
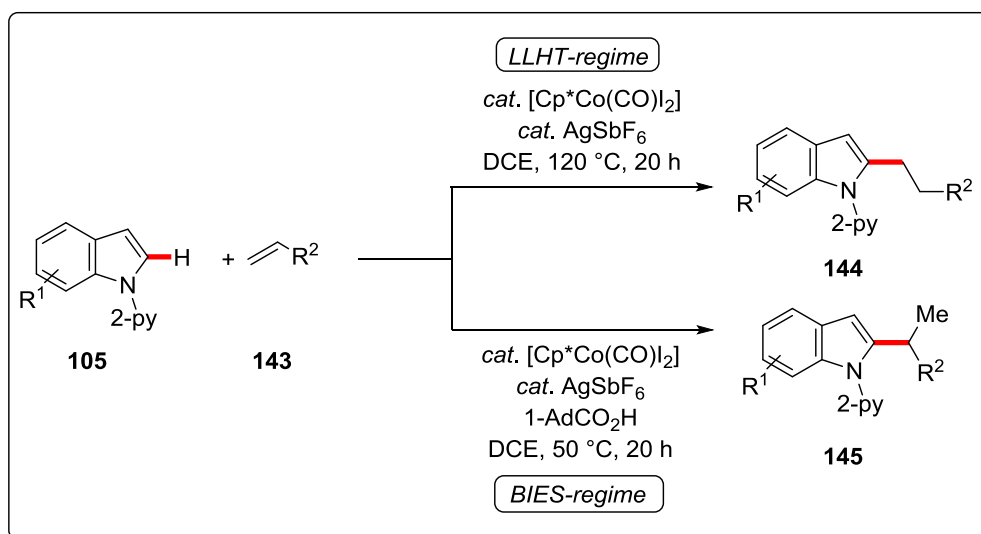
Scheme 83. Cobalt(III)-catalyzed branched/linear-selective C–H hydroarylation.

Based on this mechanistic insight, an enantioselective cobalt(III)-catalyzed hydroarylation protocol was developed by employing monoprotected amino acids (MPAAs). However, yields and enantioselectivities are overall rather moderate, which gives rise to the future development of more reactive and selective catalytic systems *e.g.* by using oligopeptides as additives.

Furthermore, cobalt(III)-catalyzed allylative and alkenylative C–H/C–F functionalizations were developed (Scheme 84).[174] A diverse set of perfluoroalkylalkenes **127** as well as valuable 1,1-difluoroalkenes **128** were successfully converted at 25 °C with ample scope and excellent functional

group tolerance. The products displayed good to excellent diastereoselectivities and the catalyst loading could be reduced to 0.25 mol % without loss of reactivity.
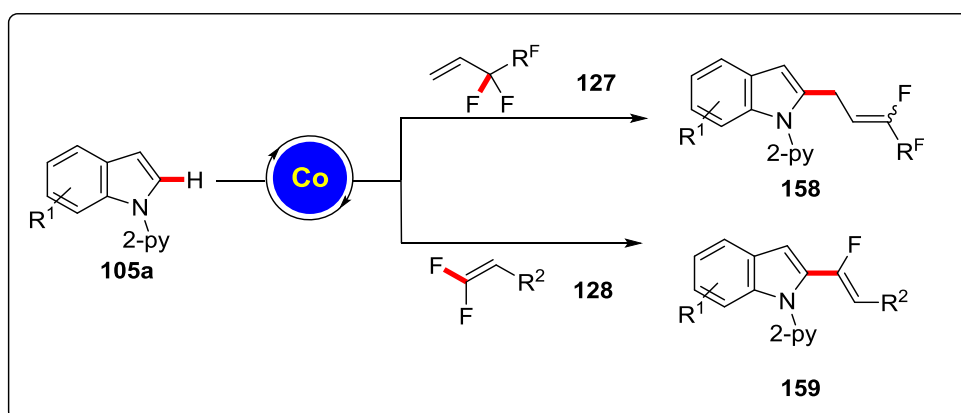
Scheme 84. Cobalt(III)-catalyzed allylative and alkenylative C–H/C–F functionalizations.

Finally, a manganese(I) complex, which obviates the use of costly Cp* ligands, was shown to be a competent catalyst in allylative and alkenylative C–H/C–F functionalizations, with overall excellent and improved diastereoselectivities as compared to the analagous cobalt(III) catalysis (Scheme 85).[176] The reaction displayed a broad applicability, including the functionalization of valuable and easily transformable ketimines **6**. Regarding a future prospect, the development of *e.g.* manganese(I)carboxylate complexes might be of great importance for studying the selectivity control in this and related reactions.
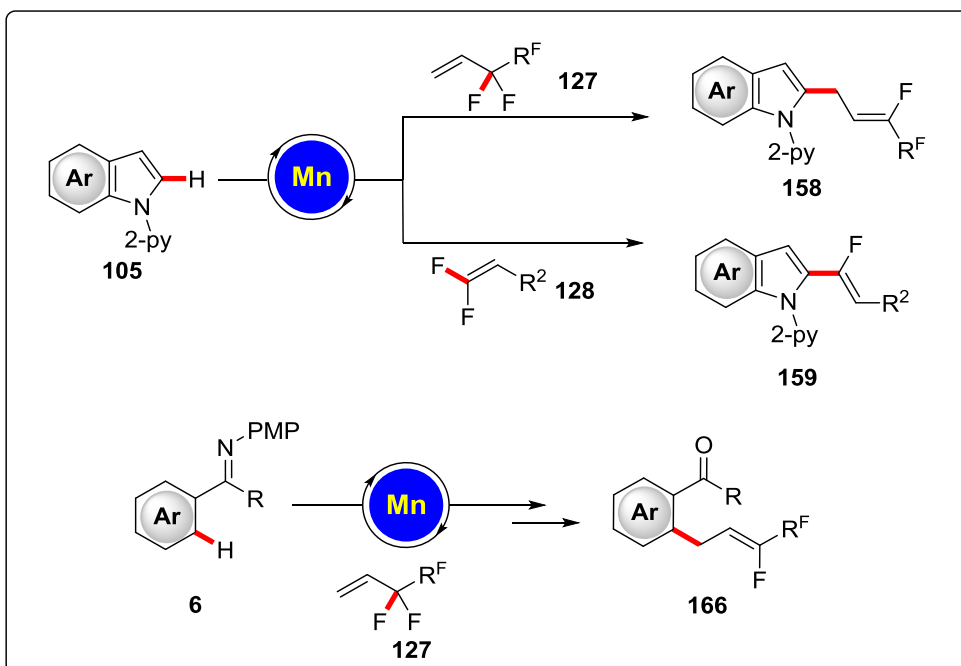
Scheme 85. Manganese(I)-catalyzed allylative and alkenylative C–H/C–F functionalizations.

5 Experimental Section

5.1 General Remarks

All reactions involving moisture- or air-sensitive reagents or products were performed under an atmosphere of nitrogen using pre-dried glassware and standard Schlenk techniques. If not otherwise mentioned, yields refer to isolated compounds, estimated to be >95% pure as determined by ^{1}H-NMR.

Vacuum

The following uncorrected pressures were measured on the used vacuum pump: membrane pump vacuum (MPV): 0.5 mbar, oil pump vacuum (OPV): 0.1 mbar.

Melting Points

Melting points were measured using a *Stuart® Melting Point Apparatus SMP3* from BARLOWORLD SCIENTIFIC. Values are uncorrected.

Column and HPLC-Chromatography

Analytical thin layer chromatography (TLC) was performed on MERCK, silica gel *60 F254* aluminum plates. Detection was performed under UV light at 254 nm or by treatment with a $KMnO_4$ solution. Chromatographic purification of products was accomplished by flash column chromatography on MERCK silica gel, grade 60 (0.040–0.063 mm and 0.063–0.200 mm, 70–230 mesh ASTM). Analytical High-Performance-Liquid-Chromatography (HPLC) for determination of enantiomeric excess was conducted on an AGILENT *1260 Infinity* system with *Chiralpak IC-3*® and *IF-3*® from DAICEL (both 3.0 μm particle size; Ø = 4.6 mm and length = 250 mm) as columns.

Gel permeation chromatography (GPC)

GPC purifications were performed on a JAI system (JAI-*LC-9260 II NEXT*) equipped with two sequential columns (*JAIGEL-2HR*, gradient rate: 5.000; *JAIGEL-2.5HR*, gradient rate: 20.000; internal diameter = 20 mm; length = 600 mm; Flush rate = 10.0 mL/min and chloroform (HPLC-quality with 0.6% ethanol as stabilizer) was used as the eluent.

Gas Chromatography

Gas chromatography or coupled gas chromatography-mass spectrometry was performed on a *5890 Series II* GC system with mass detector *HP 5972* from HEWLETT-PACKARD, a *7890 GC* system with/without mass detector *5975C* (*Triplex-Axis-Detector*) or a *7890B GC* system coupled with a *5977A* mass detector, both systems from AGILENT TECHNOLOGIES.

Nuclear Magnetic Resonance Spectroscopy

Nuclear magnetic resonance (NMR) spectra were recorded on VARIAN *Inova 500, 600*, VARIAN *Mercury 300*, *VX 300*, VARIAN *Avance 300*, VARIAN *VNMRS 300* and BRUKER *Avance III 300*, *400* and *HD 500* spectrometers. All chemical shifts are given as δ-values in ppm relative to the residual proton peak of the deuterated solvent or its carbon atom, respectively. ^{1}H- and ^{13}C-NMR spectra were referenced using the residual proton or solvent carbon peak (see table), respectively. ^{13}C- and ^{19}F-NMR were measured as proton-decoupled spectra.

	^{1}H-NMR	^{13}C-NMR
$CDCl_3$	7.26	77.16
$[D]_6$-DMSO	2.50	39.52

The detected resonance-multiplicities were described by the following abbreviations: s (singlet), d (doublet), t (triplet), q (quartet), hept (heptet), m (multiplet) or analogous representations. The coupling constants J are reported in Hertz (Hz). Analysis of the recorded spectra was carried out with *MestReNova 10* software.

Infrared Spectroscopy

Infrared spectra were recorded at a BRUKER *Alpha-P ATR FT-IR* spectrometer. Liquid samples were measured as a film, solid samples neat. The analysis of the spectra was carried out using the software from BRUKER *OPUS 6*. The absorption is given in wave numbers (cm^{-1}) and the spectra were recorded in the range of 4000–400 cm^{-1}. *In situ*-IR studies were performed on METTLER TOLEDO *ReactIR™ 15* with an *iC IR 4.3* software.

Mass Spectrometry

Electron ionization (EI) and EI high resolution mass spectra (HR-MS) were measured on a *time-of-flight* mass spectrometer *AccuTOF* from JOEL. Electrospray ionization (ESI) mass spectra were recorded on an *Ion-Trap* mass spectrometer *LCQ* from FINNIGAN, a *quadrupole time-of-flight maXis* from BRUKER DALTONIC or on a *time-of-flight mass* spectrometer microTOF from BRUKER DALTONIC. ESI-HRMS spectra were recorded on a BRUKER *Apex IV* or a BRUKER *Daltonic 7T*, fourier transform ion cyclotron resonance (FTICR) mass spectrometer. The ratios of mass to charge (m/z) are indicated and intensities relative to the base peak ($I = 100$) are written in parentheses.

Solvents

All solvents for reactions involving moisture-sensitive reagents were dried, distilled and stored under inert atmosphere (Ar or N_2) according to the following standard procedures:

1,2-Dichloroethane was dried over CaH_2 for 8 h, degassed and distilled under reduced pressure.

Dichloromethane was purified using a solvent purification system (*SPS-800*) from M. BRAUN.

Diethyl ether was purified using a solvent purification system (*SPS-800*) from M. BRAUN.

1,4-Dioxane was distilled from sodium benzophenone ketyl.

1,1,1,3,3,3-Hexafluoropropan-2-ol was distilled from 3 Å molecular sieves.

Methanol was stirred over magnesium turnings at 65 °C for 3 h prior to distillation from $Mg(OMe)_2$.

***N*-Methyl-2-pyrrolidone** was stirred over CaH_2 at 200 °C for 4 h and distilled under reduced pressure.

Tetrahydrofuran was purified using a solvent purification system (*SPS-800*) from M. BRAUN.

Toluene was purified using a solvent purification system (*SPS-800*) from M. BRAUN.

2,2,2-Trifluoroethanol was stirred over $CaSO_4$ and distilled under reduced pressure.

Water was degassed by repeated *Freeze-Pump-Thaw* degassing procedure.

Reagents

Chemicals obtained from commercial sources with purity higher than 95% were used without further purification. The following literature-known compounds were synthesized based on previously described methods:

(*E*)-2-Styrylpyridines **9**,[180] SPOs,[178] ruthenium(II)-PA complexes,[123] ketimines **6**,[36c, 181] indoles **105**[182] and 2-phenylpyridines **1**.[183]

The following chemicals were kindly provided by the persons named below:

Uttam Dhawa: 4-methoxy-1-(pyridin-2-yl)-1*H*-indole (**105h**) and 5-methoxy-(pyridin-2-yl)-1*H*-indole (**105b**).

Weiping Liu: (*E*)-1-(4-methoxyphenyl)-*N*-(4-methoxyphenyl)ethan-1-imine (**6c**), (*E*)-1-(4-fluorophenyl)-*N*-(4-methoxyphenyl)ethan-1-imine (**6f**), (*E*)-1-(4-bromophenyl)-*N*-(4-methoxyphenyl)ethan-1-imine (**6g**) and (*E*)-1-(4-iodophenyl)-*N*-(4-methoxy-phenyl)ethan-1-imine (**6h**).

Tjark Meyer: [RuCl$_2$(*p*-cymene)(Ph$_2$POH)] (**124a**), [RuCl$_2$(*p*-cymene){(*p*-FC$_6$H$_4$)$_2$POH}] (**124b**).

Valentin Müller: 5-fluoro-1-(pyridin-2-yl)-1*H*-indole (**105m**) and 5-bromo-1-(pyridin-2-yl)-1*H*-indole (**105c**).

Karsten Rauch: [RuCl$_2$(*p*-cymene)]$_2$ and [Ru(O$_2$CMes)$_2$(*p*-cymene)] (**20**).

Svenja Warratz: [RuCl$_2$(*p*-cymene)(*t*-BuPhPOH)] (**124c**) and [RuCl$_2$(*p*-cymene)(*o*-Tol$_2$POH)] (**124g**).

5.1.1   General Procedure A: Ruthenium(II)-PA-Catalyzed C–H Arylation

A suspension of (*E*)-2-styrylpyridine **9** (0.50 mmol, 1.00 equiv), aryl bromide **2** (0.75 mmol, 1.50 equiv), [RuCl$_2$(*p*-cymene)(*n*-Bu$_2$POH)] (**124e**) (11.7 mg, 25.0 μmol, 5.00 mol %) and K$_2$CO$_3$ (138 mg, 1.00 mmol, 2.00 equiv) in PhMe (2.00 mL, 0.25 M) was stirred at 120 °C for 18 h. At ambient temperature, the mixture was diluted with EtOAc (5.0 mL), filtered over Celite and the solvents were removed *in vacuo*. Isolation by column chromatography on silica gel (*n*-hexane/EtOAc) yielded the corresponding products **10**.

5.1.2   General Procedure B: Cobalt(III)-Catalyzed C−H/C−C Functionalization

A suspension of indole **105** (0.50 mmol, 1.00 equiv), vinylcyclopropanes **125** (0.60 mmol, 1.20 equiv), [Cp*Co(CO)I$_2$] (23.8 mg, 50.0 μmol, 10.0 mol %), AgSbF$_6$ (34.4 mg, 100 μmol, 20.0 mol %) and NaOPiv (12.4 mg, 100 μmol, 20.0 mol %) in DCE (1.00 mL, 0.50 M) was stirred at 50 °C for 20 h. At ambient temperature, the solvent was removed *in vacuo* and the remaining residue was purified by column chromatography on silica gel (*n*-hexane/EtOAc) to yield the desired products **130**.

5.1.3   General Procedure C: Rhodium(III)-Catalyzed C−H/C−C Functionalization

A suspension of indole **105** (0.25 mmol, 1.00 equiv), vinylcyclopropane **125** (0.30 mmol, 1.20 equiv), [Cp*Rh(CH$_3$CN)$_3$](SbF$_6$)$_2$ (19.7 mg, 25.0 μmol, 10.0 mol %) and NaOPiv (6.20 mg, 50.0 μmol, 20.0 mol %) in DCE (1.00 mL, 0.25 M) was stirred at 50 °C for 20 h. At ambient temperature, the solvent was removed *in vacuo* and the remaining residue was purified by column chromatography on silica gel (*n*-hexane/EtOAc) to afford the desired products **130**.

5.1.4   General Procedure D: Cobalt(III)-Catalyzed Linear-selective C−H Alkylation

A suspension of indole **105** (0.50 mmol, 1.00 equiv), alkene **143** (1.50 mmol, 3.00 equiv), [Cp*Co(CO)I$_2$] (23.8 mg, 50.0 μmol, 10.0 mol %) and AgSbF$_6$ (34.4 mg, 100 μmol, 20.0 mol %) in DCE (1.00 mL, 0.50 M) was stirred at 120 °C for 20 h. At ambient temperature, the reaction mixture was diluted with EtOAc (5.0 mL) and the solvents were removed *in vacuo*. The remaining residue was purified by column chromatography on silica gel (*n*-hexane/EtOAc) to afford the desired products **144**.

5.1.5   General Procedure E: Cobalt(III)-Catalyzed Branched-Selective C−H Alkylation

A suspension of indole **105** (0.50 mmol, 1.00 equiv), alkene **143** (1.50 mmol, 3.00 equiv), [Cp*Co(CO)I$_2$] (23.8 mg, 50.0 μmol, 10.0 mol %), AgSbF$_6$ (34.4 mg, 100 μmol, 20.0 mol %) and 1-AdCO$_2$H (90.1 mg, 0.50 mmol, 1.00 equiv) in DCE (0.50 mL, 1.00 M) was stirred at 50 °C for 20 h. At ambient temperature, the reaction mixture was diluted with EtOAc (5.0 mL) and the solvents were removed *in vacuo*. The remaining residue was purified by column chromatography on silica gel (*n*-hexane/EtOAc) to yield the desired products **145**.

## 5.1.6 General Procedure F: Cobalt(III)-Catalyzed Allylative C−H/C–F Functionalization

A suspension of indole **105** (0.50 mmol, 1.00 equiv), perfluoroalkylalkene **127** (0.60 mmol, 1.20 equiv), [Cp*Co(CO)I$_2$] (6.00 mg, 12.5 µmol, 2.5 mol %) and K$_2$CO$_3$ (69.1 mg, 0.50 mmol, 1.00 equiv) in TFE (0.50 mL, 1.00 M) was stirred at 25 °C for 20 h. The mixture was diluted with EtOAc (5.0 mL), filtered over Celite and the solvents were removed *in vacuo*. Isolation by column chromatography on silica gel (*n*-hexane/EtOAc) afforded the desired products **158**.

5.1.7 General Procedure G: Cobalt(III)-Catalyzed Alkenylative C−H/C–F Functionalization

A suspension of indole **105** (0.50 mmol, 1.00 equiv), 1,1-difluoroalkene **128** (0.75 mmol, 1.50 equiv), [Cp*Co(CO)I$_2$] (6.00 mg, 12.5 µmol, 2.5 mol %) and K$_2$CO$_3$ (69.1 mg, 0.50 mmol, 1.00 equiv) in TFE (0.50 mL, 1.00 M) was stirred at 25 °C for 20 h. The mixture was diluted with EtOAc (5.0 mL), filtered over Celite and the solvents were removed *in vacuo*. Isolation by column chromatography on silica gel (*n*-hexane/EtOAc) afforded the desired products **159**.

5.1.8 General Procedure H: Manganese(I)-Catalyzed Allylative C−H/C−F Functionalization

A suspension of ketimine **6** (0.50 mmol, 1.00 equiv), perfluoroalkylalkene **127** (1.50 mmol, 3.00 equiv), [MnBr(CO)$_5$] (13.7 mg, 10.0 mol %), NaOAc (16.4 mg, 40 mol %) and K$_2$CO$_3$ (104 mg, 0.75 mmol, 1.50 equiv) in 1,4-dioxane (0.50 mL, 1.00 M) was stirred at 105 °C for 20 h. At ambient temperature, the mixture was diluted with EtOAc (5.0 mL), filtered over Celite and the solvents were removed *in vacuo*. The remaining residue was purified by column chromatography on silica gel (*n*-hexane/EtOAc) to furnish the desired products **166**.

5.2 Ruthenium(II)-PA-Catalyzed C–H Arylation of (*E*)-2-Styrylpyridines

5.2.1 Characterization Data
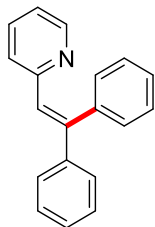
(*Z*)-2-(2,2-Diphenylvinyl)pyridine (10aa): The general procedure **A** was followed using (*E*)-2-styrylpyridine (**9a**) (90.5 mg, 0.50 mmol, 1.00 equiv) and 4-bromobenzene (**2a**) (118 mg, 0.75 mmol, 1.50 equiv). Isolation by column chromatography (*n*-hexane/EtOAc: 20/1) yielded **10aa** (103 mg, 80%) as a colorless solid.

M.p.: 206 °C.

^{1}H-NMR (300 MHz, CDCl$_3$): δ = 8.53 (ddd, *J* = 4.9, 1.9, 0.9 Hz, 1H), 7.36–7.27 (m, 9H), 7.23–7.16 (m, 2H), 7.14 (s, 1H), 6.97 (ddd, *J* = 7.4, 4.9, 1.1 Hz, 1H), 6.65 (ddd, *J* = 8.1, 1.1, 0.9 Hz, 1H).

^{13}C-NMR (75 MHz, CDCl$_3$): δ = 156.5 (C$_q$), 149.2 (CH), 145.8 (C$_q$), 142.6 (C$_q$), 139.8 (C$_q$), 135.3 (CH), 130.2 (CH), 128.8 (CH), 128.7 (CH), 128.3 (CH), 128.1 (CH), 127.8 (CH), 127.7 (CH), 123.7 (CH), 121.1 (CH).

IR (ATR): 1583, 1560, 1506, 1488, 1219, 774, 762, 698, 552, 504 cm^{-1}.

MS (EI) *m/z* (relative intensity): 257 ([M]$^+$, 40), 256 (100), 182 (10).

HR-MS (ESI): *m/z* calcd. for [C$_{19}$H$_{16}$N]$^+$ [M + H]$^+$ 258.1277, found 258.1280.

The spectral data are in accordance with those reported in the literature.[32]
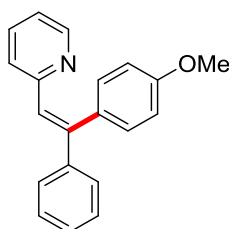
(*Z*)-2-[2-(4-Methoxyphenyl)-2-phenylvinyl]pyridine (10ab): The general procedure **A** was followed using (*E*)-2-styrylpyridine (**9a**) (90.5 mg, 0.50 mmol, 1.00 equiv) and 4-bromoanisole (**2b**) (140 mg, 0.75 mmol, 1.50 equiv). Isolation by column chromatography (*n*-hexane/EtOAc: 20/1) yielded **10ab** (138 mg, 96%) as a pale yellow solid.

M.p.: 111 °C.

^{1}H-NMR (300 MHz, CDCl$_3$): δ = 8.53 (ddd, *J* = 5.0, 1.9, 0.9 Hz, 1H), 7.39–7.29 (m, 6H), 7.16–7.08 (m, 3H), 7.04–6.96 (m, 1H), 6.92–6.85 (m, 2H), 6.76 (ddd, *J* = 8.1, 1.1, 0.9 Hz, 1H), 3.83 (s, 3H).

^{13}**C-NMR** (75 MHz, CDCl$_3$): δ = 159.1 (C$_q$), 156.7 (C$_q$), 149.0 (CH), 145.6 (C$_q$), 142.7 (C$_q$), 135.3 (CH), 131.9 (C$_q$), 131.3 (CH), 128.1 (CH), 128.0 (CH), 127.8 (CH), 127.8 (CH), 123.7 (CH), 121.0 (CH), 114.0 (CH), 55.3 (CH$_3$).

IR (ATR): 3054, 1603, 1508, 1465, 1244, 1026, 827, 773, 762, 540 cm^{-1}.

MS (EI) *m/z* (relative intensity): 287 ([M]$^+$, 40), 286 (100), 271 (10), 243 (20).

HR-MS (ESI): *m/z* calcd. for [C$_{20}$H$_{18}$NO]$^+$ [M + H]$^+$ 288.1383, found 288.1391.

The spectral data are in accordance with those reported in the literature.[184]
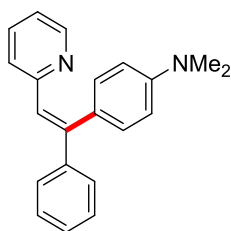
(***Z***)-***N***,***N***-**dimethyl-4-[1-phenyl-2-(pyridin-2-yl)vinyl]aniline (10ac):** The general procedure **A** was followed using (*E*)-2-styrylpyridine (**9a**) (90.5 mg, 0.50 mmol, 1.00 equiv) and 4-bromo-*N*,*N*-dimethylaniline (**2c**) (150 mg, 0.75 mmol, 1.50 equiv). Isolation by column chromatography (*n*-hexane/EtOAc: 20/1) yielded **10ac** (141 mg, 94%) as a yellow solid.

M.p.: 102 °C.

^{1}**H-NMR** (300 MHz, CDCl$_3$): δ = 8.53 (ddd, *J* = 4.9, 1.9, 0.9 Hz, 1H), 7.43–7.21 (m, 6H), 7.09–7.02 (m, 2H), 7.01 (s, 1H), 6.97 (ddd, *J* = 8.1, 1.1, 0.9 Hz, 1H), 6.87 (ddd, *J* = 8.1, 8.1, 1.1 Hz, 1H), 6.72–6.62 (m, 2H), 2.98 (s, 6H).

^{13}**C-NMR** (75 MHz, CDCl$_3$): δ = 157.3 (C$_q$), 149.9 (C$_q$), 149.1 (CH), 146.1 (C$_q$), 143.5 (C$_q$), 135.2 (CH), 131.1 (CH), 128.2 (CH), 128.1 (CH), 127.9 (CH), 127.6 (CH), 127.4 (C$_q$), 123.7 (CH), 120.8 (CH), 112.2 (CH), 40.3 (CH$_3$).

IR (ATR): 3046, 1603, 1577, 1558, 1519, 1431, 946, 766, 512 cm^{-1}.

MS (EI) *m/z* (relative intensity): 300 ([M]$^+$, 60), 299 (100), 283 (10), 149 (10).

HR-MS (ESI): *m/z* calcd. for [C$_{21}$H$_{21}$N$_2$]$^+$ [M + H]$^+$ 301.1699, found 301.1701.
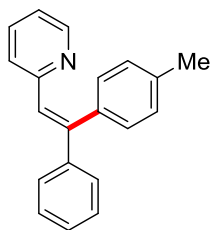
(***Z***)-**2-[2-(4-Methylphenyl)-2-phenylvinyl]pyridine (10ad):** The general procedure **A** was followed using (*E*)-2-styrylpyridine (**9a**) (90.5 mg, 0.50 mmol, 1.00 equiv) and 4-bromotoluene (**2d**) (128 mg,

0.75 mmol, 1.50 equiv). Isolation by column chromatography (*n*-hexane/EtOAc: 20/1) yielded **10ad** (126 mg, 93%) as a yellow solid.

M.p.: 86 °C.

^{1}H-NMR (300 MHz, CDCl$_3$): δ = 8.54 (ddd, J = 4.9, 1.9, 0.9 Hz, 1H), 7.37–7.25 (m, 6H), 7.16–7.08 (m, 5H), 6.97 (ddd, J = 7.5, 4.9, 1.1 Hz, 1H), 6.72 (ddd, J = 8.1, 1.1, 0.9 Hz, 1H), 2.39 (s, 3H).

^{13}C-NMR (75 MHz, CDCl$_3$): δ = 156.8 (C$_q$), 149.2 (CH), 145.8 (C$_q$), 142.8 (C$_q$), 137.5 (C$_q$), 132.8 (C$_q$), 135.2 (CH), 130.0 (CH), 129.4 (CH), 128.4 (CH), 128.2 (CH), 127.9 (CH), 127.8 (CH), 123.4 (CH), 121.0 (CH), 21.3 (CH$_3$).

IR (ATR): 3051, 1583, 1459, 775, 762, 697, 589, 521, 404 cm^{-1}.

MS (EI) *m/z* (relative intensity): 271 ([M]$^+$, 45), 270 (100), 254 (15), 127 (10).

HR-MS (ESI): *m/z* calcd. for [C$_{20}$H$_{18}$N]$^+$ [M + H]$^+$ 272.1434, found 272.1436.

The spectral data are in accordance with those reported in the literature.[184]
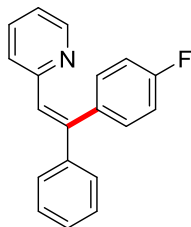
(*Z*)-2-[2-(4-Fluorophenyl)-2-phenylvinyl]pyridine (10ae): A modified general procedure **A** was followed at 140 °C using (*E*)-2-styrylpyridine (**9a**) (90.5 mg, 0.50 mmol, 1.00 equiv) and 1-bromo-4-fluorobenzene (**2e**) (131 mg, 0.75 mmol, 1.50 equiv). Isolation by column chromatography (*n*-hexane/EtOAc: 20/1) yielded **10ae** (127 mg, 92%) as a pale yellow solid.

M.p.: 95 °C.

^{1}H-NMR (300 MHz, CDCl$_3$): δ = 8.53 (ddd, J = 4.9, 1.9, 0.9 Hz, 1H), 7.42–7.28 (m, 6H), 7.21–7.12 (m, 3H), 7.09–6.98 (m, 3H), 6.71 (ddd, J = 8.1, 1.1, 0.9 Hz, 1H).

^{13}C-NMR (75 MHz, CDCl$_3$): δ = 162.5 (d, $^1J_{C-F}$ = 249 Hz, C$_q$), 156.5 (C$_q$), 149.5 (CH), 144.8 (C$_q$), 142.5 (C$_q$), 135.8 (C$_q$), 135.5 (CH), 132.0 (CH, d, $^3J_{C-F}$ = 8.0 Hz), 129.0 (CH), 128.4 (CH), 128.2 (CH), 127.8 (CH), 123.8 (CH), 121.3 (CH), 115.8 (CH, d, $^2J_{C-F}$ = 21.4 Hz).

^{19}F-NMR (282 MHz, CDCl$_3$): δ = −114.0 (tt, J = 8.7, 5.5 Hz).

IR (ATR): 1584, 1560, 1505, 1445, 1219, 1156, 760, 745, 588, 522 cm^{-1}.

MS (EI) *m/z* (relative intensity): 275 ([M]$^+$, 40), 274 (100).

HR-MS (ESI): *m/z* calcd. for [C$_{19}$H$_{15}$FN]$^+$ [M + H]$^+$ 276.1183, found 276.1187.

The spectral data are in accordance with those reported in the literature.[184]
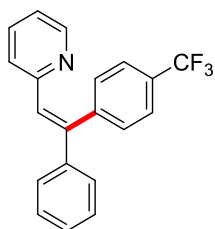
(Z)-2-{2-(4-(Trifluoromethyl)phenyl]-2-phenylvinyl}pyridine (10af): A modified general procedure **A** was followed at 140 °C using (*E*)-2-styrylpyridine (**9a**) (90.5 mg, 0.50 mmol, 1.50 equiv) and 1-bromo-4-(trifluoromethyl)benzene (**2f**) (169 mg, 0.75 mmol, 1.50 equiv). Isolation by column chromatography (*n*-hexane/EtOAc: 20/1) yielded **10af** (115 mg, 71%) as a pale yellow solid.

M.p.: 75 °C.

^{1}H-NMR (300 MHz, CDCl$_3$): δ = 8.53 (ddd, *J* = 4.9, 1.9, 0.9 Hz, 1H), 7.60 (d, *J* = 7.9 Hz, 2H), 7.41–7.27 (m, 8H), 7.20 (s, 1H), 7.03 (ddd, *J* = 7.4, 4.9, 1.1 Hz, 1H), 6.72 (ddd, *J* = 8.1, 1.1, 0.9 Hz, 1H).

^{13}C-NMR (75 MHz, CDCl$_3$): δ = 158.8 (C$_q$), 149.4 (CH), 144.2 (C$_q$) 143.9 (C$_q$), 141.9 (C$_q$), 135.5 (CH), 130.5 (CH), 129.9 (q, $^2J_{C-F}$ = 32.8 Hz, C$_q$), 129.4 (CH), 128.3 (CH), 128.3 (CH), 127.7 (CH), 125.5 (q, $^3J_{C-F}$ = 3.7 Hz, CH), 124.1 (q, $^1J_{C-F}$ = 274 Hz, C$_q$), 123.8 (CH), 121.5 (CH).

^{19}F-NMR (282 MHz, CDCl$_3$): δ = –62.5 (m).

IR (ATR): 3059, 1583, 1459, 1314, 1152, 1106, 1062, 1017, 742, 718 cm^{-1}.

MS (EI) *m/z* (relative intensity): 325 ([M]$^+$, 40), 324 (100).

HR-MS (EI): *m/z* calcd. for [C$_{20}$H$_{14}$F$_3$N]$^+$ [M]$^+$ 325.1078, found 325.1074.
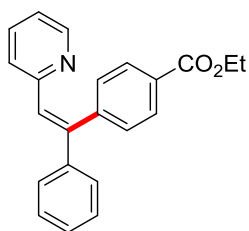
Ethyl (Z)-4-[1-phenyl-2-(pyridin-2-yl)vinyl]benzoate (10ag): The general procedure **A** was followed using (*E*)-2-styrylpyridine (**9a**) (90.5 mg, 0.50 mmol, 1.00 equiv) and ethyl 4-bromobenzoate (**2g**) (172 mg, 0.75 mmol, 1.50 equiv). Isolation by column chromatography (*n*-hexane/EtOAc: 20/1) yielded **10ag** (143 mg, 87%) as a yellow solid.

M.p.: 144 °C.

^{1}H-NMR (500 MHz, CDCl$_3$): δ = 8.50 (ddd, *J* = 4.9, 1.9, 0.9 Hz, 1H), 8.04–7.96 (m, 2H), 7.32–7.25 (m, 6H), 7.29–7.25 (m, 2H), 7.17 (s, 1H), 6.99 (ddd, *J* = 7.5, 4.9, 1.1 Hz, 1H), 6.71 (ddd, *J* = 8.1, 1.1, 0.9 Hz, 1H), 4.38 (q, *J* = 7.1 Hz, 2H), 1.37 (t, *J* = 7.1 Hz, 3H).

^{13}**C-NMR** (125 MHz, CDCl$_3$): δ = 166.4 (C$_q$), 156.0 (C$_q$), 149.4 (CH), 144.8 (C$_q$), 144.7 (C$_q$), 141.9 (C$_q$), 135.5 (CH), 130.2 (CH), 129.9 (CH), 129.8 (C$_q$), 129.3 (CH), 128.3 (CH), 128.2 (CH), 127.7 (CH), 123.8 (CH), 121.4 (CH), 61.0 (CH$_2$), 14.3 (CH$_3$).

IR (ATR): 3053, 1708, 1604, 1560, 1462, 1273, 1178, 999, 776, 691 cm^{-1}.

MS (EI) m/z (relative intensity): 329 ([M]$^+$, 40) 328 (100), 301 (70), 254 (30).

HR-MS (ESI): m/z calcd. for [C$_{22}$H$_{20}$NO$_2$]$^+$ [M + H]$^+$ 330.1489, found 330.1490.
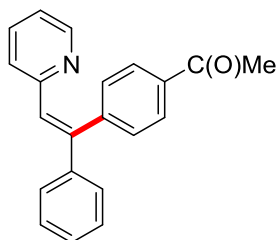
(Z)-1-{4-[1-phenyl-2-(pyridin-2-yl)vinyl]phenyl}ethan-1-one (10ah): A modified general procedure **A** was followed at 140 °C using (*E*)-2-styrylpyridine (**9a**) (90.5 mg, 0.50 mmol, 1.00 equiv) and 1-(4-bromophenyl)ethan-1-one (**2h**) (148 mg, 0.75 mmol, 1.50 equiv). Isolation by column chromatography (*n*-hexane/EtOAc: 20/1) yielded **10ah** (130 mg, 87%) as a pale yellow solid.

M.p.: 97 °C.

^{1}**H-NMR** (500 MHz, CDCl$_3$): δ = 8.50 (ddd, *J* = 4.9, 1.9, 0.9 Hz, 1H), 7.93–7.90 (m, 2H), 7.34–7.27 (m, 8H), 7.17 (s, 1H), 6.99 (ddd, *J* = 7.6, 4.9, 1.1 Hz, 1H), 6.72 (ddd, *J* = 8.1, 1.1, 0.9 Hz, 1H), 2.61 (s, 3H).

^{13}**C-NMR** (125 MHz, CDCl$_3$): δ = 197.7 (C$_q$), 156.0 (C$_q$), 149.4 (CH), 145.2 (C$_q$), 144.7 (C$_q$), 141.9 (C$_q$), 136.3 (C$_q$), 135.5 (CH), 130.5 (CH), 129.4 (CH), 128.7 (CH), 128.4 (CH), 128.3 (CH), 127.7 (CH), 123.9 (CH), 121.5 (CH), 26.6 (CH$_3$).

IR (ATR): 1681, 1583, 1264, 856, 747, 652, 599, 585 cm^{-1}.

MS (EI) m/z (relative intensity): 299 ([M]$^+$, 40), 298 (100), 254 (200).

HR-MS (ESI): m/z calcd. for [C$_{21}$H$_{18}$NO]$^+$ [M + H]$^+$ 300.1383, found 300.1386.

The spectral data are in accordance with those reported in the literature.[184]
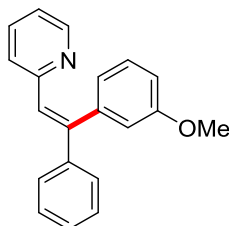
(Z)-2-[2-(3-Methoxyphenyl)-2-phenylvinyl]pyridine (10ai): The general procedure **A** was followed using (*E*)-2-styrylpyridine (**9a**) (90.5 mg, 0.50 mmol, 1.00 equiv) and 3-bromoanisole (**2i**) (140 mg,

0.75 mmol, 1.50 equiv). Isolation by column chromatography (*n*-hexane/EtOAc: 20/1) yielded **10ai** (115 mg, 80%) as a pale yellow solid.

M.p.: 108 °C.

^{1}H-NMR (300 MHz, CDCl$_3$): δ = 8.53 (ddd, *J* = 4.9, 1.9, 1.0 Hz, 1H), 7.41–7.34 (m, 2H), 7.32–7.22 (m, 5H), 7.15 (s, 1H), 6.97 (ddd, *J* = 7.5, 4.9, 1.2 Hz, 1H), 6.89 (ddd, *J* = 8.3, 2.7, 1.0 Hz, 1H), 6.79 (ddd, *J* = 8.1, 1.1, 0.9 Hz, 1H), 6.75–6.69 (m, 1H), 3.70 (s, 3H).

^{13}C-NMR (75 MHz, CDCl$_3$): δ = 159.9 (C$_q$), 156.5 (C$_q$), 149.2 (CH), 145.5 (C$_q$), 142.2 (C$_q$), 141.2 (C$_q$), 135.3 (CH), 129.8 (CH), 128.6 (CH), 128.2 (CH), 128.0 (CH), 127.6 (CH), 123.6 (CH), 122.5 (CH), 121.2 (CH), 115.1 (CH), 113.7 (CH), 55.2 (CH$_3$).

IR (ATR): 3051, 1580, 1485, 1461, 1430, 1229, 1041, 872, 742, 551 cm^{-1}.

MS (EI) *m/z* (relative intensity): 287 ([M]$^+$, 20), 286 (100), 271 (10), 243 (20).

HR-MS (ESI): *m/z* calcd. for [C$_{20}$H$_{18}$NO]$^+$ [M + H]$^+$ 288.1383, found 288.1393.
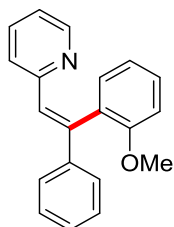
(Z)-2-[2-(2-Methoxyphenyl)-2-phenylvinyl]pyridine (10aj): A modified general procedure **A** was followed at 140 °C in PhMe (0.50 mL, 1.00 M) using (*E*)-2-styrylpyridine (**9a**) (90.5 mg, 0.50 mmol, 1.00 equiv) and 2-bromoanisole (**2j**) (140 mg, 0.75 mmol, 1.50 equiv). Isolation by column chromatography (*n*-hexane/EtOAc: 20/1) yielded **10aj** (116 mg, 81%) as a pale yellow solid.

M.p.: 114 °C.

^{1}H-NMR (500 MHz, CDCl$_3$): δ = 8.51 (ddd, *J* = 4.9, 2.0, 0.9 Hz, 1H), 7.38–7.33 (m, 3H), 7.30–7.23 (m, 5H), 7.08 (dd, *J* = 7.6, 2.0 Hz, 1H), 6.97–6.92 (m, 3H), 6.70 (ddd, *J* = 8.1, 1.1, 0.9 Hz, 1H), 3.58 (s, 3H).

^{13}C-NMR (125 MHz, CDCl$_3$): δ = 157.3 (C$_q$), 156.6 (C$_q$), 149.1 (CH), 142.1 (C$_q$), 141.8 (C$_q$), 135.3 (CH), 131.2 (CH), 129.3 (CH), 129.3 (CH), 128.7 (C$_q$), 128.1 (CH), 127.6 (CH), 126.7 (CH), 122.7 (CH), 121.1 (CH), 121.0 (CH), 111.5 (CH), 55.6 (CH$_3$).

IR (ATR): 3056, 1582, 1490, 1461, 1433, 1247, 1160, 1047, 756, 695 cm^{-1}.

MS (EI) *m/z* (relative intensity): 287 ([M]$^+$, 20), 270 (10), 257 (30), 256 (100).

HR-MS (ESI): *m/z* calcd. for [C$_{20}$H$_{18}$NO]$^+$ [M + H]$^+$ 288.1383, found 288.1385.
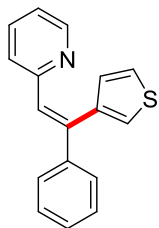
(*Z*)-2-[2-Phenyl-2-(thiophen-3-yl)vinyl]pyridine (10al): The general procedure **A** was followed using (*E*)-2-styrylpyridine (**9a**) (90.5 mg, 0.50 mmol, 1.00 equiv) and 3-bromothiophene (**9l**) (122 mg, 0.75 mmol, 1.50 equiv). Isolation by column chromatography (*n*-hexane/EtOAc: 20/1) yielded **10al** (114 mg, 87%, *Z*/*E* = 96:4) as a pale brown solid.

M.p.: 87 °C.

^{1}H-NMR (500 MHz, CDCl$_3$): δ = 8.53 (ddd, *J* = 4.9, 1.9, 0.9 Hz, 1H), 7.40–7.34 (m, 4H), 7.33–7.27 (m, 3H), 7.10 (s, 1H), 7.07 (dd, *J* = 3.0, 1.3 Hz, 1H), 7.01 (ddd, *J* = 7.5, 4.9, 1.1 Hz, 1H), 6.87 (dd, *J* = 4.9, 1.3 Hz, 1H), 6.80 (dd, *J* = 8.1, 1.1, 0.9 Hz, 1H).

^{13}C-NMR (125 MHz, CDCl$_3$): δ = 156.6 (C$_q$), 149.2 (CH), 142.2 (C$_q$), 140.4 (C$_q$), 139.8 (C$_q$), 135.4 (CH), 129.2 (CH), 129.1 (CH), 128.2 (CH), 128.1 (CH), 127.6 (CH), 125.7 (CH), 125.1 (CH), 123.5 (CH), 121.3 (CH).

IR (ATR): 3049, 1582, 1560, 1461, 1431, 863, 760, 743, 701 cm^{-1}.

MS (EI) *m/z* (relative intensity): 263 ([M]$^+$, 40), 262 (100), 230 (25), 186 (25).

HR-MS (EI): *m/z* calcd. for [C$_{17}$H$_{13}$NS]$^+$ [M]$^+$ 263.0769, found 263.0765.
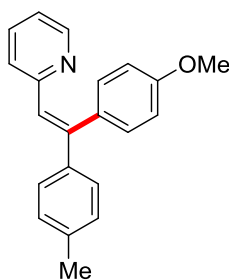
(*Z*)-2-[2-(4-Methoxyphenyl)-2-(*p*-tolyl)vinyl]pyridine (10bb): The general procedure **A** was followed using (*E*)-2-(4-methylstyryl)pyridine (**9b**) (97.7 mg, 0.50 mmol, 1.00 equiv) and 4-bromoanisole (**2b**) (140 mg, 0.75 mmol, 1.50 equiv). Isolation by column chromatography (*n*-hexane/EtOAc: 20/1) yielded **10bb** (136 mg, 90%) as a colorless solid.

M.p.: 69 °C.

^{1}H-NMR (300 MHz, CDCl$_3$): δ = 8.51 (ddd, *J* = 4.9, 1.9, 0.9 Hz, 1H), 7.31–7.26 (m, 1H), 7.25–7.22 (m, 2H), 7.14–7.07 (m, 4H), 7.06 (s, 1H), 6.95 (ddd, *J* = 7.5, 4.9, 1.1 Hz, 1H), 6.88–6.82 (m, 2H), 6.72 (ddd, *J* = 8.1, 1.1, 0.9 Hz, 1H), 3.82 (s, 3H), 2.84 (s, 3H).

^{13}C-NMR (75 MHz, CDCl$_3$): δ = 159.2 (C$_q$), 157.0 (C$_q$), 149.2 (CH), 145.4 (C$_q$), 140.0 (C$_q$), 137.9 (C$_q$), 135.2 (CH), 132.2 (C$_q$), 131.3 (CH), 128.9 (CH), 127.7 (CH), 127.5 (CH), 123.6 (CH), 120.8 (CH), 114.6 (CH), 55.2 (CH$_3$), 21.1 (CH$_3$).

IR (ATR): 3051, 1581, 1507, 1460, 1181, 1024, 848, 824, 745, 531 cm^{-1}.

MS (EI) m/z (relative intensity): 301 ([M]$^+$, 40), 300 (100), 257 (20).

HR-MS (ESI): m/z calcd. for [C$_{21}$H$_{20}$NO]$^+$ [M + H]$^+$ 302.1539, found 302.1543.
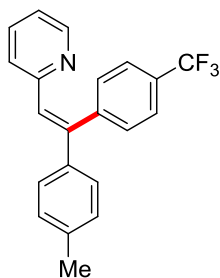
(Z)-2-{2-(*p*-Tolyl)-2-[4-(trifluoromethyl)phenyl]vinyl}pyridine (10bf): The general procedure **A** was followed using (*E*)-2-(4-methylstyryl)pyridine (**9b**) (97.7 mg, 0.50 mmol, 1.00 equiv) and 1-bromo-4-(trifluoromethyl)benzene (**2f**) (169 mg, 0.75 mmol, 1.50 equiv). Isolation by column chromatography (*n*-hexane/EtOAc: 20/1) yielded **10bf** (144 mg, 85%) as an off-white solid.

M.p.: 89 °C.

^{1}H-NMR (300 MHz, CDCl$_3$): δ = 8.50 (ddd, J = 4.9, 1.9, 0.9 Hz, 1H), 7.61–7.54 (m, 2H), 7.34–7.28 (m, 3H), 7.21–7.16 (m, 2H), 7.15 (s, 1H), 7.14–7.10 (m, 2H), 7.00 (ddd, J = 7.5, 4.9, 1.1 Hz, 1H), 6.67 (ddd, J = 8.1, 1.1, 0.9 Hz, 1H), 2.35 (s, 3H).

^{13}C-NMR (125 MHz, CDCl$_3$): δ = 156.0 (C$_q$), 149.3 (CH), 144.3 (C$_q$), 144.0 (C$_q$), 139.0 (C$_q$), 138.4 (C$_q$), 135.5 (CH), 130.6 (CH), 129.8 (q, $^2J_{C-F}$ = 32.4 Hz, C$_q$), 129.1 (CH), 128.6 (CH), 127.6 (CH), 125.5 (q, $^3J_{C-F}$ = 3.8 Hz, CH), 124.0 (q, $^1J_{C-F}$ = 271 Hz, C$_q$), 123.7 (CH), 121.4 (CH), 21.1 (CH$_3$).

^{19}F-NMR (282 MHz, CDCl$_3$): δ = –62.5 (m).

IR (ATR): 3071, 1582, 1460, 1407, 1321, 1161, 1065, 856, 837 cm^{-1}.

MS (EI) m/z (relative intensity): 339 ([M]$^+$, 35), 338 (100), 268 (10).

HR-MS (ESI): m/z calcd. for [C$_{21}$H$_{17}$F$_3$N]$^+$ [M + H]$^+$ 340.1308, found: 340.1311.
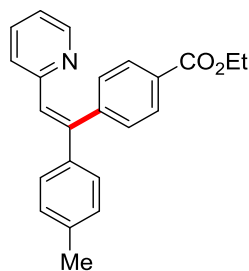
(*Z*)-Ethyl-4-[2-(pyridin-2-yl)-1-(*p*-tolyl)vinyl]benzoate (10bg): The general procedure **A** was followed using (*E*)-2-(4-methylstyryl)pyridine (**9b**) (97.7 mg, 0.50 mmol, 1.00 equiv) and ethyl 4-bromobenzoate (**2g**) (172 mg, 0.75 mmol, 1.50 equiv). Isolation by column chromatography (*n*-hexane/EtOAc: 20/1) yielded **10bg** (149 mg, 87%) as yellow solid.

M.p.: 72 °C.

^{1}H-NMR (300 MHz, CDCl$_3$): δ = 8.50 (ddd, J = 4.9, 1.9, 0.9 Hz, 1H), 8.03–7.96 (m, 2H), 7.30–7.24 (m, 3H), 7.22–7.17 (m, 2H), 7.15 (s, 1H), 7.13–7.08 (m, 2H), 6.97 (ddd, J = 7.4, 4.9, 1.1 Hz, 1H), 6.66 (ddd, J = 8.1, 1.1, 0.9 Hz, 1H), 4.37 (q, J = 7.3 Hz, 2H), 2.35 (s, 3H), 1.39 (t, J = 7.3 Hz, 3H).

^{13}C-NMR (125 MHz, CDCl$_3$): δ = 166.4 (C$_q$), 156.2 (C$_q$), 149.3 (CH), 145.0 (C$_q$), 144.7 (C$_q$), 139.0 (C$_q$), 138.2 (C$_q$), 135.4 (CH), 130.2 (CH), 129.8 (CH), 129.7 (C$_q$), 129.1 (CH), 128.4 (CH), 127.6 (CH), 123.7 (CH), 121.3 (CH), 61.0 (CH$_2$), 21.1 (CH$_3$), 14.3 (CH$_3$).

IR (ATR): 2980, 1709, 1581, 1460, 1268, 1099, 813, 772, 746 cm^{-1}.

MS (EI) *m/z* (relative intensity): 343 ([M]$^+$, 40), 342 (100), 314 (65), 268 (15).

HR-MS (ESI): *m/z* calcd. for [C$_{23}$H$_{22}$NO$_2$]$^+$ [M + H]$^+$ 344.1645, found: 344.1645.
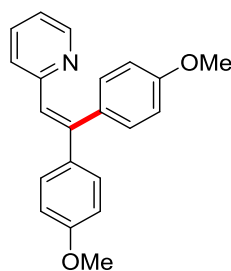
2-[2,2-Bis(4-methoxyphenyl)vinyl]pyridine (10cb): The general procedure **A** was followed using (*E*)-2-(4-methoxystyryl)pyridine (**9c**) (106 mg, 0.50 mmol, 1.00 equiv) and 4-bromoanisole (**2b**) (140 mg, 0.75 mmol, 1.50 equiv). Isolation by column chromatography (*n*-hexane/EtOAc: 20/1) yielded **10cb** (147 mg, 93%) as a colorless solid.

M.p.: 89 °C.

^{1}H-NMR (300 MHz, CDCl$_3$): δ = 8.49 (ddd, J = 4.9, 1.9, 0.9 Hz, 1H), 7.32–7.22 (m, 3H), 7.12–7.07 (m, 2H), 7.01 (s, 1H), 6.93 (ddd, J = 7.5, 4.9, 1.1 Hz, 1H), 6.87–6.80 (m, 4H), 6.69 (ddd, J = 8.1, 1.1, 0.9 Hz, 1H), 3.81 (s, 3H), 3.78 (s, 3H).

^{13}**C-NMR** (125 MHz, CDCl$_3$): δ = 159.7 (C$_q$), 159.3 (C$_q$), 157.2 (C$_q$), 149.2 (CH), 145.1 (C$_q$), 135.5 (C$_q$), 135.2 (CH), 132.2 (C$_q$), 131.4 (CH), 129.1 (CH), 126.7 (CH), 123.5 (CH), 120.8 (CH), 114.1 (CH), 113.6 (CH), 55.2 (CH$_3$), 55.1 (CH$_3$).

IR (ATR): 2999, 1601, 1507, 1459, 1240, 1172, 1148, 826 cm^{-1}.

MS (EI) *m/z* (relative intensity): 317 ([M]$^+$, 40), 316 (100), 273 (15).

HR-MS (ESI): *m/z* calcd. for [C$_{21}$H$_{20}$NO$_2$]$^+$ [M + H]$^+$ 318.1489, found 318.1489.

The spectral data are in accordance with those reported in the literature.[42]
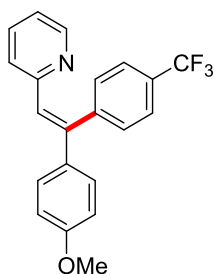
(*E*)-2-{2-(4-Methoxyphenyl)-2-[4-(trifluoromethyl)phenyl]vinyl}pyridine (**10cf**): The general procedure **A** was followed using (*E*)-2-(4-methoxystyryl)pyridine (**9c**) (106 mg, 0.50 mmol, 1.00 equiv) and 1-bromo-4-(trifluoromethyl)benzene (**2f**) (169 mg, 0.75 mmol, 1.50 equiv). Isolation by column chromatography (*n*-hexane/EtOAc: 20/1) yielded **10cf** (149 mg, 84%) as a white solid.

M.p.: 83 °C.

^{1}**H-NMR** (500 MHz, CDCl$_3$): δ = 8.48 (ddd, *J* = 4.9, 1.9, 0.9 Hz, 1H), 7.59–7.56 (m, 2H), 7.32–7.28 (m, 3H), 7.25–7.21 (m, 2H), 7.11 (s, 1H), 6.96 (ddd, *J* = 7.5, 4.9, 1.0 Hz, 1H), 6.86–6.82 (m, 2H), 6.65 (ddd, *J* = 8.1, 1.0, 0.9 Hz, 1H), 3.78 (s, 3H).

^{13}**C-NMR** (125 MHz, CDCl$_3$): δ = 159.5 (C$_q$), 156.3 (C$_q$), 149.4 (CH), 144.1 (C$_q$), 143.8 (C$_q$), 135.4 (CH), 134.3 (C$_q$), 130.6 (CH), 129.7 (q, $^2J_{C-F}$ = 32.1 Hz, C$_q$), 128.9 (CH), 127.7 (CH), 125.4 (q, $^3J_{C-F}$ = 3.5 Hz, CH), 124.2 (q, $^1J_{C-F}$ = 273 Hz, C$_q$), 123.6 (CH), 121.2 (CH), 113.8 (CH), 55.2 (CH$_3$).

^{19}**F-NMR** (282 MHz, CDCl$_3$): δ = –62.3 (m).

IR (ATR): 2963, 1608, 1579, 1510, 1409, 1239, 1108, 993, 801, 557 cm^{-1}.

MS (EI) *m/z* (relative intensity): 355 ([M]$^+$, 30), 354 (100), 311 (25).

HR-MS (ESI): *m/z* calcd. for [C$_{21}$H$_{17}$F$_3$NO]$^+$ [M + H]$^+$ 356.1257, found 356.1255.

The spectral data are in accordance with those reported in the literature.[36a]
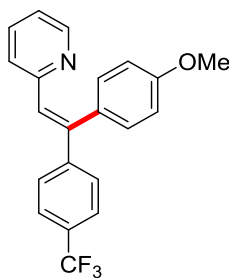
(Z)-2-[2-(4-Methoxyphenyl)-2-(4-trifluoromethyl)phenylvinyl]pyridine **(10db):** The general procedure **A** was followed using (*E*)-2-[4-(trifluoromethyl)styryl]pyridine (**9d**) (125 mg, 0.50 mmol, 1.00 equiv) and 1-bromoanisole (**2b**) (140 mg, 0.75 mmol, 1.50 equiv). Isolation by column chromatography (*n*-hexane/EtOAc: 20/1) yielded **10db** (158 mg, 90%) as a brown solid.

M.p.: 82 °C.

^{1}H-NMR (300 MHz, CDCl$_3$): δ = 8.53 (ddd, *J* = 4.9, 1.9, 0.9 Hz, 1H), 7.56–7.54 (m, 2H), 7.47–7.44 (m, 2H), 7.32 (ddd, *J* = 8.1, 7.5, 1.9 Hz, 1H), 7.11 (s, 1H), 7.10–7.04 (m, 2H), 7.00 (ddd, *J* = 7.5, 4.9, 1.1 Hz, 1H), 6.90–6.83 (m, 2H), 6.78 (ddd, *J* = 8.1, 1.1, 0.9 Hz, 1H), 3.80 (s, 3H).

^{13}C-NMR (75 MHz, CDCl$_3$): δ = 159.5 (C$_q$), 156.3 (C$_q$), 149.4 (CH), 146.6 (C$_q$), 144.1 (C$_q$), 135.4 (CH), 131.3 (CH), 131.1 (C$_q$), 130.1 (CH), 129.8 (q, $^2J_{C–F}$ = 32.1 Hz, C$_q$), 128.1 (CH), 125.1 (q, $^3J_{C–F}$ = 3.5 Hz, CH), 124.1 (q, $^1J_{C–F}$ = 273 Hz, C$_q$), 123.8 (CH), 121.5 (CH), 114.3 (CH), 55.2 (CH$_3$).

^{19}F-NMR (282 MHz, CDCl$_3$): δ = –62.5 (m).

IR (ATR): 2963, 1608, 1579, 1510, 1409, 1239, 1108, 993, 801, 557 cm^{-1}.

MS (EI) *m/z* (relative intensity): 355 ([M]$^+$, 30), 354 (100), 311 (25).

HR-MS (EI): *m/z* calcd. for [C$_{21}$H$_{16}$F$_3$NO]$^+$ [M]$^+$ 355.1184, found 355.1187.

The spectral data are in accordance with those reported in the literature.[36a]
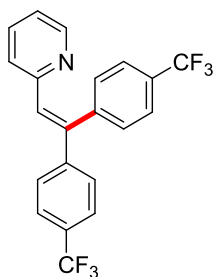
2-{2,2-Bis[4-(trifluoromethyl)phenyl]vinyl}pyridine (10df): The general procedure **A** was followed using (*E*)-2-[4-(trifluoromethyl)styryl]pyridine (**9d**) (125 mg, 0.50 mmol, 1.00 equiv) and 1-bromo-4-(trifluoromethyl)benzene (**2f**) (169 mg, 0.75 mmol, 1.50 equiv). Isolation by column chromatography (*n*-hexane/EtOAc: 20/1) yielded **10df** (151 mg, 77%) as a colorless solid.

M.p.: 109 °C.

¹H-NMR (300 MHz, CDCl₃): δ = 8.52 (ddd, J = 4.9, 1.8, 0.9 Hz, 1H), 7.67–7.59 (m, 4H), 7.47–7.38 (m, 3H), 7.37–7.32 (m, 2H), 7.26 (s, 1H), 7.09 (ddd, J = 7.5, 4.9, 1.1 Hz, 1H), 6.70 (ddd, J = 8.1, 1.1, 0.9 Hz, 1H).

¹³C-NMR (75 MHz, CDCl₃): δ = 155.3 (C$_q$), 149.6 (CH), 145.3 (C$_q$), 143.0 (C$_q$), 142.9 (C$_q$), 135.7 (CH), 131.3 (CH), 130.5 (CH), 130.0 (q, $^2J_{C–F}$ = 32.5 Hz, C$_q$), 130.0 (q, $^2J_{C–F}$ = 32.5 Hz, C$_q$), 128.0 (CH), 125.8 (q, $^3J_{C–F}$ = 3.8 Hz, CH), 125.4 (q, $^3J_{C–F}$ = 3.8 Hz, CH), 124.0 (CH), 123.9 (q, $^1J_{C–F}$ = 275 Hz, C$_q$), 123.8 (q, $^1J_{C–F}$ = 275 Hz, C$_q$), 122.0 (CH).

¹⁹F-NMR (282 MHz, CDCl₃): δ = −62.6 (m).

IR (ATR): 1578, 1319, 1163, 1103, 1064, 1017, 837, 769, 739 cm⁻¹.

MS (EI) m/z (relative intensity): 393 ([M]⁺, 40), 392 (100), 322 (15), 248 (10).

HR-MS (ESI): m/z calcd. for [C₂₁H₁₄F₆N]⁺ [M + H]⁺ 394.1025, found 394.1026.
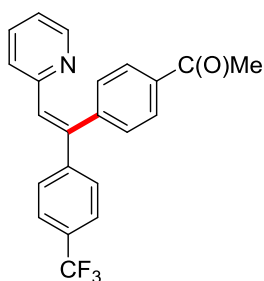
(*E*)-1-{4-[2-(Pyridin-2-yl)-1-(4-(trifluoromethyl)phenyl)vinyl]phenyl}ethan-1-one   (10dh):   The general procedure **A** was followed using (*E*)-2-[4-(trifluoromethyl)styryl]pyridine (**9d**) (125 mg, 0.50 mmol, 1.00 equiv) and 1-(4-bromophenyl)ethan-1-one (**2h**) (148 mg, 0.75 mmol, 1.50 equiv). Isolation by column chromatography (*n*-hexane/EtOAc: 20/1) yielded **10dh** (143 mg, 78%) as a colorless solid.

M.p.: 101 °C.

¹H-NMR (300 MHz, CDCl₃): δ = 8.52 (ddd, J = 4.9, 1.9, 0.9 Hz, 1H), 7.96–7.90 (m, 2H), 7.57–7.54 (m, 2H), 7.40 (d, J = 8.1 Hz, 2H), 7.34 (ddd, J = 8.1, 7.5, 1.9 Hz, 1H), 7.30–7.25 (m, 2H), 7.21 (s, 1H), 7.03 (ddd, J = 7.5, 4.9, 1.1 Hz, 1H), 6.73 (ddd, J = 8.1, 1.1, 0.9 Hz, 1H), 2.63 (s, 3H).

¹³C-NMR (75 MHz, CDCl₃): δ = 197.6 (C$_q$), 155.4 (C$_q$), 149.5 (CH), 146.3 (C$_q$), 144.3 (C$_q$), 143.3 (C$_q$), 136.6 (CH), 135.7 (C$_q$), 131.2 (CH), 130.4 (CH), 130.3 (q, $^2J_{C–F}$ = 32.5 Hz, C$_q$), 128.8 (CH), 128.0 (CH), 125.3 (q, $^3J_{C–F}$ = 3.8 Hz, CH), 124.1 (q, $^1J_{C–F}$ = 270 Hz, C$_q$), 124.0 (CH), 121.9 (CH), 26.6 (CH₃).

¹⁹F-NMR (282 MHz, CDCl₃): δ = −62.6 (m).

IR (ATR): 1672, 1322, 1268, 1162, 1136, 1109, 1017, 834, 740, 607 cm⁻¹.

MS (EI) m/z (relative intensity): 367 ([M]⁺, 30), 366 (100), 322 (15).

HR-MS (ESI): m/z calcd. for [C₂₂H₁₇F₃NO]⁺ [M + H]⁺ 368.1257, found 368.1259.
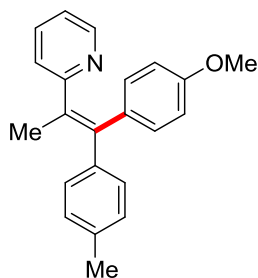
(Z)-2-[1-(4-Methoxyphenyl)-1-(p-tolyl)prop-1-en-2-yl]pyridine **(10eb)**: A modified general procedure **A** was followed at 140 °C in PhMe (0.50 mL, 1.00 M) using (E)-2-[1-(4-methylphenyl)prop-1-en-2-yl]pyridine (**9e**) (113 mg, 0.50 mmol, 1.00 equiv) and 4-bromoanisole (**2b**) (140 mg, 0.75 mmol, 1.50 equiv). Isolation by column chromatography (n-hexane/EtOAc: 20/1) yielded **10eb** (82.0 mg, 52%, Z/E = 12:1) as a pale red solid.

M.p.: 105 °C.

^{1}H-NMR (500 MHz, CDCl$_3$): δ = 8.55 (ddd, J = 4.9, 1.9, 0.9 Hz, 1H), 7.30 (ddd, J = 8.1, 7.5, 1.9 Hz, 1H), 7.15–7.12 (m, 4H), 6.97 (ddd, J = 7.5, 4.9, 1.1 Hz, 1H), 6.86 (ddd, J = 8.1, 1.1, 0.9 Hz, 1H), 6.78–6.72 (m, 2H), 6.59–6.54 (m, 2H), 3.68 (s, 3H), 2.35 (s, 3H), 2.20 (s, 3H).

^{13}C-NMR (125 MHz, CDCl$_3$): δ = 162.6 (C$_q$), 158.0 (C$_q$), 148.9 (CH), 140.7 (C$_q$), 140.3 (C$_q$), 136.4 (C$_q$), 135.4 (C$_q$), 134.8 (C$_q$), 131.8 (CH), 129.8 (CH), 129.7 (CH), 128.7 (CH), 125.4 (CH), 120.8 (CH), 113.0 (CH), 55.0 (CH$_3$), 21.5 (CH$_3$), 21.2 (CH$_3$).

IR (ATR): 3050, 1580, 1505, 1460, 1289, 1239, 1175, 746, 572 cm^{-1}.

MS (EI) m/z (relative intensity): 315 ([M]$^+$, 40), 314 (100), 300 (10), 206 (10).

HR-MS (ESI): m/z calcd. for [C$_{22}$H$_{22}$NO]$^+$ [M + H]$^+$ 316.1696, found 316.1697.

5.2.2   Mechanistic Studies

5.2.2.1   Experiments with Radical Scavengers

A suspension of (E)-2-styrylpyridine (**9a**) (90.5 mg, 0.50 mmol, 1.00 equiv), 4-bromoanisole (**2b**) (140 mg, 0.75 mmol, 1.50 equiv), [RuCl$_2$(p-cymene)(n-Bu$_2$POH)] (**124e**) (11.7 mg, 25.0 µmol, 5.00 mol %), K$_2$CO$_3$ (138 mg, 1.00 mmol, 2.00 equiv), a radical scavenger (0.50 mmol, 1.00 equiv) and n-dodecane (25 µL) as the internal standard in PhMe (2.00 mL, 0.25 M) was heated at 120 °C for 18 h. At ambient temperature, the conversion was measured by GC.

5.2.2.2   KIE Studies

Two parallel reactions of (E)-2-styrylpyridine (**9a**) (90.5 mg, 0.50 mmol, 1.00 equiv) or [D]$_1$-**9a** (91.5 mg, 0.50 mmol, 1.00 equiv), 4-bromoanisole (**2b**) (140 mg, 0.75 mmol), [RuCl$_2$(p-cymene)(n-Bu$_2$POH)] (**124e**) (11.7 mg, 25.0 µmol, 5.0 mol %), K$_2$CO$_3$ (138 mg, 1.00 mmol) and n-dodecane (25 µL) in PhMe (2.0 mL) were placed in a 25 mL Schlenk tube, equipped with the sensor of a *ReactIR™ 15* machine, and heated at 120 °C under nitrogen atmosphere. The KIE was determined by

following the corresponding initial reaction rates, which were obtained by integration of the vibrational band of the products **10ab** and [D]$_1$-**10ab** at 1520 cm^{-1}, respectively.

5.2.2.3 *Hammett* Plot Analyses

5.2.2.3.1 *Hammett* Plot with (*E*)-**2**-styrylpyridine (**9a**)

A suspension of (*E*)-2-styrylpyridine (**9a**) (90.5 mg, 0.50 mmol, 1.00 equiv), *p-X*-C$_6$H$_4$Br   **2** (0.75 mmol, 1.50 equiv), [RuCl$_2$(*p*-cymene)(*n*-Bu$_2$POH)] (**124e**) (11.7 mg, 25.0 µmol, 5.00 mol %), K$_2$CO$_3$ (138 mg, 1.00 mmol, 2.00 equiv) and *n*-dodecane (25 µL) in PhMe (2.0 mL, 0.25 M) was stirred at 120 °C. Periodic aliquots (25 µL) were removed by a syringe and the conversions were analyzed by GC up to ca. 10–20% conversion.

Table 27. Reaction rates k_X and σ_p-values for the *Hammett* plot analysis with aryl bromides **2**.

Entry	substituent *X*	σ_p	k_X / µmol min^{-1}	log (k_X / k_H)
1	NMe$_2$	−0.83	0.319	−0.340
2	OMe	−0.27	0.606	−0.062
3	H	0	0.699	0
4	Cl	0.23	0.630	−0.045
5	CO$_2$Et	0.45	0.579	−0.082
6	CF$_3$	0.54	0.557	−0.099

5.2.2.4 Kinetic Order Analysis

5.2.2.4.1 Kinetic reaction order with respect to the concentration of (*E*)-**2**-styrylpyridine (**9a**)

The kinetic order with respect to the concentration of (*E*)-2-styrylpyridine (**9a**) was examined by applying the initial rate method. A suspension of **9a** (0.500, 0.370, 0.250, 0.125 mmol), 4-bromoanisole (**2b**) (140 mg, 0.75 mmol), [RuCl$_2$(*p*-cymene)(*n*-Bu$_2$POH)] (**124e**) (11.7 mg, 25.0 µmol), K$_2$CO$_3$ (138 mg, 1.00 mmol) and *n*-dodecane (25 µL) in PhMe (2.0 mL) was stirred at 120 °C. Periodic aliquots (25 µL) were removed by a syringe and analyzed by GC up to ca. 10–20% conversion.

Table 28. Kinetic reaction order with respect to the concentration of **9a**.

Entry	*c* / mol L^{-1}	*k* / mol L^{-1} min^{-1}	log (*c* / mol L^{-1})	log (*k* / mol L^{-1} min^{-1})
1	0.250	3.319	0.602	−3.479
2	0.185	2.500	0.733	−3.602
3	0.125	1.841	−0.903	−3.735
4	0.063	0.989	−1.200	−4.004

5.2.2.4.2   Kinetic reaction order with respect to the concentration of 4-bromoanisole (2b)

The kinetic order with respect to the concentration of 4-bromoanisole (2b) was examined by the initial rate method. A suspension of (E)-2-Styrylpyridine (9a) (90.5 mg, 0.50 mmol), 4-bromoanisole (2b) (4.00, 2.00, 0.600, 0.250, 0.125 mmol), [RuCl$_2$(p-cymene)(n-Bu$_2$POH)] (124e) (11.7 mg, 25.0 µmol), K$_2$CO$_3$ (138 mg, 1.00 mmol) and n-dodecane (25 µL) in PhMe (2.0 mL) was stirred at 120 °C. Periodic aliquots (25 µL) were removed by a syringe and analyzed by GC up to ca. 10–20% conversion.

Table 29. Kinetic reaction order with respect to the concentration of 2b.

Entry	c / mol L^{-1}	k / mol L^{-1} min^{-1}	log (c / mol L^{-1})	log (k / mol L^{-1} min^{-1})
1	2.000	2.937	0.301	−3.532
2	1.000	2.831	0	−3.548
3	0.300	2.483	−0.523	−3.605
4	0.125	2.023	−0.903	−3.694
5	0.063	1.469	−1.201	−3.833

5.2.2.4.3   Kinetic reaction order with respect to concentration of [RuCl$_2$(p-cymene)(n-Bu$_2$POH)] (124e)

The kinetic order with respect to the concentration of [RuCl$_2$(p-cymene)(n-Bu$_2$POH)] (124e) was examined by the initial rate method. A suspension of (E)-2-styrylpyridine (9a) (90.5 mg, 0.50 mmol, 1.00 equiv), 4-bromoanisole (2b) (140 mg, 0.75 mmol, 1.50 equiv), [RuCl$_2$(p-cymene)(n-Bu$_2$POH)] (124e) (1.25, 2.50, 3.50, 5.00 mol %), K$_2$CO$_3$ (138 mg, 1.00 mmol, 1.00 equiv) and n-dodecane (25 µL) in PhMe (2.0 mL) was stirred at 120 °C. Periodic aliquots (25 µL) were removed by a syringe and analyzed by GC up to ca. 10–20% conversion.

Table 30. Kinetic reaction order with respect to the concentration of 124e.

Entry	c / mol L^{-1}	k / mol L^{-1} min^{-1}	log (c / mol L^{-1})	log (k / mol L^{-1} min^{-1})
1	1.25	0.697	0.097	−4.157
2	2.50	1.560	0.398	−3.807
3	3.50	2.565	0.544	−3.591
4	5.00	3.319	0.699	−3.479

5.3   Cobalt(III)-Catalyzed C−H/C−C Functionalization

5.3.1   Characterization Data
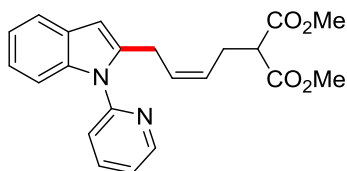
(**Z**)-**Dimethyl 2-{4-[1-(pyridin-2-yl)-1*H*-indol-2-yl]but-2-en-1-yl}malonate** (**130aa**): The general procedure **B** was followed using 1-(pyridin-2-yl)-1*H*-indole (**105a**) (97.1 mg, 0.50 mmol) and dimethyl 2-vinylcyclopropane-1,1-dicarboxylate (**125a**) (110 mg, 0.60 mmol). Isolation by column chromatography (*n*-hexane/EtOAc: 3/1) yielded **130aa** (176 mg, 93%, *E*/*Z* = 1:11) as a yellow oil.

^{1}H-NMR (300 MHz, CDCl$_3$): δ = 8.64 (ddd, *J* = 4.9, 1.9, 0.8 Hz, 1H), 7.86 (ddd, *J* = 8.0, 7.6, 1.9 Hz, 1H), 7.59–7.53 (m, 1H), 7.46–7.41 (m, 1H), 7.36–7.27 (m, 2H), 7.15–7.09 (m, 2H), 6.43 (d, *J* = 0.7 Hz, 1H), 5.64 (dtt, *J* = 10.8, 7.2, 1.0 Hz, 1H), 5.40 (dtt, *J* = 10.8, 7.6, 1.0 Hz, 1H), 3.69 (s, 6H), 3.65 (d, *J* = 7.2 Hz, 2H), 3.35 (t, *J* = 7.7 Hz, 1H), 2.62 (ddd, *J* = 7.7, 7.6, 1.0 Hz, 1.83H, *Z*), 2.54 (ddd, *J* = 7.7, 7.6, 1.0 Hz, 0.17H, *E*).

^{13}C-NMR (125 MHz, CDCl$_3$): δ = 169.0 (C$_q$), 151.1 (C$_q$), 149.5 (CH), 139.2 (C$_q$), 138.1 (CH), 137.2 (C$_q$), 128.8 (CH), 128.4 (C$_q$), 126.2 (CH), 121.9 (CH), 121.7 (CH), 120.8 (CH), 120.5 (CH), 119.9 (CH), 109.9 (CH), 102.7 (CH), 52.5 (CH$_3$), 51.5 (CH), 31.7 (CH$_2$, *E*), 30.9 (CH$_2$, *E*), 26.7 (CH$_2$, *Z*), 25.9 (CH$_2$, *Z*).

IR (ATR): 1732, 1586, 1469, 1436, 1150, 745 cm^{-1}.

MS (EI) *m*/*z* (relative intensity): 378 ([M]$^+$, 30), 247 (100), 219 (90), 206 (70).

HR-MS (EI): *m*/*z* calcd. for [C$_{22}$H$_{22}$N$_2$O$_4$]$^+$ [M]$^+$ 378.1574, found 378.1578.
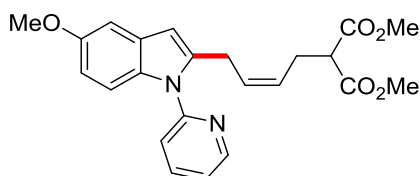
(**Z**)-**Dimethyl 2-{4-[5-methoxy-1-(pyridin-2-yl)-1*H*-indol-2-yl]but-2-en-1-yl}malonate** (**130ba**): The general procedure **B** was followed using 5-methoxy-1-(pyridin-2-yl)-1*H*-indole (**105b**) (112 mg, 0.50 mmol) and dimethyl 2-vinylcyclopropane-1,1-dicarboxylate (**125a**) (110 mg, 0.60 mmol). Isolation by column chromatography (*n*-hexane/EtOAc: 3/1) yielded **130ba** (188 mg, 92%, *E*/*Z* = 1:13) as a colorless oil.

^{1}H-NMR (500 MHz, CDCl$_3$): δ = 8.61 (ddd, *J* = 4.9, 1.9, 0.8 Hz, 1H), 7.85 (ddd, *J* = 8.1, 7.5, 1.9 Hz, 1H), 7.40 (ddd, *J* = 8.1, 1.0, 0.8 Hz, 1H), 7.26 (ddd, *J* = 7.5, 4.9, 1.0 Hz, 1H), 7.24–7.20 (m, 1H), 7.01 (d, *J* = 2.6 Hz, 1H), 6.76 (dd, *J* = 8.9, 2.6 Hz, 1H), 6.34 (d, *J* = 0.8 Hz, 1H), 5.61 (dtt, *J* = 10.7, 7.6,

1.5 Hz, 1H), 5.38 (dtt, J = 10.7, 7.7, 1.0 Hz, 1H), 3.82 (s, 3H), 3.68 (s, 6H), 3.58 (d, J = 7.6 Hz, 2H), 3.34 (t, J = 7.7 Hz, 1H), 2.61 (ddd, J = 7.7, 7.6, 1.5 Hz, 1.86H, Z), 2.52 (ddd, J = 7.7, 7.6, 1.5 Hz, 0.14H, E).

^{13}C-NMR (125 MHz, CDCl$_3$): δ = 169.2 (C$_q$), 154.8 (C$_q$), 151.4 (C$_q$), 149.5 (CH), 139.8 (C$_q$), 138.2 (CH), 132.4 (C$_q$), 129.1 (C$_q$), 129.0 (CH), 126.3 (CH), 121.7 (CH), 120.6 (CH), 111.3 (CH), 110.9 (CH), 102.7 (CH), 102.1 (CH), 55.8 (CH$_3$), 52.5 (CH$_3$), 51.5 (CH), 31.7 (CH$_2$, E), 30.6 (CH$_2$, E), 26.7 (CH$_2$, Z), 25.9 (CH$_2$, Z).

IR (ATR): 1732, 1582, 1470, 1434, 1202, 1030, 839 cm^{-1}.

MS (EI) m/z (relative intensity): 408 ([M]$^+$, 30), 277 (80), 249 (100), 236 (40).

HR-MS (EI): m/z calcd. for [C$_{23}$H$_{24}$N$_2$O$_5$]$^+$ [M]$^+$ 408.1685, found 408.1700.
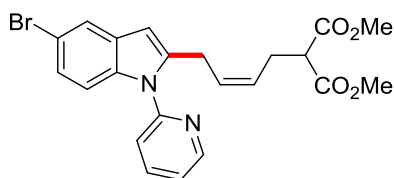
(Z)-Dimethyl 2-{4-[5-bromo-1-(pyridin-2-yl)-1H-indol-2-yl]but-2-en-1-yl}malonate (130ca): The general procedure **B** was followed using 5-bromo-1-(pyridin-2-yl)-1H-indole (**105c**) (137 mg, 0.50 mmol) and dimethyl 2-vinylcyclopropane-1,1-dicarboxylate (**125a**) (110 mg, 0.60 mmol). Isolation by column chromatography (n-hexane/EtOAc: 3/1) yielded **130ca** (203 mg, 89%, E/Z = 1:9) as a yellow oil.

^{1}H-NMR (400 MHz, CDCl$_3$): δ = 8.65 (ddd, J = 4.9, 2.0, 0.8 Hz, 1H), 7.89 (ddd, J = 7.9, 7.5, 2.0 Hz, 1H), 7.66–7.63 (m, 1H), 7.39 (ddd, J = 7.9, 1.0, 0.8 Hz, 1H), 7.35–7.30 (m, 1H), 7.19–7.16 (m, 2H), 6.34 (d, J = 0.8 Hz, 1H), 5.59 (dtt, J = 10.8, 7.6, 1.4 Hz, 1H), 5.39 (dtt, J = 10.8, 7.6, 1.2 Hz, 1H), 3.68 (s, 6H), 3.60 (d, J = 7.6 Hz, 2H), 3.34 (t, J = 7.6 Hz, 1H), 2.58 (ddd, J = 7.6, 7.6, 1.4 Hz, 1.80H, Z), 2.52 (ddd, J = 7.6, 7.6, 1.4 Hz, 0.20H, E).

^{13}C-NMR (100 MHz, CDCl$_3$): δ = 169.2 (C$_q$), 150.9 (C$_q$), 149.8 (CH), 140.7 (C$_q$), 138.5 (CH), 136.0 (C$_q$), 130.2 (C$_q$), 128.5 (CH), 127.8 (CH), 124.6 (CH), 122.4 (CH), 121.0 (CH), 113.8 (C$_q$), 111.6 (CH), 102.2 (CH), 95.7 (CH), 52.6 (CH$_3$), 51.4 (CH), 31.6 (CH$_2$, E), 30.8 (CH$_2$, E), 26.7 (CH$_2$, Z), 25.9 (CH$_2$, Z).

IR (ATR): 1731, 1586, 1470, 1435, 1148, 783, 734 cm^{-1}.

MS (EI) m/z (relative intensity): 456 ([M, ^{79}Br]$^+$, 25), 325 (100), 297 (90), 286 (40), 245 (55).

HR-MS (EI): m/z calcd. for [C$_{22}$H$_{21}$^{79}BrN$_2$O$_4$]$^+$ [M]$^+$ 456.0679, found 456.0689.
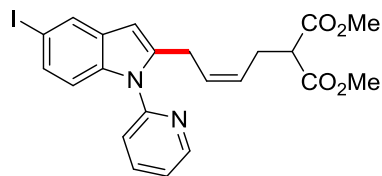
(**Z**)-**Dimethyl 2-{4-[5-iodo-1-(pyridin-2-yl)-1***H*-indol-2-yl]but-2-en-1-yl}malonate** (**130da**): The general procedure **B** was followed using 5-iodo-1-(pyridin-2-yl)-1*H*-indole (**105d**) (160 mg, 0.50 mmol) and dimethyl 2-vinylcyclopropane-1,1-dicarboxylate (**125a**) (110 mg, 0.60 mmol). Isolation by column chromatography (*n*-hexane/EtOAc: 3/1) yielded **130da** (224 mg, 89%, *E*/*Z* = 1:14) as a yellow oil.

^{1}H-NMR (500 MHz, CDCl$_3$): δ = 8.64 (ddd, *J* = 4.9, 1.9, 0.8 Hz, 1H), 7.89 (ddd, *J* = 7.9, 7.5, 2.1 Hz, 1H), 7.86 (d, *J* = 1.6 Hz, 1H), 7.39–7.30 (m, 3H), 7.08–7.04 (m, 1H), 6.32 (d, *J* = 0.8 Hz, 1H), 5.59 (dtt, *J* = 10.8, 7.6, 1.4 Hz, 1H), 5.39 (dtt, *J* = 10.8, 7.4, 1.0 Hz, 1H), 3.68 (s, 6H), 3.58 (d, *J* = 7.6 Hz, 2H), 3.33 (t, *J* = 7.5 Hz, 1H), 2.58 (ddd, *J* = 7.5, 7.4, 1.4 Hz, 1.87H, *Z*), 2.52 (ddd, *J* = 7.5, 7.4, 1.4 Hz, 0.13H, *E*).

^{13}C-NMR (125 MHz, CDCl$_3$): δ = 169.2 (C$_q$), 150.8 (C$_q$), 149.8 (CH), 140.3 (C$_q$), 138.5 (CH), 136.5 (C$_q$), 130.9 (C$_q$), 130.0 (CH), 128.7 (CH), 128.4 (CH), 126.7 (CH), 122.4 (CH), 120.1 (CH), 112.1 (CH), 101.9 (CH), 84.1 (C$_q$), 52.5 (CH$_3$), 51.4 (CH), 31.7 (CH$_2$, *E*), 30.8 (CH$_2$, *E*), 26.7 (CH$_2$, *Z*), 25.9 (CH$_2$, *Z*).

IR (ATR): 1731, 1586, 1470, 1436, 1149, 784, 730 cm^{-1}.

MS (EI) *m*/*z* (relative intensity): 504 ([M]$^+$, 40), 373 (100), 345 (95), 332 (30), 245 (45).

HR-MS (EI): *m*/*z* calcd. for [C$_{22}$H$_{21}$IN$_2$O$_4$]$^+$ [M]$^+$ 504.0541, found 504.0549.
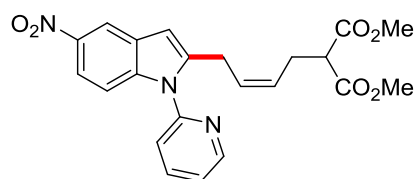
(**Z**)-**Dimethyl 2-{4-[5-nitro-1-(pyridin-2-yl)-1***H*-indol-2-yl]but-2-en-1-yl}malonate** (**130ea**): The general procedure **B** was followed using 5-nitro-1-(pyridin-2-yl)-1*H*-indole (**105e**) (120 mg, 0.50 mmol) and dimethyl 2-vinylcyclopropane-1,1-dicarboxylate (**125a**) (110 mg, 0.60 mmol). Isolation by column chromatography (*n*-hexane/EtOAc: 3/1) yielded **130ea** (187 mg, 88%, *E*/*Z* = 1:17) as a yellow oil.

^{1}H-NMR (300 MHz, CDCl$_3$): δ = 8.67 (ddd, *J* = 4.8, 2.0, 0.9 Hz, 1H), 8.48–8.43 (m, 1H), 8.00–7.91 (m, 2H), 7.44–7.38 (m, 2H), 7.28–7.24 (m, 1H), 6.55 (d, *J* = 0.8 Hz, 1H), 5.59 (dtt, *J* = 10.8, 7.5, 1.4 Hz, 1H), 5.43 (dtt, *J* = 10.8, 7.5, 1.0 Hz, 1H), 3.67 (s, 6H), 3.59 (d, *J* = 7.5 Hz, 1.89H, *Z*), 3.49 (d, *J* = 7.5 Hz, 0.11H, *E*), 3.35 (t, *J* = 7.7 Hz, 1H), 2.58 (ddd, *J* = 7.7, 7.5, 1.4 Hz, 2H).

^{13}**C-NMR** (125 MHz, CDCl$_3$): δ = 169.0 (C$_q$), 150.0 (C$_q$), 149.9 (CH), 142.8 (C$_q$), 142.3 (C$_q$), 140.1 (C$_q$), 138.7 (CH), 127.7 (C$_q$), 127.6 (CH), 127.2 (CH), 123.1 (CH), 121.1 (CH), 117.3 (CH), 116.8 (CH), 110.0 (CH), 104.0 (CH), 52.5 (CH$_3$), 51.3 (CH), 31.5 (CH$_2$, *E*), 30.9 (CH$_2$, *E*), 26.7 (CH$_2$, *Z*), 25.9 (CH$_2$, *Z*).

IR (ATR): 1732, 1587, 1511, 1436, 1326, 908, 727 cm^{-1}.

MS (EI) *m/z* (relative intensity): 423 ([M]$^+$, 20), 292 (100), 264 (80), 251 (40), 205 (25).

HR-MS (EI): *m/z* calcd. for [C$_{22}$H$_{21}$N$_3$O$_6$]$^+$ [M]$^+$ 423.1425, found 423.1420.
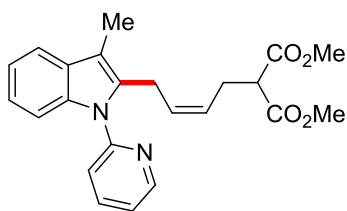
(*Z*)-**Dimethyl 2-{4-[3-methyl-1-(pyridin-2-yl)-1*H*-indol-2-yl]but-2-en-1-yl}malonate** (**130fa**): The general procedure **B** was followed using 3-methyl-1-(pyridin-2-yl)-1*H*-indole (**105f**) (104 mg, 0.50 mmol) and dimethyl 2-vinylcyclopropane-1,1-dicarboxylate (**2a**) (110 mg, 0.60 mmol). Isolation by column chromatography (*n*-hexane/EtOAc: 3/1) yielded **130fa** (182 mg, 93%, *E/Z* = 1:5) as a yellow oil.

^{1}**H-NMR** (500 MHz, CDCl$_3$): δ = 8.61 (ddd, *J* = 4.9, 1.9, 0.8 Hz, 1H), 7.85 (ddd, *J* = 8.0, 7.5, 2.0 Hz, 1H), 7.54–7.51 (m, 1H), 7.39 (ddd, *J* = 8.0, 1.0, 0.8 Hz, 1H), 7.34–7.25 (m, 2H), 7.15–7.10 (m, 2H), 5.48 (dtt, *J* = 15.2, 7.6, 1.4 Hz, 0.17H, *E*), 5.34 (dtt, *J* = 10.6, 7.6, 1.4 Hz, 0.83H, *Z*), 5.18–5.09 (m, 1H), 3.70 (s, 5.02H, *Z*), 3.69 (d, *J* = 7.6 Hz, 2H), 3.63 (s, 0.98H, *E*), 3.25 (t, *J* = 7.6 Hz, 1H), 2.50 (ddd, *J* = 7.6, 7.6, 1.4 Hz, 1.68H, *Z*), 2.42 (ddd, *J* = 7.6, 7.6, 1.4 Hz, 0.32H, *E*), 2.31 (s, 2.52H, *Z*), 2.27 (s, 0.48H, *E*).

^{13}**C-NMR** (125 MHz, CDCl$_3$): δ = 169.2 (C$_q$), 151.6 (C$_q$), 149.6 (C$_q$), 138.2 (CH), 136.5 (C$_q$), 134.7 (CH), 129.8 (C$_q$), 129.3 (CH), 125.0 (CH), 121.9 (CH), 121.6 (CH), 121.0 (CH), 120.2 (CH), 118.2 (C$_q$), 110.3 (CH), 109.8 (CH), 52.5 (CH$_3$), 51.4 (CH), 31.6 (CH$_2$, *E*), 28.0 (CH$_2$, *E*), 26.7 (CH$_2$, *Z*), 23.5 (CH$_2$, *Z*), 8.7 (CH$_3$).

IR (ATR): 1732, 1586, 1470, 1457, 1255, 1125, 1148, 738 cm^{-1}.

MS (EI) *m/z* (relative intensity): 392 ([M]$^+$, 45), 261 (70), 233 (100), 220 (65).

HR-MS (EI): *m/z* calcd. for [C$_{23}$H$_{24}$N$_2$O$_4$]$^+$ [M]$^+$ 392.1736, found 392.1725.
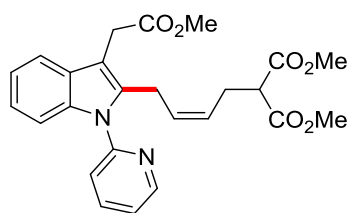
(Z)-Dimethyl 2-{4-[3-(2-methoxy-2-oxoethyl)-1-(pyridin-2-yl)-1*H*-indol-2-yl]but-2-en-1-yl}malonate (130ga): The general procedure **B** was followed using methyl 2-(1-(pyridin-2-yl)-1*H*-indol-3-yl)acetate (**105g**) (133 mg, 0.50 mmol) and dimethyl 2-vinylcyclopropane-1,1-dicarboxylate (**125a**) (110 mg, 0.60 mmol). Isolation by column chromatography (*n*-hexane/EtOAc: 3/1) yielded **130ga** (167 mg, 74%, *E/Z* = 1:11) as a colorless oil.

^{1}H-NMR (500 MHz, CDCl$_3$): δ = 8.63 (ddd, *J* = 4.9, 2.0, 0.9 Hz, 1H), 7.86 (ddd, *J* = 8.0, 7.4, 2.0 Hz, 1H), 7.60–7.57 (m, 1H), 7.40 (ddd, *J* = 8.0, 0.9, 0.9 Hz, 1H), 7.31–7.26 (m, 2H), 7.17–7.11 (m, 2H), 5.36 (dtt, *J* = 10.7, 7.6, 1.4 Hz, 1H), 5.16 (dtt, *J* = 10.7, 7.6, 1.4 Hz, 1H), 3.78 (s, 2H), 3.73 (d, *J* = 7.6 Hz, 2H), 3.70 (s, 6H), 3.66 (s, 3H), 3.25 (t, *J* = 7.6 Hz, 1H), 2.46 (ddd, *J* = 7.6, 7.6, 1.4 Hz, 1.83H, *Z*), 2.40 (ddd, *J* = 7.6, 7.6, 1.4 Hz, 0.17H, *E*).

^{13}C-NMR (125 MHz, CDCl$_3$): δ = 172.0 (C$_q$), 169.2 (C$_q$), 151.2 (C$_q$), 149.7 (CH), 138.3 (CH), 136.4 (C$_q$), 129.2 (CH), 128.3 (CH), 125.4 (C$_q$), 122.2 (CH), 122.1 (C$_q$), 121.3 (CH), 120.7 (CH), 118.4 (CH), 110.0 (CH), 107.5 (CH), 95.5 (C$_q$), 52.5 (CH$_3$), 51.9 (CH$_3$), 51.3 (CH), 31.5 (CH$_2$, *E*), 30.3 (CH$_2$), 28.1 (CH$_2$, *E*), 26.6 (CH$_2$, *Z*), 23.6 (CH$_2$, *Z*).

IR (ATR): 1730, 1586, 1470, 1458, 1147, 731 cm^{-1}.

MS (EI) *m/z* (relative intensity): 450 ([M]$^+$, 30) 319 (80), 291 (100), 259 (40), 245 (45), 219 (50).

HR-MS (EI): *m/z* calcd. for [C$_{25}$H$_{26}$N$_2$O$_6$]$^+$ [M]$^+$ 450.1791, found 450.1796.
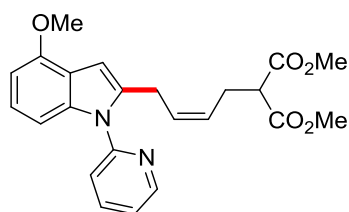
(Z)-Dimethyl 2-{4-[4-methoxy-1-(pyridin-2-yl)-1*H*-indol-2-yl}but-2-en-1-yl]malonate   (130ha): The general procedure **B** was followed using 4-methoxy-1-(pyridin-2-yl)-1*H*-indole (**105h**) (112 mg, 0.50 mmol) and dimethyl 2-vinylcyclopropane-1,1-dicarboxylate (**125a**) (110 mg, 0.60 mmol). Isolation by column chromatography (*n*-hexane/EtOAc: 3/1) yielded **130ha** (157 mg, 77%, *E/Z* = 1:13) as a colorless oil.

^{1}H-NMR (500 MHz, CDCl$_3$): δ = 8.61 (ddd, *J* = 4.9, 1.9, 0.8 Hz, 1H), 7.85 (ddd, *J* = 8.1, 7.5, 2.0 Hz, 1H), 7.41 (ddd, *J* = 8.1, 1.0, 0.8 Hz, 1H), 7.29 (ddd, *J* = 7.5, 4.9, 1.0 Hz, 1H), 7.05–7.00 (m, 1H), 6.94–6.92 (m, 1H), 6.54 (d, *J* = 7.9 Hz, 1H), 6.51 (d, *J* = 0.8 Hz, 1H), 5.61 (dtt, *J* = 10.8, 7.6, 1.4 Hz,

1H), 5.37 (dtt, J = 10.8, 7.7, 1.0 Hz, 1H), 3.93 (s, 3H), 3.68 (s, 6H), 3.61 (d, J = 7.6 Hz, 1.86H, Z), 3.51 (d, J = 7.6 Hz, 0.14H, E), 3.34 (t, J = 7.7 Hz, 1H), 2.60 (ddd, J = 7.7, 7.7, 1.4 Hz, 1.86H, Z), 2.52 (ddd, J = 7.7, 7.7, 1.4 Hz, 0.14H, E).

13C-NMR (125 MHz, CDCl$_3$): δ = 169.2 (C$_q$), 152.6 (C$_q$), 151.4 (C$_q$), 149.5 (CH), 139.6 (C$_q$), 138.2 (CH), 137.7 (C$_q$), 128.8 (CH), 126.2 (CH), 122.5 (CH), 122.1 (CH), 121.0 (CH), 118.7 (C$_q$), 103.5 (CH), 100.7 (CH), 99.8 (CH), 55.3 (CH$_3$), 52.5 (CH$_3$), 51.5 (CH), 31.6 (CH$_2$, E), 30.7 (CH$_2$, E), 26.7 (CH$_2$, Z), 25.9 (CH$_2$, Z).

IR (ATR): 1732, 1587, 1495, 1469, 1255, 1148, 765, 728 cm^{-1}.

MS (EI) m/z (relative intensity): 408 ([M]$^+$, 45), 277 (60), 249 (100), 236 (30).

HR-MS (EI): m/z calcd. for [C$_{23}$H$_{24}$N$_2$O$_5$]$^+$ [M]$^+$ 408.1680, found 408.1689.
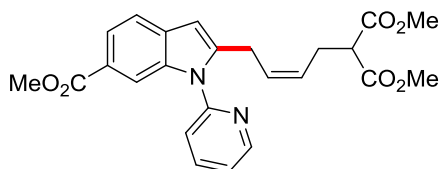
(Z)-Dimethyl 2-{4-[6-(methoxycarbonyl)-1-(pyridin-2-yl)-1H-indol-2-yl]but-2-en-1-yl}-malonate (130ia): The general procedure **B** was followed using methyl 1-(pyridin-2-yl)-1H-indole-6-carboxylate (**105i**) (126 mg, 0.50 mmol) and dimethyl 2-vinylcyclopropane-1,1-dicarboxylate (**125a**) (110 mg, 0.60 mmol). Isolation by column chromatography (n-hexane/EtOAc: 3/1) yielded **130ia** (183 mg, 84%, E/Z = 1:8) as a colorless oil.

1H-NMR (500 MHz, CDCl$_3$): δ = 8.65 (ddd, J = 4.9, 1.9, 0.8 Hz, 1H), 8.00–7.98 (m, 1H), 7.91 (ddd, J = 7.9, 7.5, 2.0 Hz, 1H), 7.80 (ddd, J = 8.2, 1.4, 0.8 Hz, 1H), 7.56–7.53 (m, 1H), 7.45 (dd, J = 7.9, 1.0 Hz, 1H), 7.35–7.32 (m, 1H), 6.45 (d, J = 0.7 Hz, 1H), 5.61 (dtt, J = 10.8, 7.6, 1.5 Hz, 1H), 5.41 (dtt, J = 10.8, 7.6, 1.0 Hz, 1H), 3.85 (s, 3H), 3.69 (s, 0.70H, E), 3.67 (s, 5.30H, Z), 3.64 (d, J = 7.6 Hz, 2H), 3.34 (t, J = 7.7 Hz, 1H), 2.59 (ddd, J = 7.7, 7.6, 1.5 Hz, 1.77H, Z), 2.53 (ddd, J = 7.7, 7.6, 1.5 Hz, 0.23H, E).

13C-NMR (125 MHz, CDCl$_3$): δ = 169.1 (C$_q$), 168.0 (C$_q$), 150.6 (C$_q$), 149.8 (CH), 143.0 (C$_q$), 138.7 (CH), 136.7 (C$_q$), 132.2 (C$_q$), 128.2 (CH), 126.9 (CH), 123.4 (C$_q$), 122.6 (CH), 121.8 (CH), 121.2 (CH), 119.5 (CH), 112.2 (CH), 102.9 (CH), 52.5 (CH$_3$, Z), 52.4 (CH$_3$, E), 51.8 (CH$_3$, Z), 51.7 (CH$_3$, E), 51.3 (CH, Z), 50.7 (CH, E), 31.6 (CH$_2$, E), 30.8 (CH$_2$, E), 26.7 (CH$_2$, Z), 25.9 (CH$_2$, Z).

IR (ATR): 1731, 1710, 1587, 1470, 1434, 1233, 909, 725 cm^{-1}.

MS (EI) m/z (relative intensity): 436 ([M]$^+$, 15), 305 (40), 277 (100), 265 (20).

HR-MS (EI): m/z calcd. for [C$_{24}$H$_{24}$N$_2$O$_6$]$^+$ [M]$^+$ 436.1629, found 436.1630.
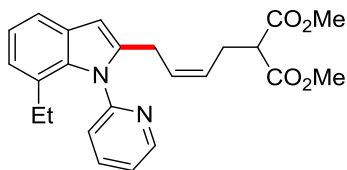
(*Z*)-Dimethyl 2-{4-[7-ethyl-1-(pyridin-2-yl)-1*H*-indol-2-yl]but-2-en-1-yl}malonate (130ja): The general procedure **B** was followed using 7-ethyl-1-(pyridin-2-yl)-1*H*-indole (**105j**) (110 mg, 0.50 mmol) and dimethyl 2-vinylcyclopropane-1,1-dicarboxylate (**125a**) (110 mg, 0.60 mmol). Isolation by column chromatography (*n*-hexane/EtOAc: 3/1) yielded **130ja** (138 mg, 68%, *E*/*Z* = 1:8) as a yellow oil.

^{1}H-NMR (500 MHz, CDCl$_3$): δ = 8.64 (ddd, *J* = 4.8, 2.0, 0.9 Hz, 1H), 7.84 (ddd, *J* = 8.0, 7.4, 2.0 Hz, 1H), 7.42–7.38 (m, 2H), 7.33 (ddd, *J* = 7.7, 1.0, 0.9 Hz, 1H), 7.05 (dd, *J* = 7.6, 7.6 Hz, 1H), 6.94–6.91 (m, 1H), 6.37 (d, *J* = 0.8 Hz, 1H), 5.61 (dtt, *J* = 10.8, 7.5, 1.4 Hz, 1H), 5.37 (dtt, *J* = 10.8, 7.5, 1.0 Hz, 1H), 3.69 (s, 0.70H, *E*), 3.67 (s, 5.30H, *Z*), 3.33 (t, *J* = 7.5 Hz, 1H), 3.25 (d, *J* = 7.5 Hz, 2H), 2.25 (ddd, *J* = 7.5, 7.5, 1.4 Hz, 2H), 2.14 (q, *J* = 7.7 Hz, 2H), 0.91 (t, *J* = 7.7 Hz, 3H).

^{13}C-NMR (125 MHz, CDCl$_3$): δ = 169.2 (C$_q$), 153.3 (C$_q$), 149.3 (CH), 140.0 (C$_q$), 137.8 (CH), 136.1 (C$_q$), 129.3 (C$_q$), 128.7 (CH), 127.4 (C$_q$), 126.3 (CH), 124.1 (CH), 123.3 (CH), 122.2 (CH), 120.3 (CH), 117.9 (CH), 102.0 (CH), 52.5 (CH$_3$), 51.4 (CH), 31.6 (CH$_2$, *E*), 30.7 (CH$_2$, *E*), 26.7 (CH$_2$, *Z*), 25.9 (CH$_2$, *Z*), 24.8 (CH$_2$), 14.5 (CH$_3$).

IR (ATR): 1733, 1584, 1436, 1150, 909, 729 cm^{-1}.

MS (EI) *m*/*z* (relative intensity): 406 ([M]$^+$, 60), 275 (90), 247 (100), 234 (45), 219 (30).

HR-MS (EI): *m*/*z* calcd. for [C$_{24}$H$_{26}$N$_2$O$_4$]$^+$ [M]$^+$ 406.1887, found 406.1888.
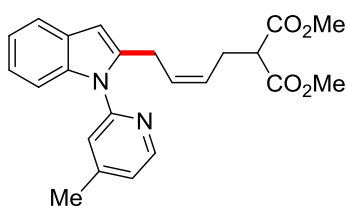
(*Z*)-Dimethyl 2-{4-[1-(5-methylpyridin-2-yl)-1*H*-indol-2-yl]but-2-en-1-yl}malonate (130ka): The general procedure **B** was followed using 1-(5-methylpyridin-2-yl)-1*H*-indole (**105k**) (104 mg, 0.50 mmol) and dimethyl 2-vinylcyclopropane-1,1-dicarboxylate (**125a**) (110 mg, 0.60 mmol). Isolation by column chromatography (*n*-hexane/EtOAc: 3/1) yielded **130ka** (159 mg, 81%, *E*/*Z* = 1:14) as an orange oil.
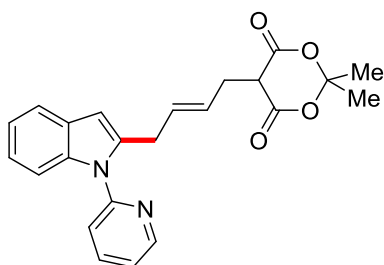
^{1}H-NMR (500 MHz, CDCl$_3$): δ = 8.49 (ddd, *J* = 4.9, 1.9, 0.8 Hz, 1H), 7.57–7.52 (m, 1H), 7.32–7.28 (m, 1H), 7.26–7.22 (m, 1H), 7.13–7.08 (m, 3H), 6.40 (d, *J* = 0.7 Hz, 1H), 5.64 (dtt, *J* = 10.7, 7.5, 1.4 Hz, 1H), 5.43–5.35 (m, 1H), 3.68 (s, 6H), 3.63 (d, *J* = 7.5 Hz, 2H), 3.35 (t, *J* = 7.7 Hz, 1H), 2.61 (ddd, *J* = 7.7, 7.6, 1.4 Hz, 1.87H, *Z*), 2.54 (ddd, *J* = 7.7, 7.6, 1.4 Hz, 0.13H, *E*), 2.42 (s, 3H).

^{13}C-NMR (125 MHz, CDCl$_3$): δ = 169.2 (C$_q$), 151.3 (C$_q$), 149.8 (C$_q$), 149.2 (CH), 139.3 (C$_q$), 137.3 (C$_q$), 129.0 (CH), 128.4 (C$_q$), 126.2 (CH), 123.1 (CH), 121.7 (CH), 121.6 (CH), 120.5 (CH), 119.9 (CH), 110.0 (CH), 102.5 (CH), 52.4 (CH$_3$), 51.4 (CH), 31.6 (CH$_2$, E), 30.9 (CH$_2$, E), 26.7 (CH$_2$, Z), 25.8 (CH$_2$, Z), 21.0 (CH$_3$).

IR (ATR): 1732, 1603, 1457, 1433, 1151, 910, 729 cm^{-1}.

MS (EI) m/z (relative intensity): 392 ([M]$^+$, 25), 261 (100), 233 (55), 220 (50).

HR-MS (EI): m/z calcd. for [C$_{23}$H$_{24}$N$_2$O$_4$]$^+$ [M]$^+$ 392.1736, found 392.1729.
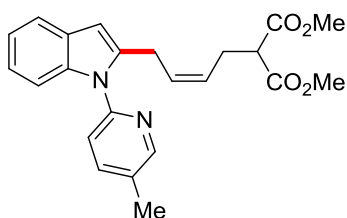
(Z)-Dimethyl 2-{4-[1-(4-methylpyridin-2-yl)-1H-indol-2-yl]but-2-en-1-yl}malonate (130la): The general procedure **B** was followed using 1-(4-methylpyridin-2-yl)-1H-indole (**105l**) (104 mg, 0.50 mmol) and dimethyl 2-vinylcyclopropane-1,1-dicarboxylate (**125a**) (110 mg, 0.60 mmol). Isolation by column chromatography (*n*-hexane/EtOAc: 3/1) yielded **130la** (180 mg, 92%, E/Z = 1:14) as an orange oil.

^{1}H-NMR (500 MHz, CDCl$_3$): δ = 8.46 (ddd, J = 4.9, 1.9, 0.8 Hz, 1H), 7.55–7.52 (m, 1H), 7.33–7.30 (m, 1H), 7.28–7.24 (m, 1H), 7.12–7.07 (m, 3H), 6.40 (d, J = 0.8 Hz, 1H), 5.63 (dtt, J = 10.7, 7.5, 1.4 Hz, 1H), 5.43–5.35 (m, 1H), 3.68 (s, 6H), 3.63 (d, J = 7.5 Hz, 2H), 3.35 (t, J = 7.7 Hz, 1H), 2.60 (ddd, J = 7.7, 7.7, 1.4 Hz, 1.87H, Z), 2.57 (ddd, J = 7.7, 7.7, 1.4 Hz, 0.13H, E), 2.44 (s, 3H).

^{13}C-NMR (125 MHz, CDCl$_3$): δ = 169.2 (C$_q$), 149.8 (CH), 148.8 (C$_q$), 139.2 (C$_q$), 138.8 (CH), 137.4 (C$_q$), 131.8 (C$_q$), 128.9 (CH), 128.3 (C$_q$), 126.2 (CH), 121.6 (CH), 120.5 (CH), 120.4 (CH), 119.9 (CH), 110.0 (CH), 102.2 (CH), 52.4 (CH$_3$), 51.4 (CH), 31.7 (CH$_2$, E), 30.9 (CH$_2$, E), 26.7 (CH$_2$, Z), 25.9 (CH$_2$, Z), 21.1 (CH$_3$).

IR (ATR): 1732, 1483, 1456, 1275, 1150, 1205, 785 cm^{-1}.

MS (EI) m/z (relative intensity): 392 ([M]$^+$, 20), 261 (100), 233 (75), 220 (60).

HR-MS (EI): m/z calcd. for [C$_{23}$H$_{24}$N$_2$O$_4$]$^+$ [M]$^+$ 392.1736, found 392.1736.
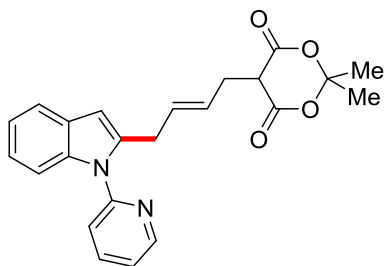
(*E*)-2,2-Dimethyl-5-{4-[1-(pyridin-2-yl)-1*H*-indol-2-yl]but-2-en-1-yl}-1,3-dioxane-4,6-dione

(130ab): The general procedure **B** was followed using 1-(pyridin-2-yl)-1*H*-indole (**105a**) (97.0 mg, 0.50 mmol and 6,6-dimethyl-1-vinyl-5,7-dioxaspiro[2.5]octane-4,8-dione (**125b**) (118 mg, 0.60 mmol). Isolation by column chromatography (*n*-hexane/EtOAc: 3/1) yielded **130ab** (162 mg, 83%, *E/Z* = 3.7:1) as an orange oil.
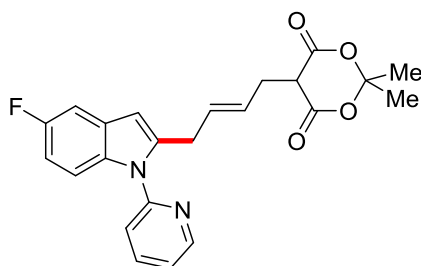
^{1}H-NMR (500 MHz, CDCl$_3$): δ = 8.63 (ddd, *J* = 4.9, 1.9, 0.8 Hz, 1H), 7.85 (ddd, *J* = 8.0, 7.4, 2.0 Hz, 1H), 7.57–7.52 (m, 1H), 7.40 (ddd, *J* = 8.0, 1.0, 0.8 Hz, 1H), 7.33–7.27 (m, 2H), 7.12–7.07 (m, 2H), 6.42 (d, *J* = 0.8 Hz, 1H), 5.72 (dtt, *J* = 15.2, 6.7, 1.2 Hz, 0.79H, *E*), 5.64 (dtt, *J* = 10.7, 7.2, 1.4 Hz, 0.21H, *Z*), 5.50 (dtt, *J* = 10.7, 7.2, 1.6 Hz, 0.21H, *Z*), 5.42 (dtt, *J* = 15.2, 7.3, 1.2 Hz, 0.79H, *E*), 3.70 (d, *J* = 7.2 Hz, 0.42H, *Z*), 3.55 (d, *J* = 6.7 Hz, 1.58H, *E*), 3.46 (t, *J* = 7.7 Hz, 1H), 2.74 (ddd, *J* = 7.7, 7.2, 1.4 Hz, 2H), 1.71 (s, 6H).

^{13}C-NMR (125 MHz, CDCl$_3$): δ = 165.0 (C$_q$), 151.4 (C$_q$), 149.6 (CH), 139.2 (C$_q$), 138.3 (CH), 137.3 (C$_q$), 131.5 (CH), 128.6 (C$_q$), 126.4 (CH), 122.2 (CH), 121.9 (CH), 121.0 (CH), 120.7 (CH), 120.1 (CH), 110.1 (CH), 105.0 (C$_q$), 103.0 (CH), 46.3 (CH), 30.9 (CH$_2$, *E*), 29.0 (CH$_2$, *E*), 28.3 (CH$_3$), 26.8 (CH$_3$), 26.5 (CH$_2$, *Z*), 25.9 (CH$_2$, *Z*).

IR (ATR): 1782, 1743, 1586, 1469, 1284, 908, 727 cm^{-1}.

MS (EI) *m/z* (relative intensity): 390 ([M]$^+$, 30), 287 (35), 259 (40), 247 (100), 219 (80), 206 (85).

HR-MS (EI): *m/z* calcd. for [C$_{23}$H$_{22}$N$_2$O$_4$]$^+$ [M]$^+$ 390.1580, found: 390.1567.

(*E*)-2,2-Dimethyl-5-{4-[1-(pyridin-2-yl)-1*H*-indol-2-yl]but-2-en-1-yl}-1,3-dioxane-4,6-dione

(130ab): The general procedure **C** was followed using 1-(pyridin-2-yl)-1*H*-indole (**105a**) (97.0 mg, 0.50 mmol) and 6,6-dimethyl-1-vinyl-5,7-dioxaspiro[2.5]octane-4,8-dione (**125b**) (118 mg,

0.60 mmol). Isolation by column chromatography (*n*-hexane/EtOAc: 3/1) yielded **130ab** (162 mg, 83%, *E*/*Z* = 5.9:1) as an orange oil.

^{1}H-NMR (500 MHz, CDCl$_3$): δ = 8.63 (ddd, *J* = 4.9, 1.9, 0.8 Hz, 1H), 7.85 (ddd, *J* = 8.0, 7.4, 2.0 Hz, 1H), 7.57–7.52 (m, 1H), 7.40 (ddd, *J* = 8.0, 1.0, 0.9 Hz, 1H), 7.33–7.27 (m, 2H), 7.12–7.07 (m, 2H), 6.42 (d, *J* = 0.8 Hz, 1H), 5.72 (dtt, *J* = 15.2, 6.7, 1.2 Hz, 0.86H, *E*), 5.64 (dtt, *J* = 10.7, 7.2, 1.4 Hz, 0.14H, *Z*), 5.50 (dtt, *J* = 10.7, 7.2, 1.6 Hz, 0.14H, *Z*), 5.42 (dtt, *J* = 15.2, 7.3, 1.2 Hz, 0.86H, *E*), 3.70 (d, *J* = 7.2 Hz, 0.29H, *Z*), 3.55 (d, *J* = 6.7 Hz, 1.71H, *E*), 3.46 (t, *J* = 7.7 Hz, 1H), 2.74 (ddd, *J* = 7.7, 7.2, 1.4 Hz, 2H), 1.71 (s, 6H).

^{13}C-NMR (125 MHz, CDCl$_3$): δ = 165.0 (C$_q$), 151.4 (C$_q$), 149.6 (CH), 139.2 (C$_q$), 138.3 (CH), 137.3 (C$_q$), 131.5 (CH), 128.6 (C$_q$), 126.4 (CH), 122.2 (CH), 121.9 (CH), 121.0 (CH), 120.7 (CH), 120.1 (CH), 110.1 (CH), 105.0 (C$_q$), 103.0 (CH), 46.3 (CH), 30.9 (CH$_2$, *E*), 29.0 (CH$_2$, *E*), 28.3 (CH$_3$), 26.8 (CH$_3$), 26.5 (CH$_2$, *Z*), 25.9 (CH$_2$, *Z*).

IR (ATR): 1782, 1743, 1586, 1469, 1284, 908, 727 cm^{-1}.

MS (EI) *m/z* (relative intensity): 390 ([M]$^+$, 30), 287 (35), 259 (40), 247 (100), 219 (80), 206 (85).

HR-MS (EI): *m/z* calcd. for [C$_{23}$H$_{22}$N$_2$O$_4$]$^+$ [M]$^+$ 390.1580, found: 390.1567.

(*E*)-5-{4-[5-fluoro-1-(pyridin-2-yl)-1*H*-indol-2-yl]but-2-en-1-yl}-2,2-dimethyl-1,3-dioxane-4,6-dione (130mb): The general procedure **B** was followed using 5-fluoro-1-(pyridin-2-yl)-1*H*-indole (**130m**) (106 mg, 0.50 mmol) and 6,6-dimethyl-1-vinyl-5,7-dioxaspiro[2.5]octane-4,8-dione (**125b**) (118 mg, 0.60 mmol). Isolation by column chromatography (*n*-hexane/EtOAc: 3/1) yielded **130mb** (165 mg, 81%, *E*/*Z* = 2.6:1) as an orange oil.

^{1}H-NMR (300 MHz, CDCl$_3$): δ = 8.62 (ddd, *J* = 4.9, 1.9, 0.8 Hz, 1H), 7.85 (ddd, *J* = 8.0, 7.4, 2.0 Hz, 1H), 7.42–7.27 (m, 2H), 7.24–7.14 (m, 2H), 6.82 (dt, *J* = 9.2, 2.6 Hz, 1H), 6.36 (d, *J* = 0.8 Hz, 1H), 5.71 (dtt, *J* = 15.3, 6.9, 1.4 Hz, 0.72H, *E*), 5.65 (dtt, *J* = 10.6, 7.5, 1.4 Hz, 0.28H, *Z*), 5.54–5.37 (m, 1H), 3.67 (d, *J* = 7.5 Hz, 0.56H, *Z*), 3.52 (d, *J* = 6.9 Hz, 1.44H, *E*), 3.47 (t, *J* = 7.7 Hz, 1H), 2.78 (ddd, *J* = 7.7, 7.6, 1.4 Hz, 0.55H, *Z*), 2.74 (ddd, *J* = 7.7, 7.6, 1.4 Hz, 1.45H, *E*), 1.75–1.64 (m, 6H).

^{13}C-NMR (125 MHz, CDCl$_3$): δ = 165.0 (C$_q$), 158.5 (d, $^1J_{C–F}$ = 236 Hz, C$_q$), 151.2 (C$_q$), 149.6 (CH), 140.8 (C$_q$), 138.4 (CH), 133.9 (C$_q$), 131.2 (CH), 129.0 (d, $^3J_{C–F}$ = 10.4 Hz, C$_q$), 126.7 (CH), 122.3 (CH), 121.0 (CH), 120.7 (CH), 110.9 (d, $^3J_{C–F}$ = 10.1 Hz, CH), 109.8 (d, $^2J_{C–F}$ = 26.3 Hz, CH), 105.0

(C$_q$), 103.0 (d, $^4J_{C-F}$ = 4.2 Hz, CH), 46.2 (CH), 30.9 (CH$_2$, E), 29.0 (CH$_2$, E), 28.3 (CH$_3$), 26.8 (CH$_3$), 26.5 (CH$_2$, Z), 25.9 (CH$_2$, Z).

^{19}F-NMR (282 MHz, CDCl$_3$): δ = –124.0 (m).

IR (ATR): 1782, 1745, 1585, 1469, 1288, 1174, 775, 729 cm^{-1}.

MS (EI) m/z (relative intensity): 408 ([M]$^+$, 10) 324 (15), 305 (15), 277 (25), 265 (85), 237 (100), 224 (80).

HR-MS (EI): m/z calcd. for [C$_{23}$H$_{21}$FN$_2$O$_4$]$^+$ [M]$^+$ 408.1485, found 408.1491.
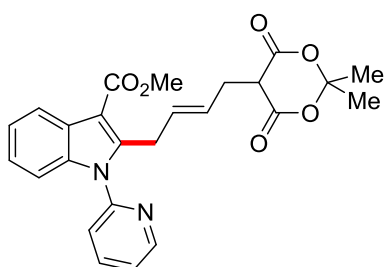
(Z)-Methyl-2-{4-[2,2-dimethyl-4,6-dioxo-1,3-dioxan-5-yl]but-2-en-1-yl}-1-(pyridin-2-yl)-1H-indole-3-carboxylate (130nb): The general procedure **B** was followed using methyl 1-(pyridin-2-yl)-1H-indole-3-carboxylate (**130n**) (126 mg, 0.50 mmol) and 6,6-dimethyl-1-vinyl-5,7-dioxaspiro[2.5]octane-4,8-dione (**125b**) (118 mg, 0.60 mmol). Isolation by column chromatography (n-hexane/EtOAc: 3/1) yielded **130nb** (168 mg, 75%, E/Z = 2.4:1) as an orange oil.

^{1}H-NMR (500 MHz, CDCl$_3$): δ = 8.68 (ddd, J = 4.9, 1.9, 0.8 Hz, 1H), 8.17–8.12 (m, 1H), 7.91 (ddd, J = 8.0, 7.4, 2.0 Hz, 1H), 7.41–7.39 (m, 2H), 7.24 (ddd, J = 9.3, 6.8, 1.5 Hz, 1H), 7.18–7.10 (m, 2H), 5.66 (dtt, J = 15.2, 7.4, 1.2 Hz, 0.71H, E), 5.50–5.42 (m, 0.58H, Z), 5.23 (dtt, J = 15.2, 7.2, 1.2 Hz, 0.71H, E), 3.98 (s, 3H), 3.92 (d, J = 7.4 Hz, 2H), 3.72 (t, J = 7.5 Hz, 0.29H, Z), 3.44 (t, J = 7.5 Hz, 0.71H, E), 2.64 (ddd, J = 7.5, 7.2, 1.2 Hz, 2H), 1.76–1.60 (m, 6H).

^{13}C-NMR (125 MHz, CDCl$_3$): δ = 166.1 (C$_q$), 165.2 (C$_q$, Z), 164.9 (C$_q$, E), 150.1 (CH), 150.0 (C$_q$), 146.9 (C$_q$, Z), 146.0 (C$_q$, E), 138.7 (CH), 136.9 (C$_q$), 130.8 (CH), 126.6 (C$_q$), 126.3 (CH), 123.6 (CH), 123.1 (CH), 122.6 (CH), 122.5 (CH), 121.8 (CH), 110.4 (CH), 106.0 (C$_q$), 104.9 (C$_q$), 50.6 (CH), 46.5 (CH$_3$, Z), 46.3 (CH$_3$, E), 29.0 (CH$_2$, E), 28.9 (CH$_2$, E), 28.8 (CH$_3$), 26.7 (CH$_3$), 24.7 (CH$_2$, Z), 23.8 (CH$_2$, Z).

IR (ATR): 1746, 1694, 1537, 1457, 1283, 1189, 1099, 909, 727 cm^{-1}.

MS (EI) m/z (relative intensity): 448 ([M]$^+$, 10), 364 (10), 305 (45), 277 (70), 264 (30), 245 (40).

HR-MS (EI): m/z calcd. for [C$_{25}$H$_{24}$N$_2$O$_6$]$^+$ [M]$^+$ 448.1634, found 448.1631.
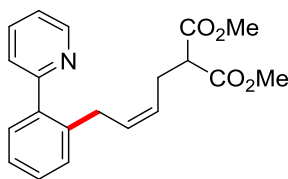
(*Z*)-Dimethyl 2-{4-[2-(pyridin-2-yl)phenyl]but-2-en-1-yl}malonate (131aa): The general procedure **B** was followed using 2-phenylpyridine (**1a**) (77.6 mg, 0.50 mmol) and dimethyl 2-vinylcyclopropane-1,1-dicarboxylate (**125a**) (110 mg, 0.60 mmol). Isolation by column chromatography (*n*-hexane/EtOAc: 3/1) yielded **131aa** (146 mg, 86%, *E*/*Z* = 1:9) as a colorless oil.

¹H-NMR (400 MHz, CDCl₃): δ = 8.68–8.63 (m, 1H), 7.73 (ddd, *J* = 8.0, 7.8, 1.9 Hz, 1H), 7.38–7.29 (m, 3H), 7.29–7.20 (m, 3H), 5.59 (dtt, *J* = 15.1, 7.5, 1.4 Hz, 0.10H, *E*), 5.51 (dtt, *J* = 10.7, 7.5, 1.4 Hz, 0.90H, *Z*), 5.32–5.20 (m, 1H), 3.69 (s, 5.40H, *Z*), 3.63 (s, 0.60H, *E*), 3.50 (d, *J* = 7.5 Hz, 1.80H, *Z*), 3.50 (d, *J* = 7.5 Hz, 0.20H, *E*), 3.31 (t, *J* = 7.7 Hz, 1H), 2.56 (ddd, *J* = 7.7, 7.7, 1.4 Hz, 2H).

¹³C-NMR (100 MHz, CDCl₃): δ = 169.3 (C$_q$), 159.9 (C$_q$), 149.2 (CH), 140.3 (C$_q$), 138.3 (C$_q$), 136.2 (CH), 131.8 (CH), 129.8 (CH), 129.6 (CH), 128.5 (CH), 126.2 (CH), 125.0 (CH), 124.2 (CH), 121.7 (CH), 52.5 (CH₃), 51.6 (CH), 31.0 (CH₂), 26.7 (CH₂).

IR (ATR): 1732, 1586, 1435, 1231, 1196, 1150, 1024, 751 cm⁻¹.

MS (EI) *m/z* (relative intensity): 339 ([M]⁺, 15), 308 (100).

HR-MS (ESI): *m/z* calcd. for [C₂₀H₂₂NO₄]⁺ [M + H]⁺ 340.1543, found 340.1547.
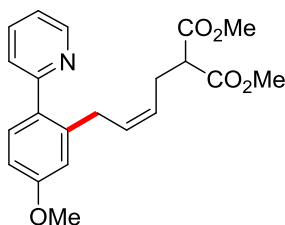
(*Z*)-Dimethyl 2-{4-[5-methoxy-2-(pyridin-2-yl)phenyl]but-2-en-1-yl}malonate (131ba): The general procedure **B** was followed using 2-(4-methoxyphenyl)pyridine (**1b**) (92.5 mg, 0.50 mmol) and dimethyl 2-vinylcyclopropane-1,1-dicarboxylate (**125a**) (110 mg, 0.60 mmol). Isolation by column chromatography (*n*-hexane/EtOAc: 3/1) yielded **131ba** (138 mg, 75%, *E*/*Z* = 1:4) as a colorless oil.

¹H-NMR (600 MHz, CDCl₃): δ = 8.68–8.63 (m, 1H), 7.69 (ddd, *J* = 8.0, 7.6, 1.9 Hz, 1H), 7.34–7.27 (m, 2H), 7.18 (ddd, *J* = 7.6, 4.9, 1.2 Hz, 1H), 6.82–6.75 (m, 2H), 5.58 (dtt, *J* = 15.8, 7.4, 1.2 Hz, 0.20H, *E*), 5.51 (dtt, *J* = 10.7, 7.6, 1.2 Hz, 0.80H, *Z*), 5.32–5.24 (m, 1H), 3.80 (s, 3H), 3.68 (s, 4.80H, *Z*), 3.65 (s, 1.20H, *E*), 3.51 (d, *J* = 7.4 Hz, 1.59H, *Z*), 3.39 (d, *J* = 7.4 Hz, 0.41H, *E*), 3.31 (t, *J* = 7.7 Hz, 1H), 2.57 (ddd, *J* = 7.7, 7.6, 1.2 Hz, 1.61H, *Z*), 2.53 (ddd, *J* = 7.7, 7.6, 1.2 Hz, 0.39H, *E*).

^{13}**C-NMR** (125 MHz, CDCl$_3$): δ = 169.2 (C$_q$), 159.5 (C$_q$), 149.0 (CH), 139.8 (C$_q$), 139.5 (C$_q$), 136.2 (CH), 132.9 (C$_q$), 132.4 (CH), 131.6 (CH), 125.1 (CH), 124.1 (CH), 121.3 (CH), 115.1 (CH), 111.4 (CH), 55.2 (CH$_3$), 52.4 (CH$_3$), 51.5 (CH), 36.2 (CH$_2$, *E*), 31.7 (CH$_2$, *E*), 31.1 (CH$_2$, *Z*), 26.6 (CH$_2$, *Z*).

IR (ATR): 1732, 1606, 1587, 1428, 1231, 1149, 988, 787 cm^{-1}.

MS (EI) *m/z* (relative intensity): 369 ([M]$^+$, 10), 238 (100), 197 (40), 193 (10), 167 (75).

HR-MS (EI): *m/z* calcd. for [C$_{21}$H$_{23}$NO$_5$]$^+$ [M]$^+$ 369.1576, found 369.1573.
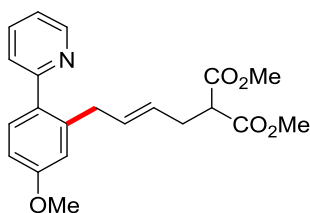
(*E*)-**Dimethyl 2-{4-[5-methoxy-2-(pyridin-2-yl)phenyl]but-2-en-1-yl}malonate (131ba')**: The general procedure **C** was followed using 2-(4-methoxyphenyl)pyridine (**1b**) (46.3 mg, 0.25 mmol) and dimethyl 2-vinylcyclopropane-1,1-dicarboxylate (**125a**) (55.2 mg, 0.30 mmol). Isolation by column chromatography (*n*-hexane/EtOAc: 5/1 → 3/1 → 2/1) yielded **131ba'** (41.6 mg, 45%, *E/Z* = 2:1) and **131ba''** (16.6 mg, 12%, *E/Z* = 3:1) as yellow oils.

^{1}**H-NMR** (500 MHz, CDCl$_3$): δ = 8.68–8.63 (m, 1H), 7.68 (ddd, *J* = 8.0, 7.8, 1.9 Hz, 1H), 7.34–7.27 (m, 2H), 7.18 (ddd, *J* = 7.8, 4.9, 1.2 Hz, 1H), 6.83–6.75 (m, 2H), 5.61–5.48 (m, 1H), 5.33–5.23 (m, 1H), 3.82 (s, 3H), 3.69 (s, 1.80H, *Z*), 3.67 (s, 4.20H, *E*), 3.51 (d, *J* = 7.4 Hz, 0.60H, *Z*), 3.39 (d, *J* = 7.4 Hz, 1.40H, *E*), 3.34 (t, *J* = 7.7 Hz, 1H), 2.58 (ddd, *J* = 7.7, 7.6, 1.4 Hz, 0.60H, *Z*), 2.53 (ddd, *J* = 7.7, 7.6, 1.4 Hz, 1.40H, *E*).

^{13}**C-NMR** (125 MHz, CDCl$_3$): δ = 169.2 (C$_q$), 159.9 (C$_q$), 149.0 (CH), 139.8 (C$_q$), 139.9 (C$_q$), 136.0 (CH), 132.4 (C$_q$), 132.2 (CH), 131.1 (CH), 125.1 (CH), 124.2 (CH), 121.3 (CH), 115.3 (CH), 111.5 (CH), 55.3 (CH$_3$), 52.7 (CH$_3$), 51.3 (CH), 36.3 (CH$_2$, *E*), 31.8 (CH$_2$, *E*), 31.2 (CH$_2$, *Z*), 26.7 (CH$_2$, *Z*).

IR (ATR): 1732, 1586, 1468, 1436, 1256, 1150, 1170, 747 cm^{-1}.

MS (ESI) *m/z* (relative intensity): 370 ([M + H]$^+$, 10), 238 (100), 197 (40).

HR-MS (ESI): *m/z* calcd. for [C$_{21}$H$_{24}$NO$_5$]$^+$ [M + H]$^+$ 370.1649, found 370.1651.
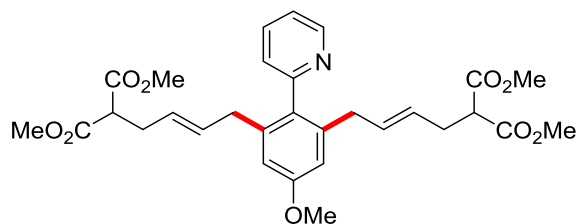
(2*E*,*Z*,2'*E*,*Z*)-Tetramethyl   [5-methoxy-2-(pyridin-2-yl)-1,3-phenylene]bis(but-2-ene-4,1-diyl)]di-malonate (131ba''):

¹H-NMR (600 MHz, CDCl₃): δ = 8.70–8.62 (m, 1H), 7.72–7.65 (m, 1H), 7.23–7.12 (m, 2H), 6.66–6.59 (m, 2H), 5.50–5.42 (m, 2H), 5.24 (dtt, *J* = 10.7, 7.6, 1.2 Hz, 1H, *Z*), 5.14 (dtt, *J* = 15.2, 7.7, 1.4 Hz, 1H, *E*), 3.79 (s, 3H), 3.66 (s, 12H), 3.33 (t, *J* = 7.7 Hz, 1.51H, *E*), 3.26 (t, *J* = 7.7 Hz, 0.49H, *Z*), 3.08 (d, *J* = 7.6 Hz, 0.95H, *Z*), 2.94 (d, *J* = 7.6 Hz, 3.05H, *E*), 2.49 (ddd, *J* = 7.7, 7.7, 1.2 Hz, 3.05H, *E*), 2.42 (ddd, *J* = 7.7, 7.6, 1.2 Hz, 0.95H, *Z*).

¹³C-NMR (125 MHz, CDCl₃): δ = 169.1 (C$_q$), 159.1 (C$_q$), 158.7 (C$_q$), 149.3 (CH), 139.7 (C$_q$), 135.7 (CH), 132.0 (C$_q$), 126.5 (CH), 125.0 (CH), 121.6 (CH), 121.6 (CH), 112.4 (CH), 55.2 (CH₃), 52.4 (CH₃), 51.5 (CH, *E*), 51.5 (CH, *Z*), 36.8 (CH₂, *E*), 31.8 (CH₂, *E*), 31.6 (CH₂, *Z*), 26.6 (CH₂, *Z*).

IR (ATR): 1730, 1602, 1459, 1434, 1230, 1148, 1021, 753 cm⁻¹.

MS (EI) *m/z* (relative intensity): 553 ([M]⁺, 10), 522 (10), 422 (100).

HR-MS (EI): *m/z* calcd. for [C₃₀H₃₅NO₉]⁺ [M]⁺ 553.2312, found 553.2310.
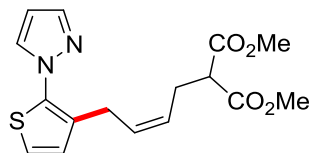
(*Z*)-Dimethyl 2-{4-[2-(1*H*-pyrazol-1-yl)thiophen-3-yl]but-2-en-1-yl}malonate (133): The general procedure **B** was followed using 1-(thiophen-2-yl)-1H-pyrazole (**131**) (75.0 mg, 0.50 mmol) and dimethyl 2-vinylcyclopropane-1,1-dicarboxylate (**125a**) (110 mg, 0.60 mmol). Isolation by column chromatography (*n*-hexane/EtOAc: 3/1) yielded **133** (67.0 mg, 40%, *E*/*Z* = 12:1) as a colorless oil.

¹H-NMR (500 MHz, CDCl₃): δ = 7.70 (dd, *J* = 1.9, 0.5 Hz, 1H), 7.63 (dd, *J* = 2.5, 0.5 Hz, 1H), 7.11 (d, *J* = 5.5 Hz, 1H), 6.84 (d, *J* = 5.5 Hz, 1H), 6.42 (dd, *J* = 2.5, 1.9 Hz, 1H), 5.56 (dtt, *J* = 10.6, 7.6, 1.0 Hz, 1H), 5.38 (dtt, *J* = 10.6, 7.6, 1.0 Hz, 1H), 3.71 (s, 6H), 3.40–3.24 (m, 3H), 2.66 (ddd, *J* = 7.6, 7.6, 1.0 Hz, 1.84H, *Z*), 2.60 (ddd, *J* = 7.6, 7.6, 1.0 Hz, 0.16H, *E*).

¹³C-NMR (75 MHz, CDCl₃): δ = 169.2 (C$_q$), 141.2 (CH), 137.5 (C$_q$), 133.3 (C$_q$), 131.7 (CH), 130.0 (CH), 127.7 (CH), 126.0 (CH), 121.9 (CH), 107.0 (CH), 52.6 (CH₃), 51.4 (CH), 31.7 (CH₂, *E*), 30.7 (CH₂, *E*), 26.9 (CH₂, *Z*), 25.8 (CH₂, *Z*).

IR (ATR): 2953, 1733, 1515, 1457, 1233, 1154, 755 cm⁻¹.

MS (EI) *m/z* (relative intensity): 334 ([M]⁺, 10), 303 (20), 203 (100).

HR-MS (ESI) *m/z* calcd. for [C₁₆H₁₈N₂O₄S]⁺ [M]⁺ 334.0987, found 334.0988.

5.3.2 Removal of the Directing Group
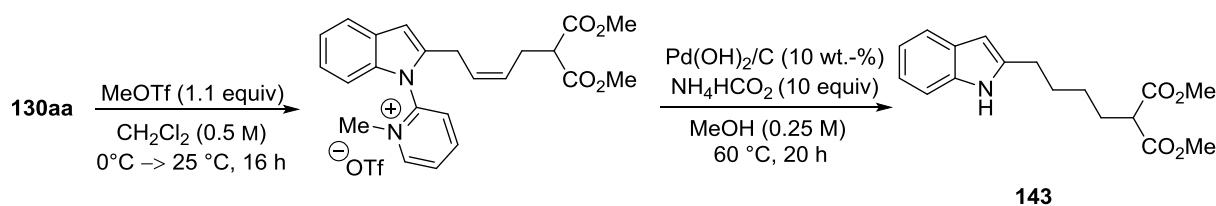
To a solution of **130aa** (189 mg, 0.50 mmol, 1.00 equiv) in CH_2Cl_2 (1.0 mL) was added MeOTf (90.3 mg, 60.0 μL, 0.55 mmol, 1.10 equiv) dropwise at 0 °C. After 30 min the mixture was allowed to warm up to 25 °C and stirred for 16 h. After removal of the solvent *in vacuo* $Pd(OH)_2/C$ (27.1 mg, 10 wt.-%) and ammonium formate (315 mg, 5.00 mmol, 10.0 equiv) were added. The mixture was diluted in MeOH (2.0 mL, 0.25 M) and heated at 60 °C for 20 h. After addition of EtOAc (10 mL) at ambient temperature, the mixture was filtered through a short pad of Celite and the solvents were removed *in vacuo*. The crude mixture was purified by flash column chromatography on silica gel (*n*-hexane/EtOAc: 3/1) to yield **143** (127 mg, 84%) as a pale yellow solid.
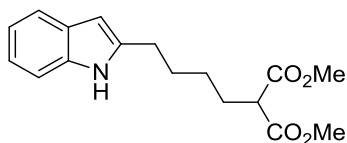
Dimethyl 2-[4-(1*H*-indol-2-yl)butyl]malonate (143):

M.p.: 75 °C

^{1}H-NMR (400 MHz, CDCl$_3$): δ = 8.08 (s, 1H), 7.56–7.52 (m, 1H), 7.32–7.26 (m, 1H), 7.15–7.05 (m, 2H), 6.22 (d, J = 1.2 Hz, 1H), 3.74 (s, 6H), 3.44 (t, J = 7.7 Hz, 2H), 2.73 (t, J = 7.3 Hz, 1H), 2.03–1.94 (m, 2H), 1.78–1.68 (m, 2H), 1.47–1.36 (m, 2H).

^{13}C-NMR (100 MHz, CDCl$_3$): δ = 169.8 (C$_q$), 139.3 (C$_q$), 135.8 (C$_q$), 128.7 (C$_q$), 120.8 (CH), 119.6 (CH), 119.4 (CH), 110.3 (CH), 99.3 (CH), 52.4 (CH$_3$), 51.4 (CH), 28.6 (CH$_2$), 28.3 (CH$_2$), 27.5 (CH$_2$), 26.6 (CH$_2$).

IR (ATR): 3387, 1726, 1459, 1289, 1139, 742, 640 cm^{-1}.

MS (EI) *m/z* (relative intensity): 303 ([M]$^+$, 30), 144 (30), 130 (100).

HR-MS (EI) *m/z* calcd. for [C$_{17}$H$_{21}$NO$_4$]$^+$ [M]$^+$ 303.1471, found 303.1465.

5.3.3   Mechanistic Studies

5.3.3.1   H/D-Exchange Experiment
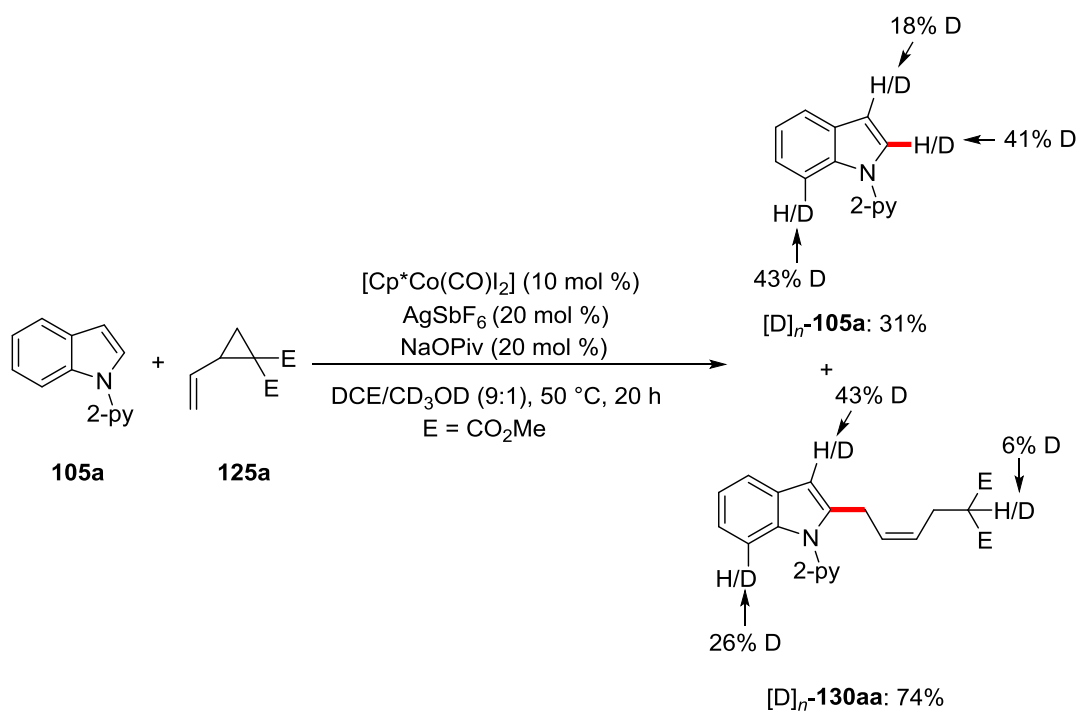
A suspension of **105a** (146 mg, 0.75 mmol, 1.50 equiv), **125a** (91.7 mg, 0.50 mmol, 1.00 equiv), [Cp*Co(CO)I$_2$] (23.8 mg, 10.0 mol %), AgSbF$_6$ (34.4 mg, 20.0 mol %) and NaOPiv (12.4 mg, 100 µmol, 20 mol %) in DCE (1.8 mL) and CD$_3$OD (0.2 mL) was stirred at 50 °C for 20 h. After removal of the solvents, the crude mixture was purified by column chromatography on silica gel (*n*-hexane/EtOAc: 10:1 → 5:1 → 3:1) to yield [D]$_n$-**130aa** (140 mg, 74%, *E/Z* = 1:5) and [D]$_n$-**105a** (45.2 mg, 31% reis.) as yellow oils.

18% D

H/D

H/D ← 41% D

N

H/D   2-py

43% D

[D]$_n$-**105a**
(CDCl$_3$, 500 MHz)

43% D

H/D

CO$_2$Me

H/D ← 6% D

CO$_2$Me

N

H/D   2-py

26% D

[D]$_n$-**130aa**
(CDCl$_3$, 500 MHz)
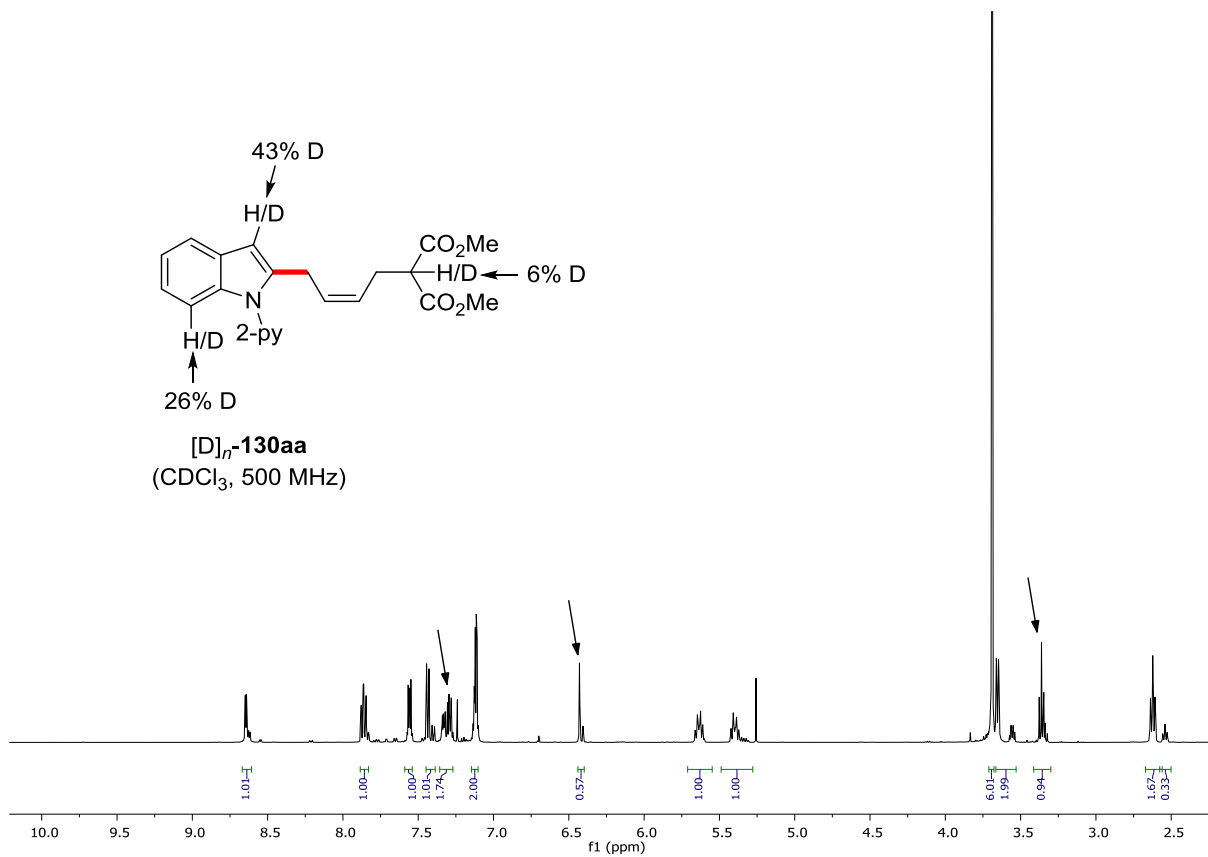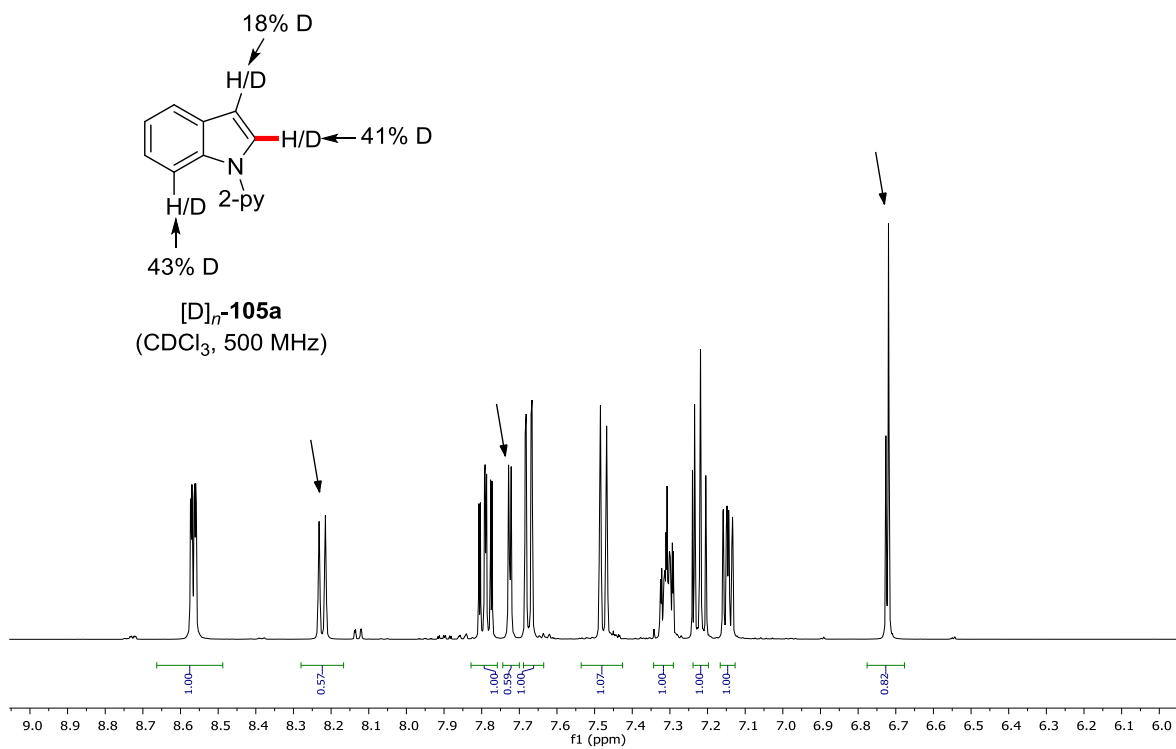
5.3.3.2   H/D-exchange in the absence of the catalyst

105a   **105a**: 85%
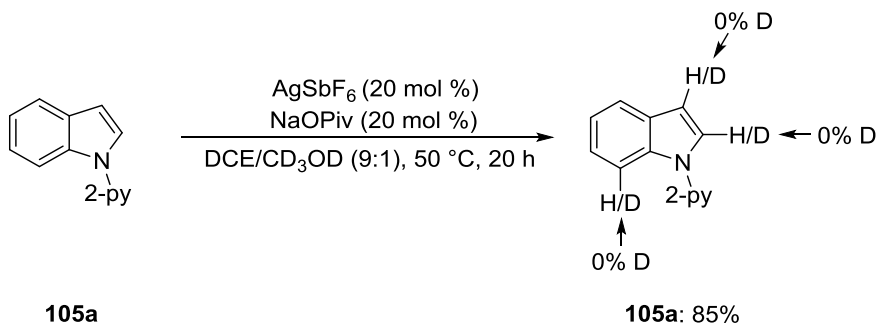
A suspension of **105a** (97.1 mg, 0.50 mmol, 1.00 equiv), AgSbF$_6$ (34.4 mg, 20.0 mol %) and NaOPiv (12.4 mg, 100 μmol, 20 mol %) in DCE (1.8 mL) and CD$_3$OD (0.2 mL) was stirred at 50 °C for 20 h. After removal of the solvents, the crude mixture was purified by column chromatography on silica gel (*n*-hexane/EtOAc: 10:1) to afford **105a** (82.9 mg, 85% reisolated).

105a
(CDCl$_3$, 500 MHz)

5.3.3.3 Kinetic Isotope Effect

105a/[D]₁-105a   **125a**   **130aa/[D]ₙ-130aa**
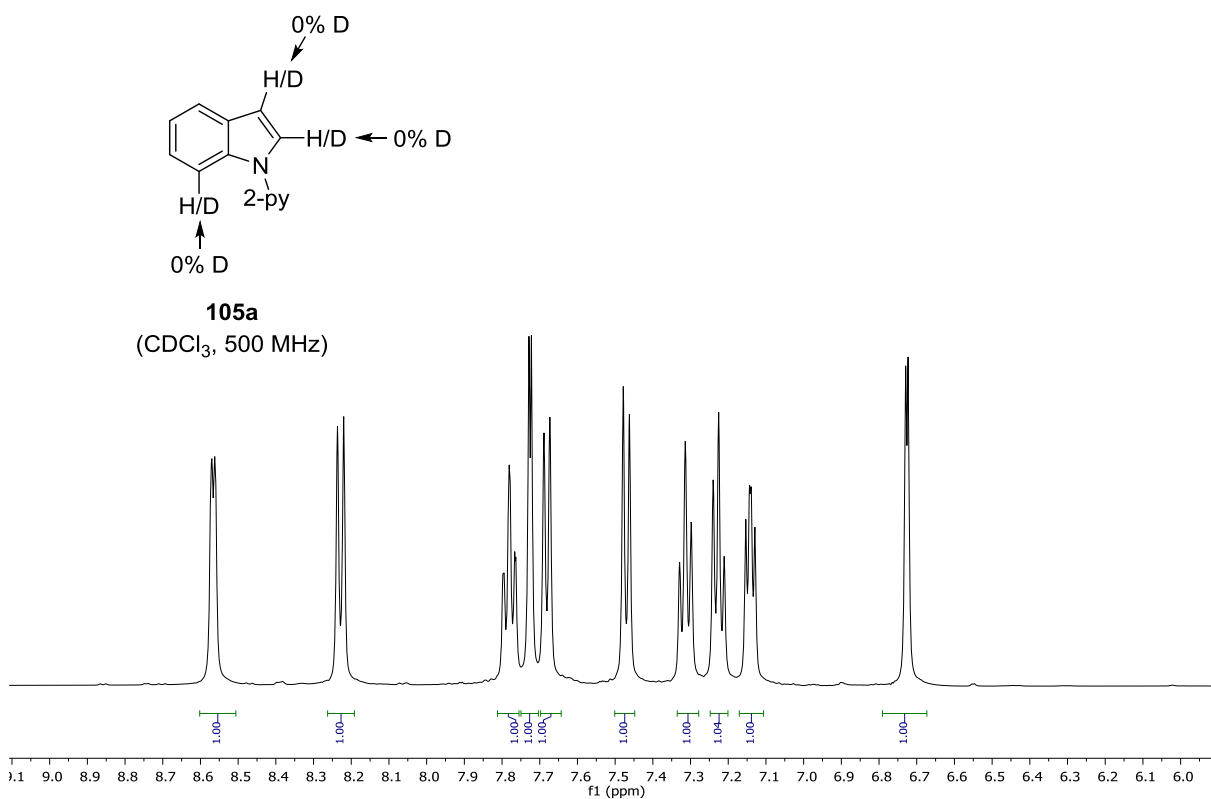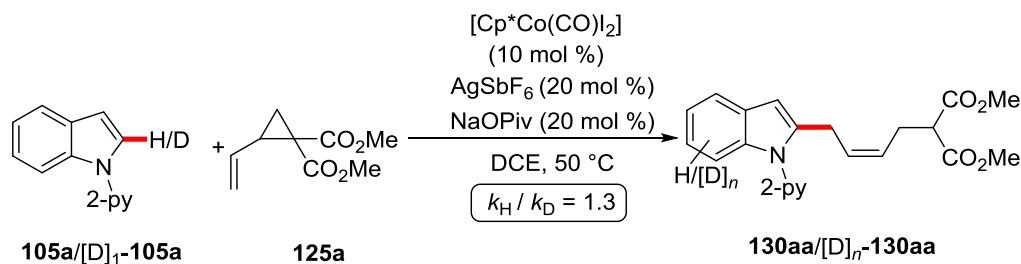
Two parallel reactions of **105a** or [D]₁-**105a**[9] were performed to determine the KIE value by comparison of the initial reaction rates. A suspension of **105a** (97.1 mg, 0.50 mmol, 1.00 equiv) or [D]₁-**105a** (97.6 mg, 0.50 mmol, 1.00 equiv), **125a** (110 mg, 0.60 mmol, 1.20 equiv), [Cp*Co(CO)I₂] (23.8 mg, 10 mol %), AgSbF₆ (34.4 mg, 20 mol %), NaOPiv (12.4 mg, 20 mol %) and *n*-dodecane (30 µL) in DCE (2.0 mL) was stirred at 50 °C. Periodic aliquots (25 µL) were removed to provide the following conversions as determined by GC-analysis:

Table 31. Conversion-time table for the KIE measurement.

t / min	5	10	15	20	25
130aa / %	6.0	10.8	16.2	19.6	26.2
[D]ₙ-**130aa** / %	3.1	7.6	11.6	15.7	18.8

5.4 Regioselective Cobalt(III)-Catalyzed C−H Alkylations

5.4.1 Characterization Data
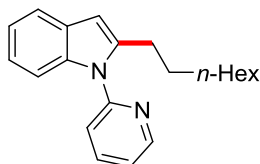
2-*n*-Octyl-1-(pyridin-2-yl)-1*H*-indole (144aa): The general procedure **D** was followed using 1-(pyridin-2-yl)-1*H*-indole (**105a**) (97.1 mg, 0.50 mmol) and oct-1-ene (**143a**) (168 mg, 1.50 mmol). Isolation by column chromatography (*n*-hexane/EtOAc: 25/1) yielded **144a** (125 mg, 82%) as a colorless oil.

^{1}H-NMR (600 MHz, CDCl$_3$): δ = 8.65 (ddd, J = 5.0, 2.1, 0.9 Hz, 1H), 7.87 (ddd, J = 7.8, 7.5, 2.1 Hz, 1H), 7.62–7.56 (m, 1H), 7.42 (ddd, J = 7.8, 1.0, 0.9 Hz, 1H), 7.36–7.27 (m, 2H), 7.16–7.10 (m, 2H), 6.46 (dt, J = 0.9, 0.9 Hz, 1H), 2.86 (t, J = 7.7 Hz, 2H), 1.58–1.50 (m, 2H), 1.31–1.17 (m, 10H), 0.85 (t, J = 7.1 Hz, 3H).

^{13}C-NMR (125 MHz, CDCl$_3$): δ = 151.5 (C$_q$), 149.5 (CH), 141.7 (C$_q$), 138.1 (CH), 137.2 (C$_q$), 128.6 (C$_q$), 121.9 (CH), 121.4 (CH), 121.0 (CH), 120.4 (CH), 119.7 (CH), 109.9 (CH), 102.0 (CH), 31.9 (CH$_2$), 29.4 (CH$_2$), 29.3 (CH$_2$), 29.2 (CH$_2$), 28.7 (CH$_2$), 27.5 (CH$_2$), 22.7 (CH$_2$), 14.2 (CH$_3$).

IR (ATR): 2925, 2854, 1584, 1468, 1455, 780, 755, 733 cm^{-1}.

MS (EI) *m/z* (relative intensity): 306 ([M]$^+$, 25), 221 (25), 207 (100), 196 (45), 168 (30).

HR-MS (EI): *m/z* calcd. for [C$_{21}$H$_{26}$N$_2$]$^+$ [M]$^+$ 306.2096, found 306.2103.

The analytical data are in accordance with those reported in literature.[185]
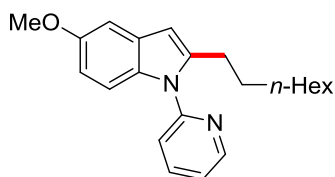
5-Methoxy-2-*n*-octyl-1-(pyridin-2-yl)-1*H*-indole (144ba): The general procedure **D** was followed using 5-methoxy-1-(pyridin-2-yl)-1*H*-indole (**105b**) (112 mg, 0.50 mmol) and oct-1-ene (**143a**) (168 mg, 1.50 mmol). Isolation by column chromatography (*n*-hexane/EtOAc: 25/1) yielded **144ba** (125 mg, 74%) as a yellow oil.

^{1}H-NMR (400 MHz, CDCl$_3$): δ = 8.63 (ddd, J = 5.0, 2.1, 0.9 Hz, 1H), 7.83 (ddd, J = 7.9, 7.5, 2.1 Hz, 1H), 7.38 (ddd, J = 7.9, 1.0, 0.9 Hz, 1H), 7.29–7.23 (m, 2H), 7.06–7.04 (m, 1H), 6.77 (dd, J = 8.9, 2.5 Hz, 1H), 6.38 (dt, J = 0.8, 0.8 Hz, 1H), 3.85 (s, 3H), 2.83 (t, J = 7.6 Hz, 2H), 1.64–1.48 (m, 2H), 1.34–1.21 (m, 10H), 0.88 (t, J = 6.8 Hz, 3H).

^{13}**C-NMR** (100 MHz, CDCl$_3$): δ = 154.7 (C$_q$), 151.6 (C$_q$), 149.5 (CH), 142.3 (C$_q$), 138.1 (CH), 132.3 (C$_q$), 129.1 (C$_q$), 121.7 (CH), 120.7 (CH), 110.9 (CH), 110.8 (CH), 102.1 (CH), 101.9 (CH), 55.8 (CH$_3$), 31.8 (CH$_2$), 29.2 (CH$_2$), 29.2 (CH$_2$), 29.1 (CH$_2$), 28.6 (CH$_2$), 27.5 (CH$_2$), 22.6 (CH$_2$), 14.0 (CH$_3$).

IR (ATR): 2924, 2853, 1582, 1470, 1450, 1173, 772 cm^{-1}.

MS (EI) m/z (relative intensity): 336 ([M]$^+$, 40), 251 (20), 237 (100), 222 (15).

HR-**MS** (EI): m/z calcd. for [C$_{22}$H$_{28}$N$_2$O]$^+$ [M]$^+$ 336.2202, found 336.2193.
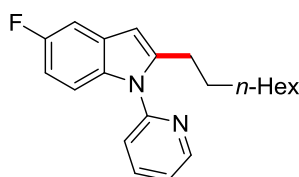
5-**Fluoro**-**2**-**n**-**octyl**-**1**-**(pyridin**-**2**-**yl)**-**1***H*-**indole** (**144ma**): The general procedure **D** was followed using 5-fluoro-1-(pyridin-2-yl)-1*H*-indole (**105m**) (106 mg, 0.50 mmol) and oct-1-ene (**143a**) (168 mg, 1.50 mmol). Isolation by column chromatography (*n*-hexane/EtOAc: 20/1) yielded **144ma** (123 mg, 76%) as a colorless oil.

^{1}**H-NMR** (300 MHz, CDCl$_3$): δ = 8.65 (ddd, J = 4.8, 2.1, 1.0 Hz, 1H), 7.83 (ddd, J = 8.0, 7.5, 2.1 Hz, 1H), 7.37 (ddd, J = 8.0, 1.3, 1.0 Hz, 1H), 7.31 (ddd, J = 7.5, 4.8, 1.3 Hz, 1H), 7.26–7.20 (m, 2H), 7.88–7.80 (m, 1H), 6.39 (dt, J = 0.8, 0.8 Hz, 1H), 2.80 (t, J = 7.6 Hz, 2H), 1.63–1.50 (m, 2H), 1.34–1.17 (m, 10H), 0.88 (t, J = 6.8 Hz, 3H).

^{13}**C-NMR** (125 MHz, CDCl$_3$): δ = 158.3 (d, $^1J_{C-F}$ = 235 Hz, C$_q$), 151.2 (C$_q$), 149.5 (CH), 143.3 (C$_q$), 138.2 (CH), 133.7 (C$_q$), 128.9 (d, $^3J_{C-F}$ = 10.2 Hz, C$_q$), 122.1 (CH), 120.9 (CH), 110.7 (d, $^3J_{C-F}$ = 10.0 Hz, CH), 109.2 (d, $^2J_{C-F}$ = 24.1 Hz, CH), 104.6 (d, $^2J_{C-F}$ = 24.2 Hz, CH), 101.9 (d, $^4J_{C-F}$ = 4.1 Hz, CH), 31.8 (CH$_2$), 29.3 (CH$_2$), 29.3 (CH$_2$), 29.1 (CH$_2$), 28.6 (CH$_2$), 27.6 (CH$_2$), 22.7 (CH$_2$), 14.1 (CH$_3$).

^{19}**F-NMR** (282 MHz, CDCl$_3$): δ = –124.2 (m).

IR (ATR): 2924, 2854, 1584, 1469, 1436, 1176, 775 cm^{-1}.

MS (EI) m/z (relative intensity): 324 ([M]$^+$, 30), 239 (25), 225 (100).

HR-**MS** (EI): m/z calcd. for [C$_{21}$H$_{25}$FN$_2$]$^+$ [M]$^+$ 324.2002, found 324.1996.
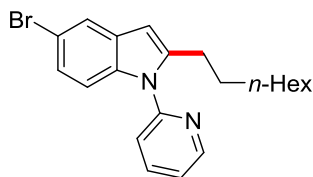
5-**Bromo**-**2**-**n**-**octyl**-**1**-**(pyridin**-**2**-**yl)**-**1***H*-**indole** (**144ca**): The general procedure **D** was followed using 5-bromo-1-(pyridin-2-yl)-1*H*-indole (**105c**) (136 mg, 0.50 mmol) and oct-1-ene (**143a**) (168 mg,

1.50 mmol). Isolation by column chromatography (*n*-hexane/EtOAc: 25/1) yielded **144ca** (152 mg, 79%) as a colorless oil.

¹H-NMR (300 MHz, CDCl₃): δ = 8.64 (ddd, *J* = 4.9, 2.1, 0.9 Hz, 1H), 7.85 (ddd, *J* = 8.0, 7.4, 2.1 Hz, 1H), 7.67 (dd, *J* = 1.5, 0.9 Hz, 1H), 7.34 (ddd, *J* = 8.0, 0.9, 0.9 Hz, 1H), 7.32 (ddd, *J* = 7.4, 4.9, 0.9 Hz, 1H), 7.18–7.16 (m, 2H), 6.37 (dt, *J* = 0.8, 0.8 Hz, 1H), 2.79 (t, *J* = 7.8 Hz, 2H), 1.58–1.48 (m, 2H), 1.31–1.19 (m, 10H), 0.87 (t, *J* = 7.1 Hz, 3H).

¹³C-NMR (125 MHz, CDCl₃): δ = 150.9 (C$_q$), 149.5 (CH), 143.0 (C$_q$), 138.6 (CH), 135.8 (C$_q$), 130.2 (C$_q$), 124.0 (CH), 122.2 (CH), 122.2 (CH), 120.9 (CH), 113.5 (C$_q$), 111.5 (CH), 101.3 (CH), 31.8 (CH₂), 29.3 (CH₂), 29.3 (CH₂), 28.5 (CH₂), 28.5 (CH₂), 27.4 (CH₂), 22.7 (CH₂), 12.1 (CH₃).

IR (ATR): 2924, 2853, 1486, 1469, 1456, 864, 780 cm⁻¹.

MS (EI) *m/z* (relative intensity): 384 ([M(⁷⁹Br)]⁺, 20), 301 (15), 287 (100), 219 (20), 205 (30).

HR-MS (EI): *m/z* calcd. for [C₂₁H₂₅⁷⁹BrN₂]⁺ [M]⁺ 384.1201, found 384.1197.
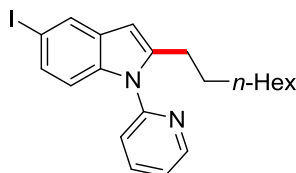
5-Iodo-2-*n*-octyl-1-(pyridin-2-yl)-1*H*-indole (144da): The general procedure **D** was followed using 5-iodo-1-(pyridin-2-yl)-1*H*-indole (**144d**) (160 mg, 0.50 mmol) and oct-1-ene (**143a**) (168 mg, 1.50 mmol). Isolation by column chromatography (*n*-hexane/EtOAc: 25/1) yielded **144da** (167 mg, 77%) as a yellowish oil.

¹H-NMR (300 MHz, CDCl₃): δ = 8.66 (ddd, *J* = 5.0, 2.1, 0.9 Hz, 1H), 7.90–7.81 (m, 2H), 7.37–7.29 (m, 3H), 7.06 (ddd, *J* = 8.2, 0.9, 0.9 Hz, 1H), 6.35 (dt, *J* = 0.8, 0.8 Hz, 1H), 2.79 (t, *J* = 7.8 Hz, 2H), 1.58–1.48 (m, 2H), 1.34–1.15 (m, 10H), 0.87 (t, *J* = 7.1 Hz, 3H).

¹³C-NMR (125 MHz, CDCl₃): δ = 150.9 (C$_q$), 149.5 (CH), 142.6 (C$_q$), 138.2 (CH), 136.3 (C$_q$), 131.0 (C$_q$), 129.6 (CH), 128.4 (CH), 122.2 (CH), 120.9 (CH), 112.0 (CH), 101.0 (CH), 84.0 (C$_q$), 31.8 (CH₂), 29.3 (CH₂), 29.2 (CH₂), 28.5 (CH₂), 27.4 (CH₂), 27.4 (CH₂), 22.7 (CH₂), 14.9 (CH₃).

IR (ATR): 2923, 2852, 1585, 1469, 1455, 867, 780 cm⁻¹.

MS (EI) *m/z* (relative intensity): 432 ([M]⁺, 60), 347 (20), 333 (100), 206 (40).

HR-MS (EI): *m/z* calcd. for [C₂₁H₂₅IN₂]⁺ [M]⁺ 432.1062, found 432.1052.
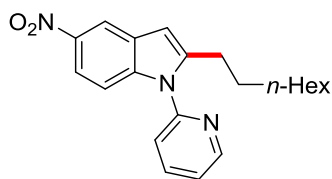
5-**Nitro**-**2**-**n**-**octyl**-**1**-**(pyridin**-**2**-**yl)**-**1***H*-**indole** (**144ea**)**:** The general procedure **D** was followed using 5-nitro-1-(pyridin-2-yl)-1*H*-indole (**105e**) (120 mg, 0.50 mmol) and oct-1-ene (**143a**) (168 mg, 1.50 mmol). Isolation by column chromatography (*n*-hexane/EtOAc: 10/1) yielded **144ea** (73.7 mg, 42%) as a yellowish oil.

¹H-NMR (300 MHz, CDCl₃): δ = 8.66 (ddd, *J* = 5.0, 2.1, 0.9 Hz, 1H), 8.48 (d, *J* = 2.1 Hz, 1H), 8.03–7.91 (m, 2H), 7.45–7.37 (m, 2H), 7.25 (ddd, *J* = 8.5, 0.9, 0.6 Hz, 1H), 6.35 (dt, *J* = 0.8, 0.8 Hz, 1H), 2.76 (t, *J* = 7.8 Hz, 2H), 1.61–1.51 (m, 2H), 1.30–1.15 (m, 10H), 0.84 (t, *J* = 7.1 Hz, 3H).

¹³C-NMR (125 MHz, CDCl₃): δ = 150.3 (C$_q$), 149.9 (CH), 145.2 (C$_q$), 142.3 (C$_q$), 140.1 (C$_q$), 138.6 (CH), 127.7 (C$_q$), 123.1 (CH), 121.3 (CH), 117.2 (CH), 116.6 (CH), 110.0 (CH), 103.3 (CH), 31.8 (CH₂), 29.3 (CH₂), 29.3 (CH₂), 29.1 (CH₂), 28.3 (CH₂), 27.5 (CH₂), 22.7 (CH₂), 14.1 (CH₃).

IR (ATR): 2926, 2855, 1586, 1512, 1470, 1331, 784 cm⁻¹.

MS (EI) *m/z* (relative intensity): 351 ([M]⁺, 20), 264 (30), 252 (100), 206 (40).

HR-**MS** (EI): *m/z* calcd. for [C₂₁H₂₅N₃O₂]⁺ [M]⁺ 351.1947, found 351.1945.
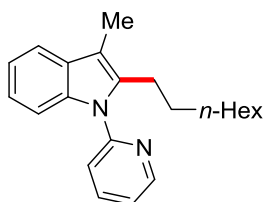
3-**Methyl**-**2**-**n**-**octyl**-**1**-**(pyridin**-**2**-**yl)**-**1***H*-**indole** (**144fa**)**:** The general procedure **D** was followed using 3-methyl-1-(pyridin-2-yl)-1*H*-indole (**105f**) (104 mg, 0.50 mmol) and oct-1-ene (**143a**) (168 mg, 1.50 mmol). Isolation by column chromatography (*n*-hexane/EtOAc: 20/1) yielded **144fa** (104 mg, 65%) as a colorless oil.

¹H-NMR (300 MHz, CDCl₃): δ = 8.64 (ddd, *J* = 4.9, 2.0, 0.9 Hz, 1H), 7.85 (ddd, *J* = 7.9, 7.4, 2.0 Hz, 1H), 7.56–7.51 (m, 1H), 7.41 (ddd, *J* = 7.9, 1.0, 0.9 Hz, 1H), 7.33–7.26 (m, 2H), 7.16–7.08 (m, 2H), 2.89 (t, *J* = 7.2 Hz, 2H), 2.31 (s, 3H), 1.32–1.13 (m, 12H), 0.85 (t, *J* = 6.7 Hz, 3H).

¹³C-NMR (125 MHz, CDCl₃): δ = 151.9 (C$_q$), 149.4 (CH), 138.0 (CH), 137.2 (C$_q$), 136.5 (C$_q$), 129.4 (C$_q$), 121.6 (CH), 121.5 (CH), 120.9 (CH), 120.0 (CH), 118.0 (CH), 109.7 (CH), 109.7 (C$_q$), 31.9 (CH₂), 29.4 (CH₂), 29.2 (CH₂), 29.2 (CH₂), 29.2 (CH₂), 24.8 (CH₂), 22.7 (CH₂), 14.2 (CH₃), 8.9 (CH₃).

IR (ATR): 2923, 2854, 1585, 1470, 1436, 1362, 738 cm⁻¹.

MS (EI) *m/z* (relative intensity): 320 ([M]⁺, 50), 235 (30), 221 (100), 207 (25).

HR-**MS** (EI): *m/z* calcd. for [C₂₂H₂₈N₂]⁺ [M]⁺ 320.2252, found 320.2251.
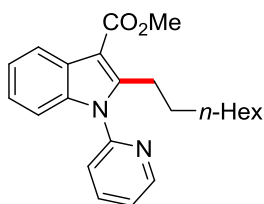
Methyl 2-*n*-octyl-1-(pyridin-2-yl)-1*H*-indole-3-carboxylate (144na): The general procedure **D** was followed using methyl 1-(pyridin-2-yl)-1*H*-indole-3-carboxylate (**105n**) (126 mg, 0.50 mmol) and oct-1-ene (**143a**) (168 mg, 1.50 mmol). Isolation by column chromatography (*n*-hexane/EtOAc: 5/1) yielded **144na** (140 mg, 77%) as a colorless oil.

^{1}H-NMR (300 MHz, CDCl$_3$): δ = 8.69 (ddd, J = 4.9, 2.1, 0.9 Hz, 1H), 8.18 (ddd, J = 7.9, 7.7, 0.9 Hz, 1H), 7.91 (ddd, J = 7.9, 0.9, 0.9 Hz, 1H), 7.45–7.38 (m, 2H), 7.28–7.21 (m, 1H), 7.18–7.08 (m, 2H), 3.97 (s, 3H), 2.81 (t, J = 7.8 Hz, 2H), 1.60–1.47 (m, 2H), 1.27–1.10 (m, 10H), 0.86 (t, J = 6.8 Hz, 3H).

^{13}C-NMR (125 MHz, CDCl$_3$): δ = 165.9 (C$_q$), 150.2 (C$_q$), 149.9 (C$_q$), 149.8 (CH), 138.4 (CH), 136.7 (C$_q$), 126.6 (C$_q$), 123.4 (CH), 122.6 (CH), 122.3 (CH), 122.2 (CH), 121.4 (CH), 110.1 (CH), 105.3 (C$_q$), 50.8 (CH$_3$), 31.8 (CH$_2$), 29.5 (CH$_2$), 29.4 (CH$_2$), 29.1 (CH$_2$), 29.0 (CH$_2$), 25.9 (CH$_2$), 22.6 (CH$_2$), 14.1 (CH$_3$).

IR (ATR): 2924, 2853, 1697, 1587, 1468, 1434, 1182, 1076 cm^{-1}.

MS (EI) *m/z* (relative intensity): 364 ([M]$^+$, 35), 305 (20), 265 (35), 250 (30), 207 (100).

HR-MS (EI): *m/z* calcd. for [C$_{23}$H$_{28}$N$_2$O$_2$]$^+$ [M]$^+$ 364.2148, found 364.2151.
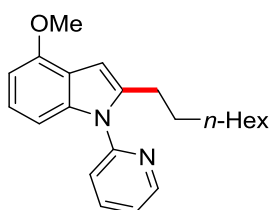
4-Methoxy-2-*n*-octyl-1-(pyridin-2-yl)-1*H*-indole (144ha): The general procedure **D** was followed using 4-methoxy-1-(pyridin-2-yl)-1*H*-indole (**105h**) (112 mg, 0.50 mmol) and oct-1-ene (**143a**) (168 mg, 1.50 mmol). Isolation by column chromatography (*n*-hexane/EtOAc: 25/1) yielded **144ha** (132 mg, 79%) as a colorless oil.

^{1}H-NMR (300 MHz, CDCl$_3$): δ = 8.64 (ddd, J = 5.0, 2.1, 0.9 Hz, 1H), 7.85 (ddd, J = 8.0, 7.5, 2.1 Hz, 1H), 7.40 (ddd, J = 8.0, 1.0, 0.9 Hz, 1H), 7.32–7.27 (m, 2H), 7.08–6.92 (m, 1H), 6.62–6.52 (m, 2H), 3.96 (s, 3H), 2.81 (t, J = 7.6 Hz, 2H), 1.61–1.51 (m, 2H), 1.32–1.21 (m, 10H), 0.88 (t, J = 6.8 Hz, 3H).

^{13}C-NMR (125 MHz, CDCl$_3$): δ = 152.4 (C$_q$), 151.6 (C$_q$), 149.4 (CH), 140.1 (C$_q$), 138.4 (C$_q$), 138.0 (CH), 122.1 (CH), 121.9 (CH), 121.1 (CH), 118.9 (C$_q$), 103.6 (CH), 100.7 (CH), 99.0 (CH), 55.4 (CH$_3$), 31.8 (CH$_2$), 29.3 (CH$_2$), 29.3 (CH$_2$), 29.1 (CH$_2$), 28.6 (CH$_2$), 27.4 (CH$_2$), 22.7 (CH$_2$), 14.1 (CH$_3$).

IR (ATR): 2923, 2854, 1585, 1470, 1435, 779, 738 cm^{-1}.

MS (EI) m/z (relative intensity): 336 ([M]$^{+}$, 45), 251 (20), 237 (100), 221 (25).

HR-MS (EI): m/z calcd. for [C$_{22}$H$_{28}$N$_2$O]$^+$ [M]$^+$ 336.2202, found 336.2205.
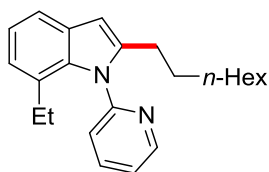
7-Ethyl-2-n-octyl-1-(pyridin-2-yl)-1H-indole (144ja): The general procedure **D** was followed using 7-ethyl-1-(pyridin-2-yl)-1H-indole (**105j**) (111 mg, 0.50 mmol) and oct-1-ene (**143a**) (168 mg, 1.50 mmol). Isolation by column chromatography (n-hexane/EtOAc: 20/1) yielded **144ja** (102 mg, 61%) as a colorless oil.

^{1}**H-NMR** (300 MHz, CDCl$_3$): δ = 8.65 (ddd, J = 4.9, 2.1, 0.9 Hz, 1H), 7.82 (ddd, J = 7.9, 7.6, 2.1 Hz, 1H), 7.45–7.36 (m, 2H), 7.32 (ddd, J = 7.6, 1.0, 0.9 Hz, 1H), 7.06 (d, J = 7.7 Hz, 1H), 6.96–6.90 (m, 1H), 6.40 (dt, J = 0.8, 0.8 Hz, 1H), 2.45 (t, J = 7.6 Hz, 2H), 2.15 (q, J = 7.5 Hz, 2H), 1.60–1.49 (m, 2H), 1.32–1.19 (m, 10H), 0.94 (t, J = 7.5 Hz, 3H), 0.87 (t, J = 7.1 Hz, 3H).

^{13}**C-NMR** (125 MHz, CDCl$_3$): δ = 153.5 (C$_q$), 149.0 (CH), 142.5 (C$_q$), 137.5 (CH), 135.9 (C$_q$), 129.4 (C$_q$), 127.3 (C$_q$), 124.0 (CH), 123.2 (CH), 121.8 (CH), 120.3 (CH), 117.7 (CH), 101.3 (CH), 31.9 (CH$_2$), 29.4 (CH$_2$), 29.3 (CH$_2$), 29.2 (CH$_2$), 28.4 (CH$_2$), 27.2 (CH$_2$), 24.9 (CH$_2$), 22.7 (CH$_2$), 14.6 (CH$_3$), 14.1 (CH$_3$).

IR (ATR): 2926, 2855, 1582, 1467, 1435, 1340, 798, 741 cm^{-1}.

MS (EI) m/z (relative intensity): 334 ([M]$^{+}$, 40), 249 (80), 235 (100), 219 (30).

HR-MS (EI): m/z calcd. for [C$_{23}$H$_{30}$N$_2$]$^+$ [M]$^+$ 334.2409, found 334.2413.
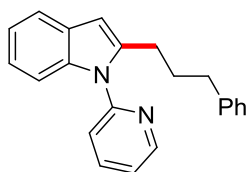
2-(3-Phenylpropyl)-1-(pyridin-2-yl)-1H-indole (144ab): The general procedure **D** was followed using 1-(pyridin-2-yl)-1H-indole (**105a**) (97.1 mg, 0.50 mmol) and allylbenzene (**143b**) (177 mg, 1.50 mmol). Isolation by column chromatography (n-hexane/EtOAc: 30/1) yielded **144ab** (133 mg, 85%) as a colorless oil.

^{1}**H-NMR** (400 MHz, CDCl$_3$): δ = 8.65 (ddd, J = 5.0, 2.1, 0.9 Hz, 1H), 7.85 (ddd, J = 8.0, 7.5, 2.1 Hz, 1H), 7.62–7.56 (m, 1H), 7.43–7.35 (m, 2H), 7.32–7.25 (m, 3H), 7.22–7.12 (m, 5H), 6.51 (dt, J = 0.8, 0.8 Hz, 1H), 2.93 (t, J = 7.7 Hz, 2H), 2.66 (t, J = 7.5 Hz, 2H), 1.93 (tt, J = 7.7, 7.5 Hz, 2H).

^{13}C-NMR (100 MHz, CDCl$_3$): δ = 151.4 (C$_q$), 149.6 (CH), 141.9 (C$_q$), 141.0 (C$_q$), 138.1 (CH), 137.2 (C$_q$), 128.5 (C$_q$), 128.3 (CH), 128.2 (CH), 125.7 (CH), 121.9 (CH), 121.6 (CH), 120.9 (CH), 120.5 (CH), 119.8 (CH), 110.0 (CH), 102.3 (CH), 35.3 (CH$_2$), 30.2 (CH$_2$), 26.9 (CH$_2$).

IR (ATR): 3025, 2932, 1584, 1468, 1455, 735, 698 cm^{-1}.

MS (EI) m/z (relative intensity): 312 ([M]$^+$, 20), 221 (100), 206 (40), 91 (20).

HR-MS (EI): m/z calcd. for [C$_{22}$H$_{20}$N$_2$]$^+$ [M]$^+$ 312.1626, found 312.1624.

The analytical data are in accordance with those reported in literature.[186]
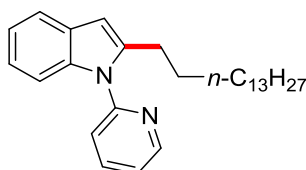
2-n-Pentadecyl-1-(pyridin-2-yl)-1H-indole (144ac): The general procedure **D** was followed using 1-(pyridin-2-yl)-1H-indole (**105a**) (97.1 mg, 0.50 mmol) and pentadec-1-ene (**143c**) (316 mg, 1.50 mmol). Isolation by column chromatography (n-hexane/EtOAc: 25/1) yielded **144ac** (159 mg, 79%) as a colorless oil.

^{1}H-NMR (300 MHz, CDCl$_3$): δ = 8.67 (ddd, J = 5.0, 2.1, 0.9 Hz, 1H), 7.86 (ddd, J = 8.0, 7.5, 2.1 Hz, 1H), 7.62–7.56 (m, 1H), 7.42 (ddd, J = 8.0, 1.0, 0.9 Hz, 1H), 7.36–7.27 (m, 2H), 7.16–7.10 (m, 2H), 6.46 (dt, J = 0.8, 0.8 Hz, 1H), 2.86 (t, J = 7.7 Hz, 2H), 1.65–1.53 (m, 2H), 1.35–1.19 (m, 24H), 0.92 (t, J = 7.1 Hz, 3H).

^{13}C-NMR (125 MHz, CDCl$_3$): δ = 151.5 (C$_q$), 149.4 (CH), 141.6 (C$_q$), 138.0 (CH), 137.1 (C$_q$), 128.6 (C$_q$), 121.8 (CH), 121.4 (CH), 121.0 (CH), 120.4 (CH), 119.7 (CH), 109.9 (CH), 102.0 (CH), 31.9 (CH$_2$), 29.7 (CH$_2$), 29.7 (CH$_2$), 29.7 (CH$_2$), 29.7 (CH$_2$), 29.6 (CH$_2$), 29.6 (CH$_2$), 29.5 (CH$_2$), 29.4 (CH$_2$), 29.4 (CH$_2$), 29.3 (CH$_2$), 28.6 (CH$_2$), 27.5 (CH$_2$), 22.7 (CH$_2$), 14.0 (CH$_3$).

IR (ATR): 2921, 2851, 1485, 1469, 1456, 780, 735 cm^{-1}.

MS (EI) m/z (relative intensity): 404 ([M]$^+$, 35), 221 (55), 207 (100), 195 (15).

HR-MS (EI): m/z calcd. for [C$_{28}$H$_{40}$N$_2$]$^+$ [M]$^+$ 404.3191, found 404.3182.
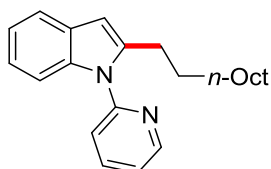
2-n-Decyl-1-(pyridin-2-yl)-1H-indole (144ad): The general procedure **D** was followed using 1-(pyridin-2-yl)-1H-indole (**105a**) (97.1 mg, 0.50 mmol) and dec-1-ene (**143d**) (210 mg, 1.50 mmol).

Isolation by column chromatography (*n*-hexane/EtOAc: 25/1) yielded **144ad** (125 mg, 75%) as a colorless oil.

^{1}H-NMR (300 MHz, CDCl$_3$): δ = 8.66 (ddd, J = 5.0, 2.1, 0.9 Hz, 1H), 7.86 (ddd, J = 8.0, 7.5, 2.1 Hz, 1H), 7.62–7.56 (m, 1H), 7.42 (ddd, J = 8.0, 1.0, 0.9 Hz, 1H), 7.36–7.27 (m, 2H), 7.16–7.10 (m, 2H), 6.45 (dt, J = 0.8, 0.8 Hz, 1H), 2.86 (t, J = 7.7 Hz, 2H), 1.65–1.51 (m, 2H), 1.35–1.18 (m, 14H), 0.89 (t, J = 7.1 Hz, 3H).

^{13}C-NMR (125 MHz, CDCl$_3$): δ = 151.5 (C$_q$), 149.4 (CH), 141.6 (C$_q$), 138.0 (CH), 137.1 (C$_q$), 128.6 (C$_q$), 121.8 (CH), 121.4 (CH), 121.0 (CH), 120.4 (CH), 119.7 (CH), 109.9 (CH), 102.0 (CH), 31.9 (CH$_2$), 29.6 (CH$_2$), 29.6 (CH$_2$), 29.5 (CH$_2$), 29.4 (CH$_2$), 29.3 (CH$_2$), 28.6 (CH$_2$), 27.5 (CH$_2$), 22.7 (CH$_2$), 14.1 (CH$_3$).

IR (ATR): 2923, 2852, 1585, 1468, 1455, 780, 735 cm^{-1}.

MS (EI) m/z (relative intensity): 334 ([M]$^+$, 45), 249 (30), 235 (100), 221 (45).

HR-MS (EI): m/z calcd. for [C$_{23}$H$_{30}$N$_2$]$^+$ [M]$^+$ 334.2409, found 334.2407.

The analytical data are in accordance with those reported in literature.[186]
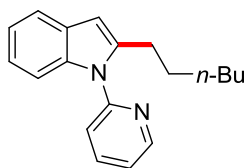
2-*n*-Hexyl-1-(pyridin-2-yl)-1*H*-indole (145ae): The general procedure **D** was followed using 1-(pyridin-2-yl)-1*H*-indole (**105a**) (97.1 mg, 0.50 mmol) and hex-1-ene (**143e**) (126 mg, 1.50 mmol). Isolation by column chromatography (*n*-hexane/EtOAc: 25/1) yielded **144ae** (90.5 mg, 65%) as a colorless oil.

^{1}H-NMR (400 MHz, CDCl$_3$): δ = 8.67 (ddd, J = 5.0, 2.1, 0.9 Hz, 1H), 7.87 (ddd, J = 8.0, 7.5, 2.1 Hz, 1H), 7.62–7.56 (m, 1H), 7.42 (ddd, J = 8.0, 1.0, 0.9 Hz, 1H), 7.36–7.27 (m, 2H), 7.16–7.10 (m, 2H), 6.46 (dt, J = 0.9, 0.9 Hz, 1H), 2.85 (t, J = 7.7 Hz, 2H), 1.63–1.53 (m, 2H), 1.36–1.20 (m, 6H), 0.87 (t, J = 7.1 Hz, 3H).

^{13}C-NMR (100 MHz, CDCl$_3$): δ = 151.5 (C$_q$), 149.5 (CH), 141.7 (C$_q$), 138.1 (CH), 137.2 (C$_q$), 128.6 (C$_q$), 121.9 (CH), 121.4 (CH), 121.1 (CH), 120.5 (CH), 119.8 (CH), 110.0 (CH), 102.0 (CH), 31.5 (CH$_2$), 28.9 (CH$_2$), 28.5 (CH$_2$), 27.4 (CH$_2$), 22.5 (CH$_2$), 14.0 (CH$_3$).
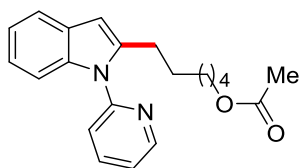
IR (ATR): 2926, 2856, 1584, 1468, 1455, 779, 735 cm^{-1}.

MS (EI) m/z (relative intensity): 278 ([M]$^+$, 25), 221 (20), 207 (100).

HR-MS (EI): m/z calcd. for [C$_{19}$H$_{22}$N$_2$]$^+$ [M]$^+$ 278.1783, found 278.1788.

The analytical data are in accordance with those reported in literature.[186]

6-[1-(Pyridin-2-yl)-1*H*-indol-2-yl]hexyl acetate (144af): The general procedure **D** was followed using 1-(pyridin-2-yl)-1*H*-indole (**105a**) (97.1 mg, 0.50 mmol) and hex-5-en-1-yl acetate (**143f**) (213 mg, 1.50 mmol). Isolation by column chromatography (*n*-hexane/EtOAc: 10/1) yielded **144af** (128 mg, 76%) as a yellowish oil.

¹H-NMR (300 MHz, CDCl$_3$): δ = 8.65 (ddd, *J* = 5.0, 2.1, 0.9 Hz, 1H), 7.85 (ddd, *J* = 8.0, 7.5, 2.1 Hz, 1H), 7.60–7.55 (m, 1H), 7.42 (ddd, *J* = 8.0, 1.0, 0.9 Hz, 1H), 7.33–7.24 (m, 2H), 7.15–7.08 (m, 2H), 6.44 (dt, *J* = 0.8, 0.8 Hz, 1H), 4.01 (t, *J* = 6.9 Hz, 2H), 2.84 (t, *J* = 7.4 Hz, 2H), 2.02 (s, 3H), 1.63–1.53 (m, 4H), 1.36–1.28 (m, 4H).

¹³C-NMR (125 MHz, CDCl$_3$): δ = 170.9 (C$_q$), 151.4 (C$_q$), 149.4 (CH), 141.3 (C$_q$), 138.1 (CH), 137.1 (C$_q$), 128.5 (C$_q$), 121.9 (CH), 121.4 (CH), 121.0 (CH), 120.4 (CH), 119.7 (CH), 109.9 (CH), 102.0 (CH), 64.4 (CH$_2$), 28.9 (CH$_2$), 28.4 (CH$_2$), 28.4 (CH$_2$), 27.3 (CH$_2$), 25.6 (CH$_2$), 21.0 (CH$_3$).

IR (ATR): 2933, 1736, 1585, 1470, 1456, 1242, 783, 748 cm^{-1}.

MS (EI) *m/z* (relative intensity): 336 ([M]$^+$, 25), 221 (25), 207 (100).

HR-MS (EI): *m/z* calcd. for [C$_{21}$H$_{24}$N$_2$O$_2$]$^+$ [M]$^+$ 336.1838, found 336.1838.
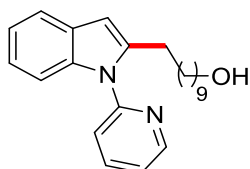
10-[1-(Pyridin-2-yl)-1*H*-indol-2-yl]decan-1-ol (144ag): The general procedure **D** was followed using 1-(pyridin-2-yl)-1*H*-indole (**105a**) (97.1 mg, 0.50 mmol) and dec-9-en-1-ol (**143g**) (234 mg, 1.50 mmol). Isolation by column chromatography (*n*-hexane/EtOAc: 5/1) yielded **144ag** (117 mg, 67%) as a yellowish oil.

¹H-NMR (300 MHz, CDCl$_3$): δ = 8.64 (ddd, *J* = 5.0, 2.1, 0.9 Hz, 1H), 7.87 (ddd, *J* = 8.0, 7.4, 2.1 Hz, 1H), 7.59–7.54 (m, 1H), 7.41 (ddd, *J* = 8.0, 1.0, 0.9 Hz, 1H), 7.33–7.27 (m, 2H), 7.14–7.07 (m, 2H), 6.43 (dt, *J* = 0.8, 0.8 Hz, 1H), 3.57 (t, *J* = 6.7 Hz, 2H), 2.82 (t, *J* = 7.6 Hz, 2H), 1.74 (bs, 1H), 1.60–1.45 (m, 4H), 1.31–1.19 (m, 12H).

¹³C-NMR (125 MHz, CDCl$_3$): δ = 151.4 (C$_q$), 149.4 (CH), 141.6 (C$_q$), 138.1 (CH), 137.1 (C$_q$), 128.5 (C$_q$), 121.9 (CH), 121.4 (CH), 121.1 (CH), 120.4 (CH), 119.7 (CH), 109.9 (CH), 101.9 (CH), 62.7 (CH$_2$), 32.7 (CH$_2$), 29.5 (CH$_2$), 29.5 (CH$_2$), 29.4 (CH$_2$), 29.3 (CH$_2$), 29.3 (CH$_2$), 28.6 (CH$_2$), 27.4 (CH$_2$), 25.7 (CH$_2$).

IR (ATR): 3375, 2925, 2852, 1699, 1585, 1469, 1455, 782, 736 cm^{-1}.

MS (EI) m/z (relative intensity): 350 ([M]$^+$, 15), 221 (25), 207 (100).

HR-MS (EI): m/z calcd. for [C$_{23}$H$_{30}$N$_2$O]$^+$ [M]$^+$ 350.2358, found 350.2354.
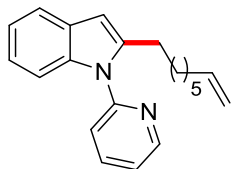
2-(Oct-7-en-1-yl)-1-(pyridin-2-yl)-1H-indole (144ah): The general procedure **D** was followed using 1-(pyridin-2-yl)-1H-indole (**105a**) (97.1 mg, 0.50 mmol) and octa-1,7-diene (**143h**) (165 mg, 1.50 mmol). Isolation by column chromatography (n-hexane/EtOAc: 40/1) yielded **144ah** (99.8 mg, 66%) as a colorless oil.

^{1}H-NMR (500 MHz, CDCl$_3$): δ = 8.65 (ddd, J = 4.9, 2.1, 0.9 Hz, 1H), 7.86 (ddd, J = 7.8, 7.8, 2.1 Hz, 1H), 7.63–7.57 (m, 1H), 7.43 (ddd, J = 7.8, 1.0, 0.9 Hz, 1H), 7.37–7.32 (m, 1H), 7.23 (ddd, J = 7.3, 5.2, 0.9 Hz, 1H), 7.17–7.10 (m, 2H), 6.47 (dt, J = 0.8, 0.8 Hz, 1H), 5.81 (ddt, J = 17.0, 10.2, 6.6 Hz, 1H), 5.00 (dd, J = 17.0, 2.0 Hz, 1H), 4.95 (dd, J = 10.2, 2.0 Hz, 1H), 2.86 (t, J = 7.8 Hz, 2H), 2.03 (tt, J = 7.8, 7.7 Hz, 2H), 1.62–1.52 (m, 2H), 1.40–1.22 (m, 6H).

^{13}C-NMR (125 MHz, CDCl$_3$): δ = 151.5 (C$_q$), 149.5 (CH), 141.6 (C$_q$), 139.0 (CH), 138.1 (CH), 137.2 (C$_q$), 128.6 (C$_q$), 121.9 (CH), 121.4 (CH), 121.1 (CH), 120.5 (CH), 119.8 (CH), 114.1 (CH$_2$), 110.0 (CH), 102.0 (CH), 33.7 (CH$_2$), 29.0 (CH$_2$), 28.7 (CH$_2$), 28.6 (CH$_2$), 28.4 (CH$_2$), 27.4 (CH$_2$).

IR (ATR): 2926, 2855, 1585, 1469, 1436, 1346, 780, 737 cm^{-1}.

MS (EI) m/z (relative intensity): 304 ([M]$^+$, 100), 221 (20), 207 (100).

HR-MS (EI): m/z calcd. for [C$_{21}$H$_{24}$N$_2$]$^+$ [M]$^+$ 304.1939, found 304.1935.
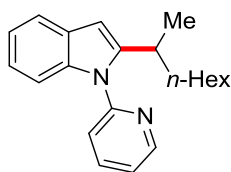
2-(Octan-2-yl)-1-(pyridin-2-yl)-1H-indole (145aa): The general procedure **E** was followed using 1-(pyridin-2-yl)-1H-indole (**105a**) (97.1 mg, 0.50 mmol) and oct-1-ene (**143a**) (168 mg, 1.50 mmol). Isolation by column chromatography (n-hexane/EtOAc: 25/1) yielded **145aa** (122 mg, 80%, 95:5) as a colorless oil. After purification by HPLC pure **145aa** could be isolated (110 mg, 72%, >99:1).

^{1}H-NMR (300 MHz, CDCl$_3$): δ = 8.67 (ddd, J = 4.9, 2.0, 0.9 Hz, 1H), 7.86 (ddd, J = 7.9, 7.5, 2.0 Hz, 1H), 7.59–7.53 (m, 1H), 7.40 (ddd, J = 7.9, 1.0, 0.9 Hz, 1H), 7.32 (ddd, J = 7.5, 4.9, 1.0 Hz, 1H), 7.24–7.21 (m, 1H), 7.12–7.06 (m, 2H), 6.46 (dd, J = 0.8, 0.8 Hz, 1H), 3.16 (tq, J = 7.6, 7.6 Hz, 0.95H,

M), 2.86 (t, J = 7.7 Hz, 0.10H, AM), 1.64–1.55 (m, 1H), 1.46–1.33 (m, 1H), 1.25–1.10 (m, 11H), 0.82 (t, J = 6.8 Hz, 3H).

^{13}**C-NMR** (125 MHz, CDCl$_3$): δ = 151.6 (C$_q$), 149.6 (CH), 147.4 (C$_q$), 138.1 (CH), 137.2 (C$_q$), 128.5 (C$_q$), 122.1 (CH), 121.7 (CH), 121.3 (CH), 120.4 (CH), 119.8 (CH), 109.9 (CH), 99.8 (CH), 37.2 (CH$_2$), 31.7 (CH$_2$), 30.8 (CH), 29.3 (CH$_2$), 27.1 (CH$_2$), 22.7 (CH$_2$), 20.6 (CH$_3$), 14.1 (CH$_3$).

IR (ATR): 2925, 2854, 1584, 1468, 1435, 780, 733 cm^{-1}.

MS (EI) m/z (relative intensity): 306 ([M]$^+$, 20), 221 (55), 207 (100).

**HR-MS** (EI): m/z calcd. for [C$_{21}$H$_{26}$N$_2$]$^+$ [M]$^+$ 306.2096, found 306.2083.

Asymmetric cobalt(III)-catalyzed C–H hydroarylation:

A suspension of 2-pyridylindole (**105a**) (0.50 mmol, 1.00 equiv), oct-1-ene (**143a**) (168 mg, 1.50 mmol), [Cp*Co(CO)I$_2$] (23.8 mg, 50.0 µmol, 10.0 mol %), AgSbF$_6$ (34.4 mg, 100 µmol, 20.0 mol %) and Phth-L-Leu-OH (130 mg, 0.50 mmol, 1.00 equiv) in DCE (0.50 mL, 1.00 M) was stirred at 50 °C for 20 h. At ambient temperature, the reaction mixture was diluted with EtOAc (5.0 mL) and the solvents were removed *in vacuo*. The remaining residue was purified by column chromatography on silica gel (*n*-hexane/EtOAc) to yield the desired product **145aa** (57.1 mg, 37%, M:AM = 93:7). The enantiomeric excess was determined by analytical HPLC (*Chiralpak*® IF-3, *n*-hexane/EtOAc 90:10, flow rate = 0.5 mL/min, λ = 280 nm) to be 25% *ee*.
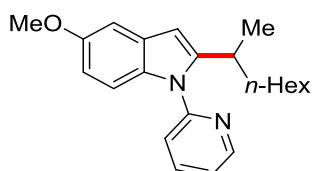
Racemic Mixture:
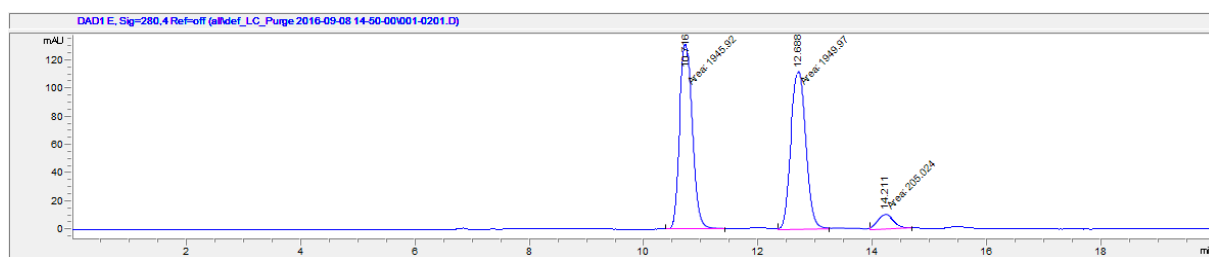
t_R / min	Area	Assignment
10.716	1946	Enantiomer 1
12.688	1950	Enantiomer 2
14.211	205	AM-product **144aa**

Enantiomeric excess of 25%:
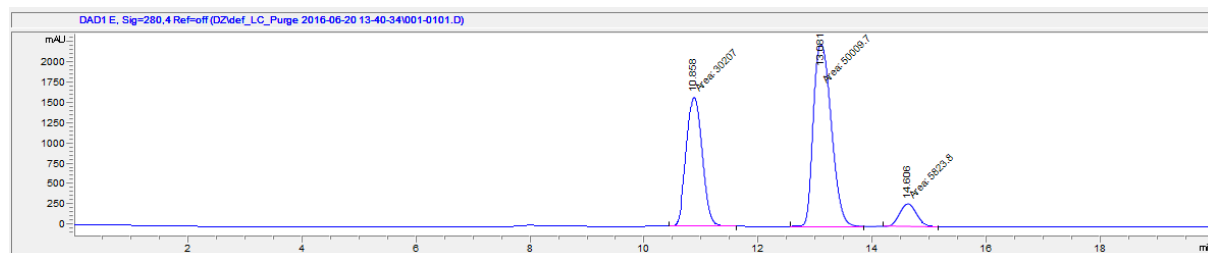
t_R / min	Area	Assignment
10.858	30207	Enantiomer 1
13.081	50010	Enantiomer 2
14.606	5824	AM-product **144aa**

5-Methoxy-2-(octan-2-yl)-1-(pyridin-2-yl)-1*H*-indole (145ba): The general procedure **E** was followed using 5-methoxy-1-(pyridin-2-yl)-1*H*-indole (**105b**) (112 mg, 0.50 mmol) and oct-1-ene (**143a**) (168 mg, 1.50 mmol). Isolation by column chromatography (*n*-hexane/EtOAc: 25/1) yielded **145ba** (116 mg, 69%, 94:6) as a colorless oil.

^{1}H-NMR (400 MHz, CDCl$_3$): δ = 8.65 (ddd, J = 4.9, 2.1, 1.0 Hz, 1H), 7.85 (ddd, J = 7.9, 7.4, 2.1 Hz, 1H), 7.38 (ddd, J = 7.9, 1.0, 0.9 Hz, 1H), 7.29 (ddd, J = 7.4, 4.9, 0.9 Hz, 1H), 7.17 (dd, J = 8.9, 0.9 Hz, 1H), 7.08–7.04 (m, 1H), 6.76 (dd, J = 8.9, 2.5 Hz, 1H), 6.39 (dd, J = 0.8, 0.8 Hz, 1H), 3.86 (s, 3H), 3.18 (tq, J = 6.8, 6.8 Hz, 0.94H, M), 2.83 (t, J = 7.6 Hz, 0.12H, AM), 1.67–1.34 (m, 2H), 1.30–1.08 (m, 11H), 0.84 (t, J = 7.1 Hz, 3H).

^{13}C-NMR (100 MHz, CDCl$_3$): δ = 154.7 (C$_q$), 151.3 (C$_q$), 149.6 (CH), 148.1 (C$_q$), 138.1 (CH), 132.4 (C$_q$), 129.0 (C$_q$), 121.9 (CH), 121.4 (CH), 111.0 (CH), 110.7 (CH), 102.1 (CH), 99.6 (CH), 55.8 (CH$_3$), 37.1 (CH$_2$), 31.6 (CH$_2$), 30.8 (CH), 29.2 (CH$_2$), 27.0 (CH$_2$), 22.6 (CH$_2$), 20.5 (CH$_3$), 14.0 (CH$_3$).

IR (ATR): 2926, 2855, 1582, 1470, 1435, 1172, 770 cm^{-1}.

MS (EI) *m/z* (relative intensity): 336 ([M]$^+$, 55), 251 (85), 237 (100).

HR-MS (EI+): *m/z* calcd. for [C$_{22}$H$_{28}$N$_2$O]$^+$ [M]$^+$ 336.2202, found 336.2213.
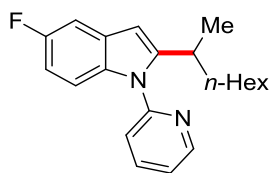
5-Fluoro-2-(octan-2-yl)-1-(pyridin-2-yl)-1*H*-indole (145ma): The general procedure **E** was followed using 5-fluoro-1-(pyridin-2-yl)-1*H*-indole (**105m**) (106 mg, 0.50 mmol) and oct-1-ene (**143a**) (168 mg, 1.50 mmol). Isolation by column chromatography (*n*-hexane/EtOAc: 20/1) yielded **145ma** (138 mg, 85%, 96:4) as a colorless oil.

^{1}H-NMR (500 MHz, CDCl$_3$): δ = 8.68 (ddd, *J* = 4.9, 2.1, 1.0 Hz, 1H), 7.88 (ddd, *J* = 7.9, 7.4, 2.1 Hz, 1H), 7.39 (ddd, *J* = 7.9, 1.0, 1.0 Hz, 1H), 7.34 (ddd, *J* = 7.4, 4.9, 1.0 Hz, 1H), 7.24 (dd, *J* = 9.1, 2.4 Hz, 1H), 7.17 (dd, *J* = 8.9, 4.5 Hz, 1H), 6.85 (dd, *J* = 8.9, 2.4 Hz, 1H), 6.44 (dd, *J* = 0.8, 0.8 Hz, 1H), 3.16 (tq, *J* = 6.8, 6.8 Hz, 0.96H, M), 2.80 (t, *J* = 7.6 Hz, 0.08H, AM), 1.70–1.59 (m, 1H), 1.50–1.36 (m, 1H), 1.32–1.06 (m, 11H), 0.84 (t, *J* = 7.1 Hz, 3H).

^{13}C-NMR (125 MHz, CDCl$_3$): δ = 158.3 (d, $^1J_{C-F}$ = 235 Hz, C$_q$), 151.4 (C$_q$), 149.7 (CH), 149.1 (C$_q$), 138.3 (CH), 133.8 (C$_q$), 128.9 (d, $^3J_{C-F}$ = 10.1 Hz, C$_q$), 122.3 (CH), 121.6 (CH), 110.6 (d, $^3J_{C-F}$ = 10.0 Hz, CH), 109.1 (d, $^2J_{C-F}$ = 24.2 Hz, CH), 104.7 (d, $^2J_{C-F}$ = 24.1 Hz, CH), 99.6 (d, $^4J_{C-F}$ = 4.3 Hz, CH), 37.0 (CH$_2$), 31.6 (CH$_2$), 30.8 (CH), 29.1 (CH$_2$), 27.0 (CH$_2$), 22.5 (CH$_2$), 20.5 (CH$_3$), 14.0 (CH$_3$).

^{19}F-NMR (282 MHz, CDCl$_3$): δ = −124.2 (m).

IR (ATR): 2926, 2855, 1584, 1469, 1435, 1177, 774 cm^{-1}.

MS (EI) *m/z* (relative intensity): 324 ([M]$^+$, 20), 239 (55), 225 (100).

HR-MS (EI): *m/z* calcd. for [C$_{21}$H$_{25}$FN$_2$]$^+$ [M]$^+$ 324.2002, found 324.2010.
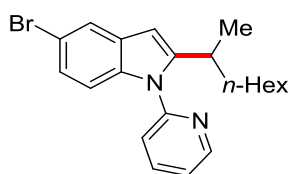
5-Bromo-2-(octan-2-yl)-1-(pyridin-2-yl)-1*H*-indole (145ca): The general procedure **E** was followed using 5-bromo-1-(pyridin-2-yl)-1*H*-indole (**105c**) (136 mg, 0.50 mmol) and oct-1-ene (**143a**) (168 mg, 1.50 mmol). Isolation by column chromatography (*n*-hexane/EtOAc: 25/1) yielded **145ca** (154 mg, 80%, 95:5) as a colorless oil.

^{1}H-NMR (400 MHz, CDCl$_3$): δ = 8.66 (ddd, *J* = 4.9, 2.1, 0.9 Hz, 1H), 7.87 (ddd, *J* = 7.9, 7.4, 2.1 Hz, 1H), 7.70 (dd, *J* = 1.9, 0.9 Hz, 1H), 7.34 (ddd, *J* = 7.9, 0.9, 0.9 Hz, 1H), 7.32 (ddd, *J* = 7.4, 4.9, 0.9 Hz, 1H), 7.20–7.08 (m, 2H), 6.38 (dd, *J* = 0.8, 0.8 Hz, 1H), 3.14 (tq, *J* = 6.9, 6.9 Hz, 0.95H, M), 2.79 (t, *J* = 7.8 Hz, 0.10H, AM), 1.64–1.37 (m, 2H), 1.29–1.10 (m, 11H), 0.84 (t, *J* = 7.1 Hz, 3H).

^{13}C-NMR (100 MHz, CDCl$_3$): δ = 151.1 (C$_q$), 149.7 (CH), 148.8 (C$_q$), 138.3 (CH), 136.0 (C$_q$), 130.2 (C$_q$), 124.0 (CH), 122.5 (CH), 122.3 (CH), 121.6 (CH), 113.5 (C$_q$), 111.4 (CH), 99.2 (CH), 36.9 (CH$_2$), 31.6 (CH$_2$), 30.8 (CH), 29.1 (CH$_2$), 26.9 (CH$_2$), 22.5 (CH$_2$), 20.4 (CH$_3$), 14.0 (CH$_3$).

IR (ATR): 2925, 2855, 1585, 1470, 1437, 863, 781, 735 cm^{-1}.

MS (EI) *m/z* (relative intensity): 384 ([M(^{79}Br)]$^+$, 25), 299 (45), 287 (100), 219 (75), 205 (15).

HR-MS (EI+): *m/z* calcd. for [C$_{21}$H$_{25}$^{79}BrN$_2$]$^+$ [M]$^+$ 384.1201, found 384.1206.
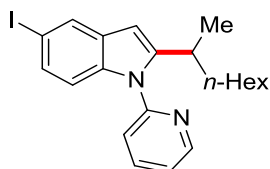
5-Iodo-2-(octan-2-yl)-1-(pyridin-2-yl)-1*H*-indole (145da): The general procedure **E** was followed using 5-iodo-1-(pyridin-2-yl)-1*H*-indole (**105d**) (160 mg, 0.50 mmol) and oct-1-ene (**143a**) (168 mg, 1.50 mmol). Isolation by column chromatography (*n*-hexane/EtOAc: 25/1) yielded **145da** (178 mg, 82%, 94:6) as a colorless oil.

^{1}H-NMR (300 MHz, CDCl$_3$): δ = 8.66 (ddd, *J* = 5.0, 2.1, 0.9 Hz, 1H), 7.91–7.84 (m, 2H), 7.38–7.32 (m, 3H), 6.99 (dd, *J* = 8.6, 0.9 Hz, 1H), 6.36 (dd, *J* = 0.8, 0.8 Hz, 1H), 3.12 (tq, *J* = 6.8, 6.8 Hz, 0.94H, M), 2.79 (t, *J* = 7.8 Hz, 0.12H, AM), 1.64–1.36 (m, 2H), 1.26–1.09 (m, 11H), 0.83 (t, *J* = 7.1 Hz, 3H).

^{13}C-NMR (125 MHz, CDCl$_3$): δ = 151.0 (C$_q$), 149.7 (CH), 148.3 (C$_q$), 138.3 (CH), 136.4 (C$_q$), 131.0 (C$_q$), 129.6 (CH), 128.5 (CH), 122.4 (CH), 121.6 (CH), 112.0 (CH), 98.9 (CH), 83.9 (C$_q$), 37.0 (CH$_2$), 31.7 (CH$_2$), 30.8 (CH), 29.2 (CH$_2$), 27.0 (CH$_2$), 22.6 (CH$_2$), 20.5 (CH$_3$), 14.2 (CH$_3$).

IR (ATR): 2924, 2854, 1584, 1469, 1436, 866, 781 cm^{-1}.

MS (EI) *m/z* (relative intensity): 432 ([M]$^+$, 60), 348 (45), 333 (100), 219 (65), 206 (20).

HR-MS (EI): *m/z* calcd. for [C$_{21}$H$_{25}$IN$_2$]$^+$ [M]$^+$ 432.1062, found 432.1067.
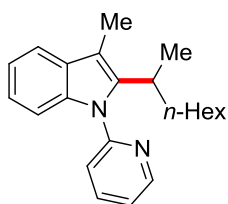
3-Methyl-2-(octan-2-yl)-1-(pyridin-2-yl)-1*H*-indole (145fa): The general procedure **E** was followed using methyl 3-methyl-1-(pyridin-2-yl)-1*H*-indole (**105f**) (104 mg, 0.50 mmol) and oct-1-ene (**143a**) (168 mg, 1.50 mmol). Isolation by column chromatography (*n*-hexane/EtOAc: 20/1) yielded **145fa** (97.6 mg, 61%, 21:79) as a colorless oil.

^{1}H-NMR (300 MHz, CDCl$_3$): δ = 8.63 (ddd, *J* = 4.9, 2.0, 0.9 Hz, 1H), 7.85 (ddd, *J* = 7.9, 7.4, 2.0 Hz, 1H), 7.56–7.51 (m, 1H), 7.41 (dt, *J* = 7.9, 0.9 Hz, 1H), 7.33–7.26 (m, 2H), 7.16–7.08 (m, 2H), 3.03–2.93 (m, 0.2H, M), 2.89 (t, *J* = 7.2 Hz, 1.6H, AM), 2.38 (s, 0.6H, M), 2.31 (s, 2.4H, AM), 1.35–1.12 (m, 12H), 0.84 (t, *J* = 6.7 Hz, 3H).

¹³C-NMR (125 MHz, CDCl₃): δ = 152.1 (C$_q$, M), 151.9 (C$_q$, AM), 149.5 (CH, M), 149.4 (CH, AM), 138.0 (CH, AM), 137.9 (CH, M), 137.2 (C$_q$, AM), 137.2 (C$_q$, M), 136.5 (C$_q$, AM), 136.5 (C$_q$, M), 129.9 (C$_q$, M), 129.4 (C$_q$, AM), 121.5 (CH, M), 122.1 (CH, M), 121.6 (CH, AM), 121.5 (CH, AM), 121.4 (CH, M), 121.0 (CH, AM), 120.0 (CH, AM), 119.8 (CH, M), 118.0 (CH, AM), 117.6 (CH, M), 109.9 (CH, M), 109.7 (CH, AM), 109.7 (C$_q$, AM), 108.2 (C$_q$, M), 36.0 (CH₂, M), 31.9 (CH₂, AM), 31.8 (CH₂, M), 31.7 (CH, M), 29.4 (CH₂, AM), 29.2 (CH₂, AM), 29.2 (CH₂, AM), 29.2 (CH₂, AM), 27.9 (CH₂, M), 24.8 (CH₂, AM), 22.7 (CH₂, AM), 20.1 (CH₃, M), 14.2 (CH₃, AM), 14.2 (CH₃, M), 9.6 (CH₃, M), 8.9 (CH₃, AM).

IR (ATR): 2924, 2854, 1586, 1470, 1436, 1362, 779, 739 cm⁻¹.

MS (EI) *m/z* (relative intensity): 320 ([M]⁺, 55), 235 (30), 221 (100), 207 (30).

HR-MS (EI): *m/z* calcd. for [C₂₂H₂₈N₂]⁺ [M]⁺ 320.2252, found 320.2253.
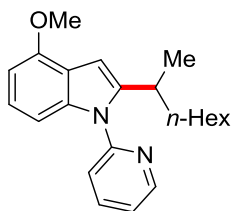
4-Methoxy-2-(octan-2-yl)-1-(pyridin-2-yl)-1*H*-indole (145ha): The general procedure **E** was followed using 4-methoxy-1-(pyridin-2-yl)-1*H*-indole (**105h**) (112 mg, 0.50 mmol) and oct-1-ene (**143a**) (168 mg, 1.50 mmol). Isolation by column chromatography (*n*-hexane/EtOAc: 25/1) yielded **145ha** (128 mg, 76%, 95:5) as a yellowish oil.

¹H-NMR (400 MHz, CDCl₃): δ = 8.65 (ddd, *J* = 4.9, 2.1, 1.0 Hz, 1H), 7.87 (ddd, *J* = 7.9, 7.4, 2.1 Hz, 1H), 7.39 (ddd, *J* = 7.9, 1.1, 1.0 Hz, 1H), 7.32 (ddd, *J* = 7.4, 4.9, 1.1 Hz, 1H), 7.01 (dd, *J* = 8.3, 7.8 Hz, 1H), 6.86 (dd, *J* = 8.3, 0.8 Hz, 1H), 6.63–6.47 (m, 2H), 3.97 (s, 3H), 3.13 (tq, *J* = 6.8, 6.8 Hz, 0.95H, M), 2.78 (t, *J* = 7.6 Hz, 0.10H, AM), 1.64–1.57 (m, 1H), 1.42–1.34 (m, 1H), 1.25–1.09 (m, 11H), 0.81 (t, *J* = 7.3 Hz, 3H).

¹³C-NMR (100 MHz, CDCl₃): δ = 152.6 (C$_q$), 151.8 (C$_q$), 149.6 (CH), 146.1 (C$_q$), 138.6 (C$_q$), 138.2 (CH), 122.2 (CH), 122.1 (CH), 121.8 (CH), 118.8 (C$_q$), 103.6 (CH), 100.6 (CH), 96.8 (CH), 55.4 (CH₃), 37.1 (CH₂), 31.7 (CH₂), 30.7 (CH), 29.2 (CH₂), 27.0 (CH₂), 22.6 (CH₂), 20.6 (CH₃), 14.0 (CH₃).

IR (ATR): 2926, 2855, 1586, 1470, 1440, 1258, 764 cm⁻¹.

MS (EI) *m/z* (relative intensity): 336 ([M]⁺, 55), 251 (85), 237 (100).

HR-MS (EI): *m/z* calcd. for [C₂₂H₂₈N₂O]⁺ [M]⁺ 336.2202, found 336.2213.
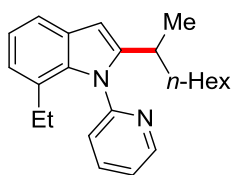
7-Ethyl-2-(octan-2-yl)-1-(pyridin-2-yl)-1*H*-indole (145ja): The general procedure **E** was followed using 7-ethyl-1-(pyridin-2-yl)-1*H*-indole (**105j**) (111 mg, 0.50 mmol) and oct-1-ene (**143a**) (168 mg, 1.50 mmol). Isolation by column chromatography (*n*-hexane/EtOAc: 20/1) yielded **145ja** (118 mg, 71%, 96:4) as a colorless oil.

^{1}H-NMR (300 MHz, CDCl$_3$): δ = 8.65 (ddd, J = 4.9, 2.0, 0.9 Hz, 1H), 7.82 (ddd, J = 7.8, 7.6, 2.0 Hz, 1H), 7.44 (dd, J = 7.8, 1.4 Hz, 1H), 7.40 (ddd, J = 7.6, 4.9, 0.9 Hz, 1H), 7.33 (ddd, J = 7.8, 0.9, 0.9 Hz, 1H), 7.06 (t, J = 7.7 Hz, 1H), 6.96–6.90 (m, 1H), 6.40 (dd, J = 0.8, 0.8 Hz, 1H), 2.52 (tq, J = 6.8, 6.8 Hz, 0.96H, M), 2.45 (t, J = 7.6 Hz, 0.08H, AM), 2.12 (q, J = 7.5 Hz, 2H), 1.72–1.59 (m, 1H), 1.46–1.35 (m, 1H), 1.27–1.10 (m, 11H), 0.94 (t, J = 7.5 Hz, 3H), 0.84 (t, J = 7.1 Hz, 3H).

^{13}C-NMR (125 MHz, CDCl$_3$): δ = 153.6 (C$_q$), 149.0 (CH), 148.3 (C$_q$), 137.4 (CH), 135.7 (C$_q$), 129.4 (C$_q$), 127.4 (C$_q$), 124.4 (CH), 123.3 (CH), 121.7 (CH), 120.3 (CH), 117.7 (CH), 99.2 (CH), 37.7 (CH$_2$), 31.7 (CH), 31.1 (CH$_2$), 29.3 (CH$_2$), 27.3 (CH$_2$), 24.8 (CH$_2$), 22.7 (CH$_2$), 21.3 (CH$_3$), 14.7 (CH$_3$), 14.1 (CH$_3$).

IR (ATR): 2925, 2854, 1583, 1467, 1435, 797, 740 cm^{-1}.

MS (EI) *m/z* (relative intensity): 334 ([M]$^+$, 50) 249 (40), 235 (100), 221 (40).

HR-MS (EI): *m/z* calcd. for [C$_{23}$H$_{30}$N$_2$]$^+$ [M]$^+$ 334.2409, found 334.2396.
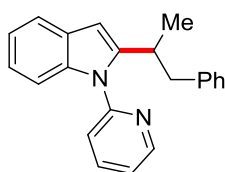
2-(1-Phenylpropan-2-yl)-1-(pyridin-2-yl)-1*H*-indole (145ab): The general procedure **E** was followed using 1-(pyridin-2-yl)-1*H*-indole (**105a**) (97.1 mg, 0.50 mmol) and allylbenzene (**143b**) (177 mg, 1.50 mmol). Isolation by column chromatography (*n*-hexane/EtOAc: 30/1) yielded **145ab** (127 mg, 82%, 99:1) as a colorless oil.

^{1}H-NMR (400 MHz, CDCl$_3$): δ = 8.69 (ddd, J = 4.9, 2.1, 0.9 Hz, 1H), 7.84 (ddd, J = 7.9, 7.5, 2.1 Hz, 1H), 7.66–7.55 (m, 1H), 7.33 (ddd, J = 7.5, 4.9, 1.0 Hz, 1H), 7.28 (ddd, J = 7.9, 1.0, 0.9 Hz, 1H), 7.24–7.21 (m, 1H), 7.18–7.08 (m, 5H), 6.93–6.88 (m, 2H), 6.52 (dd, J = 0.8, 0.8 Hz, 1H), 3.59–3.46

(m, 0.99H, M), 3.00 (dd, J = 13.2, 5.3 Hz, 1H), 2.86 (t, J = 7.7 Hz, 0.02H, AM), 2.56 (dd, J = 13.2, 8.7 Hz, 1H), 1.23 (d, J = 7.0 Hz, 3H).

^{13}**C-NMR** (100 MHz, CDCl$_3$): δ = 151.6 (C$_q$), 149.7 (CH), 146.5 (C$_q$), 140.3 (C$_q$), 138.3 (CH), 137.3 (C$_q$), 129.0 (CH), 128.5 (C$_q$), 128.1 (CH), 125.9 (CH), 122.2 (CH), 121.7 (CH), 121.6 (CH), 120.5 (CH), 120.1 (CH), 109.9 (CH), 100.4 (CH), 43.8 (CH$_2$), 32.8 (CH), 19.3 (CH$_3$).

IR (ATR): 3025, 2932, 1584, 1468, 1437, 735, 698 cm^{-1}.

MS (EI) m/z (relative intensity): 312 ([M]$^+$, 20), 221 (35), 207 (100).

HR-MS (EI): m/z calcd. for [C$_{22}$H$_{20}$N$_2$]$^+$ [M]$^+$ 312.1626, found 312.1621.
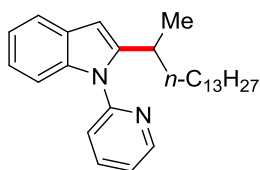
2-(Pentadecan-2-yl)-1-(pyridin-2-yl)-1H-indole (145ac): The general procedure **E** was followed using 1-(pyridin-2-yl)-1H-indole (**105a**) (97.1 mg, 0.50 mmol) and pentadec-1-ene (**143c**) (316 mg, 1.50 mmol). Isolation by column chromatography (n-hexane/EtOAc: 25/1) yielded **145ac** (154 mg, 76%, 95:5) as a yellowish oil.

^{1}**H-NMR** (300 MHz, CDCl$_3$): δ = 8.69 (ddd, J = 5.0, 2.1, 0.9 Hz, 1H), 7.87 (ddd, J = 8.0, 7.5, 2.1 Hz, 1H), 7.62–7.56 (m, 1H), 7.42 (ddd, J = 8.0, 1.0, 0.9 Hz, 1H), 7.36–7.27 (m, 2H), 7.16–7.10 (m, 2H), 6.50 (dd, J = 0.8, 0.8 Hz, 1H), 3.22 (tq, J = 6.8, 6.8 Hz, 0.95H, M), 2.86 (t, J = 7.7 Hz, 0.10H, AM), 1.72–1.62 (m, 1H), 1.50–1.40 (m, 1H), 1.35–1.12 (m, 25H), 0.93 (t, J = 7.1 Hz, 3H).

^{13}**C-NMR** (125 MHz, CDCl$_3$): δ = 151.7 (C$_q$), 149.6 (CH), 147.4 (C$_q$), 138.2 (CH), 137.4 (C$_q$), 128.6 (C$_q$), 122.1 (CH), 121.4 (CH), 121.0 (CH), 120.4 (CH), 119.7 (CH), 109.7 (CH), 99.7 (CH), 37.1 (CH$_2$), 32.0 (CH$_2$), 30.8 (CH), 29.7 (CH$_2$), 29.7 (CH$_2$), 29.7 (CH$_2$), 29.7 (CH$_2$), 29.7 (CH$_2$), 29.6 (CH$_2$), 29.5 (CH$_2$), 29.4 (CH$_2$), 27.1 (CH$_2$), 22.7 (CH$_2$), 20.6 (CH$_3$), 14.2 (CH$_3$).

IR (ATR): 2923, 2852, 1585, 1468, 1456, 780, 735 cm^{-1}.

MS (EI) m/z (relative intensity): 404 ([M]$^+$, 35), 221 (55), 207 (100), 195 (15).

HR-MS (EI): m/z calcd. for [C$_{28}$H$_{40}$N$_2$]$^+$ [M]$^+$ 404.3191, found 404.3182.
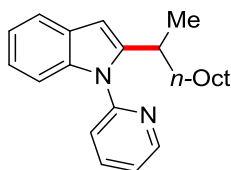
2-(Decan-2-yl)-1-(pyridin-2-yl)-1H-indole (145ad): The general procedure **E** was followed using 1-(pyridin-2-yl)-1H-indole (**105a**) (97.1 mg, 0.50 mmol) and dec-1-ene (**143d**) (210 mg, 1.50 mmol).

Isolation by column chromatography (*n*-hexane/EtOAc: 25/1) yielded **145ad** (118 mg, 71%, 94:6) as a colorless oil.

¹H-NMR (400 MHz, CDCl₃): δ = 8.68 (ddd, *J* = 5.0, 2.1, 0.9 Hz, 1H), 7.88 (ddd, *J* = 8.0, 7.5, 2.1 Hz, 1H), 7.65–7.58 (m, 1H), 7.43 (ddd, *J* = 8.0, 1.0, 0.9 Hz, 1H), 7.35–7.26 (m, 2H), 7.19–7.11 (m, 2H), 6.50 (dd, *J* = 0.8, 0.8 Hz, 1H), 3.23 (tq, *J* = 6.8, 6.8 Hz, 0.94H, M), 2.86 (t, *J* = 7.7 Hz, 0.12H, AM), 1.72–1.62 (m, 1H), 1.50–1.40 (m, 1H), 1.34–1.11 (m, 15H), 0.91 (t, *J* = 7.1 Hz, 3H).

¹³C-NMR (100 MHz, CDCl₃): δ = 151.7 (C$_q$), 149.6 (CH), 147.4 (C$_q$), 138.2 (CH), 137.4 (C$_q$), 128.6 (C$_q$), 122.1 (CH), 121.4 (CH), 121.0 (CH), 120.4 (CH), 119.7 (CH), 109.7 (CH), 99.7 (CH), 37.1 (CH₂), 31.8 (CH₂), 30.7 (CH), 29.5 (CH₂), 29.4 (CH₂), 29.3 (CH₂), 27.1 (CH₂), 22.7 (CH₂), 20.6 (CH₃), 14.1 (CH₃).

IR (ATR): 2923, 2852, 1585, 1468, 1435, 780, 735 cm⁻¹.

MS (EI) *m/z* (relative intensity): 334 ([M]⁺, 45), 249 (30), 235 (100), 221 (45).

HR-MS (EI): *m/z* calcd. for [C₂₃H₃₀N₂]⁺ [M]⁺ 334.2409, found 334.2407.
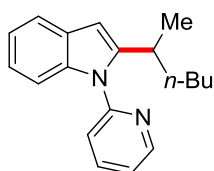
2-(Hexan-2-yl)-1-(pyridin-2-yl)-1*H*-indole (145ae): The general procedure **E** was followed using 1-(pyridin-2-yl)-1*H*-indole (**105a**) (97.1 mg, 0.50 mmol) and hex-1-ene (**143e**) (126 mg, 1.50 mmol). Isolation by column chromatography (*n*-hexane/EtOAc: 25/1) yielded **145ae** (94.6 mg, 68%, 96:4) as a colorless oil.

¹H-NMR (400 MHz, CDCl₃): δ = 8.67 (ddd, *J* = 5.0, 2.1, 0.9 Hz, 1H), 7.86 (ddd, *J* = 8.0, 7.5, 2.1 Hz, 1H), 7.62–7.56 (m, 1H), 7.42 (ddd, *J* = 8.0, 1.0, 0.9 Hz, 1H), 7.36–7.27 (m, 2H), 7.16–7.10 (m, 2H), 6.46 (dd, *J* = 0.8, 0.8 Hz, 1H), 3.17 (tq, *J* = 7.6, 7.6 Hz, 0.96H, M), 2.82 (t, *J* = 7.7 Hz, 0.08H, AM), -1.67–1.56 (m, 1H), 1.45–1.35 (m, 1H), 1.24–1.07 (m, 7H), 0.77 (t, *J* = 7.1 Hz, 3H).

¹³C-NMR (100 MHz, CDCl₃): δ = 151.7 (C$_q$), 149.7 (CH), 147.5 (C$_q$), 138.2 (CH), 137.3 (C$_q$), 128.6 (C$_q$), 122.2 (CH), 121.7 (CH), 121.4 (CH), 120.4 (CH), 119.9 (CH), 110.0 (CH), 99.8 (CH), 36.7 (CH₂), 30.7 (CH), 29.3 (CH₂), 22.6 (CH₂), 20.5 (CH₃), 13.9 (CH₃).

IR (ATR): 2928, 2857, 1584, 1469, 1436, 781, 747, 736 cm⁻¹.

MS (EI) *m/z* (relative intensity): 278 ([M]⁺, 40), 221 (80), 207 (100).

HR-MS (EI): *m/z* calcd. for [C₁₉H₂₂N₂]⁺ [M]⁺ 278.1783, found 278.1781.
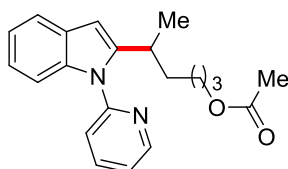
5-[1-(Pyridin-2-yl)-1*H*-indol-2-yl]hexyl acetate (145af): The general procedure **E** was followed using 1-(pyridin-2-yl)-1*H*-indole (**105a**) (97.1 mg, 0.50 mmol) and hex-5-en-1-yl acetate (**143f**) (213 mg, 1.50 mmol). Isolation by column chromatography (*n*-hexane/EtOAc: 10/1) yielded **145af** (124 mg, 73%, 99:1) as a yellowish oil.

¹H-NMR (300 MHz, CDCl₃): δ = 8.68 (ddd, J = 4.9, 2.1, 0.9 Hz, 1H), 7.87 (ddd, J = 8.0, 7.6, 2.1 Hz, 1H), 7.60–7.54 (m, 1H), 7.41 (ddd, J = 8.0, 1.0, 0.9 Hz, 1H), 7.33 (ddd, J = 7.5, 4.9, 1.0 Hz, 1H), 7.25–7.20 (m, 1H), 7.12–7.05 (m, 2H), 6.45 (dd, J = 0.8, 0.8 Hz, 1H), 3.94 (t, J = 6.7 Hz, 2H), 3.25–3.13 (m, 0.99H, M), 2.84 (t, J = 7.4 Hz, 0.02H, AM), 1.99 (s, 3H), 1.69–1.59 (m, 1H), 1.51–1.39 (m, 3H), 1.32–1.21 (m, 5H).

¹³C-NMR (100 MHz, CDCl₃): δ = 171.1 (C_q), 151.6 (C_q), 149.7 (CH), 146.9 (C_q), 140.3 (CH), 138.3 (CH), 137.3 (C_q), 128.5 (C_q), 122.2 (CH), 121.5 (CH), 120.5 (CH), 119.9 (CH), 109.9 (CH), 99.9 (CH), 64.3 (CH₂), 36.5 (CH₂), 30.7 (CH), 28.5 (CH₂), 23.4 (CH₂), 21.0 (CH₃), 20.6 (CH₃).

IR (ATR): 2933, 1736, 1585, 1470, 1437, 1242, 782, 748 cm⁻¹.

MS (EI) *m/z* (relative intensity): 336 ([M]⁺, 30), 221 (60), 207 (55), 135 (100).

HR-MS (EI): *m/z* calcd. for [C₂₁H₂₄N₂O₂]⁺ [M]⁺ 336.1838, found 336.1829.
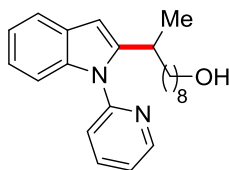
9-[1-(Pyridin-2-yl)-1*H*-indol-2-yl]decan-1-ol (145ag): The general procedure **E** was followed using 1-(pyridin-2-yl)-1*H*-indole (**105a**) (97.1 mg, 0.50 mmol) and dec-9-en-1-ol (**143g**) (234 mg, 1.50 mmol). Isolation by column chromatography (*n*-hexane/EtOAc: 5/1) yielded **145ag** (109 mg, 62%, 92:8) as a yellowish oil.

¹H-NMR (400 MHz, CDCl₃): δ = 8.65 (ddd, J = 4.9, 2.1, 0.9 Hz, 1H), 7.88 (ddd, J = 8.0, 7.5, 2.1 Hz, 1H), 7.60–7.54 (m, 1H), 7.40 (ddd, J = 8.0, 1.0, 0.9 Hz, 1H), 7.34–7.30 (ddd, J = 7.5, 4.9, 1.0 Hz, 1H), 7.25–7.21 (m, 1H), 7.13–7.06 (m, 2H), 6.44 (dd, J = 0.8, 0.8 Hz, 1H), 3.55 (t, J = 6.7 Hz, 2H), 3.16 (tq, J = 6.9, 6.9 Hz, 0.92H, M), 2.82 (t, J = 7.6 Hz, 0.16H, AM), 1.70 (bs, 1H), 1.64–1.36 (m, 4H), 1.31–1.01 (m, 13H).

¹³C-NMR (100 MHz, CDCl₃): δ = 151.6 (C_q), 149.6 (CH), 147.4 (C_q), 138.1 (CH), 137.3 (C_q), 128.5 (C_q), 122.2 (CH), 121.8 (CH), 121.4 (CH), 120.4 (CH), 119.9 (CH), 109.9 (CH), 99.8 (CH), 62.9 (CH₂), 38.6 (CH₂), 37.0 (CH₂), 36.4 (CH₂), 32.7 (CH₂), 30.7 (CH), 29.4 (CH₂), 27.0 (CH₂), 25.6 (CH₂), 20.5 (CH₃).

IR (ATR): 3374, 2924, 2852, 1699, 1586, 1468, 1436, 780, 736 cm⁻¹.

MS (EI) *m/z* (relative intensity): 350 ([M]⁺, 15), 264 (25), 252 (100), 206 (30).

HR-MS (EI): m/z calcd. for $[C_{23}H_{30}N_2O]^+$ $[M]^+$ 350.2358, found 350.2351.
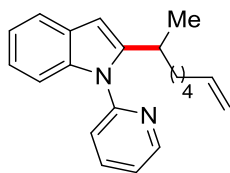
2-(Oct-7-en-2-yl)-1-(pyridin-2-yl)-1*H*-indole (145ah): The general procedure **E** was followed using 1-(pyridin-2-yl)-1*H*-indole (**105a**) (97.1 mg, 0.50 mmol) and octa-1,7-diene (**143h**) (165 mg, 1.50 mmol). Isolation by column chromatography (*n*-hexane/EtOAc: 40/1) yielded **145ah** (119 mg, 78%, 94:6) as a colorless oil.

¹H-NMR (300 MHz, CDCl₃): δ = 8.69 (ddd, J = 4.9, 2.0, 0.9 Hz, 1H), 7.88 (ddd, J = 7.8, 7.6, 2.0 Hz, 1H), 7.64−7.58 (m, 1H), 7.43 (ddd, J = 7.9, 0.9, 0.9 Hz, 1H), 7.33 (ddd, J = 7.2, 4.9, 0.9 Hz, 1H), 7.29−7.24 (m, 1H), 7.18−7.10 (m, 2H), 6.49 (dd, J = 0.8, 0.8 Hz, 1H), 5.76 (ddt, J = 17.2, 10.4, 6.8 Hz, 1H), 5.08–4.84 (m, 2H), 3.22 (tq, J = 6.9, 6.9 Hz, 0.94H, M), 2.86 (t, J = 7.6 Hz, 0.12H, AM), 2.08–1.92 (m, 3H), 1.81–1.54 (m, 2H), 1.53–1.41 (m, 1H), 1.32–1.21 (m, 5H).

¹³C-NMR (125 MHz, CDCl₃): δ = 151.6 (C_q), 149.6 (CH), 147.3 (C_q), 138.9 (CH), 138.2 (CH), 137.3 (C_q), 128.5 (C_q), 122.1 (CH), 121.7 (CH), 121.4 (CH), 120.4 (CH), 119.9 (CH), 114.1 (CH₂), 109.9 (CH), 102.0 (CH, AM), 99.8 (CH, M), 38.6 (CH₂, AM), 36.8 (CH₂, M), 36.4 (CH₂, AM), 33.5 (CH₂, M), 30.6 (CH), 28.7 (CH₂), 27.7 (CH₂, AM), 26.5 (CH₂), 20.5 (CH₃).

IR (ATR): 2926, 2854, 1584, 1469, 1455, 1435, 780, 734 cm⁻¹.

MS (EI) m/z (relative intensity): 304 ([M]⁺, 20), 263 (15), 221 (100), 207 (100).

HR-MS (EI): m/z calcd. for $[C_{21}H_{24}N_2]^+$ $[M]^+$ 304.1939, found 304.1938.
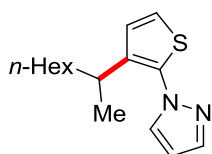
1-[3-(Octan-2-yl)thiophen-2-yl]-1*H*-pyrazole (148): A modified general procedure **E** was followed using 1-(thiophen-2-yl)-1*H*-pyrazole (**131**) (75.0 mg, 0.50 mmol) and oct-1-ene (**143a**) (168 mg, 1.50 mmol) at 80 °C. Isolation by column chromatography (*n*-hexane/EtOAc: 15/1) yielded **148** (109 mg, 83%, 79:21) as a yellowish oil.

¹H-NMR (300 MHz, CDCl₃): δ = 7.68 (dd, J = 1.9, 0.6 Hz, 1H), 7.59 (dd, J = 2.4, 0.6 Hz, 0.21H, AM), 7.57 (dd, J = 2.4, 0.6 Hz, 0.79H, M), 7.13 (dd, J = 5.7, 0.5 Hz, 0.79H, M), 7.09 (dd, J = 5.7, 0.5 Hz, 0.21H, AM), 6.89–6.83 (m, 1H), 6.41–6.38 (m, 1H), 2.73 (tq, J = 7.1, 7.1 Hz, 0.79H, M), 2.51 (t, J = 7.6 Hz, 0.42H, AM), 1.52–1.41 (m, 2H), 1.22–1.13 (m, 11H), 0.83 (t, J = 6.9 Hz, 3H).

^{13}**C-NMR** (125 MHz, CDCl$_3$): δ = 142.1 (C$_q$), 140.9 (CH), 135.9 (C$_q$, AM), 135.4 (C$_q$, M), 132.0 (CH, M), 131.5 (CH, AM), 127.5 (CH, AM), 124.8 (CH, M), 122.5 (CH, M), 121.7 (CH, AM), 106.7 (CH, AM), 106.6 (CH, M), 37.7 (CH$_2$), 32.1 (CH), 31.9 (CH$_2$, AM), 31.7 (CH$_2$, M), 30.2 (CH$_2$, AM), 29.3 (CH$_2$, AM), 29.3 (CH$_2$, AM), 29.2 (CH$_2$, M), 27.6 (CH$_2$), 22.7 (CH$_2$), 21.8 (CH$_3$), 14.1 (CH$_3$, AM), 14.1 (CH$_3$, M).

IR (ATR): 2957, 2924, 1455, 1389, 919, 746 cm^{-1}.

MS (EI) *m/z* (relative intensity): 262 ([M]$^+$, 40), 191 (40), 177 (100), 163 (90), 144 (60).

HR-MS (EI): *m/z* calcd. for [C$_{15}$H$_{22}$N$_2$S]$^+$ [M]$^+$ 262.1504, found 262.1515.

5.4.2   Removal of the Directing Group
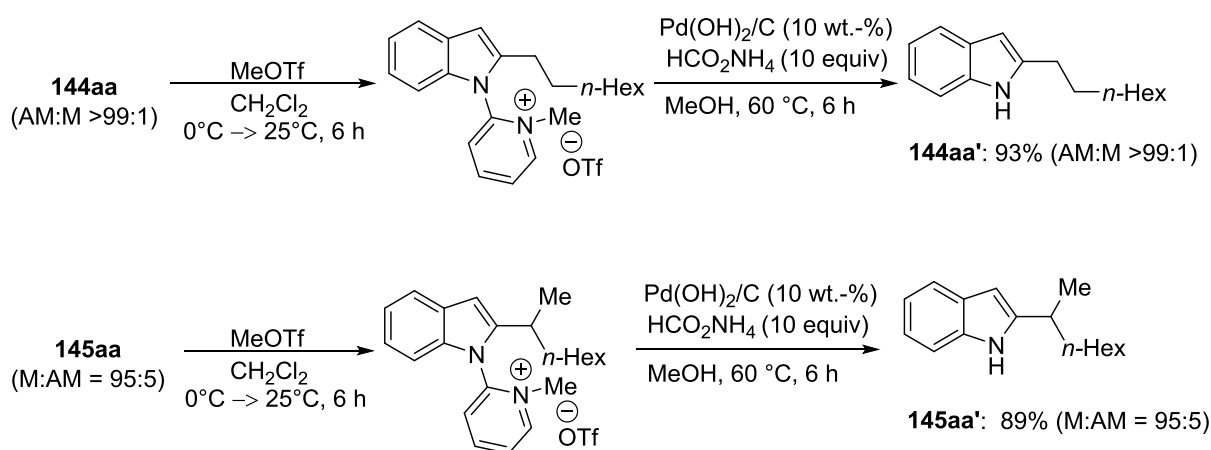
To a solution of **144aa** (153 mg, 0.50 mmol, 1.00 equiv) or **145aa** (153 mg, 0.50 mmol, 1.00 equiv) in CH$_2$Cl$_2$ (1.0 mL) was added MeOTf (90.3 mg, 60.0 µL, 0.55 mmol, 1.10 equiv) dropwise at 0 °C. After 30 min, the mixture was allowed to warm up to 25 °C and stirred for 6 h. After removal of the solvent *in vacuo*, Pd(OH)$_2$/C (19.3 mg, 10 wt.-%) and ammonium formate (315 mg, 5.00 mmol, 10.0 equiv) were added. The mixture was diluted with MeOH (2.0 mL, 0.25 M) and stirred at 60 °C for 6 h. After addition of EtOAc (10 mL) at ambient temperature, the mixture was filtered through a short pad of celite and the solvents were removed *in vacuo*. The crude mixture was purified by flash column chromatography on silica gel (*n*-hexane/EtOAc: 8/1) to yield **144aa'** (106 mg, 93%) or **145aa'** (102 mg, 89%, 95:5) as pale yellow solids, respectively.
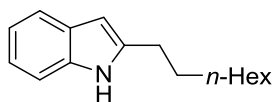
2-*n*-Octyl-1*H*-indole (144aa'):

M.p.: 58 °C

¹H-NMR (300 MHz, CDCl₃): δ = 7.69 (bs, 1H), 7.64–7.54 (m, 1H), 7.31–7.26 (m, 1H), 7.23–7.14 (m, 2H), 6.31 (dt, *J* = 0.8, 0.8 Hz, 1H), 2.74 (tt, *J* = 7.5, 7.5 Hz, 2H), 1.75 (tt, *J* = 7.5, 7.5 Hz, 2H), 1.48–1.34 (m, 10H), 1.00 (t, *J* = 7.0 Hz, 3H).

¹³C-NMR (125 MHz, CDCl₃): δ = 139.9 (C$_q$), 135.7 (C$_q$), 128.7 (C$_q$), 120.7 (CH), 119.6 (CH), 119.4 (CH), 110.2 (CH), 99.3 (CH), 31.9 (CH₂), 29.5 (CH₂), 29.4 (CH₂), 29.3 (CH₂), 29.2 (CH₂), 28.2 (CH₂), 22.7 (CH₂), 14.2 (CH₃).

IR (ATR): 3407, 2925, 2854, 1458, 1288, 779, 748 cm⁻¹.

MS (EI) *m/z* (relative intensity): 229 ([M]⁺, 30), 144 (30), 130 (100).

HR-MS (EI): *m/z* calcd. for [C₁₆H₂₃N]⁺ [M]⁺ 229.1830, found 229.1829.
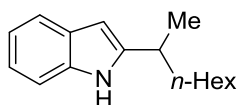
2-(Octan-2-yl)-1*H*-indole (145aa'):

M.p.: 60 °C

¹H-NMR (300 MHz, CDCl₃): δ = 7.85 (bs, 1H), 7.55–7.49 (m, 1H), 7.32–7.26 (m, 1H), 7.17–7.01 (m, 2H), 6.23 (dd, *J* = 0.8, 0.8 Hz, 1H), 2.88 (tq, *J* = 7.0, 7.0 Hz, 0.95H), 2.74 (t, *J* = 7.6 Hz, 0.05H), 1.75–1.57 (m, 2H), 1.37–1.24 (m, 11H), 0.86 (t, *J* = 7.0 Hz, 3H).

¹³C-NMR (125 MHz, CDCl₃): δ = 144.9 (C$_q$), 135.5 (C$_q$), 128.6 (C$_q$), 120.8 (CH), 119.8 (CH), 119.5 (CH), 110.2 (CH), 98.2 (CH), 37.3 (CH₂), 33.4 (CH), 31.8 (CH₂), 29.4 (CH₂), 27.4 (CH₂), 22.7 (CH₂), 20.7 (CH₃), 14.2 (CH₃).

IR (ATR): 3406, 2926, 2855, 1458, 781, 749 cm⁻¹.

MS (EI) *m/z* (relative intensity): 229 ([M]⁺, 40), 158 (20), 144 (100), 130 (45).

HR-MS (EI): *m/z* calcd. for [C₁₆H₂₃N]⁺ [M]⁺ 229.1830, found 229.1824.

5.4.3   Mechanistic Studies

5.4.3.1   Kinetic Isotope Effect

5.4.3.1.1   KIE for the linear-selective reaction
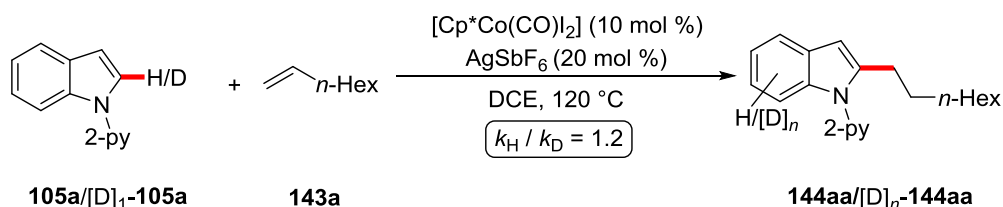
105a/[D]$_1$-**105a**   **143a**   **144aa**/[D]$_n$-**144aa**

Two parallel reactions of **105a** or [D]$_1$-**105a** with **143a** were performed respectively to determine the KIE value by comparison of the initial reaction rates by GC-analysis with *n*-dodecane as the internal standard. A suspension of **105a** (97.1 mg, 0.50 mmol, 1.00 equiv) or [D]$_1$-**105a** (97.6 mg, 0.50 mmol, 1.00 equiv), **143a** (168 mg, 235 µL, 1.50 mmol, 3.00 equiv), [Cp*Co(CO)I$_2$] (23.8 mg, 10.0 mol %) and AgSbF$_6$ (34.4 mg, 20.0 mol %) in DCE (2.00 mL) was stirred at 120 °C. Aliquots (25 µL) were periodically removed to provide the following conversions as determined by GC-analysis:

Table 32. KIE for the linear-selective reaction.

t / min	10	20	30	40	50
144aa / %	2.5	5.8	11.6	18.8	25.2
[D]$_n$-**144aa** / %	1.0	5.4	8.7	16.3	21.0

5.4.3.1.2   KIE for the branched-selective reaction
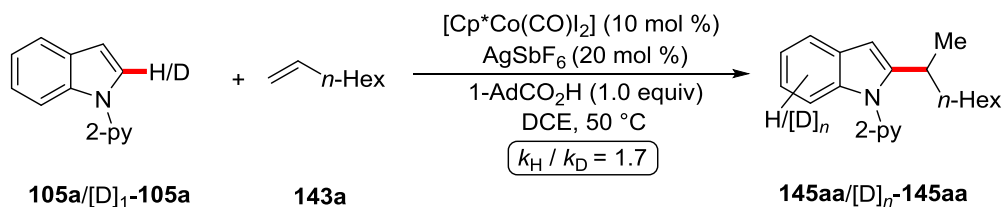
105a/[D]$_1$-**105a**   **143a**   **145aa**/[D]$_n$-**145aa**

Two parallel reactions of **105a** or [D]$_1$-**105a** with **143a** were performed respectively to determine the KIE value by comparison of the initial reaction rates by GC-analysis with *n*-dodecane as the internal standard. A suspension of **105a** (97.1 mg, 0.50 mmol, 1.00 equiv) or [D]$_1$-**105a** (97.6 mg, 0.50 mmol, 1.00 equiv), **143a** (168 mg, 235 µL, 1.50 mmol, 3.00 equiv), [Cp*Co(CO)I$_2$] (23.8 mg, 10 mol %), AgSbF$_6$ (34.4 mg, 20 mol %) and 1-AdCO$_2$H (90.1 mg, 0.50 mmol, 1.00 equiv) in DCE (2.00 mL)
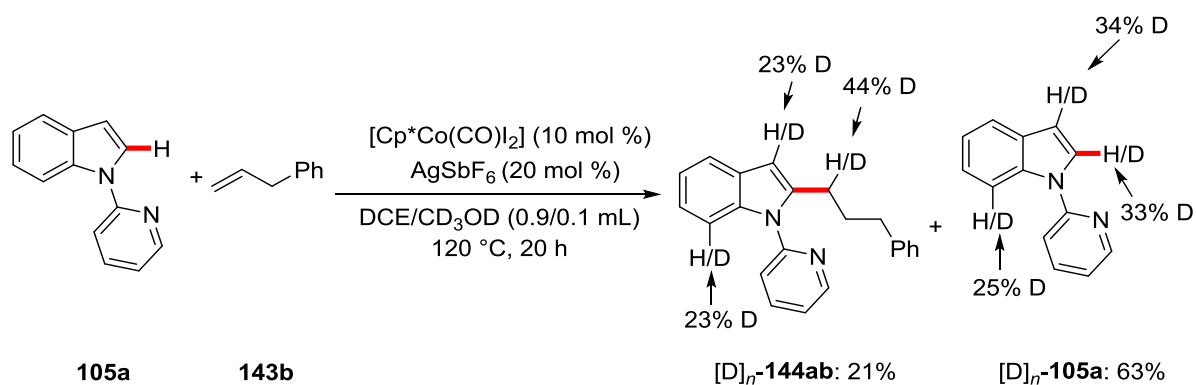
was stirred at 50 °C. Aliquots (25 µL) were periodically removed to provide the following conversions as determined by GC-analysis:

Table 33. KIE for the branched-selective reaction.

t / min	30	40	50	60	90
145aa / %	1.64	2.37	3.06	3.44	5.92
$[D]_n$-1**45aa** / %	0.76	1.36	1.67	1.98	3.38

5.4.3.2   H/D-Exchange Experiments

5.4.3.2.1   H/D-exchange for the linear-selective reaction

A suspension of **105a** (146 mg, 0.75 mmol, 1.50 equiv), allylbenzene (**143b**) (59.1 mg, 0.50 mmol, 1.00 equiv), [Cp*Co(CO)I$_2$] (23.8 mg, 10.0 mol %) and AgSbF$_6$ (34.4 mg, 20.0 mol %) in DCE (0.9 mL) and CD$_3$OD (0.1 mL) was stirred at 120 °C for 20 h. After removal of the solvents, the crude mixture was purified by column chromatography on silica gel (*n*-hexane/EtOAc: 20:1) to yield [D]$_n$-**144ab** (32.8 mg, 21%) and [D]$_n$-**105a** (92.0 mg, 63% reis.) as yellow oils.

[D]$_n$-**105a**
(CDCl$_3$, 300 MHz)

34% D

33% D

25% D

23% D   44% D

23% D

[D]$_n$-**144ab**
(CDCl$_3$, 500 MHz)
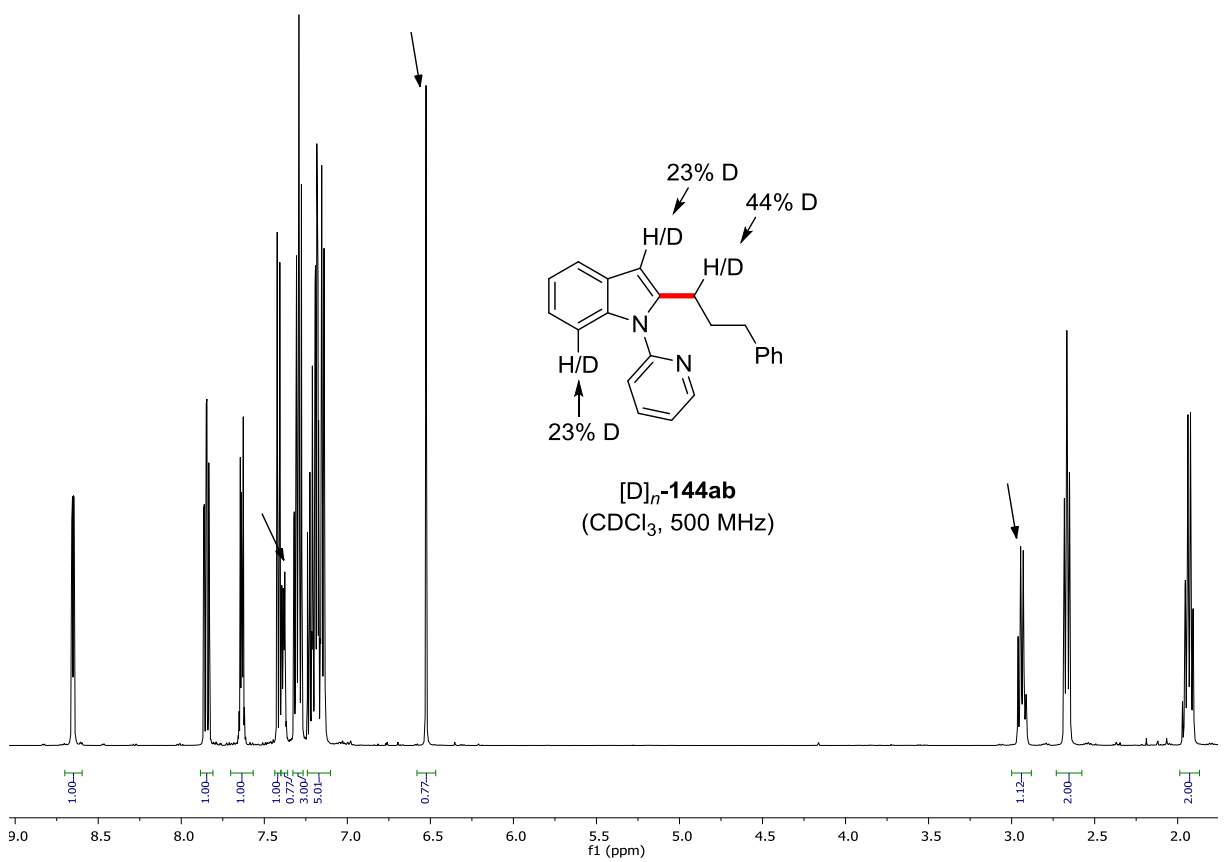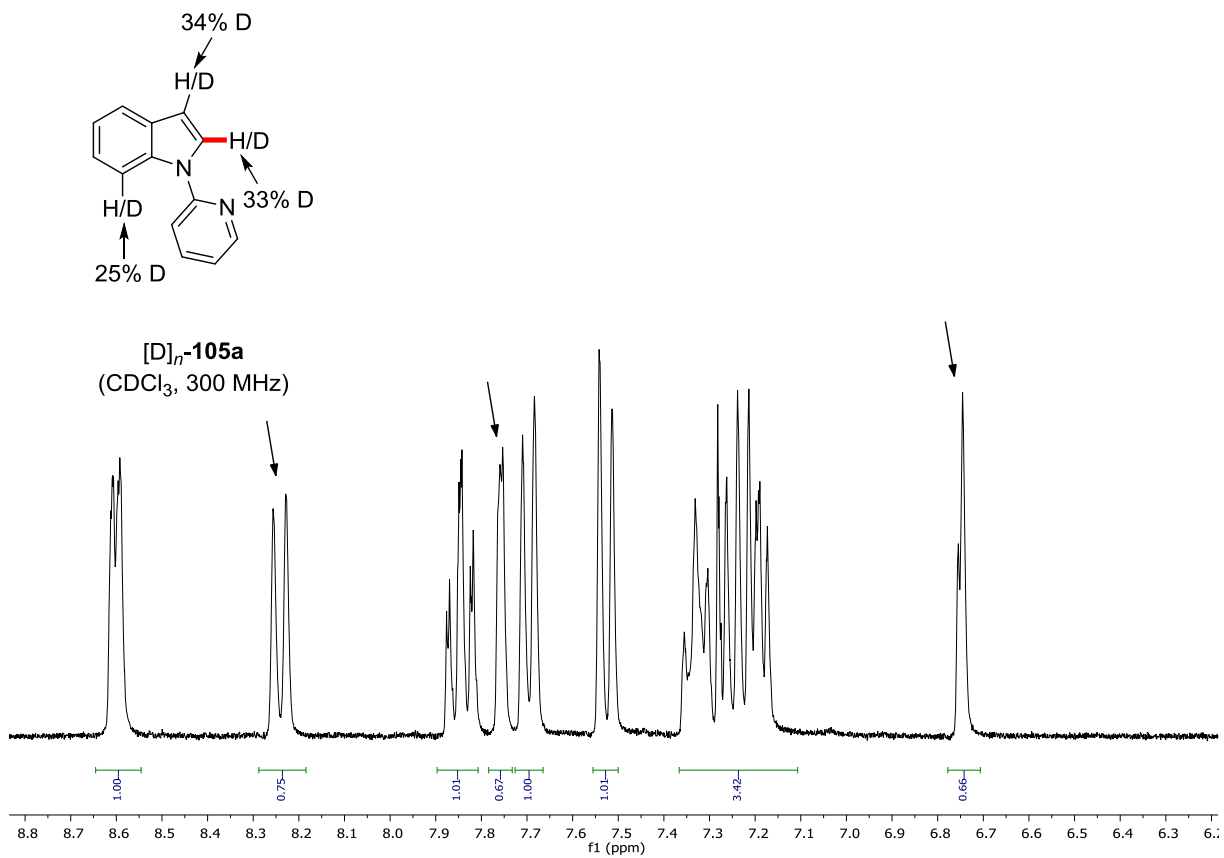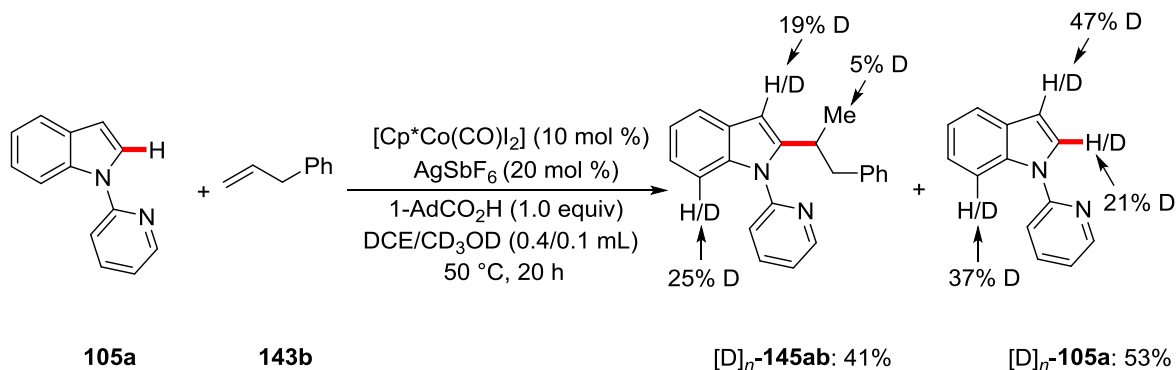
5.4.3.2.2 H/D-exchange for the branched-selective reaction

A suspension of **105a** (146 mg, 0.75 mmol, 1.50 equiv), allylbenzene (**143b**) (59.1 mg, 0.50 mmol, 1.00 equiv), [Cp*Co(CO)I$_2$] (23.8 mg, 10.0 mol %), AgSbF$_6$ (34.4 mg, 20.0 mol %) and 1-AdCO$_2$H (90.1 mg, 0.50 mmol, 1.00 equiv) in DCE (0.4 mL) and CD$_3$OD (0.1 mL) was stirred at 50 °C for 20 h. After removal of the solvents, the crude mixture was purified by column chromatography on silica gel (*n*-hexane/EtOAc: 20:1) to yield [D]$_n$-**145ab** (64.0 mg, 41%) and [D]$_n$-**105a** (77.1 mg, 53% reis.) as yellow oils.
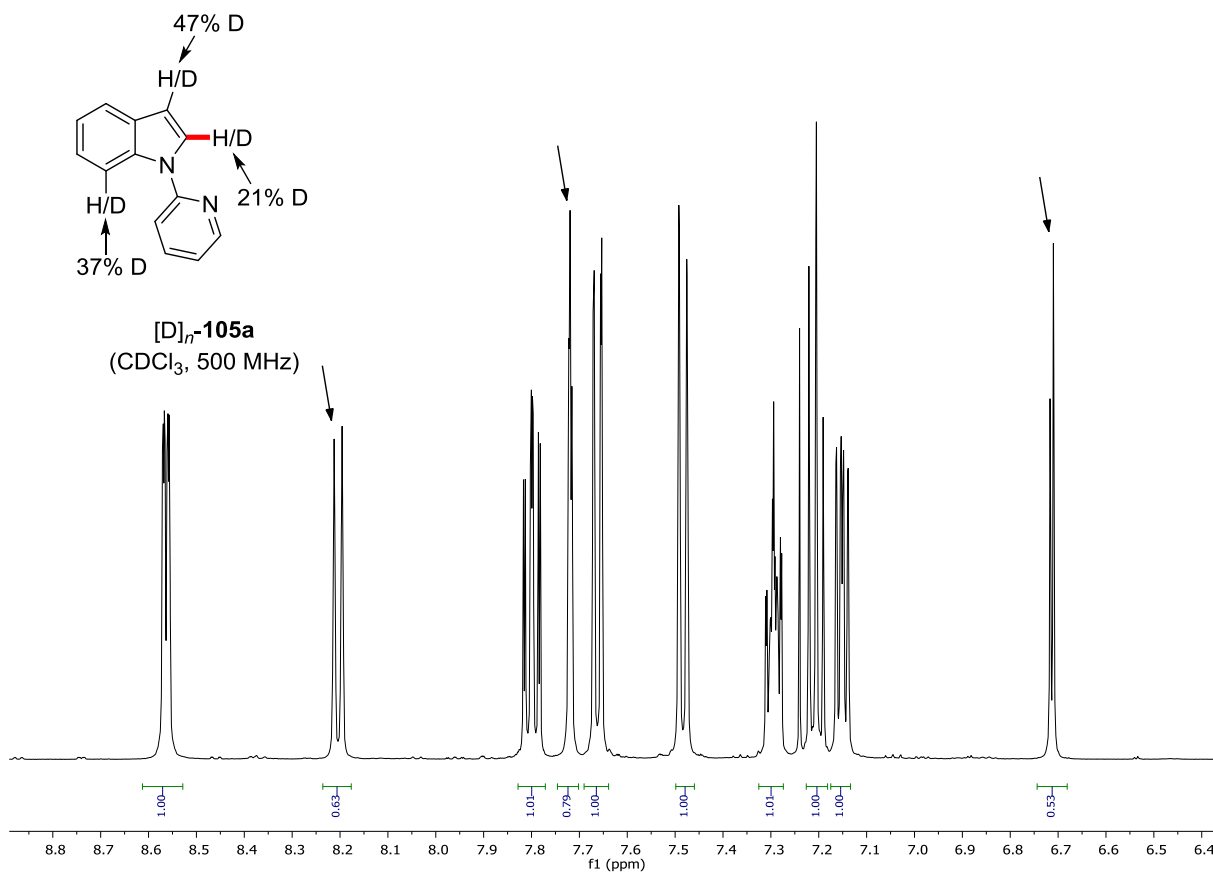
^{1}H NMR spectrum of [D]$_n$-**145ab** (CDCl$_3$, 500 MHz)
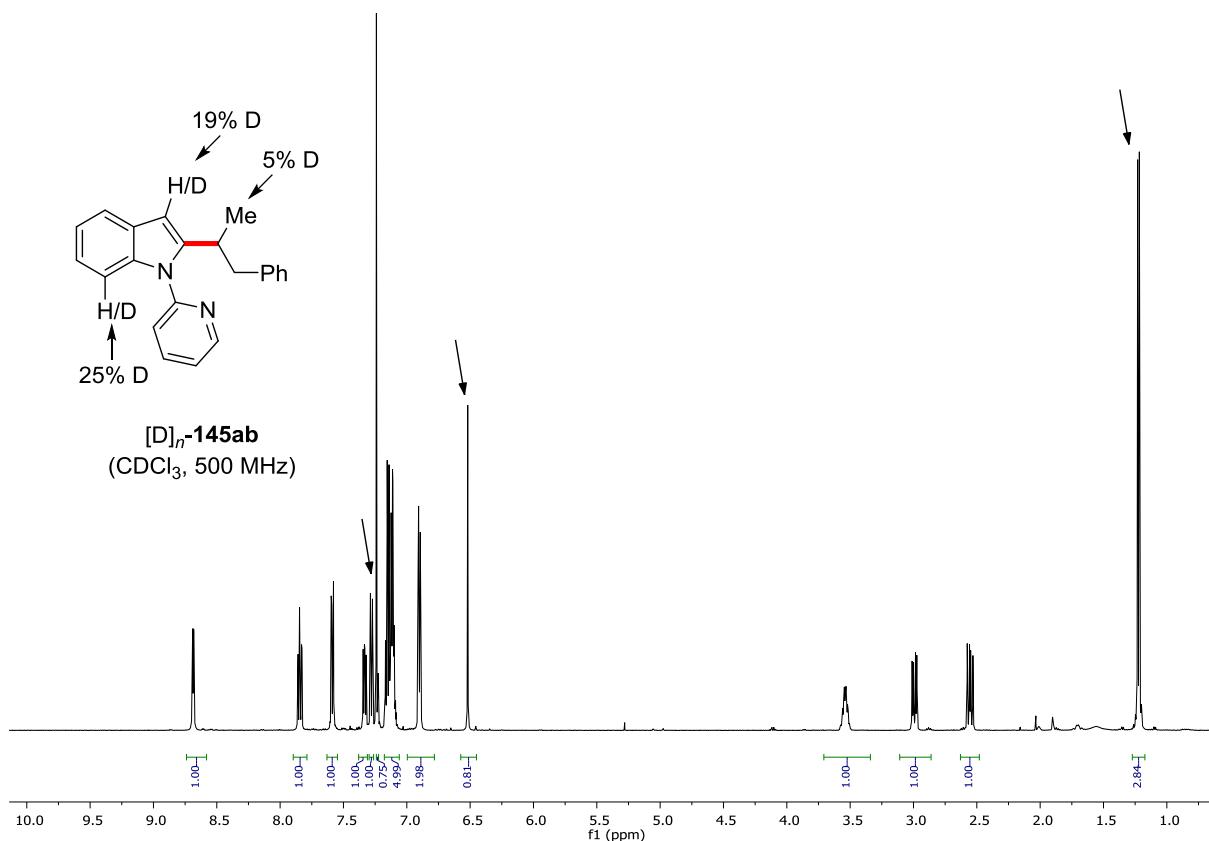
5.4.3.2.3   H/D-exchange with alkene under the linear-selective regime
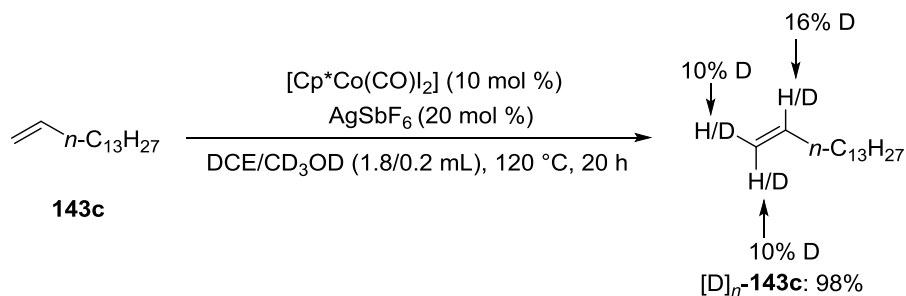
A suspension of 1-pentadecene (**143c**) (105 mg, 135 μL, 1.00 mmol, 1.00 equiv), [Cp*Co(CO)I$_2$] (23.8 mg, 10.0 mol %) and AgSbF$_6$ (34.4 mg, 20.0 mol %) in DCE (1.8 mL) and CD$_3$OD (0.2 mL) was stirred at 120 °C for 20 h. After removal of the solvents, the crude mixture was purified by column chromatography on silica gel (*n*-hexane/EtOAc: 50:1) to yield [D]$_n$-**143c** (103 mg, 98% reis.) as a colorless oil.

[D]$_n$-**143c**
(CDCl$_3$, 300 MHz)
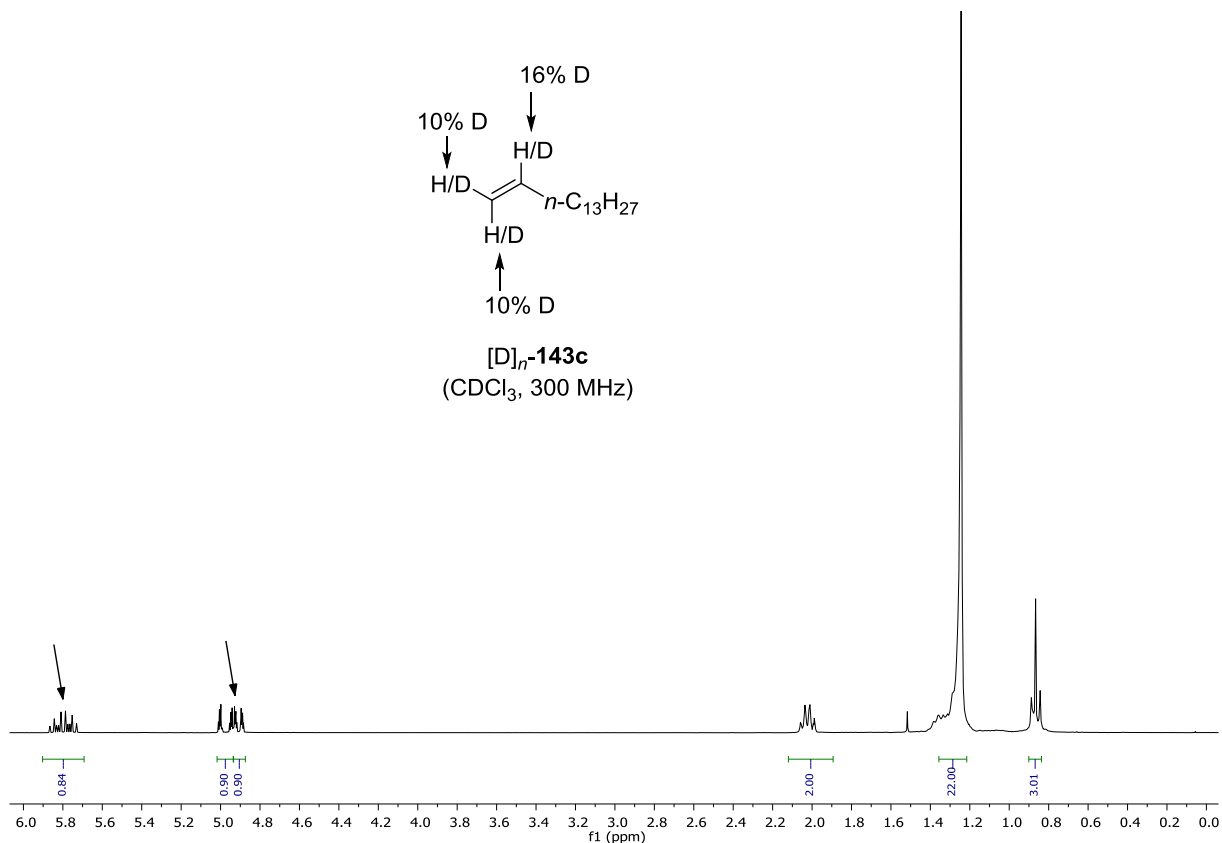
5.4.3.2.4   H/D-exchange with alkene under the branched-selective regime
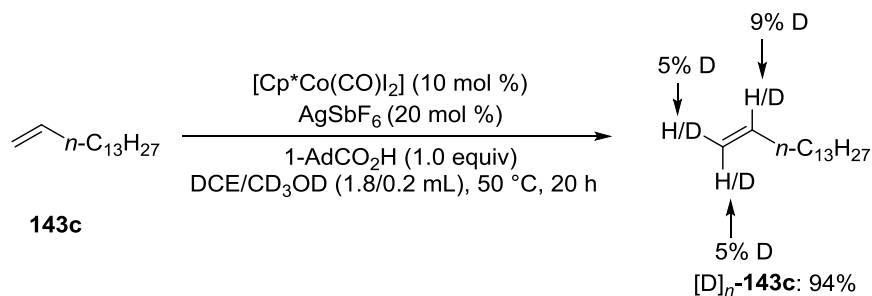
[D]$_n$-**143c**: 94%

A suspension of 1-pentadecene (**143c**) (105 mg, 135 μL, 1.00 mmol, 1.00 equiv), [Cp*Co(CO)I$_2$] (23.8 mg, 10.0 mol %), AgSbF$_6$ (34.4 mg, 20.0 mol %) and 1-AdCO$_2$H (90.1 mg, 0.50 mmol, 1.00 equiv) in DCE (1.8 mL) and CD$_3$OD (0.2 mL) was stirred at 50 °C for 20 h. After removal of the solvents, the crude mixture was purified by column chromatography on silica gel (*n*-hexane/EtOAc: 50:1) to yield [D]$_n$-**143c** (98.7 mg, 94% reisolated) as a colorless oil.

$[D]_n$-**143c**
(CDCl$_3$, 300 MHz)
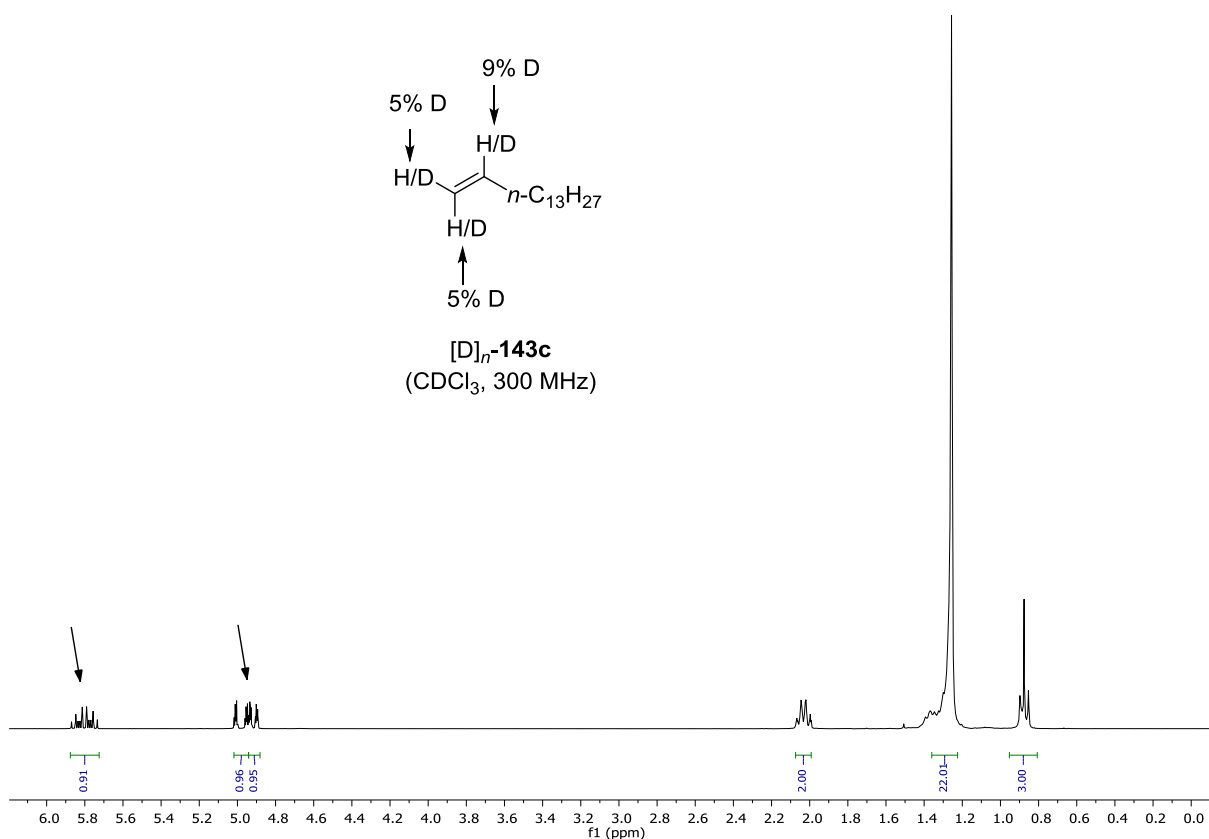
5.4.3.2.5   H/D-exchange with [D]$_1$-105a

A suspension of [D]$_1$-**105a** (97.6 mg, 0.50 mmol, 1.00 equiv), [Cp*Co(CO)I$_2$] (23.8 mg, 10.0 mol %), AgSbF$_6$ (34.4 mg, 20.0 mol %) in DCE (1.0 mL) was stirred at 120 °C for 20 h. After removal of the solvents, the crude mixture was purified by column chromatography on silica gel (*n*-hexane/EtOAc: 20:1) to yield [D]$_n$-**105a** (90.2 mg, 93% reisolated) as a colorless oil.

[D]$_n$-**105a**
(CDCl$_3$, 500 MHz)
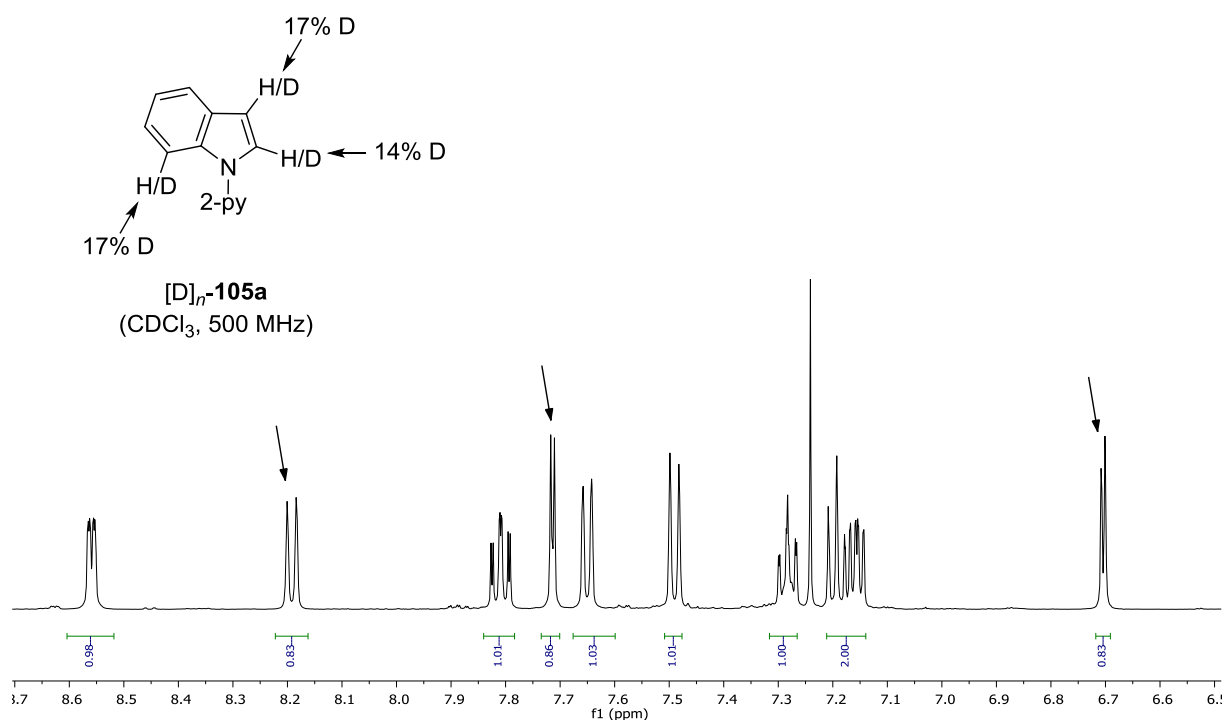
5.4.3.2.6   H/D-exchange with [D]$_1$-105a under the reaction conditions
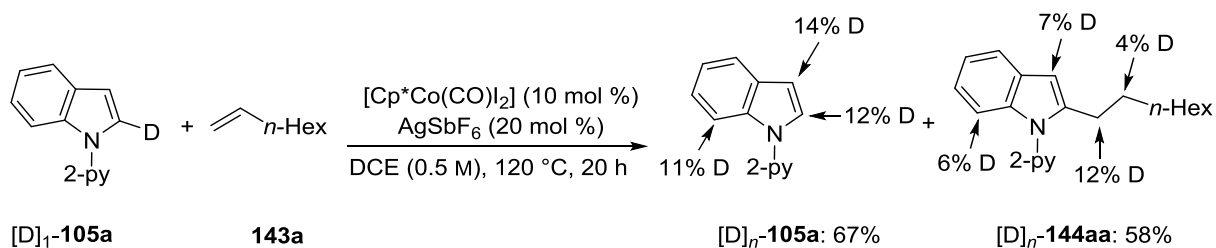
As suspension of [D]$_1$-**105a** (146 mg, 0.75 mmol, 1.50 equiv), **143a** (56.0 mg, 0.50 mmol, 1.00 equiv), [Cp*Co(CO)I$_2$] (23.8 mg, 10.0 mol %) and AgSbF$_6$ (34.4 mg, 20.0 mol %) in DCE (1.0 mL) was stirred at 120 °C for 20 h. After removal of the solvents, the crude mixture was purified by column chromatography on silica gel (*n*-hexane/EtOAc: 20:1) to yield [D]$_n$-**144aa** (88.7 mg, 58%) and [D]$_n$-**105a** (97.8 mg, 67% reisolated) as yellow oils.

[D]$_n$-**105a**
(CDCl$_3$, 400 MHz)

14% D
12% D
11% D   2-py
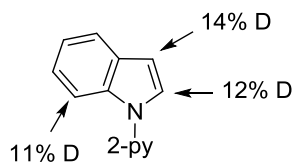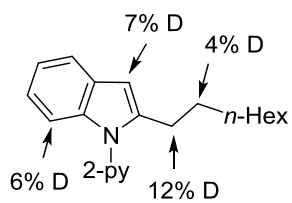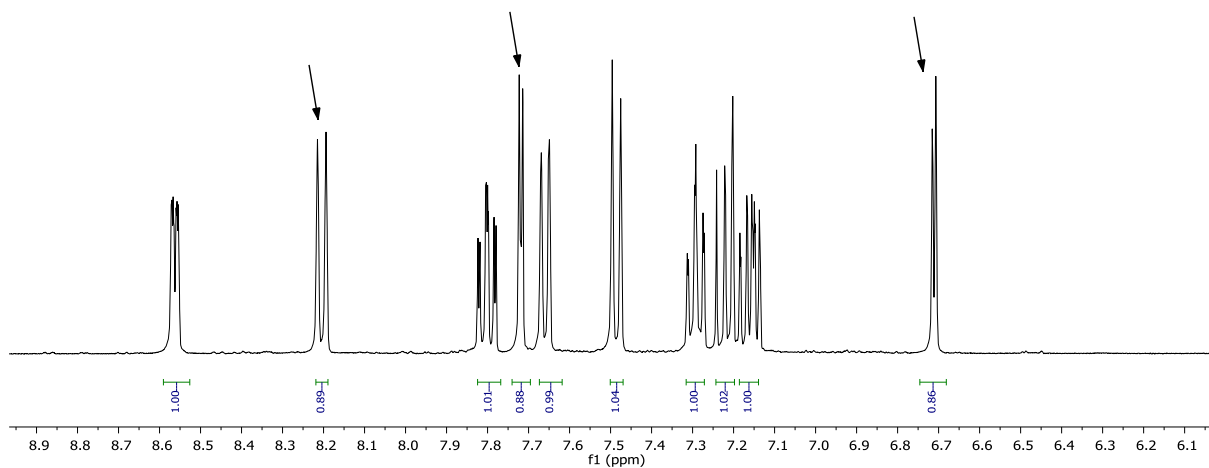
[D]$_n$-**144aa**
(CDCl$_3$, 500 MHz)

7% D
4% D
6% D   2-py
12% D
_n_-Hex
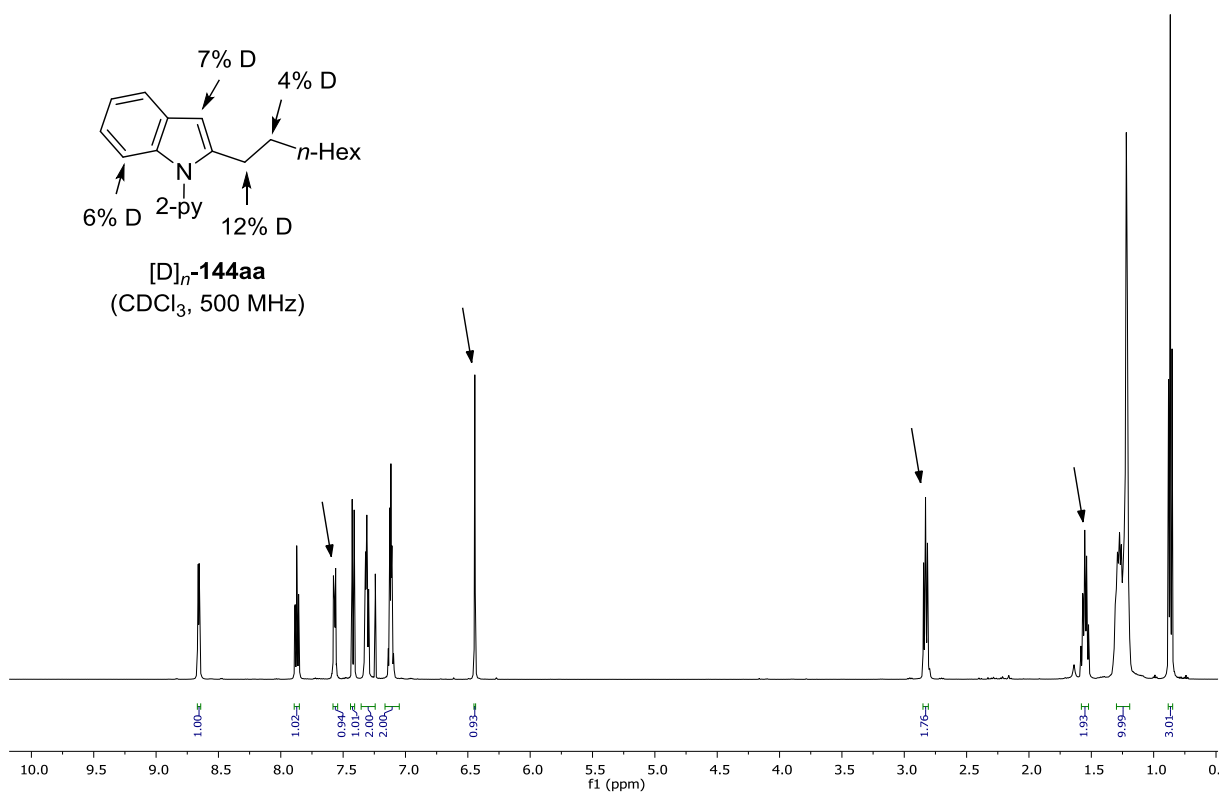
5.4.3.2.7 H/D-exchange with linear product 144ab
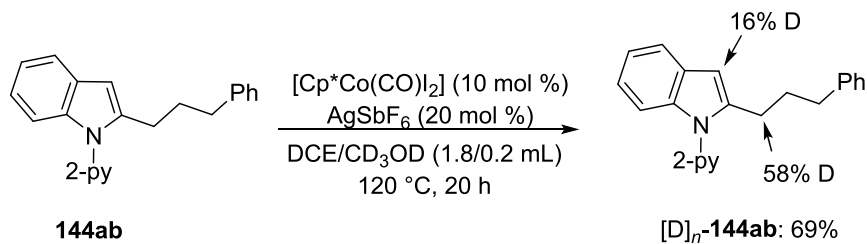
A suspension of **144ab** (156 mg, 0.50 mmol, 1.00 equiv), [Cp*Co(CO)I$_2$] (23.8 mg, 10.0 mol %), AgSbF$_6$ (34.4 mg, 20.0 mol %) in DCE (1.8 mL) and CD$_3$OD (0.2 mL) was stirred at 120 °C for 20 h. After removal of the solvents, the crude mixture was purified by column chromatography on silica gel (*n*-hexane/EtOAc: 20:1) to yield [D]$_n$-**144ab** (108 mg, 69% reisolated) as a colorless oil.
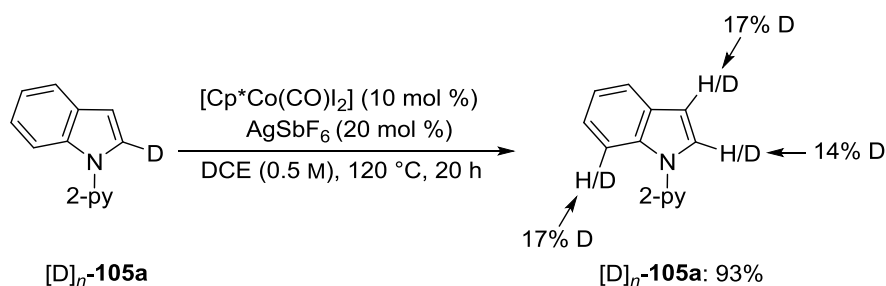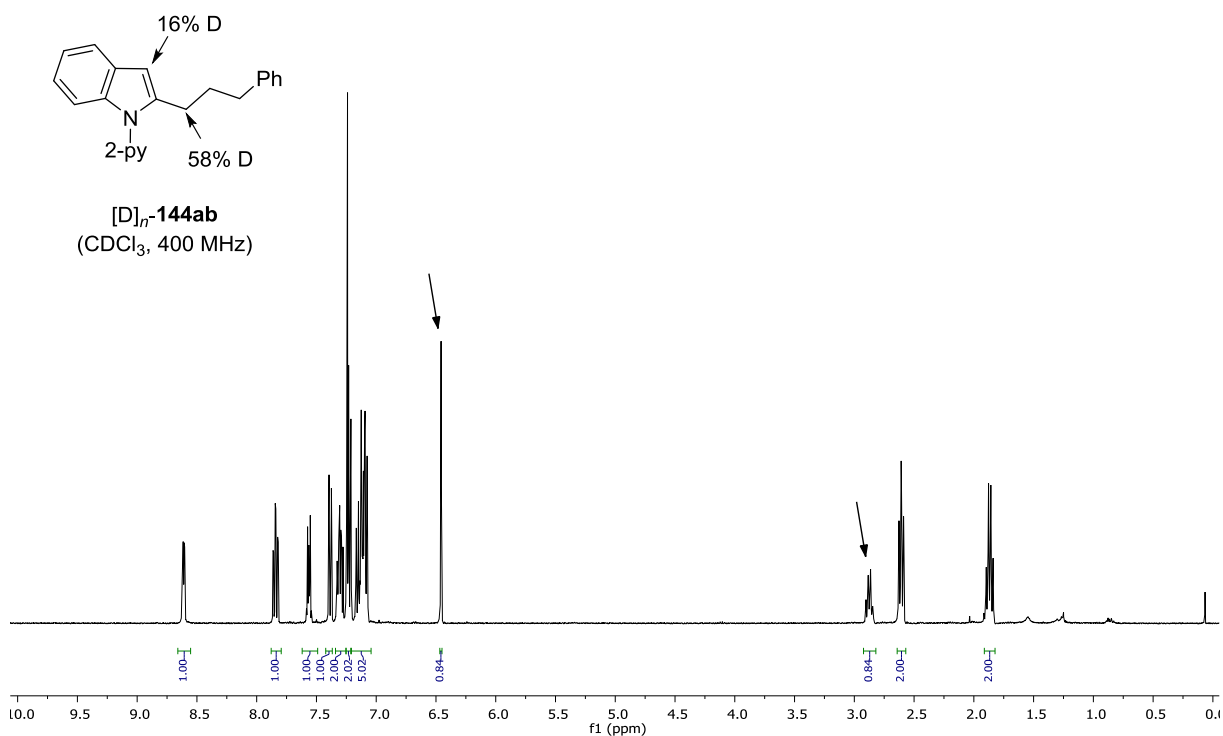
5.4.3.2.8 H/D-exchange with branched product 145ab
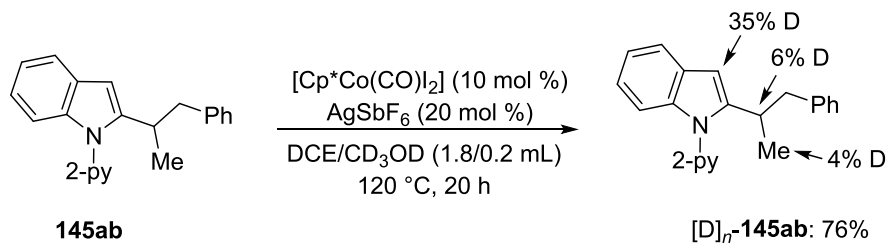
A suspension of **145ab** (156 mg, 0.50 mmol, 1.00 equiv), [Cp*Co(CO)I$_2$] (23.8 mg, 10.0 mol %), AgSbF$_6$ (34.4 mg, 20.0 mol %) in DCE (1.8 mL) and CD$_3$OD (0.2 mL) was stirred at 120 °C for 20 h. After removal of the solvents, the crude mixture was purified by column chromatography on silica gel (*n*-hexane/EtOAc: 20:1) to yield [D]$_n$-**145ab** (119 mg, 76% reisolated) as a colorless oil.

### 5.4.3.3 Intermolecular Competition Experiment

105b/105m
(each 1.0 equiv)

143a (1.0 equiv)
[Cp*Co(CO)I$_2$] (10 mol %)
AgSbF$_6$ (20 mol %)
1-AdCO$_2$H (1.0 equiv)
DCE (1.0 M), 50 °C, 20 h

145ba: 11%

+

145ma: 7%
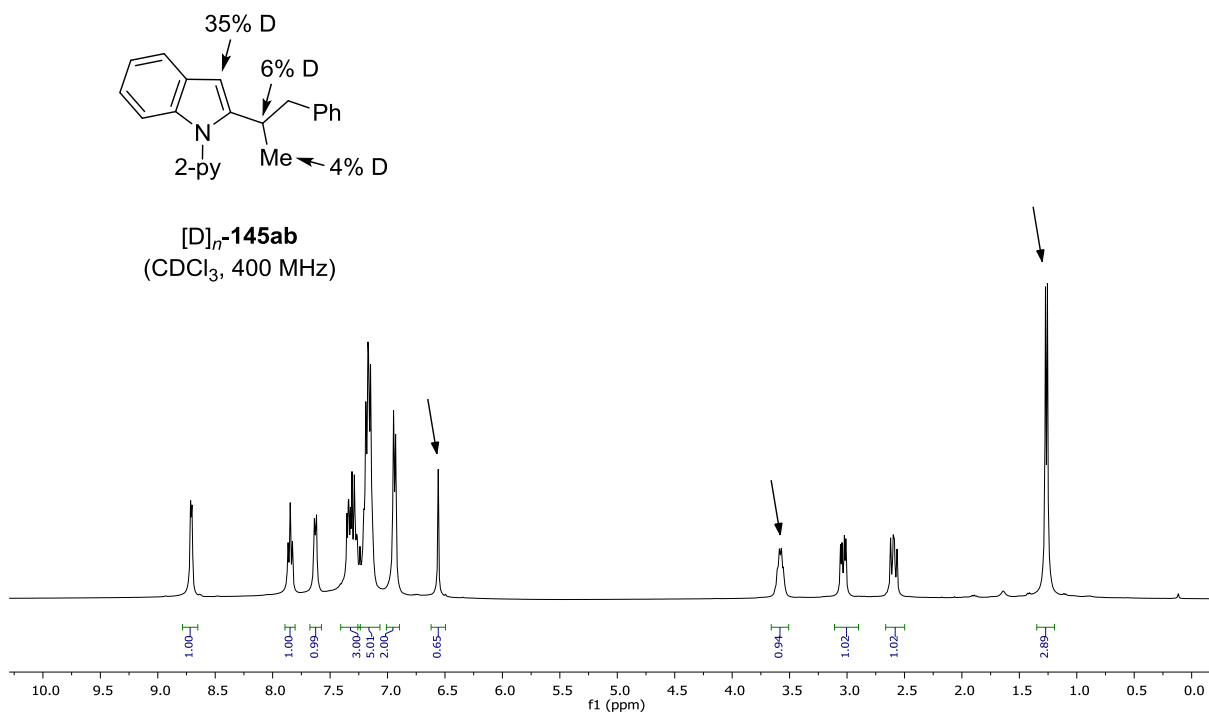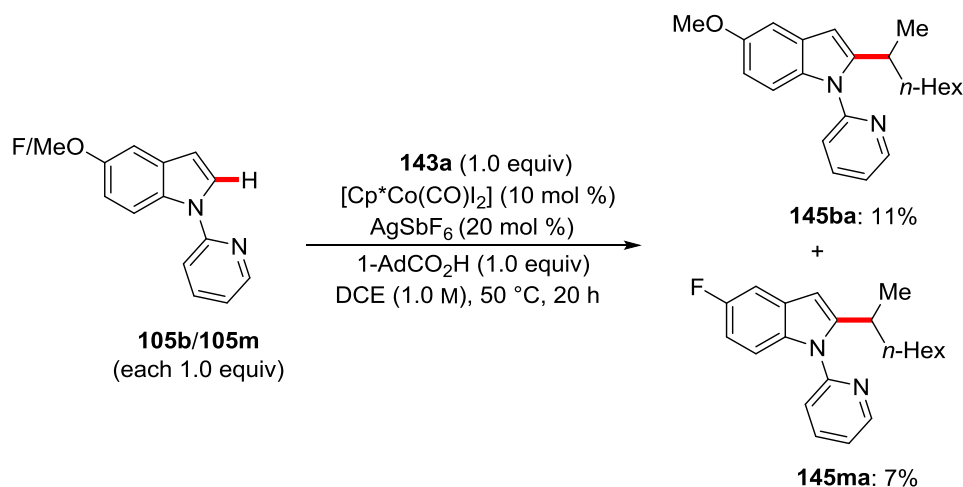
A suspension of 5-methoxy-1-(pyridin-2-yl)-1*H*-indole (**105b**) (112 mg, 0.50 mmol, 1.00 equiv), 5-fluoro-1-(pyridin-2-yl)-1*H*-indole (**105m**) (106 mg, 0.50 mmol, 1.00 equiv), *n*-octene (**143a**) (66.1 mg, 0.50 mmol, 1.00 equiv), [Cp*Co(CO)I$_2$] (23.8 mg, 10.0 mol %), AgSbF$_6$ (34.4 mg, 20.0 mol %) and 1-AdCO$_2$H (90.1 mg, 0.50 mmol, 1.00 equiv) in DCE (0.50 mL, 1.00 M) was stirred at 50 °C for 20 h. At ambient temperature, the solvent was removed *in vacuo* and the remaining residue was purified by column chromatography (*n*-hexane/EtOAc: 30/1) to afford the products **145ba** (18.5 mg, 11%) and **145ma** (11.3 mg, 7%).

5.4.3.4 Attempted Isomerization Experiments

144aa: AM:M > 99:1

[Cp*Co(CO)I$_2$] (10 mol %)
AgSbF$_6$ (20 mol %)
1-AdCO$_2$H (1.0 equiv)
DCE (1.0 M), 50 °C, 20 h

144aa: 95%, AM:M > 99:1
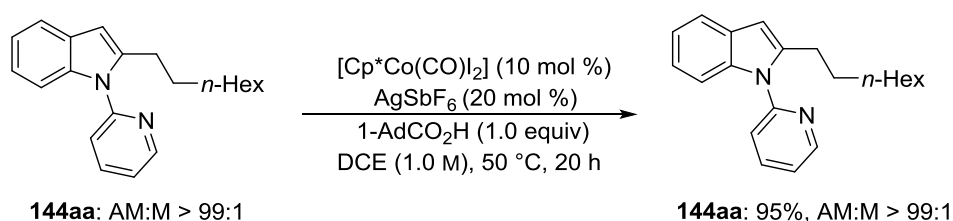
A suspension of **144aa** (153 mg, 0.50 mmol, 1.00 equiv, AM:M > 99:1), [Cp*Co(CO)I$_2$] (23.8 mg, 10.0 mol %), AgSbF$_6$ (34.4 mg, 20.0 mol %) and 1-AdCO$_2$H (90.1 mg, 0.50 mmol, 1.00 equiv) in DCE (0.5 mL, 1.0 M) was stirred at 50 °C for 20 h. At ambient temperature, the solvent was removed and the crude mixture was purified by flash column chromatography on silica gel (*n*-hexane/EtOAc: 10/1) to yield **144aa** (145 mg, 95%, AM:M > 99:1) as a yellow oil.

145aa: AM:M = 5:95   **145aa**: 94%, AM:M = 5:95
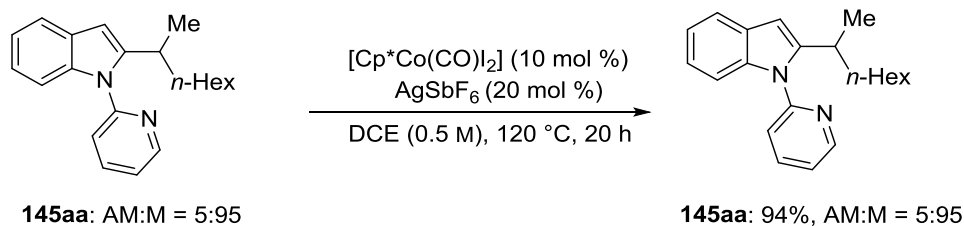
A suspension of **145aa** (153 mg, 0.50 mmol, 1.00 equiv, AM:M = 5:95), [Cp*Co(CO)I₂] (23.8 mg, 10.0 mol %) and AgSbF₆ (34.4 mg, 20.0 mol %) in DCE (1.0 mL, 0.5 M) was stirred at 120 °C for 20 h. At ambient temperature, the solvent was removed and the crude mixture was purified by flash column chromatography on silica gel (*n*-hexane/EtOAc: 10/1), yielding **145aa** (144 mg, 94%, AM:M = 5:95) as a yellow oil.

5.4.3.5   Kinetic Studies for the *anti*-*Markovnikov*-selective reaction

5.4.3.5.1   Determination of the reaction order with respect to the concentration of indole 105a

105a   **143a**   **144aa**
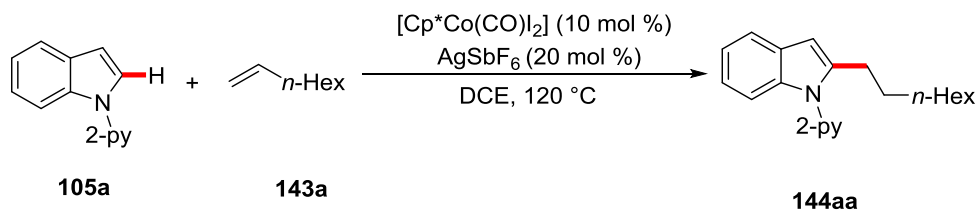
The reaction order was examined using the initial rate method. A suspension of **105a** (0.250, 0.400, 0.500, 0.600 and 0.750 mmol), **143a** (168 mg, 1.50 mmol), [Cp*Co(CO)I₂] (23.8 mg, 50.0 μmol) and AgSbF₆ (34.4 mg, 100 μmol) was stirred at 120 °C in DCE (2.0 mL). Aliquots up to ca. 10−20% conversion (25 μL; 5, 10, 15, 20, 25 min) were periodically removed by a syringe and directly analyzed by GC using *n*-dodecane (30 μL) as the internal standard.

Table 34. Reaction order in [**105a**] for the linear-selective reaction.

Entry	c / mol L^{-1}	k / mol L^{-1} s^{-1}	log (c / mol L^{-1})	log (k / mol L^{-1} s^{-1})
1	0.125	7.224E-6	-0.9031	-5.141
2	0.200	1.154E-5	-0.6990	-4.938
3	0.250	1.851E-5	-0.6021	-4.733
4	0.300	2.200E-5	-0.5229	-4.658
5	0.375	2.643E-5	-0.4260	-4.578

5.4.3.5.2 Determination of the reaction order with respect to the concentration of 1-octene (143a)

The reaction order was examined using the initial rate method. A suspension of **105a** (97.1 mg, 0.50 mmol), **143a** (0.25, 0.38, 0.50, 0.75, 1.00, 1.50, 2.00 mmol), [Cp*Co(CO)I$_2$] (23.8 mg, 50.0 µmol) and AgSbF$_6$ (34.4 mg, 100 µmol) was stirred at 120 °C in DCE (2.0 mL). Aliquots up to ca. 10−20% conversion (25 µL; 5, 10, 15, 20, 25 min) were periodically removed by a syringe and directly analyzed by GC using *n*-dodecane (30 µL) as the internal standard.

Table 35. Reaction order in [**143a**] for the linear-selective reaction.

Entry	c / mol L^{-1}	k / mol L^{-1} s^{-1}	log (c / mol L^{-1})	log (k / mol L^{-1} s^{-1})
1	0.125	1.107E-5	-0.9031	-4.956
2	0.188	1.206E-5	-0.7270	-4.919
3	0.250	1.414E-5	-0.6021	-4.850
4	0.375	1.491E-5	-0.4260	-4.826
5	0.500	1.721E-5	-0.3010	-4.764
6	0.750	1.849E-5	-0.1249	-4.733
7	1.000	2.056E-5	0	-4.687

5.4.3.5.3 Determination of the reaction order with respect to the concentration of [Cp*Co(CO)I$_2$]

The reaction order was examined using the initial rate method. A suspension of **105a** (97.1 mg, 0.50 mmol), **143a** (112 mg, 1.50 mmol), [Cp*Co(CO)I$_2$] (3.50, 5.00, 7.50, 10.0, 11.5 and 12.5 mol %), AgSbF$_6$ (34.4 mg, 20 mol %) was stirred at 120 °C in DCE (2.0 mL). Aliquots up to ca. 10−20% conversion (25 µL; 5, 10, 15, 20, 25 min) were periodically removed by a syringe and directly analyzed by GC using *n*-dodecane (30 µL) as internal standard.

Table 36. Reaction order in [Cp*Co(CO)I$_2$] for the linear-selective reaction.

Entry	n / mol %	k / mol L^{-1} s^{-1}	log (n / mol %)	log (k / mol L^{-1} s^{-1})
1	3.50	6.250E-6	0.544	-5.204
2	5.00	1.100E-5	0.699	-5.018
3	7.50	1.338E-5	0.875	-4.873
4	10.0	1.849E-5	1.000	-4.733
5	11.5	2.451E-5	1.061	-4.678

| 6 | 12.5 | 3.055E-5 | 1.097 | -4.580 |

5.4.3.6   Kinetic Studies for the *Markovnikov*-selective reaction

5.4.3.6.1   Determination of the reaction order with respect to the concentration of indole 105a
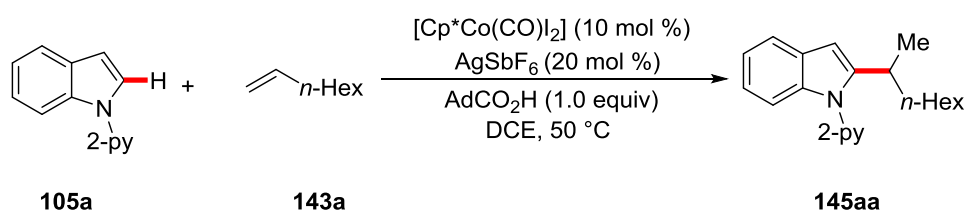
The reaction order was examined using initial rate method. A suspension of **105a** (0.150, 0.250, 0.400, 0.500 and 0.750 mmol), **143a** (168 mg, 1.50 mmol), [Cp*Co(CO)I$_2$] (23.8 mg, 50.0 µmol), AgSbF$_6$ (34.4 mg, 100 µmol) and 1-AdCO$_2$H (90.1 mg, 0.50 mmol) was stirred at 50 °C in DCE (2.0 mL). Aliquots up to ca. 10% conversion (25 µL; 15, 30, 40, 50, 60 min) were periodically removed by a syringe and directly analyzed by GC using *n*-dodecane (30 µL) as the internal standard.

Table 37. Reaction order in [**105a**] for the branched-selective reaction.

Entry	c / mol L^{-1}	k / mol L^{-1} s^{-1}	log (c / mol L^{-1})	log (k / mol L^{-1} s^{-1})
1	0.075	4.332E-6	-1.125	-5.338
2	0.125	4.797E-6	-0.903	-5.319
3	0.200	4.288E-6	-0.699	-5.368
4	0.250	5.473E-6	-0.602	-5.262
5	0.375	4.587E-6	-0.426	-5.363

5.4.3.6.2   Determination of the reaction order with respect to the concentration of 1-octene (143a)

The reaction order was examined using the initial rate method. A suspension of **105a** (97.1 mg, 0.50 mmol), **143a** (0.50, 0.75, 1.00, 1.25 and 1.50 mmol), [Cp*Co(CO)I$_2$] (23.8 mg, 50.0 µmol), AgSbF$_6$ (34.4 mg, 100 µmol) and 1-AdCO$_2$H (90.1 mg, 0.50 mmol) was stirred at 50 °C in DCE (2.0 mL). Aliquots up to ca. 10% conversion (25 µL; 15, 30, 40, 50, 60 min) were periodically removed by a syringe and directly analyzed by GC using *n*-dodecane (30 µL) as the internal standard.

Table 38. Reaction order in [**143a**] for the branched-selective reaction.

Entry	n / mol %	k / mol L^{-1} s^{-1}	log (n / mol %)	log (k / mol L^{-1} s^{-1})
1	0.250	1.547E-6	-0.6021	-5.810
2	0.375	2.261E-6	-0.4260	-5.646
3	0.500	2.834E-6	-0.3010	-5.547
4	0.625	3.689E-6	-0.2041	-5.433
5	0.750	5.473E-6	-0.1249	-5.262

5.4.3.6.3 Determination of the reaction order with respect to the concentration of [Cp*Co(CO)I$_2$]

The reaction order was examined using the initial rate method. A suspension of **105a** (97.1 mg, 0.50 mmol), **143a** (112 mg, 1.50 mmol), [Cp*Co(CO)I$_2$] (2.50, 3.50, 5.00, 7.50, 10.0 mol %), AgSbF$_6$ (34.4 mg, 100 μmol) and 1-AdCO$_2$H (90.1 mg, 0.50 mmol) was stirred at 50 °C in DCE (2.0 mL). Aliquots up to ca. 10% conversion (25 μL; 15, 30, 40, 50, 60 min) were periodically removed by a syringe and directly analyzed by GC using n-dodecane (30 μL) as the internal standard.

Table 39. Reaction order in [Cp*Co(CO)I$_2$] for the branched-selective reaction.

Entry	n / mol %	k / mol L^{-1} s^{-1}	log (n / mol %)	log (k / mol L^{-1} s^{-1})
1	2.50	1.375E-6	0.3979	-5.862
2	3.50	2.082E-6	0.5441	-5.681
3	5.00	2.980E-6	0.6989	-5.526
4	7.50	4.725E-6	0.8751	-5.326
5	10.0	5.504E-6	1.0000	-5.260

5.4.3.7 *Arrhenius* Plot Analysis

5.4.3.7.1 *Arrhenius* plot of *anti-Markovnikov*-selective reaction

A suspension of **105a** (97.1 mg, 0.50 mmol, 1.00 equiv), **143a** (112 mg, 1.50 mmol, 3.00 equiv), [Cp*Co(CO)I$_2$] (23.8 mg, 10.0 mol %) and AgSbF$_6$ (34.4 mg, 20 mol %) was stirred at different temperatures (105, 110, 115, 120, 125 and 130 °C) in DCE (2.0 mL). Aliquots up to ca. 10−25% conversion (25 μL; 15, 20, 25, 30, 35 min for 115−120 °C; 20, 25, 30, 35, 40 min for 105 °C and 110 °C) were periodically removed by a syringe and directly analyzed by GC using n-dodecane (30 μL) as internal standard.

Table 40. *Arrhenius* plot analysis for the linear-selective reaction.

Entry	Θ / °C	k / mol L^{-1} s^{-1}	$1 / T$ (K^{-1})	ln (k / mol L^{-1} s^{-1})
1	105	6.573E-6	0.002644	-11.93
2	110	9.438E-6	0.002610	-11.57
3	115	1.642E-5	0.002576	-11.02
4	120	1.849E-5	0.002544	-10.90
5	125	2.618E-5	0.002512	-10.55
6	130	4.398E-5	0.002480	-10.03

5.4.3.7.2 ***Arrhenius* plot of *Markovnikov*-selective reaction**

A suspension of **105a** (97.1 mg, 0.50 mmol, 1.00 equiv), **143a** (112 mg, 1.50 mmol, 3.00 equiv), [Cp*Co(CO)I$_2$] (23.8 mg, 10.0 mol %), AgSbF$_6$ (34.4 mg, 20 mol %) and 1-AdCO$_2$H (90.1 mg, 0.50 mmol) was stirred at different temperatures (40, 45, 50, 55 and 60 °C) in DCE (2.0 mL). Aliquots up to ca. 10% conversion (25 μL; 15, 30, 40, 50, 60 min) were periodically removed by a syringe and directly analyzed by GC using *n*-dodecane (30 μL) as the internal standard.

Table 41. *Arrhenius* plot analysis for the branched-selective reaction.

Entry	Θ / °C	k / mol L^{-1} s^{-1}	$1 / T$ (K^{-1})	ln (k / mol L^{-1} s^{-1})
1	40	2.078E-6	0.003193	-13.08
2	45	3.156E-6	0.003143	-12.67
3	50	5.473E-6	0.003095	-12.12
4	55	5.953E-6	0.003047	-12.03
5	60	8.525E-6	0.003002	-11.67

5.5 Cobalt(III)-Catalyzed C−H/C–F Functionalization

5.5.1 Characterization Data
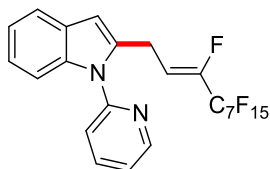
(Z)-2-(1H,1H,2H-Perfluorodec-2-en-1-yl)-1-(pyridin-2-yl)-1H-indole **(158aa)**: The general procedure **F** was followed using 1-(pyridin-2-yl)-1H-indole (**105a**) (97.1 mg, 0.50 mmol) and 1H,1H,2H-perfluorodec-1-ene (**127a**) (268 mg, 0.60 mmol). Isolation by column chromatography (*n*-hexane/EtOAc: 20/1) yielded **158aa** (301 mg, 97%, Z/E = 86:14) as a yellow oil.

^{1}H-NMR (300 MHz, CDCl$_3$): δ = 8.64 (ddd, J = 4.9, 1.9, 0.9 Hz, 1H), 7.88 (ddd, J = 7.9, 7.6, 1.9 Hz, 1H), 7.61 (ddd, J = 7.6, 4.9, 1.0 Hz, 1H), 7.41 (ddd, J = 7.9, 1.0, 0.9 Hz, 1H), 7.41–7.35 (m, 1H), 7.31 (ddd, J = 7.3, 4.9, 0.9 Hz, 1H), 7.25−7.12 (m, 2H), 6.50 (d, J = 0.9 Hz, 1H), 6.16 (dt, J = 22.3, 8.1 Hz, 0.14H, *E*), 5.82 (dt, J = 33.0, 7.5 Hz, 0.86H, *Z*), 3.90 (ddt, J = 7.5, 2.4, 1.8 Hz, 1.72H, *Z*), 3.84 (ddt, J = 8.1, 2.5, 1.8 Hz, 0.28H, *E*).

^{13}C-NMR (125 MHz, CDCl$_3$): δ = 150.8 (C$_q$), 149.6 (CH), 146.1 (dt, $^1J_{C–F}$ = 261 Hz, $^2J_{C–F}$ = 29.1 Hz, C$_q$), 138.3 (CH), 137.1 (C$_q$), 136.1 (C$_q$), 128.3 (C$_q$), 122.4 (CH), 122.1 (CH), 121.0 (CH), 120.5 (CH), 120.0 (CH), 117.0 (dt, $^1J_{C–F}$ = 288 Hz, $^2J_{C–F}$ = 31.3 Hz, C$_q$), 113.3 (dt, $^2J_{C–F}$ = 8.1 Hz, $^3J_{C–F}$ = 4.2 Hz, CH), 112.4 (m, C$_q$), 110.9 (m, C$_q$), 110.7 (m, C$_q$), 110.5 (m, C$_q$), 108.6 (m, C$_q$), 108.3 (m, C$_q$), 110.1 (CH), 106.7 (CH), 22.7 (d, $^3J_{C–F}$ = 4.3 Hz, CH$_2$).

^{19}F-NMR (282 MHz, CDCl$_3$): δ = –80.9 (m), –115.0 (m, *E*), –117.5 (m, *Z*), –122.0 (m), –122.1 (m), –122.8 (m), –123.0 (m), –126.3 (m), –130.8 (m).

IR (ATR): 3061, 1589, 1472, 1455, 1439, 1197, 1107, 736 cm^{-1}.

MS (ESI) m/z (relative intensity): 643 ([M + Na]$^+$, 20), 621 ([M + H]$^+$, 100).

HR-MS (ESI): m/z calcd. for [C$_{23}$H$_{13}$F$_{16}$N$_2$]$^+$ [M + H]$^+$ 621.0818, found 621.0809.
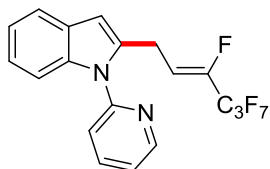
Z)-2-(1H,1H,2H-Perfluorohex-2-en-1-yl)-1-(pyridin-2-yl)-1H-indole **(158ab):** The general procedure **F** was followed using 1-(pyridin-2-yl)-1H-indole (**105a**) (97.1 mg, 0.50 mmol) and 1H,1H,2H-perfluorohex-1-ene (**127b**) (148 mg, 0.60 mmol). Isolation by column chromatography (*n*-hexane/EtOAc: 20/1) yielded **158ab** (197 mg, 94%, Z/E = 86:14) as a yellow oil.

¹H-NMR (300 MHz, CDCl₃): δ = 8.64 (ddd, J = 4.9, 1.9, 0.9 Hz, 1H), 7.88 (ddd, J = 7.9, 7.6, 1.9 Hz, 1H), 7.61 (ddd, J = 7.6, 4.9, 1.0 Hz, 1H), 7.45 (ddd, J = 7.9, 1.0, 0.9 Hz, 1H), 7.43–7.35 (m, 1H), 7.31 (ddd, J = 7.1, 4.7, 0.9 Hz, 1H), 7.25−7.14 (m, 2H), 6.50 (d, J = 0.9 Hz, 1H), 6.16 (dt, J = 22.0, 7.9 Hz, 0.14H, E), 5.82 (dt, J = 33.0, 7.4 Hz, 0.86H, Z), 3.90 (ddt, J = 7.4, 2.4, 1.8 Hz, 1.72H, Z), 3.84 (ddt, J = 7.9, 2.5, 1.8 Hz, 0.28H, E).

¹³C-NMR (125 MHz, CDCl₃): δ = 150.8 (C$_q$), 149.6 (CH), 145.8 (dt, $^1J_{C-F}$ = 261 Hz, $^2J_{C-F}$ = 29.1 Hz, C$_q$), 138.3 (CH), 137.0 (C$_q$), 136.0 (C$_q$), 128.2 (C$_q$), 122.4 (CH), 122.1 (CH), 121.0 (CH), 120.5 (CH), 120.3 (CH), 117.5 (dt, $^1J_{C-F}$ = 288 Hz, $^2J_{C-F}$ = 31.3 Hz, C$_q$), 113.3 (td, $^2J_{C-F}$ = 8.1 Hz, $^3J_{C-F}$ = 4.2 Hz, CH), 110.1 (CH), 109.9 (m, C$_q$), 108.3 (m, C$_q$), 103.6 (CH), 22.7 (d, $^3J_{C-F}$ = 4.3 Hz, CH₂).

¹⁹F-NMR (282 MHz, CDCl₃): δ = –80.8 (m), –115.9 (m, E), –118.4 (m, Z), –127.3 (m, Z), –127.9 (m, E), –131.0 (m).

IR (ATR): 3059, 1587, 1119, 782, 737 cm⁻¹.

MS (ESI) m/z (relative intensity): 421 ([M + H]⁺, 100), 197 (20).

HR-MS (ESI): m/z calcd. for [C₁₉H₁₃F₈N₂]⁺ [M + H]⁺ 421.0946, found 421.0949.
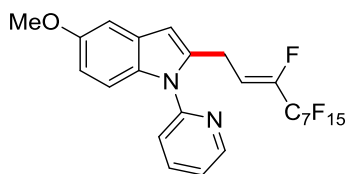
(Z)-2-(1H,1H,2H-Perfluorodec-2-en-1-yl)-5-methoxy-1-(pyridin-2-yl)-1H-indole (**158ba**): The general procedure **F** was followed using 5-methoxy-1-(pyridin-2-yl)-1H-indole (**105b**) (112 mg, 0.50 mmol) and 1H,1H,2H-perfluorodec-1-ene (**127a**) (268 mg, 0.60 mmol). Isolation by column chromatography (n-hexane/EtOAc: 20/1) yielded **158ba** (293 mg, 90%, Z/E = 86:14) as a colorless solid.

M.p.: 98 °C

¹H-NMR (500 MHz, CDCl₃): δ = 8.61 (ddd, J = 4.9, 1.9, 0.9 Hz, 1H), 7.87 (ddd, J = 7.9, 7.6, 1.9 Hz, 1H), 7.41 (ddd, J = 7.9, 1.0, 0.9 Hz, 1H), 7.31−7.23 (m, 2H), 7.05 (d, J = 2.5 Hz, 1H), 6.81 (dd, J = 9.0, 2.5 Hz, 1H), 6.41 (d, J = 0.9 Hz, 1H), 6.13 (dt, J = 22.5, 8.0 Hz, 0.14H, E), 5.76 (dt, J = 33.0, 7.5 Hz, 0.86H, Z), 3.90 (ddt, J = 7.5, 2.4, 1.8 Hz, 1.72H, Z), 3.84 (ddt, J = 8.0, 2.5, 1.8 Hz, 0.28H, E), 3.84 (s, 3H).

¹³C-NMR (125 MHz, CDCl₃): δ = 154.9 (C$_q$), 150.9 (C$_q$), 149.6 (CH), 145.8 (dt, $^1J_{C-F}$ = 261 Hz, $^2J_{C-F}$ = 29.1 Hz, C$_q$), 138.1 (CH), 136.5 (C$_q$), 132.1 (C$_q$), 128.8 (C$_q$), 121.9 (CH), 120.1 (CH), 116.8 (dt, $^1J_{C-F}$ = 287 Hz, $^2J_{C-F}$ = 31.0 Hz, C$_q$), 113.3 (dt, $^2J_{C-F}$ = 8.4 Hz, $^3J_{C-F}$ = 4.5 Hz, CH), 112.5 (m, C$_q$), 112.1 (CH), 111.0 (CH), 110.5 (m, C$_q$), 110.2 (m, C$_q$), 110.0 (m, C$_q$), 108.6 (m, C$_q$), 108.2 (m, C$_q$), 103.5 (CH), 102.3 (CH), 55.8 (CH₃), 22.8 (d, $^3J_{C-F}$ = 4.3 Hz, CH₂).

¹⁹F-NMR (376 MHz, CDCl$_3$): δ = –80.9 (m), –117.5 (m), –122.0 (m), –122.8 (m), –122.9 (m), –123.4 (m), –126.2 (m), –130.9 (m).

IR (ATR): 1474, 1450, 1438, 1237, 1201, 1146, 907, 729, 649 cm^{-1}.

MS (ESI) m/z (relative intensity): 673 ([M + Na]$^+$, 20), 651 ([M + H]$^+$, 100), 381 (15).

HR-**MS** (ESI): m/z calcd. for [C$_{24}$H$_{15}$F$_{16}$N$_2$O]$^+$ [M + H]$^+$ 651.0923, found 651.0917.
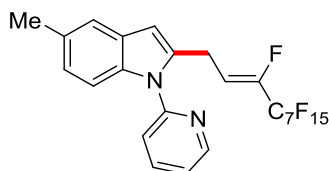
(Z)-**2**-**(1H,1H,2H**-**Perfluorodec**-**2**-**en**-**1**-**yl)**-**5**-**methyl**-**1**-**(pyridin**-**2**-**yl)**-**1H**-**indole**   **(158fa)**:   The general procedure **F** was followed using 5-methyl-1-(pyridin-2-yl)-1H-indole (**105f**) (104 mg, 0.50 mmol) and 1H,1H,2H-perfluorodec-1-ene (**127a**) (268 mg, 0.60 mmol). Isolation by column chromatography (n-hexane/EtOAc: 20/1) yielded **158fa** (244 mg, 77%, Z/E = 86:14) as a colorless oil.

¹H-NMR (400 MHz, CDCl$_3$): δ = 8.62 (ddd, J = 4.9, 1.9, 0.9 Hz, 1H), 7.84 (ddd, J = 8.0, 7.6, 1.9 Hz, 1H), 7.46 (ddd, J = 8.0, 1.0, 0.9 Hz, 1H), 7.38 (dd, J = 1.7, 0.9 Hz, 1H), 7.31–7.29 (m, 2H), 7.00 (dd, J = 8.4, 1.7 Hz, 1H), 6.41 (d, J = 0.9 Hz, 1H), 6.15 (dt, J = 22.4, 8.0 Hz, 0.14H, E), 5.80 (dt, J = 32.8, 7.6 Hz, 0.86H, Z), 3.89 (ddt, J = 7.6, 2.5, 1.7 Hz, 1.72H, Z), 3.83 (ddt, J = 8.0, 2.4, 1.7 Hz, 0.28H, E), 2.45 (s, 3H).

¹³C-NMR (100 MHz, CDCl$_3$): δ = 151.0 (C$_q$), 149.6 (CH), 146.1 (dt, $^1J_{\text{C–F}}$ = 261 Hz, $^2J_{\text{C–F}}$ = 28.3 Hz, C$_q$), 138.3 (CH), 136.2 (C$_q$), 135.5 (C$_q$), 130.4 (C$_q$), 128.6 (C$_q$), 123.9 (CH), 121.9 (CH), 120.3 (CH), 120.2 (CH), 117.4 (dt, $^1J_{\text{C–F}}$ = 289 Hz, $^2J_{\text{C–F}}$ = 33.9 Hz, C$_q$), 113.4 (dt, $^2J_{\text{C–F}}$ = 8.1 Hz, $^3J_{\text{C–F}}$ = 4.2 Hz, CH), 112.9 (m, C$_q$), 110.9 (m, C$_q$), 110.6 (m, C$_q$), 110.2 (m, C$_q$), 109.8 (CH), 108.3 (m, C$_q$), 107.8 (m, C$_q$), 103.4 (CH), 22.8 (d, $^3J_{\text{C–F}}$ = 4.2 Hz, CH$_2$), 21.3 (CH$_3$).

¹⁹F-NMR (282 MHz, CDCl$_3$): δ = –80.8 (m), –114.9 (m, E), –117.5 (m, Z), –122.0 (m), –122.1 (m), –122.8 (m), –122.9 (m), –126.2 (m), –131.1 (m).

IR (ATR): 2921, 1599, 1473, 1439, 1237, 1201, 1146, 908, 731 cm^{-1}.

MS (ESI) m/z (relative intensity): 635 ([M + H]$^+$, 100).

HR-**MS** (ESI): m/z calcd. for [C$_{24}$H$_{15}$F$_{16}$N$_2$]$^+$ [M + H]$^+$ 635.0974, found 635.0984.
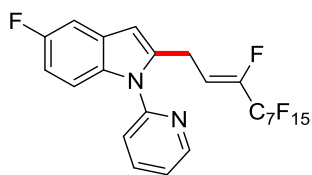
(**Z**)-**2**-(**1***H*,**1***H*,**2***H*-**Perfluorodec-2-en-1-yl**)-**5-fluoro-1-(pyridin-2-yl)-1***H*-**indole** (**158ma**): The general procedure **F** was followed using 5-fluoro-1-(pyridin-2-yl)-1*H*-indole (**105m**) (106 mg, 0.50 mmol) and 1*H*,1*H*,2*H*-perfluorodec-1-ene (**127a**) (268 mg, 0.60 mmol). Isolation by column chromatography (*n*-hexane/EtOAc: 20/1) yielded **158ma** (271 mg, 85%, *Z/E* = 86:14) as a yellow oil.

^{1}H-NMR (400 MHz, CDCl$_3$): δ = 8.62 (ddd, *J* = 4.9, 1.9, 0.9 Hz, 1H), 7.84 (ddd, *J* = 8.0, 7.5, 1.9 Hz, 1H), 7.43 (ddd, *J* = 8.0, 1.0, 0.9 Hz, 1H), 7.33 (ddd, *J* = 7.5, 1.9, 1.0 Hz, 1H), 7.29 (dd, *J* = 9.1, 4.3 Hz, 1H), 7.26 (dd, *J* = 9.3, 2.5 Hz, 1H), 6.89 (dt, *J* = 9.1, 2.5 Hz, 1H), 6.43 (d, *J* = 0.9 Hz, 1H), 6.10 (dt, *J* = 22.4, 8.2 Hz, 0.14H, *E*), 5.77 (dt, *J* = 32.5, 7.0 Hz, 0.86H, *Z*), 3.79 (ddt, *J* = 7.0, 2.4, 1.5 Hz, 1.72H, *Z*), 3.85 (ddt, *J* = 8.2, 2.5, 1.7 Hz, 0.28H, *E*).

**^{13}C-NMR** (125 MHz, CDCl$_3$): δ = 158.5 (d, $^1J_{C-F}$ = 236 Hz, C$_q$), 150.7 (C$_q$), 149.8 (CH), 146.2 (dt, $^1J_{C-F}$ = 261 Hz, $^2J_{C-F}$ = 29.0 Hz, C$_q$), 138.6 (CH), 137.7 (C$_q$), 133.7 (C$_q$), 128.8 (d, $^3J_{C-F}$ = 10.3 Hz, C$_q$), 122.4 (CH), 120.4 (CH), 117.2 (dt, $^1J_{C-F}$ = 285 Hz, $^2J_{C-F}$ = 33.3 Hz, C$_q$), 113.7 (m, C$_q$), 113.0 (dt, $^2J_{C-F}$ = 8.5 Hz, $^3J_{C-F}$ = 4.4 Hz, CH), 112.4 (m, C$_q$), 110.9 (d, $^2J_{C-F}$ = 9.5 Hz, CH), 110.5 (d, $^2J_{C-F}$ = 26.0 Hz, CH), 110.4 (m, C$_q$), 110.0 (m, C$_q$), 108.6 (m, C$_q$), 108.2 (m, C$_q$), 105.4 (d, $^2J_{C-F}$ = 23.7 Hz, CH), 103.5 (d, $^3J_{C-F}$ = 4.3 Hz, CH), 22.7 (d, $^3J_{C-F}$ = 4.3 Hz, CH$_2$).

^{19}F-NMR (470 MHz, CDCl$_3$): δ = –81.0 (m), –117.6 (m), –122.1 (m), –122.9 (m), –123.0 (m) –123.4 (m), –123.5 (m), –126.3 (m), –130.5 (m).

IR (ATR): 1473, 1450, 1439, 1235, 1143, 776, 663 cm^{-1}.

MS (ESI) *m/z* (relative intensity): 661 ([M + Na]$^+$, 15), 639 ([M + H]$^+$, 100).

HR-**MS** (ESI): *m/z* calcd. for [C$_{23}$H$_{12}$F$_{17}$N$_2$]$^+$ [M + H]$^+$ 639.0724, found 639.0731.
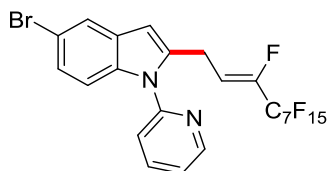
(**Z**)-**2**-(**1***H*,**1***H*,**2***H*-**Perfluorodec-2-en-1-yl**)-**5-bromo-1-(pyridin-2-yl)-1***H*-**indole** (**158ca**): The general procedure **F** was followed using 5-bromo-1-(pyridin-2-yl)-1*H*-indole (**105c**) (136 mg, 0.50 mmol) and 1*H*,1*H*,2*H*-perfluorodec-1-ene (**127a**) (268 mg, 0.60 mmol). Isolation by column chromatography (*n*-hexane/EtOAc: 10/1) yielded **158ca** (324 mg, 93%, *Z/E* = 84:16) as an off-white solid.

M.p.: 59 °C

1H-NMR (400 MHz, CDCl$_3$): δ = 8.63 (ddd, J = 4.9, 1.9, 0.8 Hz, 1H), 7.90 (ddd, J = 7.9, 7.6, 1.9 Hz, 1H), 7.70 (dd, J = 1.4, 0.4 Hz, 1H), 7.41 (ddd, J = 7.9, 1.0, 0.8 Hz, 1H), 7.34 (ddd, J = 7.6, 4.9, 1.0 Hz, 1H), 7.25−7.15 (m, 2H), 6.41 (d, J = 0.9 Hz, 1H), 6.11 (dt, J = 22.5, 8.3 Hz, 0.16H, *E*), 5.75 (dt, J = 32.7, 7.3 Hz, 0.84H, *Z*), 3.85 (ddt, J = 7.3, 2.4, 1.8 Hz, 1.68H, *Z*), 3.79 (ddt, J = 8.3, 2.5, 1.8 Hz, 0.32H, *E*).

13C-NMR (125 MHz, CDCl$_3$): δ = 150.1 (C$_q$), 149.9 (CH), 146.1 (dt, $^1J_{C-F}$ = 261 Hz, $^2J_{C-F}$ = 29.5 Hz, C$_q$), 138.6 (CH), 137.4 (C$_q$), 135.8 (C$_q$), 129.9 (C$_q$), 125.1 (CH), 122.6 (CH), 122.0 (CH), 120.5 (CH), 117.2 (dt, $^1J_{C-F}$ = 288 Hz, $^2J_{C-F}$ = 31.3 Hz, C$_q$), 114.2 (C$_q$), 112.9 (dt, $^2J_{C-F}$ = 8.1 Hz, $^3J_{C-F}$ = 4.3 Hz, CH), 112.3 (m, C$_q$), 111.6 (CH), 110.6 (m, C$_q$), 110.4 (m, C$_q$), 110.1 (m, C$_q$), 108.5 (m, C$_q$), 108.3 (m, C$_q$), 102.9 (CH), 22.6 (d, $^3J_{C-F}$ = 4.3 Hz, CH$_2$).

19F-NMR (376 MHz, CDCl$_3$): δ = −80.9 (m), −114.9 (m, *E*), −117.5 (m, *Z*), −122.0 (m), −122.0 (m), −122.7 (m), −122.9 (m), −126.2 (m), −130.4 (m).

IR (ATR): 1588, 1472, 1443, 1236, 1200, 1146, 907, 731 cm^{-1}.

MS (ESI) m/z (relative intensity): 699 ([M(^{79}Br) + H]$^+$, 100), 275 (80).

HR-MS (ESI): m/z calcd. for [C$_{23}$H$_{12}$^{79}BrF$_{16}$N$_2$]$^+$ [M + H]$^+$ 698.9923, found 698.9922.
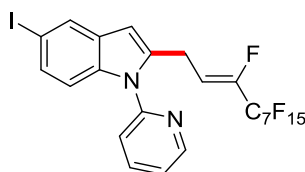
(*Z*)-2-(1*H*,1*H*,2*H*-Perfluorodec-2-en-1-yl)-5-iodo-1-(pyridin-2-yl)-1*H*-indole (158da): The general procedure **F** was followed using 5-iodo-1-(pyridin-2-yl)-1*H*-indole (**105d**) (160 mg, 0.50 mmol) and 1*H*,1*H*,2*H*-perfluorodec-1-ene (**127a**) (268 mg, 0.60 mmol). Isolation by column chromatography (*n*-hexane/EtOAc: 10/1) yielded **158da** (346 mg, 93%, *Z*/*E* = 82:18) as a yellow oil.

1H-NMR (300 MHz, CDCl$_3$): δ = 8.62 (ddd, J = 4.9, 1.9, 0.9 Hz, 1H), 7.98−7.82 (m, 2H), 7.45−7.38 (m, 2H), 7.33 (ddd, J = 7.5, 4.9, 0.9 Hz, 1H), 7.10 (dd, J = 8.7, 0.6 Hz, 1H), 6.40 (d, J = 0.9 Hz, 0.18H, *E*), 6.39 (d, J = 0.9 Hz, 0.82H, *Z*), 6.09 (dt, J = 22.5, 8.0 Hz, 0.18H, *E*), 5.76 (dt, J = 33.0, 7.5 Hz, 0.82H, *Z*), 3.90 (ddt, J = 7.5, 2.4, 1.8 Hz, 1.63H, *Z*), 3.84 (ddt, J = 8.0, 2.5, 1.8 Hz, 0.37H, *E*).

13C-NMR (125 MHz, CDCl$_3$): δ = 150.3 (C$_q$), 149.8 (CH), 146.1 (dt, $^1J_{C-F}$ = 261 Hz, $^2J_{C-F}$ = 29.1 Hz, C$_q$), 138.5 (CH), 137.0 (C$_q$), 136.3 (CH), 130.6 (C$_q$), 130.4 (C$_q$), 129.8 (CH), 122.5 (CH), 117.2 (dt, $^1J_{C-F}$ = 288 Hz, $^2J_{C-F}$ = 31.3 Hz, C$_q$), 112.1 (CH), 112.9 (dt, $^2J_{C-F}$ = 8.1 Hz, $^3J_{C-F}$ = 4.2 Hz, CH), 112.4 (m, C$_q$), 112.1 (CH), 110.7 (m, C$_q$), 110.3 (m, C$_q$), 110.2 (m, C$_q$), 108.5 (m, C$_q$), 108.2 (m, C$_q$), 102.7 (CH), 84.5 (C$_q$), 22.6 (d, $^3J_{C-F}$ = 4.3 Hz, CH$_2$).

19F-NMR (282 MHz, CDCl$_3$): δ = −80.9 (m), −117.6 (m), −122.1 (m), −121.9 (m), −122.9 (m), −123.5 (m), −126.2 (m), −130.4 (m).

IR (ATR): 3044, 1587, 1472, 1443, 1240, 1209, 1150, 904, 725 cm^{-1}.

MS (ESI) m/z (relative intensity): 769 ([M + Na]$^+$, 20), 747 ([M + H]$^+$, 100).

HR-**MS** (ESI): m/z calcd. for [C$_{23}$H$_{12}$F$_{16}$IN$_2$]$^+$ [M + H]$^+$ 746.9784, found 746.9786.
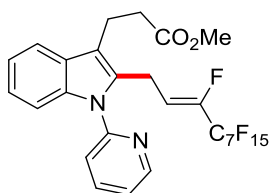
(*Z*)-**Methyl**-**2**-**[(1*H*,1*H*,2*H*-Perfluorodec-2-en-1-yl)-1-(pyridin-2-yl)-1*H*-indole-3-yl]propanoate**
(158pa): A modified general procedure **F** was followed using methyl 2-(1-(pyridin-2-yl)-1*H*-indol-3-yl)propanoate (**105p**) (140 mg, 0.50 mmol) and 1*H*,1*H*,2*H*-perfluoro-1-decene (**127a**) (268 mg, 0.60 mmol) at 70 °C. Isolation by column chromatography (*n*-hexane/EtOAc = 10:1) yielded **158pa** (237 mg, 67%, *Z/E* = 80:20) as a white solid.

M.p.: 70 °C.

^{1}H-**NMR** (400 MHz, CDCl$_3$): δ = 8.60 (ddd, J = 4.9, 1.9, 0.8 Hz, 1H), 7.87 (ddd, J = 8.1, 7.5, 1.9 Hz, 1H), 7.60–7.55 (m, 1H), 7.44 (ddd, J = 8.1, 1.0, 0.8 Hz, 1H), 7.34–7.27 (m, 2H), 7.20–7.12 (m, 2H), 5.89 (dt, J = 23.2, 8.3 Hz, 0.20H, *E*), 5.61 (dt, J = 33.3, 7.0 Hz, 0.80H, *Z*), 3.94–3.90 (m, 2H), 3.65 (s, 3H), 3.12 (t, J = 7.8 Hz, 2H), 2.69 (t, J = 7.8 Hz, 2H).

^{13}C-**NMR** (100 MHz, CDCl$_3$): δ = 173.4 (C$_q$), 150.9 (C$_q$), 149.7 (CH), 144.7 (dt, $^1J_{C-F}$ = 260 Hz, $^2J_{C-F}$ = 29.1 Hz, C$_q$), 138.5 (CH), 136.6 (C$_q$), 132.2 (d, $^4J_{C-F}$ = 2.0 Hz, C$_q$), 127.9 (C$_q$), 122.8 (CH), 122.1 (CH), 120.8 (CH), 120.7 (CH), 118.6 (CH), 116.9 (dt, $^1J_{C-F}$ = 282 Hz, $^2J_{C-F}$ = 33.0 Hz, C$_q$), 114.4 (C$_q$), 114.0 (dt, $^2J_{C-F}$ = 8.1 Hz, $^3J_{C-F}$ = 4.3 Hz, CH), 113.2 (m, C$_q$), 110.8 (m, C$_q$), 110.7 (m, C$_q$), 110.5 (m, C$_q$), 110.1 (CH), 108.1 (C$_q$), 107.4 (m, C$_q$), 51.6 (CH$_3$), 34.7 (CH$_2$), 20.2 (d, $^3J_{C-F}$ = 4.2 Hz, CH$_2$), 19.6 (CH$_2$).

^{19}F-**NMR** (376 MHz, CDCl$_3$): δ = −80.8 (m), −115.4 (m, *E*), −117.3 (m, *Z*), −122.0 (m), −122.1 (m), −122.7 (m), −122.9 (m), −126.2 (m), −131.1 (m).

IR (ATR): 2955, 1737, 1586, 1472, 1439, 1200, 1144, 732 cm^{-1}.

MS (ESI) m/z (relative intensity): 707 ([M + H]$^+$, 100), 687 (10).

HR-**MS** (ESI): m/z calcd. for [C$_{27}$H$_{19}$F$_{16}$N$_2$O$_2$]$^+$ [M + H]$^+$ 707.1186, found 707.1188.
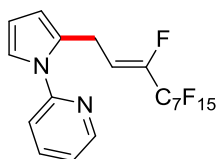
(*Z*)-**2**-**[2**-(1*H*,1*H*,2*H*-Perfluorodec-2-en-1-yl)-1*H*-pyrrol-1-yl]pyridine (160)**: The general procedure **G** was followed using 2-(1*H*-pyrrol-1-yl)pyridine (**146**) (72.1 mg, 0.50 mmol) and 1*H*,1*H*,2*H*-

perfluorodec-1-ene (**127a**) (268 mg, 0.60 mmol). Isolation by column chromatography (*n*-hexane/EtOAc: 10/1) yielded **160** (174 mg, 61%, *Z/E* = 84:16) and **160'** (40 mg, 8%, *Z/E* = 84:16) as yellow oils.

^{1}H-NMR (400 MHz, CDCl$_3$): δ = 8.47 (ddd, *J* = 4.9, 1.9, 0.9 Hz, 1H), 7.77 (ddd, *J* = 8.2, 7.5, 1.9 Hz, 1H), 7.28 (ddd, *J* = 8.2, 1.0, 0.9 Hz, 1H), 7.18 (ddd, *J* = 7.5, 4.9, 1.0 Hz, 1H), 7.01 (dd, *J* = 3.1, 1.8 Hz, 1H), 6.24 (dd, *J* = 3.1, 3.0 Hz, 1H), 6.16 (dt, *J* = 22.7, 8.2 Hz, 0.16H, *E*), 6.12–6.09 (m, 1H) 5.81 (dt, *J* = 33.4, 7.5 Hz, 0.84H, *Z*), 3.88 (ddt, *J* = 7.5, 3.9, 2.0 Hz, 1.68H, *Z*), 3.83 (ddt, *J* = 7.5, 4.0, 2.0 Hz, 0.32H, *E*).

^{13}C-NMR (100 MHz, CDCl$_3$): δ = 152.5 (C$_q$), 148.6 (CH), 145.4 (dt, $^{1}J_{C-F}$ = 260 Hz, $^{2}J_{C-F}$ = 30.1 Hz, C$_q$), 138.5 (CH), 129.1 (C$_q$), 121.2 (CH), 121.0 (CH), 116.9 (dt, $^{1}J_{C-F}$ = 285 Hz, $^{2}J_{C-F}$ = 33.3 Hz, C$_q$), 116.6 (CH), 114.6 (dt, $^{2}J_{C-F}$ = 8.3 Hz, $^{3}J_{C-F}$ = 4.3 Hz, CH), 112.2 (m, C$_q$), 111.3 (m, C$_q$), 111.2 (m, C$_q$), 110.9 (m, C$_q$), 110.7 (CH), 109.7 (CH), 108.6 (m, C$_q$), 107.8 (C$_q$), 22.9 (d, $^{3}J_{C-F}$ = 4.2 Hz, CH$_2$).

^{19}F-NMR (376 MHz, CDCl$_3$): δ = –80.8 (m), –117.5 (m), –122.0 (m), –122.8 (m), –123.0 (m), –123.5 (m), –126.2 (m), –132.3 (m).

IR (ATR): 1523, 1504, 1325, 1182, 992, 754 cm^{-1}.

MS (ESI) *m/z* (relative intensity): 593 ([M + Na]$^+$, 20), 571 ([M + H]$^+$, 100).

HR-MS (ESI): *m/z* calcd. for [C$_{19}$H$_{11}$F$_{16}$N$_2$]$^+$ [M + H]$^+$ 571.0661, found 571.0668.
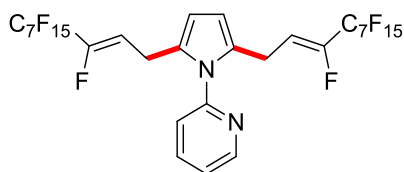
(*Z*)-2-[2,5-Di-(1*H*,1*H*,2*H*-Perfluorodec-2-en-1-yl)-1*H*-pyrrol-1-yl]pyridine (160'):

^{1}H-NMR (400 MHz, CDCl$_3$): δ = 8.59 (ddd, *J* = 4.9, 1.9, 0.9 Hz, 1H), 7.84 (ddd, *J* = 8.0, 7.8, 1.9 Hz, 1H), 7.34 (ddd, *J* = 7.8, 4.9, 1.2 Hz, 1H), 7.20 (ddd, *J* = 8.0, 1.2, 0.9 Hz, 1H), 6.00 (s, 2H), 5.91 (dt, *J* = 22.5, 8.3 Hz, 0.32H, *E*), 5.61 (dt, *J* = 33.0, 7.6 Hz, 1.68H, *Z*), 3.47 (ddt, *J* = 7.6, 2.4, 1.8 Hz, 3.36H, *Z*), 3.40 (ddt, *J* = 8.3, 2.5, 1.8 Hz, 0.64H, *E*).

^{13}C-NMR (100 MHz, CDCl$_3$): δ = 150.7 (C$_q$), 149.8 (CH), 145.7 (dt, $^{1}J_{C-F}$ = 259 Hz, $^{2}J_{C-F}$ = 30.1 Hz, C$_q$), 138.4 (CH), 129.1 (C$_q$), 123.1 (CH), 121.9 (CH), 117.4 (dt, $^{1}J_{C-F}$ = 288 Hz, $^{2}J_{C-F}$ = 33.3 Hz, C$_q$), 112.6 (dt, $^{2}J_{C-F}$ = 8.3 Hz, $^{3}J_{C-F}$ = 4.3 Hz, CH), 111.2 (m, C$_q$), 110.8 (m, C$_q$), 110.2 (m, C$_q$), 109.7 (m, C$_q$), 108.8 (m, C$_q$), 108.2 (m, C$_q$), 107.8 (CH), 21.3 (d, $^{3}J_{C-F}$ = 4.1 Hz, CH$_2$).

^{19}F-NMR (376 MHz, CDCl$_3$): δ = –81.2 (m), –117.7 (m), –121.9 (m), –122.2 (m), –123.1 (m), – 123.1 (m), –126.4 (m), –131.8 (m).

IR (ATR): 2960, 2924, 1473, 1235, 1143, 1047, 735, 559 cm^{-1}.

MS (ESI) *m/z* (relative intensity): 997 ([M + H]$^+$, 100), 573 (20), 545 (15).

HR-MS (ESI): *m/z* calcd. for [C$_{29}$H$_{13}$F$_{32}$N$_2$]$^+$ [M + H]$^+$ 997.0562, found: 997.0553.
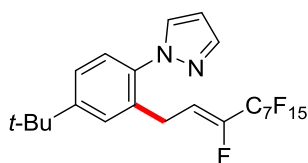
(Z)-1-[4-(*tert*-Butyl)-2-(1*H*,1*H*,2*H*-perfluorodec-2-en-1-yl)phenyl]-1*H*-pyrazole **(161c):** A modified general procedure **F** was followed using 1-[4-(*tert*-butyl)phenyl]-1*H*-pyrazole (**18c**) (100 mg, 0.50 mmol), 1*H*,1*H*,2*H*-perfluorodec-1-ene (**127a**) (268 mg, 0.60 mmol), [Cp*Co(CO)I$_2$] (23.7 mg, 10 mol %) and AgSbF$_6$ (34.4 mg, 20 mol %) at 70 °C. Isolation by column chromatography (*n*-hexane/EtOAc: 20/1) yielded **161c** (248 mg, 79%, Z/E = 87:13) as a yellow oil.

^{1}H-NMR (300 MHz, CDCl$_3$): δ = 7.70 (dd, J = 2.2, 1.7 Hz, 1H), 7.56 (d, J = 4.0, 2.4 Hz, 1H), 7.36 (dd, J = 8.2, 2.2 Hz, 1H), 7.30 (dd, J = 2.4, 2.1 Hz, 1H), 7.23 (dd, J = 8.2, 1.7 Hz, 1H), 6.42 (dd, J = 4.0, 2.1 Hz, 1H), 5.90 (dt, J = 21.8, 7.9 Hz, 0.13H, *E*), 5.67 (dt, J = 33.3, 7.6 Hz, 0.87H, *Z*), 3.79 (ddt, J = 7.6, 4.1, 2.5 Hz, 2H), 1.33 (s, 9H).

^{13}C-NMR (100 MHz, CDCl$_3$): δ = 152.2 (C$_q$), 145.7 (dt, $^1J_{C–F}$ = 259 Hz, $^2J_{C–F}$ = 29.1 Hz, C$_q$), 140.5 (CH), 137.1 (C$_q$), 132.9 (C$_q$), 130.3 (CH), 127.3 (CH), 125.8 (CH), 124.7 (CH), 117.0 (dt, $^1J_{C–F}$ = 289 Hz, $^2J_{C–F}$ = 31.3 Hz, C$_q$), 114.7 (dt, $^2J_{C–F}$ = 8.9 Hz, $^3J_{C–F}$ = 3.6 Hz, CH), 113.0 (m, C$_q$), 112.0 (m, C$_q$), 110.6 (m, C$_q$), 110.0 (m, C$_q$), 108.6 (m, C$_q$), 108.1 (m, C$_q$), 106.5 (CH), 34.7 (CH), 31.2 (CH$_3$), 26.3 (d, $^3J_{C–F}$ = 3.7 Hz, CH$_2$).

^{19}F-NMR (282 MHz, CDCl$_3$): δ = –80.9 (m), –114.5 (m, *E*), –117.5 (m), –122.1 (m), –122.1 (m), –122.9 (m, *Z*), –123.1 (m, *E*), –123.5 (m), –126.2 (m), –132.3 (m).

IR (ATR): 2968, 1522, 1238, 1201, 1146, 909, 732 cm^{-1}.

MS (EI) *m/z* (relative intensity): 626 ([M]$^+$, 100), 611 (20), 598 (10).

HR-MS (ESI): *m/z* calcd. for [C$_{23}$H$_{19}$F$_{16}$N$_2$]$^+$ [M + H]$^+$ 627.1287, found 627.1289.
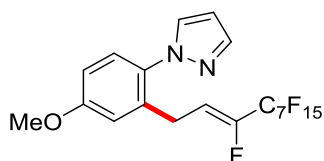
(Z)-1-[4-(Methoxy)-2-(1*H*,1*H*,2*H*-perfluorodec-2-en-1-yl)phenyl]-1*H*-pyrazole (161d): A modified general procedure **F** was followed using 1-[4-(methoxy)phenyl]-1*H*-pyrazole (**18d**) (100 mg, 0.50 mmol), 1*H*,1*H*,2*H*-perfluorodec-1-ene (**127a**) (268 mg, 0.60 mmol), [Cp*Co(CO)I$_2$] (23.7 mg, 10 mol %) and AgSbF$_6$ (34.4 mg, 20 mol %) at 70 °C. Isolation by column chromatography (*n*-hexane/EtOAc: 10/1) yielded **161d** (159 mg, 53%, Z/E = 82:18) as a colorless oil.

^{1}H-NMR (400 MHz, CDCl$_3$): δ = 7.69 (dd, J = 1.9, 0.7 Hz, 1H), 7.59 (d, J = 2.3, 0.7 Hz, 1H), 7.24–7.21 (m, 1H), 6.84 (dd, J = 8.6, 2.9 Hz, 1H), 6.79 (d, J = 2.9 Hz, 1H), 6.41 (dd, J = 2.3, 1.9 Hz, 1H), 5.88

(dt, J = 21.8, 7.9 Hz, 0.18H, E), 5.62 (dt, J = 33.3, 7.6 Hz, 0.82H, Z), 3.82 (s, 3H), 3.45 (ddt, J = 7.6, 4.1, 2.5 Hz, 2H).

^{13}C-NMR (100 MHz, CDCl$_3$): δ = 160.0 (C$_q$), 146.0 (dt, $^1J_{C-F}$ = 259 Hz, $^2J_{C-F}$ = 29.1 Hz, C$_q$), 140.6 (CH), 135.3 (C$_q$), 132.9 (C$_q$), 130.7 (CH), 127.8 (CH), 117.4 (dt, $^1J_{C-F}$ = 289 Hz, $^2J_{C-F}$ = 31.3 Hz, C$_q$), 115.4 (CH), 114.2 (dt, $^2J_{C-F}$ = 8.9 Hz, $^3J_{C-F}$ = 3.6 Hz, CH), 113.5 (m, C$_q$), 112.6 (CH), 110.9 (m, C$_q$), 110.8 (m, C$_q$), 110.6 (m, C$_q$), 108.6 (m, C$_q$), 107.7 (m, C$_q$), 106.5 (CH), 55.5 (CH$_3$), 26.0 (d, $^3J_{C-F}$ = 3.7 Hz, CH$_2$).

^{19}F-NMR (376 MHz, CDCl$_3$): δ = −80.8 (m), −114.5 (m, E), −117.4 (m), −122.0 (m), −122.0 (m), −122.7 (m), −122.9 (m), −126.2 (m), −131.5 (m).

IR (ATR): 2963, 1521, 1235, 1199, 1144, 1044, 735 cm^{-1}.

MS (ESI) m/z (relative intensity): 623 ([M + Na]$^+$, 10), 601 ([M + H]$^+$, 100).

HR-MS (ESI): m/z calcd. for [C$_{20}$H$_{13}$F$_{16}$N$_2$O]$^+$ [M + H]$^+$ 601.0767, found 601.0768.
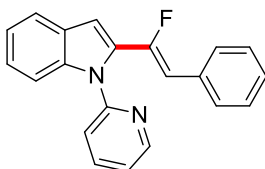
(Z)-2-(1-Fluoro-2-phenylvinyl)-1-(pyridin-2-yl)-1H-indole (159aa): The general procedure **G** was followed using 1-(pyridin-2-yl)-1H-indole (**105a**) (97.1 mg, 0.50 mmol) and 1-(2,2-difluorovinyl)-benzene (**128a**) (105 mg, 0.75 mmol). Isolation by column chromatography (n-hexane/EtOAc: 10/1) yielded **159aa** (152 mg, 97%, Z/E = 99:1) as a colorless solid.

M.p.: 68 °C.

^{1}H-NMR (300 MHz, CDCl$_3$): δ = 8.70 (ddd, J = 4.9, 2.0, 0.9 Hz, 1H), 7.86 (ddd, J = 8.1, 7.5, 2.0 Hz, 1H), 7.72 (ddd, J = 8.1, 1.0, 0.9 Hz, 1H), 7.56–7.52 (m, 4H), 7.35–7.16 (m, 6H), 7.03 (d, J = 0.9 Hz, 1H), 6.48 (d, J = 18.9 Hz, 0.03H, E), 6.04 (d, J = 38.0 Hz, 0.97H, Z).

^{13}C-NMR (125 MHz, CDCl$_3$): δ = 151.8 (C$_q$), 151.1 (d, $^1J_{C-F}$ = 257 Hz, C$_q$), 149.3 (CH), 138.4 (C$_q$), 138.2 (CH), 133.3 (d, $^4J_{C-F}$ = 3.8 Hz, C$_q$), 132.3 (d, $^2J_{C-F}$ = 30.1 Hz, C$_q$), 128.9 (d, $^4J_{C-F}$ = 7.8 Hz, CH), 128.6 (CH), 127.7 (C$_q$), 127.6 (CH), 124.4 (CH), 122.4 (CH), 121.7 (CH), 121.3 (CH), 120.7 (CH), 111.4 (CH), 110.1 (d, $^2J_{C-F}$ = 9.4 Hz, CH), 107.6 (d, $^3J_{C-F}$ = 4.5 Hz, CH).

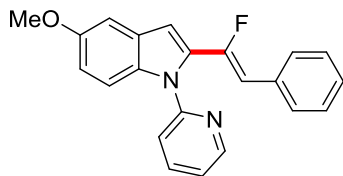**^{19}F-NMR** (376 MHz, CDCl$_3$): δ = −91.9 (d, J = 18.9 Hz), −105.9 (d, J = 38.0 Hz).

IR (ATR): 3054, 3024, 1586, 1467, 1436, 1382, 1349, 1147, 783, 739 cm^{-1}.

MS (ESI) m/z (relative intensity): 337 ([M + Na]$^+$, 100), 315 ([M + H]$^+$, 20).

HR-MS (ESI): m/z calcd. for [C$_{21}$H$_{16}$FN$_2$]$^+$ [M + H]$^+$ 315.1292, found 315.1300.

(Z)-2-(1-Fluoro-2-phenylvinyl)-5-methoxy-1-(pyridin-2-yl)-1*H*-indole **(159ba)**: The general procedure **G** was followed using 5-methoxy-1-(pyridin-2-yl)-1*H*-indole (**105b**) (112 mg, 0.50 mmol) and 1-(2,2-difluorovinyl)-benzene (**128a**) (105 mg, 0.75 mmol). Isolation by column chromatography (*n*-hexane/EtOAc: 10/1) yielded **159ba** (150 mg, 87%, *Z/E* > 99:1) as a colorless oil.

^{1}H-NMR (300 MHz, CDCl$_3$): δ = 8.64 (ddd, *J* = 4.9, 2.0, 0.8 Hz, 1H), 7.82 (ddd, *J* = 8.0, 7.6, 2.0 Hz, 1H), 7.51–7.46 (m, 3H), 7.58 (ddd, *J* = 8.0, 1.0, 0.9 Hz, 1H), 7.35–7.27 (m, 3H), 7.26–7.19 (m, 1H), 7.09 (d, *J* = 2.5 Hz, 1H), 6.94 (d, *J* = 0.9 Hz, 1H), 6.92 (dd, *J* = 9.0, 2.5 Hz, 1H), 6.02 (d, *J* = 37.9 Hz, 1H, *Z*), 3.86 (s, 3H).

^{13}C-NMR (125 MHz, CDCl$_3$): δ = 155.2 (C$_q$), 151.6 (C$_q$), 150.8 (d, $^1J_{C–F}$ = 258 Hz, C$_q$), 149.2 (CH), 138.2 (CH), 133.7 (C$_q$), 133.2 (d, $^4J_{C–F}$ = 3.9 Hz, C$_q$), 132.3 (d, $^2J_{C–F}$ = 30.1 Hz, C$_q$), 128.7 (d, $^4J_{C–F}$ = 7.6 Hz, CH), 128.4 (CH), 128.2 (C$_q$), 127.4 (CH), 122.0 (CH), 120.3 (CH), 114.5 (CH), 112.2 (CH), 109.8 (d, $^2J_{C–F}$ = 9.7 Hz, CH), 107.2 (d, $^3J_{C–F}$ = 3.9 Hz, CH), 102.3 (CH), 55.7 (CH$_3$).

^{19}F-NMR (282 MHz, CDCl$_3$): δ = –106.0 (d, *J* = 37.9 Hz).

IR (ATR): 3056, 2949, 1586, 1467, 1435, 1216, 1201, 1031, 839 cm^{-1}.

MS (ESI) *m/z* (relative intensity): 345 ([M + H]$^+$, 100), 325 (20).

HR-MS (ESI): *m/z* calcd. for [C$_{22}$H$_{18}$FN$_2$O]$^+$ [M + H]$^+$ 345.1398, found 345.1405.
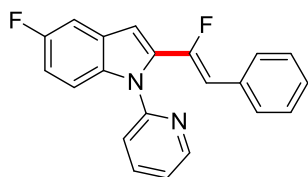
(Z)-2-(1-Fluoro-2-phenylvinyl)-5-fluoro-1-(pyridin-2-yl)-1*H*-indole **(159ma)**: The general procedure **G** was followed using 5-fluoro-1-(pyridin-2-yl)-1*H*-indole (**105m**) (106 mg, 0.50 mmol) and 1-(2,2-difluorovinyl)-benzene (**128a**) (105 mg, 0.75 mmol). Isolation by column chromatography (*n*-hexane/EtOAc: 10/1) yielded **159ma** (153 mg, 92%, *Z/E* > 99:1) as a colorless oil.

^{1}H-NMR (300 MHz, CDCl$_3$): δ = 8.66 (ddd, *J* = 4.9, 2.0, 0.8 Hz, 1H), 7.85 (ddd, *J* = 8.0, 7.6, 2.0 Hz, 1H), 7.52–7.45 (m, 3H), 7.41 (ddd, *J* = 8.0, 1.0, 0.8 Hz, 1H), 7.36–7.30 (m, 3H), 7.29–7.21 (m, 2H), 7.01 (ddd, *J* = 9.0, 2.5, 0.7 Hz, 1H), 6.96 (dd, *J* = 0.9, 0.9 Hz, 1H), 6.04 (d, *J* = 37.8 Hz, 1H, *Z*).

^{13}C-NMR (125 MHz, CDCl$_3$): δ = 158.6 (d, $^1J_{C–F}$ = 238 Hz, C$_q$), 151.4 (C$_q$), 150.4 (d, $^1J_{C–F}$ = 256 Hz, C$_q$), 149.3 (CH), 138.4 (CH), 135.0 (C$_q$), 133.5 (d, $^2J_{C–F}$ = 30.3 Hz, C$_q$), 133.0 (d, $^4J_{C–F}$ = 4.0 Hz, C$_q$), 128.8 (d, $^4J_{C–F}$ = 8.2 Hz, CH), 128.5 (CH), 128.1 (d, $^3J_{C–F}$ = 10.2 Hz, C$_q$), 127.6 (CH), 122.4 (CH),
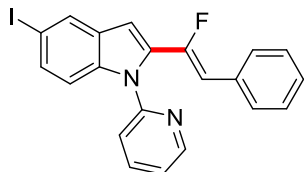
120.4 (CH), 112.6 (d, $^2J_{C-F}$ = 26.0 Hz, CH), 112.2 (d, $^3J_{C-F}$ = 9.9 Hz, CH), 110.4 (d, $^2J_{C-F}$ = 8.8 Hz, CH), 107.0 (d, $^3J_{C-F}$ = 4.6 Hz, CH), 105.9 (d, $^2J_{C-F}$ = 23.9 Hz, CH).

^{19}F-NMR (282 MHz, CDCl$_3$): δ = –106.4 (d, J = 37.8 Hz), –122.2 (m).

IR (ATR): 3057, 1585, 1465, 1436, 1382, 1185, 782, 744, 662 cm^{-1}.

MS (EI) m/z (relative intensity): 332 ([M]$^+$, 100), 311 (80), 255 (35).

HR-MS (EI): m/z calcd. for [C$_{21}$H$_{14}$F$_2$N$_2$]$^+$ [M]$^+$ 332.1125, found 332.1125.

(Z)-2-(1-Fluoro-2-phenylvinyl)-5-iodo-1-(pyridin-2-yl)-1H-indole (159da): A modified procedure **G** was followed using 5-iodo-1-(pyridin-2-yl)-1H-indole (**105d**) (160 mg, 0.50 mmol) and 1-(2,2-difluorovinyl)-benzene (**128a**) (105 mg, 0.75 mmol) at 50 °C. Isolation by column chromatography (n-hexane/EtOAc: 10/1) yielded **159da** (183 mg, 83%, Z/E = 98:2) as a yellow oil.

^{1}H-NMR (300 MHz, CDCl$_3$): δ = 8.64 (ddd, J = 4.9, 2.0, 0.8 Hz, 1H), 7.98 (dd, J = 1.7, 0.5 Hz, 1H), 7.84 (ddd, J = 8.0, 7.6, 2.0 Hz, 1H), 7.50 (ddd, J = 4.9, 1.0, 0.8 Hz, 1H), 7.47–7.40 (m, 2H), 7.38 (ddd, J = 8.0, 1.7, 0.8 Hz, 1H), 7.36–7.30 (m, 3H), 7.30–7.21 (m, 2H), 6.90 (d, J = 0.9 Hz, 1H), 6.47 (d, J = 18.7 Hz, 0.02H, E), 6.03 (d, J = 37.9 Hz, 0.98H, Z).

^{13}C-NMR (125 MHz, CDCl$_3$): δ = 151.1 (C$_q$), 150.1 (d, $^1J_{C-F}$ = 258 Hz, C$_q$), 149.4 (CH), 138.4 (CH), 137.6 (C$_q$), 132.9 (d, $^4J_{C-F}$ = 4.6 Hz, C$_q$), 132.8 (d, $^2J_{C-F}$ = 30.3 Hz, C$_q$), 132.4 (CH), 130.0 (C$_q$), 129.8 (CH), 128.8 (d, $^4J_{C-F}$ = 7.7 Hz, CH), 128.4 (CH), 127.6 (CH), 122.5 (CH), 120.4 (CH), 113.2 (CH), 110.6 (d, $^2J_{C-F}$ = 8.8 Hz, CH), 106.1 (d, $^3J_{C-F}$ = 4.3 Hz, CH), 84.4 (C$_q$).

^{19}F-NMR (282 MHz, CDCl$_3$): δ = –93.1 (d, J = 18.7 Hz, E), –106.7 (d, J = 37.9 Hz, Z).

IR (ATR): 3056, 1587, 1470, 1469, 1379, 1239, 1207, 732, 693 cm^{-1}.

MS (ESI) m/z (relative intensity): 441 ([M + H]$^+$, 100), 436 (15).

HR-MS (ESI): m/z calcd. for [C$_{21}$H$_{15}$FN$_2$I]$^+$ [M + H]$^+$ 441.0258, found 441.0251.
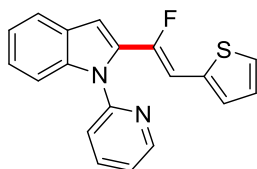
(Z)-2-[1-Fluoro-2-(thiophen-2-yl)vinyl]-1-(pyridin-2-yl)-1H-indole (159ab): The general procedure **G** was followed using 1-(pyridin-2-yl)-1H-indole (**105a**) (97.1 mg, 0.50 mmol) and 2-(2,2-

difluorovinyl)thiophene (**128b**) (110 mg, 0.75 mmol). Isolation by column chromatography (*n*-hexane/EtOAc: 10/1) yielded **159ab** (154 mg, 96%, *Z/E* = 96:4) as a yellow oil.

¹H-NMR (300 MHz, CDCl₃): δ = 8.64 (ddd, *J* = 4.9, 2.0, 0.8 Hz, 1H), 7.84 (ddd, *J* = 8.0, 7.6, 2.0 Hz, 1H), 7.67 (ddd, *J* = 7.7, 1.2, 0.9 Hz, 1H), 7.56–7.51 (m, 1H), 7.42 (ddd, *J* = 8.0, 1.0, 0.8 Hz, 1H), 7.37–7.35 (m, 1H), 7.32 (ddd, *J* = 7.6, 4.9, 1.0 Hz, 1H), 7.29–7.23 (m, 3H), 7.20 (dd, *J* = 7.1, 1.2 Hz, 1H), 6.99 (d, *J* = 0.9 Hz, 1H), 6.51 (d, *J* = 17.9 Hz, 0.04H, *E*), 6.11 (d, *J* = 37.7 Hz, 0.96H, *Z*).

**¹³C-NMR** (75 MHz, CDCl₃): δ = 151.8 (C$_q$), 150.2 (d, $^1J_{C-F}$ = 260 Hz, C$_q$), 149.4 (CH), 138.6 (C$_q$), 138.3 (CH), 133.9 (d, $^4J_{C-F}$ = 3.3 Hz, C$_q$), 131.8 (d, $^2J_{C-F}$ = 29.7 Hz, C$_q$), 128.2 (d, $^4J_{C-F}$ = 5.8 Hz, CH), 127.8 (C$_q$), 125.3 (CH), 124.1 (CH), 124.0 (CH), 122.3 (CH), 121.6 (CH), 121.2 (CH), 120.6 (CH), 111.2 (CH), 107.1 (d, $^3J_{C-F}$ = 4.4 Hz, CH), 104.7 (d, $^2J_{C-F}$ = 13.5 Hz, CH).

¹⁹F-NMR (282 MHz, CDCl₃): δ = –93.5 (d, *J* = 17.9 Hz, *E*), –106.0 (d, *J* = 37.7 Hz, *Z*).

IR (ATR): 3053, 1585, 1467, 1435, 1347, 1294, 1072, 773, 728 cm⁻¹.

MS (EI) *m/z* (relative intensity): 320 ([M]⁺, 100), 299 (90), 241 (15).

HR-MS (EI): *m/z* calcd. for [C₁₉H₁₃FN₂S]⁺ [M]⁺ 320.0783, found 320.0788.
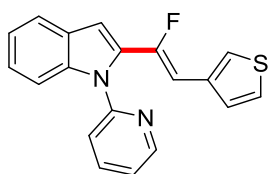
(Z)-2-[1-Fluoro-2-(thiophen-3-yl)vinyl]-1-(pyridin-2-yl)-1*H*-indole (159ac): The general procedure **G** was followed using 1-(pyridin-2-yl)-1*H*-indole (**105a**) (97.1 mg, 0.50 mmol) and 3-(2,2-difluorovinyl)thiophene (**128c**) (110 mg, 0.75 mmol). Isolation by column chromatography (*n*-hexane/EtOAc: 10/1) yielded **159ac** (159 mg, 99%, *Z/E* = 90:10) as a yellow oil.

¹H-NMR (400 MHz, CDCl₃): δ = 8.64 (ddd, *J* = 4.9, 2.0, 0.8 Hz, 1H), 7.87 (ddd, *J* = 8.0, 7.6, 2.0 Hz, 1H), 7.65 (ddd, *J* = 7.9, 1.3, 0.9 Hz, 1H), 7.56–7.54 (m, 1H), 7.41 (ddd, *J* = 8.0, 1.0, 0.8 Hz, 1H), 7.34 (ddd, *J* = 7.6, 4.9, 1.0 Hz, 1H), 7.27 (dd, *J* = 5.1, 1.0 Hz, 1H), 7.22–7.16 (m, 2H), 7.03 (dd, *J* = 3.6, 1.0 Hz, 1H), 6.99 (d, *J* = 0.9 Hz, 1H), 6.98 (dd, *J* = 5.1, 3.6 Hz, 1H), 6.67 (d, *J* = 17.9 Hz, 0.10H, *E*), 6.27 (d, *J* = 37.7 Hz, 0.90H, *Z*).

¹³C-NMR (75 MHz, CDCl₃): δ = 151.6 (C$_q$), 149.4 (d, $^1J_{C-F}$ = 260 Hz, C$_q$), 148.4 (CH), 138.5 (C$_q$), 138.3 (CH), 135.5 (d, $^4J_{C-F}$ = 3.3 Hz, C$_q$), 131.4 (d, $^2J_{C-F}$ = 29.7 Hz, C$_q$), 127.8 (C$_q$), 127.3 (CH), 126.9 (CH), 126.3 (d, $^4J_{C-F}$ = 9.5 Hz, CH), 124.3 (CH), 122.5 (CH), 121.6 (CH), 121.2 (CH), 120.6 (CH), 111.2 (CH), 107.3 (d, $^3J_{C-F}$ = 4.4 Hz, CH), 104.2 (d, $^2J_{C-F}$ = 13.5 Hz, CH).

¹⁹F-NMR (376 MHz, CDCl₃): δ = –92.1 (d, *J* = 17.9 Hz, *E*), –104.6 (d, *J* = 37.7 Hz, *Z*).

IR (ATR): 3058, 1586, 1469, 1450, 1437, 1382, 1214, 780 cm⁻¹.

MS (EI) *m/z* (relative intensity): 320 ([M]⁺, 80), 299 (100).

HR-MS (EI): *m/z* calcd. for [C₁₉H₁₃FN₂S]⁺ [M]⁺ 320.0783, found 320.0775.
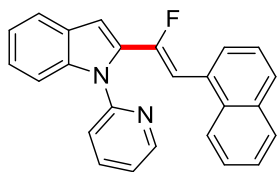
(Z)-2-[1-Fluoro-2-(naphthalen-1-yl)vinyl]-1-(pyridin-2-yl)-1H-indole (159ad): A modified general procedure **G** was followed using 1-(pyridin-2-yl)-1H-indole (**105a**) (97.1 mg, 0.50 mmol) and 1-(2,2-difluorovinyl)naphthalene (**128d**) (143 mg, 0.75 mmol) at 70 °C. Isolation by column chromatography (n-hexane/EtOAc: 30/1 → 20/1) yielded **159ad** (93.1 mg, 51%, Z/E = 92:8) as a white solid.

M.p. = 75 °C.

^{1}H-NMR (400 MHz, CDCl$_3$): δ = 8.72 (ddd, J = 4.9, 1.9, 0.8 Hz, 1H), 7.90 (ddd, J = 8.1, 7.6, 1.9 Hz, 1H), 7.86−7.77 (m, 4H), 7.72 (d, J = 7.4 Hz, 1H), 7.54 (ddd, J = 8.1, 1.0, 0.8 Hz, 1H), 7.51−7.44 (m, 4H), 7.34 (ddd, J = 7.6, 4.9, 1.3 Hz, 1H), 7.29 (ddd, J = 7.2, 7.1, 1.3 Hz, 1H), 7.26–7.24 (m, 1H), 7.15 (d, J = 0.9 Hz, 1H), 6.92 (d, J = 17.9 Hz, 0.08H, E), 6.64 (d, J = 36.0 Hz, 0.92H, Z).

^{13}C-NMR (125 MHz, CDCl$_3$): δ = 151.9 (C$_q$), 151.6 (d, $^1J_{C-F}$ = 255 Hz, C$_q$), 149.7 (CH), 138.9 (C$_q$), 138.6 (CH), 133.7 (C$_q$), 132.3 (d, $^2J_{C-F}$ = 32.3 Hz, C$_q$), 131.3 (C$_q$), 129.2 (d, $^4J_{C-F}$ = 3.3 Hz, C$_q$), 128.7 (d, $^4J_{C-F}$ = 8.2 Hz, CH), 128.1 (CH), 127.8 (C$_q$), 127.4 (CH), 127.3 (CH), 126.1 (CH), 125.7 (CH), 125.6 (CH), 124.4 (CH), 123.8 (CH), 121.7 (CH), 121.4 (CH), 121.1 (CH), 111.3 (CH), 107.6 (d, $^3J_{C-F}$ = 4.2 Hz, CH), 106.3 (d, $^2J_{C-F}$ = 10.5 Hz, CH).

^{19}F-NMR (282 MHz, CDCl$_3$): δ = –94.2 (d, J = 17.9 Hz, E), –107.3 (d, J = 36.0 Hz, Z).

IR (ATR): 3056, 1586, 1467, 1437, 1213, 1143, 908, 732 cm^{-1}.

MS (EI) m/z (relative intensity): 364 ([M]$^+$, 80), 343 (100), 266 (20).

HR-MS (EI): m/z calcd. for [C$_{25}$H$_{17}$FN$_2$]$^+$ [M]$^+$ 364.1376, found 364.1378.

5.5.2   Mechanistic Studies for the Allylative Cobalt(III)-Catalyzed C−H/C–F Activation

5.5.2.1   H/D-Exchange Experiments
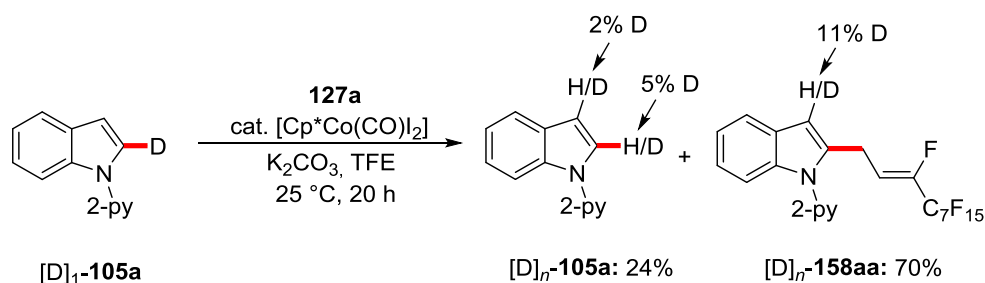
A suspension of [D]$_1$-**105a** (117 mg, 0.60 mmol, 1.20 equiv), **127a** (223 mg, 0.50 mmol, 1.00 equiv), [Cp*Co(CO)I$_2$] (6.0 mg, 2.5 mol %) and K$_2$CO$_3$ (69.0 mg, 0.50 mmol, 1.00 equiv) in TFE (0.5 mL) was stirred at 25 °C for 20 h. After removal of the solvents, the crude mixture was purified by column

chromatography on silica gel (*n*-hexane/EtOAc: 30:1 → 20:1) to yield [D]$_n$-**158aa** (214 mg, 70%) and [D]$_n$-**105a** (28.1 mg, 24% reisolated) as yellow oils.
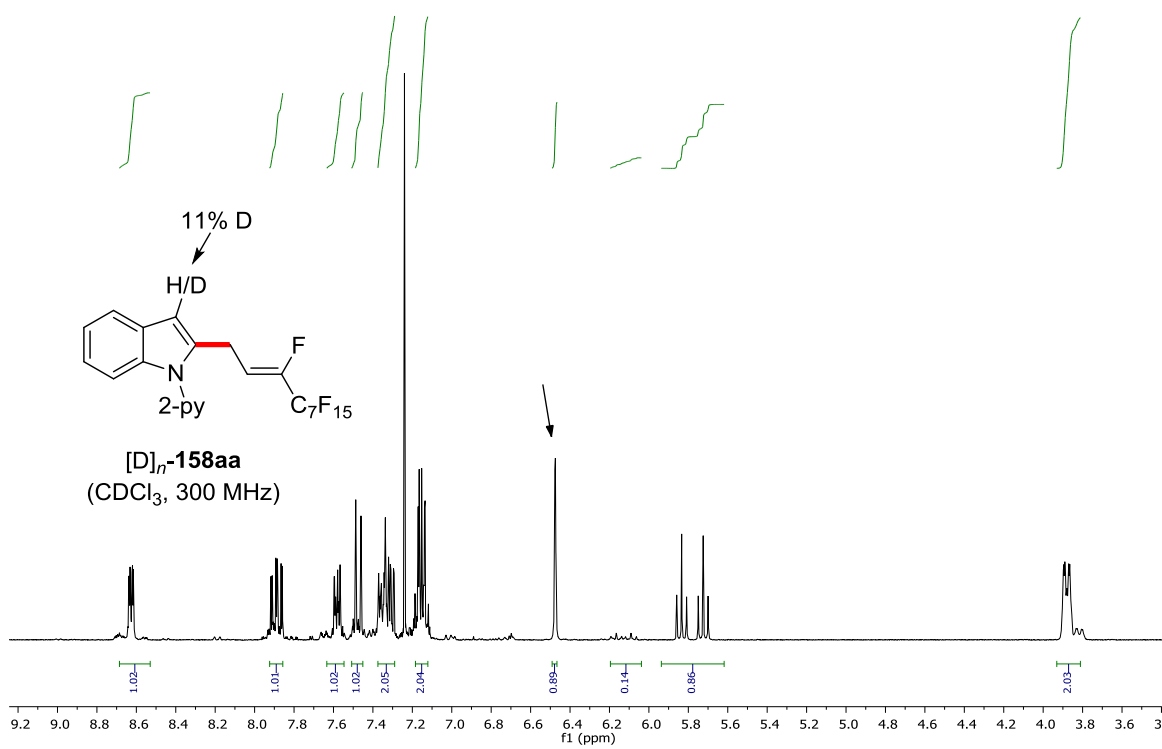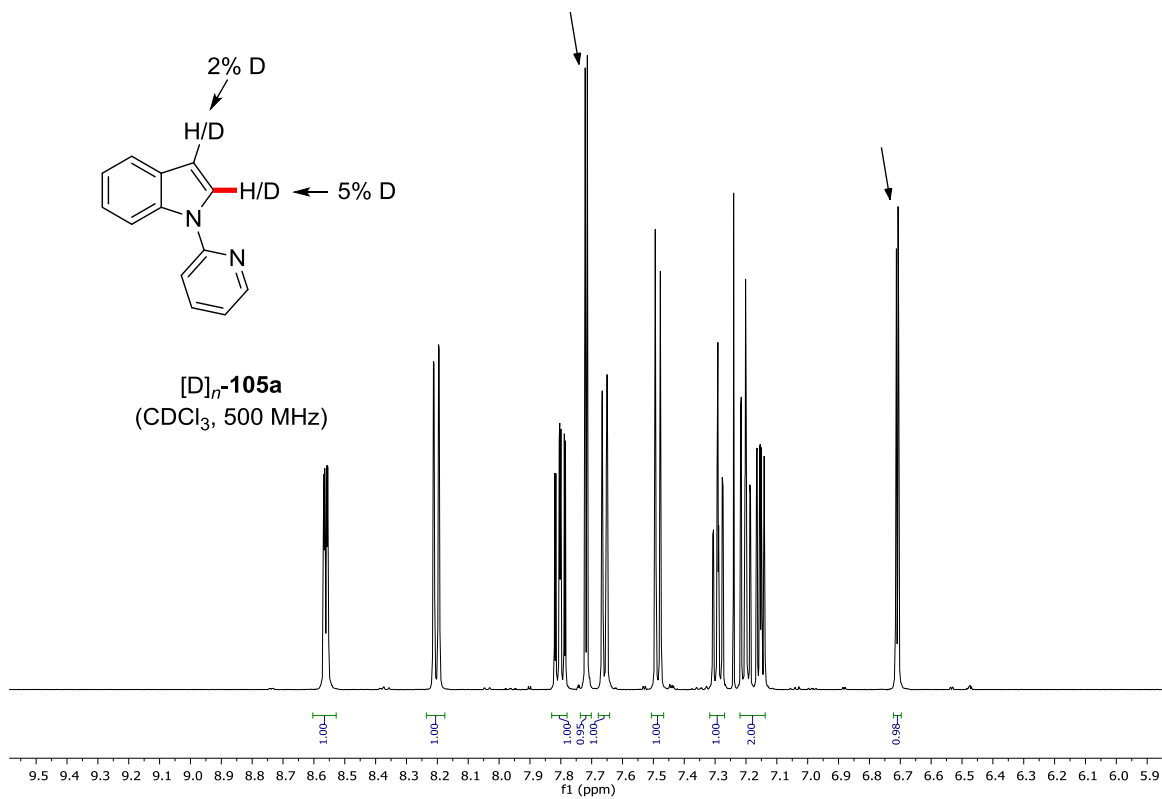
5.5.2.2   KIE Studies
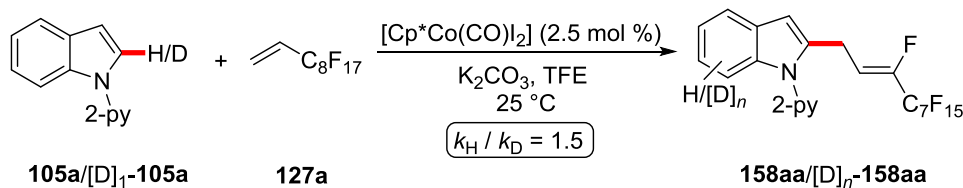
Two parallel reactions of **105a** and [D]₁-**105a** with **127a** were performed respectively to determine the KIE value by comparison of the initial reaction rates. A suspension of **105a** (97.1 mg, 0.50 mmol, 1.00 equiv) or [D]₁-**105a** (97.5 mg, 0.50 mmol, 1.00 equiv), **127a** (268 mg, 0.75 mmol, 1.50 equiv), [Cp*Co(CO)I₂] (6.00 mg, 2.5 mol %), K₂CO₃ (69.1 mg, 1.00 equiv) and *n*-dodecane (30 µL) as the internal standard in TFE (2.00 mL) was stirred at 25 °C. Aliquots (25 µL) were periodically removed to provide the following conversions as determined by GC-analysis:

Table 42. Conversion-time table for determination of the KIE.

t / min	10	20	30	40	50	60
158aa / %	4.8	5.7	8.7	11.8	13.9	16.8
[D]ₙ-**158aa** / %	3.5	5.9	6.9	9.0	10.3	12.1

5.5.2.3   Intermolecular Competition Experiment
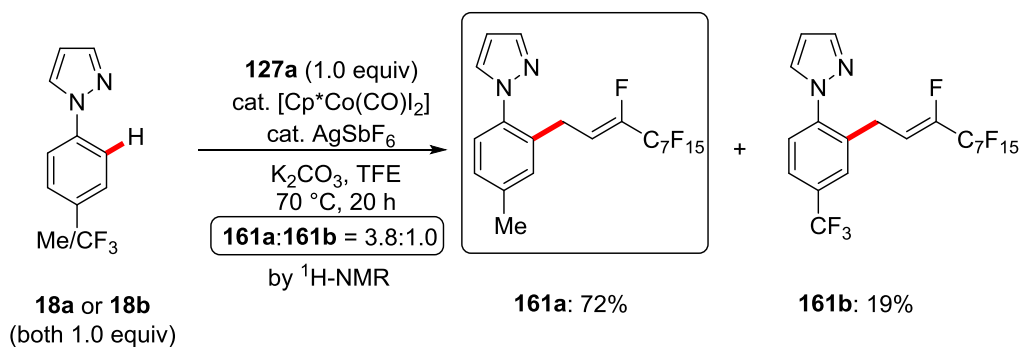
A suspension of 1-(*p*-tolyl)-1*H*-pyrazole (**18a**) (79.0 mg, 0.50 mmol, 1.00 equiv), 1-(4-(trifluoromethyl)phenyl)-1*H*-pyrazole (**18b**) (106 mg, 0.50 mmol, 1.00 equiv), **127a** (223 mg, 0.50 mmol, 1.00 equiv), [Cp*Co(CO)I₂] (23.8 mg, 10.0 mol %), AgSbF₆ (34.0 mg, 20 mol %) and K₂CO₃ (69.0 mg, 0.50 mmol, 1.00 equiv) in TFE (0.5 mL) was stirred at 70 °C for 20 h. After

filtration over Celite and removal of the solvents, the crude mixture was analyzed by means of ^{1}H-NMR spectroscopy with 1,3,5-trimethoxybenzene (16.8 mg, 0.10 mmol) as the internal standard to furnish the following conversions: **161a**: 72% (*Z/E* = 87:13) and **161b**: 19% (*Z/E* = 86:14).

5.6   Manganese(I)-Catalyzed Allylative C−H/C–F Functionalization

5.6.1   Characterization Data
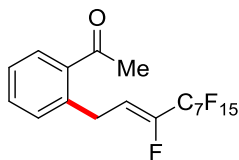
(Z)-1-[2-(1H,1H,2H-Perfluorodec-2-en-1-yl)phenyl]ethan-1-one (166a): The general procedure **H** was followed using *N*-(4-methoxyphenyl)-1-phenylethan-1-imine (**6a**) (113 mg, 0.50 mmol) and 1*H*,1*H*,2*H*-perfluorodec-1-ene (**127a**) (669 mg, 1.50 mmol). Isolation by column chromatography (*n*-hexane/EtOAc: 25/1) yielded **166a** (197 mg, 72%, *Z/E* = 97:3) as a yellow oil.

^{1}H-NMR (400 MHz, CDCl$_3$): δ = 7.77 (dd, *J* = 7.4, 1.4 Hz, 1H), 7.44 (ddd, *J* = 7.6, 7.4, 1.4 Hz, 1H), 7.34 (ddd, *J* = 7.6, 7.5, 1.4 Hz, 1H), 7.27 (dd, *J* = 7.5, 1.4 Hz, 1H), 6.14 (dt, *J* = 23.5, 9.5 Hz, 0.03H, *E*), 5.91 (dt, *J* = 33.5, 8.0 Hz, 0.97H), 3.81 (ddt, *J* = 8.0, 4.1, 2.1 Hz, 2H), 2.59 (s, 3H).

^{13}C-NMR (100 MHz, CDCl$_3$): δ = 201.0 (C$_q$), 145.9 (dt, $^1J_{C-F}$ = 257 Hz, $^2J_{C-F}$ = 29.1 Hz, C$_q$), 137.9 (C$_q$), 136.8 (C$_q$), 132.4 (CH), 131.5 (CH), 130.1 (CH), 127.1 (CH), 117.4 (dt, $^1J_{C-F}$ = 288 Hz, $^2J_{C-F}$ = 34.0 Hz, C$_q$), 115.3 (dt, $^2J_{C-F}$ = 7.8 Hz, $^3J_{C-F}$ = 4.1 Hz, CH), 113.5 (m, C$_q$), 113.1 (m, C$_q$), 111.3 (m, C$_q$), 110.9 (m, C$_q$), 110.2 (m, C$_q$), 108.3 (m, C$_q$), 29.1 (CH$_3$), 28.7 (d, $^3J_{C-F}$ = 3.5 Hz, CH$_2$).

^{19}F-NMR (376 MHz, CDCl$_3$): δ = –81.0 (m), –117.5 (m), –122.1 (m), –122.1 (m), –122.9 (m), –123.1 (m), –126.3 (m), –132.5 (m).

IR (ATR): 1686, 1358, 1236, 1199, 1144, 1106, 759, 732 cm^{-1}.

MS (ESI) *m/z* (relative intensity): 569 ([M + Na]$^+$, 100), 547 ([M + H]$^+$, 45), 373 (15).

HR-MS (ESI): *m/z* calcd. for [C$_{18}$H$_{11}$F$_{16}$O]$^+$ [M + H]$^+$ 547.0549, found 547.0543.
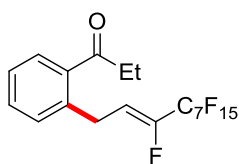
(Z)-1-[2-(1H,1H,2H-Perfluorodec-2-en-1-yl)phenyl]propan-1-one (166b): The general procedure **H** was followed using *N*-(4-methoxyphenyl)-1-phenylpropan-1-imine (**6b**) (120 mg, 0.50 mmol) and 1*H*,1*H*,2*H*-perfluorodec-1-ene (**127a**) (669 mg, 1.50 mmol). Isolation by column chromatography (*n*-hexane/EtOAc: 30/1) yielded **166b** (181 mg, 65%, *Z/E* = 97:3) as a yellow oil.

^{1}H-NMR (400 MHz, CDCl$_3$): δ = 7.71 (dd, *J* = 8.0, 1.4 Hz, 1H), 7.43 (ddd, *J* = 7.7, 7.5, 1.4 Hz, 1H), 7.33 (ddd, *J* = 8.0, 7.5, 1.3 Hz, 1H), 7.27 (dd, *J* = 7.7, 1.3 Hz, 1H) 6.13 (dt, *J* = 22.3, 8.8 Hz, 0.03H, *E*), 5.92 (dt, *J* = 33.8, 7.7 Hz, 0.97H, *Z*), 3.76 (ddt, *J* = 7.7, 4.1, 2.1 Hz, 2H), 2.94 (q, *J* = 7.3 Hz, 2H), 1.18 (t, *J* = 7.3 Hz, 3H).

13C-NMR (100 MHz, CDCl$_3$): δ = 204.2 (C$_q$), 145.2 (dt, $^1J_{\text{C–F}}$ = 259 Hz, $^2J_{\text{C–F}}$ = 28.0 Hz, C$_q$), 137.6 (C$_q$), 137.1 (C$_q$), 131.9 (CH), 131.4 (CH), 129.1 (CH), 127.0 (CH), 117.4 (dt, $^1J_{\text{C–F}}$ = 288 Hz, $^2J_{\text{C–F}}$ = 34.9 Hz, C$_q$), 115.5 (dt, $^2J_{\text{C–F}}$ = 8.9 Hz, $^3J_{\text{C–F}}$ = 3.6 Hz, CH), 113.2 (m, C$_q$), 110.9 (m, C$_q$), 110.7 (m, C$_q$), 110.2 (m, C$_q$), 108.5 (m, C$_q$), 107.5 (m, C$_q$), 34.3 (CH$_2$), 28.6 (d, $^3J_{\text{C–F}}$ = 3.6 Hz, CH$_2$), 8.20 (CH$_3$).

19F-NMR (376 MHz, CDCl$_3$): δ = –80.9 (m), –117.5 (m), –122.0 (m), –122.1 (m), –122.8 (m), –123.0 (m), –126.2 (m), –132.5 (m).

IR (ATR): 1687, 1238, 1203, 1148, 907, 729 cm^{-1}.

MS (ESI) m/z (relative intensity): 583 ([M + Na]$^+$, 100), 561 ([M + H]$^+$, 60), 381 (15).

HR-MS (ESI): m/z calcd. for [C$_{19}$H$_{13}$F$_{16}$O]$^+$ [M + H]$^+$ 561.0705, found 561.0707.
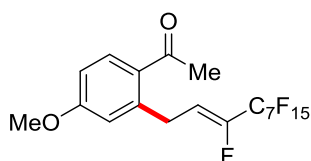
(*Z*)-1-[4-Methoxy-2-(1*H*,1*H*,2*H*-perfluorodec-2-en-1-yl)phenyl]ethan-1-one (166c): The general procedure **H** was followed using *N*-bis(4-methoxyphenyl)ethan-1-imine (**6c**) (128 mg, 0.50 mmol) and 1*H*,1*H*,2*H*-perfluorodec-1-ene (**127a**) (669 mg, 1.50 mmol). Isolation by column chromatography (*n*-hexane/EtOAc: 30/1) yielded **166c** (181 mg, 63%, *Z*/*E* = 97:3) as a yellow oil.

1H-NMR (500 MHz, CDCl$_3$): δ = 7.81 (d, J = 8.8 Hz, 1H), 7.82 (dd, J = 8.8, 2.6 Hz, 1H), 7.75 (d, J = 2.6 Hz, 1H), 6.15 (dt, J = 23.8, 8.6 Hz, 0.03H, *E*), 5.92 (dt, J = 33.9, 7.7 Hz, 0.97H, *Z*), 3.86 (ddt, J = 7.7, 4.1, 1.7 Hz, 2H), 3.84 (s, 3H), 2.55 (s, 3H).

13C-NMR (125 MHz, CDCl$_3$): δ = 198.9 (C$_q$), 162.4 (C$_q$), 145.9 (dt, $^1J_{\text{C–F}}$ = 258 Hz, $^2J_{\text{C–F}}$ = 29.0 Hz, C$_q$), 141.1 (C$_q$), 133.1 (CH), 128.8 (C$_q$), 116.9 (CH), 116.5 (dt, $^1J_{\text{C–F}}$ = 287 Hz, $^2J_{\text{C–F}}$ = 31.3 Hz, C$_q$), 115.1 (dt, $^2J_{\text{C–F}}$ = 8.9 Hz, $^3J_{\text{C–F}}$ = 3.6 Hz, CH), 112.8 (m, C$_q$), 111.5 (CH), 110.5 (m, C$_q$), 110.3 (m, C$_q$), 110.0 (m, C$_q$), 108.2 (m, C$_q$), 107.9 (m, C$_q$), 55.2 (CH$_3$), 29.2 (d, $^3J_{\text{C–F}}$ = 3.7 Hz, CH$_2$), 28.7 (CH$_3$).

19F-NMR (470 MHz, CDCl$_3$): δ = –81.0 (m), –117.5 (m), –122.1 (m), –122.2 (m), –122.9 (m), –123.1 (m), –126.3 (m), –132.6 (m).

IR (ATR): 1676, 1604, 1585, 1235, 1199, 1144, 1106, 733, 706 cm^{-1}.

MS (ESI) m/z (relative intensity): 599 ([M + Na]$^+$, 90), 577 ([M + H]$^+$, 100).

HR-MS (ESI): m/z calcd. for [C$_{19}$H$_{13}$F$_{16}$O$_2$]$^+$ [M + H]$^+$ 577.0655, found 577.0661.
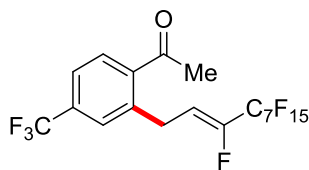
(*Z*)-1-[4-Trifluoromethyl-2-(1*H*,1*H*,2*H*-perfluorodec-2-en-1-yl)phenyl]ethan-1-one (166d): The general procedure **H** was followed using 1-(4-trifluoromethylphenyl)-*N*-(4-methoxyphenyl)ethan-1-imine (**6d**) (147 mg, 0.50 mmol) and 1*H*,1*H*,2*H*-perfluorodec-1-ene (**127a**) (669 mg, 1.50 mmol). Isolation by column chromatography (*n*-hexane/EtOAc: 30/1) yielded **166d** (157 mg, 51%, *Z*/*E* = 97:3) as a yellow oil.

^{1}H-NMR (400 MHz, CDCl$_3$): δ = 7.83 (d, *J* = 8.0 Hz, 1H), 7.61 (dd, *J* = 8.0, 1.4 Hz, 1H), 7.51 (d, *J* = 1.4 Hz, 1H), 6.10 (dt, *J* = 22.6, 8.5 Hz, 0.03H, *E*), 5.87 (dt, *J* = 33.4, 7.8 Hz, 0.97H, *Z*), 3.83 (ddt, *J* = 7.8, 4.0, 2.0 Hz, 2H), 2.62 (s, 3H).

^{13}C-NMR (100 MHz, CDCl$_3$): δ = 200.3 (C$_q$), 146.5 (dt, $^1J_{C-F}$ = 261 Hz, $^2J_{C-F}$ = 29.5 Hz, C$_q$), 139.9 (C$_q$), 138.5 (C$_q$), 133.7 (q, $^2J_{C-F}$ = 33.0 Hz, C$_q$), 130.0 (CH), 128.0 (q, $^3J_{C-F}$ = 3.8 Hz, CH), 124.1 (q, $^3J_{C-F}$ = 3.7 Hz, CH), 123.4 (d, $^1J_{C-F}$ = 273 Hz, C$_q$), 117.0 (dt, $^1J_{C-F}$ = 286 Hz, $^2J_{C-F}$ = 22.3 Hz, C$_q$), 114.2 (dt, $^2J_{C-F}$ = 7.8 Hz, $^3J_{C-F}$ = 3.7 Hz, CH), 113.2 (m, C$_q$), 111.1 (m, C$_q$), 110.7 (m, C$_q$), 110.2 (m, C$_q$), 108.6 (m, C$_q$), 107.7 (m, C$_q$), 29.3 (CH$_3$), 28.3 (d, $^3J_{C-F}$ = 3.7 Hz, CH$_2$).

^{19}F-NMR (376 MHz, CDCl$_3$): δ = –63.5 (m), –80.9 (m), –117.6 (m), –122.1 (m), –122.1 (m), –122.8 (m), –123.1 (m), –126.3 (m), –130.6 (m).

IR (ATR): 1695, 1334, 1238, 1201, 1172, 1130, 1093, 833, 720 cm^{-1}.

MS (EI) *m*/*z* (relative intensity): 614 ([M]$^+$, 100), 599 (85), 579 (20).

HR-MS (ESI): *m*/*z* calcd. for [C$_{19}$H$_9$F$_{19}$O + Na]$^+$ 637.0242, found 637.0222.
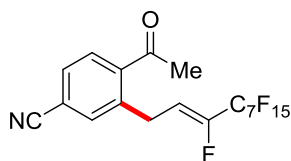
(*Z*)-4-Acetyl-3-(1*H*,1*H*,2*H*-perfluorodec-2-en-1-yl)benzonitrile (166e): The general procedure **H** was followed using 4-{1-[(4-methoxyphenyl)imino]ethyl}benzonitrile (**6e**) (125 mg, 0.50 mmol) and 1*H*,1*H*,2*H*-perfluorodec-1-ene (**127a**) (669 mg, 1.50 mmol). Isolation by column chromatography (*n*-hexane/EtOAc: 20/1) yielded **166e** (134 mg, 47%, *Z*/*E* = 97:3) as a yellow oil.

^{1}H-NMR (400 MHz, CDCl$_3$): δ = 7.81 (d, *J* = 7.7 Hz, 1H), 7.66 (dd, *J* = 7.7, 1.9 Hz, 1H), 7.56 (d, *J* = 1.9 Hz, 1H), 6.07 (dt, *J* = 23.8, 8.6 Hz, 0.03H, *E*), 5.86 (dt, *J* = 33.0, 7.7 Hz, 0.97H, *Z*), 3.79 (ddt, *J* = 7.7, 4.2, 2.1 Hz, 2H), 2.61 (s, 3H).

13C-NMR (100 MHz, CDCl$_3$): δ = 199.9 (C$_q$), 146.6 (dt, $^1J_{C-F}$ = 261 Hz, $^2J_{C-F}$ = 28.7 Hz, C$_q$), 140.5 (C$_q$), 138.8 (C$_q$), 134.7 (CH), 130.9 (CH), 130.0 (CH), 117.4 (C$_q$), 116.8 (dt, $^1J_{C-F}$ = 289 Hz, $^2J_{C-F}$ = 33.8 Hz, C$_q$), 115.8 (dt, $^2J_{C-F}$ = 8.9 Hz, $^3J_{C-F}$ = 3.6 Hz, CH), 113.9 (m, C$_q$), 113.0 (m, C$_q$), 111.2 (m, C$_q$), 110.7 (m, C$_q$), 110.3 (m, C$_q$), 108.3 (m, C$_q$), 107.6 (m, C$_q$), 29.4 (CH$_3$), 28.2 (d, $^3J_{C-F}$ = 3.7 Hz, CH$_2$).

19F-NMR (376 MHz, CDCl$_3$): δ = –80.8 (m), –117.5 (m), –122.0 (m), –122.0 (m), –122.8 (m), –122.9 (m), –126.1 (m), –130.0 (m).

IR (ATR): 3051, 2920, 1585, 1467, 1435, 1380, 1348 cm^{-1}.

MS (ESI) m/z (relative intensity): 594 ([M + Na]$^+$, 20), 572 ([M + H]$^+$, 100).

HR-MS (ESI): m/z calcd. for [C$_{19}$H$_{10}$F$_{16}$NO]$^+$ [M + H]$^+$ 572.0501, found 572.0498.
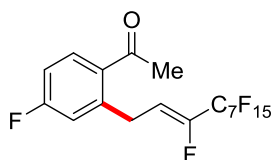
(*Z*)-1-[4-Fluoro-2-(1*H*,1*H*,2*H*-perfluorodec-2-en-1-yl)phenyl]ethan-1-one (166f): The general procedure **H** was followed using 1-(4-fluorophenyl)-*N*-(4-methoxyphenyl)ethan-1-imine (**6f**) (122 mg, 0.50 mmol) and 1*H*,1*H*,2*H*-perfluorodec-1-ene (**127a**) (669 mg, 1.50 mmol). Isolation by column chromatography (*n*-hexane/EtOAc: 30/1) yielded **166f** (195 mg, 69%, *Z*/*E* = 97:3) as a colorless oil.

1H-NMR (500 MHz, CDCl$_3$): δ = 7.82 (dd, J = 8.4, 5.7 Hz, 1H), 7.02 (ddd, J = 10.1, 8.4, 2.4 Hz, 1H), 6.96 (dd, J = 9.4, 2.4 Hz, 1H), 6.11 (dt, J = 23.5, 8.5 Hz, 0.03H, *E*), 5.89 (dt, J = 33.6, 7.6 Hz, 0.97H, *Z*), 3.83 (ddt, J = 7.6, 4.1, 1.7 Hz, 2H), 2.58 (s, 3H).

13C-NMR (125 MHz, CDCl$_3$): δ = 200.3 (C$_q$), 161.6 (d, $^1J_{C-F}$ = 254 Hz, C$_q$), 145.7 (dt, $^1J_{C-F}$ = 260 Hz, $^2J_{C-F}$ = 29.5 Hz, C$_q$), 139.3 (d, $^3J_{C-F}$ = 3.2 Hz, C$_q$), 128.3 (d, $^3J_{C-F}$ = 8.6 Hz, CH), 125.2 (d, $^4J_{C-F}$ = 3.8 Hz, CH), 124.6 (d, $^2J_{C-F}$ = 16.8 Hz, CH), 118.9 (d, $^2J_{C-F}$ = 23.7 Hz, CH), 116.8 (dt, $^1J_{C-F}$ = 287 Hz, $^2J_{C-F}$ = 32.8 Hz, C$_q$), 113.9 (dt, $^2J_{C-F}$ = 8.9 Hz, $^3J_{C-F}$ = 3.6 Hz, CH), 113.2 (m, C$_q$), 111.3 (m, C$_q$), 110.8 (m, C$_q$), 110.2 (m, C$_q$), 108.3 (m, C$_q$), 107.5 (m, C$_q$), 29.4 (CH$_3$), 20.3 (dd, $^3J_{C-F}$ = 5.8, 4.4 Hz, CH$_2$).

19F-NMR (470 MHz, CDCl$_3$): δ = –80.8 (m), –105.8 (m), –117.4 (m), –122.0 (m), –122.0 (m), –122.8 (m), –123.0 (m), –126.2 (m), –131.4 (m).

IR (ATR): 1692, 1456, 1237, 1199, 1144, 791, 730 cm^{-1}.

MS (ESI) m/z (relative intensity): 587 ([M + Na]$^+$, 100), 565 ([M + H]$^+$, 15).

HR-MS (ESI): m/z calcd. for [C$_{18}$H$_{10}$F$_{17}$O]$^+$ [M + H]$^+$ 565.0455, found 565.0457.
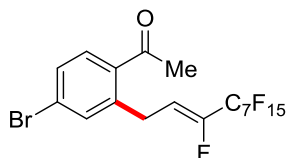
(Z)-1-[4-Bromo-2-(1H,1H,2H-perfluorodec-2-en-1-yl)phenyl]ethan-1-one (166g): The general procedure **H** was followed using 1-(4-bromophenyl)-N-(4-methoxyphenyl)ethan-1-imine (**6g**) (152 mg, 0.50 mmol) and 1H,1H,2H-perfluorodec-1-ene (**127a**) (669 mg, 1.50 mmol). Isolation by column chromatography (n-hexane/EtOAc: 30/1) yielded **166g** (218 mg, 71%, Z/E = 97:3) as a yellow oil.

^{1}H-NMR (300 MHz, CDCl$_3$): δ = 7.64 (d, J = 8.5 Hz, 1H), 7.49 (dd, J = 8.5, 2.0 Hz, 1H), 7.42 (d, J = 2.0 Hz, 1H), 6.11 (dt, J = 22.3, 8.8 Hz, 0.03H, E), 5.86 (dt, J = 33.3, 7.8 Hz, 0.97H, Z), 3.79 (ddt, J = 7.8, 4.1, 2.0 Hz, 2H), 2.57 (s, 3H).

^{13}C-NMR (125 MHz, CDCl$_3$): δ = 199.7 (C$_q$), 145.8 (dt, $^1J_{C-F}$ = 259 Hz, $^2J_{C-F}$ = 28.4 Hz, C$_q$), 140.0 (C$_q$), 135.3 (C$_q$), 134.4 (CH), 131.4 (CH), 130.2 (CH), 126.9 (C$_q$), 117.0 (dt, $^1J_{C-F}$ = 288 Hz, $^2J_{C-F}$ = 32.3 Hz, C$_q$), 114.4 (dt, $^2J_{C-F}$ = 8.9 Hz, $^3J_{C-F}$ = 3.6 Hz, CH), 112.5 (m, C$_q$), 110.8 (m, C$_q$), 110.7 (m, C$_q$), 110.3 (m, C$_q$), 108.7 (m, C$_q$), 107.4 (m, C$_q$), 29.1 (CH$_3$), 28.6 (d, $^3J_{C-F}$ = 3.5 Hz, CH$_2$).

^{19}F-NMR (282 MHz, CDCl$_3$): δ = –80.9 (m), –117.5 (m), –122.0 (m), –122.1 (m), –122.8 (m), –123.1 (m), –126.3 (m), –131.3 (m).

IR (ATR): 1686, 1238, 1203, 1148, 906, 729 cm^{-1}.

MS (ESI) m/z (relative intensity): 647 ([M(^{79}Br) + Na]$^+$, 20), 625 ([M(^{79}Br) + H]$^+$, 100), 450 (50).

HR-MS (ESI): m/z calcd. for [C$_{18}$H$_{10}$^{79}BrF$_{16}$O]$^+$ [M + H]$^+$ 624.9654, found 624.9643.
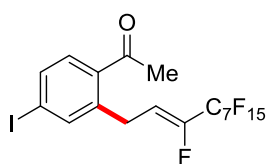
(Z)-1-[4-Iodo-2-(1H,1H,2H-perfluorodec-2-en-1-yl)phenyl]ethan-1-one (166h): The general procedure **H** was followed using 1-(4-iodophenyl)-N-(4-methoxyphenyl)ethan-1-imine (**6h**) (176 mg, 0.50 mmol) and 1H,1H,2H-perfluorodec-1-ene (**127a**) (669 mg, 1.50 mmol). Isolation by column chromatography (n-hexane/EtOAc: 30/1) yielded **166h** (248 mg, 74%, Z/E = 97:3) as a yellow oil.

^{1}H-NMR (300 MHz, CDCl$_3$): δ = 7.74 (dd, J = 8.2, 1.7 Hz, 1H), 7.66 (d, J = 1.7 Hz, 1H), 7.50 (d, J = 8.2 Hz, 1H), 6.10 (dt, J = 22.3, 8.8 Hz, 0.03H, E), 5.88 (dt, J = 33.3, 7.7 Hz, 0.97H, Z), 3.78 (ddt, J = 7.7, 4.1, 2.1 Hz, 2H), 2.62 (s, 0.09H, E), 2.58 (s, 2.91H, Z).

^{13}C-NMR (75 MHz, CDCl$_3$): δ = 199.9 (C$_q$), 145.9 (dt, $^1J_{C-F}$ = 260 Hz, $^2J_{C-F}$ = 28.9 Hz, C$_q$), 140.4 (CH), 139.6 (C$_q$), 136.3 (CH), 135.9 (C$_q$), 131.2 (CH), 117.0 (dt, $^1J_{C-F}$ = 288 Hz, $^2J_{C-F}$ = 32.3 Hz, C$_q$),

114.5 (dt, $^2J_{C-F}$ = 8.9 Hz, $^3J_{C-F}$ = 3.6 Hz, CH), 113.0 (m, C_q), 111.1 (m, C_q), 110.6 (m, C_q), 110.3 (m, C_q), 108.7 (m, C_q), 107.4 (m, C_q), 99.6 (C_q), 29.1 (CH$_3$), 28.4 (d, $^3J_{C-F}$ = 3.5 Hz, CH$_2$).

^{19}F-NMR (376 MHz, CDCl$_3$): δ = –80.7 (m), –117.4 (m), –122.0 (m), –122.0 (m), –122.9 (m), –123.0 (m), –126.1 (m), –131.0 (m).

IR (ATR): 1687, 1581, 1551, 1235, 1198, 1143, 720, 707 cm^{-1}.

MS (ESI) m/z (relative intensity): 695 ([M + Na]$^+$, 100), 673 ([M + H]$^+$, 20).

HR-MS (ESI): m/z calcd. for [C$_{18}$H$_{10}$F$_{16}$IO]$^+$ [M + H]$^+$ 672.9515, found 672.9506.
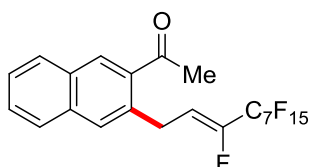
(Z)-1-[3-(1H,1H,2H-Perfluorodec-2-en-1-yl)naphthalen-2-yl]ethan-1-one (166i): The general procedure **H** was followed using *N*-(4-methoxyphenyl)-1-(naphthalen-2-yl)ethan-1-imine (**6i**) (138 mg, 0.50 mmol) and 1H,1H,2H-perfluorodec-1-ene (**127a**) (669 mg, 1.50 mmol). Isolation by column chromatography (*n*-hexane/EtOAc: 30/1) yielded **166i** (179 mg, 60%, Z/E = 98:2) as a red oil.

^{1}H-NMR (300 MHz, CDCl$_3$): δ = 8.32 (s, 1H), 7.89 (dd, J = 8.0, 1.3 Hz, 1H), 7.79 (dd, J = 7.9, 1.4 Hz, 1H), 7.67 (s, 1H), 7.59 (ddd, J = 8.0, 6.9, 1.4 Hz, 1H), 7.52 (ddd, J = 7.9, 6.9, 1.3 Hz, 1H), 6.24 (dt, J = 33.2, 8.2 Hz, 0.02H, *E*), 5.99 (dt, J = 33.5, 7.6 Hz, 0.98H, *Z*), 3.99 (ddt, J = 7.6, 4.1, 2.1 Hz, 2H), 2.73 (s, 3H).

**^{13}C-NMR** (125 MHz, CDCl$_3$): δ = 200.5 (C_q), 145.5 (dt, $^1J_{C-F}$ = 258 Hz, $^2J_{C-F}$ = 28.3 Hz, C_q), 134.8 (C_q), 134.7 (C_q), 134.0 (C_q), 131.8 (CH), 131.4 (C_q), 130.1 (CH), 128.7 (CH), 128.6 (CH), 127.2 (CH), 126.7 (CH), 117.1 (dt, $^1J_{C-F}$ = 287 Hz, $^2J_{C-F}$ = 32.8 Hz, C_q), 115.5 (dt, $^2J_{C-F}$ = 8.9 Hz, $^3J_{C-F}$ = 3.6 Hz, CH), 113.2 (m, C_q), 110.9 (m, C_q), 110.8 (m, C_q), 109.9 (m, C_q), 108.7 (m, C_q), 108.2 (m, C_q), 29.0 (CH$_3$), 28.9 (d, $^3J_{C-F}$ = 3.1 Hz, CH$_2$).

^{19}F-NMR (282 MHz, CDCl$_3$): δ = –80.9 (m), –117.4 (m), –122.0 (m), –122.1 (m), –122.8 (m), –123.0 (m), –126.2 (m), –132.3 (m).

IR (ATR): 1681, 1238, 1201, 1149, 906, 728 cm^{-1}.

MS (ESI) m/z (relative intensity): 619 ([M + Na]$^+$, 100), 597 ([M + H]$^+$, 40).

HR-MS (ESI): m/z calcd. for [C$_{22}$H$_{13}$F$_{16}$O]$^+$ [M + H]$^+$ 597.0705, found 597.0704.
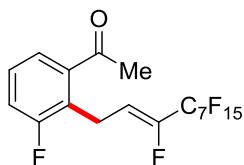
(Z)-1-[3-Fluoro-2-(1H,1H,2H-perfluorodec-2-en-1-yl)phenyl]ethan-1-one (166j): The general procedure **H** was followed using 1-(3-fluorophenyl)-N-(4-methoxyphenyl)ethan-1-imine (**6j**) (122 mg, 0.50 mmol) and 1H,1H,2H-perfluorodec-1-ene (**127a**) (669 mg, 1.50 mmol). Isolation by column chromatography (n-hexane/EtOAc: 30/1) yielded **166j** (149 mg, 53%, Z/E = 97:3) as a yellow oil.

^{1}H-NMR (400 MHz, CDCl$_3$): δ = 7.53 (dd, J = 7.8, 0.9 Hz, 1H), 7.33 (ddd, J = 7.8, 7.8, 5.3 Hz, 1H), 7.21 (ddd, J = 8.4, 7.8, 0.9 Hz, 1H), 5.98 (dt, J = 23.5, 8.1 Hz, 0.03H, E), 5.79 (dt, J = 33.0, 7.3 Hz, 0.97H, Z), 3.81 (ddt, J = 7.3, 4.1, 2.0 Hz, 2H), 2.59 (s, 3H).

^{13}C-NMR (100 MHz, CDCl$_3$): δ = 200.3 (C$_q$), 161.6 (d, $^1J_{C–F}$ = 254 Hz, C$_q$), 145.7 (dt, $^1J_{C–F}$ = 260 Hz, $^2J_{C–F}$ = 29.5 Hz, C$_q$), 139.3 (d, $^3J_{C–F}$ = 3.2 Hz, C$_q$), 128.3 (d, $^3J_{C–F}$ = 8.6 Hz, CH), 125.2 (d, $^4J_{C–F}$ = 3.8 Hz, CH), 124.6 (d, $^2J_{C–F}$ = 16.8 Hz, C$_q$), 118.9 (d, $^2J_{C–F}$ = 23.7 Hz, CH), 116.8 (dt, $^1J_{C–F}$ = 287 Hz, $^2J_{C–F}$ = 32.8 Hz, C$_q$), 113.9 (dt, $^2J_{C–F}$ = 8.9 Hz, $^4J_{C–F}$ = 3.6 Hz, CH), 113.2 (m, C$_q$), 111.3 (m, C$_q$), 110.8 (m, C$_q$), 110.2 (m, C$_q$), 108.3 (m, C$_q$), 107.5 (m, C$_q$), 29.4 (CH$_3$), 20.3 (dd, $^3J_{C–F}$ = 5.8, 4.4 Hz, CH$_2$).

^{19}F-NMR (376 MHz, CDCl$_3$): δ = –80.8 (m), –115.1 (m), –117.5 (m), –122.0 (m), –122.1 (m), –122.8 (m), –123.0 (m), –126.2 (m), –131.0 (m).

IR (ATR): 1692, 1456, 1237, 1199, 1144, 791, 730 cm^{-1}.

MS (ESI) m/z (relative intensity): 587 ([M + Na]$^+$, 40), 441 (100), 419 (30).

HR-MS (ESI): m/z calcd. for [C$_{18}$H$_{10}$F$_{17}$O]$^+$ [M + H]$^+$ 565.0455, found 565.0452.
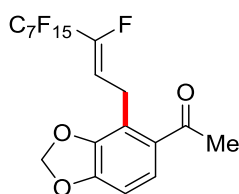
(Z)-1-[4-(1H,1H,2H-Perfluorodec-2-en-1-yl)benzo[d][1,3]dioxol-5-yl]ethan-1-one (166k): The general procedure **H** was followed using 1-(benzo[d][1,3]dioxol-5-yl)-N-(4-methoxyphenyl)ethan-1-imine (**6k**) (135 mg, 0.50 mmol) and 1H,1H,2H-perfluorodec-1-ene (**127a**) (669 mg, 1.50 mmol). Isolation by column chromatography (n-hexane/EtOAc: 20/1) yielded **166k** (193 mg, 65%, Z/E = 98:2) as a yellow oil.

^{1}H-NMR (300 MHz, CDCl$_3$): δ = 7.43 (d, J = 8.2 Hz, 1H), 6.75 (d, J = 8.2 Hz, 1H), 6.02 (s, 2H), 5.85 (dt, J = 33.5, 7.4 Hz, 1H), 3.85 (ddt, J = 7.4, 4.1, 2.1 Hz, 2H), 2.53 (s, 3H).

^{13}C-NMR (125 MHz, CDCl$_3$): δ = 198.6 (C$_q$), 150.2 (C$_q$), 147.8 (C$_q$), 145.3 (dt, $^1J_{C–F}$ = 260 Hz, $^2J_{C–F}$ = 29.5 Hz, C$_q$), 130.8 (C$_q$), 126.5 (CH), 119.6 (C$_q$), 116.8 (dt, $^1J_{C–F}$ = 287 Hz, $^2J_{C–F}$ = 32.8 Hz, C$_q$), 114.1

(dt, $^2J_{C-F}$ = 8.9 Hz, $^3J_{C-F}$ = 3.6 Hz, CH), 113.2 (m, C$_q$), 110.9 (m, C$_q$), 110.8 (m, C$_q$), 109.9 (m, C$_q$), 108.7 (m, C$_q$), 108.2 (m, C$_q$), 106.2 (CH), 101.8 (CH$_2$), 28.8 (CH$_3$), 21.8 (d, $^3J_{C-F}$ = 4.0 Hz, CH$_2$).

^{19}F-NMR (282 MHz, CDCl$_3$): δ = –80.9 (m), –117.5 (m), –122.0 (m), –122.1 (m), –122.8 (m), –123.1 (m), –126.2 (m), –131.7 (m).

IR (ATR): 1675, 1453, 1237, 1200, 1146, 1058, 939, 731 cm^{-1}.

MS (ESI) *m/z* (relative intensity): 613 ([M + Na]$^+$, 80), 591 ([M + H]$^+$, 100).

HR-MS (ESI): *m/z* calcd. for [C$_{19}$H$_{11}$F$_{16}$O$_3$]$^+$ [M + H]$^+$ 591.0447, found 591.0451.
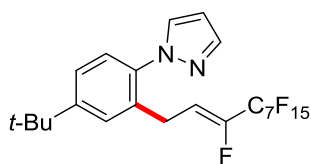
(*Z*)-1-[4-(*tert*-Butyl)-2-(1*H*,1*H*,2*H*-perfluorodec-2-en-1-yl)phenyl]-1*H*-pyrazole **(161c):** The general procedure **H** was followed using 1-[4-(*tert*-butyl)phenyl]-1*H*-pyrazole (**18c**) (100 mg, 0.50 mmol) and 1*H*,1*H*,2*H*-perfluorodec-1-ene (**127a**) (315 mg, 0.75 mmol). Isolation by column chromatography (*n*-hexane/EtOAc: 20/1) yielded **161c** (241 mg, 77%, *Z/E* = 87:13) as a colorless solid.

M.p.: 80 °C.

^{1}H-NMR (300 MHz, CDCl$_3$): δ = 7.70 (dd, *J* = 2.2, 1.7 Hz, 1H), 7.56 (dd, *J* = 4.0, 2.4 Hz, 1H), 7.36 (dd, *J* = 8.2, 2.2 Hz, 1H), 7.30 (dd, *J* = 2.4, 2.1 Hz, 1H), 7.23 (dd, *J* = 8.2, 1.7 Hz, 1H), 6.42 (dd, *J* = 4.0, 2.1 Hz, 1H), 5.90 (dt, *J* = 21.8, 7.9 Hz, 0.13H, *E*), 5.67 (dd, *J* = 33.3, 7.6 Hz, 0.87H, *Z*), 3.79 (ddt, *J* = 7.6, 4.1, 2.5 Hz, 2H), 1.33 (s, 9H).

^{13}C-NMR (125 MHz, CDCl$_3$): δ = 152.2 (C$_q$), 145.7 (dt, $^1J_{C-F}$ = 259 Hz, $^2J_{C-F}$ = 29.1 Hz, C$_q$), 140.5 (CH), 137.1 (C$_q$), 132.9 (C$_q$), 130.3 (CH), 127.3 (CH), 125.8 (CH), 124.7 (CH), 117.0 (dt, $^1J_{C-F}$ = 289 Hz, $^2J_{C-F}$ = 31.3 Hz, C$_q$), 114.7 (dt, $^2J_{C-F}$ = 8.9 Hz, $^3J_{C-F}$ = 3.6 Hz, CH), 113.0 (m, C$_q$), 112.0 (m, C$_q$), 110.6 (m, C$_q$), 110.0 (m, C$_q$), 108.6 (m, C$_q$), 108.1 (m, C$_q$), 106.5 (CH), 34.7 (CH), 31.2 (CH$_3$), 26.3 (d, $^3J_{C-F}$ = 3.7 Hz, CH$_2$).

^{19}F-NMR (282 MHz, CDCl$_3$): δ = –80.9 (m), –114.5 (m, *E*), –117.5 (m, *Z*), –122.1 (m), –122.1 (m), –122.9 (m, *Z*), –123.1 (m, *E*), –123.5 (m), –126.2 (m), –132.3 (m).

IR (ATR): 2968, 1522, 1238, 1201, 1146, 909, 732 cm^{-1}.

MS (EI) *m/z* (relative intensity): 626 ([M]$^+$, 100), 611 (20), 598 (10).

HR-MS (ESI): *m/z* calcd. for [C$_{23}$H$_{19}$F$_{16}$N$_2$]$^+$ [M + H]$^+$ 627.1287, found 627.1289.

5.6.2   Mechanistic Studies

5.6.2.1   H/D-Exchange Experiments

5.6.2.1.1   H/D-Exchange Experiment with CD₃OD
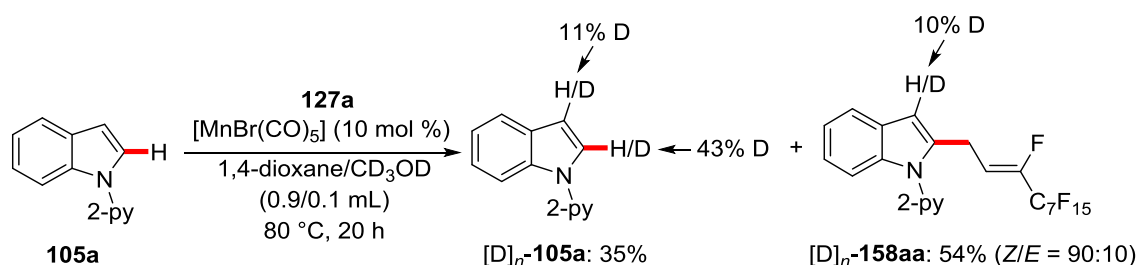
A suspension of **105a** (116 mg, 0.60 mmol, 1.20 equiv), **127a** (224 mg, 0.50 mmol, 1.00 equiv), [MnBr(CO)₅] (13.7 mg, 10.0 mol %) and K₂CO₃ (69.0 mg, 0.50 mmol, 1.00 equiv) in 1,4-dioxane (0.9 mL) and CD₃OD (0.1 mL) was stirred at 80 °C for 20 h. After removal of the solvents, the crude mixture was purified by column chromatography on silica gel (*n*-hexane/EtOAc: 30:1 → 20:1) to yield [D]*ₙ*-**158aa** (167 mg, 54%, *Z/E* = 90:10) and [D]*ₙ*-**105a** (40.7 mg, 35% reisolated) as yellow oils.

[D]$_n$-**158aa**
(CDCl$_3$, 500 MHz)
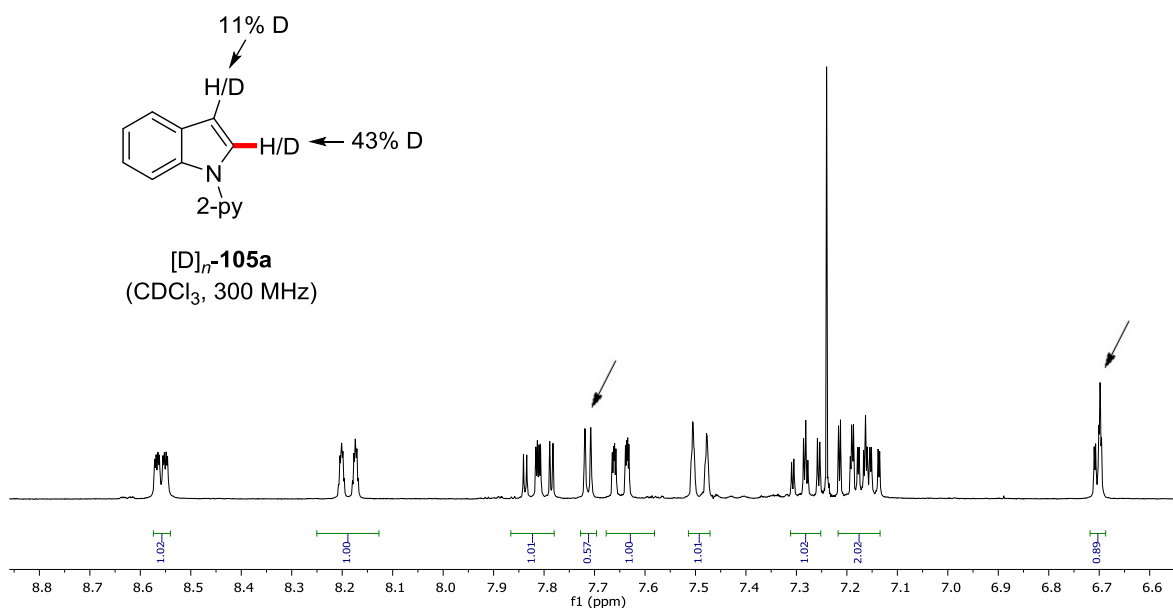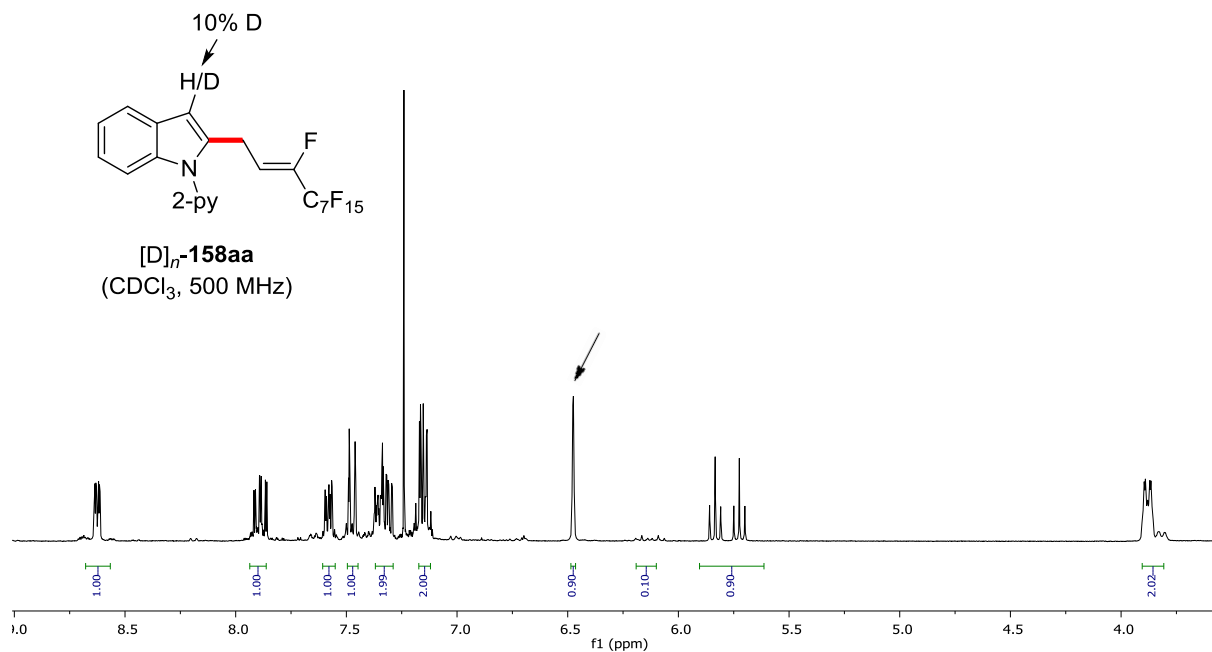
5.6.2.1.2 H/D-Exchange Experiment with CD$_3$OH
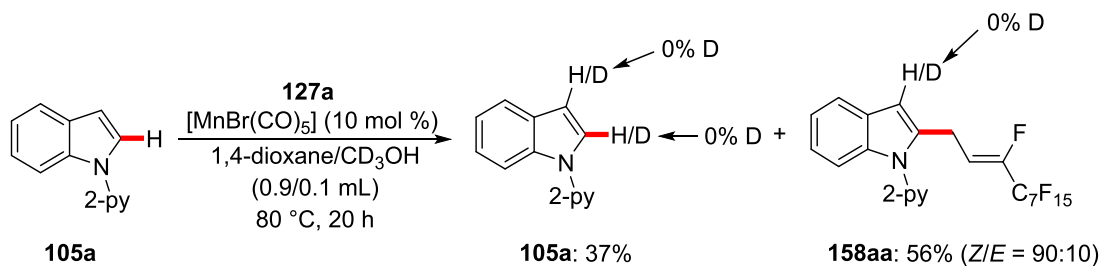
A suspension of **105a** (97.0 mg, 0.50 mmol, 1.00 equiv), **127a** (268 mg, 0.60 mmol, 1.20 equiv), [MnBr(CO)$_5$] (13.7 mg, 10.0 mol %) and K$_2$CO$_3$ (69.0 mg, 0.50 mmol, 1.00 equiv) in 1,4-dioxane (0.9 mL) and CD$_3$OH (0.1 mL) was stirred at 80 °C for 20 h. After removal of the solvents, the crude mixture was purified by column chromatography on silica gel (*n*-hexane/EtOAc: 30:1→20:1) to yield **158aa** (171 mg, 56%, *Z/E* = 90:10) and **105a** (43.0 mg, 37% reisolated) as yellow oils.
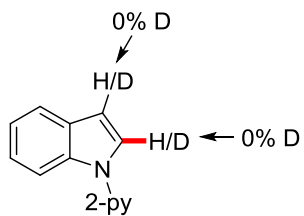
105a
(CDCl$_3$, 300 MHz)
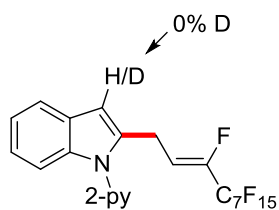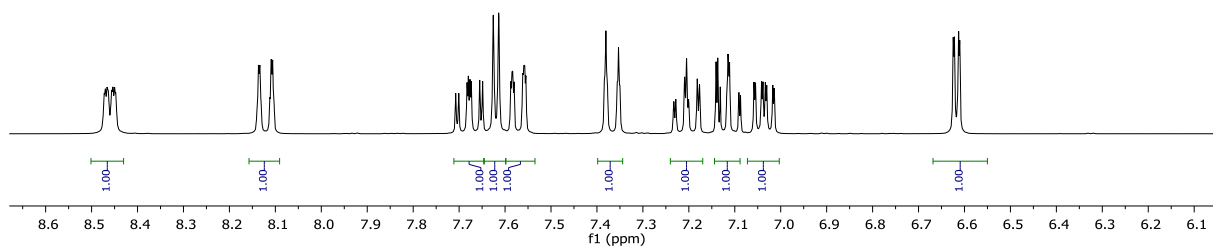
158aa
(CDCl$_3$, 300 MHz)
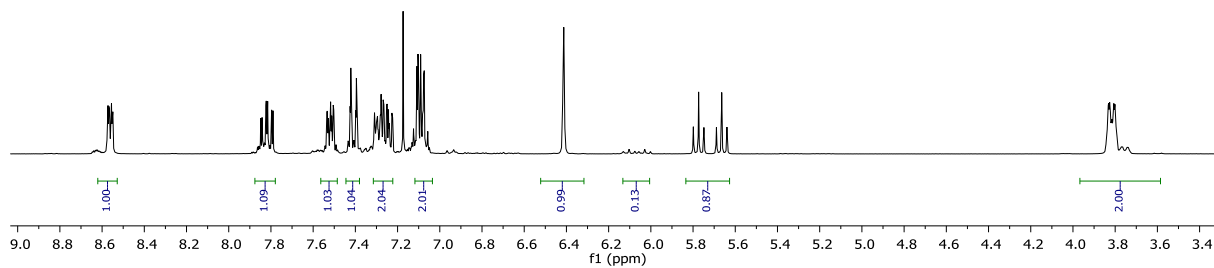
5.6.2.2 KIE Studies
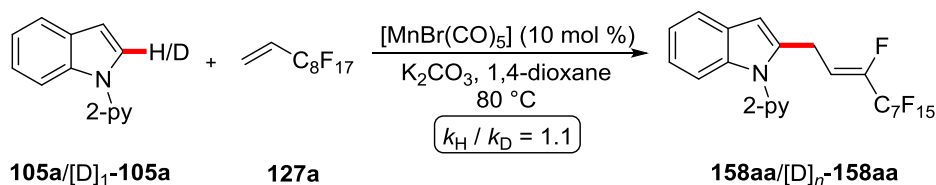
Two parallel reactions of **105a** or [D]$_1$-**105a** with **127a** were performed respectively to determine the KIE value by comparison of the initial reaction rates by GC-analysis with *n*-dodecane as the internal standard. A suspension of **105a** (97.1 mg, 0.50 mmol, 1.00 equiv) or [D]$_1$-**105a** (97.6 mg, 0.50 mmol, 1.00 equiv), **127a** (268 mg, 0.60 mmol, 1.20 equiv), [MnBr(CO)$_5$] (13.7 mg, 10 mol %), K$_2$CO$_3$ (69.1 mg, 1.00 equiv) and *n*-dodecane (30 μL) in 1,4-dioxane (2.00 mL) was stirred at 80 °C. Aliquots (30 μL) were periodically removed to provide the following conversions as determined by GC-analysis:

Table 43. Conversion-time table for determination of the KIE.

t / min	40	60	80	100	120
158aa / %	5.19	8.00	13.2	17.9	20.9
[D]$_n$-**158aa** / %	3.25	5.69	9.98	14.4	17.7

5.6.2.3 Experiments with Cyclometalated Complex 167

5.6.2.3.1 Complex 167 as Catalyst
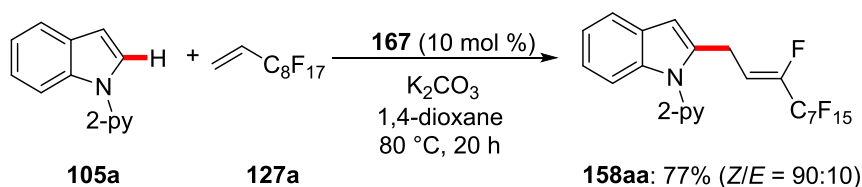
A suspension of indole **105a** (97.1 mg, 0.50 mmol, 1.00 equiv), 1*H*,1*H*,2*H*-perfluorodecene (**127a**) (268 mg, 0.60 mmol, 1.20 equiv), **167** (18.0 mg, 10.0 mol %) and K$_2$CO$_3$ (69.1 mg, 0.50 mmol, 1.00 equiv) in 1,4-dioxane (0.50 mL, 1.00 M) was stirred at 80 °C for 20 h. At ambient temperature, the solvent was removed *in vacuo* and the remaining residue was purified by column chromatography on silica gel to afford the desired product **158aa** (240 mg, 77%, *Z/E* = 90:10).

5.6.2.3.2   Stoichiometric Reaction with Complex 167
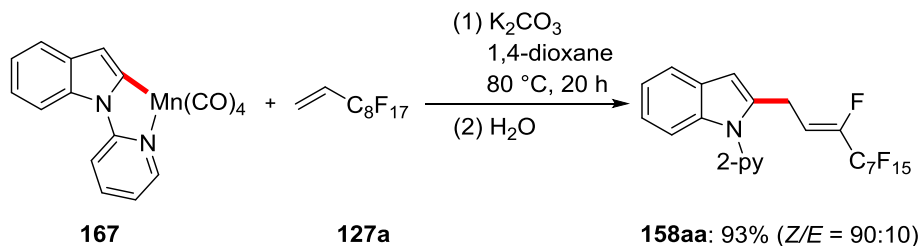
167   **127a**   **158aa**: 93% (*Z/E* = 90:10)

A suspension of complex **167** (72.0 mg, 0.20 mmol, 1.00 equiv), 1*H*,1*H*,2*H*-perfluorodecene (**127a**) (107 mg, 0.24 mmol, 1.20 equiv), K₂CO₃ (27.6 mg, 0.20 mmol, 1.00 equiv) in 1,4-dioxane (0.20 mL, 1.00 M) was stirred at 80 °C for 20 h. At ambient temperature, the reaction mixture was diluted with water (5.0 mL) and extracted with EtOAc (3 x 10 mL). After removal of the solvents *in vacuo*, the remaining residue was purified by column chromatography on silica gel to afford the desired product **158aa** (115 mg, 93%, *Z/E* = 90:10).

5.6.2.3.3   Stoichiometric Reaction with Complex 167 in the absence of K₂CO₃
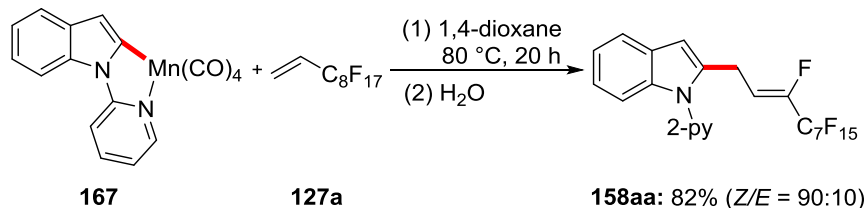
167   **127a**   **158aa:** 82% (*Z/E* = 90:10)

A suspension of complex **167** (72.0 mg, 0.20 mmol, 1.00 equiv), 1*H*,1*H*,2*H*-perfluorodecene (**127a**) (107 mg, 0.24 mmol, 1.20 equiv) in 1,4-dioxane (0.20 mL, 1.00 M) was stirred at 80 °C for 20 h. At ambient temperature, the reaction mixture was diluted with water (5.0 mL) and extracted with EtOAc (3 x 10 mL). The solvents were removed *in vacuo* and the remaining residue was purified by column chromatography on silica gel to afford the desired product **158aa** (102 mg, 82%, *Z/E* = 90:10)

6 References

[1]   a) M. Fujita, T. Hiyama, *J. Org. Chem.* **1988**, *53*, 5415–5421; b) T. Hiyama, M. Obayashi, I. Mori, H. Nozaki, *J. Org. Chem.* **1983**, *48*, 912–914.

[2]   a) R. J. P. Corriu, J. P. Masse, *J. Chem. Soc., Chem. Commun.* **1972**, 144; b) K. Tamao, K. Sumitani, M. Kumada, *J. Am. Chem. Soc.* **1972**, *94*, 4374–4376.

[3]   R. F. Heck, J. P. Nolley, *J. Org. Chem.* **1972**, *37*, 2320–2322.

[4]   S. Baba, E. Negishi, *J. Am. Chem. Soc.* **1976**, *98*, 6729–6731.

[5]   K. Sonogashira, *J. Organomet. Chem.* **2002**, *653*, 46–49.

[6]   a) D. Milstein, J. K. Stille, *J. Am. Chem. Soc.* **1978**, *100*, 3636–3638; b) M. Kosugi, Y. Shimizu, T. Migita, *Chem. Lett.* **1977**, *6*, 1423–1424; c) D. Azarian, S. S. Dua, C. Eaborn, D. R. M. Walton, *J. Organomet. Chem.* **1976**, *117*, C55–C57.

[7]   a) N. Miyaura, K. Yamada, A. Suzuki, *Tetrahedron Lett.* **1979**, *20*, 3437–3440; b) N. Miyaura, A. Suzuki, *J. Chem. Soc., Chem. Commun.* **1979**, 866–867.

[8]   a) C. A. Busacca, D. R. Fandrick, J. J. Song, C. H. Senanayake, *Adv. Synth. Catal.* **2011**, *353*, 1825–1864; b) C. Torborg, M. Beller, *Adv. Synth. Catal.* **2009**, *351*, 3027–3043; c) K. Nicolaou, P. G. Bulger, D. Sarlah, *Angew. Chem. Int. Ed.* **2005**, *44*, 4442–4489.

[9]   a) L. Ackermann, *Modern Arylation Methods*, Wiley-VCH, Weinheim, **2009**; b) A. de Meijere, F. Diederich, *Metal-Catalyzed Cross-Coupling Reactions*, Wiley-VCH, Weinheim, **2004**.

[10]   a) B. M. Trost, *Angew. Chem. Int. Ed.* **1995**, *34*, 259–281; b) B. M. Trost, *Science* **1991**, *254*, 1471–1477.

[11]   a) P. A. Wender, B. L. Miller, *Nature* **2009**, *460*, 197–201; b) P. A. Wender, M. P. Croatt, B. Witulski, *Tetrahedron* **2006**, *62*, 7505–7511.

[12]   a) L. Ackermann, A. R. Kapdi, H. K. Potukuchi, S. I. Kozhushkov, in *Handbook of Green Chemistry,* Ed.: P. T. Anastas, Wiley-VCH, Weinheim **2012**, pp. 259–305; b) P. Anastas, J. Warner, *Green Chemistry: Theory and Practice*, Oxford University Press, New York, **1998**.

[13]   For reviews on C–H functionalization: a) L. Vaccaro, S. Santoro, L. Ackermann, S. Kozhushkov, *Green Chem.* **2016**, *18*, 5025–5030; b) C. Borie, L. Ackermann, M. Nechab, *Chem. Soc. Rev.* **2016**, *45*, 1368–1386; c) B. Ye, N. Cramer, *Acc. Chem. Res.* **2015**, *48*, 1308–1318; d) K. Shin, H. Kim, S. Chang, *Acc. Chem. Res.* **2015**, *48*, 1040–1052; e) Y. Segawa, T. Maekawa, K. Itami, *Angew. Chem. Int. Ed.* **2015**, *54*, 66–81; f) B. Liu, F. Hu, B.-F. Shi, *ACS Catal.* **2015**, *5*, 1863–1881; g) O. Daugulis, J. Roane, L. D. Tran, *Acc. Chem. Res.* **2015**, *48*, 1053–1064; h) V. S. Thirunavukkarasu, S. I. Kozhushkov, L. Ackermann, *Chem. Commun.* **2014**, *50*, 29–39; i) S. A. Girard, T. Knauber, C.-J. Li, *Angew. Chem. Int. Ed.* **2014**, *53*, 74–100; j) S. De Sarkar, W. Liu, S. I. Kozhushkov, L. Ackermann, *Adv. Synth. Catal.* **2014**, *356*, 1461–1479; k) J. Wencel-Delord, F. Glorius, *Nat. Chem.* **2013**, *5*, 369–375; l) G. Rouquet, N. Chatani, *Angew. Chem. Int. Ed.* **2013**, *52*, 11726–11743; m) J. Yamaguchi, A. D. Yamaguchi, K. Itami, *Angew. Chem. Int. Ed.* **2012**, *51*, 8960–9009; n) C. S. Yeung, V. M. Dong, *Chem. Rev.* **2011**, *111*, 1215–1292; o) T. Satoh, M. Miura, *Chem. Eur. J.* **2010**, *16*, 11212–11222; p) R. Giri, B.-F. Shi, K. M. Engle, N. Maugel, J.-Q. Yu, *Chem. Soc. Rev.* **2009**, *38*, 3242–3272; q) R. G. Bergman, *Nature* **2007**, *446*, 391–393; r) D. Alberico, M. E. Scott, M. Lautens, *Chem. Rev.* **2007**, *107*, 174–238; s) L. Ackermann, *Synlett* **2007**, 507–526; t) L. Ackermann, in *Chelation-Assisted Arylation via C–H Bond Cleavage,* Ed.: N. Chatani, Springer Berlin, Heidelberg, **2007**, pp. 35–60.

[14]   a) W. Liu, L. Ackermann, *ACS Catal.* **2016**, *6*, 3743–3752; b) C. Wang, *Synlett* **2013**, *24*, 1606–1613.

[15]   a) M. Moselage, J. Li, L. Ackermann, *ACS Catal.* **2015**, *6*, 498–525; b) L. Ackermann, *J. Org. Chem.* **2014**, *79*, 8948–8954; c) K. Gao, N. Yoshikai, *Acc. Chem. Res.* **2014**, *47*, 1208–1219.

[16]   a) D. Balcells, E. Clot, O. Eisenstein, *Chem. Rev.* **2010**, *110*, 749–823; b) Y. Boutadla, D. L. Davies, S. A. Macgregor, A. I. Poblador-Bahamonde, *Dalton Trans.* **2009**, 5820–5831; c) Z. Lin, *Coord. Chem. Rev.* **2007**, *251*, 2280–2291.

[17]   a) T. R. Cundari, T. R. Klinckman, P. T. Wolczanski, *J. Am. Chem. Soc.* **2002**, *124*, 1481–
        1487; b) J. L. Bennett, P. T. Wolczanski, *J. Am. Chem. Soc.* **1997**, *119*, 10696–10719.
[18]   J. Kua, X. Xu, R. A. Periana, W. A. Goddard, *Organometallics* **2002**, *21*, 511–525.
[19]   J. Oxgaard, W. J. Tenn, R. J. Nielsen, R. A. Periana, W. A. Goddard, *Organometallics* **2007**,
        26, 1565–1567.
[20]   a) L. Ackermann, *Chem. Rev.* **2011**, *111*, 1315–1345; b) D. Lapointe, K. Fagnou, *Chem. Lett.*
        2010, *39*, 1118–1126; c) S. I. Gorelsky, D. Lapointe, K. Fagnou, *J. Am. Chem. Soc.* **2008**, *130*,
        10848–10849.
[21]   a) Y. Boutadla, D. L. Davies, S. A. Macgregor, A. I. Poblador-Bahamonde, *Dalton Trans.*
        2009, 5887–5893; b) D. L. Davies, S. M. Donald, S. A. Macgregor, *J. Am. Chem. Soc.* **2005**,
        127, 13754–13755.
[22]   a) D. García-Cuadrado, A. A. Braga, F. Maseras, A. M. Echavarren, *J. Am. Chem. Soc.* **2006**,
        128, 1066–1067; b) L.-C. Campeau, M. Parisien, A. Jean, K. Fagnou, *J. Am. Chem. Soc.* **2006**,
        128, 581–590; c) L.-C. Campeau, M. Parisien, M. Leblanc, K. Fagnou, *J. Am. Chem. Soc.*
        2004, *126*, 9186–9187.
[23]   a) K. Raghuvanshi, D. Zell, L. Ackermann, *Org. Lett.* **2017**, *19*, 1278–1281; b) K.
        Raghuvanshi, D. Zell, K. Rauch, L. Ackermann, *ACS Catal.* **2016**, *6*, 3172–3175; c) H. Wang,
        M. Moselage, M. J. González, L. Ackermann, *ACS Catal.* **2016**, *6*, 2705–2709; d) R. Mei, J.
        Loup, L. Ackermann, *ACS Catal.* **2016**, *6*, 793–797; e) W. Ma, R. Mei, G. Tenti, L.
        Ackermann, *Chem. Eur. J.* **2014**, *20*, 15248–15251.
[24]   S. De Sarkar, W. Liu, S. I. Kozhushkov, L. Ackermann, *Adv. Synth. Catal.* **2014**, *356*, 1461–
        1479.
[25]   a) W. Ma, P. Gandeepan, J. Li, L. Ackermann, *Org. Chem. Front.* **2017**, DOI:
        10.1039/C1037QO00134G; b) F. Zhang, D. R. Spring, *Chem. Soc. Rev.* **2014**, *43*, 6906–6919.
[26]   a) M. Seki, *Org. Process Res. Dev.* **2016**, *20*, 867–877; b) L. Ackermann, *Org. Process Res.
        Dev.* **2015**, *19*, 260–269; c) J. Yamaguchi, A. D. Yamaguchi, K. Itami, *Angew. Chem. Int. Ed.*
        2012, *51*, 8960–9009; d) J.-Q. Yu, Z. Shi, *C–H Activation*, Springer Berlin, Heidelberg, **2010**.
[27]   a) L. Ackermann, *Acc. Chem. Res.* **2014**, *47*, 281–295; b) P. B. Arockiam, C. Bruneau, P. H.
        Dixneuf, *Chem. Rev.* **2012**, *112*, 5879–5918.
[28]   S. Oi, S. Fukita, N. Hirata, N. Watanuki, S. Miyano, Y. Inoue, *Org. Lett.* **2001**, *3*, 2579–2581.
[29]   S. Oi, R. Funayama, T. Hattori, Y. Inoue, *Tetrahedron* **2008**, *64*, 6051–6059.
[30]   S. Oi, Y. Ogino, S. Fukita, Y. Inoue, *Org. Lett.* **2002**, *4*, 1783–1785.
[31]   S. Oi, E. Aizawa, Y. Ogino, Y. Inoue, *J. Org. Chem.* **2005**, *70*, 3113–3119.
[32]   S. Oi, K. Sakai, Y. Inoue, *Org. Lett.* **2005**, *7*, 4009–4011.
[33]   S. G. Ouellet, A. Roy, C. Molinaro, R. Angelaud, J.-F. Marcoux, P. D. O'Shea, I. W. Davies,
        J. Org. Chem. **2011**, *76*, 1436–1439.
[34]   F. Kakiuchi, S. Kan, K. Igi, N. Chatani, S. Murai, *J. Am. Chem. Soc.* **2003**, *125*, 1698–1699.
[35]   F. Kakiuchi, Y. Matsuura, S. Kan, N. Chatani, *J. Am. Chem. Soc.* **2005**, *127*, 5936–5945.
[36]   a) L. Ackermann, R. Vicente, A. Althammer, *Org. Lett.* **2008**, *10*, 2299–2302; b) L.
        Ackermann, A. Althammer, R. Born, *Angew. Chem. Int. Ed.* **2006**, *45*, 2619–2622; c) L.
        Ackermann, *Org. Lett.* **2005**, *7*, 3123–3125.
[37]   a) S. I. Kozhushkov, H. K. Potukuchi, L. Ackermann, *Catal. Sci. Technol.* **2013**, *3*, 562–571;
        b) J. Kerr, *Chem. Rev.* **1966**, *66*, 465–500.
[38]   V. Sokolov, L. L. Troitskaya, O. A. Reutov, *J. Organomet. Chem.* **1979**, *182*, 537–546.
[39]   a) M. Lafrance, S. I. Gorelsky, K. Fagnou, *J. Am. Chem. Soc.* **2007**, *129*, 14570–14571; b) M.
        Lafrance, K. Fagnou, *J. Am. Chem. Soc.* **2006**, *128*, 16496–16497.
[40]   a) H. Nandivada, X. Jiang, J. Lahann, *Adv. Mater.* **2007**, *19*, 2197–2208; b) Y. L. Angell, K.
        Burgess, *Chem. Soc. Rev.* **2007**, *36*, 1674–1689.
[41]   F. Požgan, P. H. Dixneuf, *Adv. Synth. Catal.* **2009**, *351*, 1737–1743.
[42]   L. Ackermann, R. Vicente, H. K. Potukuchi, V. Pirovano, *Org. Lett.* **2010**, *12*, 5032–5035.
[43]   L. Ackermann, A. V. Lygin, *Org. Lett.* **2011**, *13*, 3332–3335.
[44]   a) P. B. Arockiam, C. Fischmeister, C. Bruneau, P. H. Dixneuf, *Angew. Chem. Int. Ed.* **2010**,
        122, 6629–6632; b) L. Ackermann, J. Pospech, H. K. Potukuchi, *Org. Lett.* **2012**, *14*, 2146–
        2149.

[45]   a) M. Seki, *Synthesis* **2012**, *44*, 3231–3237; b) M. Seki, M. Nagahama, *J. Org. Chem.* **2011**, *76*, 10198–10206.

[46]   M. K. Lakshman, A. C. Deb, R. R. Chamala, P. Pradhan, R. Pratap, *Angew. Chem. Int. Ed.* **2011**, *50*, 11400–11404.

[47]   a) L. Ackermann, A. Althammer, R. Born, *Tetrahedron* **2008**, *64*, 6115–6124; b) L. Ackermann, A. Althammer, R. Born, *Synlett* **2007**, 2833–2836.

[48]   N. Luo, Z. Yu, *Chem. Eur. J.* **2010**, *16*, 787–791.

[49]   O. Roelen, Chemische Verwertungsgesellschaft Oberhausen mbH, DE 849548, **1938/1952**.

[50]   F. Hebrard, P. Kalck, *Chem. Rev.* **2009**, *109*, 4272–4282.

[51]   I. Khand, G. Knox, P. Pauson, W. Watts, *J. Chem. Soc. D, Chem. Commun.* **1971**, 36.

[52]   A. Y. Khodakov, W. Chu, P. Fongarland, *Chem. Rev.* **2007**, *107*, 1692–1744.

[53]   M. Hawkins, *Appl. Earth Sci.* **2001**, *110*, 66–70.

[54]   D. S. Avila, R. L. Puntel, M. Aschner, in *Interrelations between Essential Metal Ions and Human Diseases, Vol. 13,* Eds.: A. Sigel, H. Sigel, K. O. R. Sigel, Springer Netherlands, Dordrecht, **2013**, pp. 199–227.

[55]   a) S. Murahashi, S. Horiie, *J. Am. Chem. Soc.* **1956**, *78*, 4816–4817; b) S. Murahashi, *J. Am. Chem. Soc.* **1955**, *77*, 6403–6404.

[56]   H. F. Klein, S. Schneider, M. He, U. Floerke, H. J. Haupt, *Eur. J. Inorg. Chem.* **2000**, 2295–2301.

[57]   a) R. Beck, H. Sun, X. Li, S. Camadanli, H. F. Klein, *Eur. J. Inorg. Chem.* **2008**, 3253–3257; b) S. Camadanli, R. Beck, U. Flörke, H.-F. Klein, *Dalton Trans.* **2008**, 5701–5704; c) H. F. Klein, S. Camadanli, R. Beck, D. Leukel, U. Flörke, *Angew. Chem. Int. Ed.* **2005**, *44*, 975–977; d) H. F. Klein, R. Beck, U. Flörke, H. J. Haupt, *Eur. J. Inorg. Chem.* **2003**, 1380–1387.

[58]   U. Koelle, B. Fuss, M. Rajasekharan, B. Ramakrishna, J. Ammeter, M. Böhm, *J. Am. Chem. Soc.* **1984**, *106*, 4152–4160.

[59]   a) G. Song, F. Wang, X. Li, *Chem. Soc. Rev.* **2012**, *41*, 3651–3678; b) F. W. Patureau, J. Wencel-Delord, F. Glorius, *Aldrichim. Acta* **2012**, *45*, 31–41.

[60]   T. Yoshino, H. Ikemoto, S. Matsunaga, M. Kanai, *Angew. Chem. Int. Ed.* **2013**, *52*, 2207–2211.

[61]   a) M. E. Tauchert, C. D. Incarvito, A. L. Rheingold, R. G. Bergman, J. A. Ellman, *J. Am. Chem. Soc.* **2012**, *134*, 1482; b) Y. Li, X.-S. Zhang, H. Li, W.-H. Wang, K. Chen, B.-J. Li, Z.-J. Shi, *Chem. Sci.* **2012**, *3*, 1634–1639.

[62]   A. Allred, *J. Inorg. Nucl. Chem.* **1961**, *17*, 215–221.

[63]   T. Yoshino, H. Ikemoto, S. Matsunaga, M. Kanai, *Chem. Eur. J.* **2013**, *19*, 9142–9146.

[64]   J. R. Hummel, J. A. Ellman, *J. Am. Chem. Soc.* **2015**, *137*, 490–498.

[65]   H. Wang, J. Koeller, W. Liu, L. Ackermann, *Chem. Eur. J.* **2015**, *21*, 15525–15528.

[66]   J. Park, S. Chang, *Angew. Chem. Int. Ed.* **2015**, *54*, 14103–14107.

[67]   Y. Liang, Y. F. Liang, C. Tang, Y. Yuan, N. Jiao, *Chem. Eur. J.* **2015**, *21*, 16395–16399.

[68]   B. Sun, T. Yoshino, M. Kanai, S. Matsunaga, *Angew. Chem. Int. Ed.* **2015**, *54*, 12968–12972.

[69]   M. Sen, D. Kalsi, B. Sundararaju, *Chem. Eur. J.* **2015**, *21*, 15529–15533.

[70]   N. R. Candeias, L. C. Branco, P. M. P. Gois, C. A. Afonso, A. F. Trindade, *Chem. Rev.* **2009**, *109*, 2703–2802.

[71]   B. Sun, T. Yoshino, S. Matsunaga, M. Kanai, *Adv. Synth. Catal.* **2014**, *356*, 1491–1495.

[72]   B. Sun, T. Yoshino, S. Matsunaga, M. Kanai, *Chem. Commun.* **2015**, *51*, 4659–4661.

[73]   P. Anbarasan, T. Schareina, M. Beller, *Chem. Soc. Rev.* **2011**, *40*, 5049–5067.

[74]   J. Li, L. Ackermann, *Angew. Chem. Int. Ed.* **2015**, *54*, 3635–3638.

[75]   D.-G. Yu, T. Gensch, F. de Azambuja, S. Vásquez-Céspedes, F. Glorius, *J. Am. Chem. Soc.* **2014**, *136*, 17722–17725.

[76]   U. Kazmaier, *Transition Metal Catalyzed Enantioselective Allylic Substitution in Organic Synthesis, Vol. 38*, Springer Berlin, Heidelberg, **2011**.

[77]   M. Moselage, N. Sauermann, J. Koeller, W. Liu, D. Gelman, L. Ackermann, *Synlett* **2015**, *26*, 1596–1600.

[78]   Y. Suzuki, B. Sun, K. Sakata, T. Yoshino, S. Matsunaga, M. Kanai, *Angew. Chem. Int. Ed.* **2015**, *54*, 9944–9947.

[79]   T. Gensch, S. Vásquez-Céspedes, D.-G. Yu, F. Glorius, *Org. Lett.* **2015**, *17*, 3714–3717.

[80]   G. Halbritter, F. Knoch, A. Wolski, H. Kisch, *Angew. Chem. Int. Ed.* **1994**, *33*, 1603–1605.

[81]   K. Gao, P.-S. Lee, T. Fujita, N. Yoshikai, *J. Am. Chem. Soc.* **2010**, *132*, 12249–12251.

[82]   P.-S. Lee, T. Fujita, N. Yoshikai, *J. Am. Chem. Soc.* **2011**, *133*, 17283–17295.

[83]   Z. Ding, N. Yoshikai, *Angew. Chem. Int. Ed.* **2012**, *51*, 4698–4701.

[84]   K. Gao, N. Yoshikai, *J. Am. Chem. Soc.* **2011**, *133*, 400–402.

[85]   L. Ilies, Q. Chen, X. Zeng, E. Nakamura, *J. Am. Chem. Soc.* **2011**, *133*, 5221–5223.

[86]   V. Galamb, G. Palyi, F. Ungvary, L. Marko, R. Boese, G. Schmid, *J. Am. Chem. Soc.* **1986**, *108*, 3344–3351.

[87]   Q. Chen, L. Ilies, E. Nakamura, *J. Am. Chem. Soc.* **2011**, *133*, 428–429.

[88]   P.-S. Lee, N. Yoshikai, *Org. Lett.* **2015**, *17*, 22–25.

[89]   J. F. Teichert, B. L. Feringa, *Angew. Chem. Int. Ed.* **2010**, *49*, 2486–2528.

[90]   D. J. Schipper, M. Hutchinson, K. Fagnou, *J. Am. Chem. Soc.* **2010**, *132*, 6910–6911.

[91]   H. Ikemoto, T. Yoshino, K. Sakata, S. Matsunaga, M. Kanai, *J. Am. Chem. Soc.* **2014**, *136*, 5424–5431.

[92]   S. B. Goldhaber, *Regul. Toxicol. Pharm.* **2003**, *38*, 232–242.

[93]   J. Emsley, *Oxygen. Nature's Building Blocks: An A–Z Guide to the Elements*, Oxford University Press, Oxford, **2001**.

[94]   M. Bruce, M. Iqbal, F. Stone, *J. Chem . Soc. A: Inorg. Phys. Theor.* **1970**, 3204–3209.

[95]   L. S. Liebeskind, J. R. Gasdaska, J. S. McCallum, S. J. Tremont, *J. Org. Chem.* **1989**, *54*, 669–677.

[96]   a) G. J. Depree, L. Main, B. K. Nicholson, *J. Organomet. Chem.* **1998**, *551*, 281–291; b) W. Tully, L. Main, B. K. Nicholson, *J. Organomet. Chem.* **1995**, *503*, 75–92.

[97]   R. C. Cambie, M. R. Metzler, P. S. Rutledge, P. D. Woodgate, *J. Organomet. Chem.* **1992**, *429*, 41–57.

[98]   Y. Kuninobu, Y. Nishina, T. Takeuchi, K. Takai, *Angew. Chem. Int. Ed.* **2007**, *46*, 6518–6520.

[99]   B. Zhou, Y. Hu, C. Wang, *Angew. Chem. Int. Ed.* **2015**, *54*, 13659–13663.

[100]   W. Liu, J. Bang, Y. Zhang, L. Ackermann, *Angew. Chem. Int. Ed.* **2015**, *54*, 14137–14140.

[101]   W. Liu, S. C. Richter, R. Mei, M. Feldt, L. Ackermann, *Chem. Eur. J.* **2016**, *22*, 17958–17961.

[102]   P. Anbarasan, H. Neumann, M. Beller, *Angew. Chem. Int. Ed.* **2011**, *50*, 519–522.

[103]   B. Zhou, H. Chen, C. Wang, *J. Am. Chem. Soc.* **2013**, *135*, 1264–1267.

[104]   B. Zhou, P. Ma, H. Chen, C. Wang, *Chem. Commun.* **2014**, *50*, 14558–14561.

[105]   R. He, Z. T. Huang, Q. Y. Zheng, C. Wang, *Angew. Chem. Int. Ed.* **2014**, *53*, 4950–4953.

[106]   W. Liu, D. Zell, M. John, L. Ackermann, *Angew. Chem. Int. Ed.* **2015**, *54*, 4092–4096.

[107]   a) L. Kiss, F. Fülöp, *Chem. Rev.* **2013**, *114*, 1116–1169; b) D. Seebach, J. Gardiner, *Acc. Chem. Res.* **2008**, *41*, 1366–1375.

[108]   W. Liu, S. C. Richter, Y. Zhang, L. Ackermann, *Angew. Chem. Int. Ed.* **2016**, *55*, 7747–7750.

[109]   a) L. Ackermann, *Org. Process Res. Dev.* **2015**, *19*, 260–269; b) L. Ackermann, *Acc. Chem. Res.* **2013**, *47*, 281–295.

[110]   a) L. Souillart, N. Cramer, *Chem. Rev.* **2015**, *115*, 9410–9464; b) M. Murakami, T. Matsuda, *Chem. Commun.* **2011**, *47*, 1100–1105; c) V. Ritleng, C. Sirlin, M. Pfeffer, *Chem. Rev.* **2002**, *102*, 1731–1770.

[111]   a) T. F. Schneider, J. Kaschel, D. B. Werz, *Angew. Chem. Int. Ed.* **2014**, *53*, 5504–5523; b) M. Rubin, M. Rubina, V. Gevorgyan, *Chem. Rev.* **2007**, *107*, 3117–3179.

[112]   N. A. Foley, J. P. Lee, Z. Ke, T. B. Gunnoe, T. R. Cundari, *Acc. Chem. Res.* **2009**, *42*, 585–597.

[113]   a) G. M. Crisenza, O. O. Sokolova, J. F. Bower, *Angew. Chem. Int. Ed.* **2015**, *54*, 14866–14870; b) G. M. Crisenza, N. G. McCreanor, J. F. Bower, *J. Am. Chem. Soc.* **2014**, *136*, 10258–10261.

[114]   K. Gao, N. Yoshikai, *J. Am. Chem. Soc.* **2010**, *133*, 400–402.

[115]   H. Amii, K. Uneyama, *Chem. Rev.* **2009**, *109*, 2119–2183.

[116]   a) W. K. Hagmann, *J. Med. Chem.* **2008**, *51*, 4359–4369; b) K. Müller, C. Faeh, F. Diederich, *Science* **2007**, *317*, 1881–1886; c) P. Kirsch, *Modern Fluoroorganic Chemistry: Synthesis, Reactivity, Applications*, Wiley-VCH, Weinheim, **2004**.

[117] a) Q. Lu, F. J. Klauck, F. Glorius, *Chem. Sci.* **2017**, *8*, 3379–3383; b) D. Zell, Q. Bu, M. Feldt, L. Ackermann, *Angew. Chem. Int. Ed.* **2016**, *55*, 7408–7412; c) J.-Q. Wu, Z.-P. Qiu, S.-S. Zhang, J.-G. Liu, Y.-X. Lao, L.-Q. Gu, Z.-S. Huang, J. Li, H. Wang, *Chem. Commun.* **2015**, *51*, 77–80; d) T. H. Meyer, W. Liu, M. Feldt, A. Wuttke, R. A. Mata, L. Ackermann, *Chem. Eur. J.* **2017**, *23*, 5443–5447.

[118] Selected examples: a) G. Yin, X. Mu, G. Liu, *Acc. Chem. Res.* **2016**, *49*, 2413–2423; b) T. Ahrens, J. Kohlmann, M. Ahrens, T. Braun, *Chem. Rev.* **2015**, *115*, 931–972; c) H. Egami, M. Sodeoka, *Angew. Chem. Int. Ed.* **2014**, *53*, 8294–8308; d) T. Besset, T. Poisson, X. Pannecoucke, *Chem. Eur. J.* **2014**, *20*, 16830–16845; e) T. Liang, C. N. Neumann, T. Ritter, *Angew. Chem. Int. Ed.* **2013**, *52*, 8214–8264; f) J. Wang, M. Sánchez-Roselló, J. L. Aceña, C. del Pozo, A. E. Sorochinsky, S. Fustero, V. A. Soloshonok, H. Liu, *Chem. Rev.* **2013**, *114*, 2432; g) T. Stahl, H. F. T. Klare, M. Oestreich, *ACS Catal.* **2013**, *3*, 1578–1587; h) T. Furuya, A. S. Kamlet, T. Ritter, *Nature* **2011**, *473*, 470–477; i) T. Braun, F. Wehmeier, *Eur. J. Inorg. Chem.* **2011**, *2011*, 613–625; j) H. Amii, K. Uneyama, *Chem. Rev.* **2009**, *109*, 2119–2183; k) K. Müller, C. Faeh, F. Diederich, *Science* **2007**, *317*, 1881–1886; l) T. Braun, R. N. Perutz, *Chem. Commun.* **2002**, 2749–2757.

[119] a) D. J. Harrison, G. M. Lee, M. C. Leclerc, I. Korobkov, R. T. Baker, *J. Am. Chem. Soc.* **2013**, *135*, 18296–18299; b) M. F. Kühnel, D. Lentz, *Angew. Chem. Int. Ed.* **2010**, *49*, 2933–2936; c) A. A. Peterson, K. McNeill, *Organometallics* **2006**, *25*, 4938–4940; d) K. Sakoda, J. Mihara, J. Ichikawa, *Chem. Commun.* **2005**, 4684–4686; e) L. A. Gharat, A. R. Martin, *Heterocycles* **1996**, *1*, 185–189; f) W. Heitz, A. Knebelkamp, *Macromol. Rapid Commun.* **1991**, *12*, 69–75.

[120] Y. F. Liang, L. Massignan, W. Liu, L. Ackermann, *Chem. Eur. J.* **2016**, *22*, 14856–14859.

[121] a) J.-R. Pouliot, F. Grenier, J. T. Blaskovits, S. Beaupré, M. Leclerc, *Chem. Rev.* **2016**, *116*, 14225–14274; b) Y. Segawa, T. Maekawa, K. Itami, *Angew. Chem. Int. Ed.* **2015**, *54*, 66–81; c) L. G. Mercier, M. Leclerc, *Acc. Chem. Res.* **2013**, *46*, 1597–1605; d) W. Lu, J. Kuwabara, T. Kanbara, *Macromol. Rapid Commun.* **2013**, *34*, 1151–1156.

[122] a) E. Tomás-Mendivil, V. Cadierno, M. I. Menéndez, R. López, *Chem. Eur. J.* **2015**, *21*, 16874–16886; b) S. M. M. Knapp, T. J. Sherbow, R. B. Yelle, J. J. Juliette, D. R. Tyler, *Organometallics* **2013**, *32*, 3744–3752; c) E. Y. Chan, Q.-F. Zhang, Y.-K. Sau, S. M. Lo, H. H. Sung, I. D. Williams, R. K. Haynes, W.-H. Leung, *Inorg. Chem.* **2004**, *43*, 4921–4926.

[123] D. Zell, S. Warratz, D. Gelman, S. J. Garden, L. Ackermann, *Chem. Eur. J.* **2016**, *22*, 1248–1252.

[124] J. P. Wagner, P. R. Schreiner, *Angew. Chem. Int. Ed.* **2015**, *54*, 12274–12296, and references cited therein.

[125] L. Ackermann, P. Novák, R. Vicente, V. Pirovano, H. K. Potukuchi, *Synthesis* **2010**, *2010*, 2245–2253.

[126] A. B. Flynn, W. W. Ogilvie, *Chem. Rev.* **2007**, *107*, 4698–4745, and references cited therein.

[127] S. Warratz, PhD thesis, Georg-August-Universität Göttingen **2016**.

[128] T. Tsou, J. Kochi, *J. Am. Chem. Soc.* **1979**, *101*, 6319–6332.

[129] G. Manolikakes, P. Knochel, *Angew. Chem. Int. Ed.* **2009**, *48*, 205–209.

[130] T. L. Hall, M. F. Lappert, P. W. Lednor, *J. Chem. Soc., Dalton Trans.* **1980**, 1448–1456.

[131] J. Hubrich, L. Ackermann, *Eur. J. Org. Chem.* **2016**, 3700–3704.

[132] P. L. Anelli, F. Montanari, S. Quici, *Org. Synth.* **1990**, *49*, 212.

[133] L. P. Hammett, *J. Am. Chem. Soc.* **1937**, *640*, 96–103.

[134] C. Hansch, A. Leo, *Substituent Constants for Correlation Analysis in Chemistry and Biology*, John Wiley & Sons Inc., Hoboken, New Jersey, **1979**.

[135] a) Z. Ruan, S. Lackner, L. Ackermann, *Angew. Chem. Int. Ed.* **2016**, *55*, 3153–3157; b) Y. Aihara, N. Chatani, *Chem. Sci.* **2013**, *4*, 664–670.

[136] E. M. Simmons, J. F. Hartwig, *Angew. Chem. Int. Ed.* **2012**, *51*, 3066–3072.

[137] a) M. Brasse, J. Cámpora, J. A. Ellman, R. G. Bergman, *J. Am. Chem. Soc.* **2013**, *135*, 6427; b) Y. Tan, F. Barrios-Landeros, J. F. Hartwig, *J. Am. Chem. Soc.* **2012**, *134*, 3683; c) E. V. Anslyn, D. A. Dougherty, *Modern Physical Organic Chemistry*, University Science Books, Sausalito, **2006**.

[138] M. Simonetti, G. Perry, X. C. Cambeiro, F. Juliá-Hernández, J. N. Arokianathar, I. Larrosa, *J. Am. Chem. Soc.* **2016**, *138*, 3596–3606.

[139] C. Wang, *Synlett* **2013**, *24*, 1606–1613.

[140] a) X. Wang, A. Lerchen, F. Glorius, *Org. Lett.* **2016**, *18*, 2090–2093; b) D. Zhao, J. H. Kim, L. Stegemann, C. A. Strassert, F. Glorius, *Angew. Chem. Int. Ed.* **2015**, *54*, 4508–4511.

[141] X.-G. Liu, S.-S. Zhang, J.-Q. Wu, Q. Li, H. Wang, *Tetrahedron Lett.* **2015**, *56*, 4093–4095.

[142] S. Grimme, A. Hansen, J. G. Brandenburg, C. Bannwarth, *Chem. Rev.* **2016**, *116*, 5105–5154.

[143] M. Feldt, L. Ackermann, unpublished results.

[144] H. McNab, *Chem. Soc. Rev.* **1978**, *7*, 345–358, and references cited therein.

[145] P. Gandeepan, J. Koeller, L. Ackermann, *ACS Catal.* **2017**, *7*, 1030–1034.

[146] a) T. Zhou, Y. Wang, B. Li, B. Wang, *Org. Lett.* **2016**, *18*, 5066–5069; b) L. Xu, C. Zhang, Y. He, L. Tan, D. Ma, *Angew. Chem. Int. Ed.* **2016**, *55*, 321–325.

[147] L. Xu, L. Tan, D. Ma, *J. Org. Chem.* **2016**, *81*, 10476–10483.

[148] I. Krossing, I. Raabe, *Angew. Chem. Int. Ed.* **2004**, *43*, 2066–2090.

[149] S. Kozuch, S. Shaik, *Acc. Chem. Res.* **2010**, *44*, 101–110.

[150] a) G. M. Crisenza, J. F. Bower, *Chem. Lett.* **2016**, *45*, 2–9; b) F. Kakiuchi, S. Murai, *Acc. Chem. Res.* **2002**, *35*, 826–834.

[151] a) Y. Ebe, T. Nishimura, *J. Am. Chem. Soc.* **2015**, *137*, 5899–5902; b) B. Ye, P. A. Donets, N. Cramer, *Angew. Chem. Int. Ed.* **2014**, *53*, 507–511; c) P. S. Lee, N. Yoshikai, *Angew. Chem. Int. Ed.* **2013**, *52*, 1240–1244; d) S. Pan, N. Ryu, T. Shibata, *J. Am. Chem. Soc.* **2012**, *134*, 17474–17477; e) Y. Nakao, N. Kashihara, K. S. Kanyiva, T. Hiyama, *Angew. Chem. Int. Ed.* **2010**, *49*, 4451–4454; f) T. Mukai, K. Hirano, T. Satoh, M. Miura, *J. Org. Chem.* **2009**, *74*, 6410–6413; g) Y. Uchimaru, *Chem. Commun.* **1999**, 1133–1134.

[152] V. Müller, L. Ackermann, unpublished results.

[153] E. V. Dehmlow, M. Lissel, *Synthesis* **1979**, *5*, 372–374.

[154] A. Isidro Llobet, M. Álvarez Domingo, F. Albericio Palomera, *Chem. Rev.* **2009**, *109* 2455–2504.

[155] J. Li, S. Warratz, D. Zell, S. De Sarkar, E. E. Ishikawa, L. Ackermann, *J. Am. Chem. Soc.* **2015**, *137*, 13894–13901.

[156] a) G.-J. Cheng, Y.-F. Yang, P. Liu, P. Chen, T.-Y. Sun, G. Li, X. Zhang, K. Houk, J.-Q. Yu, Y.-D. Wu, *J. Am. Chem. Soc.* **2014**, *136*, 894–897; b) G. Li, D. Leow, L. Wan, J. Q. Yu, *Angew. Chem. Int. Ed.* **2013**, *52*, 1245–1247.

[157] B. F. Shi, N. Maugel, Y. H. Zhang, J. Q. Yu, *Angew. Chem. Int. Ed.* **2008**, *47*, 4882–4886.

[158] B. Ye, N. Cramer, *Angew. Chem. Int. Ed.* **2014**, *53*, 7896–7899.

[159] J. Zheng, S.-B. Wang, C. Zheng, S.-L. You, *J. Am. Chem. Soc.* **2015**, *137*, 4880–4883.

[160] S. Reddy Chidipudi, D. J. Burns, I. Khan, H. W. Lam, *Angew. Chem. Int. Ed.* **2015**, *54*, 13975–13979.

[161] D. Zell, M. Bursch, V. Müller, S. Grimme, L. Ackermann, *Angew. Chem. Int. Ed.* **2017**, *56*, under revision.

[162] a) D. Zell, F. Pescialioli, V. Müller, L. Ackermann, unpublished results; b) V. Müller, Master-Thesis, Georg-August-Universität Göttingen, **2016**.

[163] a) M. Sen, B. Emayavaramban, N. Barsu, J. R. Premkumar, B. Sundararaju, *ACS Catal.* **2016**, *6*, 2792–2796; b) J. Zhang, H. Chen, C. Lin, Z. Liu, C. Wang, Y. Zhang, *J. Am. Chem. Soc.* **2015**, *137*, 12990–12996.

[164] a) G. l. Erdogan, D. B. Grotjahn, *J. Am. Chem. Soc.* **2009**, *131*, 10354–10355; b) J. Zhou, J. F. Hartwig, *Angew. Chem. Int. Ed.* **2008**, *47*, 5783–5787; c) C. M. Yung, M. B. Skaddan, R. G. Bergman, *J. Am. Chem. Soc.* **2004**, *126*, 13033–13043.

[165] K. J. Laidler, in *Chemical Kinetics*, McGraw-Hill, New York, **1977**, pp. 310–311.

[166] S. Arrhenius, *Z. Phys. Chem.* **1889**, *4*, 226–248.

[167] J. Wang, M. Sánchez-Roselló, J. L. Aceña, C. del Pozo, A. E. Sorochinsky, S. Fustero, V. A. Soloshonok, H. Liu, *Chem. Rev.* **2014**, *114*, 2432–2506.

[168] a) C.-Q. Wang, L. Ye, C. Feng, T.-P. Loh, *J. Am. Chem. Soc.* **2017**, *139*, 1762–1765; b) J.-Q. Wu, S.-S. Zhang, H. Gao, Z. Qi, C.-J. Zhou, W.-W. Ji, Y. Liu, Y. Chen, Q. Li, X. Li, *J. Am. Chem. Soc.* **2017**, *139*, 3537–3545; c) L. Kong, X. Zhou, X. Li, *Org. Lett.* **2016**; d) P. Tian, C. Feng, T.-P. Loh, *Nat. Commun.* **2015**, *6*, 7472.

[169]   J. A. Gladysz, D. P. Curran, I. T. Horváth, *Handbook of Fluorous Chemistry*, John Wiley & Sons Inc., Hoboken, New Jersey, **2006**.

[170]   A. Berkessel, J. A. Adrio, D. Hüttenhain, J. M. Neudörfl, *J. Am. Chem. Soc.* **2006**, *128*, 8421–8426.

[171]   D. A. Wynn, M. M. Roth, B. D. Pollard, *Talanta* **1984**, *31*, 1036–1040.

[172]   a) T. K. Hyster, D. M. Dalton, T. Rovis, *Chem. Sci.* **2015**, *6*, 254–258; b) T. Piou, T. Rovis, *J. Am. Chem. Soc.* **2014**, *136*, 11292.

[173]   a) G. Landelle, M. Bergeron, M.-O. Turcotte-Savard, J.-F. Paquin, *Chem. Soc. Rev.* **2011**, *40*, 2867–2908; b) C. E. Jakobsche, G. Peris, S. J. Miller, *Angew. Chem. Int. Ed.* **2008**, *47*, 6707–6711.

[174]   D. Zell, V. Müller, U. Dhawa, M. Bursch, R. R. Presa, S. Grimme, L. Ackermann, *Chem. Eur. J.* **2017**, *23*, submitted.

[175]   L. Ackermann, N. Hofmann, R. Vicente, *Org. Lett.* **2011**, *13*, 1875–1877.

[176]   D. Zell, U. Dhawa, V. Müller, M. Bursch, S. Grimme, L. Ackermann, *ACS Catal.* **2017**, *7*, 4209–4213.

[177]   a) M. Moselage, J. Li, F. Kramm, L. Ackermann, *Angew. Chem. Int. Ed.* **2017**, *56*, 5341–5344; b) C. Kashima, S. Hibi, T. Maruyama, K. Harada, Y. Omote, *J. Heterocycl. Chem.* **1987**, *24*, 637–639.

[178]   D. García-Cuadrado, P. de Mendoza, A. A. Braga, F. Maseras, A. M. Echavarren, *J. Am. Chem. Soc.* **2007**, *129*, 6880–6886.

[179]   a) H. Clavier, S. P. Nolan, *Chem. Commun.* **2010**, *46*, 841–861; b) A. C. Hillier, W. J. Sommer, B. S. Yong, J. L. Petersen, L. Cavallo, S. P. Nolan, *Organometallics* **2003**, *22*, 4322–4326.

[180]   J. L. R. Williams, R. E. Adel, J. M. Carlson, G. A. Reynolds, D. G. Borden, J. A. Ford Jr., *J. Org. Chem.* **1963**, *28*, 387–390.

[181]   G. Ghattas, D. Chen, F. Pan, J. Klankermayer, *Dalton Trans.* **2012**, *41*, 9026–9028.

[182]   a) V. K. Tiwari, N. Kamal, M. Kapur, *Org. Lett.* **2015**, *17*, 1766–1769; b) S. Xu, X. Huang, X. Hong, B. Xu, *Org. Lett.* **2012**, *14*, 4614–4617.

[183]   a) J. Y. Kim, S. H. Park, J. Ryu, S. H. Cho, S. H. Kim, S. Chang, *J. Am. Chem. Soc.* **2012**, *134*, 9110–9113; b) V. P. Böhm, T. Weskamp, C. W. Gstöttmayr, W. A. Herrmann, *Angew. Chem. Int. Ed.* **2000**, *39*, 1602–1604.

[184]   L. Ackermann, R. Born, P. Álvarez-Bercedo, *Angew. Chem. Int. Ed.* **2007**, *46*, 6364–6367.

[185]   B. Punji, W. Song, G. A. Shevchenko, L. Ackermann, *Chem. Eur. J.* **2013**, *19*, 10605–10610.

[186]   V. Soni, R. A. Jagtap, R. G. Gonnade, B. Punji, *ACS Catal.* **2016**, *6*, 5666–5672.

Danksagung

Curriculum Vitae

Personal Information

Name:	Daniel Zell
Date of Birth:	19.11.1988
Place of Birth:	Bad Karlshafen
Nationality:	German

Academic Education

11/2013–06/2017	Ph.D. thesis (Mentor: Prof. Dr. L. Ackermann) at the Georg-August-University Göttingen Title: C–H Activation by Ruthenium(II), Cobalt(III) and Manganese(I) Catalysis
10/2011–09/2013	**Master of Science** in chemistry at the Georg-August-University Göttingen Master thesis (Mentor: Prof. Dr. L. Ackermann) at the Georg-August-University Göttingen Title: Mechanistic Studies of Ruthenium-Catalyzed C–H Functionalizations grade: 1.2 (awarded with distinction)
10/2008–07/2011	**Bachelor of Science** in chemistry at the Georg-August University Göttingen grade: 1.7

School Education

09/2005–07/2008	Friedrichsgymnasium Kassel Abitur grade: 1.2
09/1999–06/2005	High School in Beverungen
08/1994–07/1999	Primary School in Trendelburg

Teaching Experience

11/2013–03/2014	Lecture assistant of the course "Heterocyclic Chemistry"
04/2014–09/2014	Lecture assistant of the course "Reaction Mechanisms"
10/2014–03/2015	Lecture assistant of the course "Synthetic Methods of Organic Chemistry"
04/2015–09/2015	Lecture assistant of the course "Reaction Mechanisms"
10/2015–03/2016	Lecture assistant of the course "Synthetic Methods of Organic Chemistry"
04/2016–09/2016	Lecture assistant of the course "Organic Chemistry I"
10/2016–03/2017	Lecture assistant of the course "Heterocyclic Chemistry"
04/2017–present	Lecture assistant of the course "Organic Chemistry I"

Publications

11. **D. Zell**, V. Müller, U. Dhawa, M. Bursch, R. R. Presa, S. Grimme, L. Ackermann, *"Mild Cobalt(III)-Catalyzed Allylative C–F/C–H Functionalizations at Room Temperature" Chem. Eur. J.* **2017**, *23*, submitted.

10. **D. Zell**, M. Bursch, V. Müller, S. Grimme, L. Ackermann, *"Switch of C−H Activation Mechanism for Full Selectivity Control in Cobalt(III)-Catalyzed C−H Alkylations" Angew. Chem. Int. Ed.* **2017**, *56*, under revision.

9. **D. Zell**,' U. Dhawa,' V. Müller, M. Bursch, S. Grimme, L. Ackermann, *"C–F/C–H Functionalization by Manganese(I) Catalysis: Expedient (Per)Fluoro-Allylations and Alkenylations" ACS Catal.* **2017**, *7*, 4209–4213.

8. K. Raghuvanshi, **D. Zell**, L. Ackermann, *"Ruthenium(II)-Catalyzed C–H Oxygenations of Reusable Sulfoximine Benzamides" Org. Lett.* **2016**, *18*, 1278–1281.

7. D. Tonin,' **D. Zell**,' V. Müller, L. Ackermann, *"Ruthenium(II)-Catalyzed C−H Methylation with Trifluoroborates" Synthesis* **2017**, *49*, 127–134.

6. **D. Zell**,' Q. Bu,' M. Feldt, L. Ackermann, *"Mild C–H/C–C Activation by (Z)-Selective Cobalt-Catalysis" Angew. Chem. Int. Ed.* **2016**, *55*, 7408–7412.

5. K. Raghuvanshi, **D. Zell**, K. Rauch, L. Ackermann, *"Ketone-Assisted Ruthenium(II)-Catalyzed C–H Imidation: Access to Primary Aminoketones by Weak Coordination" ACS Catal.* **2016**, *6*, 3172–3175.

4. **D. Zell**,' S. Warratz,' D. Gelman, S. J. Garden, L. Ackermann, *"Single-Component Phosphinous Acid Ruthenium(II) Catalysts for Versatile C–H Activations by Metal-Ligand Cooperation" Chem. Eur. J.* **2016**, *22*, 1248–1252.

3. J. Li, S. Warratz, **D. Zell**, S. De Sarkar, E. E. Ishikawa, L. Ackermann, *"N-Acyl Amino Acid Ligands for Ruthenium(II)-catalyzed meta-C–H tert-Alkylation with Removable Auxiliaries" J. Am. Chem. Soc.* **2015**, *137*, 13894–13901.

2. T. Niklas, C. Steinmetzger, W. Liu, **D. Zell**, D. Stalke, L. Ackermann, M. John, *"Determination of the Relative Configuration of β-Amino Acid Esters Based on Residual Dipolar Couplings" Eur. J. Org. Chem.* **2015**, 6801–6805.

1. W. Liu, **D. Zell**, M. John, L. Ackermann, *"Manganese-Catalyzed Synthesis of cis-β-Amino Acid Esters through Organometallic C–H Activation of Ketimines" Angew. Chem. Int. Ed.* **2015**, *54*, 4092–4096.

' both authors contributed equally.

Conferences

07/2014	Second Symposium on C–H Activation, Rennes, France (Poster Presentation), **Green Chemistry Poster Prize**
10/2014	Lower Saxony Catalysis Symposium, Göttingen (Poster Presentation)
09/2015	GDCh-Wissenschaftsforum, Dresden (Poster Presentation)
10/2015	Workshop DFG SPP 1807, Göttingen (Poster Presentation)
05/2016	Summerschool DFG SPP 1807, Bremen (Oral Presentation)
07/2016	XXVII European Colloquium on Heterocyclic Chemistry, Amsterdam (Poster Presentation)
10/2016	Workshop DFG SPP 1807, Köln (Poster Presentation)
02/2017	CaRLa Winterschool, Heidelberg (Oral Presentation)